Ontario Geological Survey
Miscellaneous Paper 103

Geoscience Research Grant Program

Summary of Research 1981-1982

edited by
E.G. Pye

1982

Ontario
Ministry of Natural Resources

Hon. Alan W. Pope
Minister

W. T. Foster
Deputy Minister

Printed in Canada

ISSN 0704-2752
SUBSERIES ISSN 0225-5316

Publications of the Ontario Ministry of Natural Resources are available from the following sources. Orders for publications should be accompanied by cheque or money order payable to the Treasurer of Ontario.

Reports, maps, and price lists (personal shopping or mail order):

Public Service Centre, Ministry of Natural Resources
Room 1640, Whitney Block, Queen's Park
Toronto, Ontario M7A 1W3

Reports and accompanying maps (personal shopping):

Ontario Government Bookstore
Main Floor, 880 Bay Street
Toronto, Ontario

Reports and accompanying maps (mail order or telephone orders):

Publications Services Section, Ministry of Government Services
5th Floor, 880 Bay Street
Toronto, Ontario M7A 1N8
Telephone (local calls), 965-6015
Toll-free long distance, 1-800-268-7540
Toll-free from area code 807, 0-ZENITH-67200

Every possible effort is made to ensure the accuracy of the information contained in this report, but the Ministry of Natural Resources does not assume any liability for errors that may occur. Source references are included in the report and users may wish to verify critical information.

Parts of this publication may be quoted if credit is given. It is recommended that reference to this report be made in the following form for each individual author:

West, G.F.
1982: Model Studies of EM Prospecting; Grant 124, p.210-212 in Geoscience Research Grant Program, Summary of Research 1981-1982, edited by E.G. Pye, Ontario Geological Survey, Miscellaneous Paper 103, 219p.

1200-300-82-TRI GRAPHIC

CONTENTS

Introductory Remarks

The Ontario Geoscience Research Grants Program was initiated in early 1978 as a means of supporting mission-oriented research at Ontario universities to complement the work of the Ontario Geological Survey in response to the various issues within its mandate.

> *"To stimulate exploration for and facilitate sound planning in all matters related to mineral and other earth resources by providing an inventory and analysis of the geology and mineral deposits of Ontario."*

The Grants Program is administered by a committee reporting to the Director of the Ontario Geological Survey and is made up of three representatives of the minerals industry, three representatives of the university community, four representatives of the Survey, and a chairman. Appointments of industry and Ontario university representatives are up to three years, renewable once. The members of the present committee are:

Dr. N. Paterson, Chairman	Paterson, Grant & Watson Ltd.
Dr. A. Becker	Questor Surveys Limited
S.N. Charteris	Falconbridge Nickel Mines Ltd.
Dr. J.H. Crocket	McMaster University
Dr. P.F. Karrow	University of Waterloo
Dr. W.S. Fyfe	University of Western Ontario
Dr. J.A. Coope	Newmont Explorations of Canada Ltd.
Dr. A.C. Colvine	Ontario Geological Survey
Dr. P.C. Thurston	Ontario Geological Survey
Dr. P.G. Telford	Ontario Geological Survey
Dr. I. Thomson	Ontario Geological Survey

The role of the committee is to receive, review, and rank proposals from research workers at Ontario universities with respect to scientific merit and relevance to the objectives and activities of the Ontario Geological Survey, and to recommend funding or rejection. A feature of the appraisal process is that each submission is referred by the committee to at least four geoscientists in industry, the university community, and/or government outside the Ontario Geological Survey, and one member of the Survey for critical review and comment to ensure the most thorough and objective appraisal possible.

Proposals for projects up to three years duration are acceptable. Original and renewal applications must be submitted by November 15 preceding the fiscal year (April 1 - March 31) for which grants are awarded. Successful applicants are expected to submit a brief report for publication in an annual Summary of Research and to participate in an annual seminar to present the results of his/her research, to the community at large. Publication in scientific journals is encouraged, and a final report is required by the Ontario Geological Survey within six months of the termination of funding.

Nineteen final reports on research projects partially or wholly funded under the Ontario Geoscience Research Grant Program in 1981-1982 will be placed on Ontario Geological Survey Open File Reports. Those reports already on open file are:

OFR 5374, Grant 7: Horizontal Deep Drains to Stabilize Clay Slopes; T.C. Kenney
OFR 5384, Grant 8: Interpretational Support for Electromagnetic Prospecting; G.F. West
OFR 5380, Grant 17: Platinum Group Elements in Magnetic Sulphide Deposits; A.J. Naldrett
OFR 5365, Grant 20: Magnetism and Stratigraphy in the Blake River Volcanics; D.W. Strangway, J.W. Geissman, J. Bambrick, S. Letros, and A. Tasillo
OFR 5366, Grant 28: Immobilization of U-Th-Ra in Mine Wastes by Mineralization; W.S. Fyfe, J.R. Brown, B.I. Kronberg, and F. Murray
OFR 5376, Grant 30: Gold Exploration Using CO_2, H_2O and Alkali "Anomalies"; R.E. Whitehead
OFR 5368, Grant 38: Radon Decay Products - U Exploration; K. Bell and H.W. Card
OFR 5367, Grant 54: Regional Alteration in Archean Greenstone Belts of the Superior Province: Applications to Exploration for Massive Cu-Zn Sulphide Deposits; A.E. Beswick
OFR 5369, Grant 55: Evolution of an Archean Felsic Volcanic-Plutonic Complex; R.W. Hodder

OFR 5375, Grant 84: Sedimentology of the Matinenda Formation; A.D. Miall

The final reports listed below were about to be placed on open file as this publication went to press:

Grant 5: Component Magnetization of Iron; D.T. Symons
Grant 11: Gold Ore Formation at Red Lake; C.J. Hodgson
Grant 27: Field Relations and Geochemistry of Au, Ni and Cr Deposits; R.W. Hutchinson
Grant 32: Alteration and Gold Vein Environments; R.G. Roberts
Grant 46: Potential for Deposits of Chromite in Ontario; P.R. Mainwaring, and D.H. Watkinson
Grant 68: Model Study of Archean Greenstone Granite Gneiss Belts; J.M. Dixon
Grant 75: Asbestos Fibre Degradation in Laboratory Solutions; H.W. Nesbitt
Grant 87: Stability of Compressed Shales in Ontario; R.H. Mills
Grant 88: Metallogeny and Economic Potential of Western Lake St. Joseph Greenstone Belt; R.S. Shegelski

This publication is the fourth annual Summary of Research, and presents brief descriptions of the projects funded for the fiscal year ending March 31, 1982. Of the 21 projects approved for funding in 1981-1982, 10 were renewal projects.

UNIVERSITY	APPROVED		REJECTED	
Brock	$ 19,270*	2	$ 24,720	2
Carleton	22,750	1		0
Lakehead		0		0
Laurentian	7,500	1	45,450	2
McMaster	22,400	1		0
Ottawa		0	15,701	1
Queen's	35,000*	1	25,750	2
Toronto	186,346	8	59,328	4
Waterloo	34,070	2	32,000	1
Western	74,463	4	43,900	3
Windsor	16,490	1	39,680	3
York		0	7,182	1
Total	$418,289	21	$293,711	19

*A grant for 6,370 was submitted by Brock University but was held jointly with Queen's University.

The following are new projects initiated in fiscal 1981-82, by the principal applicant named:

Grant 100: The Petrology, Geochemistry and Economic Potential of the Nipissing Gabbro; A.D. Edgar, University of Western Ontario
Grant 105: Latter-Stage Decay Products of ^{222}Rn-Use in Radioactive Waste Management; K. Bell, Carleton University
Grant 106: Platinum Group Elements in Layered Intrusions; A.J. Naldrett, University of Toronto
Grant 108: Palynostratigraphy of Lignites Near Adam Creek and Onakawana Moose River Basin; G. Norris, University of Toronto
Grant 109: Interpretation of Gravity Data from Northern Ontario; L. Mansinha, University of Western Ontario
Grant 112: Petrographic Number Re-evaluation: P.P. Hudec, University of Windsor
Grant 113: Field Investigation of Factors Controlling Changes of Groundwater Pressure in Clay Slopes; T.C. Kenney, University of Toronto
Grant 114: Source, Correlation and Thermal Maturation History of Hydrocarbon Mineral Deposits of Southern Ontario; J.F. Barker, University of Waterloo
Grant 115: Characterization of Assimilation-type Uraniferous Pegmatites, Bancroft Region; S.J. Haynes, Brock University
Grant 118: Surface Electromagnetic Mapping in Selected Positions of Northern Ontario; D.W. Strangway, University of Toronto
Grant 124: Simulation of Complex E.M. Targets, G.F. West, University of Toronto

The undersigned would like to thank the chairman and the members of the committee for their hard work and participation in the program during the past year, and to the large number of dedicated scientists who gave freely of their time and expertise to review the proposals and provide objective appraisals to serve as a basis for selecting the projects reported on in this publication. The work of the individual researches also is gratefully acknowledged, for it is only through their endeavours, and commitment to scientific excellence, that the objectives of the program can be achieved. Finally, special thanks are due to Ms. W. Paquette, who served as Grants Administrator and Secretary.

E.G. Pye
Director
Ontario Geological Survey

1981-1982 Geoscience Research Grant Recipients

PRINCIPAL APPLICANT	UNIVERSITY		TITLE
Dr. J.H. Crocket	McMaster	Grant 49	Stable isotope studies to gold metallogeny in the Timmins Camp
Dr. W.S. Fyfe	Western	Grant 56	Geochemistry and field relations to lode gold deposits in felsic igneous intrusions
Dr. R.F. Mereu	Western	Grant 57	A Micro-earthquake survey of the Gobles oil field of S.W. Ontario
Dr. D. York	Toronto	Grant 62	Direct Dating of Ore Minerals
Dr. Ian Nichol	Queen's	Grant 76	Speciation of free gold in glacial overburden as a key to exploration
Dr. R.W. Dalrymple	Queen's	Grant 78	Terrain characteristics and physical processes in small lagoon complexes
Dr. Ian Campbell	Toronto	Grant 80	Rare Earth Elements in Acid Volcanics
Dr. W.M. Schwerdtner	Toronto	Grant 82	Structural controls of uranium deposits in the Bancroft-Goderham area
Dr. J.E. Gale	Waterloo	Grant 92	Impact of Groundwater on mining activities in the Niagara Escarpment
Dr. D.H. Rousell	Laurentian	Grant 96	Mineralization in the Whitewater Group, Sudbury Basin
Dr. A.D. Edgar	Western	Grant 100	The petrology, geochemistry and economic potential of the Nipissing Gabbro, Ontario
Dr. Keith Bell	Carleton	Grant 105	Latter-stage decay products of ^{222}Rn – use in radioactive waste management.
Dr. A.J. Naldrett	Toronto	Grant 106	Platinum group elements in layered intrusions
Dr. G. Norris	Toronto	Grant 108	Palynostratigraphy of lignites near Adam Creek and Onakawana, Moose River Basin
Dr. L. Mansinha	Western	Grant 109	Interpretation of gravity data from Northern Ontario
Dr. P.P. Hudec	Windsor	Grant 112	Petrographic number re-evaluation
Dr. T.C. Kenney	Toronto	Grant 113	Field investigation of factors controlling changes of groundwater pressure in clay slopes
Dr. J.F. Barker	Waterloo	Grant 114	Source, correlation and thermal maturation history of hydrocarbon mineral deposits of S. Ontario.
Dr. S.J. Haynes	Brock	Grant 115	Characterization of assimilation-type uraniferous pegmatites, Bancroft region
Dr. D.W. Strangway	Toronto	Grant 118	Surface electro-magnetic mapping in selected positions in N. Ontario
Dr. G.F. West	Toronto	Grant 124	Simulation of complex EM targets

Grant 82 Structural Controls of U-Ore Bearing Pegmatite Dikes at Madawaska Mine, Bancroft, Ontario

R.L. Bedell and W.M. Schwerdtner
Department of Geology, University of Toronto

ABSTRACT

Pegmatite dikes at the Madawaska Mine (the former Faraday Mine) were emplaced after the height of Grenville metamorphism, and were presumably generated from the granitic gneisses during anatexis.

All ore grade pegmatite dikes are confined to the Faraday Metagabbro Complex (FMC) and are generally concordant to the fabrics developed during ductile deformation of the Grenville Orogeny. Throughout the FMC, these fabrics are defined by strained mafic mineral aggregates. Foliations were measured in different domains and proved to be broadly concordant to the trend of the local pegmatites. Lineations have a consistent regional trend, but have plunge values that vary with the foliation plane. Commonly, pegmatites plunge parallel to mineral lineations.

Pegmatite emplacement was relatively passive, without disruption of local FMC fabrics. Numerous metagabbroic xenoliths and their disaggregation in pegmatites show that replacement and assimilation were important modes of emplacement. Little evidence of dilation was found in most exposures. Microstructures of plagioclase within the pegmatites suggest brittle deformation. This is consistent with pegmatite emplacement into the FMC after the ductile deformation that occurred during Grenville metamorphism.

The FMC was a preferred host rock for uranium-bearing pegmatite dikes because of its mechanical competence and ability to provide iron and sulphur for reduction and uranium fixation.

INTRODUCTION

The peak of metamorphism throughout the Madawaska Mine area corresponds to upper amphibolite to granulite facies. This high-grade regional event involved remobilization of large volumes of granitic crust during the Grenville metamorphism (Chesworth 1971). The pegmatites at the Madawaska Mine and throughout the area are thought to have been generated during this anatectic event.

There are presently three schools of thought as to the ultimate source of the uranium in the pegmatite dikes of the region. Bright (1980), suggested that the uraniferous pegmatites were initially derived at depth by partial melting of basal arenites of the Anstruther Lake group during Grenville metamorphism. Along the flanks of basement gneiss domes, where metamorphism was high, those pegmatites which were emplaced concordantly within the Hermon Group are thought to have also extracted uranium metasomatically from their host rocks.

S.B. Lumbers (Curator of Geology, Royal Ontario Museum, personal communication, 1981) suggested that the source of uranium is related to the alkalic rocks of the area and regional fenitization.

S.J. Haynes (Brock University, personal communication, 1981) suggested that all the uranium necessary to produce the quantity found in the pegmatites was present in the granitic gneisses. Processes of anatexis, particularly during granitic gneiss dome formation, thus may have concentrated the uranium in sufficient quantity to account for that presently found in the pegmatites.

CRITIQUE OF PREVIOUS STRUCTURAL MODEL

The Madawaska Mine is located within the Faraday Metagabbro Complex (FMC) just north of the Faraday Granite, a semi-circular gneiss dome. The rocks at the southern margin of the Faraday Granite display fenitization and are associated with the alkalic belt running through that area (Figure 1).

The diverse modal compositions and textures associated with the FMC as well as the complex geometries associated with the pegmatites, have prompted mine geologists to study merely the pegmatite distributions. Little *et al.* (1972) suggested that the pegmatite bodies are associated with a plunging synformal fold and an antiform to the north (Figure 2).

Our detailed mapping in 1980 defined the arcuate southeast border of the FMC (Figure 3). Pegmatite dikes are confined to, and are concordant with, the southeast border of the FMC along the south "limb" of the synform postulated by Little *et al.* (1972). This relationship holds for all levels of the mine. Away from this contact pegmatites have a distinct northeast trend. What Little *et al.* (1972) regarded as a fold is simply an intersection between the northeast-trending pegmatites and those that are following the arcuate southeast border contact.

The antiform postulated by Little *et al.* (1972) to the north in Figure 2 is nonexistent. This area (as shown by the cross-cut heading to the northernmost pegmatite) was not accessible until 1981, when consistent northeast-trending, southeast-plunging foliations were recorded.

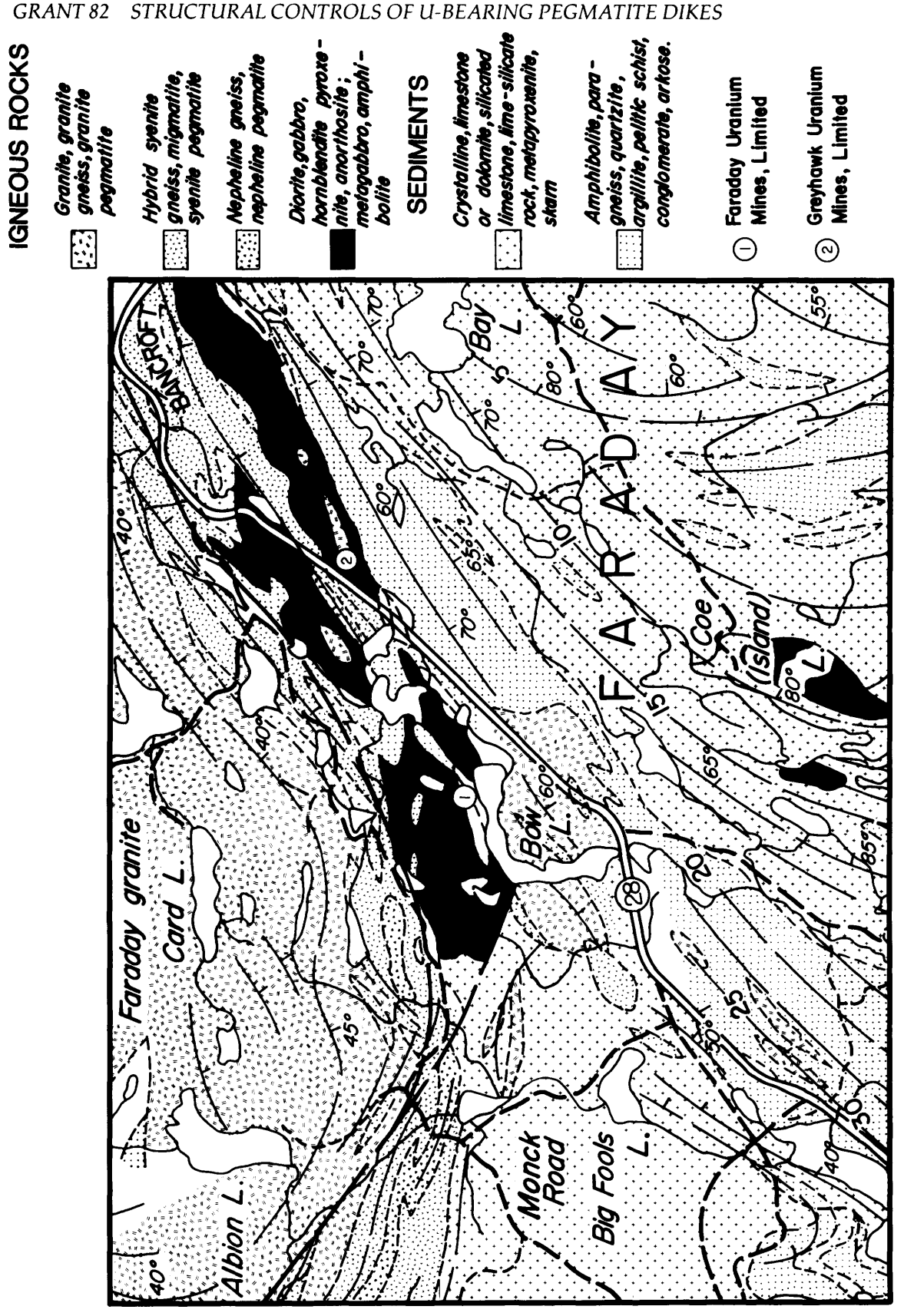

Figure 1. *Geology of the Bancroft area (after Hewitt and Satterly 1957).*

Our field work demonstrates that the pegmatites are confined to the FMC and have two dominant trends: (1) along the southeast arcuate contact of the FMC, and (2) a distinct northeast trend, away from the contact. Careful examination of the host FMC was undertaken to examine its structural properties in hope of elucidating pegmatite distribution and improving our understanding of the interaction of pegmatite and host rock during emplacement.

PETROGRAPHY AND MICROSTRUCTURE OF THE FMC

The Faraday Metagabbro Complex is texturally and modally diverse. It ranges in composition from anorthositic gabbro to amphibolite and contains relict massive to layered enclaves reflecting its premetamorphic history. The rocks of some areas exhibit greater than 100 percent tensile strain.

An original thesis done on the mine property (Morris 1956), interpreted portions of the FMC as being amphibolite of sedimentary origin. The mine geologists initially started mapping the host rocks to the pegmatites, referring to them as "gneiss 1-6", but soon abandoned this difficult task.

In the anorthositic rocks the mafic minerals appear as aggregates of amphibole, some of which still contain relict clinopyroxene cores. Rare orthopyroxene can be found and, when plotted on the pyroxene quadrilateral phase diagram (Figure 4), the electron microprobe analyses fall within the 600-900°C isotherms as outlined by Ross and Huebner (1975). These pyroxenes fall in the

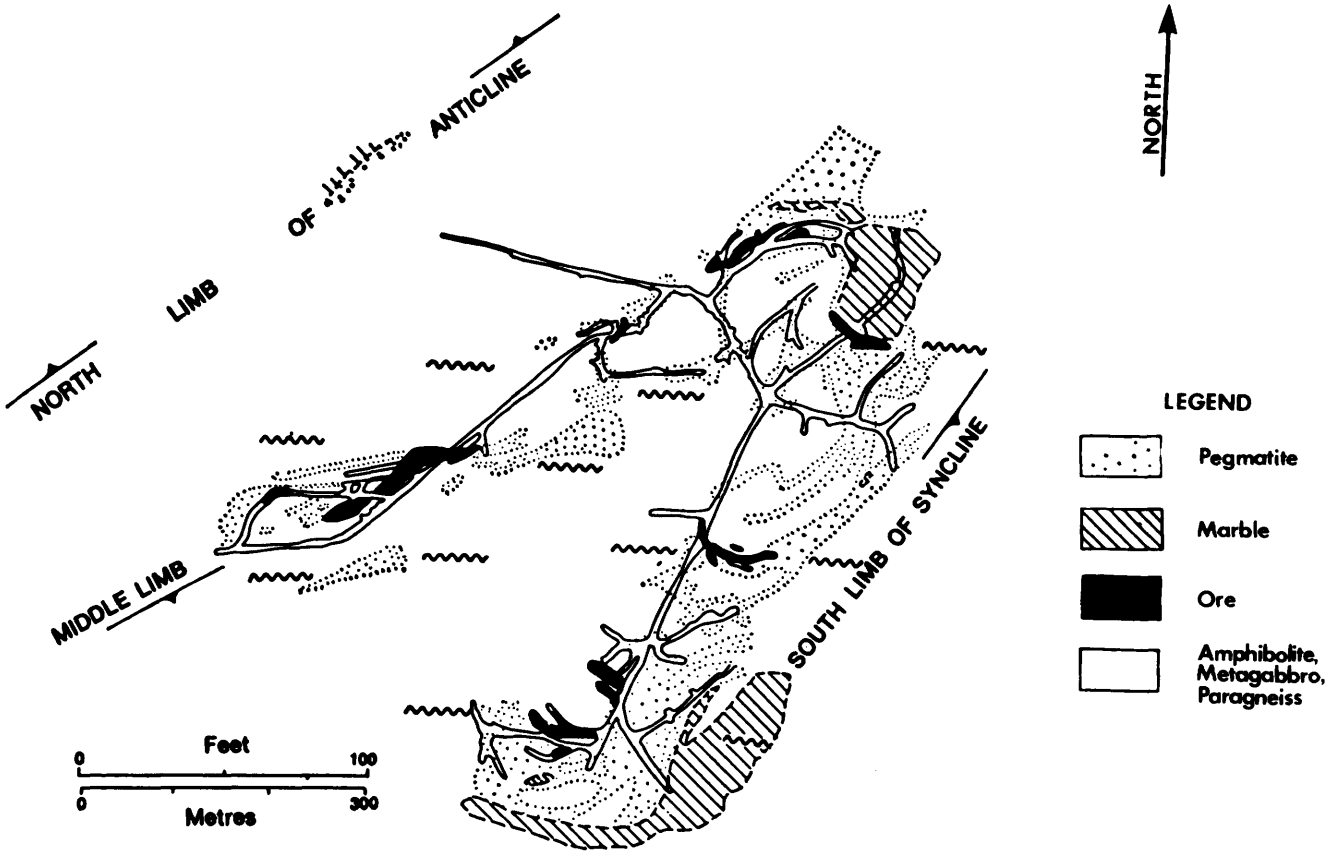

Figure 2. *Geology of the Madawaska Mine at the 450-foot level according to Little et al.* (1972).

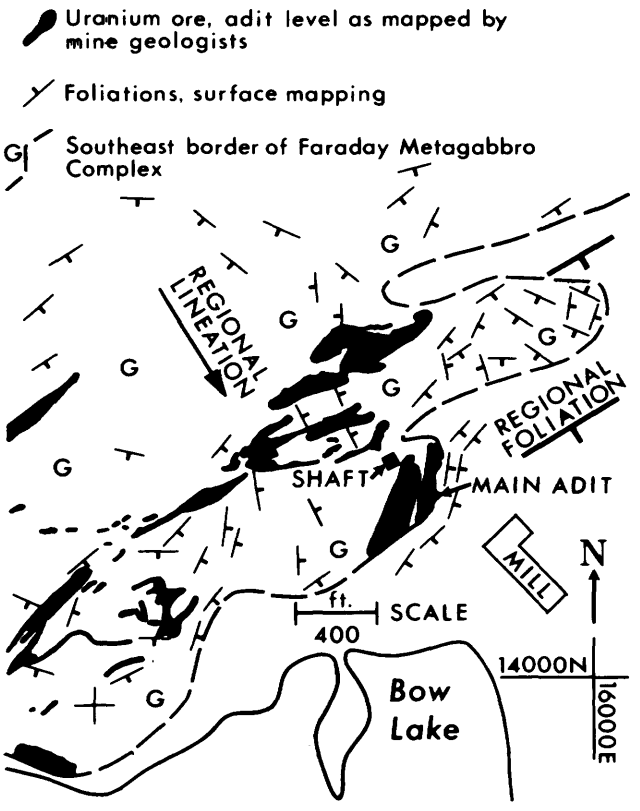

Figure 3. *Geological sketch map of the Madawaska Mine area showing that pegmatites are confined to the Faraday Metagabbro Complex. Pegmatites along the contact are concordant to the arcuate FMC border and those away from the contact have a northeast trend.*

same temperature range and have similar compositions with respect to both major and minor elements as those reported by Ashwal (1982) in the Marcy anorthosite massif of the Adirondacks in New York, also of Grenville age and metamorphosed to granulite facies.

The pyroxenes are rimmed by a slightly more sodic amphibole that often occurs as randomly oriented aggregates. Associated with the amphibole are sporadic occurrences of opaques, including magnetite (showing no exsolution textures) and monoclinic pyrrhotite. Sphene aggregates are commonly associated with magnetite cores. Biotite is also associated with these mafic segregations but often occurs as euhedral or rarely kinked crystals, indicative of a later origin relative to the bulk of the recrystallized mafic aggregates.

Plagioclase occurs in a diverse range of textures grading from relict igneous laths into grains dominated by mechanical twins, to a completely recrystallized texture (Bedell and Schwerdtner 1981). The composition of the plagioclase as determined by electron microprobe analyses ranges from labradorite (An_{60}) to andesine (An_{20}).

Scapolite is a common constituent that replaces plagioclase only, in the first stages along cleavage planes and twin boundaries, but complete replacement is common. The abundance of scapolite appears to increase in modal abundance with intensity of recrystallization of plagioclase as also reported by Appleyard and Williams (1981).

Apatite occurs sporadically and is found usually as subhedral grains within the plagioclase matrix.

Deformation microstructures have recently been examined in experimentally deformed Maryland diabase (Kronenberg and Shelton 1980) that closely resembles deformed rocks having similar composition and metamorphosed under upper greenschist to almandine-amphibolite facies conditions. With an experimental strain

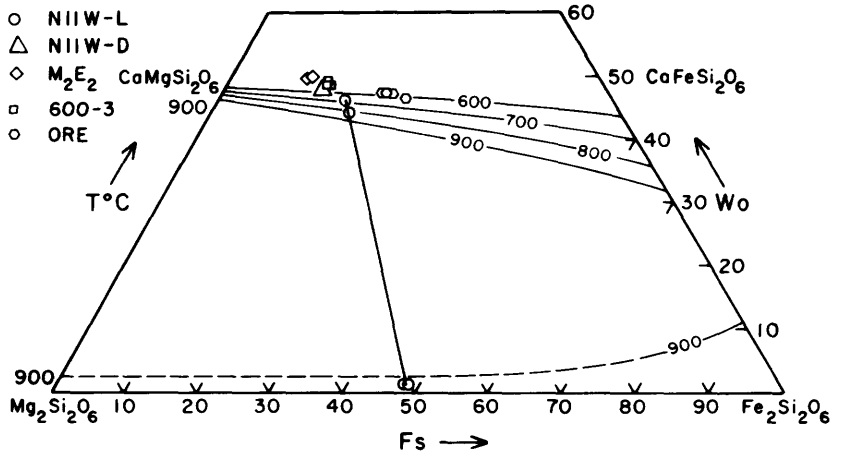

Figure 4. *Pyroxene quadrilateral with compositions obtained by electron microprobe analyses. Isotherms as designated by Ross and Huebner (1975).*

rate of $3x10^{-6}$/sec and a confining pressure of 15 Kbar, plagioclase was found to become weaker than pyroxene at temperatures greater than roughly 700°C. At much lower strain rates (geologically applicable) this transition occurs at somewhat lower temperatures. Heard and Raleigh (1972) have shown experimentally that less heat is needed at lower strain rates to produce a given amount of strain in ductile rocks. Therefore, under crustal conditions in which gabbro is ductile, plagioclase is relatively weaker than pyroxene and deformation behavior is controlled by the mechanisms of plagioclase deformation.

This is consistent with observations made by Bedell in thin sections throughout the FMC, whereby plagioclase responds earlier to deformation than the mafic minerals as revealed by a series of plastic deformation effects (Bedell and Schwerdtner 1981). This has allowed us to determine relative deformation states of individual samples, the details of which will be reported elsewhere.

FMC FABRICS

Throughout the Faraday Metagabbro Complex, the mappable fabrics are strained mafic mineral aggregates best seen on orthogonally cut slabs (Figure 5). On one surface, the aggregates are strung out as rods (Figure 5a) and, on the orthogonal face, they appear as flattened ellipses (Figure 5b). The rodding effect is known as a lineation which is parallel to the long axis (A) of the strain ellipsoid. The flattening that we see in most rock exposures defines the A-B plane of local principle strain. These fabrics were mapped throughout the FMC.

S-tectonites exhibit planes along which, in addition to the foliation, one may find ductile to brittle shearing effects, boudinage, and distinct compositional layering. Figure 6 shows many of the textures associated with S-tectonite fabrics. In this photograph the foliation plane is near vertical and at right angles to the page. On the left, notice a felsic vein hooking to the left (concave down) and which is abruptly cut off. This represents a ductile shear within the foliation plane. Also notice the diversity in changes of modal mineralogy that occur at right angles to the foliation plane. Another feature to notice is the boudinage effect of the mafic (and apparently more competent) layer. These features are typical of the S-tectonites, and their attitudes were measured throughout the FMC.

A rose net of all the readings obtained throughout the FMC are plotted in Figure 7. It contains over 900 readings from underground and surface mapping. This distinct northeast trend correlates with the overall elongation of the FMC and the distinct northeast trend of pegmatites observed away from the arcuate southeast contact.

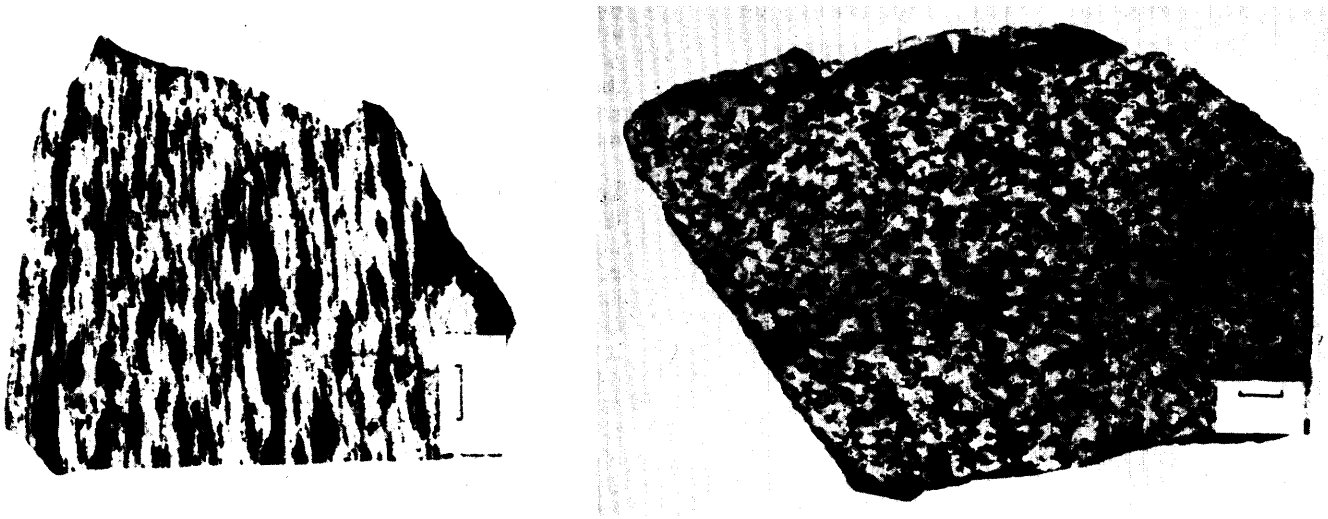

Figure 5. *Orthogonal slabs of typical metagabbro cut parallel to principal directions of the strain ellipsoid.* ***a.*** *(left) This slab contains the A-C plane.* ***b.*** *(right) Shows the A-B plane of the strain ellipsoid. Scale on slabs is 1 cm.*

Figure 6. *Outcrop showing various features of S-tectonites. The foliation plane is vertical and perpendicular to the plane of the page. Scale is indicated by 12cm long pen toward the lower left in the photograph.*

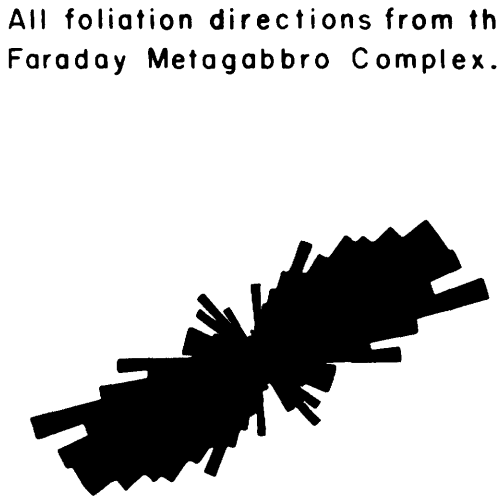

Figure 7. *Rose net diagram representing over 900 measured S-tectonite orientations from both surface and underground throughout the FMC. The north direction is vertical in the plane of the page.*

Figure 8 shows the borders of the FMC in the mine vicinity as determined in this study. Further outcrops of the gabbro are found to the north and east of Bentley Lake, and have been studied by others (e.g. Appleyard and Williams 1981). The rose nets represent individual domains where the foliation readings were taken, and indicate southeast dips with only rare readings beyond vertical and dipping to the northwest. The pegmatite distribution is shown as mapped by Morris (1956) and verified by this study. Even with limited exposure, it is apparent that the pegmatites near the southeast margin of the FMC are concordant to the arcuate southeast and south borders, whereas the pegmatites away from the margin have an overall northeast trend.

The domain in the southeast of the area, along the arcuate southeast border, has a poor clustering of foliation directions because here the fabrics tend to mimic contact complexities. The southwest domain also exhibits poor clustering and this is due to a circular plug of nepheline gneiss which intruded this part of the FMC prior to Grenville metamorphism. It is interesting to note that pegmatites are symmetrically distributed around this body displaying a strong structural control. The central rose net represents the entire middle part of the FMC from the north contact down to Bow Lake. This domain exhibits a strong northeast trend and is parallel to the general distribution of pegmatites. The rose net displays an anomalous cluster along the northwest-southeast direction. This is due to a unique zone of particularly well developed fabric, just to the west of the rose net, and which has a zone of roughly concordant pegmatites. The northwest and northeast domains have relatively few pegmatites, but the

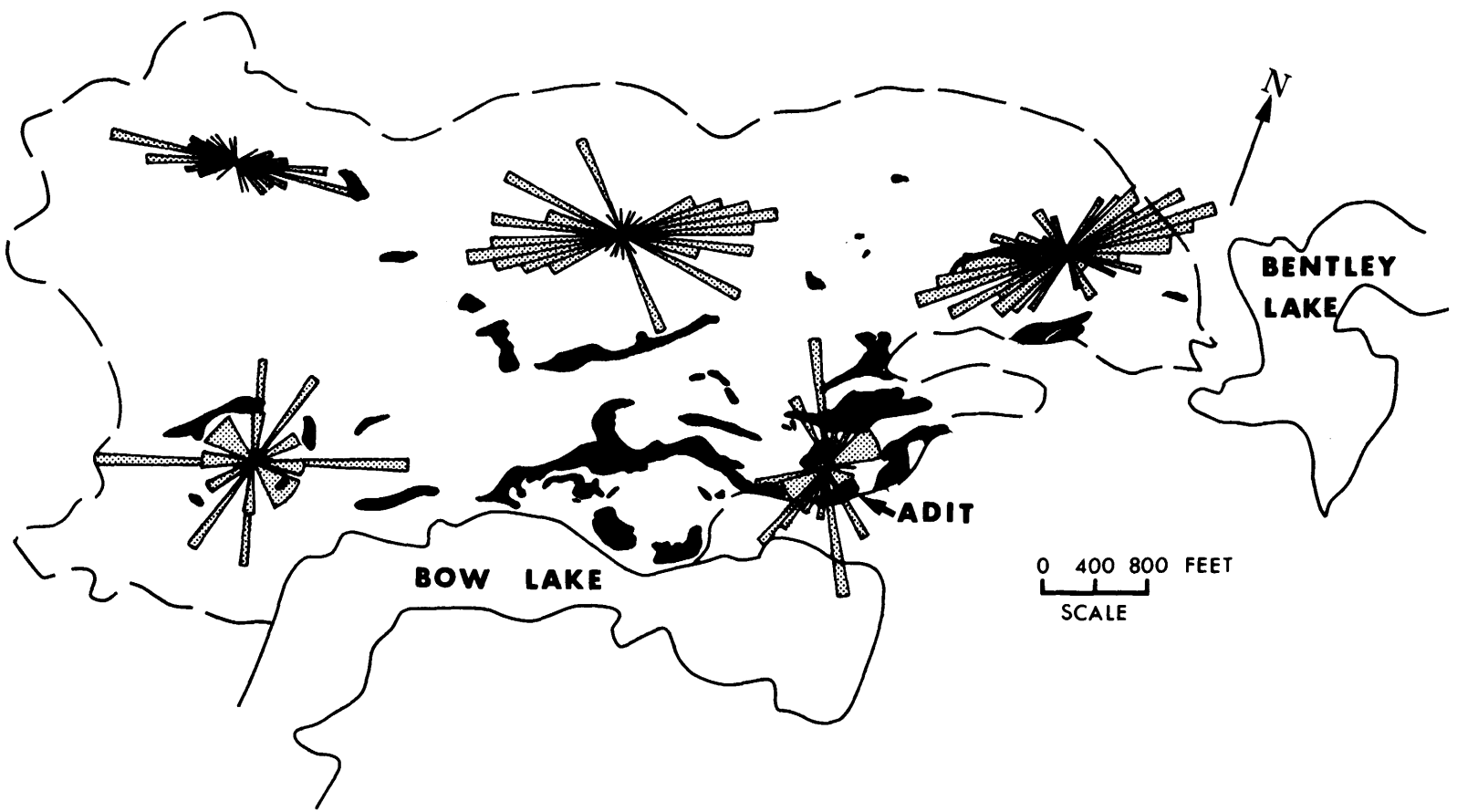

Figure 8. *Rose net diagram representing S-tectonite fabrics from different domains throughout the FMC. The pegmatite distribution is indicated by the dark coloured irregular bodies as mapped on the surface. The border of the FMC is indicated by the heavy line north of Bow Lake.*

few bodies that do occur are approximately parallel to the local host-rock fabric. The three northern domains define a broad arc, which could be attributed to a late stage diapiric mobilization of the Faraday Granite along the northern contact of the FMC. The FMC has a relatively higher melting temperature and would have behaved as a ductile unit, while the granitic gneiss dome, a relatively lower-temperature body, would still be flowing and could have imposed this late-stage strain pattern. The pegmatite distribution is roughly parallel to the trend of the regional strain pattern.

L-tectonics control the local geometry of pegmatites. Their lineation is a regional feature that has a consistent azimuth of 140° plunging to the southeast (Figure 9). Underground and surface mapping often show pegmatite plunge parallel to the regional lineation. This is well demonstrated in Figure 10, which is the first outcrop north of the mine on the southeast side of Highway 28 towards Bancroft. Here we can see the lineations as striations on the overhanging portions of the outcrop, plunging into the outcrop towards the southeast.

In review, it can be demonstrated that there is an important structural control over the distribution of uranium-bearing pegmatite dikes as documented by their concordance to the dominant S- and Ltectonite fabrics throughout the Faraday Metagabbro Complex.

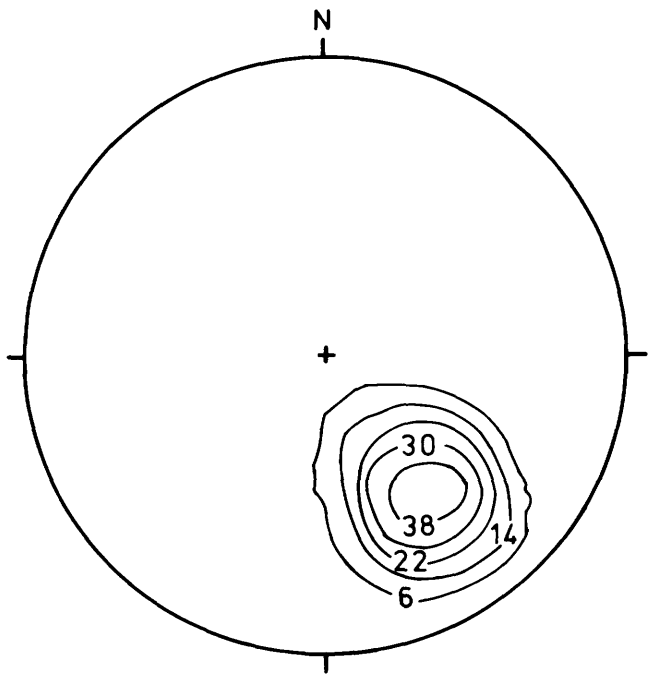

Figure 9. *Equal area meridian projection of L-tectonite orientations measured throughout the FMC.*

PEGMATITE DIKE EMPLACEMENT

Emplacement of pegmatite dikes was examined using the criteria as outlined by Kretz (1968) to differentiate between replacement and dilation. There are several problems with applying these criteria at the Madawaska Mine. First of all, as has already been demonstrated, the pegmatite dikes are dominantly concordant to the host rock fabric. If older discordant features are not available, dilation lines cannot be drawn to assess the amount of dilation versus replacement. Other criteria are dependent on the existence of sharp planar boundaries and the ability to view contacts on both sides of a pegmatite body. Such dikes are rarely found on a megascopic scale. Small veinlets show indications of dilation, but the dominant emplacement mechanism was probably replacement.

Numerous xenoliths of the FMC are found throughout the pegmatite dikes and often display the process of disaggregation and dispersion of the mafic minerals. Many of the relict fabrics still detectable in the xenoliths have not been rotated with respect to the fabric in the wall rock. This suggests a relatively passive replacement.

Macroscopic examination of pegmatite fabrics reveals that they are weakly strained as compared to the host FMC. This has been verified by examination of the plagioclase microstructure. The plagioclase ranges from albite to oligoclase (An_{15}), the oligoclase compositions having crystallized as peristerites. These grains are optically negative suggesting a high-temperature disordered structure, and are texturally hypidiomorphic and granular, with growth twins predominant. The deformation of pegmatite plagioclase consists only of brittle faulting (Figure 11) and this plagioclase therefore has not experienced the earlier ductile deformation as described for the more intermediate plagioclase in the host FMC.

Hinge zones of fold-shaped pegmatite bodies and crook structures were examined and sampled, because these areas would have been the most susceptible to deformation. These domains have undergone the same degree of brittle deformation observed in the limbs. Therefore these pegmatites must have passively emplaced themselves along a combination of structures after the high-grade ductile deformation associated with the peak of Grenville metamorphism.

The following sequence of events can now be suggested:

(1)The FMC intruded marbles and various metasediments.

(2)The height of regional metamorphism (Grenville Orogeny) imposed a pervasive S- and L-tectonite fabric on the FMC and generated pegmatites during anatexis of granitic gneisses.

(3)The more competent FMC contained well-developed structural pathways along which the uraniferous pegmatite magma preferred to intrude, and emplaced itself during late stages of Grenville metamorphism under conditions below the ductile/brittle transition for plagioclase.

THE IMPORTANCE OF HOST ROCK CONTROL IN ORE FORMATION

The emplacement of pegmatite bodies was controlled by the pre-existing ductile-deformation structure of the host rock. Thus, pegmatites followed paths of least resistance and mimicked available structures.

The most important property of the host rock in the Madawaska Mine area was its high competency relative to the metasediments. It was, therefore, able to provide the structural traps to accomodate the pegmatites attempting to force their way to a lower pressure environment.

Another major feature of the FMC is its geochemistry. The association of high grades of U-ore with the most mafic portions of the pegmatite and along contacts with the most mafic host rock have been well documented (Ralph Alexander, personal communication, 1980; Satterly 1957).

A comparable analogue to the Bancroft district is the Rossing district of South West Africa (Berning *et al.* 1976). In Africa, the highest grades of uranium in anatectically derived pegmatites are found against mafic host rocks in a terrain that is dominated by marbles and amphibolites similar to those at Bancroft. This suggests reduction of the uranyl complex by ferrous iron fixation.

Detailed petrography and geochemistry of two uranium-rich granites in South Carolina (Speer *et al.* 1981) have demonstrated that one granite retained only one eighth of its original magmatic uranium content because it lacked the ferrous iron minerals and sulphides to reduce and immobilize the U^{6+} to U^{4+} before migration out of the body.

The FMC has abundant iron-bearing mafic minerals and locally has abundant sulphides, particularly pyrrhotite. Large scale assimilation of such phases would explain the intimate association of uranium phases with Fe-Ti-Si compounds and sulphides as shown in the scanning electron microscope photos published by Rimsaite (1980) from the Madawaska Mine area.

Additional detailed petrographic evidence demonstrating the association of uranium mineralization with Fe-bearing phases is well documented by Fyson (1980).

Therefore the FMC acted as an important geochemical as well as structural trap. If future demand for uranium warrants further development in this region then mafic bodies would make preferable exploration targets.

CONCLUSIONS

This study was initiated to gain an understanding of the structural controls of pegmatite distribution at the only recently active uranium mine in the Bancroft camp. It was anticipated that knowledge of the structural controls would assist in locating preferable settings for the formation of ore grade pegmatites elsewhere.

This study has successfully demonstrated that there is a strong structural control of the distribution and orientation of the uranium bearing pegmatites at Madawaska Mine. In terms of applying what we have learned in this study to other areas we can say that the competency of the host rock appears to be a factor in controlling prefer-

Figure 10. *Road cut showing relationship of pegmatites with L-tectonites. The lineation is detectable on the overhanging portions of the outcrop, plunging into the outcrop surface to the southeast. The field of view is approximately 15 m of horizontal outcrop surface.*

Figure 11. *Photomicrograph, under crossed polarizers, of brittle deformation in optically negative albite. Field of view is approximately 2.7 mm. across.*

able zones of intrusion along pre-existing structures. Therefore, structural geology is critical in determining settings in which sufficient volumes of pegmatite are allowed to form a potential ore deposit, and is essential in determining pegmatite distribution and geometry.

Structural geology however, cannot tell us why one pegmatite is ore grade and others are not (e.g. Fyson 1980). This is a chemical problem related to uranium fixation and the importance of iron and associated phases often found in mafic rocks, in the Bancroft camp and similar settings throughout the world.

In conclusion, we believe that mafic host rocks are preferable structurally and geochemically for the emplacement of economic uraniferous pegmatites in the Madawaska Mine area.

ACKNOWLEDGMENTS

The authors would like to thank the staff of Madawaska Mines Limited for their constant assistance and for information provided. We would also like to thank staff at the Royal Ontario Museum, Dr. S.B. Lumbers and V. Vertolli, for sharing time in the field, and T. Ottaway and Dr. R.I. Gait, for access to the mineral collections. We are also indebted to the staff at the Ontario Geological Survey, particulary W. Paquette and J. Robertson.

REFERENCES

Appleyard, E.C. and Williams, S.E.
1981:Metasomatic Effects in the Faraday Metagabbro, Bancroft, Ontario, Canada; Tzchermaks Min. Petr. Mitt., Vol. 28. p.81-97.
Ashwal, L.D.
1982: Mineralogy of Mafic and Fe-Ti Oxide Rich Differentiates of the Marcy Anorthosite Massif, Adirondacks, New York; American Mineralogist, Vol 67. p.14-27.
Bedell, R.L. and Schwerdtner, W.M.
1981: Structural Controls of U-ore Bodies in the Madawaska Mines Area, Bancroft, Ontario; p.13-17 in Summary of Research, 1980-1981, edited by E.G. Pye, Ontario Geological Survey, Miscellaneous Paper 98.
Berning, J., Cooke, R., Hiemstra, S.A. and Hoffman, U.
The Rossing Uranium Deposit, South West Africa; Economic Geology Vol. 71, p.351-368.
Bright, E.G.
1980: Uranium Mineralization Associated with Mafic to Alkalic Volcanism within the Late Precambrian Grenville Supergroup, Bancroft Area, Ontario; Ontario Geological Survey, Geoscience Research Abstracts.
Chesworth, W.
1971:Metamorphic Conditions in a part of the Haliburton Highlands of Ontario; Lithos, Vol. 4, p.219-29.
Fyson, W.K., Baer, A.J. and Habib, M.K.
1980: Grant 47, Structural Fabric and Uranium Distribution in Shear Zones near Cardiff, Ontario; p.83-85 in Summary of Research, 1979-1980, edited by E.G. Pye, Ontario Geological Survey, Miscellaneous Paper 93.

Heard, H.C. and Raleigh, C.B.
1972:Steady-state Flow in Marble at 500°C-800°C; Geological Society of America, Bulletin, Vol. 83. p.935-956.
Hewitt, D. and Satterly, J.
1957: Haliburton-Bancroft Area, Ontario Department of Mines, Map No. 1957b.
Kretz, R.
1968:Study of Pegmatite Bodies and Enclosing Rocks, Yellowknife-Beaulieu Region, District of Mackenzie; Geological Survey of Canada, Bulletin 159. 108p.
Kronenberg, A.K. and Shelton, G.L.
1980:Deformation Microstructures in Experimentally Deformed Maryland Diabase; Journal of Structural Geology, Vol. 2, p.341-353.
Little, H.W., Smith, E.E.N. and Barnes, F.Q.
1972:Uranium Deposits of Canada; International Geological Congress, Guidebook for 24th Excursion C67.
Morris, H.R.
1956:Surface Geology of the Faraday Uranium Mine, Bancroft, Ontario; Unpublished M.Sc. Thesis, University of Toronto.
Rimsaite, J.Y.H.
1980: Mineralogy of Radioactive Occurrences in the Grenville Structural Province, Bancroft Area, Ontario: A Progress Report; p.253-264 in Current Research, Part A, Geological Survey of Canada, Paper 80-1A.
Ross, M.R. and Huebner, J.S.
1975: A Pyroxene Geothermometer Based on Composition-Temperature Relationships of Naturally Occurring Orthopyroxene, Pigeonite and Augite; International Conference on Geothermometry and Geobarometry, Extended Abstracts, Pennsylvania State University, University Park, Pa.
Satterly, J.
1957: Radioactive Mineral Occurrences in the Bancroft Area; Ontario Department of Mines, Annual Report, Vol. 65, part 6.
Speer, J.A., Solberg, T.N. and Becker, S.W.
1981: Petrography of the Uranium-bearing Minerals of the Liberty Hill Pluton, South Carolina: Phase Assemblages and Migration of Uranium in Granitoid Rocks; Economic Geology, Vol. 76. p.2162-2175.

Grant 106 Platinum Group Elements in the Layered Intrusion at Big Trout Lake

A.A. Borthwick and A.J. Naldrett
Department of Geology, University of Toronto

ABSTRACT

The Big Trout Lake layered intrusion appears to consist of numerous incomplete cyclic units and one complete cyclic unit. The first two cyclic units have been investigated in detail. Chromite and olivine are the major cumulus phases. Each cycle begins with chromitite-rich dunite or chromitite, and grades into chromite-rich peridotite. The top of cycle 1 is marked by unusually large, anhedral olivine crystals. The distribution of platinum group elements (PGE), gold, nickel, copper, cobalt, chrome and sulphur has been determined for the first two cyclic units and the base of cycle 3. Within each cycle, the PGE concentration shows a distinct differentiation trend. Ru, Ir and Os have nearly identical distribution patterns. The (Pt + Pd)/(Ru + Ir + Os) ratio shows an increasing trend from the base to the top of each cycle. Overall, the PGE concentrations in sulphides resemble those of gabbro-related massive Ni-Cu sulphide ores rather than those of enriched Merensky-type ores.

INTRODUCTION

Platinum group elements (Os, Ir, Ru, Rh, Pt and Pd) have become a valuable resource and are considered to be strategic mineral commodities by many industrialized nations. World production is controlled by South Africa and the U.S.S.R. The increasing importance of metals and the vulnerability of supplies has prompted further exploration in the Western Hemisphere. Canadian production of PGE, mainly from the Sudbury area, is closely tied to the world demand for Ni and Cu. A better understanding of the distribution of PGE in layered intrusions can assist in future exploration programs (Vermaak 1976; von Gruenewald 1979; Keays and Campbell 1981).

A number of models have been proposed to explain the occurrence of PGE deposits but each model has difficulty in accounting for various features of these deposits. The Big Trout Lake layered intrusion is being investigated in detail to further define the model constraints. This paper describes the geology of the intrusion, and the relationship between the PGE concentrations and the silicate petrography. The variation in proportions of different PGE is also described.

GEOLOGY

The Big Trout Lake intrusion is situated 500 km north of Thunder Bay, on the east shore of, and extending south from, Big Trout Lake (Figure 1). Surface exposures were mapped by Hudec (1964) and more recently by geologists of Canadian Nickel Company Limited (Canico). The map in Figure 1 is based on aeromagnetic surveys and drill core data provided by Canico.

Part of the intrusion is exposed along the eastern shore of the lake but most of it lies either beneath the lake or beneath glacial overburden. Past work has shown the intrusion to be nearly 60 km long and folded into a "Z" shape. It is enclosed by Archean mafic and felsic metavolcanics, metasediments, and felsic gneiss.

The northern part of the fold structure is interpreted to be synclinal about an east-trending axis. The southern part of the fold structure is an anticline with a northwest-trending axis. Drilling data and geophysical surveys reveal numerous shear zones and faults at the hinge of the anticline.

The northern limb of the southern anticline is hidden beneath Big Trout Lake and its interpretation is not clear. Geophysical data suggest that the ultramafic rocks are restricted to the southern limb of the anticline. Drilling data from a cross-section of the southern limb shows four major rock types: chromitite, peridotite, gabbro, and anorthosite. Surface exposures of the intrusion along the northern limb of the syncline are mainly of quartz diorite which is stratigraphically the uppermost rock type of the intrusion.

This study has concentrated on the mineralized southern limb of the intrusion, which is composed largely of peridotite. Figure 2 illustrates the cross-section of the part of the intrusion which has been studied in detail.

SILICATE MINERALOGY

OLIVINE

Olivine is invariably altered and is the dominant mineral in the samples studied by the authors. Its grain-size ranges from 1 mm to 10 mm. The crystals are mainly euhedral, however a small section of the ultramafic zone has a very unusual anhedral olivine. Most of the olivine crystals have reaction rims. All the crystals have altered to serpentine, antigorite, or talc and can only be identified by their crystal outline.

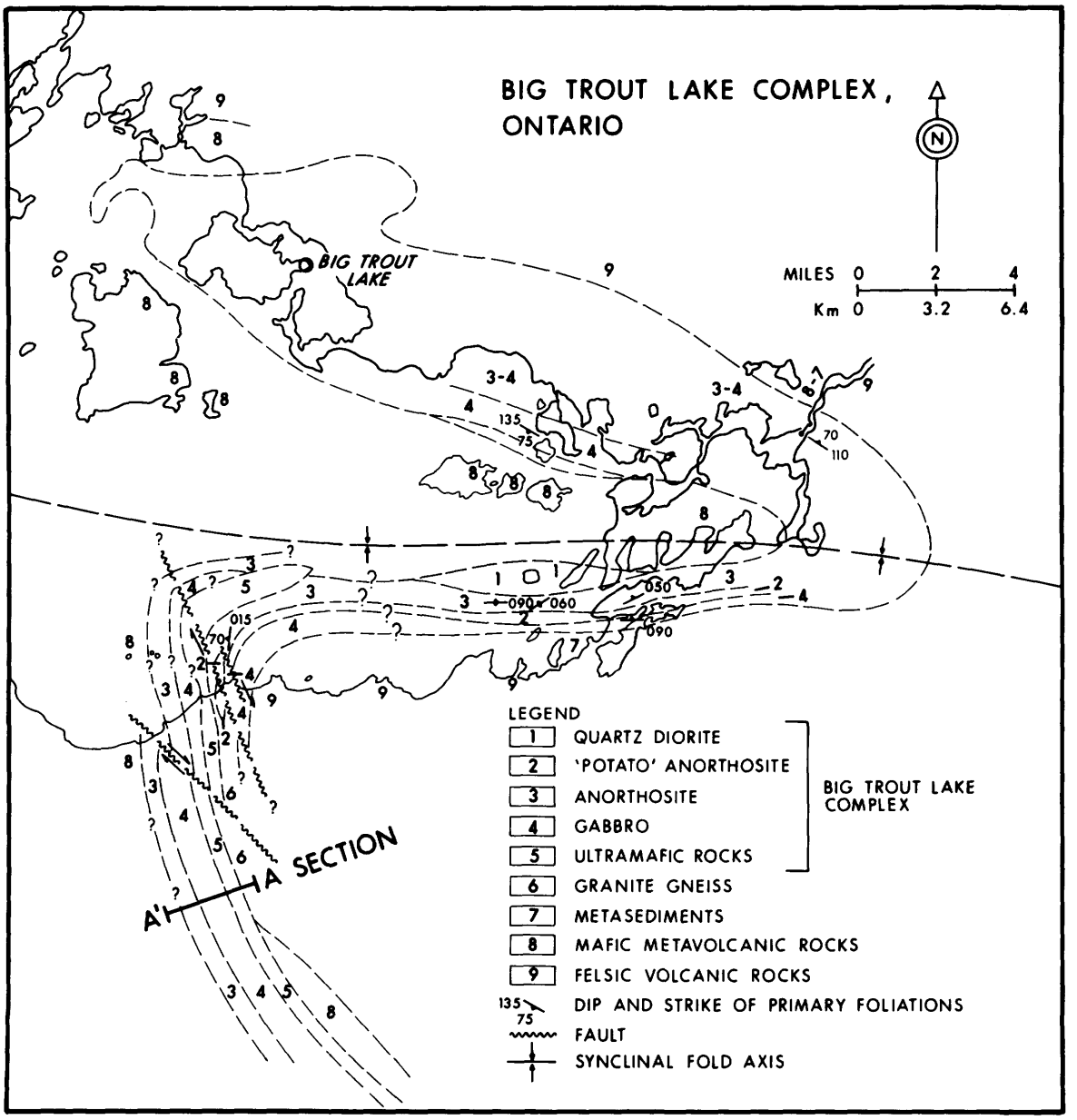

Figure 1. *Map showing the geology of Big Trout Lake layered intrusion (adapted from Sage and Troup 1974).*

PYROXENE

Pyroxene occurs interstitially to olivine crystals and is mainly intercumulus in form. Inclusions of chromite grains are common in pyroxene. The pyroxene appears to have reacted with the olivine. All the pyroxene has altered to amphibole.

CHROMITE

Chromite grains are euhedral and their diameter ranges from < 1 mm to 3 mm. Some of the grains are fractured. Silicate inclusions are common and are invariably situated at the centre of the grains. Chromite appears to be unaffected by low temperature alteration. The silicate inclusions, however, have been altered to a hydrous phase, usually amphibole.

SULPHIDES

The dominant sulphide mineral is pyrrhotite. The sulphides appear to have separated out of the host magma as immiscible droplets and crystallized interstitially to the silicate minerals. They commonly occur as isolated minerals; however net-textured ore is present in places. A minor amount of pyrrhotite has been altered to magnetite. Other sulphides include pyrite, and pentlandite exsolved from pyrrhotite.

ANALYTICAL RESULTS

Thirty-two samples were analysed. Ni, Cu, Cr, and S were determined by XRF; Co was determined by atomic absorption. The PGE concentrations were determined by the combined fire assay – neutron activation method of Hoffman *et al.* (1978) which has the advantages of a relatively large, and therefore "representative", subsample and of low detection limits. A 50 g split of a 500 g bulk rock sample was used to prepare a doré bead by fire assay. An acid leach of the bead was followed by neutron activation analysis. Duplicate determinations provided a measure of precision. If duplicate determinations differed by more than 10 percent, they were discarded and the samples prepared for re-analysis. The results have been recalculated to a metal content in 100 percent sulphide and then averaged for each sample (Table 1). The data are also presented diagrammatically in Figures 3 and 4 in order to emphasize the trends.

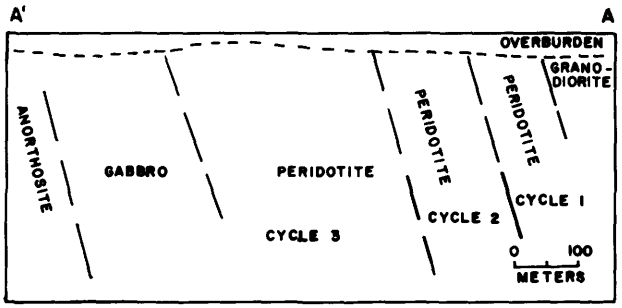

Figure 2. *A cross-section of the Big Trout Lake intrusion. Refer to Figure 1 for the location of the cross-section.*

STRATIGRAPHY

Much of the portion of the intrusion investigated so far is composed of equant, 1 to 3 mm diameter, olivine grains (now entirely altered to serpentine) surrounded poikilitically by pyroxene (also altered). Zones of coarse-grained, resorbed-looking olivine, associated with very coarse poikilitic pyroxene, appear to define distinctive horizons, one 90-110 m above the base and the other 354-434 m above the base. Chromite is a common accessory in the interval 0 to 78 m above the base, where numerous chromitite layers are interbanded with peridotite. Other chromitites occur at 250 m, 358 m, 396 m, 419 m, and 469 m above the base.

In the portion of the intrusion investigated in detail, sulphides (as indicated by the analytical data for S and Cu in Figure 3) are concentrated in the intervals 35-50, 78-110, and 190-250 m above the base. Net-texture is prominent in the sulphides in the uppermost mineralized interval.

In conformity with previous publications (e.g. Naldrett *et al.* 1979; Naldrett and Duke 1980; Naldrett 1981) analytical data for Ni, Cu, Co, PGE, and Au have been recalculated in terms of metal content in 100 percent sulphide. While it is reasonable assumption that the vast majority of the Cu, PGE, and Au are present in sulphide, this is not true for Ni and Co, which also substitute readily for other elements in silicates. Ni was plotted against both S and Cu. Regression of the data and extrapolation to zero S and Cu gave values of 0.166 and 0.268 weight percent respectively. These figures are regarded as an approximation for the Ni originally present in silicates at the magmatic stage (Ni may have been redistributed subsequently between sulphides and silicates during alteration). Since Ni should follow S more closely than Cu, this amount (0.166 weight percent) has been subtracted from the whole-rock Ni analysis to give an approximation for that originally present in sulphide and this value has been recalculated to Ni in 100 percent sulphide, for plotting on Figure 3.

Study of Figures 3 and 4 indicate no marked trends except that, at the 110 m level, above the lowermost zone of resorbed peridotite, the S and Cu contents are much reduced, the concentrations of PGE in sulphides decrease up to this point, as does the Au concentration, and the Cr content of the rock increases abruptly.

The overall level of PGE in sulphide is not particularly high. This is illustrated in Figure 5 where the average PGE contents in 100 percent sulphides are compared with data for typical Sudbury, flood-basalt related, and Merensky-type deposits. It can be seen that the metal contents are more like the massive Sudbury ores than the sparsely

Table 1. *Analyses of sulphide-bearing samples from the Big Trout Lake intrusion, recalculated to concentration of metal in 100 percent sulphides.*

Height (meters)	Ni	Cu	Co	Cr	S	Pt	Pd	Rh	Ru	Ir	Os	Au	Pt / Pt+Pd	Pt+Pd / Ru+Ir+Os
	wt. per cent					parts per billion								
40	3.32	1.41	0.14	0.26	0.99	1,696	8,112	300	760	191	346	954	0.173	7.56
41	1.83	4.87	0.06	0.23	1.22	2,308	7,657	268	803	206	301	1,046	0.232	7.61
50	6.38	3.50	0.19	0.91	0.90	3,344	7,486	416	719	389	447	661	0.309	6.96
53	0.23	2.33	0.00	1.04	0.60	*	*	*	*	*	*	*		
58	4.02	8.02	0.15	0.56	0.47	*	*	*	*	*	*	*		
80	13.73	0.87	0.31	0.34	0.80	6,846	11,244	337	547	248	359	1,028	0.378	15.68
87	5.14	1.86	0.32	0.33	1.32	2,599	5,820	369	371	80	125	331	0.309	14.62
91	3.93	2.43	0.24	0.41	1.44	1,471	5,772	328	207	71	51	292	0.203	22.02
95	3.67	2.11	0.13	0.35	1.66	938	5,579	221	158	27	48	53	0.144	27.97
102	2.88	2.79	0.04	0.28	1.63	4,949	3,508	253	182	54	54	311	0.585	29.16
108	3.37	2.19	0.04	0.35	1.60	3,948	3,970	186	201	37	44	284	0.499	28.08
124	2.90	n.d.	0.24	0.74	0.29	*	*	*	*	*	*	*		
130	n.d.	1.75	0.12	0.35	0.60	2,538	4,025	221	700	76	99	460	0.387	7.5
160	n.d.	1.43	0.21	0.21	0.49	1,893	4,928	229	421	79	136	350	0.278	10.7
175	8.44	1.80	0.45	0.36	0.39	3,051	5,698	296	691	79	180	377	0.349	9.2
183	2.90	2.15	0.22	0.31	0.65	1,103	7,107	194	436	54	86	312	0.134	14.25
185	4.99	2.08	0.31	0.33	1.01	1,473	3,967	166	249	38	42	228	0.271	16.54
190	2.76	1.30	0.26	0.35	0.81	1,325	*	*	n.d.	35	n.d.	257		
191	1.22	3.04	0.15	0.34	0.69	1,951	*	*	n.d.	51	n.d.	251		
194	4.24	1.84	0.23	0.31	1.52	1,544	*	*	n.d.	31	n.d.	127		
199	4.00	0.77	0.31	0.33	0.91	741	*	*	n.d.	24	n.d.	185		
209	4.23	3.18	0.45	0.28	0.77	1,811	5,863	497	287	81	81	321	0.236	17.09
214	3.04	1.65	0.26	0.37	2.12	2,258	1,857	322	n.d.	36	n.d.	376	0.549	114.55
219	2.69	5.19	0.17	0.41	1.62	1,657	2,949	234	n.d.	47	n.d.	358	0.360	97.61
225	0.82	3.09	0.21	0.35	1.02	1,049	*	*	n.d.	30	n.d.	722		
228	1.21	5.79	0.19	0.39	1.27	3,222	*	*	n.d.	22	n.d.	800		
230	2.33	4.32	0.19	0.41	1.86	1,600	5,768	180	n.d.	26	n.d.	373	0.217	289.04
232	2.43	2.02	0.15	0.38	2.94	1,617	2,523	218	n.d.	32	n.d.	279	0.391	131.32
241	1.91	1.42	0.13	0.05	2.46	2,010	6,779	210	n.d.	13	n.d.	276	0.229	684.77
243	1.38	1.87	0.13	0.06	1.87	994	13,541	214	n.d.	18	n.d.	381	0.068	786.02
250	n.d.	n.d.	0.00	15.30	0.07	*	*	*	*	*	*	*		
256	n.d.	n.d.	0.00	3.32	0.11	5,258	*	*	10,258	1,209	1,582	380		

*=not analysed, n.d.=not detected

Analyses, except for chrome, have been recalculated to reflect the concentration of metal in the sulfide fraction.

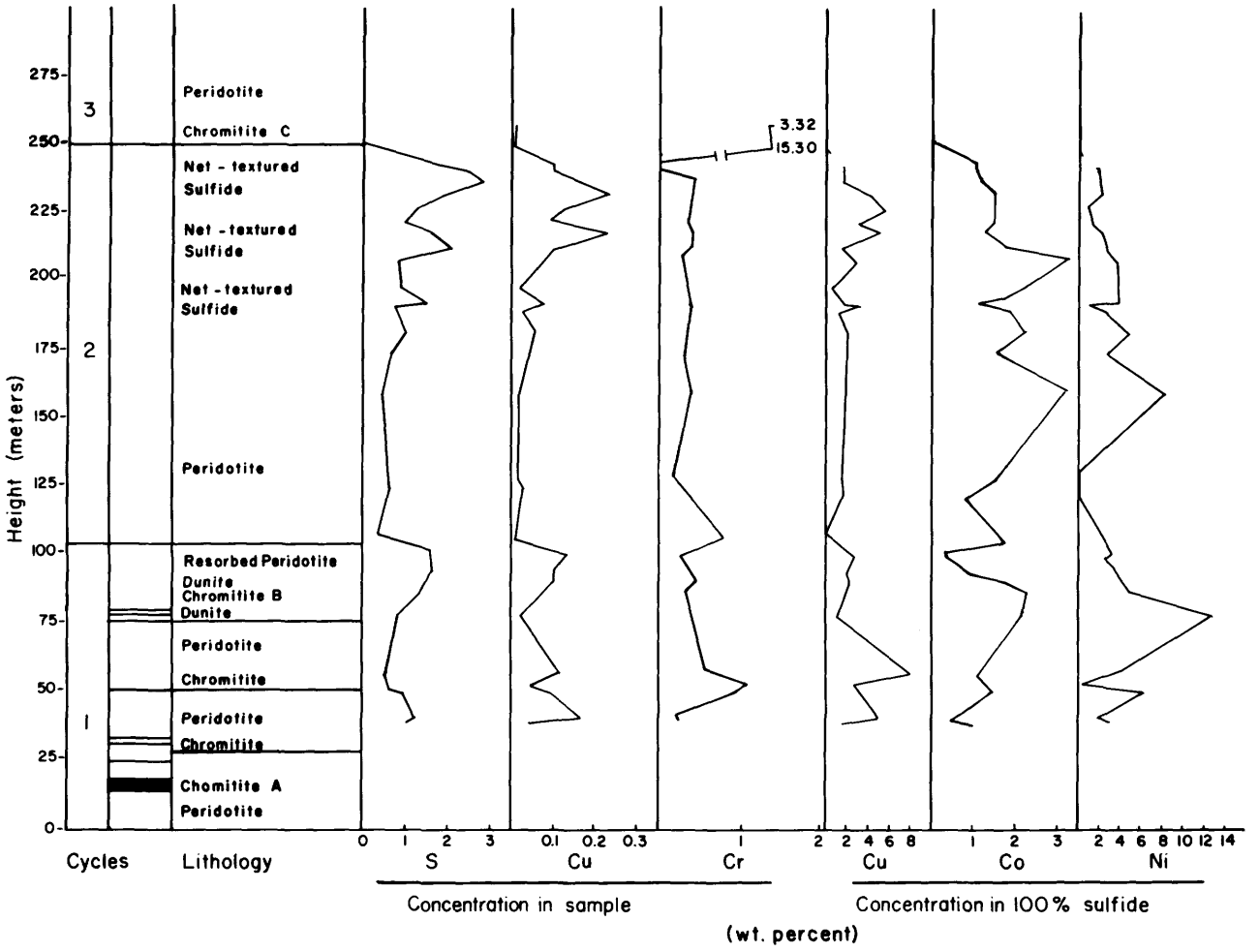

Figure 3. *Concentrations of S, Ni, Cu, Co and Cr versus height in the Big Trout Lake intrusion. S, Cu and Cr are expressed as weight percent in the sample. Ni, Cu, and Co are expressed as weight percent in 100 percent sulphide.*

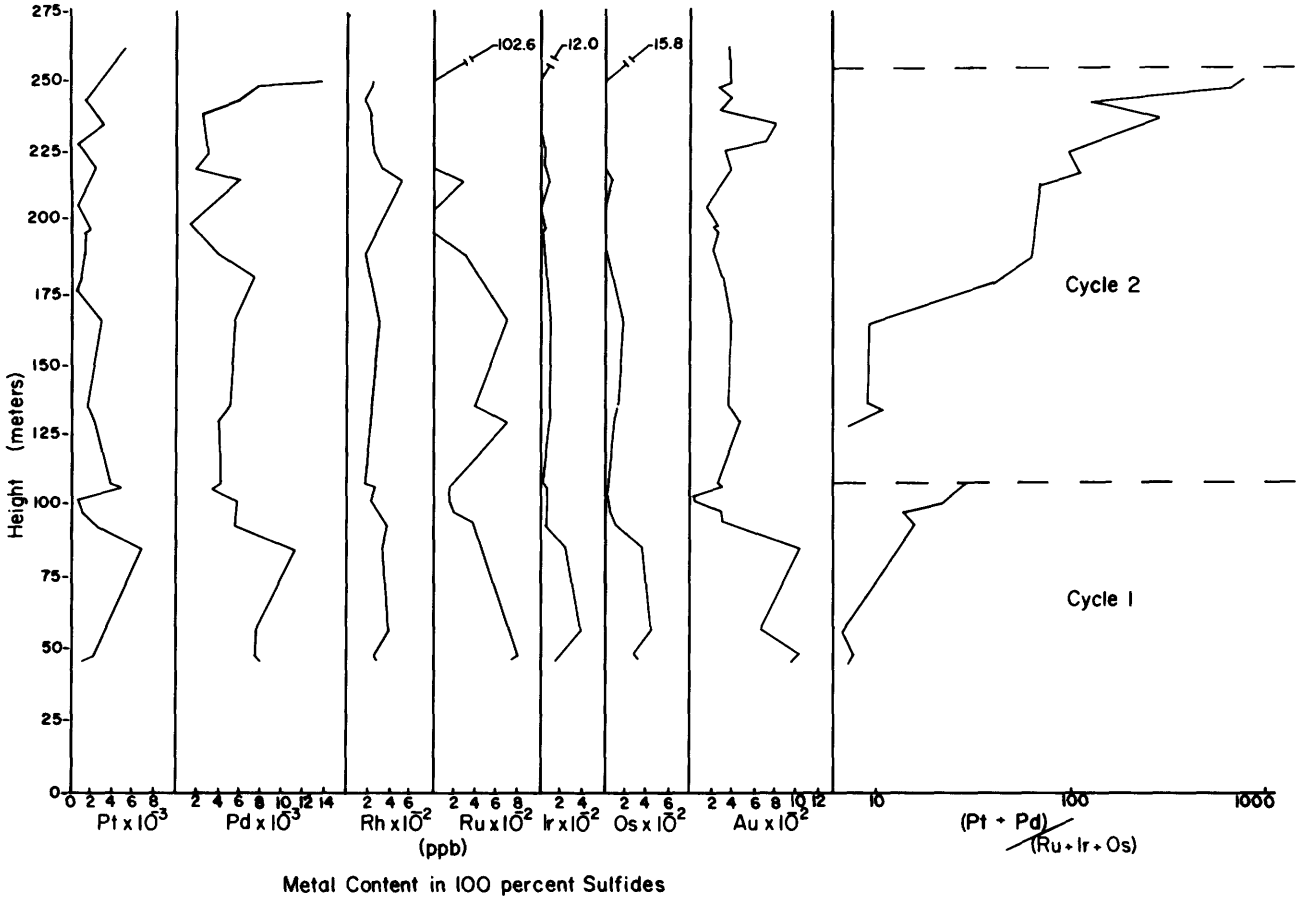

Figure 4. *Concentrations of Pt, Pd, Rh, Ru, Ir, Os and Au in 100 percent sulphide versus height in the Big Trout Lake intrusion. Also shown in the variation of the (Pt + Pd)/(Ru + Ir + Os) ratio vs height.*

disseminated Merensky ores, despite the weakly disseminated nature of the Trout Lake mineralization. The steep slope of the data from left to right of the diagram is consistent with a high average (Pt + Pd)/(Ru + Ir + Os) ratio and is consistent with Naldrett's (1981) conclusion that high ratios characterize ores derived from basaltic magmas. Perhaps the most interesting feature of the data is illustrated in Figure 4 where the (Pt + Pd)/(Ru + Ir + Os) ratio is plotted against height in the intrusion. This rises systematically from near the base to the 110 m level at which point it drops sharply before rising again up to the 250 m level.

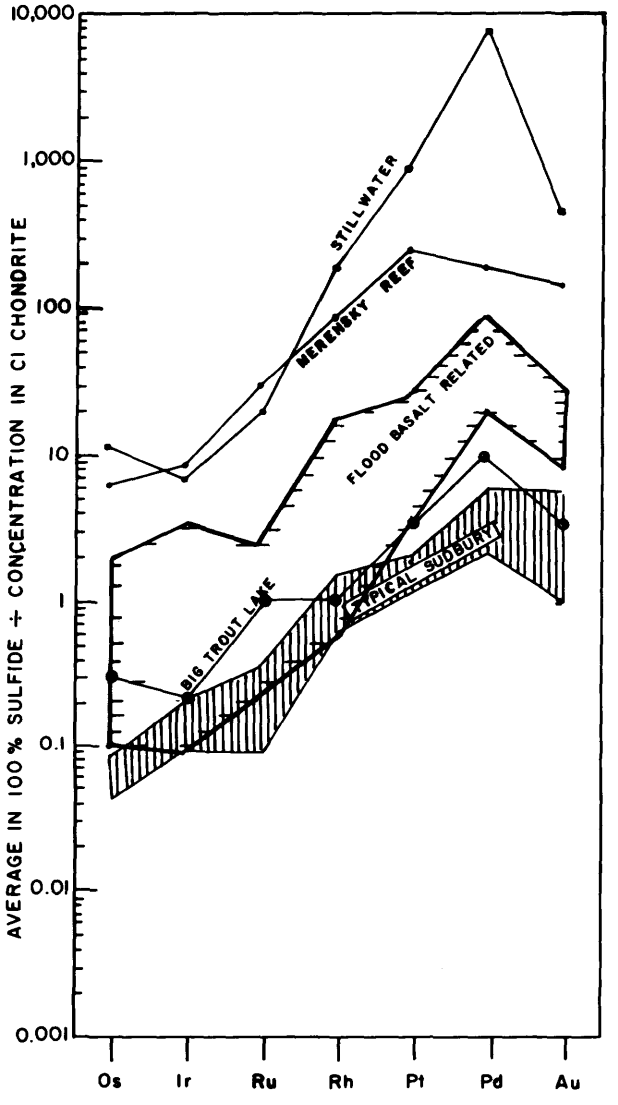

Figure 5. *Average chondrite-normalized PGE and Au concentrations originally in the sulphide in Big Trout Lake intrusion relative to the Merensky Reef, Stillwater, Sudbury, and intrusions related to flood basalt activity (open box).*

CYCLIC UNITS

Determining the number and boundaries of igneous cycles within a layered intrusion is of vital importance in interpreting its crystallization history and the relationship of mineralization to this. At Big Trout Lake, such determinations are hampered by the highly altered nature of the rocks; this alteration prevents microprobe determinations of mineral compositions. In many intrusions, chromitite layers define the base of a cyclic unit. However the variations in the S, Cu, PGE, Au, and Cr concentrations in the peridotite lead us to conclude tentatively that the top of the zone of resorbed olivine at the 110 m level marks the top of the first cycle. The top of the second cycle has yet to be established, since our studies have not been completed above the 250 m level, although it is possible that the chromitite at this level, chromitite C in Figure 3, may represent the base of cycle 3. Possibly the zones of resorbed olivine higher in the intrusion represent the tops of successive cycles.

If our definitions of cycles is correct, the marked upward increase in the (Pt + Pd)/(Ru + Ir + Os) ratio is perplexing. Although experimental data are lacking, it has been customary to regard Pd as the PGE with the greatest tendency to partition into sulphide, and Ru, Ir, and Os the PGE with the least tendency. If this were so, one might expect Pd to become more depleted from a given body of magma than Ru, Ir, and Os as crystallization proceeded, so that with continued segregation, the reverse trend in ratio would result. On the other hand, Keays and Davison (1976) and Naldrett *et al.* (1979) have speculated that Ru, Ir, and Os may be more compatible in olivine and/or chromite than Pt and Pd so that crystallization of olivine should increase the (Pt + Pd)/(Ru + Ir + Os) ratio.

Slated for further study are (1) fractionation of PGE, just described; (2) the reason for the resorbed olivine; (3) definition of the cycles using variations in major elements and trace elements other than those studied so far; and (4) the upper levels of the intrusion.

CONCLUSIONS

The metal content of 32 sulphide-bearing samples have been studied. When calculated to metal content in 100 percent sulphide, the PGE levels are not very much higher than those observed in many massive Ni-Cu ores and not nearly as high as in the Merensky-type ores. The (Pt + Pd)/(Ru + Ir + Os) ratios are consistent with the ores being derived from a basaltic parent magma. Two cyclic units, within which pronounced fractionation of the PGE appears to have occurred, have been tentatively identified.

REFERENCES

Hoffman, E.L., Naldrett, A.J., Van Loon, J.C., Hancock, R.G.V., and Manson, A.
1978: The Determination of all the Platinum Group Elements and Gold in Rocks and Ores by Neutron Activation Analysis after Preconcentration by a Nickel Sulfide Fire Assay Technique on Large Samples; Analytical Chimica Acta, Vol. 102, p. 157-166.

Hudec, P.P.
1964: Geology of the Big Trout Lake Area, District of Kenora (Patricia Portion); Ontario Department of Mines, Geological Report 23.

Keays, R.R., and Campbell, I.H.
1981: Precious Metals in the Jimberlana Intrusion, Western Australia: Implications for the Genesis of Platiniferous Ores in Layered Intrusions; Economic Geology, Vol. 76, No. 5, p. 1118-1141.

Keays, R.R., and Davison, R.M.
1976: Palladium, Iridium and Gold in the Ores and Host Rocks of Nickel Sulfide Deposits of Western Australia; Economic Geology, Vol. 71, p. 1214-1228.

Naldrett, A.J.
1981: Nickel Sulfide Deposits: Classification, Composition, and Genesis; Economic Geology, Seventy-Fifth Anniversary Volume, p. 628685.

Naldrett, A.J., and Duke, J.M.
1980: Platinum Metals in Magmatic Sulfide Ores; Science, Vol. 208, p. 1417-1428.

Naldrett, A.J., Hoffman, E.L., Green, A.H., Chou, C.L., Naldrett, S.R., and Alcock, R.A.
1979: The Composition of Ni-Sulfide Ores with Particular Reference to their Content of PGE and Au; Canadian Mineralogist, Vol. 17, p.403416

Sage, R.P., and Troup, W.R.
1974: Operation Winisk Lake, Big Trout Lake Area, Patricia Kenora District, Ontario; Ontario Division of Mines, Preliminary Map P.860, scale 1 inch to 1 mile.

Vermaak, C.F.
1976: The Merensky Reef — Thoughts on its Environment and Genesis; Economic Geology, Vol. 71, p. 1270-1298.

von Gruenewald, G.
1979: A Review of some Recent Concepts of the Bushveld Complex with Particular Reference to the Sulfide Minerlization; Canadian Mineralogist, Vol. 17, p. 233-256.

Grant 80 Rare Earth Elements in Felsic Volcanic Rocks Associated with Cu-Zn Massive Sulphide Mineralization

I.H. Campbell[1], P. Coad[2], J.M. Franklin[3], M.P. Gorton[1], T.R. Hart[1], J. Sowa[1] and P.C. Thurston[4]

[1]Department of Geology, University of Toronto
[2]Kidd Creek Mines Limited
[3]Economic Geology Division, Geological Survey of Canada
[4]Ontario Geological Survey

ABSTRACT

A study of host felsic volcanic rocks and alteration pipes associated with Cu-Zn massive sulphide deposits has produced no evidence of REE mobility in the felsic volcanic rocks adjacent to massive sulphide deposits. However they can be mobile in the alteration pipes below the orebodies. Where REE mobility has been observed, all of the REE are leached from the system, but the middle REE, centered on Tb, are preferentially removed producing $(Yb/Tb)_n$ ratios greater than 1. Eu^{2+} has been found to be more mobile than the +3 REE, resulting in a marked increase in the size of the Eu anomaly where alteration is intense. Other "immobile" elements such as Th, Zr, Y and Hf may also be mobile in the alteration pipe.

Preliminary data suggest that REE mobility increases with the size of the deposit. Thus REE mobility is potentially a method of identifying large massive sulphide deposits at an early stage in exploration.

INTRODUCTION

In the previous report (Campbell *et al.* 1981) it was suggested that the geochemistry of immobile trace elements, such as Y, Zr, Hf, Ti and the rare earth elements (REE), can be used to classify the felsic rocks associated with massive Cu-Zn sulphide deposits. It was shown that the felsic volcanic rocks which host ore have flat REE patterns with well developed Eu anomalies whereas Archean felsic volcanic rocks, not associated with ore, usually have steep REE patterns with little or no Eu anomaly. If full advantage is to be taken of this technique it is essential that we have a sound understanding of trace element mobility in the altered rocks adjacent to massive sulphides. This paper presents some preliminary results of a study of trace element mobility, placing special emphasis on the REE. It will be shown that the elements normally regarded as mobile (Rb, Sr, Na, K, Fe, MgO, etc.) are mobile under the conditions of pervasive alteration which accompany massive sulphide deposits. Under the same conditions, the immobile trace elements show little or no evidence of mobility. There is, however, clear evidence that the "immobile" trace elements can be mobile in the highly altered rocks found in the alteration pipes which underly some massive sulphide deposits. It will be shown that mobility of these "immobile" trace elements may be used as a prospecting tool.

FACTORS CONTROLLING TRACE ELEMENT MOBILITY

Four factors control the mobility of a trace element: its diffusion rate in a solid, its solubility in metasomatic fluids, the amount of fluid passing through the rock, and the stability of the phases which host the element. The immobile trace elements characteristically have a charge of +3 or greater which affects their mobility in two ways. Firstly they have low rates of diffusion, and secondly they do not substitute readily into major rock-forming minerals but are concentrated instead in minor accessory phases. Little is known about the stability of accessory phases during metasomatism or about the solubility of REE in metasomatic fluid. The work which is available on REE solubilities in fluids suggests that it is low (Flynn and Burnham 1978). Solubilities will, of course, vary with the temperature and composition of the fluid and with the nature of the element. An element which is immobile under one set of conditions may be mobile under another.

PREVIOUS WORK

In recent years the concept of immobile trace elements has been questioned by a number of authors including Hellman *et al.* (1979), Alderton *et al.* (1980), Dostal *et al.* (1980), MacGeeham and McLean (1980) and McLennan and Taylor (1979, 1980). These papers have demonstrated, with varying degrees of success, that the so-called "immobile" elements can be mobile under certain conditions.

A convincing demonstration of REE mobility should satisfy two criteria:

(1) The range of trace element concentrations in the rock before alteration or metamorphism must be known with complete confidence.

(2) Mobile trace element ratios should be different in altered and unaltered rocks. Diffusion rates and solubility in

solution vary from one element to the next. Elements are also concentrated in different minerals in rocks. For these reasons the mobility of elements will be variable. Where alteration takes the form of ionic exchange between selected elements or infilling of vesicules or fractures, the ratio of elements not involved in the processes should remain constant. Their absolute abundances in the rock may change because of the diluting effect of the added material, or the concentrating effect of leaching, but their ratios should remain constant. On the other hand, ratios of elements which are directly involved in the alteration process can be expected to change during alteration, because of variations in mobility.

Few of the papers listed above satisfy both these criteria. The problems involved in demonstrating trace element mobility can be illustrated using the data of Hellman *et al.* (1979), one of the most widely quoted papers on REE mobility.

Hellman *et al.* (1979) have studied the effects of burial metamorphism on the trace element geochemistry of selected suites of basaltic rocks. Their most detailed work is on the Maddina Volcanics, a suite of Proterozoic flood lavas from Western Australia, where they have shown that altered rocks have a distinctly lower REE content than unaltered rocks. REE ratios in both altered and unaltered samples however remain the same.

In their description of the alteration process, Hellman *et al.* (1979) stated that "The most obvious metamorphic adjustment (in these rocks) is the filling of vesicles and cavities by metamorphic minerals such as pumpellyite, quartz and epidote and the development of heterogeneities dominated by varying proportions of pumpellyite and quartz throughout the flow tops." This suggests that the immobile trace elements may have been diluted by the infilling process.

To test the dilution hypothesis we have calculated the amount of SiO_2 which must be added and the amount of FeO and MgO which must be removed to convert 10139, an unaltered sample, to 10144, an altered sample (Figure 1). These two samples were selected because the calculation is simplest as most of the variation between the samples can be accounted for by the three elements considered. This iterative calculation gives a dilution factor of 0.56 in close agreement with the depletion factors calculated by Hellman *et al.* for Y (0.62), ΣLREE (0.51) and ΣHREE (0.65) but somewhat less than the values for Ti and Zr (0.73). If the possible effects of dilution are taken into account, the difference between the REE patterns for altered and unaltered samples is negligible (Figure 1).

We do not wish to imply that there was no mobility of the "immobile" trace elements during alteration of the Maddina Volcanics, since variations in the REE/Zr and the REE/Ti ratios require some mobility. However the effects are minimal when the combined contributions of analytical error, sampling error, and dilution are taken into account. Considering the high degree of alteration in these rocks (in the type area SiO_2 changes from 52 percent to 71 percent, ΣFeO from 9.1 to 2.8, K_2O from 1.63 to 0.08 etc.), the "immobile" elements show amazing coherence. In altered rocks they are certainly far more likely to reflect the original chemistry of the sample than the mobile elements such as SiO_2, FeO, MgO, Na_2O, K_2O, Rb etc. Thus, although the "immobile" elements may not be totally immobile, they are certainly the least mobile of the elements Hellman *et al.* have analysed.

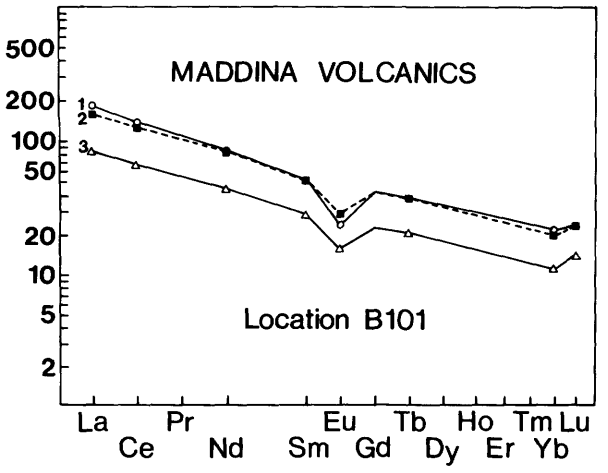

Figure 1. *Chondrite normalized REE patterns for altered and unaltered basalts from the Maddina Volcanics, Fortescue Group, Western Australia. 1 is the unaltered center of a flow (sample 10139), 3 is the altered flow top (sample 10144) and 2 is the recalculated pattern for the flow top assuming SiO_2 addition and loss of FeO and MgO. Data from Hellman et al. (1979).*

IMMOBILE ELEMENTS IN ALTERATION PIPES

Three factors make alteration pipes below massive sulphide deposits an ideal place to look for REE mobility.

(1) The alteration pipes are discordant replacement features, allowing samples of the same rock type to be collected from both inside and outside the pipe.

(2) The degree of alteration within a pipe can be intense. For example, a rhyolite with 75 percent SiO_2, 2 percent FeO and 4 percent Na_2O can alter to a chloritic rock with 16 percent SiO_2, 42 percent ΣFe_2O_3 and 0.2 percent Na_2O.

(3) Alteration is believed to result from a large amount of hot saline fluid passing through the system, i.e. a high water/rock ratio. For a given solubility of an element in a fluid, the greater the volume of fluid passing through the system, the greater the leaching effect.

This study suffers from two important limitations. Firstly, the surrounding rocks which host the massive sulphide deposits investigated have undergone low-grade regional metamorphism and metasomatism. This probably has resulted in some pre- or post-ore element mobility, especially of highly mobile elements such as Na, K, Rb and Sr. Secondly, poor outcrop exposure and structural complexity often make detailed correlation in the mine

area difficult. Thus, while it is possible to follow a mappable rhyolite unit into an alteration pipe, it is not normally possible to follow individual flows or pyroclastic beds with any degree of confidence. For these reasons, a study of this type can only be expected to identify major examples of trace element mobility. Subtle examples of trace element mobility may go unnoticed.

1. UCHI LAKE (SOUTH BAY) MINE

Three types of quartz-feldspar porphyry (QFP) are recognised in the area of the Uchi Lake Mine; QFP, QFP-1 and QFP-2. Normal QFP, away from the mine, has dark green chlorite which is characteristic of the regional chloritization in the Uchi Lake area. The chlorite in QFP-2, which is only found in the alteration pipe adjacent to ore, is black. QFP-1 is also found in the alteration pipe, but not as close to ore as QFP-2. The dark green chlorite in this rock has been partially converted to black chlorite.

Analyses of a representative selection of elements for the three types of QFP are given in Table 1. At the bottom of the table, element/La ratios are presented. The choice of La is arbitrary as any immobile trace element would have served the purpose. Ratios of mobile elements, such as Na, Rb and Sr, vary erratically both inside and outside the alteration pipe. Na/La ratios in QFP, for example, vary between 564 and 1020 and between 6 and 546 for samples collected from the alteration pipe. Where the concentrations of these elements are anomalous for felsic rocks they are low, indicating that they are being leached from the system by the metasomatic solutions. The irregular variations in Na/La, Rb/La and Sr/La ratios suggest that Na, Rb and Sr are mobile under both low-grade regional metasomic conditions and the more intense hydrothermal conditions associated with the alteration pipe.

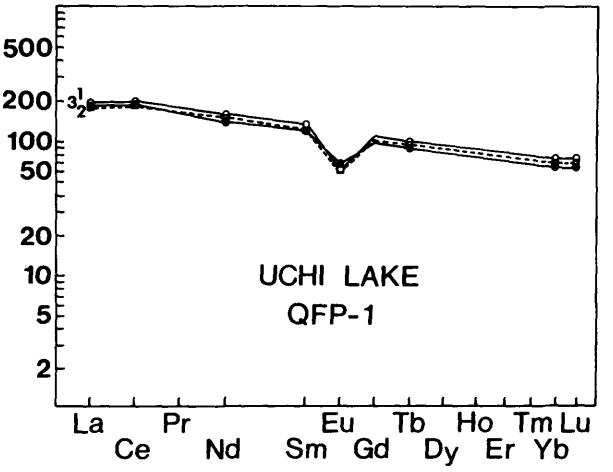

Figure 3. *Chondrite normalized REE patterns for QFP1 from the alteration pipe at Uchi Lake. 1 = sample G80-12, 2 = G80-10, 3 = G80-11.*

Ratios of the immobile elements (Y, Zr, REE, Hf, U and Th), on the other hand, show a remarkable coherence. The variations in element/La ratios for samples collected inside the alteration pipe, with one or two exceptions (e.g. Y in G80-7 and U in G80-10), are no greater than for those collected from outside the pipe. These elements have clearly undergone little or no mobilization during alteration, a conclusion consistent with a comparison between the REE plots for the different types of QFP (Figures 2, 3 and 4).

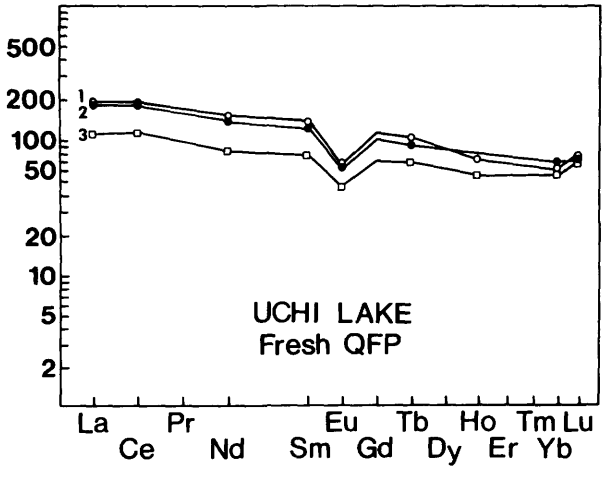

Figure 2. *Chondrite normalized REE patterns for QFP collected near the Uchi Lake Mine but well away from ore and the alteration pipe. 1 = sample G80-20, 2 = G80-14, 3 = G80-15.*

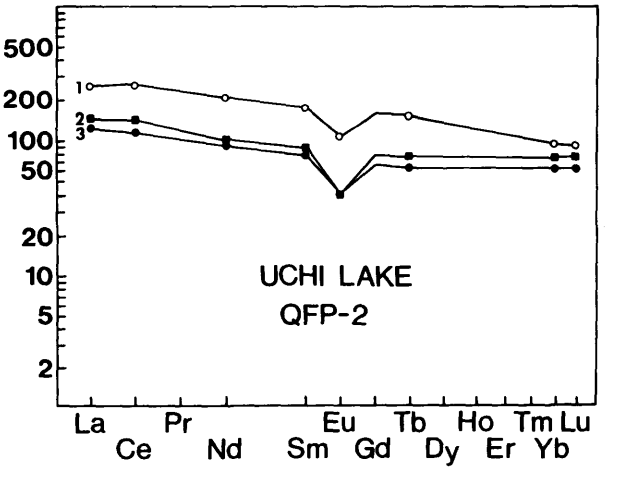

Figure 4. *Chondrite normalized REE patterns for QFP2 from the alteration pipe at Uchi Lake. 1 = sample G80-9, 2 = G80-4, 3 = G80-6.*

Table 1. *ΣFe_2O_3, Na_2O, trace elements and element/La ratios for selected rhyolites from the Uchi Lake Mine.*

Sample No.	G80-14	G80-15	G80-18	G80-19	G80-20	G80-10	G80-11	G80-12	G80-6	G80-7	G80-9
Rock Type	QFP	QFP	QFP	QFP	QFP	QFP-1	QFP-1	QFP-1	QFP-2	QFP-2	QFP-2
$\sum Fe_2O_3$%	.78	8.34	4.66	3.07	4.02	4.97	4.31	3.97	6.87	1.42	1.65
Na_2O%	5.05	3.68	5.34	3.43	3.44	.83	.71	3.22	.76	1.62	1.39
Rb	11.1	3.0	3.3	34.5	31.6	32	33	23	11	8	20
Sr	65	210	112	68.7	67	49	52	67	33	58	56
Y	133	117	167	143.7	143	114	136	149	110	100	184
Zr	520	450	732	490	485	478	488	509	390	521	547
La	55	36	57	59	61	56	56	59	36	66	80
Ce	143	90	138	157	147	147	143	151	88	170	211
Sm	24	14.4	21.3	24.7	25.5	24	25	25	14	25	24
Eu	4.4	3.2	4.2	4.8	4.5	4.9	4.6	4.4	2.8	11	7.6
Tb	4.3	3.2	5	5.2	5	4.2	4.4	4.8	2.5	4.0	7.4
Yb	14	11	16	13.2	12.6	12.8	14	15	12.2	12.5	19
Hf	12	10.5	17	12.3	12.2	12.2	11	12	9.4	14	11.3
U	1.8	0.9	1.7	1.2	1.2	4.6	1.5	1.5	1.0	1.9	1.6
Th	5.1	3.8	6.1	5.6	5.3	5.2	4.9	5.4	4.6	5.1	5.6
Sc	3.9	9.6	4.6	3.7	3.4	3.5	3.5	3.7	5.6	3.6	2.8
Eu/Eu*	.60	.61	.48	.56	.54	.65	.57	.53	.56	1.36	.66
$(Yb/Tb)^1_n$	.77	.81	.75	.60	.59	.72	.75	.74	1.15	.74	.60
Zr/Hf	43.3	42.9	43.1	39.8	39.8	39.2	44.4	42.4	41.5	37.2	48.4
					Element/La ratio						
Na_2O	918	1020	937	581	564	148	127	546	211	6	174
Rb	.20	.083	.058	.59	.52	.57	.59	.39	.30	.12	.25
Sr	1.18	5.83	1.97	1.16	1.10	.88	.93	1.14	.92	.88	.70
Y	2.42	3.25	2.93	2.44	2.34	2.04	2.43	2.53	3.06	1.52	2.30
Zr	9.5	12.5	12.8	8.3	7.95	8.54	8.71	8.63	10.8	7.89	6.84
Ce	2.60	2.5	2.42	2.66	2.41	2.63	2.55	2.56	2.44	2.57	2.64
Sm	.44	.40	.37	.42	.42	.43	.45	.42	.39	.38	.030
Eu	.080	.089	.074	.081	.074	.088	.082	.075	.078	.167	.095
Tb	.078	.089	.088	.088	.082	.075	.079	.081	.069	.061	.093
Yb	.26	.31	.28	.22	.21	.229	.250	.254	.339	.189	.238
Hf	.22	.29	.30	.21	.20	.218	.196	.203	.26	.21	.141
U	.033	.025	.030	.02	.02	.082	.027	.025	.028	.029	.020
Th	.093	.11	.11	.10	.09	.092	.088	.092	.128	.077	.070
Sc	.067	.27	.081	.063	.056	.063	.063	.063	.156	.055	.035

Notes: [1]Chondrite normalised ratio

2. STURGEON LAKE (MATTABI MINE)

At Sturgeon Lake, the rhyolite which hosts the massive sulphide deposit can be traced from outside the mine area into the alteration pipe. Analyses of rhyolites away from the mine and from the alteration pipe are given in Table 2 and REE patterns in Figure 5 and 6. The data show clear evidence of "immobile" element mobility within the Sturgeon Lake alteration pipe. Element/La ratios show a much greater variation for samples collected within the alteration pipe than for stratigraphically equivalent samples collected away from the mine. Of special interest is the behaviour of the REE shown in Figures 5 and 6. The effect of alteration is to lower the REE content of the rock, but the middle REE's, centered on Tb, appear to be preferentially removed. The result is a reversal in slope of the pattern between Tb and Yb, not normally seen in igneous rocks. Note that changes in the Zr/Hf ratio are small compared with element/La ratios, suggesting that elements with a +4 charge may be less mobile than those with a +3 charge.

3. KIDD CREEK MINE

Analyses of two types of rhyolite from the Kidd Creek alteration pipe, chloritized rhyolite and rhyolites from the stringer zone, are presented in Table 3. The chloritized samples were collected close to ore and have undergone intense alteration. A rock, assumed to have been a rhyolite with 75 percent SiO_2, 2 percent ΣFe_2O_3 and 4 percent Na_2O is altered to a rock with 18 percent SiO_2, 40 percent ΣFe_2O_3 and 0.1 percent Na_2O. The stringer zone samples are more typical of the alteration pipe below the ore body. Unfortunately, it is not possible to collect, from outside the mine area, rhyolites that are stratigraphically equivalent to those in the alteration pipe, due to poor outcrop and structural complexity near the mine. Instead we have collected samples of a footwall rhyolite, believed to be geochemically similar to the mine rhyolite before alteration. Experience with other massive sulphide deposits has shown that rhyolites which are geochemically similar to the mine rhyolite extend to appreciable distances both down dip and along strike (Campbell *et al.* 1982).

The evidence for mobility of the "immobile" elements in the Kidd Creek Mine alteration pipe is quite spectacular. Element/La ratio are reasonably coherent for the footwall rhyolites but vary erratically in the stringer zone and chloritized rhyolites. Zr/La ratios, for example, range between 4.45 and 6.46 in the footwall rhyolites, between 6.2 and 21.5 in the stringer zone and between 0.61 and 4.9 in the chloritized rhyolites. By comparison Zr/Hf ratios show remarkably little variation, supporting the argument that the alteration zone rhyolites were similar to footwall rhyolites before they were altered. Variations in REE geochemistry under the different degrees of alteration are illustrated in Figures 7, 8 and 9. The stringer zone rhyolites have lower total REE than footwall rhyolites, larger Eu anomalies and higher $(Yb/Tb)_n$ ratios. The chloritized rhyolites have similar REE patterns to the stringer zone rhyolites but the light REE are less affected. The Kidd Creek Mine data confirm the conclusion reached from the Sturgeon Lake data that REE were leached from the alteration pipe by the ore-forming solutions, with middle REE centered on Tb, being preferentially removed. The steepening Eu anomaly with increased alteration indicates that Eu^{2+} was removed faster than the trivalent REE.

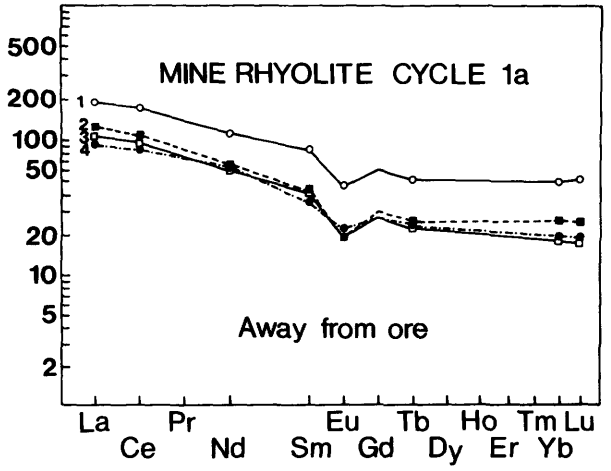

Figure 5. *Chondrite normalized REE patterns for samples of the Mine Rhyolite at Sturgeon Lake collected from outside the alteration pipe. 1 = sample 83-300, 2 = 56-13, 3 = SL-10 and 4 = SL-34.*

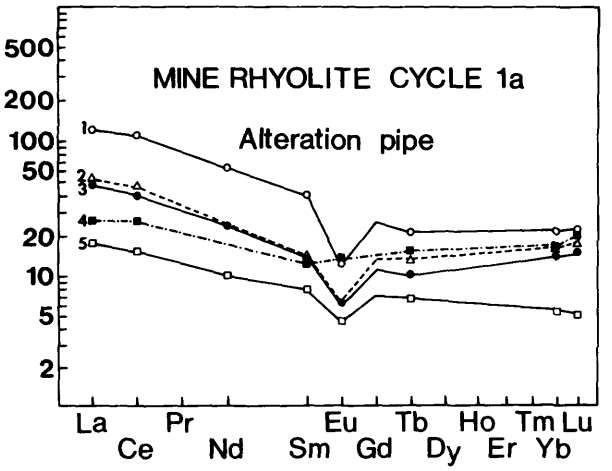

Figure 6. *Chondrite normalized REE patterns for samples of the Mine Rhyolite at Sturgeon Lake collected from the alteration pipe. 1 = sample SL-21-50, 2 = SL-25-175, 3 = SL-25-150, 4 = SL-21-175 and 5 = SL-25-125.*

Table 2. *ΣFe_2O_3, Na_2O, trace elements and element/La ratios for selected rhyolites from Sturgeon Lake Mine.*

Sample No.	83-300	SL-34	SL-10	SL-13	21-50	21-175	25-125	25-150	25-175
Rock Type	F	F	F	F	A	A	A	A	A
$\sum Fe_2O_3$%	2.49	6.01	7.02	5.69	6.33	16.1	2.71	1.64	.32
Na_2O%	.40	1.67	.16	.15	.18	.58	.17	.17	.21
Rb	3	76	12.2	31	40	139	13	9	14
Sr	64	108	134	35	127	138	85	92	157
Y	76	36	33	52	37	36	12	26	34
Zr	787	296	332	412	355	253	66	156	180
La	59	29	34	38	37	7.3	5.6	14.1	16.5
Ce	136	67	75	85	89	20	12.4	32	37
Sm	16	6.7	7.4	7.9	7.4	2.3	1.5	2.5	2.7
Eu	3.2	1.6	1.4	1.4	.86	.96	.32	.44	.46
Tb	2.5	1.1	1.1	1.2	1.0	.73	.34	.48	.64
Yb	9.9	4.0	3.6	5.4	4.4	3.3	1.1	2.8	3.2
Hf	18	6.6	7.2	9.0	8.7	5.5	1.7	3.5	4.1
U	4.7	1.7	2.7	1.9	2.2	1.9	.79	1.1	1.1
Th	15	5.5	6.7	7.6	7.5	2.0	1.1	3.2	3.5
Sc	9.2	10.5	10.2	6.3	7.1	33	2.5	1.7	1.9
Eu/Eu*	.66	.72	.64	.55	.39	1.00	.59	.50	.50
$(Yb/Tb)^1_n$	.93	.86	.77	1.06	.94	1.07	.76	1.37	1.18
Zr/Hf	43.7	44.9	46.1	45.8	40.8	46	38.8	44.6	43.9
				Element/La ratio					
Na_2O	68	576	47	39	49	795	304	121	127
Rb	.051	2.62	0.36	0.82	1.08	19	2.32	.64	.85
Sr	1.08	3.72	3.94	0.92	3.43	19	15.2	6.5	9.5
Y	1.29	1.24	0.97	1.37	1.0	4.9	2.1	1.8	2.06
Zr	13.3	10.2	9.76	10.8	9.6	35	11.8	11.1	10.9
Ce	2.31	2.31	2.21	2.24	2.41	2.74	2.21	2.27	2.24
Sm	.271	.23	.218	.21	.20	.32	.27	.18	.16
Eu	.054	.055	.041	.037	.023	.13	.057	.031	.029
Tb	.042	.038	.032	.032	.027	.10	.060	.034	.039
Yb	.168	.138	.106	.142	.119	.45	.20	.20	.194
Hf	.31	.23	.21	.24	.24	.75	.30	.25	.25
U	.080	.059	.079	.05	.059	.26	.14	.08	.067
Th	.25	.19	.20	.20	.20	.27	.20	.23	.21
Sc	.16	.36	.30	.17	.19	4.5	.45	.12	.12

Notes: [1]Chondrite normalised ratios; [2]Rock types, F = rhyolites away from mine, A = rhyolites from alteration pipe.

Table 3. *ΣFe_2O_3, Na_2O, trace elements and element/La ratios for selected rhyolites from Kidd Creek Mine.*

Sample No.	E	J	F	G	H	8	9	10	11	13	1	2	3	6	5
Rock Type[2]	F	F	F	F	F	S	S	S	S	S	C	C	C	C	C
$\sum Fe_2O_3$%	1.76	1.46	1.75	3.42	1.37	5.18	10.8	2.57	8.11	2.87	37.2	42.1	38.0	40.3	40.9
Na_2O %	2.88	.125	1.43	.08	2.76	.87	.23	.41	.42	.33	.25	.10	.17	.09	.06
Rb	54	91	82	216	67	50	29.57	31	27	21	34	13.2	13.7	3	3.7
Sr	32	23	26	26	45	36	22.6	18	13	9.4	33	16	7.7	1.7	4.5
Y	85	75	111	145	204	30	32	35	55	29	38	50	36.1	6.1	14
Zr	244	193	228	465	241	223	124.7	143	173	100	290	240	278	17	42
La	47.8	29.88	51.2	89.2	53.33	20.4	7.02	23.2	8.03	4.93	59.3	94.5	65.4	28	39.9
Ce	114.5	75.0	128.9	232.6	137.3	56.2	20.2	62.5	21.54	14.9	167.5	256.8	176.4	71	105
Sm	13.96	8.60	15.75	28.88	17.38	6.8	3.10	7.45	4.71	2.20	14.7	20.8	16.7	5.4	11
Eu	1.84	1.13	1.97	3.96	2.20	.33	.21	.33	.23	.16	.38	.58	.41	1.7	.41
Tb	2.57	2.00	3.21	5.05	4.41	.89	.67	.86	1.35	.52	.95	1.36	.88	.18	.52
Yb	8.89	8.82	12.2	16.55	21.65	6.43	4.29	5.24	8.87	4.24	8.96	10.9	10.2	.95	2.5
Hf	7.82	6.66	7.75	16.0	7.65	7	3.55	4.31	5.52	3.29	10.3	9.23	10.3	.64	1.59
U	1.67	1.37	1.57	3.43	1.61	1.52	.79	.68	1.22	1	3.2	2.05	2.57	ND	ND
Th	6.11	5.33	5.98	12.5	5.69	5.1	2.9	3.3	4.3	2.4	8.3	7.9	8.3	1	1.65
Sc	1.41	1.24	1.56	3.75	1.95	1.87	.85	.89	1.11	.61	2.37	1.57	1.98	.14	.50
Eu/Eu*	.38	.38	.35	.43	.36	.27	.19	.17	.13	.13	.12	.12	.11	.20	.18
$(Yb/Tb)_n$[1]	.81	1.04	.90	.77	1.16	1.70	1.51	1.44	1.55	1.94	2.22	1.89	2.73	1.46	1.13
Zr/Hf	31.2	29.0	29.4	29.1	31.5	31.9	35.1	33.2	31.3	30.4	28.2	26	27	26.6	26.4
							Element/La ratio								
Na_2O	603	42	280	9	521	430	329	530	520	670	42	20	26	32	15
Rb	1.13	3.05	1.61	2.42	1.26	2.45	4.2	1.34	3.36	4.26	.57	.14	.21	.11	.093
Sr	.67	.77	.51	.29	.84	1.76	3.22	.77	1.6	1.9	.56	.17	.12	.06	.113
Y	1.79	2.51	2.17	1.63	3.83	1.47	4.56	1.5	6.85	5.9	.64	.53	.55	.22	.35
Zr	5.10	6.46	4.45	5.21	4.52	10.9	17.7	6.2	21.5	20.3	4.9	2.54	4.25	.61	1.05
Ce	2.4	2.5	2.52	2.6	2.57	2.75	2.9	2.7	2.7	3.02	2.8	2.7	2.7	2.54	2.63
Sm	.29	.29	.308	.324	.32	.33	.44	.32	.59	.45	.25	.22	.255	.19	.276
Eu	.038	.038	.038	.044	.041	.016	.030	.014	.029	.032	.006	.006	.006	.06	.010
Tb	.054	.067	.063	.057	.083	.044	.095	.037	.17	.105	.016	.014	.013	.006	.013
Yb	.186	.295	.24	.186	.406	.315	.61	.226	1.10	.86	.15	.115	.156	.034	.063
Hf	.164	.223	.15	.18	.14	.343	.50	.186	.69	.67	.174	.098	.157	.023	.040
U	.035	.046	.031	.038	.030	.075	.11	.29	.15	.203	.054	.022	.039	ND	ND
Th	.13	.18	.12	.14	.107	.25	.41	.14	.53	.49	.14	.084	.13	.036	.041
Sc	.029	.415	.030	.042	.037	.092	.12	.038	.14	.124	.040	.017	.030	.005	.012

Notes: [1]Chondrite normalised ratio; [2] F = least altered footwall rhyolites, S = stringer zone rhyolites, C = chloritised rhyolites.

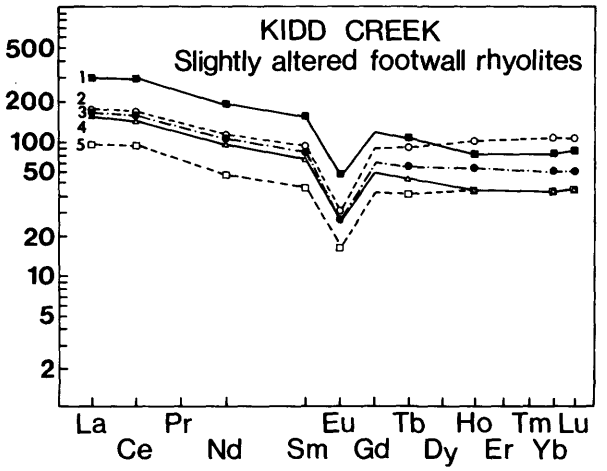

Figure 7. *Chondrite normalized REE patterns of the host altered footwall rhyolites at Kidd Creek Mine. 1 = sample G, 2 = H, 3 = F, 4 = E, 5 = J.*

DISCUSSION

Elements normally regarded as mobile (Rb, Sr, Na, K, etc.), show marked variations in element/La ratios even under the conditions of pervasive low-grade alteration found outside the alteration pipes. Other elements, such as Y, Zr, Th, U, Hf and the REE show no unexpected variations in element/La ratios, suggesting that they are not mobile under these conditions and that it is safe to use these elements to classify Archean rocks which have undergone low to moderate degrees of alteration.

Under the extreme conditions of alteration found below the Kidd Creek deposit even the most "immobile" elements become mobile. Factors controlling REE mobility were discussed above. Preferential mobility of the middle REE, as seen at Kidd Creek and to a lesser extent at Sturgeon Lake, could be due to these elements being more soluble than the light or heavy REE. Alternatively, it could be due to the preferential solution of a phase rich in the middle REE, provided the resulting fluids do not re-equilibrate with the host rocks. Whatever the cause, there is clear evidence that the hydrothermal solutions which formed the ore deposits can preferentially leach the middle REE from the underlying volcanic pile.

Perhaps the most convincing demonstration of REE mobility is the study of shale-hosted hydrothermal uranium deposits by McLennan and Taylor (1979, 1980). Chondrite-normalized REE patterns for shales are typically light REE-enriched and show a limited range of abundances. If normalised to PAAS (post Archean average sediment) the patterns should be flat at a level of 0.5 to 2.0 times PAAS. The U-enriched shales studied by McLennan and Taylor do not show this type of pattern. They have been leached of light REE, whereas middle REE, centred on Tb-Dy, have been added along with the uranium by the ore-forming solutions (Figure 10). The REE added to U-rich shales are the exact compliment to those removed from the felsic volcanic rocks which underly massive sulphide deposits. It appears that certain hydrothermal solutions can preferentially mobilize the middle REE.

For the three deposits we have studied, the degree of mobility of the REE increases with the size of the deposit. The implication is that the REE are immobile unless

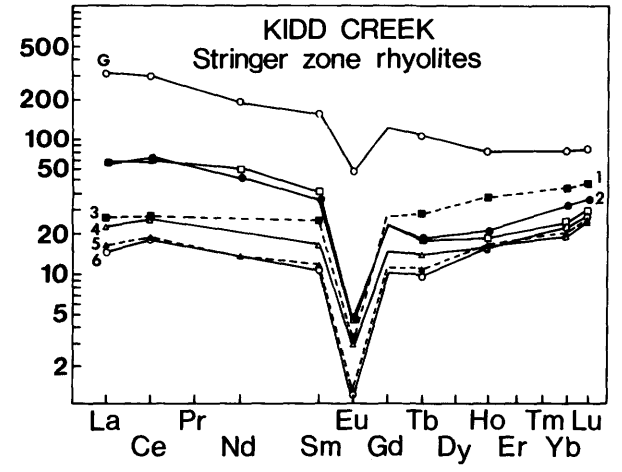

Figure 8. *Chondrite normalized REE patterns of stringer zone rhyolites from the alteration pipe, Kidd Creek Mine. 1 = sample 600-11, 2 = 600-8, 3 = 600-10, 4 = 600-9, 5 = 600-13, 6 - 13. G = pattern 1 from Figure 7 for comparison.*

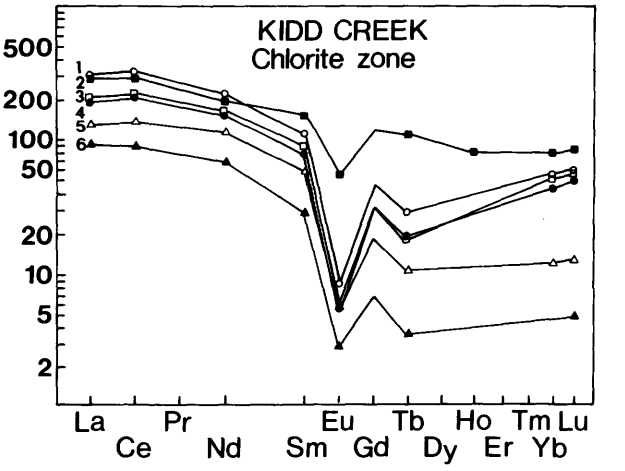

Figure 9. *Chondrite normalized REE patterns for samples from the chlorite zone of the alteration pipe at Kidd Creek Mine. 1 = sample 600-2, 2 = pattern 1 from Figure 7, 3 = 600-3, 4 = 600-1, 5 = 600-5, 6 = 600-6.*

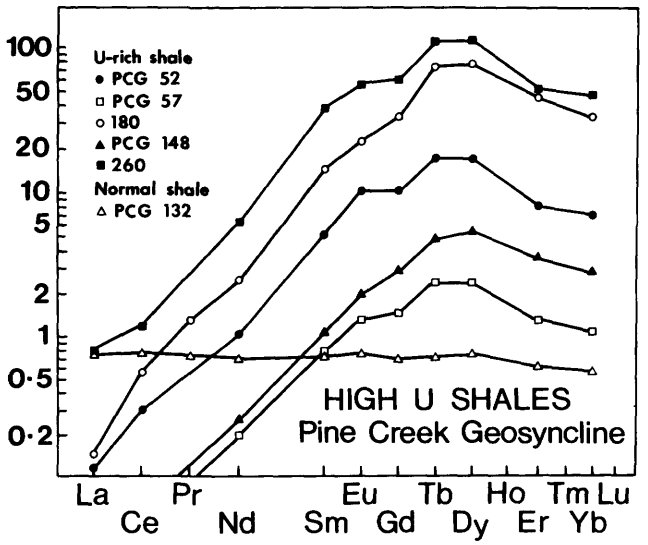

Figure 10. *REE patterns for U-rich shales from the Pine Creek U deposit normalized to PAAS (post Archean average sediment). After McLennan and Taylor (1980).*

the degree of alteration is intense. The hydrothermal system which produced the small South Bay deposit was not large enough to produce significant REE mobility. On the other hand the Kidd Creek Mine ore body, the largest known massive sulphide deposit, was logically produced by a very large hydrothermal system, capable of mobilising the REE. This gives rise to the interesting possibility that REE mobility could be used to distinguish between large and small massive sulphide deposits at an early stage of exploration.

REFERENCES

Alderton, D.H.M., Pearce, J.A., and Potts, P.J.
1980: Rare Earth Element Mobility During Granite Alteration: Evidence from Southwest England; Earth and Planetary Science Letters, Vol. 49, p. 149-165.
Campbell, I.H., Coad, P., Franklin, J.M., Gorton, M.P., Hart, T.R., Scott, S.D., Sowa, J., and Thurston, P.C.
1981: Rare Earth Elements in Felsic Volcanic Rocks Associated with Cu-Zn Massive Sulphide Mineralization; Grant 80 p. 45-53 in Geoscience Research Grant Program, Summary of Research 1980-81, edited by E.G. Pye, Ontario Geological Survey, Miscellaneous Paper 98, 340p.
Campbell, I.H., Coad, P., Franklin, J.M., Gorton, M.P., Scott, S.D., Sowa, J. and Thurston, P.C.
1982: Rare Earth Elements in Volcanic Rocks Associated with Cu-Zn Massive Sulfide Mineralization: A Preliminary Report; Canadian Journal of Earth Sciences, Vol. 19, p. 619-623.
Dostal, J., Strong, D.F., and Jamieson, R.A.
1980: Trace Element Mobility in the Mylonite Zone within the Ophiolite Aureole, St. Anthony Complex, Newfoundland; Earth and Planetary Science Letters, Vol. 49, p. 188-192.
Flynn, R.T., and Burnham, C.W.
1978: An Experimental Determination of Rare Earth Partition Coefficients Between a Chloride Containing Vapour Phase and Silicate Melts; Geochemica et Cosmochimica Acta, Vol. 42, p. 685-701.
Hellman, P.L., Smith, R.E., and Henderson, P.
1979: The Mobility of the Rare Earth Elements: Evidence and Implications from Selected Terrains Affected by Burial Metamorphism; Contributions to Mineralogy and Petrology, Vol. 71, p. 23-44.
MacGeehan, P.J., and MacLean, W.H.
1980: An Archean Sub-Seafloor Geothermal System, 'Calc-Alkali' Trends, and Massive Sulfide Genesis; Nature, Vol. 286, p. 767-771.
McLennan, S.M., and Taylor, S.R.
1979: Rare Earth Mobility Associated with Uranium Mineralization; Nature, Vol. 282, p. 247-250.
1980: Rare Earth Elements in Sedimentary Rocks, Granites and Uranium Deposits of the Pine Creek Geosyncline; Proceedings of International Uranium Symposium on the Pine Creek Geosyncline, Vienna, p. 175-190.

Grant 105 Latter-Stage Decay Products of ^{222}Rn — Use in Radioactive Waste Management

J.W. Card and Keith Bell
Department of Geology, Carleton University

ABSTRACT

Analytical procedures have been developed for the measurement of ^{210}Po in soil and mill tailings samples, using the tendency of ^{210}Po to plate out on copper and silver surfaces from acidic solutions. Laboratory tests have shown that copper and silver collect similar amounts of ^{210}Po from leach solutions and that a plating interval of two hours at 90°C is optimum.

^{210}Po measurements from soils overlying a uranium occurrence near South March, Ontario, delineated an anomaly consistent with others outlined by more conventional methods. A ^{210}Pb survey, by re-analysis of aged leach solutions, also outlined the anomaly.

Data from soil above a uranium-bearing pegmatite in Palmerston Township, Ontario, also yielded a ^{210}Po anomaly coincident with both radon and radium anomalies. A second pegmatite, in Blithfield Township, Ontario, yielded a strong in-situ ^{222}Rn anomaly, but negligible radium values. A subtle anomaly indicated by ^{210}Po data may possibly be related to decay products deposited by migrating radon.

^{210}Po and ^{210}Pb analyses of tailings from the Nordic tailings containment area near Elliot Lake, Ontario, yielded large numbers of counts; ^{210}Po and ^{210}Pb values showed sympathetic variations.

The work to date has confirmed the analytical feasibility of the ^{210}Po and ^{210}Pb methods, and has shown their usefulness as geochemical techniques.

INTRODUCTION

An evaluation of ^{210}Pb, ^{210}Bi, and ^{210}Po as possible indicators of radon migration in the vicinity of radioactive waste disposal areas and as pathfinders in uranium exploration is now in progress. All three nuclides are "latter-stage decay products" of ^{222}Rn, which is itself a radiogenic decay product of ^{226}Ra.

A literature review showed that ^{210}Po in weakly acidic solutions is spontaneously deposited onto silver or copper surfaces (United States Atomic Energy Commission 1961; Millard 1963; Bagnall 1966; Flynn 1968; Smithson *et al.* 1978). During the first year of the present investigation, laboratory tests demonstrated the feasibility of measuring ^{210}Po by deposition from leachates using soil and mill tailings samples. Included in the present work are the refinements of the analytical procedures and the completion of a few test surveys.

DEVELOPMENT OF ANALYTICAL METHOD

The three steps required to make a ^{210}Po measurement are: (i) leaching, (ii) plating, and (iii) counting. A detailed summary of the procedures is given in the Appendix. Some of the more important features to emerge during the course of this work are as follows.

(1) STRENGTH OF ACID USED FOR LEACHING. Different strengths of nitric acid (0.1 percent, 1.0 percent,

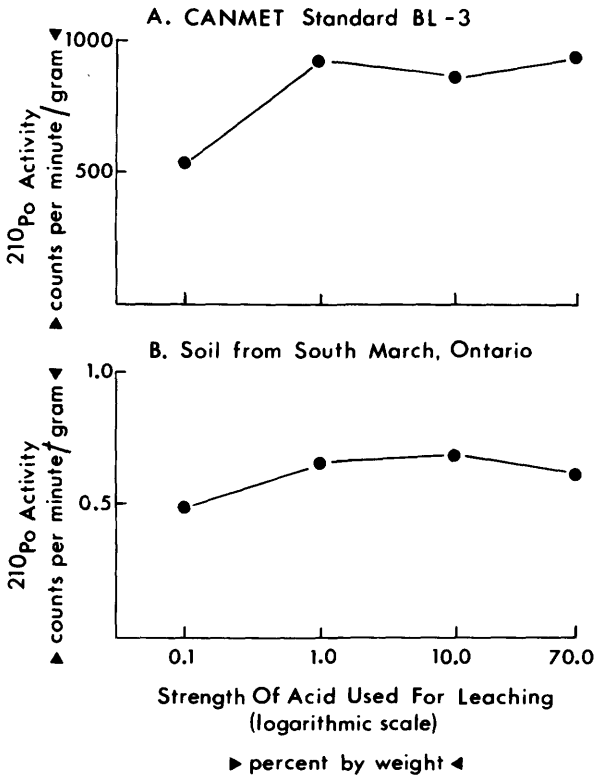

Figure 1. *^{210}Po activity following initial leaching using nitric acid of different strengths.*

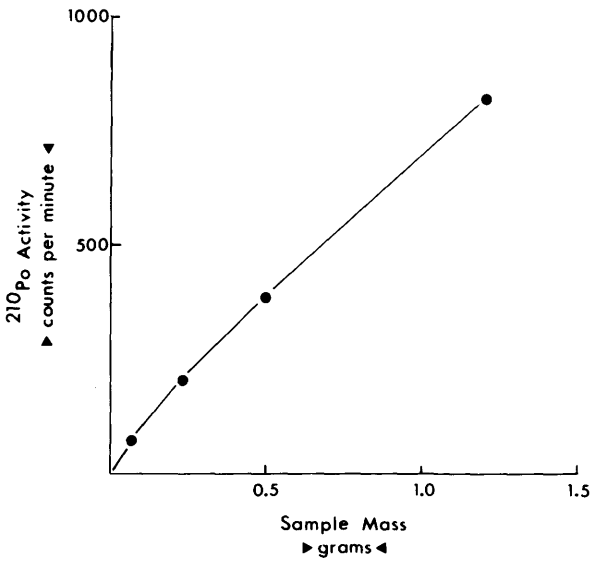

Figure 2. *^{210}Po activity following plating using leach solutions from different masses of CANMET Standard BL-3, bearing 1.02% U.*

10 percent, and 70 percent by weight) were evaluated for the initial leaching experiments, using samples of CANMET Standard BL-3 (a crushed ore bearing 1.02 percent U) and soil associated with a uranium occurrence near South March, Ontario. Surprisingly, similar amounts of activity were observed in those samples leached with 1.0 percent, 10 percent, and 70 percent nitric acid (Figure 1). The 0.1 percent acid, however, resulted in somewhat fewer counts for both the ore and the soil material. 10 percent nitric acid was thus used for most of the leaching experiments reported here.

(2) LINEAR RELATIONSHIP BETWEEN ACTIVITY AND MASS OF SAMPLE. When different aliquots of the CANMET Standard were leached with 10 percent nitric acid, the relationship between ^{210}Po activity and sample mass was found to be almost linear (Figure 2).

(3) PLATING CONDITIONS (TEMPERATURE AND TIME). Leach solutions from identical aliquots of the CANMET Standard were plated for various time periods ranging from 0.5 to 5.5 hours, and at temperatures of 45°C and 90°C. The higher-temperature plating was found to be more effective (Figure 3). After 2.0 hours of plating the activity remained fairly constant.

(4) HCl LEACHING TIME. The time for the HCl leaching phase was varied from 1.0 to 5.0 hours, and overnight tests were carried out. Although activities were not substantially different for any of the leaching times, overnight intervals were found to be the most convenient.

(5) MATERIALS AND GEOMETRIES. Both copper and silver discs (2.5 cm in diameter) were initially tested to evaluate their efficiency in collecting ^{210}Po. The activities from leach solutions from 1.0 g aliquots of CANMET Standard BL-3 using both copper and silver were virtually identical (about 700 cpm/g). Because of this, copper was used for most of our studies, as copper has the advantage of being inexpensive and disposable. Additional tests showed that copper plates 1.5 cm wide by 5.0 cm long were equally effective, and were more convenient than the discs for use in our procedures.

(6) PLATING EFFICIENCY. After ^{210}Po was initially plated onto the copper plates, fresh plates were exposed to the same leach solutions for a second trial. The total activities measured from the second set of trials were only 1 to 2 percent of the total activities measured initially, a feature that confirms the effectiveness of the plating procedure.

(7) REPRODUCIBILITY. Using the CANMET Standard, reproducibilities to within 1.5 percent, expressed as relative standard deviation, were readily achieved. Reproducibilities from soil samples, with smaller concentrations of the nuclides, tend to be lower, but can be improved using longer counting intervals. For the work to date, ten-minute counting intervals have been used; this involves counting the alpha-particle activity on each side of the plates for a period of five minutes. It has been noted that the activity measured from each side of the plate can be significantly different, varying up to a factor of two.

(8) EVALUATION OF POSSIBLE CONTAMINATION BY ^{212}Bi. ^{212}Bi, with a 60.60 minute half-life, from the ^{232}Th decay series, may also become deposited onto the copper plates. Because it is an alpha-emitter, the presence of ^{212}Bi could produce erroneous results. To avoid the effects of ^{212}Bi the copper plate is always counted twice: once immediately after plating, and a second time at least 24 hours later. Any ^{212}Bi activity after this period of time will have dropped to negligible levels. The presence

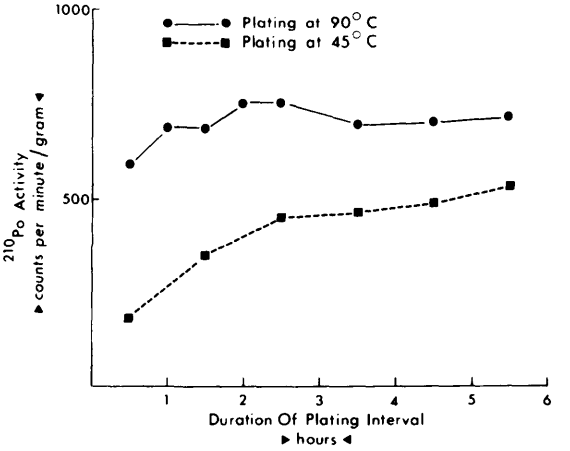

Figure 3. *^{210}Po activity following plating at two different temperatures for different time intervals.*

Table 1. *^{210}Po activity measured in a second counting interval, 60-70 days after plating.*

Experimental Conditions	Waiting Period (days)	Initial Activity (cpm/g)	Predicted Activity After Waiting Period (cpm/g)	Observed Activity After Waiting Period (cpm/g)	% Observed/ Predicted
5.0 x 1.5 cm copper plates; CANMET Standard BL-3 (1.02% U); mean of 4 trials	62	737.7	540.7	551.7	102.0
2.5 cm diameter copper discs; CANMET Standard BL-3 (1.02% U); mean of 4 trials	70	705.4	496.6	512.2	103.0
2.5 cm diameter silver discs; CANMET Standard BL-3 (1.02% U); mean of 4 trials	71	736.4	516.2	547.9	106.1
5.0 x 1.5 cm copper plates; CANMET Standard BL-3 (1.02% U); different strengths of nitric acid:					
0.1% by weight	61	533.5	393.1	395.3	100.6
1.0% by weight	61	922.5	679.7	695.0	102.3
10.0% by weight	61	853.0	628.4	605.3	96.3
70 % by weight	61	935.8	689.5	643.9	93.4
5.0 x 1.5 cm copper plates; CANMET Standard DH-1 (0.177% U; 0.104% Th); mean of 4 trials; initial activity is after correcting for Bi-212 contamination	60	154.0	114.0	117.4	103.0

of ^{212}Bi has been detected in very few cases throughout the course of this work. In one experiment, copper plates were exposed with leach solutions from CANMET Standard DH-1 (which contains both ^{232}Th, 0.104 percent, and ^{238}U, 0.177 percent). The initial activities, from four trials, averaged 178 cpm/g, while the total activities on the following day were significantly lower, averaging 154 cpm/g. These results indicate the presence of ^{212}Bi and emphasize the importance of counting for a second time, particularly when samples are suspected of containing ^{232}Th series nuclides.

(9) EVALUATION OF POSSIBLE CONTAMINATION BY ^{226}Ra. Possible effects of the presence of ^{226}Ra in the leach solutions were tested using the CANMET BL-3 Standard. Both the solutions and the plates, after the plating procedure, were placed in the bottom of 226 ml glass jars, and left for one week so that any short-lived ^{222}Rn decay products could be deposited onto collectors suspended above (Card and Bell 1979). Substantial levels of radon decay product activity were measured from the collectors exposed above the leach solutions, whereas negligible activity was observed from those exposed with the ^{210}Po-bearing plates. From these observations it seems clear that ^{226}Ra, if present in solutions, does not collect on the copper plates.

(10) EVALUATION OF POSSIBLE CONTAMINATION BY LONG-LIVED NUCLIDES. To confirm that long-lived nuclides in the ^{238}U and ^{232}Th decay series were not plated out during the experiments, a number of used plates were counted after an interval of about ten weeks (Table 1). The activity predicted from the half-life of ^{210}Po (138.4 days) was then compared with the observed activity. The table shows that the observed and predicted values were in close agreement and, accordingly, that long-lived nuclides have not contributed significantly to the total number of counts.

(11) EFFECT OF DISSOLVED ORGANIC MATTER. After the soil samples were leached, the leachates were found to be yellow in colour, a feature attributed to dissolved organic matter. To evaluate the effect of organic material on the ^{210}Po plating procedure, experiments were carried out using a mixture of soil (and hence organic matter) and CANMET Standard BL-3. The ^{210}Po activity from the standard was found to be unaffected by the presence of the organic matter.

(12) AVOIDANCE OF CONTAMINATION OF LABWARE. The temporary deposition of ^{210}Po, ^{210}Bi, and ^{210}Pb on labware and their later release could produce contamination, and procedures were adopted to avoid such problems. These include (i) the use of teflon beakers and stirring bars for plating, (ii) heating of labware in 70 percent nitric acid for two or three hours when necessary, and (iii) frequent running of blanks. Tests have shown, however, that even without precautions, the contamination is less than 1 percent of the measured value of the ^{210}Po activity.

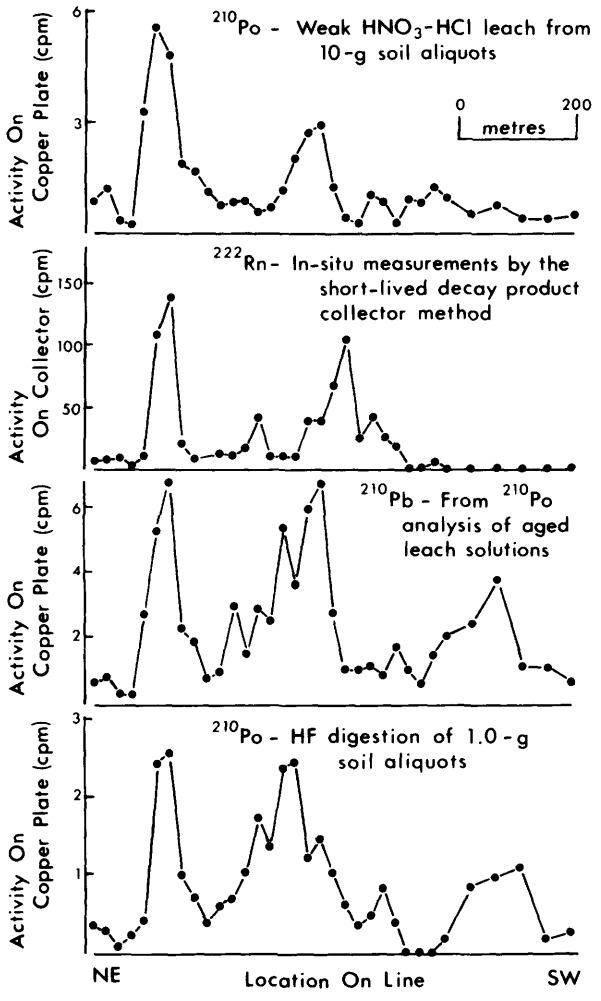

Figure 4. *Comparative profiles along a line across the South March uranium-copper occurrence.*

APPLICATIONS TO TEST SITES

A number of test surveys were carried out on soil samples from known uranium occurrences, and mill tailings samples from the Elliot Lake area.

Soil samples from a test site at South March, Ontario, previously studied by a number of workers (Grasty *et al.* 1973; Steacy *et al.* 1973; Jonasson and Dyck 1974; Charbonneau *et al.* 1975; Ford 1975; Harder 1976; Jonasson *et al.* 1977; Card and Bell 1979; Bradley 1979; Wilson 1979; Christie 1980; Gratton 1980; Bell and Card 1981), were analyzed using the ^{210}Po plating technique. The results are shown as a profile in Figure 4, along with data from an in-situ radon survey. The anomaly, represented by two peaks, reflects two mineralized layers in the Paleozoic sedimentary rocks underlying the soil. The ^{210}Po profile has quite effectively delineated these two peaks, and agrees nicely with the in-situ radon profile.

Seven months later, plating experiments were conducted using the leach solutions retained after the initial ^{210}Po plating. Any ^{210}Pb (half-life 22.3 years) present in these solutions will decay slowly to ^{210}Po. As a first approximation the amount of ^{210}Po will increase to half the equilibrium amount expected from the quantity of ^{210}Pb present, after 138.4 days (one half-life of ^{210}Po). From the ^{210}Pb profile in Figure 4 it is clear that a ^{210}Pb anomaly has been delineated in addition to the ^{210}Po anomaly. The two highest peaks are coincident with the ^{210}Po peaks, and also with peaks from in-situ radon measurements and from uranium and radium abundances in soil samples. It thus appears that the leaching procedures have been effective in removing both ^{210}Pb and ^{210}Po.

An interesting feature of the ^{210}Pb profile is the presence of a third peak corresponding to the south-west end of the traverse; this has not been documented by any of the other analytical methods. The reasons for the additional peak are not known, although the high organic content of these samples may be a factor in collecting and storing ^{210}Pb and/or ^{210}Po.

Preliminary tests involving leaching of different size fractions of a bulk sample from South March showed that the greatest activity was measured from the intermediate part of the size-fraction range (Figure 5). Although the reasons for this are not clear it may result from the adsorption of ^{210}Po onto the large surface area of the smallest size fractions. Further work is required to clarify this point. Additional aliquots of each size fraction digested by a hydrofluoric acid method yielded substantially higher numbers of counts from all size fractions, with the smaller fractions yielding the larger numbers of counts.

Another test involved analysis of all samples from the South March profile, following hydrofluoric acid digestion (see Figure 4). The two main peaks of the anomaly were once again outlined, as well as the third peak, first identified by the ^{210}Pb analyses. On a per-gram basis, the

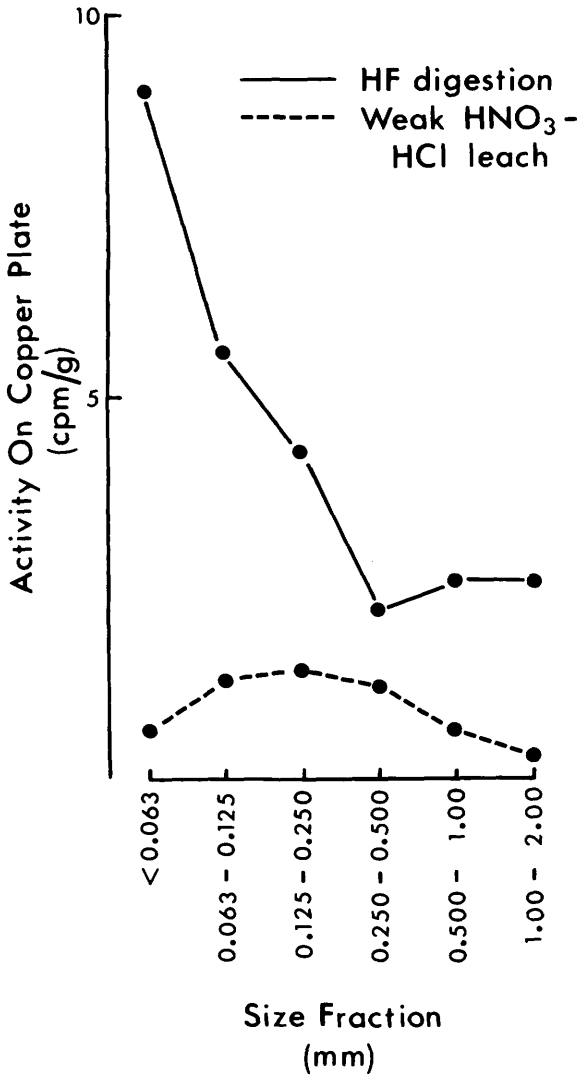

Figure 5. *^{210}Po measurements from different size fractions of the soil from the South March uranium-copper occurrence.*

hydrofluoric acid digestion resulted in about five times as many counts as those obtained using the weak nitric and hydrochloric acid leaching method.

The South March data confirms the analytical feasibility of the leaching and plating method for measuring ^{238}U series nuclide dispersion patterns. As a further test, ^{210}Po profiles were also made using soil samples from two uraniferous pegmatite occurrences in Grenville gneisses and marbles, one in Palmerston Township, and the other in Blithfield Township, Ontario. Previous work showed that although both pegmatites gave strong in-situ anomalies, only one, the Palmerston pegmatite, yielded a clear soil-radium anomaly. Comparative profiles from the two pegmatites are shown in Figure 6. The Palmerston pegmatite shows a clear ^{210}Po anomaly coincident with the ^{222}Rn and ^{226}Ra peaks. Results from Blithfield are less clear, but the highest ^{210}Po readings seem to coincide with the position of the pegmatite. From the data collected so far it seems that the South March occurrence (discussed earlier) and the Palmerston Township pegmatite show similar dispersion patterns. Profiles from the analyses for all three nuclides, ^{210}Po, ^{222}Rn, and ^{226}Ra, show peaks that coincide with the mineralization. The Blithfield occurrence, however, shows a clear ^{222}Rn anomaly, a weak though probably significant ^{210}Po anomaly, and negligible ^{226}Ra values. In both the South March and Palmerston cases perhaps a significant component of ^{210}Po has been provided from soil material containing an assemblage of ^{238}U series nuclides, whereas in the Blithfield example ^{210}Po may have been provided by diffusion of ^{222}Rn from ^{226}Ra-bearing material below, followed by decay in the pore spaces and deposition of ^{210}Pb and ^{210}Po. If this interpretation is correct then the present analytical work may provide an indirect method for monitoring ^{222}Rn migration.

To evaluate the approach over a third type of geological environment, soils were collected along a line cutting the discovery showing of the Quirke deposit near Elliot Lake. Although the soil overlying the uraniferous site has probably been affected by contamination from the mining and milling operations, the results of both ^{210}Po and ^{226}Ra analyses show an anomaly near the outcrop of the discovery showing (Figure 7).

The data so far obtained from soils overlying various types of uranium-bearing environments are encouraging. In all cases, ^{210}Po anomalies have been documented, and the initial tests using the ^{210}Pb technique have proven to be successful.

An initial application and orientation of the project towards mine waste monitoring involved collecting a suite of samples from the Nordic Mine tailings containment area at Elliot Lake, Ontario. The tailings area is about 1.5 km long by 0.5 km wide, and the placement of tailings terminated about 14 years ago. It has since been stabilized by vegetation. Twenty tailings samples were collected, at 25 m intervals across the short axis of the area, from a depth of about 35 cm. Tailings analyses involved the measurement of ^{210}Po, ^{210}Pb (by the ^{210}Po method), and ^{226}Ra by the collector method. An interesting feature of the ^{210}Po results (Figure 8) is the high signal obtained, which is many times greater than that observed from the soil samples. A comparison of the ^{210}Po and ^{210}Pb data shows similar orders of magnitude as well as coincident peaks, and it thus appears that similar information is provided by each of the two kinds of analysis. The ^{226}Ra results, however, are different, in detail, from the other two methods. In addition, samples taken at different depths from one of the stations (10 cm to 70 cm in 10 cm increments) gave values that ranged from 200 to 850 counts per minute for ^{210}Po. The ^{210}Pb and ^{210}Po results tended to vary sympathetically.

Most of the present work, using both soil samples and mill tailings, has involved weak acid leaching of the samples, in the hope of selectively leaching loosely-bound ^{210}Po and ^{210}Pb nuclides. If the loosely-bound

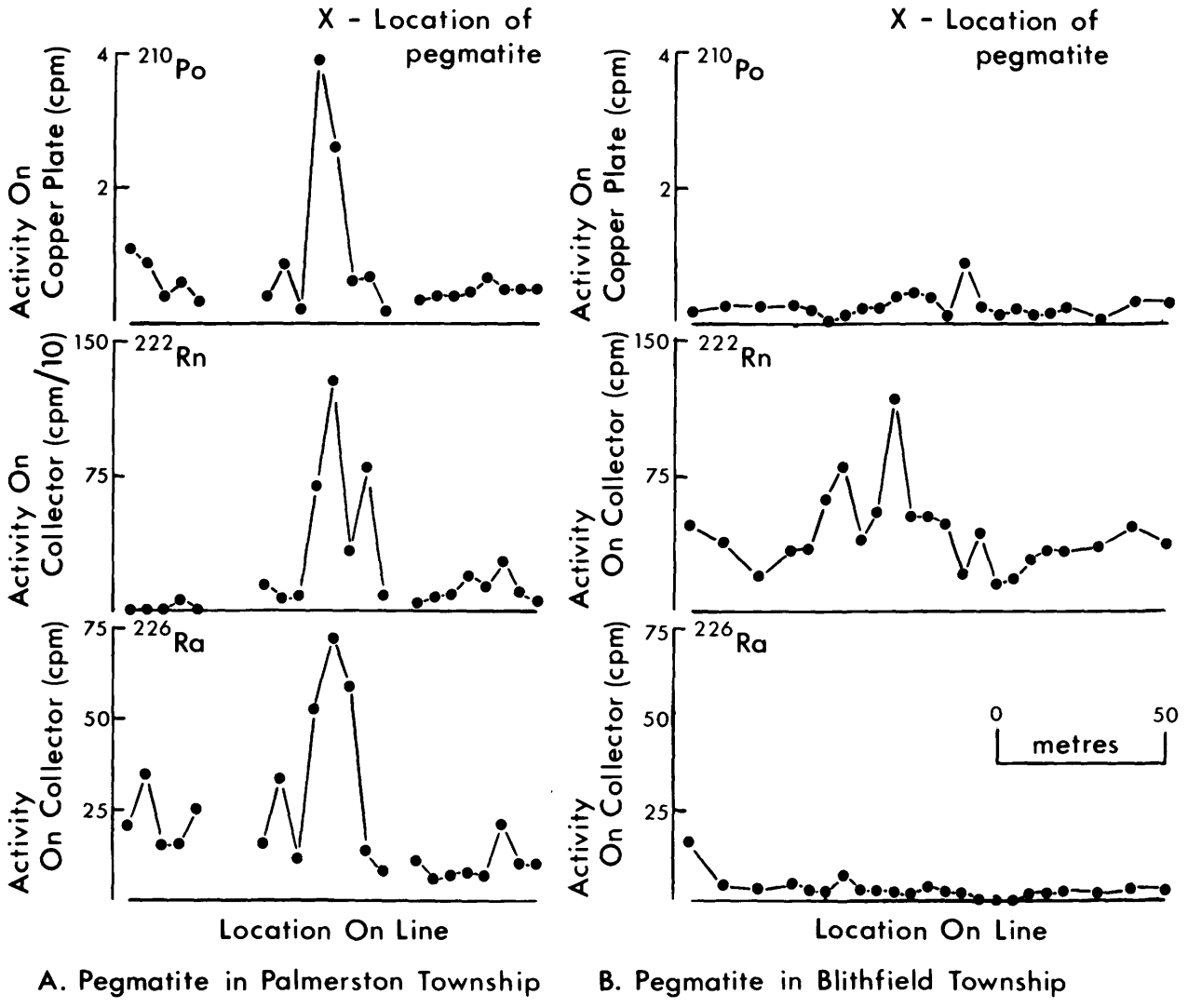

Figure 6. *Comparative profiles from two Grenville pegmatite occurrences.*

nuclides can be discriminated from those that are firmly-bound in this way, a dispersion model involving the deposition of ^{210}Po and ^{210}Pb by radon migrating through the soil pore-space network can be further evaluated. The occurrence of ^{210}Po and ^{210}Pb in loosely-bound positions may represent an easily-detectable "residue" deposited by the migrating radon, and hence would be of considerable practical importance in both uranium exploration and in monitoring patterns of radio-nuclide dispersion potentially associated with uranium mine wastes. Some evidence for the deposition of such a "residue" has been given by the results from the soils overlying the pegmatite occurrence in Blithfield Township.

CONCLUSIONS

Substantial progress has been made in working out analytical procedures for the measurement of ^{210}Po and ^{210}Pb in soil samples. The ^{210}Po anomalies have been delineated in soils associated with a variety of geological environments. Of particular interest is the apparent production of a weak ^{210}Po anomaly in soils in Blithfield Township that may be related to ^{222}Rn migration. In addition, the observation that ^{210}Po and ^{210}Pb can be readily measured in uranium mill tailings means that patterns of dispersion of the radio-nuclides away from mine-waste sites and into the environment may be evaluated.

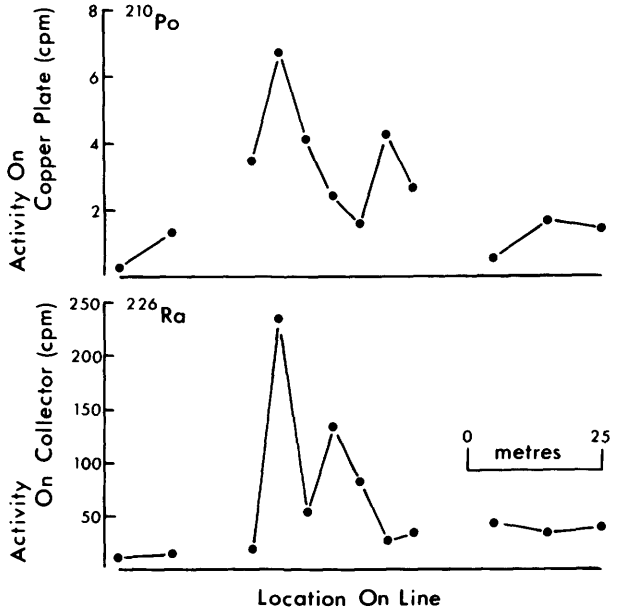

Figure 7. *Profiles across the discovery showing of the Quirke Mine, near Elliot Lake, Ontario.*

The technique itself is straightforward, requiring only inexpensive apparatus, common reagents, and a minimum of technical skill.

ACKNOWLEDGEMENTS

The authors are grateful to Rio Algom Mines Limited for permission to collect samples from their properties, and in particular to Mr. D. Sprague, Chief Geologist, who kindly pointed out many features of the geology and waste management operations.

APPENDIX - PROCEDURES FOR MAKING ^{210}PO MEASUREMENTS

A. LEACHING

1. Weigh sample into beaker (10 g, for soils).
2. Add 10 ml of 10 percent HNO_3.
3. Heat gently, evaporating to dryness.
4. Add 20 ml of 0.5 N HCl.
5. Let stand overnight.

B. PLATING

1. Separate solution from residue by centrifuging, and decant into a teflon beaker.
2. Dilute solution to about 75 ml with 0.5 N HCl.
3. Add about 0.2 g of L-ascorbic acid (to reduce Fe).

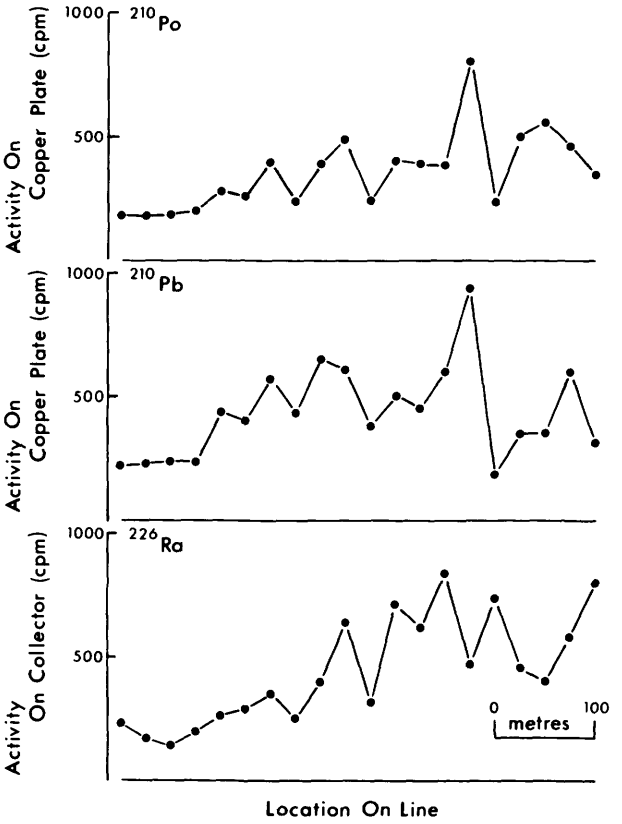

Figure 8. *^{210}Po, ^{210}Pb, and ^{226}Ra measurements from samples from the Nordic tailings containment area, near Elliot Lake, Ontario.*

4. Suspend copper plate in the solution and stir magnetically for 2 hours at 90°C.
5. Remove plate, and rinse first in distilled water and then in alcohol.

C. COUNTING

1. Place plate under alpha-particle scintillation detector and count both sides for 5 minutes.

REFERENCES

Bagnall, K.W.
1966: The Chemistry of Selenium, Tellurium and Polonium; Elsevier Publishing Company, 200p.
Bell, K., and Card, J.W.
1981: Radon Decay Products and Uranium Exploration; Grant 38, p. 18-24 in Geoscience Research Grant Program, Summary of Research, 1980-1981, edited by E.G. Pye, Ontario Geological Survey, Miscellaneous Paper 98, 340p.

Bradley, C.J.
1979: Delineation of a Soil Radium Anomaly: An Evaluation of a Soil-Immersion Technique; unpublished B.Sc. thesis, Carleton University, Ottawa, Ontario, 43p.
Card, J.W., and Bell, K.
1979: Radon Decay Products and their Application to Uranium Exploration; Canadian Institute of Mining and Metallurgy Bulletin, Vol. 72, No. 812, p.81-87
Charbonneau, B.W., Jonasson, I.R., and Ford, K.L.
1975: Cu-U Mineralization in the March Formation Paleozoic Rocks of the Ottawa-St. Lawrence Lowlands; p. 229-233 in Report of Activities, Geological Survey of Canada, Paper 75-1A, 602p.
Christie, D.S.
1980: Radon-Thoron Survey of a Known Uranium-Copper Occurrence: An Evaluation of a Soil-Gas-Suction Emanometry Technique; unpublished B.Sc. thesis, Carleton University, Ottawa, Ontario, 37p.
Flynn, W.W.
1968: The Determination of Low Levels of Polonium-210 in Environmental Materials; Analytica Chimica Acta, Vol. 43, p. 221-227.
Ford, K.L.
1975: Petrography, Geochemistry and Geophysics of a Uranium-Copper Occurrence, South March, Ontario; unpublished B.Sc. thesis, Carleton University, Ottawa, Ontario, 62p.
Grasty, R.L., Charbonneau, B.W., and Steacy, H.R.
1973: A Uranium Occurrence in Paleozoic Rocks West of Ottawa; p.286-289 in Report of Activities, Geological Survey of Canada, Paper 73-1A, 297p.
Gratton, F.J.
1980: Radon Variations in Soil Gas at the South March Uranium-Copper Occurrence; unpublished B.Sc. thesis, Carleton University, Ottawa, Ontario, 45p.
Harder, D.G.
1976: A Study of Two Uranium Occurrences at Marchhurst and Harwood Plains; unpublished B.Sc. thesis, University of Ottawa, Ottawa, Ontario, 48p.
Jonasson, I.R., Charbonneau, B.W., and Ford, K.L.
1977: On the Nature and Formation of Radioactive Hydrocarbons from the Ordovician Rocks of the Ottawa Area; p. 109-111 in Report of Activities, Geological Survey of Canada, Paper 77-1B, 350p.
Jonasson, I.R., and Dyck, W.
1974: Some Studies of Geochemical Dispersion about a Small Uranium Showing, March Township, Ontario; p. 61-63 in Report of Activities, Geological Survey of Canada, Paper 74-1B, 297p.
Millard, H.T.
1963: Quantitative Radiochemical Procedure for Analysis of Polonium-210 and Lead-212 in Minerals; Analytical Chemistry, Vol. 35, p. 1017-1023.
Smithson, G.L., Dalton, J.L., and Mason, G.L.
1978: Radiochemical Procedures for Determination of Selected Members of the Uranium and Thorium Series; CANMET Report No. 78-22, 65p.
Steacy, H.R., Boyle, R.W., Charbonneau, B.W., and Grasty, R.L.
1973: Mineralogical Notes on the Uranium Occurrences at South March and Eldorado, Ontario; p. 103-105 in Report of Activities, Geological Survey of Canada, Paper 73-1B, 216p.
United States Atomic Energy Commission
1961: The Radiochemistry of Polonium; United States Atomic Energy Commission, Nuclear Science Series, 68p.
Wilson, J.S.
1979: Soil-Radium Geochemistry of a Uranium-Copper Occurrence, South March, Ontario; unpublished B.Sc. thesis, Carleton University, Ottawa, Ontario, 26p.

Grant 108 Palynostratigraphic Comparison of Cretaceous of the Moose River Basin, Ontario, with Marginal Marine Assemblages from the Scotian Shelf and Alberta

R.A. Fensome and G. Norris
Department of Geology, University of Toronto

ABSTRACT

Spore-pollen assemblages from the mid-Cretaceous Mattagami Formation in the Moose River Basin are compared with coeval assemblages from three wells on the Scotian Shelf. The latter are similar to the Moose River floras but more diverse and associated with marine dinoflagellates in a near-shore marine environment. The dinoflagellates confirm that the earliest floras from the Mattagami Formation are Albian in age but strengthen the possibility that some might be Aptian. The highest floras from the Mattagami Formation are probably late Albian or early Cenomanian in age by comparison with those on the Scotian Shelf. In general, the spore-pollen floras from the Moose River Basin are more restricted in taxonomic diversity compared with both the mid-Cretaceous of the Scotian Shelf and correlative nearshore marine sections in Alberta. It is tentatively concluded that this may be a function of the environment of deposition; floras in nearshore marine sections reflect regional floras contributing spores and pollen via air currents and river systems discharging into the adjacent shallow seas.

INTRODUCTION

The Mattagami Formation of the Moose River Basin has yielded rich spore-pollen floras which have proved to be useful for correlation of surface sections in the southern and western parts of the basin (Norris 1979; Norris, in press; Norris *et al.* 1976; Hopkins and Sweet 1976; Norris and Dobell 1980; Richardson and Norris 1981).

These floras have generally been considered to be Albian in age, but doubt remains as to their exact correlation with marine standards because the Mesozoic Moose River Basin comprises exclusively terrestrial sediments.

LOCATION AND ZONATION

A reconnaissance study of mid-Cretaceous intervals intersected by three drill holes in the Scotia Shelf has yielded important new information on terrestrially derived palynofloras interdigitating and mixed with marine dinoflagellate assemblages. The three wells used for this study are:
Shell Triumph P-50 (Geological Survey of Canada Locality D 12)
Shell Wyandot E-53 (Geological Survey of Canada Locality D 18)
Shell Mississauga H-54 (Geological Survey of Canada Locality D 9)
For the locations of these wells see Barss *et al.* (1979, Figure 4).

The intervals studied are indicated in Table 1, which gives details of depths studied and the palynofloral zonation and age determinations made by Bujak and Williams (1978) and Barss *et al.* (1979). The *Subtilisphaera perlucida-Systematophora schindewolfii* Zone is believed to be Aptian in age by Bujak and Williams. Our analyses indicate that the following dinoflagellates are present in this zone:

**Aptea attadalica* (Cookson and Eisenack)
**Aptea polymorpha* Eisenack
Canningia colliveri Cookson and Eisenack
Canningia reticulata Cookson and Eisenack
Canningia sp.A
Cyclonephelium distinctum Deflandre and Cookson
Escharisphaeridia? sp.
Gardodinium eisenackii Alberti
**Muderongia simplex* Cookson and Eisenack
**Muderongia* sp.
Odontochitina sp. A (top)
Oligosphaeridium anthophorum (Cookson and Eisenack)
Oligosphaeridium asterigerum (Gocht)
Oligosphaeridium complex (White)
Oligosphaeridium pulcherrimum Deflandre and Cookson
**Ovoidinium* sp.
**Pareodinia ceratophora* (Deflandre)
**Pareodinia* sp.
Protoellipsodinium williamsii Fasola (in prep.) subsp. B

*Elements denoted by an asterisk in this and subsequent lists throughout this work are those reported by Barss *et al.* (1979) from these wells, but not found during the present study.

Table 1. *Palynofloral zonation and age determinations of mid-Cretaceous intervals intersected by three drill holes on the Scotia Shelf. (Adapted from data in Barss et al.* 1979).

		WELLS (with depths in metres)		
ZONE	SUBZONE	WYANDOT	MISSISSAUGA	TRIUMPH
Cleistosphaeridium polypes ZONE (CENOMANIAN)		594 ↕ 818	1242 ↕ 1481	1940 ↕ 2423
Spinidinium cf. S. vestitum -Eucommiidites minor ZONE (ALBIAN)	Rugubivesiculites rugosus SUBZONE (LATE ALBIAN)	837 ↕ 1195	1507 ↕ 1774	2438 ↕ 3231
	(EARLY ALBIAN)		1812 ↕ 2263	
Subtilisphaera perlucida - Systematophora Schindewolfii ZONE (APTIAN)	Aptea attadalica SUBZONE (EARLY APTIAN)	1201 ↕ 1411 ↕ 1420	2283 ↕ 2403	3353 ↕ 3484

**Pseudoceratium pelliferum* Gocht
Spinidinium vestitum Brideaux
Spinidinium cf. *vestitum* Brideaux (top)
Subtilisphaera perlucida (Alberti)
**Subtilisphaera* cf. *perlucida* (Alberti)
Subtilisphaera pirnaensis (Alberti)
**Subtilisphaera pirnaensis sensu* Millioud
**Systematophora* cf. *schindewolfii*

These assemblages are in accord with Bujak and Williams' age determination of Aptian, but our data may require revision of certain species ranges, for example the extension of that of *Spinidinium vestitum* which hitherto has only been reported from Middle Albian and higher strata.

The *Spinidinium* cf. *S. vestitum-Eucommiidites minor* Zone is determined as Albian in age by Bujak and Williams and has yielded the following dinoflagellates which accord with this age:

**Aptea polymorpha* Eisenack
Canningia reticulata Cookson and Eisenack
Canningia sp.C
Coronifera oceanica? hebospina Yun
Coronifera oceanica oceanica Cookson and Eisenack
Cribroperidinium intricatum Davey
**Cribroperidinium orthoceras* (Eisenack)
Cyclonephelium brevispinatum (Millioud)
Cyclonephelium distinctum Deflandre and Cookson
**Cyclonephelium pauciospinosum* Davey
Florentinia cooksoniae (Singh 1971)
**Florentinia mantellii* (Davey and Williams)
Hafniasphaera sp. A
Odontochitina porifera Cookson
Odontochitina striatoperforata Clarke and Verdier
Odontochitina sp. A
Oligosphaeridium albertense (Pocock)

Oligosphaeridium anthophorom Cookson and Eisenack
Oligosphaeridium asterigerum (Gocht)
Oligosphaeridium complex (White)
Oligosphaeridium cf. *complex* (White)
Oligosphaeridium pulcherimum Deflandre and Cookson
Oligosphaeridium totum Brideaux
**Palaeoperidinium cretaceum* Pocock
Protoellipsodinium williamsii Fasola (in prep.) subsp. A.
Protoellipsodinium sp.
Spiniferites ramosus gracilis (Davey)
**Subtilisphaera perlucida* (Alberti)
Surculosphaeridium longifurcatum (Firtion)
Xiphophoridium alatum (Cookson and Eisenack)

Our analyses indicate that some species ranges may require readjustment, but in general these assemblages show close resemblances to Albian assemblages described by Brideaux (1971) and Singh (1971) from Alberta, and by Davey and Verdier (1971, 1973) from northwest Europe.

The *Cleistosphaeridium polypes* Zone is believed by Bujak and Williams (1978) to be Cenomanian, and has yielded the following dinoflagellates:

**Canningia colliveri* Cookson and Eisenack
Canningia reticulata Cookson and Eisenack
Canningia sp. A
Canningia sp. B
Canningia sp. C
Cleistosphaeridium huguoniotii (Valensi)
**Cleistosphaeridium polypes* (Cookson and Eisenack)
Aff *Coronifera* sp.
**Cribroperidinium orthoceras* (Eisenack)
Cyclonephelium vannophorum Davey
**Epelidosphaeridia spinosa* Davey
**Florentinia cooksoniae* (Singh)
Hafniasphaera crassipellis (Deflandre and Cookson)
Hafniasphaera cf. *gabonensis* (Boltenhagen)
Odontochitina porifera Cookson
Odontochitina striatoperforata Cookson and Eisenack
Odontochitina sp. A
Oligosphaeridium anthophorum (Cookson and Eisenack)
Oligosphaeridium complex (White)
Oligosphaeridium pulcherrimum Deflandre and Cookson
Oligosphaeridium sp. A
Oligosphaeridium totum minor (Brideaux)
Oligosphaeridium totum totum (Brideaux)
Palaeohystrichophora infusurioides Deflandre
Palaeoperidinium cretacum Pocock
Palaeoperidinium pyrophorum (Ehrenberg)
**Palaeoperidinium* sp. A
Proteollipsodinium williamsii Fasola (in prep.)
**Spinidinium vestitum* Brideaux
Spiniferites ramosus granomembranaceus (Davey and Williams)
Spiniferites ramosus multibrevis (Davey and Williams)
Spiniferites cf. *supparas* (Drugg)
**Subtilisphaera pontis-mariae* (Deflandre)
Surculosphaeridium longifurcatum (Firtion)

Age determination on this zone does not completely conform with pre-existing data on assemblages and ranges. In particular, we draw attention to the presence of a single *Palaeoperidinium pyrophorum* which has not been reported below the Coniacian elsewhere. In general however, the assemblages resemble Cenomanian assemblages described by Davey (1969 and 1970) from western Europe and Saskatchewan, by Fasola (in preparation) from Manitoba, and by Below (1981) from Germany.

SPORE-POLLEN ASSEMBLAGES

The Aptian *Subtilisphaera perlucida-Systematophora schindewolfii* Zone contains the following species (those restricted to the subzones are so indicated):

Aequitriradites cf. *spinulosus* (Cookson and Dettmann)
Aequitriradites sp. A (*attadalica* Subzone)
?Couperisporites tabulatus Dettmann (*attadalica* Subzone)
**Appendicisporites bifurcatus* Singh
Appendicisporites concentricus Kemp (above *attadalica* Subzone)
Appendicisporites potomacensis Brenner
Appendicisporites sp. of Kemp 1970 (above *attadalica* Subzone)
Appendicisporites sp. B
Biretisporites potoniaei Delcourt and Sprumont
Concavissimisporites variverrucatus Couper (above *attadalica* Subzone)
Concavissimisporites sp. (*attadalica* Subzone)
Deltoidospora australis (Couper)
Distaltriangulisporites perplexus Singh (*attadalica* Subzone)
Impardecispora apiverrucata Couper (above *attadalica* Subzone)
Impardecispora marylandensis (Brenner)
Impardecispora purverulenta (Verbitskaya) (above *attadalica* Subzone)
'Ischyosporites' pseudoreticulatus (Couper) (above *attadalica* Subzone)
Ischyosporites variegatus (Couper) (above *attadalica* Subzone)
Nodosisporites sp. (*attadalica* Subzone)
Pilosisporites trichopapillosus (Thiergart)
Stereisporites crassus (Cookson) (*attadalica* Subzone)
**Callialasporites dampieri* (Balme)

Callialasporites trilobatus (Balme) (*attadalica* Subzone)
Callialasporites turbatus (Balme) (*attadalica* Subzone)
Pityosporites sp.(above *attadalica* Subzone)
Podocarpidites dettmanniae Kemp
Fungal spores

It must be emphasized that this is not a complete list, being based on a reconnaissance study. However, previous publications on Scotian Shelf Mesozoic palynology (e.g. Barss *et al.* 1979) have given only very abbreviated details of terrestrial palynofloras. It is noteworthy that many of the species reported by Richardson and Norris (1981) from the Adam Creek boreholes as entering the Moose River Basin in the lowest Zone A occur in dated Aptian units of the Scotian Shelf. Norris (in press) indicated that the lowest floras are probably Middle Albian but his determinations were based on information which did not include details of Aptian floras other than that of the work by Kemp (1970) on selected elements from northwest Europe. Clearly, further detailed work is necessary on the Aptian assemblages from the Scotian Shelf to determine a correlation with the lowest Cretaceous palynofloras from the Moose River Basin.

The Albian *Spinidium* cf. *S. vestitum-Eucommiidites minor* Zone contains the following spore-pollen species:

Aequitriradites cf. *spinulosus* Cookson and Dettmann
Aequitriradites sp. B
?Couperisporites tabulatus Dettmann
Triporoletes reticulatus (Pocock)
**Triporoletes triangularis* (Pocock)
Acanthotriletes varispinosus Pocock
Apiculatisporis babsae Brenner
Appendicisporites concentricus Kemp
Appendicisporites cf. *dentimarginatus* Brenner
**Appendicisporites potomacensis* Brenner
**Appendicisporites problematicus* (Burger)
**Appendicisporites unicus* (Markova)
Appendicisporites sp. of Kemp 1970
Appendicisporites sp. B
Auritulinasporites? sp.
**Baculatisporites comaumensis* (Cookson)
Biretisporites potoniaei Delcourt and Sprumont
Camarozonosporites insignis Norris
Cicatricosisporites abacus Burger
Cicatricosisporites augustus Singh
Cicatricosisporites hughesii Dettmann
**Cicatricosisporites subrotundus* Brenner
Cicatricosisporites venustus Deák
Cicatricosisporites sp. A
Cicatricosisporites sp. B
Cicatricosisporites sp. C
Cicatricososporites sp.
Cicatricososporites auritus Singh
Concavisporites sp.
Concavissimisporites granulatus Tralau (*rugosus* Subzone)
Concavissimisporites variverrucatus (Couper)
Concavissimisporites sp.
**Contignisporites cooksoniae* (Balme)
Contignisporites glebulentus Dettmann (*rugosus* Subzone)
Costatoperforosporites fistulosus Deák
Costatoperforosporites foveolatus Deák
Deltoidospora australis (Couper)
**Densoisporites velatus* Weyland and Krieger
Dictyophyllidites harrisii Couper
**Distaltriangulisporites perplexus* Singh
Distaltriangulisporities sp. A
**Foveotriletes subtriangulatus* Brenner
Gleicheniidites senonicus Ross
Impardecispora apiverrucata (Couper)
Impardecispora marylandensis (Brenner)
Impardecispora tribotrys (Dettmann)
Ischyosporites disjunctus Singh
**'Ischyosporites' foveolatus* (Pocock)
Ischyosporites pseudoreticulatus (Couper)
Ischyosporites cf. *neovariegatus* Filatoff
Ischyosporites variegatus Couper
Ischyosporites sp.
Nodosisporites sp.
Osmundacidites wellmanii Couper
Pilosisporites trichopapillosus (Thiergart)
**Pilosisporites verus* Delcourt and Sprumont
Retitriletes austroclavatidites (Cookson)
Staplinisporites caminus (Balme)
Tappanispora scurranda (Norris)
Taurocusporites segmentatus Stover
Trilobosporites canadensis Pocock
Callialasporites dampieri (Balme)
Cerebropollenites macroverrucosus (Thiergart)
Classopollis classoides Pflug
Cycadopites sp.
Eucommiidites minor Groot and Penny
Eucommiidites troedssonii Erdtman
Exesipollenites tumulus Balme
**Alisporites grandis* (Cookson)
Podocarpidites dettmanniae (Kemp) (*rugosus* Subzone)
Rugubivesiculites rugosus Pierce
Vitreisporites pallidus (Reissinger)
**Vitreisporites* sp. of Singh 1971
**Liliacidites textus* Norris
**Liliacidites peroreticulatus* (Brenner)
**Retitricolpites georgensis* Brenner
**Striatopollis paraneus* (Norris)
**Tricolpites micromunus* (Groot and Penny)
**Tricolpites parvus* Stanley
Schizophacus spriggii (Cookson and Dettmann)
Schizosporis reticulatus Cookson and Dettmann (*rugosus* Subzone)
Fungal ?hypha & spores

These assemblages resemble Albian assemblages from Alberta (Singh 1971; Brideaux 1971; Norris *et al.* 1975) in their high degree of diversity and taxonomic content. It is noteworthy that the putatively coeval Moose River assemblages are less diverse.

The Cenomanian *Cleistosphaeridium polypes* Zone contains the following species:

Aequitriradites cf. *spinulosus* Cookson and Dettman
Triporoletes reticulatus (Pocock)
Triporoletes sp.
**Appendicisporites bilateralis* Singh
Appendicisporites cf. *concentricus* Kemp
Appendicisporites cf. *crimensis* (Bolkhovitina)
**Appendicisporites jansonii* Pocock
**Appendicisporites problematicus* (Burger)
Appendicisporites sp. A
Camarozonosporites insignis Norris
**Cicatricosisporites hallei* Delcourt and Sprumunt [=*?C. venustus* Deák]
Cicatricosisporites hughesii Dettmann
**Cicatricosisporites pseudotripartitus* (Bolkhovitina)
Concavisporites sp.
Concavisporites toralis Leschik
?Deltoidospora australis (Couper)
Gleicheniidites minor Doring
Ischyosporites disjunctus Singh
Ischyosporites cf. *neovariegatus* Filatoff
Laegivatosporites haardtii (Potonie and Venitz)
Nodosisporites sp.
Ornamentifera sp. A
Pilosisporites trichopapillosus (Thiergart)
Polycingulatisporites sp. A
Retitriletes austroclavatidites (Cookson)
Retitriletes quasitrabeculatus Fensome (in prep.)
Retitriletes rosewoodensis (de Jersey)
cf. *Rogalskaisporites cicatricosus* (Rogalska)
Staplinisporites sp.
Trilete spore gen. *et* sp. indet. A
Classopollis classoides Pflug
Eucommiidites minor Groot and Penny
Exesispollenites tumulus Balme
Monosulcites sp.
Alisporites bilateralis Rouse
Pityosporites sp.
Rugubivesiculites rugosus Pierce
Carpinipites sp.
Extratriporopollenites sp. (top of zone)
Liliacidites dividuus (Pierce)
**Liliacidites peroreticulatus* (Brenner)
**Retitricolpites vulgaris* Pierce
**Retitricolpites maximus* Singh
**Retitricolpites virgeus* (Groot *et al.*)
**Tricolpites micromunus* (Groot and Penny)
**Tricolpites parvus* Stanley
Tricolpites sagax Norris (bordering on Turonian)
Arcellites sp.
Schizophacus parvus (Cookson and Dettmann)
Schizophacus? sp.

A number of species of *Appendicisporites* and *Cicatricosisporites* characterize these assemblages but their significance is not certain pending a thorough revision of these striate grains.

It is noteworthy that several angiospermous pollen species belonging to *Liliacidites, Tricolpites,* and *Retitricolpites* occur in this and the subjacent zone. In general, tricolpate angiosperms appear in northwest Europe and North America in the late early or early middle Albian (Doyle and Robbins 1977; Brenner 1976; Laing 1975, 1976) and in the Moose River Basin only in Zone B (species of *Rouseia* and *Cupuliferoidaepollenites* as reported by Richardson and Norris 1981.)

COMPARISONS BETWEEN MOOSE RIVER BASIN, SCOTIAN SHELF, AND ALBERTA

The highly diverse assemblages reported herein from the Scotia Shelf show a strong resemblance to coeval assemblages from the Aptian, Albian, and possibly Cenomanian of western Canada. Both areas were occupied by marginal marine and nearshore marine conditions. In contrast, the Moose River Basin is entirely terrestrial and does not contain certain spore-pollen species which are common to the east and to the west. Furthermore, terrestrial palynofloral resemblances are strong between the Scotian Shelf and northwest Europe (Couper 1958; Kemp 1970).

We tentatively conclude that the more limited assemblages which characterize the Moose River Basin may be the result of a more localized derivation of the floras from a terrestrial basin compared with more diverse assemblages which were derived from a larger region fed in part by rivers discharging into shallow seas.

ACKNOWLEDGMENTS

Material from the Scotian Shelf was kindly supplied by the Geological Survey of Canada.

REFERENCES

Barss, M.S., Bujak, J.P., and Williams, G.L.
1979: Palynological Zonation and Correlation of Sixty-seven Wells, Eastern Canada; Geological Survey of Canada Paper 78-24, 118p.
Below, R.
1981: Dinoflagellatien-Zysten aus dem Oberen Hauterive bis Unteren Cenoman Sud-West-Marokkos; Palaeontographica, Vol. 176B, p. 1-145, pl. 1-15
Brenner, G.J.
1976: Middle Cretaceous Floral Provinces and Early Migrations of Angiosperms; p. 23-47 in Origin and Early Evolution of Angiosperms, edited by C.B. Beck, Columbia University Press, N.Y.
Brideaux, W.W.
1971: Palynology of the Lower Colorado Group, Central Alberta, Canada, I. Introductory Remarks, Geology, and Microplankton Studies; Palaeontographica, Vol. 135B, p. 53-114, pl. 21-30
Bujak, J., and Williams, G.L.
1978: Cretaceous Palynostratigraphy of Offshore Southeastern Canada; Geological Survey of Canada, Bulletin 297, 19p. 3 pl.
Couper, R.A.
1958: British Mesozoic Microspores and Pollen Grains, A Systematic and Stratigraphic Study; Palaeontographica, Vol. 103B, p. 75-179.

Davey, R.J.
1969a: Non-Calcareous Microplankton from the Cenomanian of England, Northern France and North America, Part 1; Bulletin of British Museum of Natural History (Geology), Vol. 17, p. 103-180, pl. 1-11.
1970: Non-Calcareous Microplankton from the Cenomanian of England, Northern France and North America, Part 2; Bulletin of British Museum of Natural History (Geology), Vol. 18, p. 333-397, pl. 1-10.
Davey, R.J., and Verdier, J.P.
1971: An Investigation of Microplankton Assemblages from the Albian of the Paris Basin; Verhandelingen der K. Nederlandsche Akademie van Wetenschappen Afdeling Natuurkunde, Eerste Reeks, Vol. 26, p. 1-58, pl. 1-7.
1973: An Investigation of Microplankton Assemblages from the Latest Albian (Vraconian) Sediments; Revista Espanola de Micropaleontologia, Vol. 5, p. 173-212, pl. 1-5.
Doyle, J.A. and Robbins, E.I.
1977: Angiosperm Pollen Zonation of the Continental Cretaceous of the Atlantic Coastal Plain and its Application to Deep Wells in the Salisbury Embayment; Palynology, Vol. 1, p. 43-78.
Fasola, A.
In Press: Biostratigraphy and Paleoecology of Dinoflagellate Cysts in Late Cenomanian to Early Campanian Deposits in Southwestern Manitoba; Palaeontographica Canadiana.
Hopkins, W.S. and Sweet, A.R.
1976: Miospores and Megaspores from the Lower Cretaceous Mattagami Formation of Ontario; Geological Survey of Canada, Bulletin 256, p. 55-71.
Kemp, E.M.
1970: Aptian and Albian Miospores from Southern England; Palaeontographica, Vol. 131B, p. 73-143.
Laing, J.F.
1975: Mid-Cretaceous Angiosperm Pollen from Southern England and Northern France; Palaeontology, Vol. 18, p. 775-808.
1976: The Stratigraphic Setting of Early Angiosperm Pollen; p.1526, 3 pl. in The Evolutionary Significance of the Exine, edited by Ferguson, I.K. and Muller, J., Linnean Society Symposium Series No. 1, Academic Press, London.
Norris, G.
1979: Palynostratigraphy of Lignite-bearing Mesozoic Sediments, Moose River Basin, James Bay Lowland; Ontario Geological Survey Miscellaneous Paper 87, p. 67-68.
In Press: Mesozoic Palynology of the Moose River Basin, Ontario; in Aspects of the Mesozoic Geology of the Moose River Basin, James Bay Lowland, edited by Telford, P.G. and Verma, H., Ontario Geological Survey Geoscience Study.
Norris, G., and Dobell, P.
1980: Palynostratigraphic Correlation of Cretaceous Lignitic Strata, Southern Moose River Basin, Ontario; Ontario Geological Survey Miscellaneous Paper 93, p. 179-184.
Norris, G., Jarzen, D.M., and Awai-Thorne, B.V.
1975: Evolution of the Cretaceous Terrestrial Palynoflora in Western Canada; Geological Association of Canada, Special Publication 13, p. 333-364.
Norris, G., Telford, P.G., and Vos, A.M.
1976: An Albian Microflora from the Mattagami Formation, James Bay Lowlands, Ontario; Canadian Journal of Earth Sciences, Vol. 13, p. 400-403.
Richardson, M.L. and Norris, G.
1981: Palynostratigraphic Working Standard for Intra-basinal Correlation of Albian Lignitic Strata, Moose River Basin, Ontario; p.216-221 in Geoscience Research Program, Summary of Research 1980-1981, edited by E.G. Pye, Ontario Geological Survey, Miscellaneous Paper 98, 340p.
Singh, C.
1971: Lower Cretaceous Microfloras of the Peace River Area, Northwestern Alberta; Research Council of Alberta, Bulletin 28, p. 301-542.

Grant 100 Petrology, Geochemistry, and Economic Potential of the Nipissing Diabase

G.C. Finn[1], A.D. Edgar[2], and W.F. Rowell[2]

[1]Department of Earth Sciences, Memorial University
[2]Department of Geology, University of Western Ontario

ABSTRACT

The Wanapitei intrusion, a Nipissing-type diabase located northeast of Sudbury, Ontario, consists predominantly of gabbronorite over its 822 m thickness. Minor felsic phases are present in the upper levels of the intrusion. Principal minerals of the gabbronorite are clinopyroxene, orthopyroxene and plagioclase with actinolite, epidote and minor alteration minerals. Microprobe analyses of the pyroxenes and plagioclase define an inverse cryptic layering, with increasing Mg/(Mg + ΣFe) and An component, respectively, with increasing height. Whole rock analyses define a reverse differentiation trend relative to most otherwise similar mafic intrusions: in the Wanapitei intrusion, MgO, CaO, Ni, Cr and Cu increase with increasing stratigraphic height. Distinct breaks in the trends define at least four cycles in the intrusion.

The reverse differentiation trends are interpreted to be due to the presence of one or more auxiliary magma chambers containing liquids derived by partial melting of a mantle source. Within each chamber a process of crystallization, mixing and resorption occurred to produce a new liquid richer in Mg and poorer in Fe than the original liquid. The liquids were removed from the chamber to the site of intrusion over a short time interval, approximately 2-5 Ma (million years).

Preliminary results on the economic potential of the intrusion indicate Au, Pt and Pd to be enriched in sulphide-bearing phases, but only slightly above previously recorded values for these metals in altered and unaltered gabbronorite.

INTRODUCTION

This report summarizes the work completed during the first year of Grant 100 on the origin and economic potential of the gabbronorite intrusion from the Lake Wanapitei – Portage Bay area of Ontario (Figure 1). This area was recently mapped by Dressler (1978, 1980), who recorded two anomalous features of the intrusion:

1. reverse differentiation, i.e. increasing MgO, $Fe_2O_3^T$*, Ni, Cr and Cu values with increasing height in three of four vertical cliff sections.
2. high values of Au, Pt and Pd within the intrusion.

These preliminary results form the basis of this study. Major and trace element analyses for 141 samples and over 350 mineral analyses have been completed (see Finn 1981 for sample locations). A further 65 samples, taken from altered zones on the cliff face exposures and from sulphide-bearing locations of the intrusion, were used for the preliminary evaluation of the economic potential of the area. Models are presented to explain the origin of the intrusion.

*$Fe_2O_3^T$ = Total Fe as Fe_2O_3.

GEOLOGICAL SETTING

The Wanapitei intrusion is one of over ninety intrusions of tholeiitic composition that occur between Lake of the Woods and Cobalt, Ontario, and belongs to the Nipissing Diabase intrusive suite (Miller 1911). Rb/Sr whole rock ages of 2160 ± 60 Ma (Fairbairn *et al.* 1969) and 2150 ±

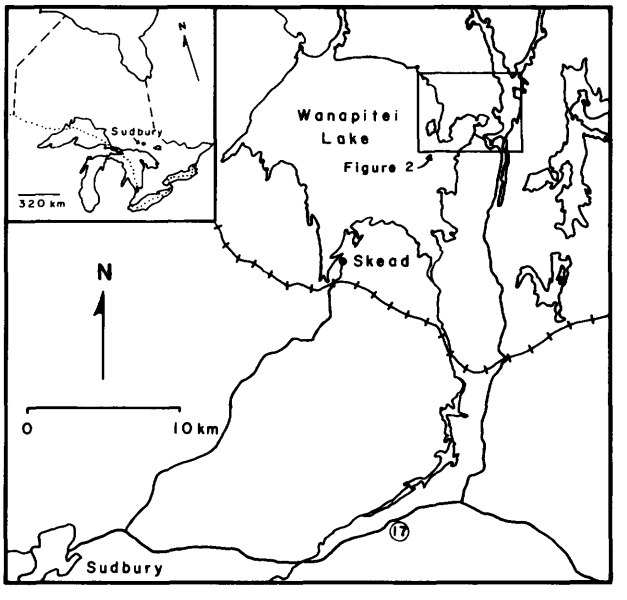

Figure 1. *Location and access to the study area, centred on Portage Bay, Lake Wanapitei, Ontario.*

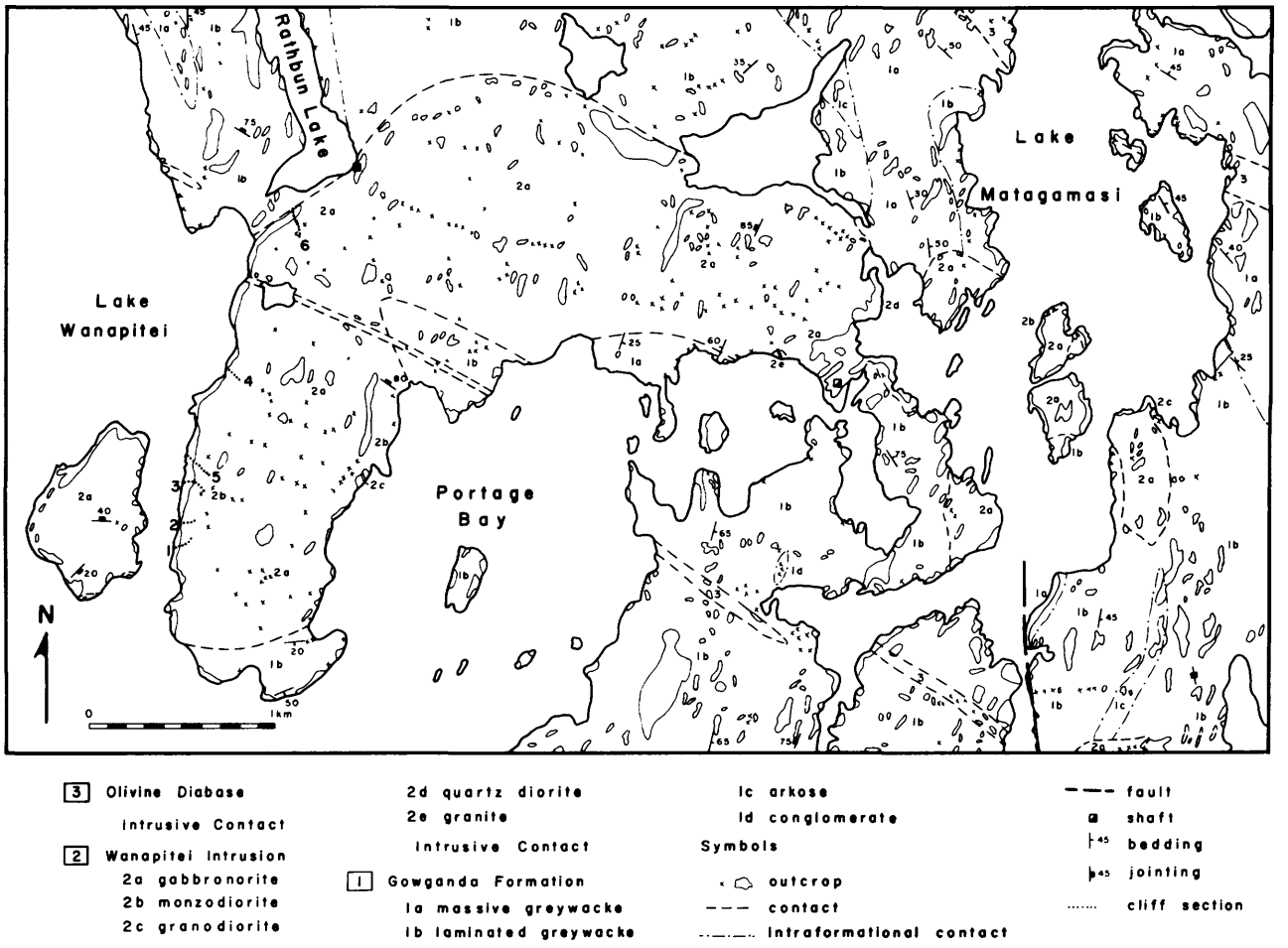

Figure 2. *Geology of the Lake Wanapitei-Portage Bay area (after Dressler 1978)*

50 Ma (Van Schmus 1965) for the Nipissing Diabase from the Cobalt and Blind River areas, respectively, mark the upper limit of Huronian sedimentation (Card *et al.* 1972). Within the Southern Province the Nipissing Diabase intrusions occur as dikes, sills and irregularly shaped bodies (Card and Pattison 1973) emplaced into the less competent Gowganda and Bruce Formations. The Wanapitei intrusion, situated near the southwest margin of the Cobalt embayment, occurs as an irregularly shaped, open ring structure (Dressler 1980). Emplacement of the Nipissing Diabase was later than an early faulting episode which occurred during the latter stages of an early major folding of the Huronian Supergroup about a north-south axis (Card 1966, 1969, 1976a, Church 1966). Following emplacement, east-west folding during the Hudsonian (Penokean) Orogeny (Church 1966), affected the Southern Province from Blind River to Sudbury. Faults within the area were reactivated at this time.

Within the area shown in Figure 2 Dressler (1978, 1980) recognized three major units; the Gowganda Formation, the Wanapitei intrusion and several olivine diabase dikes. The Gowganda Formation, consisting of laminated and massive greywacke, arkose and conglomerate lenses, is the host for the Wanapitei intrusion. The lower contact of the intrusion with the Gowganda Formation, exposed at the base of Section 6 (Figure 2), is sharp, striking north-northeast and dipping 25° southeast. Contact metamorphism is restricted to "baking" within 2 m of the contact. An exploration shaft has been sunk 325 m northeast of Section 6 into a massive sulphide occurrence at the lower contact (Figure 2).

The Wanapitei intrusion forms an arcuate shape within the Gowganda Formation and has a stratigraphic thickness of 822 m (see Figure 7). The intrusion is best exposed in the cliff face on the western side of the peninsula between Portage Bay and Lake Wanapitei; approximately 35 percent of the inland area here is outcrop.

A northwest-trending olivine diabase dike of the Sudbury Swarm (1460 ± 130 Ma, Gates and Hurley 1973), forms a linear valley across the peninsula (Figure 2). The

dike consists of plagioclase (An_{65}), olivine, augite and opaque minerals, is 20-30 m wide and has sharp contacts with the Wanapitei intrusion and the Gowganda Formation.

Structurally the area in the immediate vicinity of the Wanapitei intrusion is gently folded, with the major portion of the folding having occurred prior to emplacement. Faults of the regional Onaping Fault system bound the intrusion on the southwest and northeast and were active after its emplacement. These faults may have acted as conduits for groundwater circulation.

GENERAL FEATURES OF THE WANAPITEI INTRUSION

Sixty modal analyses (average of 1200 counts per sample) of the Wanapitei intrusion (Table 1) have been plotted on the QAP and orthopyroxene-clinopyroxene-plagioclase diagrams of Streckiesen (1976) (Figure 3) to classify the intrusion. Gabbronorite is the predominate rock type, with minor monzodiorite, granodiorite, quartz diorite and granite. In Figure 3b the extent of alteration of samples from the intrusion has been determined using the alteration index (AI) of Dressler (1980).

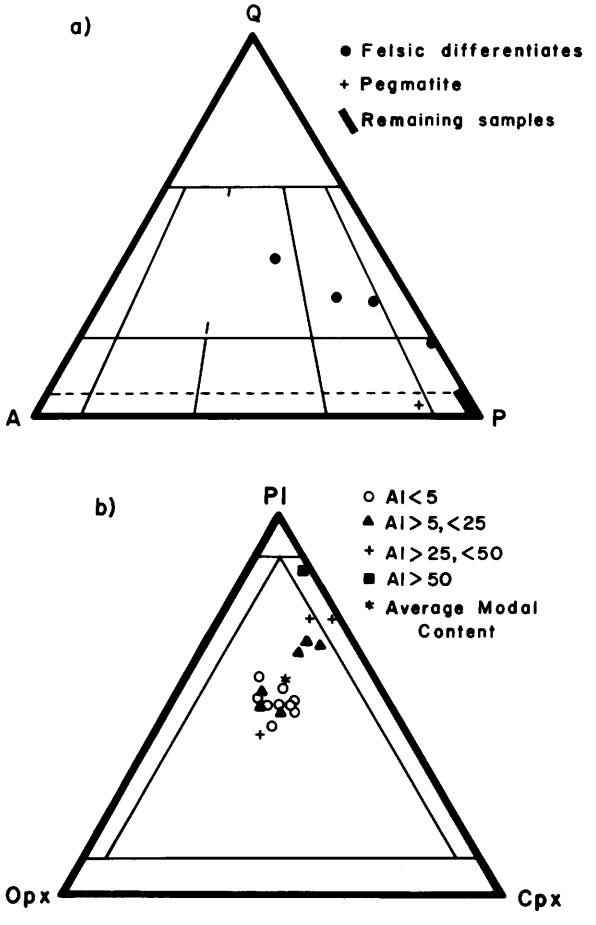

Figure 3. *Classification of samples from the Wanapitei intrusion in accordance with I.U.G.S. system (Streckeisen 1976).* ***a.*** *QAP triangle,* ***b.*** *orthopyroxene-clinopyroxene-plagioclase triangle.*

The gabbronorite has a uniform grain size (1-3 mm) and is separable into unaltered (AI < 50) and altered (AI > 50) varieties (Table 1). The unaltered gabbronorite consists of two pyroxenes, plagioclase (An_{40-70}) and minor quartz and pyrite; this assemblage becomes progressively replaced by actinolite, plagioclase (An_{0-5}), epidote and chlorite with increasing alteration. Alteration of the gabbronorite appears to be due to deuteric processes occurring on a scale ranging from pervasive to thin bands along cross-cutting fractures.

The monzodiorite (Table 1) occurs as pegmatitic schlieren (1.5 by 3.0 m) within the gabbronorite, generally found in the upper levels of the intrusion. Mineralogically the monzodiorite resembles the altered gabbronorite, and has a grain size that varies from 0.5 to 1.5 cm, with amphiboles reaching 7 cm in length. The contact separating the monzodiorite from the gabbronorite is diffuse, and is marked by a gradual increase in grain size suggesting contemporaneous crystallization.

The very minor felsic phases (Figure 3) occur in the upper levels of the intrusion and consist of plagioclase (An_{30}), microcline, and quartz ± chlorite, carbonates and opaques (Table 1). Contacts with the enclosing gabbronorite are sharp, giving the felsic phases the appearance of dikes. Dressler (1980) suggested that these phases are genetically related to quartz and quartz-carbonate veins which also cut the intrusion, are gold bearing and enriched in platinum group elements (PGE, see "Economic Potential"). Formation of these veins is related to the deuteric processes producing the altered gabbronorite.

Plagioclase, the most abundant phase within the Wanapitei intrusion (Table 1), occurs as prismatic laths having a composition, determined by optical methods, of An_{72} to An_{38} within gabbronorite. The An content of the plagioclase increases with increasing height in the vertical cliff sections. Orthopyoxene and clinopyroxene occur in equal proportions and together with plagioclase account for most of the gabbronorite (Table 1). The pyroxenes exhibit an ophitic to sub-ophitic texture with the plagioclase. Optical measurement of the $2V_x$ for the orthopyroxene (Dressler 1980) corresponds to an Mg number† of 72 to 82, for samples from the bottom and top, respectively, of cliff Sections 1 and 3. The $2V_z$ for the clinopyroxenes decreases with increasing height in the cliff sections corresponding to a decrease in the Ca component of the clinopyroxenes. Bushveld-type exsolution textures (Hess and Philips 1938) are present within several samples from the lower half of Section 5.

†Mg Number = 100 Mg/(Mg + Fe^{2+} + Fe^{3+} + Mn), with all values in molecular percent.

Table 1. *Modal analyses of whole rock samples from the Wanapitei intrusion.*

Sample No.	A-9	A-4	G-1-V	47F3	G-1-I	41F1	38F3	M-1	41F5	36E13	37E4B2	49E9A	65E13
Quartz	0.4		2.3	5.4	1.2	5.0	4.1	5.5	3.1	35.0	20.6	26.5	1.4
Plagioclase	47.9	35.2	39.8	50.9	40.3	31.3	24.5	9.4	5.5	29.6	35.9	40.9	69.2
Microcline	-	-	-	-	-	-	-	-	-	21.5	10.5	11.1[3]	10.0
Orthopyroxene	19.9	21.0	23.2	9.7	1.0	0.4	-	-	-	-	-	-	-
Clinopyroxene	28.0	16.6	16.2	12.8	14.2	4.5	4.1	9.0	-	-	-	-	-
Primary Hornblende	1.3	-	2.0	-	1.1	-	-	-	-	-	-	-	-
Biotite	-	-	0.7	1.4	2.5	3.6	0.9	0.3	-	-	-	3.5	-
Actinolite[1]	-	18.3	13.5	16.2	28.0	28.8	44.4	33.5	49.9	-	-	-	-
Epidote[1]	-	0.2	0.1	0.9	6.1	12.7	15.4	34.8	38.9	-	-	1.3	-
Chlorite[1]	-	-	-	-	3.8	-	1.8	1.0	-	5.1	27.4	12.3	-
Sericite and/or Muscovite	tr	8.3	0.1	-	0.9	-	3.4	5.3	1.3	6.7	-	-	-
Apatite	-	-	-	-	-	-	-	-	-	tr	-	tr	0.4
Sphene	-	-	-	-	-	-	-	-	-	-	0.4	0.3	-
Zircon	-	-	-	-	-	-	-	-	-	-	tr	-	-
Carbonate[1]	-	-	-	-	-	-	-	-	-	0.5	3.9	3.3	17.4
Opaque Minerals	0.6	0.4	1.3	2.2	0.4	3.7	1.9	1.2	1.3	1.6	1.3	0.9	1.6
Plagioclase Rim Composition Care[2]	An70	An54	An50 An60	An54	An43 An63	An47	An53-58	An0-5	An0-5	An30	An30	An30	An30
Alteration Index[4]	0.0	26.9	15.0	19.0	39.4	56.4	68.8	90	100	-	-	-	-
I.U.G.S. Classification (Streckiesen 1976)			Gabbronorite (Unaltered)		Gabbronorite (Altered)			Granite		Granodiorite	Qtz Diorite		Monzodiorite

(1) Secondary Mineral

(2) Plagioclase compositions by optical determinations

(3) Granophyric intergrowth of quartz and plagioclase

(4) Alteration Index after Dressler (1980).

Preliminary whole rock chemistry and optical determinations of mineral compostions from the Wanapitei intrusion indicated a reversal of the normal differentiation trend, relative to other mafic intrusions (Dressler 1980). To further investigate this reversal 148 rocks were analyzed for major and trace elements by X-ray fluorescence methods at the University of Western Ontario and the Ontario Geological Survey. Over 350 mineral analyses were obtained using the MAC Model 400 electron microprobe at the University of Western Ontario. A complete set of analyses are given in Finn (1981).

MINERAL CHEMISTRY

ORTHOPYROXENE

Selected orthopyroxene analyses are given in Table 2 and average analyses for samples from five cliff sections are plotted (Figure 4) on a Mg-Ca-ΣFe‡ (in atom percent) diagram of Poldevaart and Hess (1951). The Ca component of the orthopyroxenes is fairly constant (4-5 atom

‡ΣFe = atom percent total iron as FeO, from mineral analysis.

Table 2. *Selected microprobe analyses of orthopyroxene from the Wanapitei intrusion.*

				W-8									
	1	2	3	4	5	6	7	8	9	10	11	12	13
Sample	G-III	G-V	Edge	Inter-mediate	Core	G-XI	G-XI	W-5	G-IX	C-IX	W-3	GF-6	GF-4
SiO_2	53.50	55.55	53.90	54.86	55.32	55.50	53.12	56.00	54.01	53.45	54.73	51.28	51.78
TiO_2	0.36	0.23	0.34	0.07	0.11	0.05	9.27	0.05	0.10	0.20	0.09	0.33	0.45
Al_2O_3	0.91	1.79	0.95	1.12	1.29	1.12	1.06	1.52	1.68	0.98	1.25	0.73	0.89
Cr_2O_3	0.05	0.10	0.07	0.05	0.09	0.21	0.21	0.00	0.21	0.12	0.00	0.00	0.03
FeO*	14.27	16.80	20.38	17.15	13.21	11.28	18.63	13.76	12.64	16.32	16.20	24.32	23.37
MnO	0.25	0.29	0.45	0.31	0.26	0.25	0.36	0.00	0.29	0.20	0.00	0.52	0.54
MgO	25.00	23.66	22.78	24.94	27.34	29.32	23.57	26.75	29.04	26.14	25.39	19.92	19.99
CaO	3.79	1.22	2.08	2.34	2.32	2.59	2.12	2.32	2.23	2.05	2.07	1.89	1.98
Na_2O	0.52	0.00	0.00	0.13	9.00	0.00	0.00	0.00	0.00	0.00	0.13	0.00	0.00
Total	98.90	99.67	100.97	100.97	99.94	100.32	99.34	100.40	100.20	99.45	99.86	99.02	99.03
Number of ions based on 6 oxygen atoms													
Si	1.965	2.013	1.976	1.980	1.979	1.962	1.967	1.993	1.921	1.950	1.984	1.959	1.969
Al	0.035	0.000	0.021	0.020	0.021	0.038	0.033	0.007	0.070	0.042	0.016	0.033	0.031
Al	0.004	0.076	0.017	0.027	0.034	0.009	0.013	0.056	0.000	0.000	0.037	0.000	0.008
Ti	0.012	0.006	0.009	0.002	0.003	0.001	0.008	0.001	0.003	0.005	0.002	0.009	0.012
Cr	0.000	0.003	0.002	0.001	0.003	0.006	0.000	0.006	0.003	0.000	0.000	0.000	0.000
Fe3+	0.000	0.000	0.000	0.000	0.000	0.020	0.000	0.000	0.059	0.028	0.000	0.014	0.000
Mg	1.367	1.278	1.245	1.341	1.458	1.545	1.301	1.419	1.539	1.422	1.372	1.134	1.133
Fe2+	0.438	0.509	0.625	0.518	0.395	0.313	0.577	0.409	0.317	0.470	0.491	0.763	0.742
Mn	0.008	0.009	0.014	0.009	0.008	0.007	0.011	0.000	0.009	0.080	0.080	0.077	0.082
Ca	0.148	0.047	0.082	0.090	0.089	0.098	0.084	0.088	0.085	0.000	0.009	0.000	0.000
Na	0.035	0.000	0.000	0.009	0.000	0.000	0.000	0.000	0.000	0.000	0.000	0.001	0.000
K	0.012	0.011	0.000	0.000	0.000	0.000	0.000	0.000	0.000				
Mg/Fe+Mg	75.7	71.20	66.10	71.80	78.30	81.90	68.90	77.60	80.00	73.80	73.60	58.80	60.04
Mg	69.9	69.66	63.79	68.81	75.07	78.98	68.30	74.02	79.30	72.09	70.59	57.0	57.90
ΣFe	22.4	27.76	32.02	26.55	20.35	16.00	29.41	21.37	16.32	23.85	25.27	39.0	38.00
Ca	7.7	2.58	4.19	4.64	4.58	5.02	4.29	4.62	4.38	4.06	4.14	3.90	4.10

* Total Fe as FeO.

Total Number of analyses by electron microprobe 181.

Table 3. *Selected microprobe analyses of clinopyroxene from the Wanapitei intrusion.*

Analysis No.	1	2	3	4	5	6	7	8	9	10
Sample No.	GF-20	GF-24	G-I-V	A-9	A-9	A-5	G-I-V	G-I-IX	G-I-III	GF-3
			Augite				Salite		Subcalcic Augite	Pigeonite
SiO_2	51.90	53.14	51.47	52.82	53.36	52.21	54.18	51.66	52.72	50.58
TiO_2	0.63	0.16	0.36	0.31	0.17	0.54	0.00	0.53	0.26	0.30
Al_2O_3	1.47	1.89	1.78	2.00	2.07	1.86	0.51	2.08	1.55	1.02
Cr_2O_3	0.00	0.39	0.15	0.41	0.44	0.39	0.04	0.40	0.00	0.22
FeO*	19.00	7.10	9.83	11.26	8.11	8.94	8.41	8.06	14.59	22.58
MnO	0.37	0.26	0.23	0.25	0.29	0.30	0.00	0.22	0.32	0.54
MgO	12.38	15.97	14.83	18.21	19.80	15.18	13.71	14.67	19.67	19.00
CaO	15.63	22.52	22.07	13.12	15.57	21.21	23.50	22.97	11.65	5.10
Na_2O	0.09	0.17	0.07	0.12	0.16	0.35	0.16	0.14	0.12	0.00
K_2O	0.03	0.01	0.01	0.00	0.01	0.00	0.00	0.00	0.01	0.25
Total	101.50	101.61	100.80	98.50	99.98	100.98	100.51	100.73	100.89	99.59
Number of ions based on 6 oxygen atoms										
Si	1.961	1.929	1.908	1.968	1.944	1.919	2.022	1.906	1.931	1.932
Al	0.039	0.071	0.078	0.032	0.056	0.081	0.000	0.090	0.067	0.046
Al	0.026	0.009	0.000	0.055	0.033	0.000	0.022	0.000	0.000	0.000
Ti	0.018	0.004	0.010	0.009	0.005	0.015	0.000	0.015	0.007	0.009
Cr	0.000	0.011	0.004	0.012	0.013	0.011	0.001	0.012	0.000	0.007
Fe^{3+}	0.000	0.054	0.058	0.000	0.013	0.064	0.000	0.059	0.061	0.022
Mg	0.697	0.864	0.819	1.011	1.075	0.831	0.756	0.807	1.074	1.082
Fe^{2+}	0.600	0.162	0.246	0.351	0.234	0.210	0.260	0.189	0.386	0.699
Mn	0.012	0.008	0.007	0.008	0.009	0.009	0.000	0.007	0.010	0.017
Ca	0.633	0.876	0.877	0.524	0.608	0.835	0.932	0.908	0.457	0.209
Na	0.007	0.012	0.005	0.009	0.011	0.025	0.011	0.010	0.009	0.000
K	0.001	0.000	0.000	0.000	0.000	0.000	0.000	0.000	0.000	0.012
Mg/Mg+ΣFe	53.20	79.20	72.40	73.80	80.80	74.50	74.40	75.90	70.20	60.00
Mg	36.11	45.44	42.18	53.62	56.08	44.29	38.81	42.37	56.02	53.77
ΣFe	31.10	8.50	12.69	18.61	12.22	11.21	13.36	9.94	20.13	36.70
Ca	32.78	46.07	45.13	27.78	31.70	44.50	47.83	47.69	23.85	10.40

* Total Fé as FeO

Total number of analyses by electron microprobe - 151.

Table 4. *Selected microprobe analyses of plagioclase from the Wanapitei intrusion.*

Analysis No.	1	2	3	4	5	6
Sample No.	A-10	G-1-X	G-1-III	W-8	GF-23	G-1-I
SiO_2	47.31	47.55	50.39	49.70	53.55	52.10
Al_2O_3	33.19	33.39	31.54	31.63	28.75	29.94
CaO	16.70	17.23	14.86	15.16	11.89	12.74
K_2O	0.07	0.06	0.06	0.13	0.22	0.69
Na_2O	2.28	1.82	3.22	2.84	4.38	3.48
Total	99.55	100.05	100.07	99.46	98.79	98.96
Number of ions based on 32 oxygen atoms						
Si	8.728	8.725	9.181	9.119	9.789	9.548
Al	7.215	7.219	6.772	6.839	6.193	6.452
Al	0.000	0.000	0.000	0.000	0.000	0.013
Na	0.816	0.647	1.137	1.010	1.552	1.236
K	0.016	0.014	0.014	0.030	0.051	0.061
Ca	3.301	3.387	2.901	2.980	2.329	2.503
Ab	10.65	8.44	15.91	14.02	24.17	18.79
Or	0.22	0.19	0.20	0.44	0.83	2.54
An	89.13	91.37	83.89	85.54	75.00	78.67

Total number of analyses by electron microprobe - 24.

percent), identifying them as clinohypersthenes. The Mg number** ranges from 81.9 to 58.8. With fairly constant (4-5 atom percent), identifying them as clinohypersthenes. The Mg number** ranges fro 81.9 to 58.8. With decreasing Mg number, representing increasing differentiation, there is a decrease in SiO_2 and Al_2O_3, and an increase in TiO_2 and MnO contents of the orthopyroxenes (Table 2). The Mg number of the orthopyroxenes increases with increasing height in the cliff sections, as well as increasing from the bottom to top of the intrusion, confirming the optical determinations. The orthopyroxenes show normal compositional zoning from Mg-rich cores to Fe-rich rims.

CLINOPYROXENE

The average composition of the clinopyroxenes is augite (Figure 4) with minor salite, subcalcic augite and intermediate pigeonite (Table 3). The Mg number of the clinopyroxenes range from 53.2 to 80.8 (Table 3), and the majority are between 70 and 75. In two cliff sections the Mg number increases with height, in the remaining sections there is no distinct trend. Excepting the pigeonite, the Ca component of the clinopyroxenes varies from 24 to 48

**Mg number = 100 Mg/(Mg + ΣFe), in atom percent.

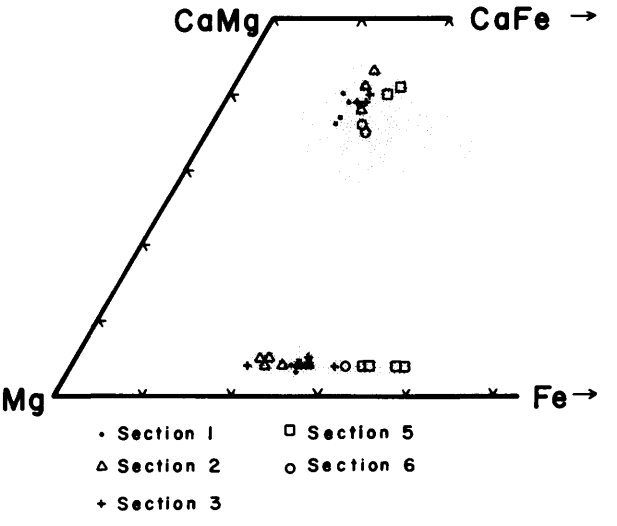

Figure 4. *Average compositions of orthopyroxene and clinopyroxene for each sample analyzed, from five cliff sections, plotted on a portion of the Ca-Mg-Fe (atom percent) triangle of Poldevaart and Hess (1951). The shaded areas define the overall fields of clinopyroxene (top) and orthopyroxene (bottom) compositions.*

Table 5. *Selected chemical analyses of whole rock samples from the Wanapitei intrusion (see Finn 1981 for complete listing of analyses).*

Analysis No.	1	2	3	4	5	6	7	8	9	10	11	12
Sample No.	G-19A	GF-27	G-2-IV	GF-1	GF-9	G-1-III	G-1-III	W-6	A-4	37E4B1	65E13	48E9A
SiO_2	51.97	52.54	49.90	52.22	50.49	50.10	50.20	50.00	49.90	61.90	59.90	68.70
TiO_2	0.65	0.48	0.49	0.28	0.27	0.33	0.35	0.13	0.20	0.71	1.57	0.74
Al_2O_3	14.76	13.08	14.40	15.86	16.41	15.30	15.00	16.70	15.00	17.80	17.20	12.50
Fe_2O_3*	10.43	10.10	10.00	6.15	8.46	8.64	8.29	7.53	0.96	5.18	0.04	1.65
FeO	n.d.	n.d.	n.d.	n.d.	n.d.	n.d.	n.d.	n.d.	6.15	n.d.	0.40	4.10
MnO	0.17	0.18	0.19	0.13	0.16	0.17	0.17	0.15	0.18	0.06	0.05	0.07
MgO	8.39	10.62	9.33	7.94	9.51	10.50	11.20	10.20	12.10	3.01	1.89	1.63
CaO	9.24	11.44	10.90	10.12	12.43	12.50	12.20	13.10	11.10	0.94	3.07	1.24
Na_2O	1.21	1.39	2.01	1.96	1.35	1.17	0.86	1.23	1.29	7.77	9.64	3.00
K_2O	0.81	0.21	0.57	0.44	0.08	0.34	0.50	0.13	0.60	0.73	1.16	2.59
CO_2	n.d.	n.d.	0.58	n.d.	n.d.	0.09	0.11	n.d.	n.d.	0.67	3.32	0.42
S	n.d.	n.d.	0.04	n.d.	n.d.	0.06	0.04	n.d.	n.d.	0.01	0.01	0.03
$H_2O\pm$	0.61	0.22	1.98	1.33	0.68	0.35	0.25	0.10	1.60	1.22	0.65	1.87
Total	98.64	100.26	100.39	96.43	99.84	99.55	99.17	99.39	99.08	99.83	99.25	98.64
Trace Elements (ppm)												
Co	72	70	40	51	74	43	41	41	40	n.d.	7	15
Cr	244	311	520	307	526	590	750	292	387	n.d.	6	35
Ni	99	162	142	105	140	163	178	145	141	n.d.	5	9
Cu	73	199	133	154	167	130	123	126	128	n.d.	8	20

*Total Fe as Fe_2O_3 where FeO is not determined (n.d.)
Analyses 1-9 - gabbronorite
Analysis 10 - granodiorite
Analysis 11 - monzodiorite
Analysis 12 - quartz diorite

atom percent and is greatest at the top of each cliff section. Average compositions for the clinopyroxenes show steady Fe, but variable Mg and Ca components. Lines joining average orthopyroxene and clinopyroxene pairs (not drawn on Figure 4) suggest mixing occurred during crystallization.

PLAGIOCLASE

The An component of plagioclase (Table 4) ranges from An_{91} to An_{75}, considerably higher than the optically determined compositions (see Finn 1981 for discussion). The relative results of both methods are similar and confirm the progressive increase in An content with height in the cliff sections. Based on the plagioclase system (Ab-An, Bowen 1913, Lindsley 1968) the relative differences in crystallization temperature between the An-rich and An-poor plagioclase from the top and bottom of the cliff section is 90-100°C. This suggests the entire section may have consolidated within this range of temperatures.

Analyses of the sulphide and oxide phases of the intrusions are presently underway.

WHOLE ROCK CHEMISTRY

Selected analyses of the Wanapitei intrusion (Table 5) indicate:

1. the intrusion has a tholeiitic compostion;
2. SiO_2 is generally low (basaltic) over the whole intrusion;
3. a moderate iron enrichment trend;
4. increasing MgO, CaO, Ni, Cr and Cu with increasing height in the cliff sections; and

5. decreasing $Fe_2O_3^T$, Na_2O, K_2O and Al_2O_3 with increasing height in the cliff sections.

The latter two characteristics are the reverse of the normal differentiation trend observed in other mafic intrusions, e.g. Skaergaard, East Greenland (Wager and Deer 1939) and the Palisades Sill, New Jersey (Walker 1940, Walker 1969).

The majority of samples from the Wanapitei intrusion fall within the tholeiitic field of Irvine and Barager (1971) on an AFM diagram with the felsic phases plotting in the calc-alkaline field (Figure 5). A moderate iron enrichment trend, similar to the Palisades Sill (Walker *et al.* 1973), is evident.

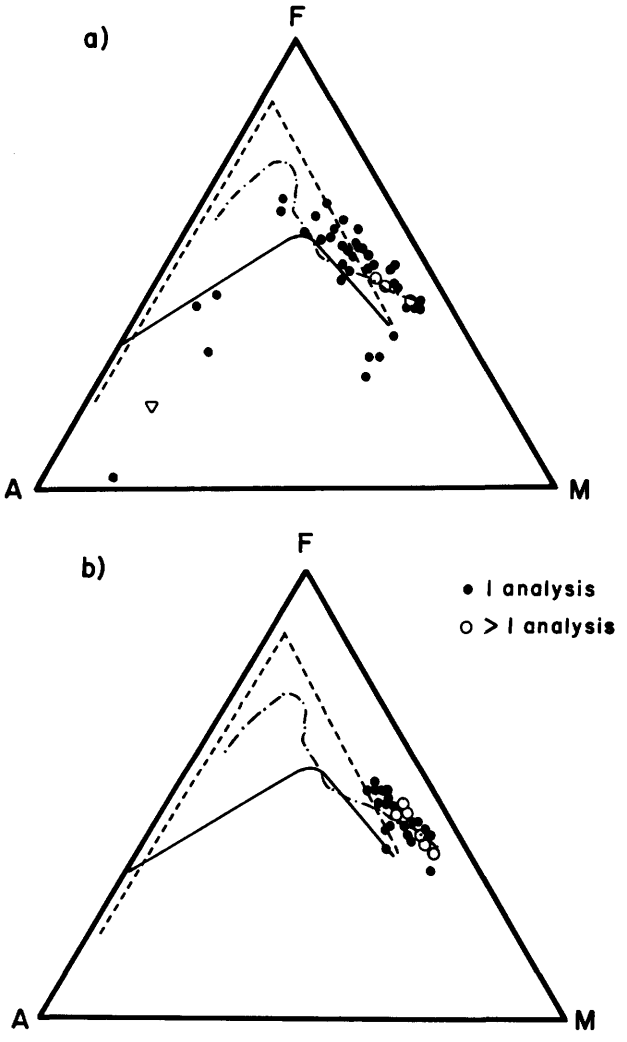

Figure 5. *AFM diagrams for the Wanapitei intrusion. The solid line separates the tholeiitic and calc-alkaline fields (Irvine and Barager 1971). The iron enrichment trends for the Skaergaard intrusion (dashed line, Wager and Brown 1968) and the Palisades sill (dot-dashed line, Walker 1969) are shown for comparison. a) surface sampled b) cliff section samples.*

CHEMICAL VARIATIONS IN CLIFF SECTIONS

The variations of CaO, Na_2O (weight percent) and MgO/(MgO + $Fe_2O_3^T$) (molecular percent) with height for each cliff section are shown in Figure 6. Overall the concentration of Mg over Fe and CaO increases towards the top of the intrusion, while Na_2O decreases, confirming the reverse differentiation. The cliff sections, as shown in Figure 6, do not represent a true stratigraphic section of the intrusion. To obtain a true section, a projection of sample locations onto a stratigraphic section was made (Finn 1981), as shown in Figure 7. The trends shown in the cliff sections hold for the stratigraphic section and show at least four cycles.

COMPARISON OF THE WANAPITEI INTRUSION WITH OTHER MAFIC INTRUSIONS

The Wanapitei intrusion can be compared with the Skaergaard intrusion (Wager and Brown 1968), the Palisades Sill (Walker 1940, Walker 1969), the Bushveld Complex (Willemse 1969, Cameron 1980) and with Nipissing Diabase intrusions in Henwood Township (Thomson 1966, Jambor 1971), and Janes Township (Dressler 1979). A comparison of similarities and differences in mineralogy, textures and chemistry is given in Finn (1981). The major difference between the Wanapitei intrusion and most of the other mafic intrusions is reverse differentiation; however a similar trend occurs within the Bushveld Complex (Cameron 1980) and possibly the Janes Township intrusion (Dressler 1979). The Wanapitei intrusion also differs from the others in the lack of olivine, cumulate textures, and rhythmic layering. The Wanapitei intrusion in similar in all other respects to the intrusions listed above. Reverse differentiation has been observed in the Stillwater complex, Montana (Jackson 1961), the Jimberlana intrusion, Australia (Campbell 1977), and was recently reported by Wilson *et al.* (1981) for the Fongen-Hyllingen complex of Norway.

DISCUSSION

None of the various hypotheses suggested for the reverse differentiation of other mafic intrusions (e.g. physically overturned, an overlying heat source, variations in liquid densities or changes in P_{Total}) sufficiently explain the trends observed in the Wanapitei intrusion.

The concept of auxiliary magma chambers has been suggested for the Bushveld complex (Kuschke 1939, Vander Walt 1941), although it was later rejected by Turner and Verhoogen (1951), and for the Stillwater complex (Jackson 1961). Recent investigators (Smith and Bailey 1966, Hildreth 1979, Ritchey 1980) of Tertiary volcanic deposits hypothesized that a differentiated, vertically zoned liquid within a magma chamber would explain zonation patterns in ash flow tuffs. In applying these

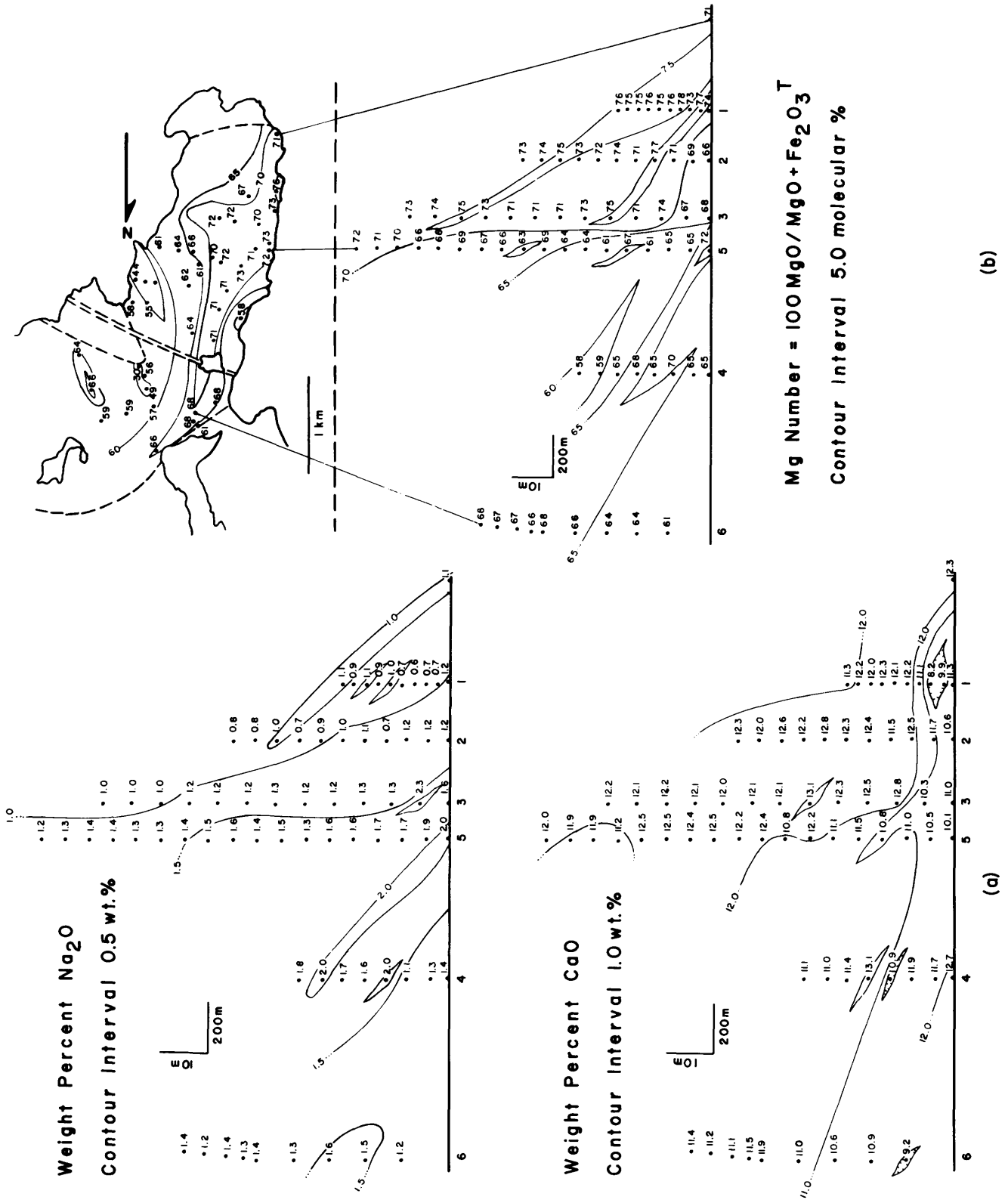

Figure 6. a. *Contoured whole rock Na_2O and CaO values (weight percent) for samples from the six cliff sections.*
b. *Contoured Mg number (molecular percent) from whole rock analyses of surface and cliff section samples.*

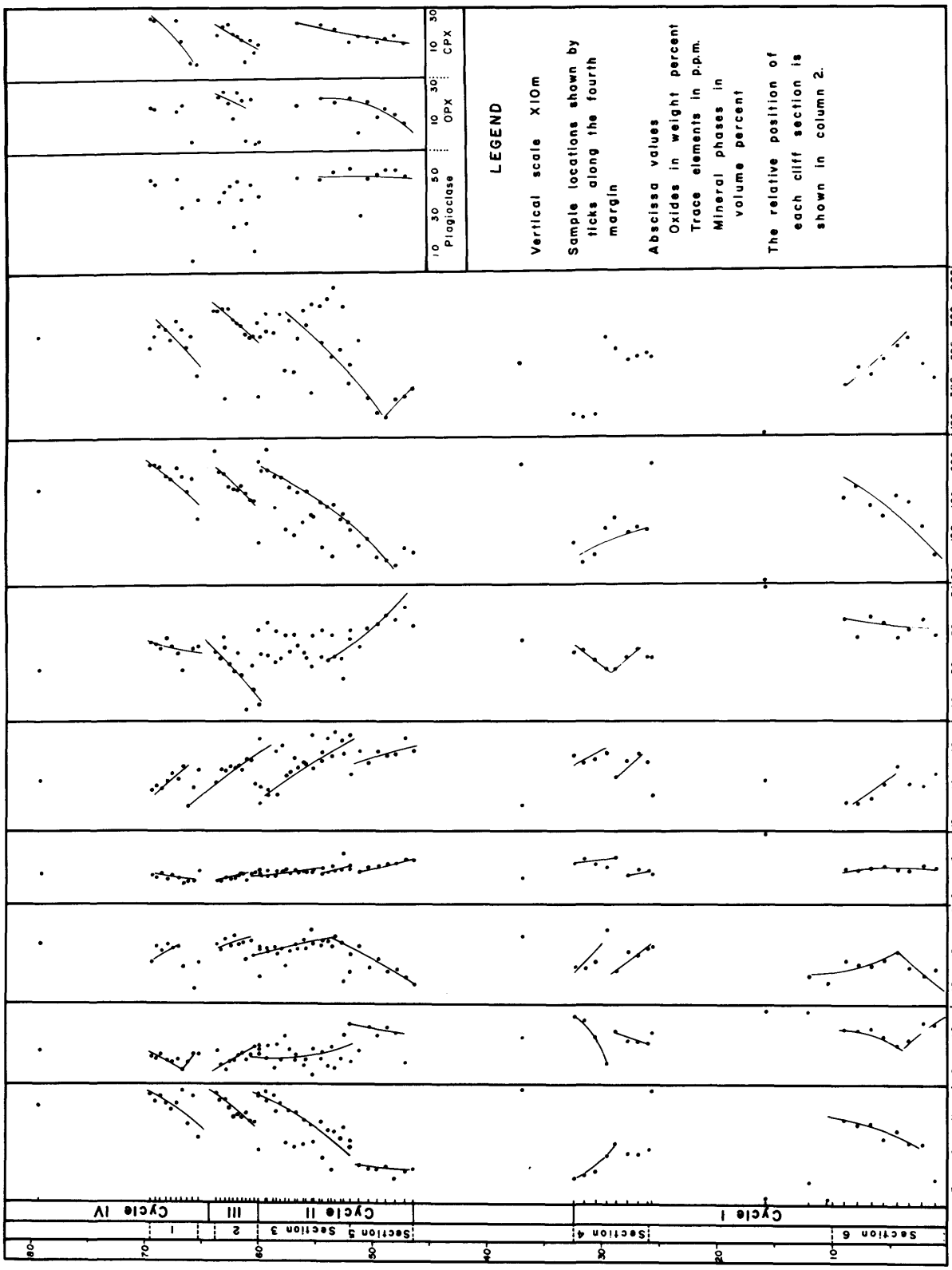

Figure 7. *Composite stratigraphic section of the Wanapitei intrusion.*

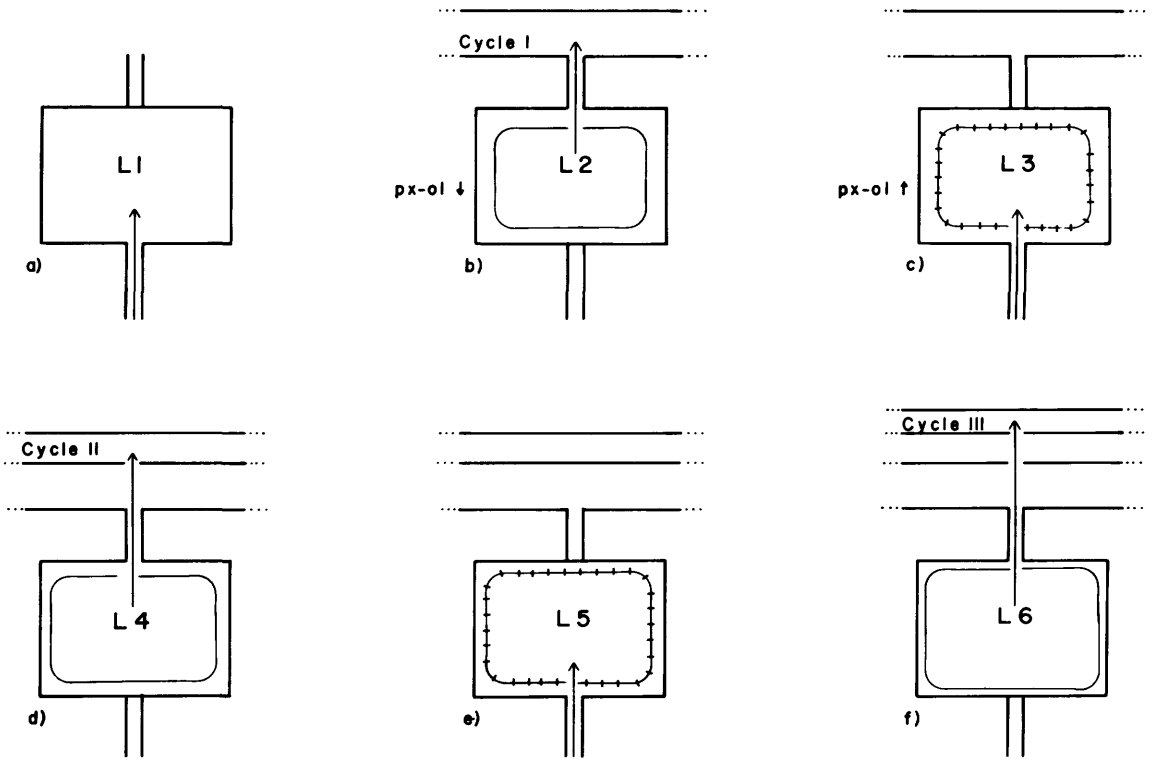

Figure 8. *Schematic diagram showing the stages of evolution of the Wanapitei intrusion, based on Model I. Symbols, px-pyroxene, ol-olivine.*

concepts to the Wanapitei intrusion two models are proposed.

MODEL I

Model I is shown schematically in Figure 8. Each stage begins with emplacement of an Mg-rich liquid (L1, L3, L5) into the auxiliary magma chamber and ends with intrusion of liquid (L2, L4, L6) at the site of crystallization of the Wanapitei intrusion.

Liquid 1 originates in the mantle and rises via faults of the regional Onaping, Temiskaming, and Murray systems (Card *et al.* 1973) into the auxiliary chamber (Figure 8a). Crystallization of Mg-rich pyroxene and olivine at the cooler edges of the chamber produces a residual liquid (L2), depleted in Mg, enriched in Fe and with comparable SiO_2 relative to the initial liquid (L1). At this stage the conduit from the chamber to the site of crystallization is opened causing L2 to evacuate the chamber (Figure 8b). This liquid crystallizes as the Mg-poor, Fe-rich layer at the base of the intrusion (Cycle I, Figure 7). Emplacement is passive, gently displacing the surrounding sedimentary rocks. This low Mg, high Fe liquid is reflected in the compositions of the pyroxenes from this cycle (Mg_{36} $\Sigma Fe_{31}Ca_{33}$, Mg_{62} $\Sigma Fe_{39}Ca_4$).

The second stage begins with emplacement of L3 from the mantle source, at a higher temperature and more Mg-rich than L1 or L2, into the auxiliary chamber (Figure 8c). Liquid 3 reacts with the previously crystallized pyroxene and olivine, resorbing these Mg-rich minerals, which increases the Mg content of L3 to produce L4. This new liquid is removed from the chamber to the site of crystallization (Figure 8d) to form Cycle II of the intrusion, which extends from 477 to 600 m above the lower contact (see Figure 7).

In the lower 45 m of Cycle II, MgO, $Fe_2O_3^T$ and CaO increase slightly, whereas above this level MgO increases, reaching a maximum of 11.80 weight percent at the top of the cycle, while $Fe_2O_3^T$ and CaO decrease (see Figure 7). These variations are reflected in the compositions of the pyroxenes and plagioclase. Repetition of the process of refilling and resorption occurs to complete the intrusion.

MODEL II

Model II involves a series of magma chambers between the mantle source and the site of the Wanapitei intrusion (Figure 9). Each cycle in the intrusion originates from a liquid that has risen through each chamber. This model is

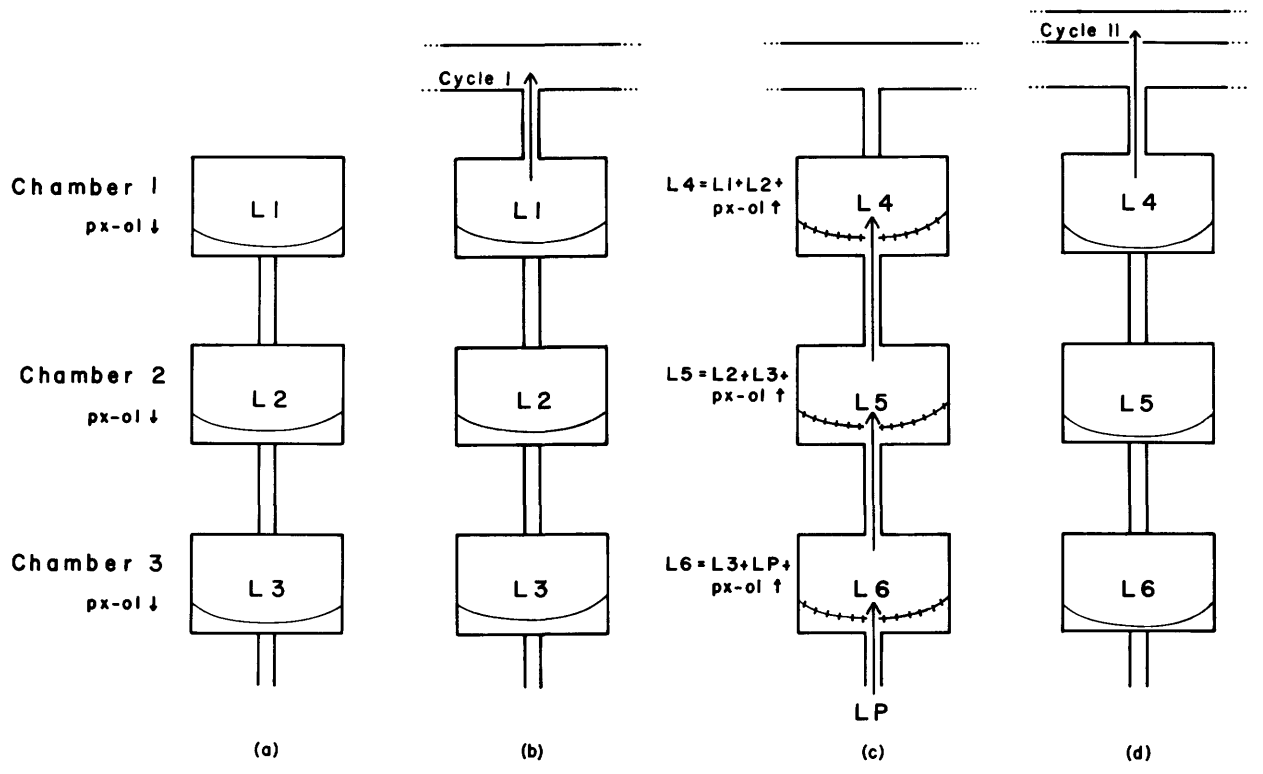

Figure 9. *Schematic diagram showing the stages of evolution of the Wanapitei intrusion, based on Model II. Symbols as in Figure 8.*

a more complex variation of Model I in which liquids within each chamber show an increase in Mg and a decrease in Fe with depth. The source of all liquids is the mantle, with variations in Mg and Fe produced by the degree of differentiation each liquid has undergone, the degree of partial melting of the source and/or the tapping of deeper levels of the mantle.

Chamber 1 (Figure 9a) is closest to the intrusion and contains an Fe-rich, Mg-poor liquid (L1). Liquid 2, in chamber 2, contains approximately equal amounts of Mg and Fe and L3, in chamber 3, has a higher Mg and lower Fe content than L1 or L2. Differentiation by crystallization of Mg-pyroxene and olivine is occurring in all chambers.

Opening of the conduit between chamber 1 and the site of the intrusion, triggered by folding, faulting or other tectonic events, permits L1 to partially evacuate chamber 1 to form Cycle I of the intrusion (Figure 9b). The resultant decrease in pressure produced by this evacuation will cause some of L2 to rise into chamber 1, where it mixes with residual L1 and resorbs previously crystallized pyroxene and olivine. This produces a new liquid (L4) richer in Mg than L1. Crystallization during mixing will seal the conduit between chambers 1 and 2. With the partial evacuation of chamber 2, L3, from chamber 3, rises and mixes with residual L2 producing L5. Evacuation of chamber 3 allows primitive liquid (LP) to rise from the mantle source into chamber 3, where it mixes with residual L3 to give L6 (Figure 9c). At this stage all chambers are again filled with liquids and the conduit between the site of intrusion and chamber 1 opens allowing L4 to rise and crystallize as Cycle II of the intrusion. The process of rising liquids, mixing with residual liquids, resorption of earlier formed minerals and renewal of liquid supply from the mantle source continues until the entire sequence of gabbronorites in the Wanapitei intrusion has been produced. A similar process of mixing and resorption has been suggested for the Fongen-Hyllingen complex of Norway (Wilson *et al.* 1981).

Both models explain the progressive enrichment in Mg and depletion in Fe with increasing stratigraphic height in the intrusion. These models require that the processes must have been fairly rapid to permit the flow of liquids without sealing the conduit and to explain the lack of cumulate textures. The origin of the true felsic phases is still unresolved.

Table 6.*Chemical analyses of unaltered gabbronorite, altered gabbronorite, and sulphide-bearing samples to evaluate the economic potential of the Wanapitei intrusion.*

	S43G	S10B	S23A	S5A	S2A	S48D	S57D	S59E	S60E
SiO_2	50.56	51.05	51.64	50.30	51.03	46.76	36.30	31.90	47.56
TiO_2	0.39	0.43	0.39	0.38	0.44	0.79	0.06	0.56	1.24
Al_2O_3	15.90	14.97	16.14	18.59	14.73	14.19	2.40	11.04	18.90
Fe_2O_3	1.47	1.65	1.45	1.56	2.95	1.43	0.17	41.76(1)	15.92(1)
FeO	5.86	5.83	5.54	5.41	6.39	5.98	0.86	--	--
MnO	0.14	0.15	0.14	0.14	0.14	0.14	0.16	0.06	0.04
MgO	9.12	8.93	9.07	8.92	8.33	7.74	1.63	6.76	8.64
CaO	12.65	12.88	13.07	12.78	11.25	9.52	34.00	--	0.26
K_2O	0.23	0.24	0.20	0.24	0.07	1.93	--	--	1.44
Na_2O	1.50	1.10	1.20	1.30	1.60	0.05	--	0.30	2.30
P_2O_5	--	--	0.01	--	0.01	--	0.01	--	--
H_2O^+	0.90	0.85	0.53	0.75	0.97	11.43	24.60	13.44	6.42
CO_2	0.10	0.15	0.25	0.25	0.20	0.40	1.53	0.37	0.28
S	--	--	--	--	--	--	--	10	4.90
Total	98.82	98.23	99.63	100.62	98.11	100.36	101.72	(2)	(2)

Trace elements (as ppm except where indicated)

Cr	576	764	541	580	514	191	61	148	279
Co	57	56	61	54	59	40	7	422	86
Ni	152	148	156	140	131	116	29	14,174	7,720
Cu	135	132	121	99	46	153	--	39,989	15,147
Zn	59	59	52	54	50	127	16	65	44
Pb	-	10	4	15	-	41	5	47	35
Rb	14	8	9	9	-	50	-	13	45
Sr	126	134	118	132	239	54	8	28	53
Y	13	16	12	13	10	14	13	10	8
Zr	35	37	31	30	30	39	13	45	36
Nb	4	5	2	6	12	29	-	11	4
Ba	67	58	58	69	5	346	1	17	96
Au(3)	2	4	3	15	5	2	2	1,200	2,100
Pt(3)	13	22	16	30	28	10	10	10,000	2,400
Pd(3)	27	50	29	27	23	2	70	6,700	10,000
Ag	1	1	1	1	1	1	1	6	1

Additional samples analysed only for Au, Pt, Pd and Ag

	S52D	S54D	S58D
Au	7	20	11
Pt	35	31	19
Pd	22	15	12
Ag	1	1	1

Samples of unaltered gabbronorite -- S43C, S10B, S23A, S5A, S52D, S54D, S58D.

Samples of altered gabbronorite -- S48D, S57D, S59E, S60E.

Sulphide rich samples -- S59E, S60E.

(1) Iron as Fe_2O_3 only

(2) Total is meaningless as FeO could not be determined, due to presence of sulphides. Volatiles by L.O.I. are very high.

(3) As p.p.b.

ECONOMIC POTENTIAL

The second phase of this project, begun in May 1981, is an evaluation of the economic potential of the Wanapitei intrusion. Dressler (1980) noted Au values were commonly <10 ppb in four of the cliff sections, but some samples contain >200 times background values. Based on these latter values Dressler (1980) proposed a "gold reef" within the gabbronorite. Palladium values are also enriched within this "reef".

Sixty-five samples from the gabbronorite, and from poorly defined shear zones of altered gabbronorite within the intrusion, have been analyzed for major and minor elements (including Ag, Au, Pt and Pd). Results (Table 6) indicate that Ag, Au, Pt and Pd are enriched in sulphide-bearing samples relative to both unaltered and altered gabbronorite. Preliminary results show that the non-sulphide bearing samples contain <2-20 ppb Au, <1 ppm Ag, <10-35 ppb Pt and <10-70 ppb Pd. Analyses of sulphide-bearing samples yield 520-2100 ppb Au, 1-7 ppm Ag, 98->10,000 ppb Pt and 6700->10,000 ppb Pd. An extensively altered sample (Table 6, Sample S57D) has slightly higher Pd values but is depleted in all trace elements relative to less altered samples. These results are in agreement with those of Dressler (1980) for the non-sulphide bearing gabbronorite, but suggest these elements occur in the sulphide phases. This relationship is evident in a sulphide-rich grab sample, from a sulphide lens near Rathbun Lake (see Figure 2) which yielded >10 000 ppb Pd (34 ounces Pd per ton, Dressler 1980).

CONCLUSIONS AND FUTURE PLANS

The Wanapitei intrusion consists predominantly of gabbronorite and shows a reverse differentiation trend. This is believed to be due to the presence of a slightly differentiated melt, from a mantle source, in one or more auxiliary magma chambers which were periodically tapped to produce the trend in the Wanapitei intrusion. Preliminary evaluation of the economic potential of the intrusion suggests that the enrichment in Au, Ag, Pt and Pd is pronounced in sulphide-bearing samples. Altered gabbronorite samples are slightly enriched in these elements.

Future studies on this grant will concentrate on:

1. delineating the mineralized zones within the intrusion;
2. establishing the relationship between the slightly greater than normal Ag, Au, Pt and Pd values in the non-sulphide bearing gabbronorite and the exceptionally high values of these elements in the sulphide-bearing gabbronorite;
3. the relationship of the "gold reef" and the sulphide-rich zone near Rathbun Lake; and
4. remapping and extensive sampling of the intrusion.

ACKNOWLEDGMENTS

We are grateful to R.L. Barnett, John Forth, Barb McKinnon, Glen Robinson and Alan Noon for technical assistance. The encouragement of B.O. Dressler of the Ontario Geological Survey is gratefully acknowledged.

REFERENCES

Bowen, N.L.
1913: The Melting Phenomena of the Plagioclase Feldspars: American Journal of Science, Fourth Series, Vol. 34, p. 577-599.

Cameron, E.N.
1980: Evolution of the Lower Critical Zone, Central Sector Eastern Bushveld Complex, and its Chromite Deposits; Economic Geology, Vol. 75, p. 845-871.

Campbell, I.H.
1977: A Study of Macro-Rhythmic Layering and Cumulate Processes in the Jimberlana Intrusion, Western Australia, Part I: The Upper Layered Series; Journal of Petrology, Vol. 18, p. 183-215.

Card, K.D.
1966: Huronian Geology (Abstract); Ninth Conference on Great Lakes Research, Chicago, p.24.
1969: Geology of the McGregor Bay-Bay of Islands Area, Districts of Sudbury and Manitoulin; Ontario Department of Mines, Open File Report 5038.
1976a: Geology of the Sudbury-Manitoulin Area, Districts of Sudbury and Manitoulin; Ontario Division of Mines, Open File Report 5123.
1976b: Metamorphism of the Middle Precambrian (Aphebian) Rocks of the eastern Southern Province; p. 269-282 in Metamorphism in the Canadian Shield, Geological Survey of Canada, Paper 78-10.

Card, K.D., Church, W.R., Franklin, J.M., Frarey, M.J., Robertson, J.A., West, G.F., and Young, G.M.
1972: The Southern Province; p. 335-380 in Variations in Tectonic Styles in Canada, edited by R.A. Price and R.J.W. Douglas, Geological Association of Canada Special Paper 11.

Card, K.D., McIlwaine, H.W., and Meyn, H.D.
1973: Geology of the Maple Mountain Area, Districts of Timiskaming, Nipissing and Sudbury, Ontario Department of Mines, Geology Report 106, 133p.

Card, K.D. and Pattison, E.F.
1973: Nipissing Diabase of the Southern Province, Ontario; Geological Association of Canada, Special Paper 12, p. 7-30.

Church, W.R.
1966: The Status of the Penokean Orogeny in Ontario (Abstract); Ninth Conference on Great Lake Research, p. 25.

Dressler, B.O.
1978: Rathbun Township, District of Sudbury, Ontario; Ontario Geological Survey, Preliminary Map P. 1609, Scale 1 inch to 1/4 mile.
1979: Geology of McNish and Janes Townships, District of Sudbury; Ontario Geological Survey, Report 191, 91p.
1980: Geology of the Wanapitei Lake Area, District of Sudbury; Ontario Geological Survey, Open File Report 5287.

Fairbairn, H.W., Hurley, P.M., Card, K.D. and Knight, C.J.
1969: Correlation of Radiometric Ages of Nipissing Diabase and Huronian Metasediments with Proterozoic Orogenic Events in Ontario; Canadian Journal of Earth Sciences, Vol. 6, p. 489-497.

Finn, G.C.
1981: Petrogenesis of the Wanapitei Gabbronorite Intrusion, a Nipissing-type Diabase, from Northeastern Ontario; Unpublished M.Sc. Thesis, University of Western Ontario, 213p.

Gates, T.M. and Hurley, P.M.
1973: Evaluation of Rb-Sr Dating Method Applied to the Matachewan, Abitibi, Mackenzie and Sudbury Dike Swarms of Canada; Canadian Journal of Earth Sciences, Vol. 10, p. 900-919.

Hess, H.H. and Philips, A.H.
1938: Orthopyroxene of the Bushveld Type; American Mineralogist, Vol. 23, p. 450-456.
Hildreth, E.W.
1979: The Bishop Tuff: Evidence for the Origin of Compositional Zonation in Silicic Magma Chambers; p.43-75 in Ash Flow Tuffs, C.E. Chapin and E.W. Elston editors, Geological Society of America, Special Paper 180.
Irvine, T.N. and Barager, W.R.A.
1971: Guide to the Chemical Classification of the Common Volcanic Rocks; Canadian Journal of Earth Sciences, Vol. 8, p. 523-548.
Jackson, E.D.
1961: Primary Textures and Mineral Associations in the Ultramafic Zone of the Stillwater Complex, Montana; United States Geological Survey, Professional Paper 358, 106p.
Jambor, J.L.
1971: The Nipissing Diabase; Canadian Mineralogist, Vol. 11, p. 34-75.
Kuschke, G.S.J.
1939: The Critical Zone of the Bushveld Igneous Complex, Lydenburg District; Geological Society of South Africa, Transactions, Vol. 42, p. 57-81.
Lindsley, D.H.
1968: Melting Relations of Plagioclase at High Pressure; New York State Museum and Science Service Memoir 18, p. 39-46.
Miller, W.G.
1911: Notes on the Cobalt Area; Engineering and Mining Journal, Vol. 92, p. 645-649.
Poldevaart, A. and Hess, H.H.
1951: Pyroxenes in the Crystallization of Basaltic Magma; Journal of Geology, Vol. 59, p. 472-489.
Ritchey, J.L.
1980: Divergent Magmas of Crater Lake, Oregon: Products of Fractional Crystallization and Vertical Zoning in a Shallow, Water Under-Saturated Chamber; Journal of Volcanological and Geothermal Research, Vol. 7, p. 373-386.
Smith, R.L. and Bailey, R.A.
1966: The Bandalier Tuff: A Study of Ash-Flow Eruption Cycles from Zones Magma Chambers; Bulletin Volcanologique, Vol. 29, p. 83-104.
Streckiesen, A.
1976: To Each Plutonic Rock Its Proper Name; Earth Science Reviews, Vol. 12, p. 1-33.
Thomson, R.
1966: Geology of Henwood Township, District of Timiskaming; Ontario Department of Mines, Miscellaneous Paper 5, 48 p.
Turner, F.J. and Verhoogen, J.
1951: Igneous and Metamorphic Petrology; McGraw-Hill, New York, 602p.
Vander Walt, C.F.J.
1941: Chrome Ores of the Western Bushveld Complex; Geological Society of South Africa, Transactions, Vol. 44, p. 79-112.
Van Schmus, W.R.
1965: The Geochronology of the Blind River - Bruce Mines Area, Ontario, Canada; Journal of Geology, Vol. 73, p. 755-780.
Wager, L.R. and Brown, G.M.
1968: Layered Igneous Rocks; Oliver and Boyd, Edinburg, 588p.
Wager, L.A. and Derr, W.A.
1939: Geological Investigations in East Greenland, Part III, The Petrology of the Skaergaard Intrusion, Kanderdluqssuaq, East Greenland; Meddelelser on Greenland, Vol. 105, 352p.
Walker, F.
1940: Differentiation of the Palisade Diabase, New Jersey; Geological Society of America, Bulletin, Vol. 51, p. 1059-1106.
Walker, K.R.
1969: The Palisades Diabase, New Jersey: A Reinvestigation; Geological Society of America, Special Paper 111, 178p.
Walker, K.R., Ware, N.G., and Lovering, J.F.
1973: Compositional Variations in the Pyroxenes of the Differentiated Palisades Sill, New Jersey; Geological Society of America, Bulletin, Vol. 84, p. 89-110.
Willemse, J.
1969: The Geology of the Bushveld Complex, the Largest Repository of Magmatic Ore Deposits in the World; Economic Geology, Monograph 4, p. 1-22.
Wilson, J.R., Esbensen, K.H. and Thy, P.
1981: Igneous Petrology of the Synorogenic Fongen-Hyllingen Layered Basic Complex, South-Central Scandinavian Caledonides; Journal of Petrology, Vol. 22, p. 584-627.

Grant 49 Gold Exploration Potential Using Oxygen, Carbon, and Hydrogen Stable Isotope Systematics of Carbonatized Rock and Quartz Veins, Timmins Area

J.A. Fyon, H.P. Schwarcz, J.H. Crocket, and M. Knyf
Department of Geology, McMaster University

ABSTRACT

Oxygen-18 content of vein quartz and vein-hosted and replacement dolomites increases with increasing stratigraphic height in the volcanic pile. This trend possibly reflects buffering of the $\delta^{18}O$ of the metamorphic fluid, from which the vein quartz precipitated, by the host rock. Oxygen-18 exchange took place between the pre-metamorphic replacement dolomite and the metamorphic fluid. No correlation exists with gold tenor. The carbon isotope composition of the dolomites is very uniform in all deposits except those from the Hollinger Mine, which is also the richest gold deposit investigated. Hydrogen isotope variations in water derived from fluid inclusions suggest the presence of H_2 or CH_4.

Hydrogen isotope systematics may closely monitor the oxidation state of the hydrothermal fluid and hence, may be useful in gold exploration. Oxygen and carbon isotope systematics appear less useful in this regard.

INTRODUCTION

This paper reports on the continuation of stable isotope and field studies being carried out in the Timmins area (Fyon *et al.* 1981, 1980) to resolve the origin of the carbonate alteration and to establish the usefulness of stable isotopes of oxygen, hydrogen and carbon as exploration tools for gold mineralization in the Timmins area. The approach is to determine the stable isotope characteristics of the individual components of an altered and veined zone. For example, for quartz veins, we determine the $\delta^{18}O$ composition of the vein quartz and accompanying silicates, the $\delta^{18}O$ and $\delta^{13}C$ of the vein-hosted carbonates, and the δD and $\delta^{13}C$ compositions of water and CO_2 gas respectively which are trapped within fluid inclusions in the quartz veins. A similar set of isotopic data is obtained from the phases which comprise the altered rock in which the quartz vein was emplaced.

Changes in the isotopic and geochemical characteristics of the altered rocks and accompanying veins reflect complex changes in the chemical constitution of the hydrothermal fluid and the conditions of phase precipitation. It is conceivable, then, that by studying these isotopic characteristics of the vein and alteration system, criteria might be identified which would permit discrimination between vein systems which are auriferous and those which are barren. This assumes, of course, that there has been no post-precipitation isotopic exchange during later, superimposed hydrothermal events or during cooling of hydrothermal systems.

A number of mining properties have been studied to date (Figure 1). They have been subdivided on the basis of their past gold production into prospects (those having no previous gold production or established gold reserves), and producers (those which have produced gold or have proven gold reserves). This does not mean that the prospects have no future potential, but rather, that no proven gold reserves have yet been developed.

STABLE ISOTOPE SYSTEMATICS

VEIN-HOSTED AND REPLACEMENT DOLOMITES

Illustrated in Figure 2 are the oxygen and carbon isotopic compositions of the vein-hosted and replacement dolomites. Only data from dolomitic alteration zones in basaltic rocks are included. Stable isotope data for calcite, present in alteration assemblages outside the dolomite zone,

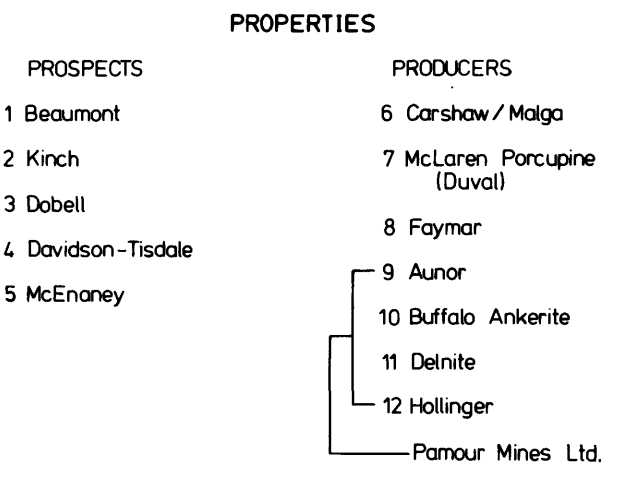

Figure 1. *Mining properties which have been included in the stable isotopic study to date (1981).*

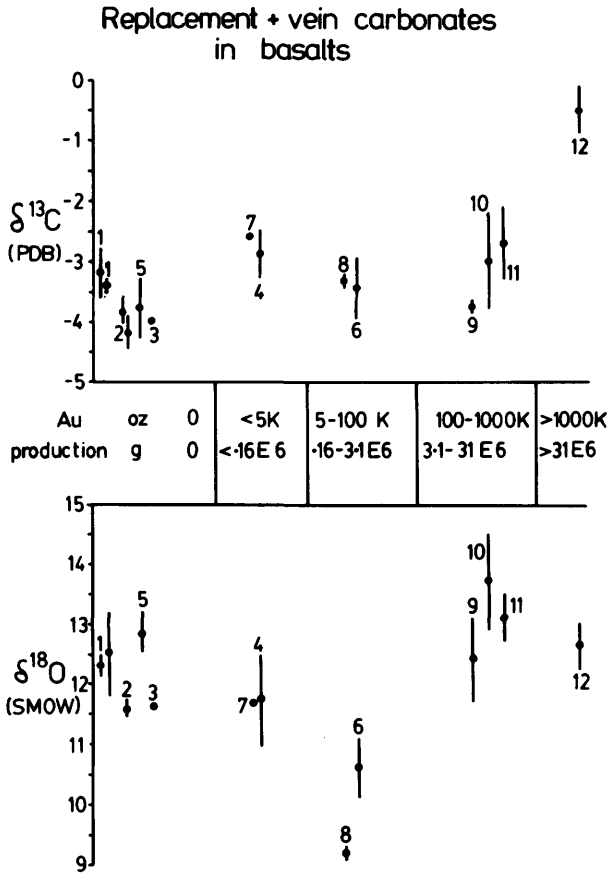

Figure 2. *Carbon and oxygen isotope compositions of vein-hosted carbonates and replacement dolomites, indexed against property gold production. Sample numbers refer to properties listed in Figure 1. E6 = 1,000,000; K = 1000.*

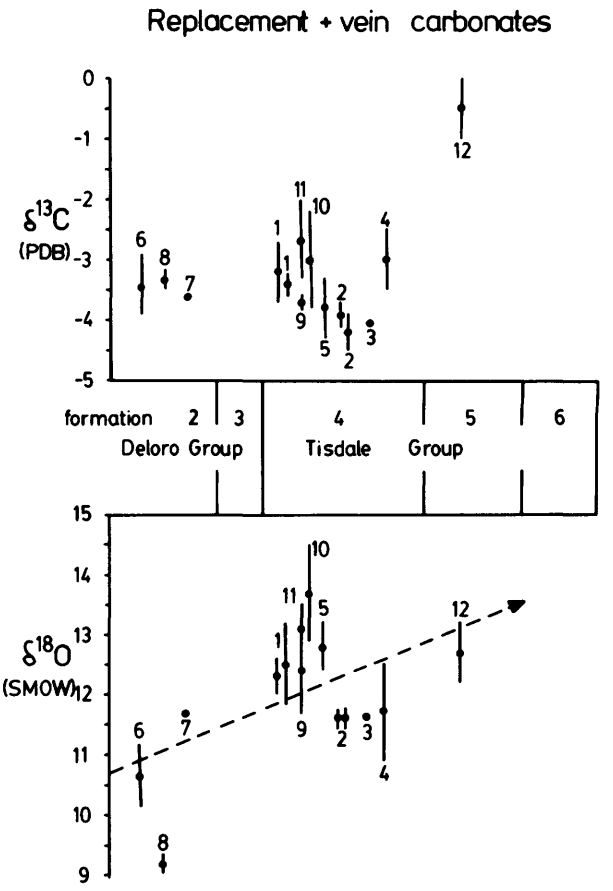

Figure 3. *Carbon and oxygen isotope compositions of vein-hosted carbonates and replacement dolomites, indexed against stratigraphic position. Sample numbers refer to properties listed in Figure 1.*

have been discussed by Fyon *et al.* (1981) and will not be considered here. The isotopic data are indexed against an arbitrary scale representing the approximate gold production or reserves from each property. The following observations may be made:

(1) $\delta^{13}C$ of the carbonates appears to be uniform over all properties and therefore is independent of gold production or reserves. An exception to this trend is the sample suite from the Hollinger Mine which is distinctly richer in both ^{13}C and gold.

(2) $\delta^{18}O$ of the carbonates is also independent of gold tenor although there is more scatter of data.

Hence, to a first approximation, neither $\delta^{18}O$ nor $\delta^{13}C$ compositions of the vein-hosted and replacement dolomites appears to reflect the gold tenor of a property.

By plotting these same data as a function of stratigraphic position within the volcanic pile (Figure 3), it is apparent that $\delta^{18}O$ composition of the carbonates shows a general increase with stratigraphic height. No such correlation exists for the $\delta^{13}C$ compositions of the carbonates which occur in the Deloro Group and lower part of the Tisdale Group. Note however, that the Hollinger, which is stratigraphically the highest deposit, is also the most enriched in in $\delta^{13}C$.

VEIN QUARTZ

Illustrated in Figure 4 are the $\delta^{18}O$ values of vein quartz, indexed against the property gold production in the top diagram and against stratigraphic height in the bottom diagram. With the exception of the Hollinger Mine suite, there is a general decrease in $\delta^{18}O$ of the vein quartz with increasing property gold tenor. The properties with the lightest $\delta^{18}O$ values of vein quartz also lie lowest in the stratigraphy (Figure 4). A similar correlation between stra-

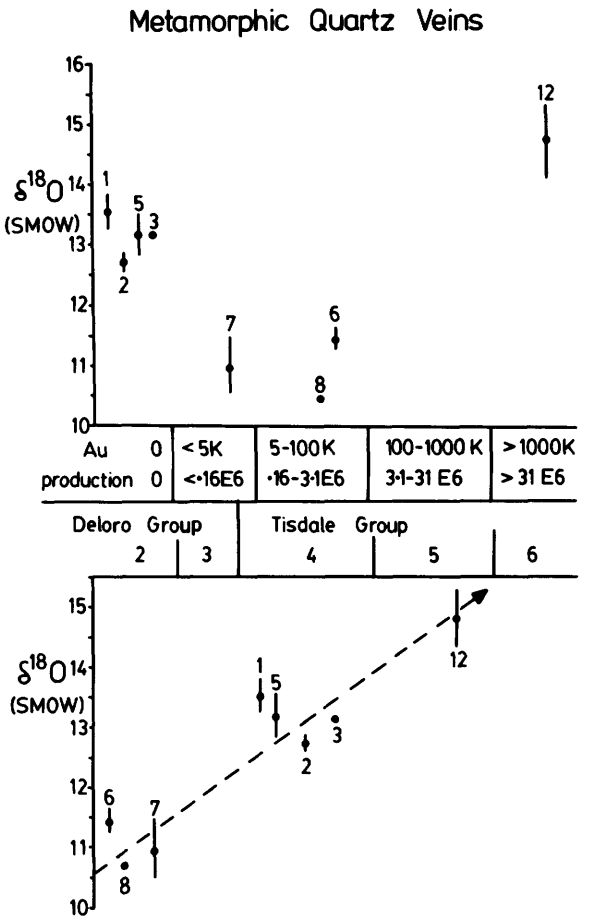

Figure 4. *Oxygen isotope composition of vein quartz indexed against both property production and stratigraphic position. Sample numbers refer to properties listed in Figure 1. E6 = 1,000,000 g; K = 1000 ounces.*

tigraphic height and $\delta^{18}O$ in the whole rock composition was previously noted by Beaty (1980), who attributed this covariation to decreasing reaction temperatures between a seawater-derived hydrothermal fluid and the rock.

FLUID INCLUSIONS

Illustrated in Figure 5 are δD analyses of fluid inclusions within the quartz veins. Only the range of data is indicated and the data are indexed against the property gold production and stratigraphic height. For individual properties, the range of data varies from about 5 ‰ on the McEnaney to 50 ‰ for the Faymar. These data suggest that δD of fluid inclusions may not be a useful tool to discriminate between barren and auriferous quartz veins. Nor does there appear to be any correlation between δD of the fluid and stratigraphic position of the vein.

The large range of δD analyses (Figure 5) is of some interest. One might ask whether this reflects a mixing of light and heavy fluids or if some other process is at work. Illustrated in Figure 6 are the δD values of the fluid inclusions, plotted against the calculated $\delta^{18}O$ composition of the fluid from which the quartz vein precipitated. Two arbitrary temperatures were used for this calculation: 350°C and 450°C. The indicated fields on Figure 6 correspond to those empirically determined or observed for juvenile water, metamorphic water and seawater.

It would be tempting to interpret the observed δD variations in terms of fluid mixing between seawater (δD = 0) and metamorphic or juvenile water. However, such cannot be the case because fluid mixing would certainly involve shifts in both δD and $\delta^{18}O$ compositions of the mixture and this is not observed in the limited data suite. What is required then is a process that would induce changes in the δD compositions of the water, but would have little if any effect on the $\delta^{18}O$ of the water. Such an effect can be achieved if either H_2 or CH_4 (methane) is present in the hydrothermal fluid (Figure 7). If we start with an initial δD water of -65 ‰ (juvenile or metamorphic), we can achieve δD water compositions as heavy as 0 ‰, if as little as 10-15 mole percent H_2 is present. The effects are less dramatic if CH_4 (methane) is present. We are presently quantitatively determining the volatile species in the fluid inclusions.

If the large range of δD of fluid inclusions reflects changes in the fluid chemistry, notably the presence of variable proportions of either H_2 or CH_4, this could be of significance for exploration in that changes of the fluid redox state might have a significant effect on the fluid's ability to transport gold.

DISCUSSION

CARBON ISOTOPES

The gold deposits of the Timmins area differ both in type and size (Fryer *et al.* 1979; Karvinen 1981) and it would not be surprising to find significant differences in $\delta^{13}C$ between deposits. However, with the exception of the Hollinger Mine suite, the $\delta^{13}C$ of the replacement dolomites is remarkably uniform, showing less than 2 ‰ variation over a wide range of stratigraphic height, size of deposit, and associated gold tenor.

The Hollinger Mine is unusual not only in terms of the carbon and oxygen isotope compositions of the replacement and vein dolomites, but also in the variety of deposit types: stratiform cherty dolomitic exhalite, quartz-carbonate veins, stratabound pyritic "flow-ore", and stratiform pyritic graphitic units. These ores are hosted within Mg-tholeiitic basalts at the top of Formation III, Tisdale Group, and in Fe-tholeiites of Formation IV, and occur in proximity to large bodies of schistose quartz-feldspar porphyry. Deformation in this area is intense.

The Hollinger Mine sample suite was collected from the pyritic "flow-ore" and graphitic ore whereas the sample suites for the other properties considered in this study represent barren carbonate alteration zones and carbonatized rock associated with quartz vein and cherty

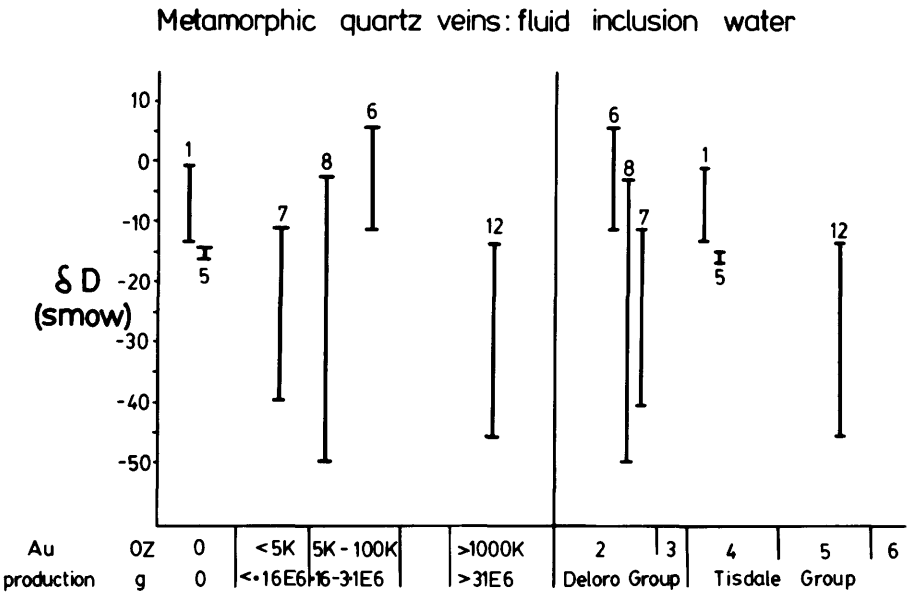

Figure 5. *Hydrogen isotope composition of fluid inclusion water hosted in vein quartz, indexed against property production and stratigraphic height. Sample numbers refer to properties listed in Figure 1. E6 = 1,000,000; K = 1000.*

dolomite mineralization. Presently, it is not known if the distinct isotopic signature of the Hollinger replacement carbonates reflects the different habit of associated gold mineralization at this site or if the structural-stratigraphic setting of Hollinger influenced the alteration process in such a way as to impart significantly different oxygen and carbon isotopic signatures to the replacement carbonates.

Additional samples from the McIntyre and Hollinger Mines are being analysed to determine if an isotope gradient exists in the replacement carbonates across the transition from Formation IV to Formation V of the Tisdale Group.

The $^{13}C/^{12}C$ ratios of hydrothermal carbonates depend critically on the pH, oxidation state, and isotopic composition of the hydrothermal fluid ($\delta^{13}C_{\Sigma}$) (Sakai 1968; Ohmoto 1972). The striking uniformity of the $\delta^{13}C$ of the hydrothermal dolomites from the Timmins area contrasts with the systematic increase in $\delta^{18}O$ of both the carbonates and vein quartz with increasing stratigraphic height of the samples. This suggests that all these occurrences of carbonatized metavolcanics were formed under essentially identical conditions in the presence of a fluid having a very uniform carbon isotopic composition. While it is possible that this fluid might have contained a mixture of seawater and mantle- or metamorphic-derived carbon, it seems fortuitous that the proportions of these components were so well regulated by the mixing process as to produce a constant $\delta^{13}C$ in the resultant carbonates. We would therefore surmise that the hydrothermal carbon was dominantly from one source, either directly from the mantle or from dehydration of carbonate-bearing volcanic and sedimentary rocks during burial metamorphism, as suggested by Kerrich and Fyfe (1981).

A critical appraisal of mantle and metamorphic carbon sources will be presented elsewhere; however, neither of these simple systems adequately accomodate the observed $\delta^{13}C$ relationships observed in the altered rocks from the Timmins area. For a mantle derived CO_2 gas, having a $\delta^{13}C$ of -7 ‰ (PDB), reaction temperatures as low as 100°C are required to produce replacement dolomite having a $\delta^{13}C$ of -3.5 ‰. Alternatively, simple decarbonatization of volcanic rock containing calcite having a $\delta^{13}C$ of 0 to -2 ‰ (PDB)(recycled marine carbonate), would produce pure CO_2 gas having a $\delta^{13}C$ of +3 to +1 ‰ (Bottinga 1968; Shieh and Taylor 1969). Such a gas would have to react with the volcanic rocks at temperatures exceeding 500°C to produce the observed -3.5 ‰ $\delta^{13}C$ in the replacement dolomite. Such high reaction temperatures are untenable in light of the mineralogy of the alteration assemblages (Fyon and Crocket 1981; Fyon *et al.* 1980). Thus, although simple metamorphic derivation of CO_2 gas is intuitively reasonable, it is difficult to reconcile with the available stable isotope data. However, buffering of a C-O-H-bearing metamorphic fluid by CH_4, CO or C (graphite), a more realistic metamorphic system, would produce isotope effects different from those expected by simple decarbonatization yielding pure CO_2. Such effects are presently being considered in light of the δD analyses.

OXYGEN ISOTOPES

In view of the uniformity of $\delta^{13}C$, it is surprising that the $\delta^{18}O$ of the carbonates and vein quartz varies so markedly (see Figure 2). It had been previously noted that $\delta^{18}O$ of whole rock samples increases with increasing stratigraphic height and this covariation was attributed to decreasing reaction temperatures between a seawater-derived hydrothermal fluid and the volcanic rock (Beaty 1980). That metamorphic quartz veins show the same $\delta^{18}O$ trend, suggesting that the $\delta^{18}O$ of the metamorphic fluid, from which the quartz veins precipitated, was buffered by the $\delta^{18}O$ of the country rock. Now, it has been argued that field relationships suggest that much, although not all, pervasive carbonate alteration predated the regional metamorphism and deformation of the volcanic pile (Fyon and Crocket 1981; Fyon *et al.* 1981). It follows that the increasing $\delta^{18}O$ of the replacement carbonates might reflect widespread oxygen isotope exchange between the carbonates and the metamorphic pore fluid. Such exchange was documented on the Gowganda Resources Limited's iron formation-hosted gold deposit southeast of Timmins (Fyon *et al.* 1981).

It should be noted that increasing $\delta^{18}O$ of quartz can also be accomplished by decreasing the precipitation temperature from a metamorphic fluid having a uniform $\delta^{18}O$. However, not all the $\delta^{18}O$ variation of the vein quartz can be attributed to temperature effects; precipitation temperatures required for the +10.5 ‰ $\delta^{18}O$ of vein quartz in the Deloro Group would have exceeded 650°C, assuming a $\delta^{18}O$ of +11 ‰ for the metamorphic fluid as calculated by Kerrich and Fryer (1979).

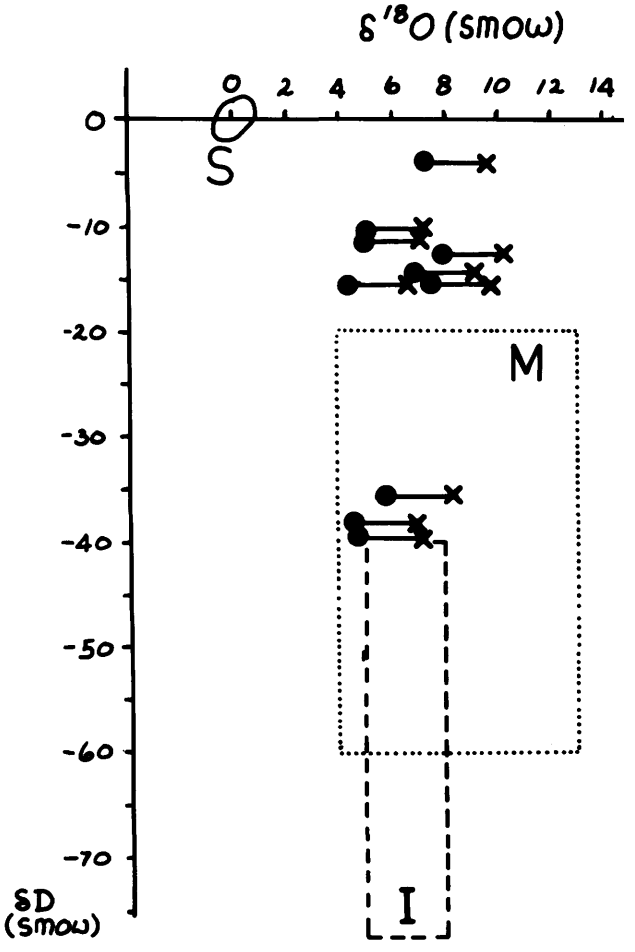

Figure 6. *Hydrogen isotope composition of fluid inclusion water plotted against the calculated oxygen isotope composition of the water which precipitated the quartz host. Calculations carried out at 350°C (•) and 450°C (x). The outline fields S, M, and I correspond to the observed seawater range (modern and inferred Archean sea water), the calculated field for metamorphic water and the empirically deduced field for juvenile or igneous water.*

CONCLUSIONS

The following preliminary conclusions can be made regarding the carbon and oxygen isotope systematics of replacement dolomite and vein quartz in the Timmins area:

(1) $\delta^{18}O$ of vein quartz and vein-hosted and replacement dolomites increases with increasing stratigraphic height in the volcanic pile. This is attributed to buffering, by the volcanic rock, of the $\delta^{18}O$ of the metamorphic fluid from which the quartz veins precipitated and to oxygen isotope exchange between the metamorphic fluid and the replacement dolomites which predate regional metamorphism.

(2) $\delta^{13}C$ of replacement and vein carbonates is very uniform and constant in all but one of the mining properties studied; the single exception, the Hollinger Mine, is significantly enriched in $\delta^{13}C$. It is also distinctly richer in gold. The uniformity of $\delta^{13}C$ suggests that the rocks underlying all the properties were carbonatized under very similar conditions and that a large uniform hydrothermal carbon reservoir was available. The source of this hydrothermal carbon remains unresolved, although it is unlikely to be a first generation, simple mixture involving seawater carbon. Marine carbon or mantle carbon, recycled by a complex metamorphic decarbonatization process, is a possible source, but constraints on the process are unknown.

(3) Very large variations are observed in δD of water from fluid inclusions. These variations could be explained by the presence of H_2 or CH_4 in the hydrothermal fluid. This aspect is very intriguing for it suggests that the hydrothermal fluids, responsible for the quartz vein precipitation, had variable redox states. Such fluid redox variations might have profoundly affected the transport-precipitation characteristics of the gold ligands. This avenue is presently being investigated.

(4) Neither the oxygen nor carbon isotopic systematics of the replacement dolomites and vein quartz appears to reflect the gold tenor of a property.

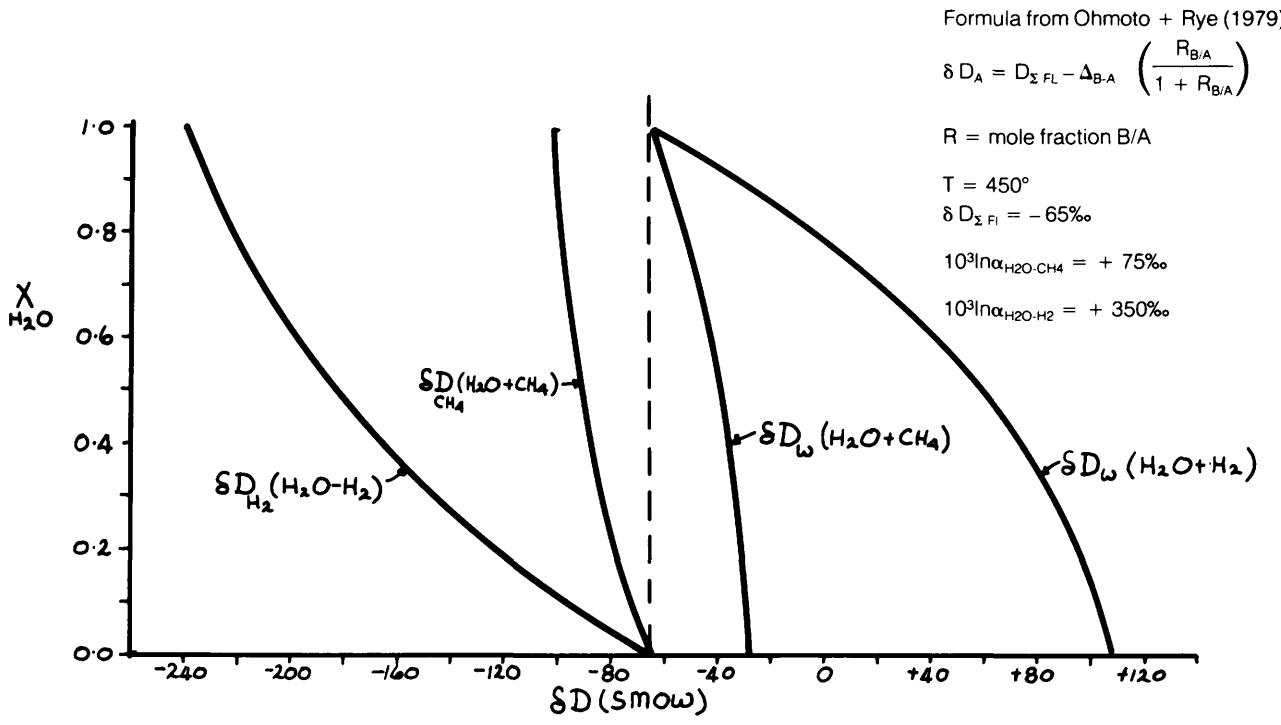

Figure 7. *Effect of a methane (CH_4) or hydrogen (H_2) mixture with water on the hydrogen isotope compositions of the coexisting water.*

REFERENCES

Beaty, D.W.
1980: The Oxygen Isotope Geochemistry of the Abitibi Greenstone Belt; Unpublished Ph.D. Thesis, California Institue of Technology, Part II.

Bottinga, Y.
1968: Calculation of Fractionation Factors for Carbon and Oxygen Isotope Exchange in the System Calcite — Carbon Dioxide — Water; Journal of Physical Chemistry, Vol. 72, p. 800-808.

Fryer, B.J., Kerrich, R., Hutchinson, R.W., Peirce, M.G. and Rogers, D.S.
1979: Archean Precious-Metal Hydrothermal Systems, Dome Mine, Abitibi Greenstone Belt, 1. Patterns of Alteration and Metal Distribution; Canadian Journal of Earth Sciences, Vol. 16, p. 421439.

Fyon, J.A. and Crocket, J.H.
1981: Volcanic Environment of Carbonate Alteration and Stratiform Gold Mineralization, Timmins Area; p. 47-58 in Genesis of Archean, Volcanic-Hosted Gold Deposits, Symposium held at the University of Waterloo, March 7, 1980, Ontario Geological Survey, Miscellaneous Paper 97, 175p.

Fyon, J.A., Crocket, J.H., Schwarcz, H.P., Kabir, A., and Knyfe, M.
1981: Trace Element and Stable Isotope Geochemistry of Auriferous Iron Formations in the Timmins Area; Grant 49, p. 90-107 in Geoscience Research Grant Program, Summary of Research, 1980-1981, edited by E.G. Pye, Ontario Geological Survey. Miscellaneous Paper 98, 340p.

Fyon, J.A., Schwarcz, H.P., and Crocket J.H.
1980: Carbon and Oxygen Isotope Geochemistry of Replacement Carbonates from the Timmins-Porcupine Gold Camp; Grant 49, p. 72-82 in Geoscience Research Grant Program, Summary of Research, 1979-1980, edited by E.G. Pye, Ontario Geological Survey, Miscellaneous Paper 93, 262p.

Karvinen, W.O.
1981: Geology and Evolution of Gold Deposits, Timmins Area, Ontario; p. 29-46 in Genesis of Archean, Volcanic-Hosted Gold Deposits, Symposium held at the University of Waterloo, March 7, 1980, Ontario Geological Survey, Miscellaneous Paper 97, 175p.

Kerrich, R. and Fryer, B.J.
1979: Archean Precious Metal Hydrothermal Systems, Dome Mine, Abitibi Greenstone Belt. II. REE and Oxygen Isotope Relations; Canadian Journal of Earth Science, Vol. 16, p. 440-458.

Kerrich, R. and Fyfe, W.S.
1981: The Gold-Carbonate Association: Source of CO_2 and CO_2-Fixation Reactions in Archean Lode Deposits; Chemical Geology, Vol. 33, p. 265-294.

Ohmoto, H.
1972: Systematics of Sulfur and Carbon Isotopes in Hydrothermal Ore Deposits; Economic Geology, Vol. 67, No. 5, p. 551-578.

Ohmoto, H. and Rye, R.O.
1979: Isotopes of Sulfur and Carbon; p. 509-567 in Geochemistry of Hydrothermal Ore Deposits, 2nd edition, edited by H.L. Barnes, J. Wiley and Sons, New York, 798p.

Sakai, H.
1968: Isotopic Properties of Sulfur Compounds in Nature; Geochimica Cosmochimica Acta, Vol. 12, p. 150-169.

Shieh, Y.N., and Taylor, H.P.
1969: Oxygen and Carbon Isotope Studies of Contact Metamorphism of Carbonate Rocks; Journal of Petrology, Vol. 10, p. 307-331.

Grant 76 Speciation of Free Gold in Glacial Overburden

D.L. Guindon and I. Nichol
Department of Geology, Queen's University

ABSTRACT

The investigation is designed to (1) test the hypothesis that the pattern of trace element concentrations in gold grains is characteristic of the deposit-type in which the gold is located, (2) determine if gold grains in the overburden exhibit the same characteristic patterns, and (3) evaluate the feasibility of using these patterns as an exploration guide by determining the provenance of gold in overburden.

Trace element concentration patterns were established for Cu, Hg, Pb, Pd, and Fe by electron microprobe analysis. Other elements were generally below the instrumental detection limit.

Samples have been classified into ten deposit-types based on a combination of vein mineralogy and host rock type. Discriminant analysis is used to determine the minimum number of elements required to identify Au according to deposit-type. Although no relationship has been found to exist between the trace elements in the gold and in associated vein samples, there is a relationship with the host rock type. Gold grains from ultramafic host rocks have higher concentrations of Hg and Cu than gold grains from mafic rocks. Gold grains from felsic to intermediate host rock sources have lower Hg and Cu and higher Pb concentrations than the gold from ultramafic host rocks. Gold grains from mafic host rocks can be distinguished from those in felsic to intermediate rocks by their lower Cu concentrations. Once the host rock type has been determined, the gold can be further classified according to deposit-type using the characteristic pattern of trace element concentrations. Calculation of discriminant scores shows that approximately 72 percent of the samples were correctly classified according to host rock and, of these, 75 to 80 percent are correctly classified according to deposit-type.

Analysis of gold grains, obtained from tills over the Martin Bird property, suggests that the gold grains maintain their characteristic pattern of trace element concentrations in overburden. The trace element composition of gold grains from a sample collected on the Munro Esker, near East Ford Lake, indicates that three deposit-types may have supplied the gold grains.

Further analyses are required to support the present findings, and to fully evaluate the feasibility of using trace element patterns to determine the provenance of gold in overburden.

INTRODUCTION

This work reported in this paper is a continuation of that described last year (Guindon and Nichol 1981). It was established that gold in the Abitibi "greenstone" belt occurs in a number of deposit-types, based on mineralogy, and that the trace element concentrations associated with the gold can be used to identify gold according to deposit-type. Variations in the trace element chemistry of gold may be related to the concentration of Ag and minor elements in the ore fields, the mineralogy of the vein material, or the nature of the wallrock.

METHOD OF INVESTIGATION

Samples from present and past producing mines and prospects were collected and classified into deposit-types based on their "vein" mineralogy. It was assumed that differences in the vein mineralogy would be reflected in the levels of trace elements associated with the gold. The following deposits-types were defined: quartz, quartz-carbonate, quartz-green carbonate (fuchsite), quartz-albite, disseminated pyrite in mafic metavolcanics, massive sulphide (pyrite), graphite and sericite schist.

In the first phase of the program, as many deposit-types as possible were sampled, to establish variations between different deposit-types within an area, and then to establish variations between different deposits of the same deposit type. In the second phase of the program, the variation in trace element chemistry for gold within the same deposit-type was examined. An investigation was also made to determine if gold obtained from overburden retained a characteristic pattern of trace element concentrations.

Overburden samples approximately 0.03 m^3 (1 cubic foot) in volume, were collected from the tills overlying the Martin Bird prospect south of Larder Lake. The samples were collected just above bedrock at 30 m (100 foot) stations along a line trending approximately north, starting about 60 m north of the main vein. A large bulk sample was collected on the Munro Esker near East Ford Lake. In this area, up to 30 gold grains per cubic foot (0.03 m^3) had previously been noted (Assessment Files Research Office, Ontario Geological Survey, Toronto, file 63a.467). The source of this gold is unknown but it was of interest to determine if there were several sources and what its trace element characteristics are.

Gold grains were located and marked in polished sections of hand samples. It was suspected that the top

microlayer of the gold would be affected by smearing and inclusions entrapped by polishing. A simple test, described last year (Guindon and Nichol 1981), confirmed the need for further preparation. Samples for analysis by electron microprobe are commonly prepared as polished sections or thin sections. Since most analyses are performed to determine concentrations of major and minor elements (> 0.1 weight percent), the problems of secondary fluorescence are generally minor. When dealing with trace quantities of elements, there are problems. The Fe content of very small grains of gold, which occur as inclusions in pyrite, was extremely high (up to 10 percent) whereas gold away from pyrite was found to have very much lower concentrations of Fe (generally > 0.1 weight percent). If the secondary fluorescence causes an increase in measured concentration, then it is possible that the concentrations of other elements may be affected by other minerals in the samples.

Another problem encountered in the preparation of polished sections is associated with the natural distribution of gold in a sample. To overcome the paucity of gold in host rock samples, a technique of crushing the samples and concentrating the gold grains was devised. This also had the benefit of eliminating most of the minerals that could cause secondary fluorescence, and thus improving the quality of analyses. Bedrock samples were crushed using a jaw crusher, and particle size was further reduced to –500 μm using a disk mill with steel plates. The –500 μm fraction was then superpanned. The gold grains concentrated at the tip of the heavy mineral train were then removed with an eye dropper and mounted in epoxy resin in 2.5 cm diameter glass disks. (The choice of the glass disks was based on convenience. This size allowed six disks to be loaded in the probe at one time.) After the epoxy set, the mount was ground to expose the gold grains and then polished with alumina powder. Disks with the gold grains were etched and carbon coated for analysis. A 25 g split of the crushed rock was taken and pulverized in a shatter box for later use in atomic absorption analysis.

Two analytical techniques were employed. All of the trace element concentrations in gold grains were determined by electron microprobe. Atomic absorption spectroscopy was used to analyse vein material.

Conditions of analyses are as reported in Guindon and Nichol (1981). In addition to Cu, Pb, Pd, Hg, and Fe, attempts were made to detect Te, W, Ti, Bi, and Sn in the gold. Hansen (1958, *in* Gay 1963) has shown that the maximum solubility of Te in gold is 60 ppm, well below the detection limits for the probe. X-ray images of gold grains that contained analytically detectable Te, showed that it occurs as inclusions in the gold. Since Te occurs as inclusions in the gold and is only inconsistently detected, it was deleted from the analytical scheme. The other elements, W, Ti, and Bi, were not detected in the samples analysed and were also omitted.

Forty-five vein samples were prepared for analysis by atomic absorption spectroscopy. Samples weighing 250 mg were dissolved using nitric-perchlorite-hydrofluoric acid digestion. The solution was evaporated to dryness and leached with a 10 percent hydrochloric acid solution. Elemental concentrations were determined using an IL-250 atomic absorption spectrometer.

TRACE ELEMENT COMPOSITION OF GOLD GRAINS

The National Bureau of Standards (NBS) gold-silver wire electron microprobe standards were used to calculate background values for the trace elements. The minimum value, maximum value, mean and standard deviation for each of the trace elements in the NBS goldsilver wires are listed in Table 1. As reported in Guindon and Nichol (1981), background corrections for the trace elements vary approximately linearly with fineness. Allowance was made for the slight curvature in background with these corrections using multiple linear regression, thus setting the mean values for the concentration of all the trace elements in the NBS standards to zero. It is not known if the concentrations of the trace elements in the NBS standards are zero but this assumption allows for a comparison with all other electron microprobe results. After the corrected values were obtained, univariate statistics were calculated for each sample. If the average concentration for an element was found to be greater than the standard deviation for that element in NBS gold-silver wires, then that element was considered to be present. These calculations were only made on the analyses of gold in grain mounts where the contributions from secondary fluorescence would be minimal. The only trace elements detected in the gold were Cu, Hg, Pb, Pd, and Fe. Guindon and Nichol (1981) suggested that Zn and As were important in identifying gold from different deposit-types. Zn and As were not detected in analyses of gold grains from host rocks, although As is present in amounts up to 1.0 weight percent in analyses of native silver from the Ross Mine; thus it must be assumed that the As and

Table 1. *Trace element statistical parameters (top) and fineness (bottom) of NBS gold-silver wire series.*

Element	N	Min	Max	Mean	Std. Dev.
Cu	163	-.027	.023	.000	.008
Ni	163	-.017	.015	.000	.005
Hs	163	-.048	.039	.000	.020
Pb	163	-.042	.039	.000	.015
Pd	163	-.030	.025	.000	.010
Pt	163	-.043	.037	.000	.016
Zn	163	-.030	.052	.000	.014
As	163	-.051	.039	.000	.014
Fe	163	-.016	.015	.000	.004
Recom'd Fineness	**N**	**Min**	**Max**	**Mean**	**Std. Dev.**
0	30	-.200	.300	.043	.143
224	25	215	240	226.8	5.85
400	25	393	441	403.8	9.35
600	26	596	612	605.0	4.97
800	26	798	809	805.1	3.14
1000	31	999	1000	1000	.18

Zn previously detected were due to secondary fluorescence.

The ranges in concentrations of trace elements for the majority of samples are Cu 0.040 to 0.170 percent, Hg 0.050 to 0.700 percent, Pb 0.050 to 0.100 percent, Pd 0.050 to 0.070 percent, and Fe 0.020 to 0.100 percent. Samples with concentrations of Cu > 0.200 weight percent, Pb > 0.100 percent, Pd > 0.100 percent or Fe > 0.100 percent are suspected to contain inclusions of pyrite, chalcopyrite or a lead mineral such as galena or altaite. No samples contained Pd > 0.100 percent. It is possible that some samples contain inclusions of Hg minerals, such as coloradoite, but they are less easily identified.

Table 1 also lists the statistical parameters for the fineness of each of the gold-silver wires. These results show that the mean fineness for each of the NBS gold-silver wires is approximately 1 percent high, but that the corrected concentrations are acceptable.

Analyses of unknowns were obtained at two different times, April, 1981, and February, 1982. Gold grains from the first batch of samples were analyzed mainly in polished sections of host rock, whereas the second set were in the form of grain mounts. Comparison of results for gold grains from the sample deposit and from the deposit-type showed very similar trace element concentration patterns. Large variations did exist for the small gold grains found as inclusions in pyrite or in contact with chalcopyrite. These grains had previously been suspected of causing secondary fluorescence interference problems. The analytical precision for a single grain may not be as good as expected, but the reproducibility over time suggests that analytical conditions can be reproduced.

CLASSIFICATION OF DEPOSIT-TYPES AND THEIR TRACE ELEMENT CHEMISTRY

Results suggest that there are differences in the pattern of trace element concentrations for gold from mines of one deposit-type at different locations, as well as for different deposit-types. Classification on the basis of deposit-type alone would result in an excessive number of categories of deposit-type, making classification of gold grains on the basis of trace elements difficult. A new method for classification of samples was required. Using Gay's (1964) suggestion that wall rock may also affect the trace element composition of gold, a system of classification using both host rock and vein associations was devised. The resulting classification scheme uses 10 groups of associations. The range, mean and standard deviation for the trace elements, for each of the deposit-types, are presented in Table 2. Two sets of statistical parameters are given for the category "all mines" in each deposit-type. The first set includes all analyses and the second includes analyses considered unaffected by secondary fluorescence. The second set of analyses were used to calculate the discriminant functions discussed below.

Using the new classification, discriminant analysis was performed on pairs of groups to determine what differences exist in their trace element chemistry and to what degree the groups can be separated. The results, along with the elements providing the discrimination, are listed in Table 3. Discrimination between groups generally gives greater than 70 percent correct classifications, suggesting that significant differences in trace element chemistry do exist. The major drawback to this scheme is that 45 discriminant functions are required to differentiate between all possible pairs of deposit types. The probability is low that any one analysis will be correctly classified into the right group for each of the nine functions required to separate one deposit-type from the other nine. If the discriminant scores do not indicate that a sample or analysis definitely belongs to one group, it is difficult to determine a correct classification. With an output of 45 scores per sample, just the number of scores makes interpretation difficult. Thus, a method to reduce the number of groupings was required, and it was decided to determine if there were differences in the trace element patterns of the gold grains, based on host rock alone.

DISCRIMINATION OF DEPOSIT-TYPES

All analyses of gold grains from similar host rocks were grouped and discriminant analysis was performed to determine if differences existed. The results indicate that gold grains from ultramafic host rocks contain the highest concentrations of Hg and Cu but lower concentrations of Pb. Gold grains from mafic host rocks contain the lowest concentrations of Hg and Cu, and the gold grains from felsic to intermediate host rocks generally contain intermediate levels. Figures 1 to 4 show the concentrations of the elements in two dimensional plots, and the lines of best separation as determined by discriminant analysis. This information allowed a hierarchal system of classification to be developed. Two two-dimensional plots are required to show the discrimination between the ultramafic and intermediate to felsic groups because the discrimination is based on Pb, Hg and Cu (Figures 3 and 4). A flow sheet showing the host rock system of classification used is presented in Figure 5. The listing of results and the plotting of the two element diagrams showed that modifications were required, because descriminant analysis shows the best straight line or plane to separate two groups. The modifications are shown in Figure 5. The use of curved lines or planes may be more suitable at times, to obtain better separation. The diagrams (Figure 1 to 4) show where the line or plane of separation needs modification and the modifications are indicated in Figure 5.

It can be seen in Figures 2 to 4 that, there is a break in the concentration of Hg for gold grains from mafic and felsic to intermediate source rocks: the majority of the grains contain Hg in concentrations below 0.250 percent, and most of the remainder contain more than 0.340 percent. It is proposed that some of the analyses above 0.340 percent contain inclusions of coloradoite in the gold. Many of these grains are from the Kirkland Lake

Table 2. *Statistical parameters for trace element concentrations and fineness (Au/(Au + Ag) x 1000) for the deposit-types and each sample classified in the deposit-type. The data is arranged in the following manner:*

minimum maximum
mean standard deviation

Two sets of parameters are given for the "all mines" category. The first set is for all analyses and the second is for only those analyses considered unaffected by secondary fluorescence. All analyses in the deposit-type "felsic-intermediate-felsite" were affected by secondary fluorescence. Samples containing less than 0.2 weight percent Cu were used to calculate discriminant functions but Fe was not included in the calculations.

ULTRA MAFIC - QUARTZ - GREEN CARBONATE

SAMPLE	N	Cu		Hg		Pb		Pd		Fe		Fin	
All Mines	113	.019	.538	.054	.651	−.026	.551	−.045	.061	−.018	.365	941	952
		.102	.074	.301	.162	.014	.056	.001	.020	.032	.062	945.9	2.3
	96	.019	.145	.054	.644	−.026	.082	−.045	.061	−.010	.080	941	952
		.085	.025	.290	.159	.008	.022	.000	.020	.017	.020	946.0	2.4
Kerr Addis-4	14	.074	.538	.397	.489	−.005	.551	−.017	.061	−.018	.043	944	949
		.151	.117	.446	.026	.083	.138	.025	.023	.018	.021	945.6	1.3
Kerr Addis-7	4	.057	.117	.200	.570	−.002	.041	−.002	.028	.136	.318	946	947
		.074	.029	.446	.178	.023	.019	.014	.013	.248	.082	946.5	0.6
Kerr Addis-8	14	.019	.114	.506	.651	−.008	.036	−.003	.026	.017	.218	946	949
		.076	.023	.587	.038	.016	.013	.016	.009	.057	.054	947.0	0.9
Kerr Addis-11	56	.031	.459	.140	.245	−.026	.025	−.031	.043	−.004	.365	941	947
		.099	.083	.206	.024	−.002	.013	−.007	.012	.018	.057	949.9	1.3
Martin Bird-0	10	.071	.132	.296	.390	−.021	.027	−.045	−.006	.016	.100	943	946
		.089	.016	.336	.029	−.007	.013	−.024	.014	.032	.024	944.0	0.9
Davey Lowe-2	12	.094	.122	.054	.127	−.009	.021	−.012	.016	−.004	.011	950	952
		.111	.008	.091	.020	.009	.003	.004	.008	.005	.005	951.2	0.6

MAFIC - QUARTZ VEIN

All Mines	198	−.030	.161	−.024	.162	−.041	1.805	−.042	.034	−.015	.625	675	957
		.027	.027	.057	.032	.024	.129	−.002	.015	.016	.056	876.7	74
	186	−.030	.142	−.024	.162	−.041	.098	−.042	.034	−.015	.089	675	957
		.026	.026	.057	.033	.014	.023	−.002	.016	.006	.016	876.9	74
Ross-3	1		.034		.032		.007		−.015		.326		710
Ross-5	1		.003		.006		.007		.017		.000		761
Ross-8	40	−.009	.161	−.024	.103	−.041	.041	−.029	.034	−.007	.124	675	759
		.017	.035	.048	.004	.009	.017	.018	.013	.005	.021	738.8	18
McIntyre -0	22	−.030	.026	.033	.092	.011	.098	−.028	.010	−.015	.625	899	901
		.000	.018	.059	.014	.052	.022	−.014	.011	.034	.136	899.9	0.8
McIntyre -1	5	.027	.039	.001	.057	−.001	.061	−.021	.002	−.007	.127	934	936
		.034	.005	.033	.023	.029	.028	−.006	.009	.021	.059	934.8	0.8
Holling -0	29	−.011	.074	−.005	.109	−.002	1.805	−.024	.015	−.010	.144	893	902
		.041	.025	.046	.036	.081	.332	−.005	.009	.026	.035	896.4	2.1
Holling -1	26	−.026	.030	.040	.153	−.008	.061	−.024	.011	−.011	.117	900	905
		.013	.014	.078	.022	.023	.016	−.007	.009	.020	.032	903.5	1.2
Holling -2	5	.002	.015	.072	.100	−.031	.012	−.013	.010	−.006	−.003	890	893
		.008	.005	.084	.012	−.008	.016	−.002	.009	−.005	.001	891.8	1.1
Pamour-2	23	.011	.040	.052	.162	−.023	.038	−.017	.023	−.005	.063	912	920
		.027	.007	.096	.028	.004	.015	.004	.012	.004	.014	915.9	2.6
Matach. Con.-3	7	.011	.056	.025	.083	−.036	.001	−.021	.004	−.011	.051	928	931
		.038	.017	.063	.019	−.017	.013	−.006	.010	.013	.021	930.0	1.3
Dome-0	12	.047	.084	.033	.078	−.013	.029	−.042	−.011	.010	.089	921	926
		.061	.011	.062	.015	.004	.015	−.023	.010	.024	.021	924.1	1.7
Ashley-1	27	.026	.073	−.012	.059	−.036	.038	−.022	.015	−.004	.024	934	957
		.045	.012	.022	.017	.008	.019	−.005	.009	.002	.007	943.4	8.3

Table 2. *Continued*

MAFIC - DISSEMINATED PYRITE

SAMPLE	N	Cu		Hg		Pb		Pd		Fe		Fin	
All Mines	21	-.048	.804	.055	.598	-.024	.035	-.020	.024	.008	2.295	890	940
		.100	.173	.361	.183	.009	.015	.003	.013	.885	.678	918.4	15
	5	.045	.053	.055	.090	.004	.035	.011	.024	.008	.031	939	940
		.048	.003	.073	.015	.018	.012	.017	.005	.016	.010	939.6	0.5
Kerr Addis-2	12	.004	.804	.210	.493	-.024	.025	-.016	.024	.795	2.043	908	922
		.132	.222	.417	.077	.009	.015	.001	.011	1.205	.398	916.3	5.1
Kerr Addis-12	5	.045	.053	.055	.090	.004	.035	.011	.024	.008	.031	939	940
		.048	.003	.073	.015	.018	.012	.017	.005	.016	.010	939.6	0.5
Barber Larder-6	4	-.048	.181	.518	.598	-.015	.017	-.020	-.002	.401	2.295	990	901
		.069	.094	.554	.033	-.003	.014	-.001	.007	1.011	.893	898.3	5.5

MAFIC - MASSIVE PYRITE

Holling -3	4	.009	.019	.023	.045	-.040	-.001	-.026	-.003	-.005	.000	939	940
		.014	.004	.036	.009	-.018	.016	-.011	.010	-.003	.003	939.8	0.5

MAFIC - QUARTZ - CARBONATE

Pamour-1	18	.010	.050	.073	.139	-.001	.034	.004	.025	.000	.176	921	930
		.037	.012	.107	.020	.014	.010	.013	.006	.032	.065	926.4	2.9
	15	.010	.046	.073	.135	.001	.034	.007	.025	.000	.006	921	930
		.035	.012	.104	.019	.016	.009	.014	.005	.003	.002	927.0	2.8

FELSIC - INTERMEDIATE - QUARTZ VEIN

All Mines	84	.000	.132	.003	1.723	-.009	4.987	-.035	.037	-.012	.181	909	954
		.064	.031	.173	.245	.135	.603	.002	.012	.021	.033	939.0	13
	73	.000	.132	.003	.805	-.009	.084	-.027	.037	-.012	.071	909	954
		.064	.032	.150	.175	.031	.020	.002	.012	.012	.015	939.7	11
Toburn-1	14	.082	.132	.052	.145	.003	.260	-.008	.037	.011	.028	944	954
		.104	.015	.092	.027	.061	.018	.009	.011	.020	.006	950.1	3.1
Macassa -0	6	.052	.069	.031	.092	.051	4.987	-.022	.009	.011	.107	940	948
		.060	.007	.054	.022	1.320	2.037	-.001	.011	.065	.040	943.7	2.7
Macassa -2	38	.018	.115	.003	.155	-.009	.061	-.027	.022	-.004	.060	937	948
		.059	.027	.088	.036	.031	.017	.002	.011	.012	.016	941.5	3.1
Baldwin Con.-6	13	.000	.120	.422	1.723	-.009	.557	-.035	.014	-.012	.181	909	923
		.044	.037	.641	.358	.076	.149	-.008	.014	.043	.063	913.4	3.9
Lake-shore-0	8	.029	.071	.020	.135	.006	.040	-.017	.011	-.012	.010	949	951
		.052	.015	.102	.036	.021	.012	-.001	.012	.004	.007	950.5	0.8
Moffatt-Hall-0	5	.046	.079	.046	.133	.034	.060	-.004	.024	.002	.015	926	943
		.059	.015	.083	.033	.046	.012	.011	.011	.007	.006	930.4	7.1

FELSIC - INTERMEDIATE - QUARTZ VEINS WITH DISSEMINATED PYRITE

All Mines	20	.003	.096	-.006	.572	-.031	.073	-.017	.034	-.001	3.849	713	946
		.046	.021	.230	.245	.007	.027	.000	.011	.490	1.056	900.4	84
	16	.013	.096	-.006	.572	-.031	.011	-.017	.016	-.001	.042	934	946
		.050	.019	.270	.260	-.005	.011	-.001	.008	.014	.012	941.1	5.2
Canadian Arrow-4	12	.003	.053	.042	.572	-.031	.073	-.013	.034	-.001	3.849	713	946
		.033	.015	.369	.244	.011	.035	.004	.013	.802	1.289	876.3	103
Silver-stack-1	8	.052	.096	-.006	.058	-.009	.011	-.017	.003	.011	.042	934	944
		.064	.014	.020	.022	.001	.007	-.006	.006	.022	.010	936.6	3.3

Table 2. *Continued*

FELSIC - INTERMEDIATE - FELSITE (QUARTZ-ALBITE)

SAMPLE	N	Cu		Hg		Pb		Pd		Fe		Fin	
All Mines	17	.046	1.107	-.022	.414	-.012	.038	-.002	.014	.253	4.198	929	955
		.218	.342	.147	.181	.012	.015	.006	.004	1.156	.920	942.5	9.4
	14	.046	.099	-.002	.414	-.012	.038	-.002	.014	NOT		934	955
		.067	.017	.096	.158	.013	.016	.006	.005	INCLUDED		945.4	7.6
Kerr Addis-3	6	.046	1.107	.351	.414	-.004	.017	.001	.008	1.156	1.674	929	936
		.487	.490	.384	.024	.004	.008	.005	.003	1.346	.214	932.0	3.3
Buffonta -4	11	.051	.099	-.002	.034	-.012	.038	-.002	.014	.253	4.198	938	955
		.072	.017	.017	.013	.016	.016	.007	.005	1.053	1.139	948.3	5.8

FELSIC - INTERMEDIATE - SERICITE SCHIST

Bousquet -1	15	.043	.089	-.006	.057	-.033	.023	-.018	.002	-.004	.016	951	988
		.070	.011	.023	.019	-.008	.017	-.007	.007	.006	.006	957.3	13

FELSIC - INTERMEDIATE - MASSIVE PYRITE

All Mines	39	.021	.660	-.017	.242	-.049	.013	-.032	.006	-.008	.776	924	949
		.075	.105	.074	.094	-.016	.017	-.010	.011	.039	.131	940.7	7.5
	37	.021	.118	-.017	.242	-.049	.013	-.032	.006	-.008	.079	924	949
		.058	.025	.071	.016	-.016	.017	-.010	.011	.027	.028	940.6	7.6
Briscoe-Bryce-1	16	.018	.660	.024	.242	-.034	.013	-.029	.002	-.008	.039	941	949
		.098	.152	.158	.019	-.011	.015	-.009	.009	.004	.013	946.0	3.0
Silver-stack-2	7	.050	.188	-.010	.020	-.032	.007	-.020	.006	.004	.079	942	947
		.080	.029	.006	.012	-.014	.016	-.008	.010	.029	.028	944.7	1.8
Bousquet -2	16	.021	.058	-.017	.037	-.049	.013	-.032	.003	-.003	.776	924	940
		.037	.009	.009	.015	-.021	.018	-.012	.012	.068	.192	933.8	5.4

Table 3. *Discriminant analysis of host rock and "vein" type for trace element concentrations in gold grains. The elements providing the discrimination and the percentages of each group correctly classified into each group are shown for each category. The table was calculated using samples that were considered unaffected by secondary fluorescence. For the deposit-type "felsic-intermediate-felsite", all samples were affected by secondary fluorescence. Only analyses with less than 0.2 weight percent Cu were used and Fe was not included in the calculations.*

DEPOSIT TYPE	Mafic Qtz Vein	Mafic Dis.Sulf	Mafic Ms.Sulf	Mafic Qtz-Carb	Fel-Int Qtz Vein	Fel-Int Qtz + D.Su	Fel-Int Ser-Sch	Fel-Int Ms.Sulf	Fel-Int Felsite
Ultra Mafic	Hg Cu 99/100	Cu Pd Hg 95/100	Cu 97/100	Cu Pd 95/100	Pb Cu Hg 91/84	Cu 73/94	Hg 87/100	Hg 80/73	Hg Cu Pb 79/81
Mafic Qtz Vein		Pd Cu Hg 86/100	Pb 75/75	Hg Pd Cu 87/100	Cu Hg Pb 93/81	Hg Cu 100/50	Cu 79/93	Pb Cu 81/91	Cu Hg 88/71
Mafic Dis.Sulf			Cu 100/100	Fe Cu 80/100	Pd Cu Pb 100/80	Pd Pb 100/94	Pd 100/100	Pd 100/97	Pb Cu 100/93
Mafic Ms.Sulf				Hg 100/100	Pb 100/85	Cu Hg Fe 100/100	Cu 100/93	Cu 100/76	Cu 100/100
Mafic Qtz.Carb					Pd Cu Pb 100/84	Pd Hg Cu 100/100	Hg 100/100	Pd 100/94	Cu Pd 100/93
Fel-Int Qtz Vein						Pb 80/100	Pb 81/87	Pb 85/91	Pb Hg 69/71
Fel-Int Qtz + D.Su							Hg Fe 80/100	Hg 50/73	Pb 81/64
Fel-Int Ser-Schi								Cu Hg Fe 93/76	Pb Hg 87/71
Fel-Int Mas.Sulf									Pb 76/71

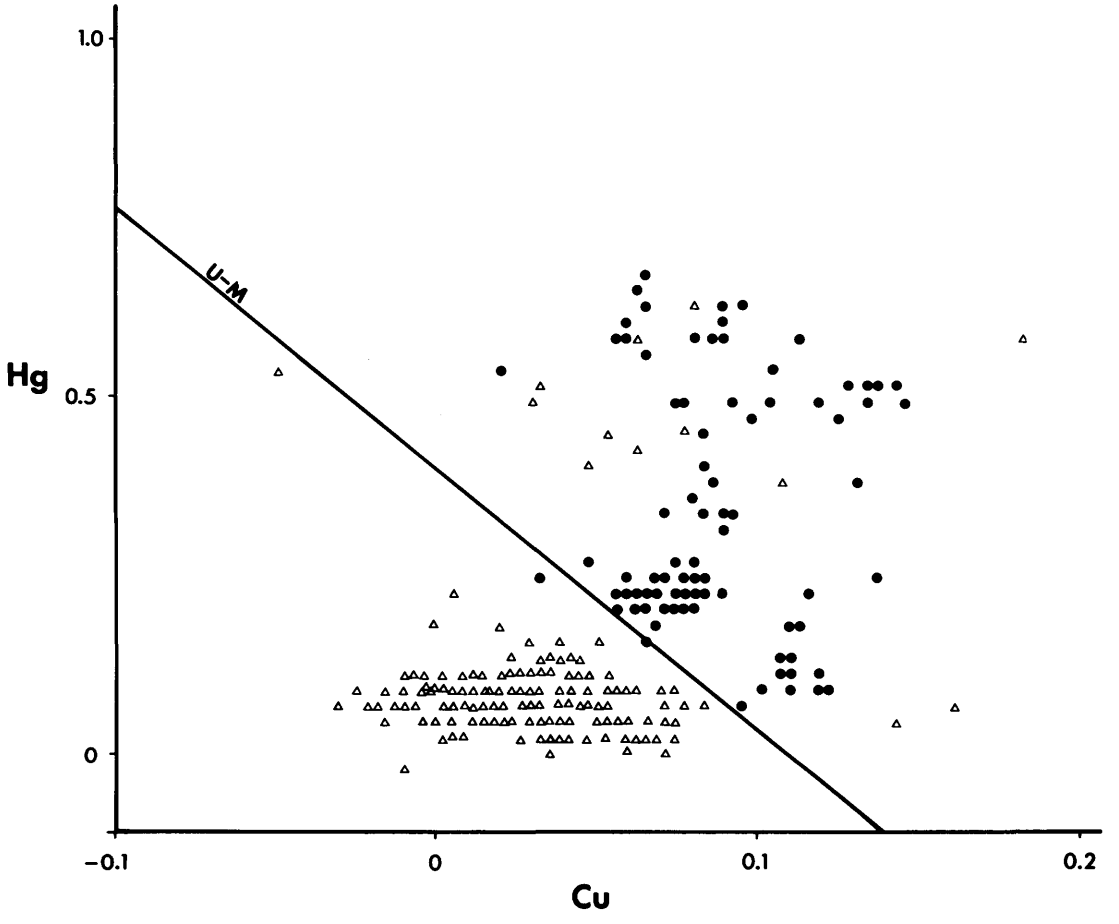

Figure 1. *Best line (U-M) to separate gold grains from ultramafic host rock (solid dots) and gold grains from mafic host rocks (open triangles) based on Hg and Cu as determined by discriminant analysis. Concentrations in weight percent.*

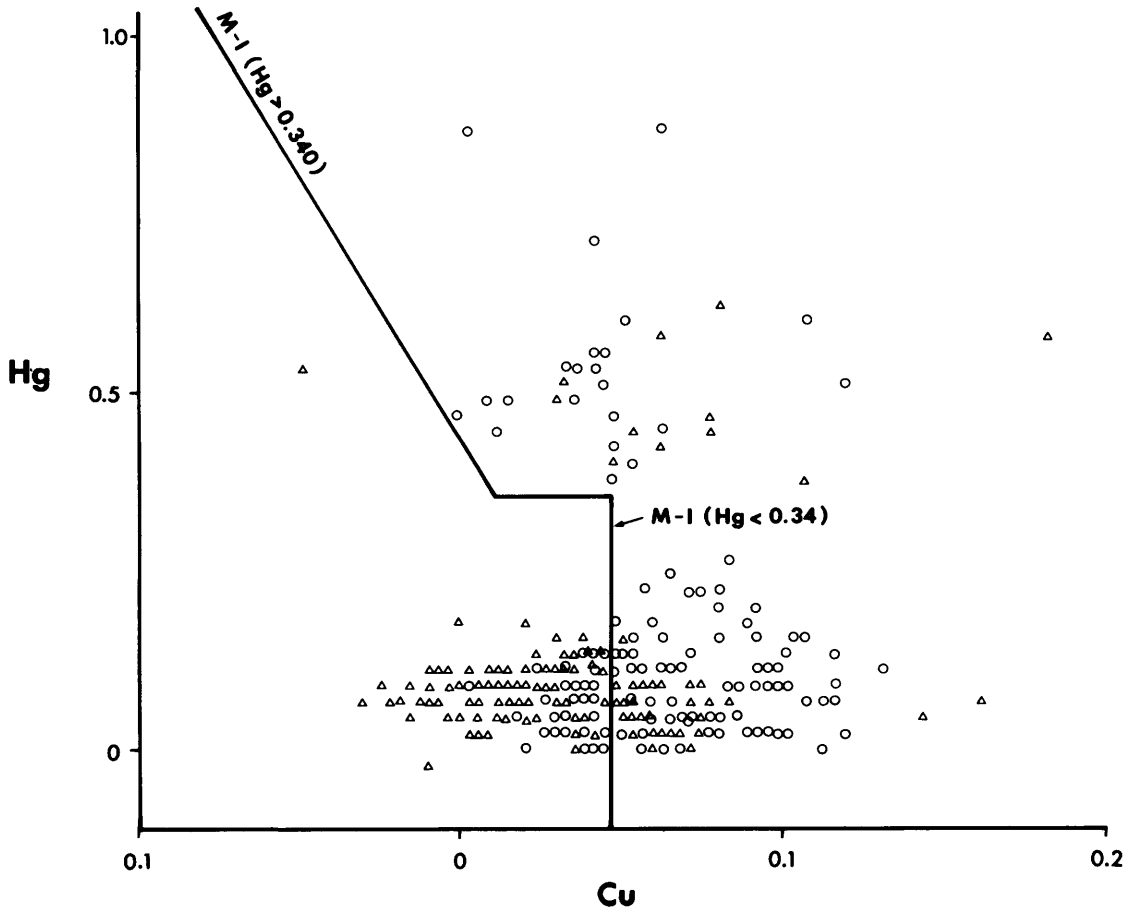

Figure 2. *Best line (M-I) to separate gold grains from mafic host rocks (open triangles) and gold grains from felsic to intermediate host rocks (open circles) as determined by discriminant analysis. Concentrations in weight percent. Lower line based on analyses with Hg concentrations less than 0.340 weight percent.*

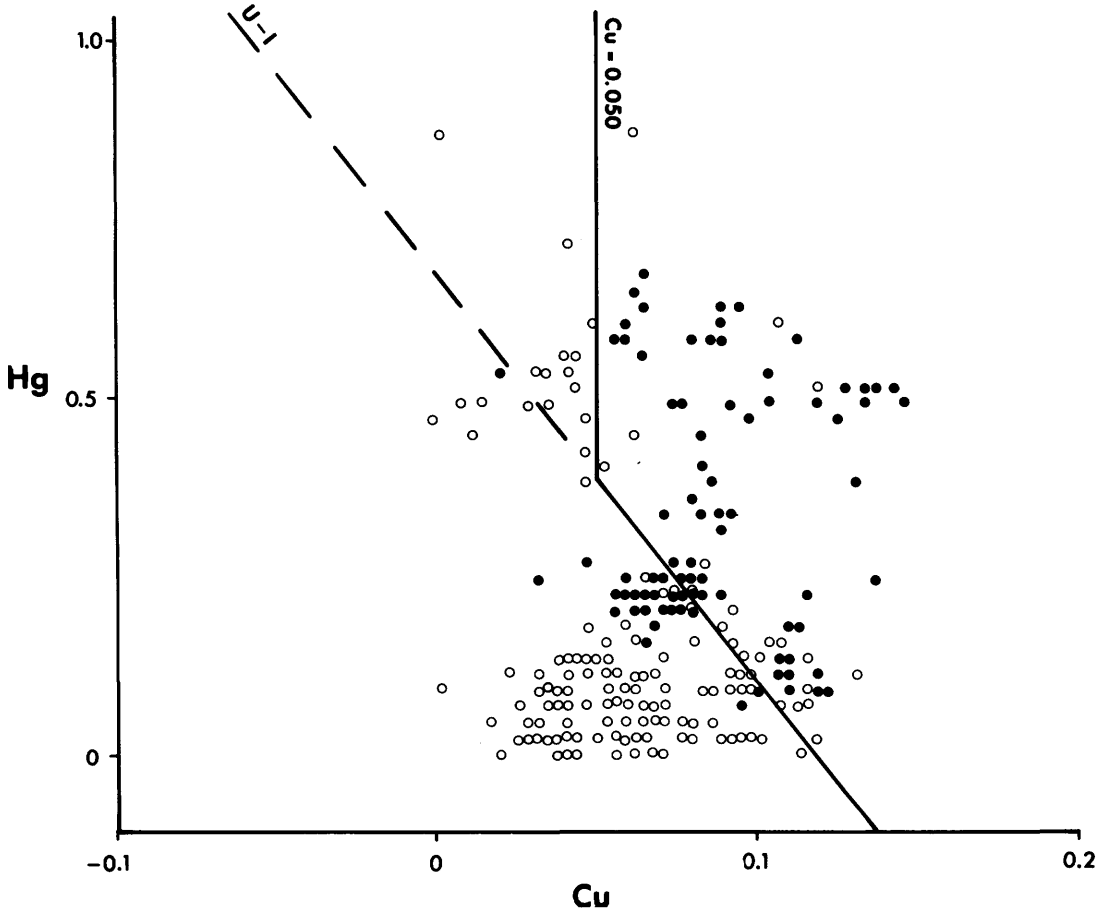

Figure 3. *Best line (U-I) to separate gold grains from ultramafic host rocks (solid dots) and gold grains from felsic to intermediate host rocks (open circles) based on Cu and Hg, as determined by discriminant anlysis. Gold grains from felsic to intermediate host rocks, classifying as ultramafic, with Hg > 0.340 percent weight percent contain Cu < 0.050 weight percent.*

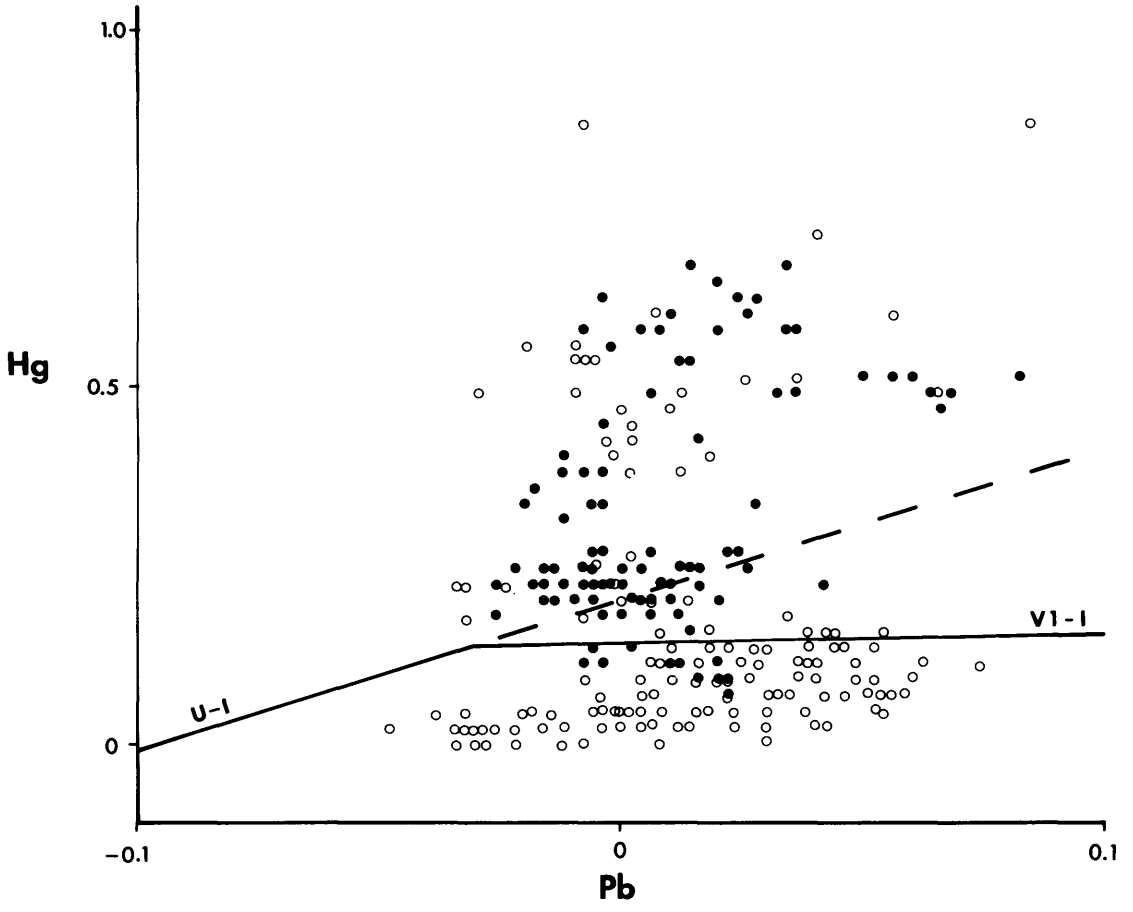

Figure 4. *Best line (U-I) to separate gold grains from ultramafic host rocks (solid dots) and gold grains from felsic to intermediate host rocks (open circles) based on Pb and Hg as determined by discriminant analysis. Gold grains from ultramafic host rocks, classifying as felsic to intermediate, can be differentiated by the function V1-I.*

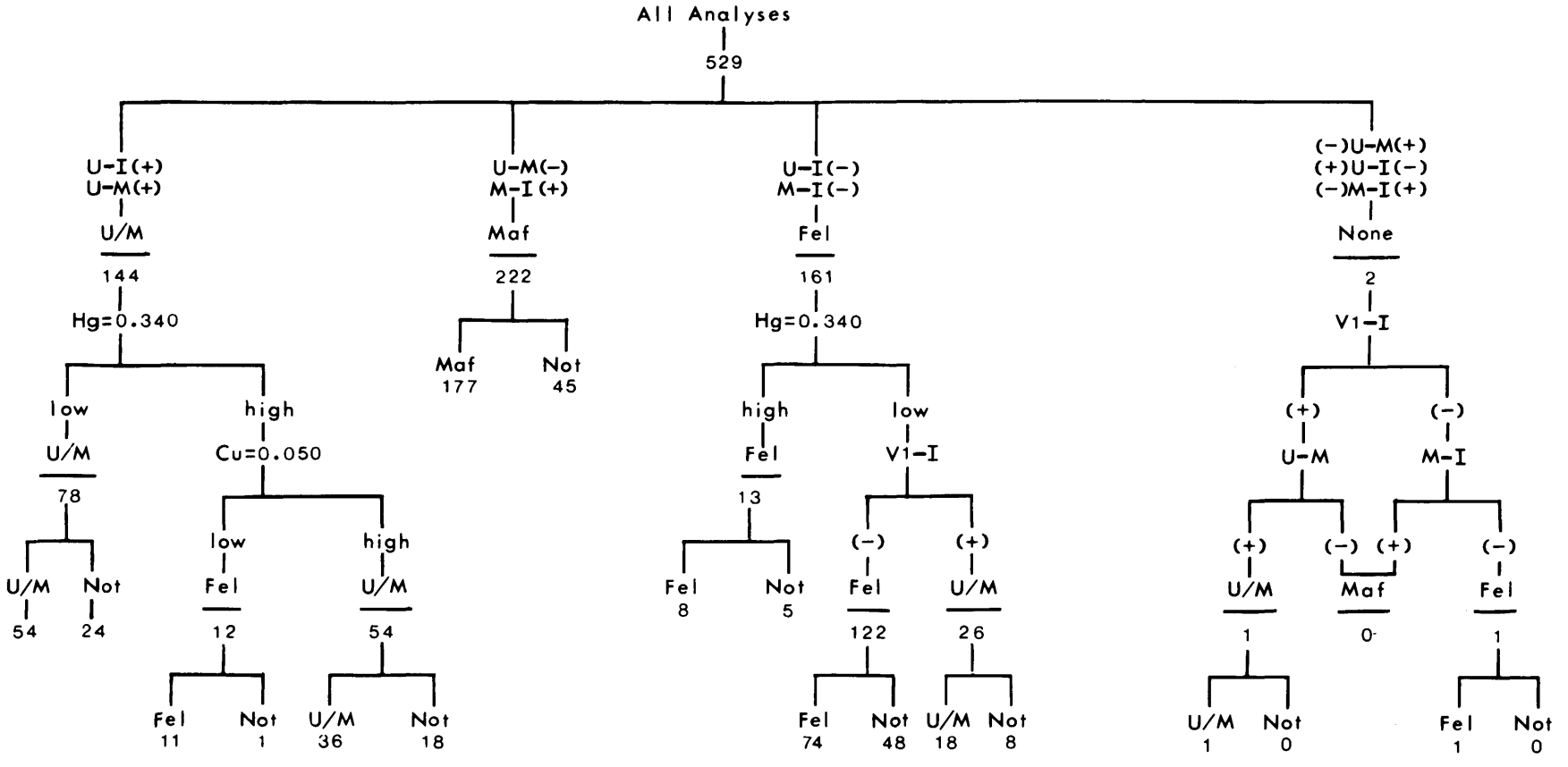

	Number Classified	Number Correctly Classified	Percent Correctly Classified
Ultramafic (U/M)	158	109	69
Mafic (Maf)	222	177	80
Felsic - Intermediate (Fel)	147	94	64
Total	529	380	72

Figure 5. *Decision tree showing the first stage of classification of analyses into deposit-types. The following stage involves the further breakdown into individual deposit-types. Approximately 72 percent of all analyses are correctly classified according to host rock. Of these 75-85 percent are correctly classified according to deposit-type. U-I, M-I, and U-M refer to dividing lines on Figures 1 to 4; + and – refer to above or below the lines.*

camp, where coloradoite is present in the ore. Coloradoite inclusions can be detected in the gold by preparing X-ray images of the gold for Hg and Te, looking for the Hg "hot spots", and checking for the associated Te inclusions. Most of these analyses are from the earlier analytical batch. When comparing analyses of the two batches, it was noted that some samples appeared to have increased levels of Hg relative to the later batch. It is possible that Hg contamination occurred during sample preparation and appears to have affected only a few of the samples.

Figure 5 also shows the path of the 529 analyses of gold grains through the classification scheme. Although the results may be biased due to the disproportionate number of samples in each host rock group, approximately 72 percent of the samples are correctly classified on the basis of host rock associations. Listings of analyses according to host rock can be made, using the criteria selection of "LISTER", a program in the QGAS system. Only the appropriate discriminant score needs be listed for each of the groups, thus making the decision of deposit-type classification easier. Of the analyses correctly classified into the host rock grouping, 75-80 percent are correctly grouped into their deposit-type classification. Therefore, about 55 percent of all samples are correctly classified according to deposit-type and about 20 percent of the remainder are correctly classified according to host rock association.

TRACE ELEMENT CONTENT OF GOLD IN OVERBURDEN

Only a few grains of gold from overburden near a known source were recovered. The gold from the Martin Bird prospect was classified as being from a "quartz-green carbonate" deposit-type. Seven gold grains were recovered from tills in a direction down-ice from the main vein. Of these, six had very similar patterns of trace element concentrations and finenesses to gold from the vein, and were classified as being from this deposit-type using the system of discriminant scores. The other grain was classified as being hosted in the deposit-type "felsite with disseminated pyrite". The fineness of this grain is similar to that of the other grains, but its Hg content is much lower. Felsite veins have been reported near the main quartz vein on the Long Lac property and they also carry some gold (Pegg, personal communication). It cannot be said with certainty that this gold grain came from one of these veins, but its trace element chemistry suggests it did.

Gold grains recovered from an esker sample on the Munro Esker near East Ford Lake vary in size and trace element concentrations, suggesting that they are from more than one source. Three deposit-types were identified: (1) ultramafic rocks, quartz-green carbonate, (2) mafic metavolcanics, massive pyrite, and (3) felsic to intermediate metavolcanics, quartz vein. In addition to the differences in trace element concentrations, the finenesses of the grains suggest different sources.

COMPARISON OF VEIN CHEMISTRY AND GOLD

Samples of vein material were analysed to compare the trace element compositions of the veins to those of the gold grains. Elements determined were Ag, Fe, Cu, Pb, Zn, and Ni. Zn and Ni were not considered in later calculations since they were undetected in the gold grains. Of the forty-five samples analysed, gold grains were recovered and analysed from fifteen. No relationship was found to exist between the trace elements in the gold and those of the vein samples. It was noted that samples containing higher concentrations of Cu in gold generally contain low (< 500 ppm) Cu in the veins, although the reverse is not necessarily true. The time of emplacement of gold in the paragenetic sequence may determine the amount of Cu available in the solution for the gold to absorb.

The amount of Ag in the vein sample was used to estimate the amount of gold present, knowing the average fineness of the gold grains. A range for the concentration of the elements associated with the gold could then be calculated. In general, the amount of Cu contained in the gold compared to the amount in the vein is < 0.2 percent; Pb is < 0.2 percent and Fe is < 0.001 percent. Thus, the concentration of the elements associated with the gold is extremely low when compared to the total amount in the vein.

CONCLUSIONS AND FUTURE PLANS

The results indicate that it is possible to differentiate gold from different deposit-types on the basis of trace element patterns. Analyses of gold grains from the Martin Bird prospect suggest that there is no loss of trace elements from gold grains in the overburden environment. Differences were found in the patterns of trace element concentrations for gold from different host rocks. The resulting grouping of deposits is very similar to the classification of gold deposits for the Superior Province as proposed by Hodgson *et al.* (1982), based on the geological characteristics of the deposits. Results from this study may be biased by the disproportionate number of analyses in each host rock group, but Figures 1 to 4 indicate that differences do exist in the trace element chemistry of gold. It is uncertain how much of an influence host rock composition has, compared to regional differences. The majority of samples of the quartz-green carbonate deposit-type are from the Larder Lake area, most of the felsic to intermediate deposit-type from the Kirkland Lake area, and most of the mafic metavolcanic deposit-type from the Timmins area. Further sampling in each of these areas would be required to draw more confident conclusions. It is hoped that subsequent analyses of gold grains will establish whether or not the differences in the patterns of trace element concentrations for gold found in different host rocks apply in other areas.

A plot of fineness verses Cu concentration shows an increase in Cu content with fineness greater than 850, but

the significance of this is not clear. Gold grains from the Timmins area tend to have a lower fineness and Cu content than gold from the Kirkland Lake – Larder Lake areas. Similarly, T. Solberg (Virginia Polytechnic Institute, personal communication, 1981) has found a relationship between fineness and Cu concentration in analyses of gold from the State of Virginia.

It was suggested by Guindon and Nichol (1981) and by W.S. Fyfe of the Grant Review Committee, that ion probe analyses be completed to determine what trace elements are in gold. Ion probe analyses completed for Solberg were found to be extremely complicated, making the identification of the trace elements impossible in some cases. (Solberg, personal communication, 1981).

Some X-ray imaging is required for samples from the Baldwin prospect and for some samples from the Kerr Addison mine, to try to locate Hg-telluride inclusions and to determine if some of the early analyses of gold, from the felsite deposit-type, were contaminated by Hg.

ACKNOWLEDGMENTS

We would like to thank all the companies and individuals who gave their time and supplied samples for this project. We would also like to thank Todd Solberg, of Virginia Polytechnic Institute for information about Virginia gold and the considerable time and expertise given for the electron microprobe analyses of gold.

REFERENCES

Gay, N.C.
1963: A Review of the Geochemical Characteristics of Gold in Ore Deposits; University of Witwatersrand, Economic Geology Research Unit, Information Circular 12, 70p.
1964: The Composition of Gold from the Barberton Mountain Land; University of Witwatersrand, Economic Geology Research Unit, Information Circular 19, 53p.

Guindon, D.L. and Nichol, I.
1981: Speciation of Free Gold in Glacial Overburden; Grant 76, p.125-131 in Geoscience Research Grant Program, Summary of Research 1980-1981, edited by E.G. Pye, Ontario Geological Survey, Miscellaneous Paper 98, 340p.

Hodgson, C.J., Chapman, R.S.G., and MacGeehan, P.J.
1982: Application of Exploration Criteria for Gold Deposits in the Superior Province of the Canadian Shield to Gold Exploration in the Cordillera; Precious Metals in the Northern Cordillera, Association of Exploration Geochemists, p. 173-206.

Grant 115 Characterization of Assimilation-Type Uraniferous Pegmatites, Bancroft Region

S.J. Haynes
Department of Geological Sciences, Brock University

ABSTRACT

Assimilation-type uraniferous pegmatites are broadly defined as those pegmatites in which uranium minerals are directly associated with assimilated and metasomatically altered country rocks. Field studies indicate that two main types are present: border metasomatic, and schlieren-swarm. The schlieren-swarm type comprise large bulbous pegmatitic masses, more than 50 m thick, containing significant quantities of both resorbed and unresorbed xenoliths of a wide variety of rock types. The border metasomatic type consists of sheet or dike-like pegmatites, generally much less than 50 m wide, with a "pseudo pegmatite" texture of metasomatically altered "schlieren" forming radioactive border zones of variable width. All uraniferous assimilation-type pegmatites display the following characteristics: (1) sulphides are present in the country rocks and in the metasomatic uraniferous zones; (2) carbonates are present in the country rock successions; (3) molybdenite is associated with higher uranium values; and (4) potassic metasomatic assemblages are K-feldspar + biotite ± magnetite.

The border metasomatic deposits studied (Farcroft-South showing, Lazlo, and Eels Creek) all occur in the mantling paragneisses of the migmatitic Anstruther Gneiss Dome. Uranium in the pegmatites of the area progressively increases from the margins of the dome to a zone 2 to 4 km from the dome margin.

It is postulated that uranium was partitioned into a fluid phase of the leucosome of the gneiss dome during anatectic melting and moved outwards into the paragneisses with the pegmatite sheets. Uranium precipitated where these fluids were reduced by low Eh reactions involving sulphides ± magnetite in the presence of carbonate (higher pH).

INTRODUCTION

This report details the results obtained from one year's funding of the project. Only those assimilation-type uraniferous pegmatites associated with the Anstruther Gneiss Dome were examined, as well as their regional geological setting. These include Farcroft-South showing, Lazlo, Eels Creek, Blott and Cavendish properties. Of these only Farcroft-South showing, and Lazlo and Cavendish properties were studied in detail.

GEOLOGICAL SETTING

All the assimilation-type pegmatites examined are related to the Anstruther Gneiss Dome in Anstruther and Cavendish Townships, Peterborough County. The Anstruther "pluton" (Figure 1) is one of four granitic masses that comprises the Harvey-Cardiff Arch (Hewitt 1962) with which most of the uraniferous pegmatites of the Bancroft region are associated.

ANSTRUTHER GNEISS DOME

Mapping in the Anstruther Lake area (Figure 2) indicates that the Anstruther Gneiss Dome is texturally zoned from

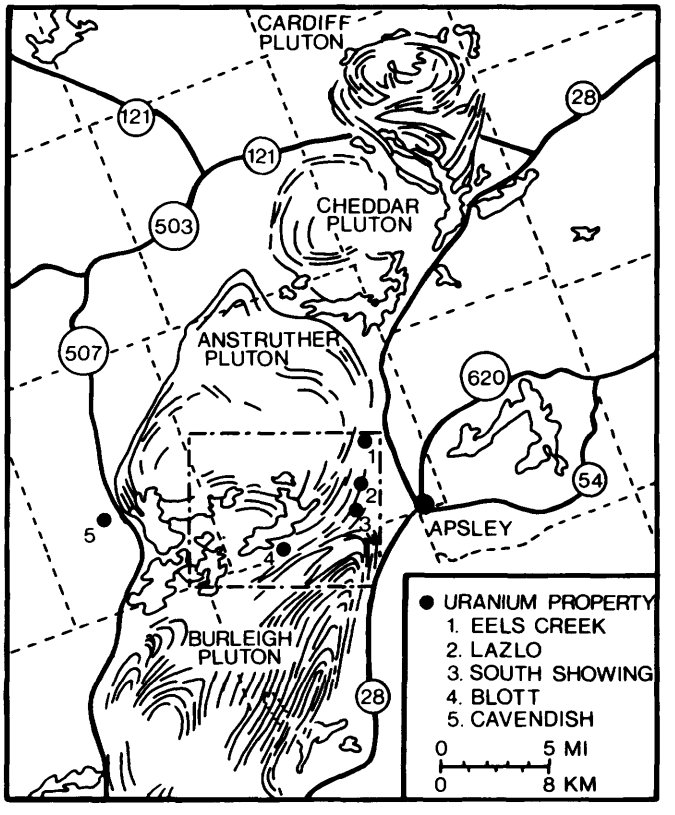

Figure 1. *Regional geology of the Harvey-Cardiff Arch and location of study area.*

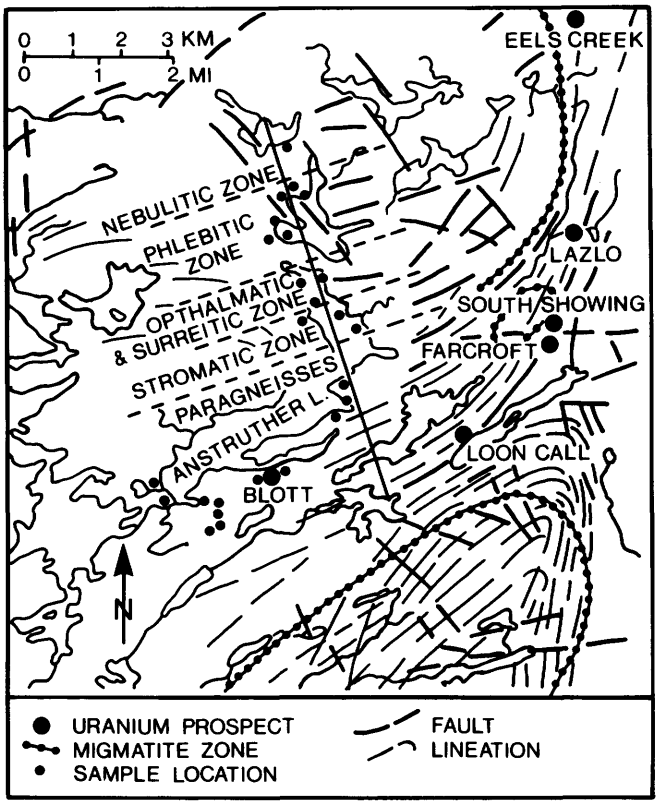

Figure 2. *Relation of uraniferous pegmatites to the structure of the Anstruther Gneiss Dome.*

a nebulitic core outwards through successive migmatite zones: phlebitic (includes phlebitic, ptygmatic and folded structures); opthalmatic and surreitic; and stromatic. These migmatites are mantled by paragneisses, often with locally developed incipient migmatization in the felsic layers near the dome. These migmatite zones represent homogeneous (nebulite zone) and inhomogeneous (phlebitic zone) diatexic melting of the central parts of the dome and metatectic melting of the outer zones, similar to the anatectic massif in the Black Forest of Germany (Mehnert 1968). Pegmatitic material is common in all zones, but large sheets and dikes of pegmatite only occur in the outer migmatite zones and in the mantling paragneisses.

URANIFEROUS PEGMATITES

BORDER METASOMATIC TYPE

The border metasomatic pegmatites are sheet-like uraniferous bodies, generally much less than 50 m wide, with a "pseudo pegmatite" texture of potassic-metasomatized alteration zones bordering country rock paragneisses. These zones are of variable width within each deposit. Although the exact alteration assemblages differ from deposit to deposit, assemblages of K-feldspar + biotite + sulphides are always present. Also, the highest values of both uranium and thorium are always associated with these alteration zones. Close inspection of the alteration zones reveals that they consist of a mixture of both pegmatite (represented by randomly-oriented crystals of granite minimum-melt composition) and resorbed "schlieren" of country rocks (displaying relict foliation, parallel to foliation in the country rocks).

Figures 3 and 4 are simplified geological maps of the Farcroft-South showing and Lazlo property synthesized from detailed mapping. In both properties biotite ± garnet quartzofeldspathic gneiss is the most abundant country rock. Hornblende gneiss and amphibolite are also present but are more common on the Farcroft-South showing. Marble occurs in country rock successions but is only minor on the Farcroft-South showing; marble is of greatest extent on the Lazlo property where it encloses uraniferous pegmatites. Migmatite outcrops in the western part of the Farcroft-South showing. The migmatite represents an outlier from the main Anstruther Gneiss Dome (see Figure 2).

Pegmatite sheets, roughly concordant to the regional foliation, are abundant on both properties. However, many of these are barren and consist of coarse-grained

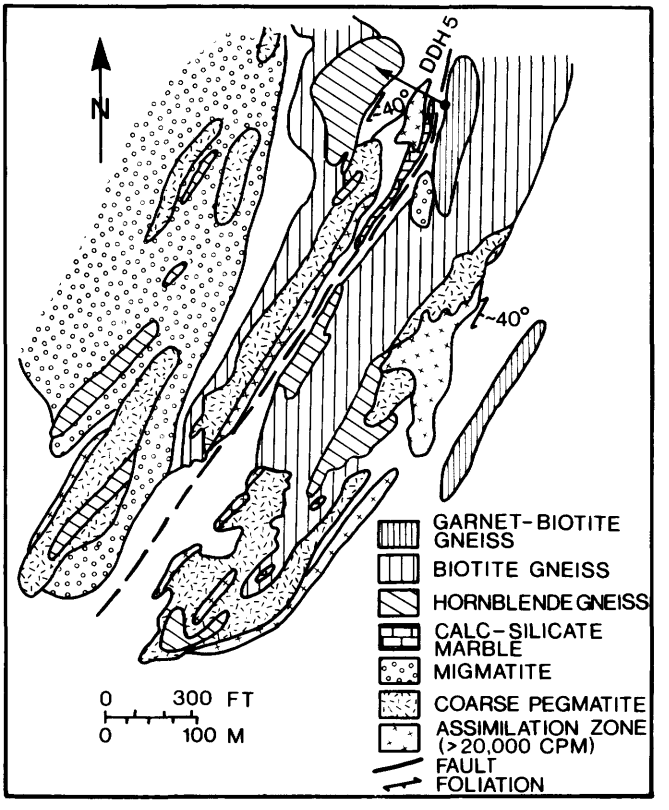

Figure 3. *Simplified geology of the south showing of the Farcroft property.*

randomly-oriented crystals of quartz and feldspars (biotite-free). Scintillometer surveys reveal that the most radioactive areas are the zones of metasomatic alteration which are restricted to the borders of the pegmatite sheets.

At the Farcroft-South showing (Figure 3) the highest radioactivity is associated with assimilated garnet-biotite gneiss. In the alteration zones, garnets are pseudomorphed by secondary biotite, and plagioclases by K-feldspar in resorbed schlieren of country rock. In addition, more coarsely crystalline K-feldspar and biotite are developed, giving rise to a granular texture in which biotite is parallel to the country-rock foliation. In the most radioactive parts, fine-grained pyrite, and minor pyrrhotite, chalcopyrite and molybdenite, are associated with small grains of uranothorite and cyrtolite. Fine-grained sulphides are also present in the country rocks adjacent to the higher radioactive zones.

At the Lazlo property (Figure 4), the highest radioactivity is associated with thin pegmatite bodies, characterized by an alteration assemblage of coarse K-feldspar + biotite + hornblende interspersed between schlieren of country rock (replaced by finer-grained K-feldspar + biotite) displaying relict country-rock foliation. In addition, coarse molybdenite rosettes are abundant. Pyrite is common but usually fine-grained. Crystals of cyrtolite and uranothorite, up to 2 cm in size, are locally present. Pyrite-bearing biotite gneiss comprises the hanging wall, while marble with intercalated metasediments forms the footwall.

Examination of the Eels Creek and Blott properties (see Figure 2) reveals geological conditions and alteration assemblages similar to the Farcroft-South and Lazlo properties, but hornblende-rich rocks have been assimilated in the alteration zones and, in addition to pyrite, magnetite is abundant in discrete masses. In all the properties examined, magnetite grains were observed in polished sections from the alteration zones, usually associated with biotite.

SCHLIEREN-SWARM TYPE

The only deposit of this type examined is at the Cavendish property. The deposit is characterized by large (100 m wide) bulbous masses of "pegmatite" intruding a sequence of amphibolite, gneiss and marble (Figure 5). The bulk of the "pegmatite" comprises resorbed schlieren of gneiss, potassically altered to K-feldspar + biotite assemblages, and displaying relict foliation. Xenoliths of amphibolite, with biotite developed along their borders are also common. Although pegmatitic "melt" material (coarse, randomly oriented feldspars and quartz) sepa-

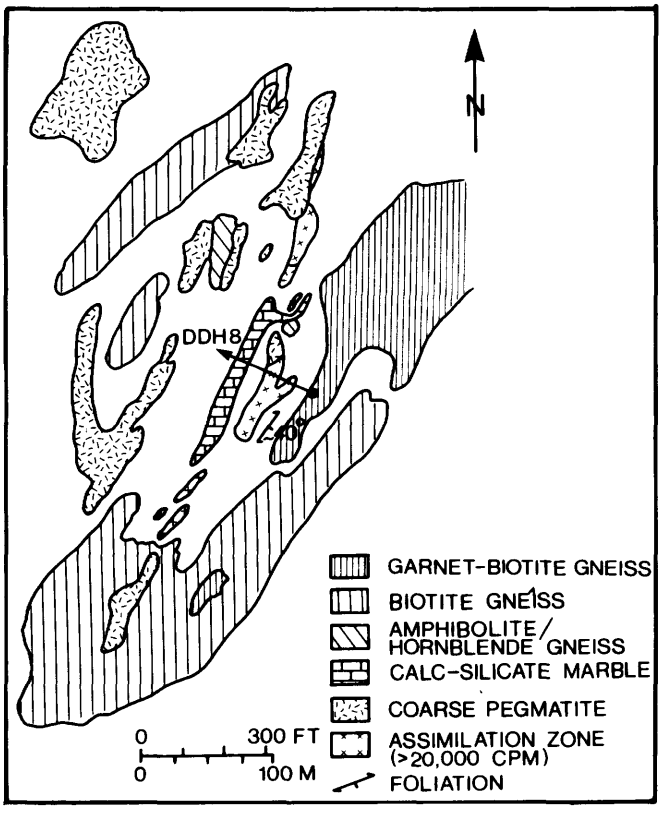

Figure 4. *Simplified geology of the Lazlo property.*

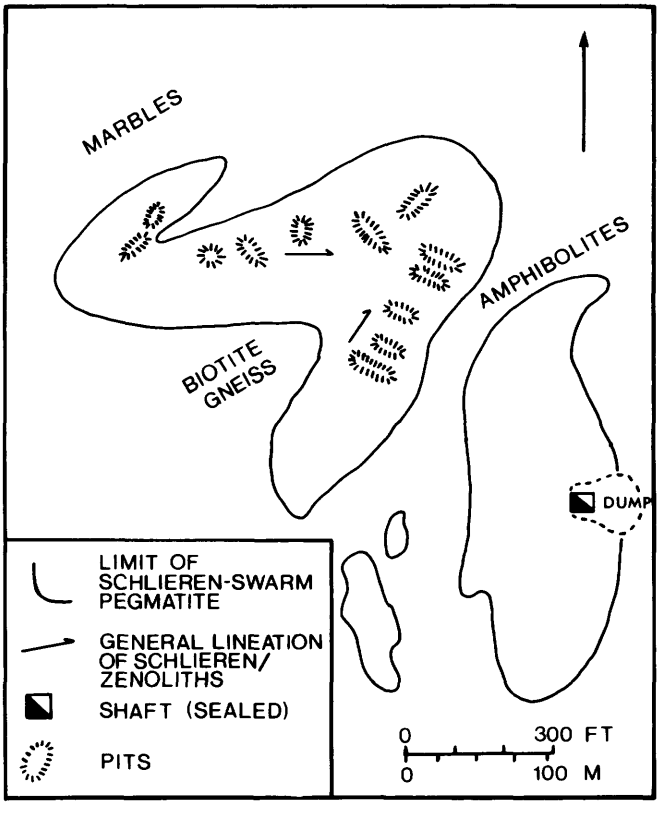

Figure 5. *Simplified geology of the Cavendish property.*

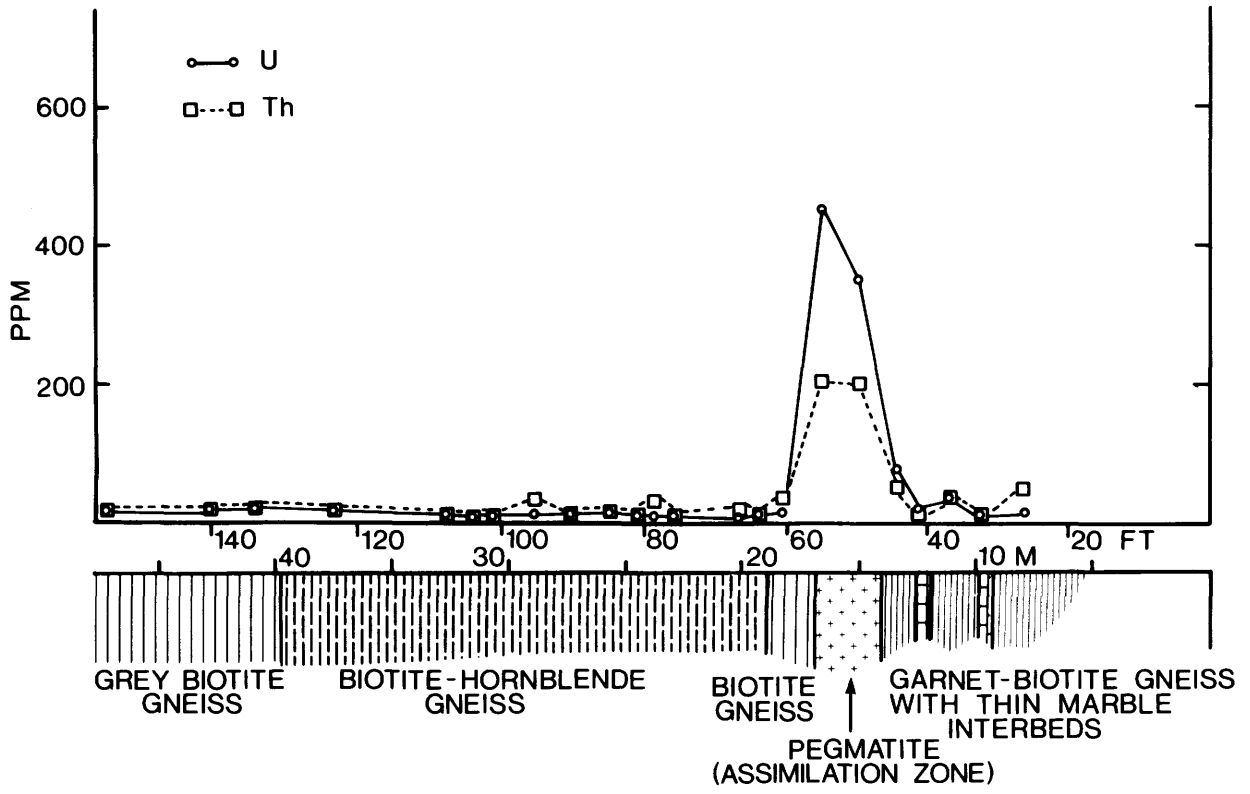

Figure 6. *Lithology and U and Th distribution in Northgate Exploration Limited's drill hole DDH5, Farcroft-South showing. Hole inclined 45°W (see Figure 3). Distances measured from collar.*

rates individual schlieren and xenoliths, it comprises only about 40 percent of the total body. Orientation of the schlieren suggests that the pegmatite was either emplaced into the hinge of a fold or was itself folded. Radioactivity is highly erratic but is highest in areas of biotitized schlieren containing masses of magnetite. Although access to the old mine workings is not possible, examination of the dump material indicates that the highest radioactivity is associated with massive magnetite and sulphides (Haynes 1979; Haynes and Frankovitch 1980).

URANIUM AND THORIUM DISTRIBUTION

BORDER METASOMATIC PEGMATITES

Drill core from Northgate Exploration Limited's DDH5 (Farcroft-South showing) and DDH8 (Lazlo property) was sampled over 1 to 1.5 m intervals, thin sectioned, and crushed. Twenty-two samples from DDH5 and 41 samples from DDH8 were submitted to N.A.C. Limited for delayed neutron counting (U) and neutron activation (Th) analyses. At the Farcroft-South showing, DDH5 intersected only the assimilated zone of the pegmatite (Figure 6). U and Th values in the country rock follow identical trends (concentrations less than 50 ppm) suggesting that uranothorite is the main radioactive mineral. In the pegmatite zone, uranium is more abundant than thorium but both are significantly enriched. This is probably due to the presence of uranothorite, cyrtolite and trace uraninite.

At the Lazlo property, DDH8 intersects two pegmatite sheets with well-developed assimilation border zones and one thin pegmatite unit (Figure 7). In the country rocks, uranium and thorium have identical patterns but in the pegmatites uranium is significantly enriched. In the lower pegmatite, uranium is enriched in the hanging wall and footwall assimilation zones but thorium shows a more erratic distribution. In the upper pegmatite, both uranium and thorium are enriched in the hanging wall and footwall, with very high values of both elements in the hanging wall. The uranium patterns in the pegmatites are closely mirrored by the distribution of molybdenum (Figure 7). Similar high Mo concentrations have been reported from Polish uranium ores (Parus *et al.* 1981). Enriched thorium and uranium values are due to the abundance of uranothorite and cyrtolite in the assimilation zones, but the very high values of uranium in the upper pegmatite result from the presence of discrete grains

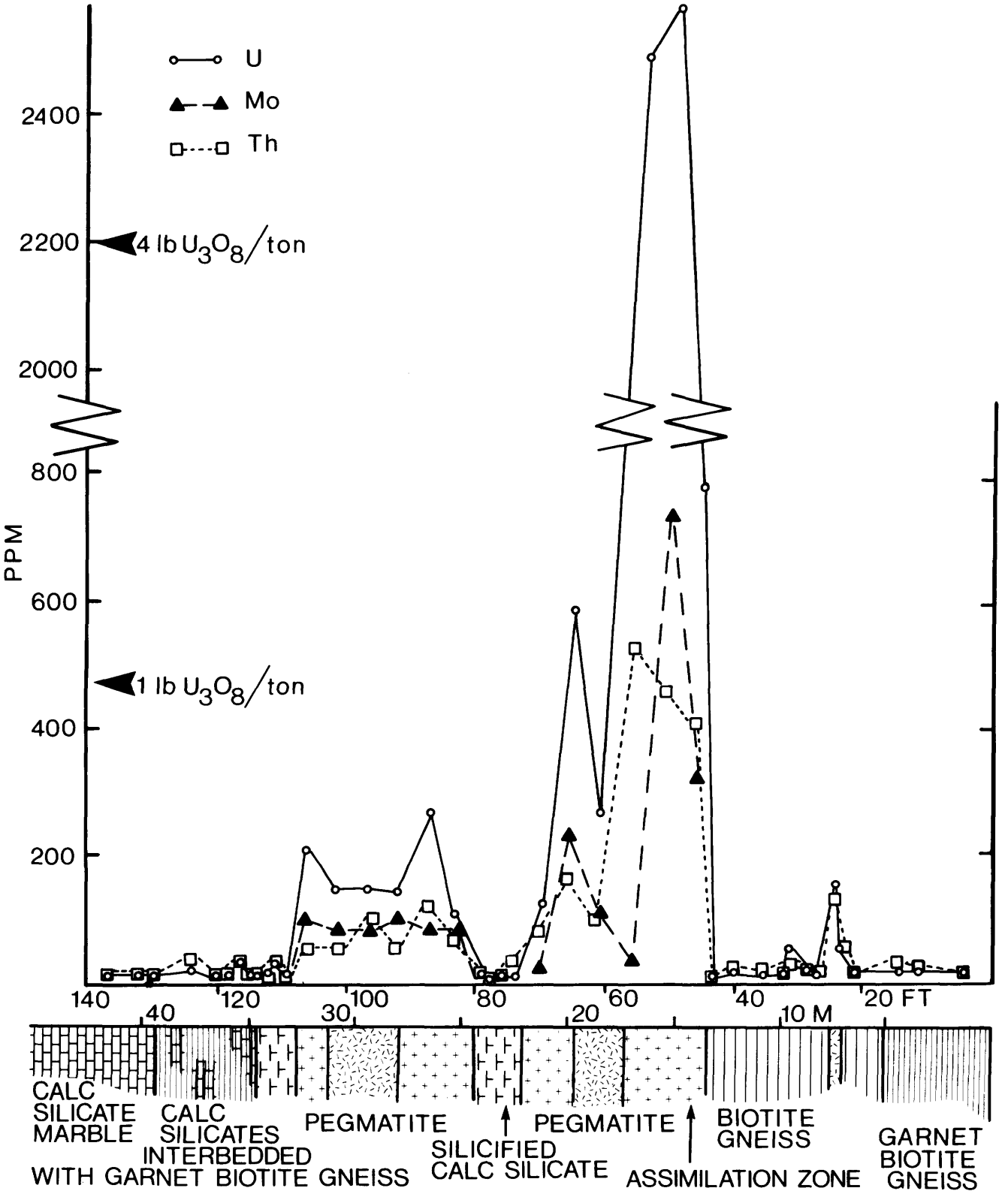

Figure 7. *Lithology and U, Th and Mo distribution in Northgate Exploration Limited's drill hole DDH8, Lazlo property. Hole inclined 45°W (see Figure 4). Distances measured from collar.*

of uraninite associated with abundant pyrite and molybdenite.

ANSTRUTHER GNEISS DOME

Forty samples of migmatite, paragneiss and barren pegmatite were taken from a section across Anstruther Lake (see Figure 2). These and radioactive samples from the Blott property were analysed by N.A.C. Limited for uranium. Values from the migmatites and paragneisses are generally less than 10 ppm U (Figure 8). The barren pegmatites increase in uranium content from 12 ppm, at the margin of the gneiss dome, to 30 to 50 ppm, 3-4 km from the margin. This is mirrored by a systematic increase in K_2O, and decrease in Na_2O, in the pegmatites (Anderson 1981).

DISCUSSION

All the uraniferous assimilation-type pegmatites display the following characteristics, not exhibited by barren pegmatites:

(1) Assimilated country rocks are potassically altered to K-feldspar + biotite ± magnetite assemblages.

(2) Sulphides, mainly pyrite ± molybdenite, are present in the metasomatic assimilation zones.

(3) Carbonates are present in the country-rock succession.

(4) The pegmatites and their assimilation zones are devoid of muscovite.

The width of the alteration zones in the uraniferous pegmatites, compared to their absence in the barren pegmatites, suggests the presence of an abundant H_2O fluid phase. The ubiquitous K-feldspar + biotite alteration assemblage appears analagous to the metasomatic potassium silicate alteration of porphyry deposits (e.g. Meyer and Hemley 1967) although formed at K^+/H^+ ratios well above the sericite - K-feldspar boundary. The systematic increase of K_2O with corresponding decrease of Na_2O, in all the pegmatites, away from the Anstruther Gneiss Dome (Anderson 1981), suggests that the border metasomatic pegmatites in the area were derived from the leucosomal material of the gneiss zone, and that a potassium-rich fluid phase was progressively partitioned from the pegmatite melts as the melts cooled upon outward migration. Further evidence for progressive H_2O fluid partitioning is the lack of alteration zones in the pegmatites close to, or within, the gneiss dome. This fluid-phase potassium would have deuterically replaced plagioclases within the pegmatites (Orville 1963) resulting in the systematic substitution of K_2O for Na_2O. As uranium in highly mobile, it is likely that it followed potassium into the fluid phase giving rise to a similar increase outwards from the gneiss dome. Numerous minor occurrences of radioactive pegmatites occur in a zone 2 to 5 km from the margin of the Anstruther Gneiss Dome, however one or more of the parameters displayed by uraniferous assimilation-type pegmatites (defined above) are lacking. This can be explained by the hypothesis that although uranium was efficiently transported in the fluid phase of the more H_2O-rich pegmatites, its precipitation was controlled by other parameters. Thermodynamic calculations for the system U-K-Ca-Fe-S-C-O-H at 300°C by Romberger (1978) indicate that uranium species precipitate at low P_{O2} and high pH (Figure 9). Although not directly applicable to pegmatite conditions in the katazone, involving water above the critical point (371°C), Romberger's data indicate that the K-feldspar + pyrite + magnetite assemblages present in the assimilation-type pegmatites could have formed at Eh and pH conditions within the stability field of uraninite. Such a complicated system depends primarily on temperature, pressure, activity of different uranium complexes, the activity of potassium (relative K^+/H^+ ratio) and sulphur fugacity so it is virtually impossible to deduce absolute values for the different degrees of freedom. However, the system can be applied empirically in that uranium is likely to precipate from a potassic pegmatitic fluid encountering reducing, relatively alkaline, environments below the magnetite-hematite oxygen fugacity buffer at pH values within the stability fields of K-feldspar and calcite.

The much higher uranium values of the Lazlo property compared to the Farcroft-South showing may have resulted not only from direct contact with marble, but also from the greater abundance of sulphides (both pyrite and molybdenite). Because the highest values at the Lazlo

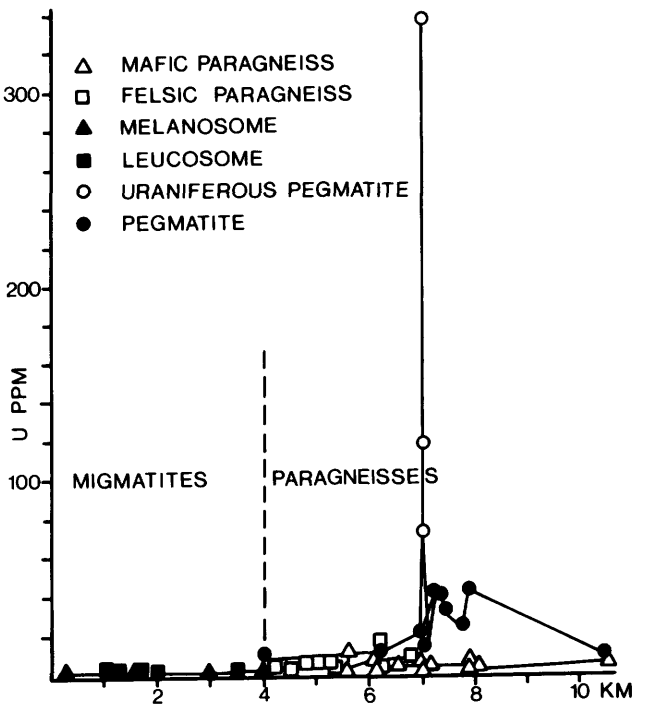

Figure 8. *Uranium concentration in migmatites, paragneisses and pegmatites relative to distance from core of Anstruther Gneiss Dome.*

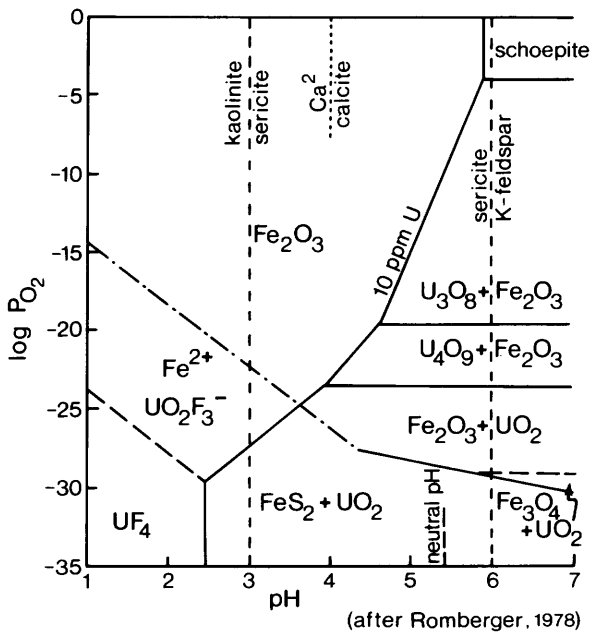

Figure 9. *Composite log P_{O2} - pH diagram for the system U-K-Ca-Fe-S-C-O-H at 300°C.*

property are present on the hanging wall of the upper pegmatite, where the pegmatite abuts sulphide-bearing gneisses, it is likely that, given the right pH conditions, the main control on the amount of uraninite precipitated is the degree of reduction. It is interesting to note that higher uranium values at the Madawaska mine, at Bancroft, are often associated with sulphide-rich country rocks; also xenoliths of marble are present and the pegmatite contains molybdenite (personal observations).

CONCLUSIONS

Exploration for uraniferous pegmatites in the Bancroft area should concentrate on pegmatites with K-feldspar + biotite ± magnetite alteration zones (containing abundant pyrite and molybdenite) adjacent to country rock successions containing both marble and sulphide-bearing gneiss or amphibolite.

Although the uraniferous pegmatites may be "stratigraphically controlled" by the distribution of marble, they occur in a variety of sulphide-bearing country rocks. Thus, their arcuate distribution about the Anstruther Gneiss Dome probably results from transport of uranium, derived from anatectic melting of the dome, by mobile pegmatitic melt. As the pegmatites cooled on moving outward from the dome, potassium and uranium partitioned into a progressively separating fluid phase. Where this fluid phase became abundant (2-4 km from the dome margin) the pegmatites became enriched in uranium, but only reached ore-level values where the fluids were reduced by reactions, with assimilated country rocks, that decreased Eh and raised pH.

ACKNOWLEDGMENTS

The author is indebted to W.W. Weber and Northgate Exploration Limited for their assistance and permission to publish work on Northgate's property. J. Pirie (Esso Minerals Canada), L. LaPrairie (Rare Earth Resources) and W. Blott kindly allowed the author to visit their properties. Appreciation is extended to F. Gombos for drafting and A.M. Fulton for typing (Brock University).

REFERENCES

Anderson, M.R.
1981: Structure, Petrography and Chemistry of a Zoned Migmatite Complex, Bancroft Region, Ontario: Relationship to Uraniferous Pegmatites; unpublished B.Sc. Thesis, Brock University, St. Catharines, Ontario, 89p.

Haynes, S.J.
1979: Genesis of the Cavendish and Crystal Lake Uranium Deposits; Summary of Geoscience Research Activities for 1978, Ontario Geological Survey, Miscellaneous Paper 87, p. 14-20.

Haynes, S.J. and Frankovitch, M.
1980: Genesis of the Cavendish and Crystal Uranium Deposits: Final Report Ontario Geoscience Research Grant GR3; Ontario Geological Survey, Open File Report 5302.

Hewitt, D.F.
1962: Some Tectonic Features of the Grenville Province; The Tectonics of the Canadian Shield, Royal Society of Canada, Special Publication No. 4, p. 102-117.

Mehnert, K.R.
1968: Migmatites and the Origin of Granitic Rocks; Elsevier, New York, 393p.
1967: Wall Rock Alteration; p. 166-235 in Geochemistry of Hydrothermal Ore Deposits, edited by H.L. Barnes, Holt, Rinehart and Winston, New York, 670p.

Orville, P.M.
1963: Alkali Ion Exchange Between Vapour and Feldspar Phases; American Journal of Science, Vol.261, p. 201-237.

Parus, J., Zoltowski, T., Kierzek, J., and Ratynski, W.
1981: Applicability of U L X-ray Lines for the Determination of Low Uranium Concentrations; Advances in X-ray Analysis, Plenum Press, Vol. 24, p. 311-312.

Romberger, S.B.
1978: Hydrothermal Transport and Deposition of Uranium, and the Origin of Vein Uranium Deposits; Geological Society of America/Geological Association of Canada Joint Annual Meeting, Toronto. Abstracts with Program.

Grant 112 Petrographic Number Re-Evaluation

P.P. Hudec
Department of Geology, University of Windsor

ABSTRACT

The Petrographic Number (PN) test as used by the Province of Ontario is one of the primary means of discriminating between acceptable and unacceptable aggregate material for use in construction. The test assigns a multiplier factor to a portion or percentage of the sample belonging to a particular rock type. The factors are 1 (best), 3, 6, and 10 (worst, or deleterious). The sum of the products is the PN of the sample.

The multiplier factors are considered to be too inflexible to give a good indication of aggregate quality. The purpose of this research was to test the established factors, and to suggest a new set of factors that would define the PN of the aggregate with greater precision.

Thirty-one aggregate samples, each representing a different petrographic type, were obtained from the Ontario Ministry of Transportation and Communications. The samples were subjected to a variety of tests to determine their basic properties and resistance to freezing, impact, and wear. The results were analyzed using a multivariate statistical technique of "best stepwise regression". The established factors, as dependent variables, were compared to the test results, as independent variables. An empirical relationship was obtained which allowed calculation of a new factor for each rock type.

The comparison of currently used and calculated PN factors showed a wide disparity in certain rock types. For instance, medium hard sandstone (current category 1) shows a calculated PN factor of 3.3; siltstone (currently 6), gives a calculated PN factor of 2.5.

The results indicate that the factors of some of the rock-types need to be re-defined. Ideally, a full range of factors from 1 to 10 should be used rather than just the four categories.

INTRODUCTION

Each rock-type behaves somewhat differently in a weathering environment because of its unique properties, e.g. mineralogy, crystal structure, and pore shape and size. Differences in rock behaviour can be expected depending on its origin: igneous, metamorphic, or sedimentary. The degree of weathering that a particular rock has undergone also determines its resistance to further physical and chemical deterioration.

Experience has shown that it is possible to estimate the probable behaviour of rock when used as aggregate material (in concrete, bituminous mix, or as road base or fill) by determining its type, degree of weathering, hardness, and potential chemical reactivity. The Ontario Ministry of Transportation and Communications (MTC) has assigned a durability factor to various rocks commonly used as crushed stone or crushed gravel. Depending on the proportion of the various rock types and their durability factors, an overall estimate of the behaviour of the aggregate in service can be established.

This procedure is referred to as Petrographic Number, or PN, determination. MTC has established four categories of rocks, and assigned to them durability factors: Good (1), Fair (3), Poor (6), and Deleterious (10). The factors are changed for a given rock type according to intended use. Figure 1 shows the form used to calculate the PN by MTC. Hot mix, mulch, and concrete PN have the most stringent requirements, whereas granular and 5/8 inch (16 mm) crushed aggregate have lower durability factor multipliers.

Although the PN test can clearly differentiate between what are obviously good and bad aggregates, the rock-types that fall into "grey" areas defy classification into one of the four durability classes above. Even the 'good' (or 'bad') rock-types don't have identical responses to weathering stress. The purpose of this research was to determine the individual durability factors for each rock-type so that the PN technique of aggregate evaluation can be improved.

SAMPLE SELECTION

Over the last several years, the MTC aggregate laboratories have accumulated samples representing each of the rock-types that are listed in Figure 1. The collecting was done as part of normal PN determination, during which each aggregate sample submitted was divided into its constituent rock-types according to the categories listed in the PN test. A total of 31 separate samples were thus accumulated representing a Province-wide sampling of each rock-type. For instance, MTC aggregate type 24 represents slightly weathered, crystalline carbonate; the individual particles in the sample come from many different sources across the Province and represent both crushed stone and crushed gravel. The proportion of the sample from any one source depends on the frequency of use of that source and the frequency of testing of the source.

Each sample, therefore, is a mixture of materials, the only common characteristic being the petrographic type of the individual grains. Since various technicians contri-

buted to the sample, some personal bias may also have been introduced.

Most of the samples represent the -19 mm, +9.5 mm size. Few of the samples were -9.5 mm, +6.7 mm, for lack of the smaller size material in sufficient quantity.

TESTING METHODS

The aggregates were subjected to tests that determined their various properties and durability. The tests used were:

COARSE AGGREGATE PETROGRAPHIC ANALYSIS

PIT NAME _____ LAB NO. _____

DATE _____ FRACTION _____ ANALYST _____

TYPE NO	TYPE	WEIGHT	%	GRANULAR & 5/8" CRUSHED CORRECTION	
1	CARBONATES (hard)				
20	CARBONATES (slightly weathered)				
2	CARBONATES (sandy, hard)				
21	CARBONATES (sandy, medium hard)				
23	CARBONATES CRYSTALLINE (hard)				
3	SANDSTONE (hard)				
22	SANDSTONE (medium hard)				
4	GNEISS - SCHIST (hard)				
5	QUARTZITE (coarse and fine grained)				
6	GREYWACKE - ARKOSE (hard and medium hard)				
7	VOLCANIC (hard and slightly weathered)				
8	GRANITE - DIORITE - GABBRO				
9	TRAP				
	TOTAL GOOD AGGREGATE				
24	CARBONATES CRYSTALLINE (slightly weathered)			x 2	
40	CARBONATES (soft, slightly shaley)			x 2	
41	CARBONATES (sandy, soft and soft pitted)			x 2	
42	CARBONATES (deeply weathered)				
25	GNEISS (soft) SCHIST (medium hard)			x 2	
26	CHERT - CHERTY CARBONATES			x 2	
27	GRANITE - DIORITE - GABBRO (brittle)			x 2	
28	VOLCANIC (soft)			x 2	
52	ENCRUSTATION			x 2	
29	ARGILLITE			x 2	
	TOTAL FAIR AGGREGATE				
43	CARBONATES (shaley or clayey)				
44	CARBONATES (ochreous)				
45	CHERT - CHERTY CARBONATES (leached)			x 5	
46	SANDSTONE (soft friable)			x 3	
48	VOLCANIC (very soft, porous)			x 3	
49	CARBONATES CRYSTALLINE (soft)			x 3	
50	GNEISS (friable)			x 3	
51	GRANITE - DIORITE - GABBRO (friable)			x 3	
53	CEMENTATIONS			x 3	
54	CEMENTATIONS (total)			x 3	
55	SCHIST (soft)			x 3	
56	SILTSTONE			x 3	
	TOTAL POOR AGGREGATE				
60	OCHRE				
61	SHALE				
62	CLAY				
63	VOLCANIC OR SCHIST (decomposed)				
	TOTAL DELETERIOUS AGGREGATE				
	TOTALS				

% GOOD _____ x 1 = _____

% FAIR _____ x 3 = _____

% POOR _____ x 6 = _____

% DELETERIOUS _____ x 10 = _____

EST PERCENT CRUSHED

EST PERCENT FLATS & ELONGATED

HOT MIX, MULCH AND CONCRETE P N

CORRECTED GRANULAR AND 5/8" CRUSHED P N

Figure 1. *Ontario Ministry of Transportation and Communications standard form for coarse aggregate petrographic analysis.*

Water adsorption
Water absorption (24 hour immersion)
Water absorption (vacuum saturation)
Specific gravity
Bulk expansion
Freeze-thaw loss
Impact strength (wet and dry aggregate)

The tests were chosen to reflect several criteria, which included: relationship of the test to basic properties of aggregates; ability of the test to replicate natural environments of aggregate degradation; and past experience with the usefulness of the test in aggregate evaluation.

FREEZE-THAW TESTS

Freeze-thaw tests simulate the response of the aggregate to freezing and thawing in nature. Although the conditions of laboratory freezing and thawing may differ from those encountered in nature, the tests attempt to replicate these conditions as closely as possible. The freeze-thaw tests were performed on unconfined aggregate, because concrete freezing tests are much more involved, costly, and time consuming. The process and effects of freezing of unconfined aggregate may be quite different than those of the same aggregate in Portland cement concrete, but tests on unconfined aggregate are the best practical alternative.

Sodium chloride salt was used at 5 percent by weight concentration to accelerate the test. Mason jars of 1 pint (approximately 500 ml) were used to contain, saturate, and freeze the sample. About 300 g of sample was used for each test. The samples were saturated in the salt solution for 24 hours and then drip-drained prior to first freezing. One-hundred percent relative humidity condition was maintained over drained samples by sealing the jars. A cycle of 16 hours freezing at –20°C or less, and thawing at room temperature (22°C) was used. Freezing and thawing was repeated for five cycles. The jars, placed on their sides, were rotated one quarter turn after each cycle. Following the final cycle, the samples were dried for 24 hours at 105°C, cooled, and back-sieved on 9.5 mm (3/8 inch) sieve. The percent loss was determined in the usual way (ASTM 1981, C88).

SORPTION TESTS

Water adsorption, absorption, and degree of saturation are some of the basic properties of aggregate. Much of the degradation experienced by aggregate is the result of rock-water (ice) interaction. The water enters and occupies the internal pores of the rock, and it is the response of the rock-water system to environmental changes that dictates the aggregate durability.

Adsorption of water vapour on internal pore surfaces gives an approximation of the internal surface area of the aggregate fragments, and thus also an indication of the dominant pore size. It has been recognized that a dominance of small pore sizes is deleterious. Thus, adsorption can be used as a measure of potential lack of durability of the aggregate.

Water adsorption was determined by placing a dry, cool sample in a humidity chamber maintained at 95 percent relative humidity at room temperature (about 22 °C). The humidity in the chamber was maintained by saturated copper sulphate solution. Three days (72 hours) were deemed sufficient for near-equilibrium to be achieved. The sample was then weighed, and the percent difference between dry and equilibrated weight was determined. Temperature control of the chamber to within 1 degree is essential for precision in this test.

Absorption, in addition to its importance in mix design and bitumen absorptiveness, also has a bearing on durability. The amount of water and degree of saturation may determine the degree of expansion of the aggregate on freezing, and expulsion of water (ice) into surrounding cement paste. Absorption, of course, is already in use as a specification criterion. Degree of saturation, as determined by vacuum absorption or boiling, is not commonly used as a test of durability.

Water absorption is determined in the established manner after 24 hour saturation on a surface dried sample (ASTM 1981, C127). Vacuum saturation can be done in two ways: by placing a dry sample in a vacuum dessicator, evacuating the air, and introducing water into the chamber while the sample is under vacuum. De-gassed water is used. The water is able to fill all the pores, since air does not block the passages. After 24 hour saturation in the dessicator, the sample is surface dried and weighed, and absorption reported as percent weight gain over dry sample.

An alternate method, requiring less equipment, and suitable for multiple sample testing is the boiling method. It can only be used on samples that do not react with boiling water; this includes the vast majority of aggregates. Any means of bringing a container with water-covered sample to boil is suitable. In this case, the same canning jars used for freeze-thaw tests were used. A sample of about 300 g was placed in each jar. The jar was filled with water to 3 cm above the sample, and covered lightly to decrease evaporation. Twenty to thirty jars were placed in a convection oven at 120-130°C until the water began to boil vigorously. After boiling for 10 minutes, the samples were removed and allowed to cool for 24 hours. The water of absorption was then determined in the usual way. The water vapour has pressure equivalent to atmospheric pressure at boiling, thus displacing all the air in the pores of the sample. On cooling, water displaces the vapour, filling the pores.

BULK SPECIFIC GRAVITY

Bulk specific gravity was determined by two methods: ASTM C127 (1981), and by use of large-mouth pycnometer bottle. The above methods are fairly standard and need not be described here.

BULK EXPANSIVITY

An aggregate may undergo large volume changes from dry to saturated state (and vice versa). Prior research by the author (Hudec 1980a) has shown that expansions (or contractions) are potentially equivalent to several tens of degrees thermal expansion, even though they take place at a constant temperature. Thus, a confined, dry aggregate can exert considerable stress due to its expansion on saturation.

It is relatively easy to measure linear expansion of dimensioned sample such as core. However, core is seldom representative of the total crushed bulk sample. Therefore, a method was devised to measure the bulk expansion of a crushed sample. A steel cylinder 40 cm high, with 10.3 cm inside diameter and 0.5 cm wall thickness was fitted with perforated screen at the bottom to allow water access into the cylinder. Crushed sample was placed into the cylinder in 5 cm layers. After each layer, the sample was shaken and tamped down to insure maximum packing. A total thickness of approximately 20 cm was used for most tests. In some cases, insufficient sample was available, so spacers were used to compensate for the smaller mass. The thickness of the sample was determined to within 0.5 cm. A spring-loaded platten connected to a micrometer gauge sensitive to 0.00002 cm was placed on top of the sample, and the gauge mechanism fixed in place by expanding friction shoes. The gauge was set to zero, and the cylinder was carefully lowered into a tall tank of water until the water level came to the level of the platten, completely covering the sample. Readings were taken at 1, 5, and 30 minute intervals. Since the only variable was the sample thickness, the result were expressed in terms of the linear thickness, although the measurement represents a bulk, or three-dimensional expansion of the sample. A dimensionless number, representing an expansion/contraction coefficient, was thus obtained.

Most samples showed no change, or slight initial contraction. Few samples showed significant expansion. The amount of the expansion is perhaps less significant than the fact that expansion does take place. Those samples that showed significant expansion were generally those with poor aggregate properties.

Table 1. *Results of tests for properties and durability of aggregate samples.*

Sample Description	MTC Type	PN Factor	Adsorption, %$	Absorption, 24 hr. Sat.	Absorption, Vac. Sat.	Specific Gravity, pyc.	Specific Gravity, imm.	Bulk expan., x 10-6	Freeze-Thaw Loss, %	Impact Loss 1, Dry Loss, %	Impact Loss 1, Wet Loss, %	Impact Loss 2 Dry Loss, %	Impact Loss 2 Wet Loss, %
HARD GNEISS	4	1	0.058	0.117	0.265	2.725	2.717	0.033	0.133	28.40	25.88	21.71	27.64
M.HARD CARB.	21	1	0.957	1.203	1.836	2.686	2.690	0.732	8.850	18.07	20.38	20.20	22.62
HRD.SANDY 1	2	1	1.015	0.857	1.210	2.661	3.015	0.033	4.420	13.70	13.60	19.40	16.30
SOFT CARB.	40	3	0.487	1.950	2.122	2.635	2.666	1.930	11.600	25.10	26.00	24.00	27.70
HRD.SST.	3	1	0.262	0.824	1.286	2.623	2.636	0.033	5.140	12.90	24.60	19.50	33.30
DW CARB	42	3	0.772	2.740	3.300	2.632	2.620	2.290	9.720	28.40	27.60	21.10	35.90
HARD VOLC.	7	1	0.283	0.300	0.480	2.840	2.810	0.166	1.030	7.08	1.20	8.50	10.30
UNWTH CHT.	26	3	0.390	1.617	1.761	2.614	2.622	0.030	3.150	18.10	17.20	15.50	16.00
MD.HD.SST.	22	1	0.280	1.518	1.963	2.602	2.582	2.500	6.300	31.90	32.70	26.30	32.60
GRANITE	8	1	0.190	0.124	0.483	2.710	2.752	0.030	2.164	25.08	23.80	22.50	29.20
M.H.SND.CARB.	21	1	0.980	2.119	2.324	2.612	2.605	0.831	4.700	21.50	15.70	19.60	18.30
LCHD. CHRT.	45	6	0.220	4.225	5.078	2.492	2.467	0.066	8.209	12.20	11.60	16.70	14.20
MD.HD.CARB.	21	1	0.500	1.326	1.732	2.696	2.732	0.931	3.725	18.20	21.60	16.50	21.70
QUARTZITE	5	1	0.202	0.157	0.224	2.669	2.667	0.033	2.164	18.30	21.50	20.50	20.90
HRD.SND.CARB.	3	1	0.750	0.481	0.964	2.660	2.631	0.599	2.396	18.70	24.60	22.80	24.70
GWCKY & ARKOSE	6	1	0.190	0.090	0.187	2.733	2.734	0.199	0.432	7.78	12.80	7.37	10.90
ENCRUSTED	52	3	0.517	0.046	0.623	2.686	2.675	0.070	4.900	15.90	19.70	18.80	20.10
SHALEY-CLAY	43	6	1.087	3.147	4.198	2.602	2.586	5.692	11.980	28.80	31.50	30.70	33.90
SILTSTONE	56	6	0.277	2.475	2.349	2.567	2.579	0.070	3.300	18.80	26.80	18.90	26.20
CLAY	62	10	1.197	3.417	4.654	2.569	2.488	3.800	16.700	51.30	38.60	51.80	32.90
TRAP	9	1	0.450	0.050	0.060	3.142	3.083	0.133	1.461	10.60	8.90	6.40	8.70
SFT.WTH.CARB.	24	3	0.827	1.235	1.692	2.699	3.115	1.400	6.600	21.00	22.60	28.40	25.10
BRIT.GRANITE	27	3	0.325	0.746	0.722	2.668	2.636	0.070	5.400	35.10	36.20	34.20	36.30
SHALE	61	10	1.062	2.407	3.359	2.552	2.521	5.689	33.400	29.30	34.90	29.90	40.20
SFT.GNEISS	25	3	0.160	0.492	0.265	2.732	2.730	0.070	4.200	38.10	34.60	33.90	36.83
FRIAB.SST.	46	6	0.572	3.186	4.317	2.492	2.483	7.400	10.400	47.70	40.50	44.00	41.80
HRD.SANDY CARB.	2	1	1.200	1.240	2.134	2.611	2.676	0.230	6.400	13.50	16.00	14.00	13.40
HARD CRS CARB.	23	1	0.175	0.037	0.367	2.799	2.787	0.030	1.900	21.90	26.00	22.00	25.40
FRIAB.GNEISS	50	6	0.477	1.572	2.241	2.722	2.677	5.923	18.500	50.50	54.40	49.10	51.40
HARD CARB.	1	1	0.375	0.549	1.195	2.725	2.717	0.030	3.400	19.60	20.90	18.05	2.30
SFT.SNDY.CARB.	41	3	0.662	3.000	3.424	2.573	2.525	3.683	7.100	22.00	29.20	27.10	27.70

AGGREGATE IMPACT TEST

From previous work, it was established that the impact test simulates the "Los Angeles Abrasion" test. Since insufficient sample was available for the Los Angeles test, the "Aggregate Impact" test was substituted. The apparatus used was imported from England. The procedure used was that recommended by the British Standards Institute (BS 812) with slight modifications. The test consists of dropping a 5 kg weight on a sample contained in a cup from a 38 cm height, a total of 15 times. The sample is removed and backsieved on a #8 (2.36 mm) sieve. The loss is reported as percent fines passing relative to original weight.

Duplicate tests were run on both dry and saturated samples. Thus a total of four test results are available for most samples. The sample was saturated for 24 hours in water prior to the test, and dried prior to back-sieving.

DISCUSSION OF RESULTS

The results of the tests are given in Table 1. The results were grouped according to the current Ontario Ministry of Transportation and Communications durability factors.

Table 2. *Statistical means of tests, listed by durability category.*

	Durability Category			
Tests:	1	3	6	10
Adsorption, %, 95% RH	0.49	0.52	0.53	1.13
Absorption, %, Immersion	0.71	1.53	2.92	2.91
Absorption, %, Vac. Sat.	1.05	1.74	3.64	4.01
Bulk Expansion Coef. x 10 -6	0	0.63	0.63	4.5
Freeze-Thaw, %, Loss	3.42	6.60	10.46	25.08
Spec. Gravity (Pyconmeter)	2.72	2.66	2.58	2.56
Spec. Gravity (Suspension)	2.74	2.70	2.56	2.51
Impact Loss, %, Dry Sample	13.60	25.42	31.74	38.51
Impact Loss, %, Wet Sample	21.36	27.41	30.61	36.65

The statistical means for each subgroup in each test were calculated (Table 2). As can be seen, there are significant differences between the test results for different durability categories, but the differences between categories are not always consistent from test to test. Thus, no significant difference can be found in the results of adsorption tests between durability categories 1, 3 and 6, but a doubling of adsorption is seen in category 10. Absorption after 24 hour saturation is seen to approximately double from category 1 to 3 and again double from category 3 to 6, but remains unchanged from category 6 to 10.

Specific gravity decreases as the durability factor increases. This suggests that the more porous, weathered rocks are less durable, a trend well in keeping with observations. The freeze-thaw results show the most dramatic change between different categories, approximately doubling with each higher category. Impact loss on dry samples shows the largest jump from category 1 to 3, then a steady increase from category 3 to 10. Impact loss an a wet sample follows a similar pattern.

It is evident that the durability factors assigned to the various rock types by MTC do reflect to a large degree their properties. The results show that the PN procedure is a useful one.

To illustrate the relationships existing between different properties and test results, a simple linear regression analysis was done on pair of test results. Those with the greatest correlation were selected and are presented in Figures 2 through 6. In each figure, the pertinent statistical parameters are given for the variables and the correlation. A line of best fit (dotted line) is drawn in each case.

Figure 2 shows the relationship between 24 hour immersion absorption and vacuum saturation. The solid black line is a "no change" line. The dotted line is the line of best fit drawn through the points (asterisks). The position of the points and the dotted line, and its angle with respect to the "no change" line, indicate that, on the average, the greater the normal saturation, the proportionately greater the vacuum saturation.

Figure 3 shows the relationship between loss in the freeze-thaw test as measured on the original 9.5 mm (3/8 inch) sieve and on the #12 sieve (1.7 mm). The loss on the 9.5 mm sieve measures the number of particles affected by the freeze-thaw action; the loss on the 1.7 mm sieve, on the other hand, determines the degree of surface spalling or complete deterioration due to the frost action.

Figure 4 gives the relationship between the freeze-thaw loss and water adsorption. The correlation is rather low, but still significant. It serves to illustrate that the breakdown due to frost action is, to a large measure, due to the adsorbed water content, which in turn is related to internal surface area of the sample. In carbonate rocks, the internal surface area is related to the clay content.

Figure 5 illustrates the relationship between specific gravity of the sample and its absorption. The more porous the material, the lower the specific gravity, and greater the absorption. Signficantly, no relationship was found between absorption and freeze-thaw loss. Likewise, no relationship exists between absorption and adsorption (Figure 6). This indicates that the larger pore space does

not necessarily imply larger internal surface area, and that it is the internal surface area rather than absolute porosity that determines the durability of rock.

STEPWISE REGRESSION ANALYSIS

To determine the relationship of the various test results to the PN category, a statistical procedure called stepwise regression analysis was performed. The current Ministry of Transportation and Communications PN category for each sample was considered as the dependent variable and all the test results as independent variables. The computer-aided analysis selects those independent variables (tests) that have the greatest bearing on the dependent variable (PN category), and produces an empirical equation of the relationship. The results of the analysis are given in Table 3. The empirical relationship has a high correlation, and can therefore be considered quite reliable.

The variables that most effect the PN category determination are, in order of significance, adsorption, vacuum absorption, specific gravity, freeze-thaw loss, and impact loss. The first three variables are inherent properties of the aggregate material, the last two are durability tests. This suggests that more attention should be paid to the properties of the samples than to results of simulation tests. In fact, the first three variables, i.e. adsorption, vacuum absorption, and specific gravity alone can define the durability factor. The last two improve the relationship only slightly.

The derived empirical relationship can be used to calculate the PN durability factors for each petrographic type. The calculated factors are in all probability more reliable than the arbitrary factors used to date. The calculated factors are shown in Table 4. As can be seen, some rock-types have calculated factors that are relatively close to the original factors. Others, however, have calculated factors that are one to three times more or less than the original factors.

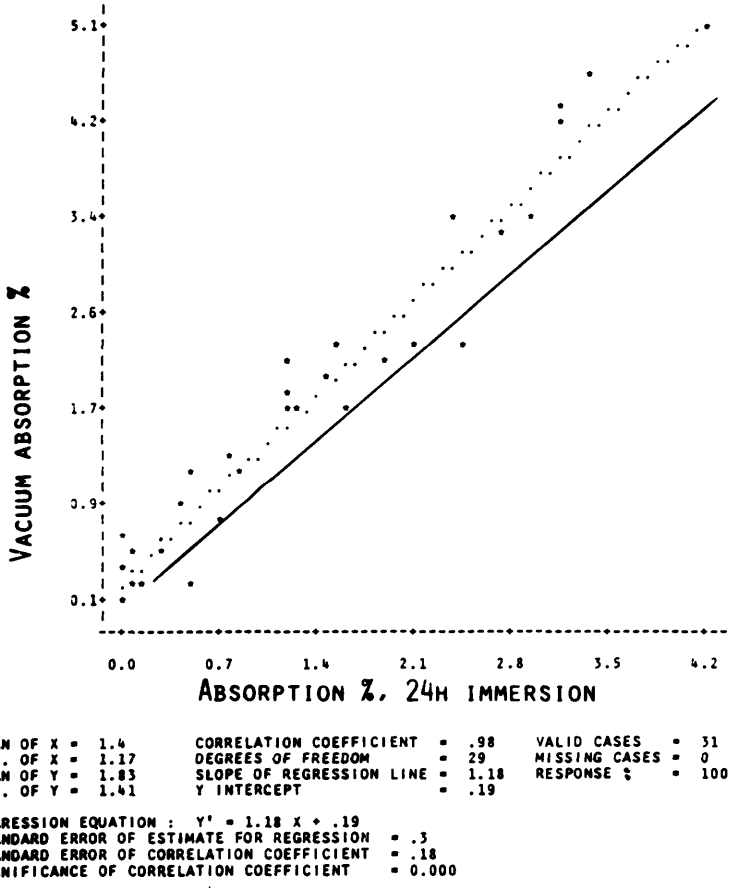

Figure 2. *Relationship between normal and vacuum saturation. Solid line represents "no change"; dotted line is calculated regression line; asterisks are data points.*

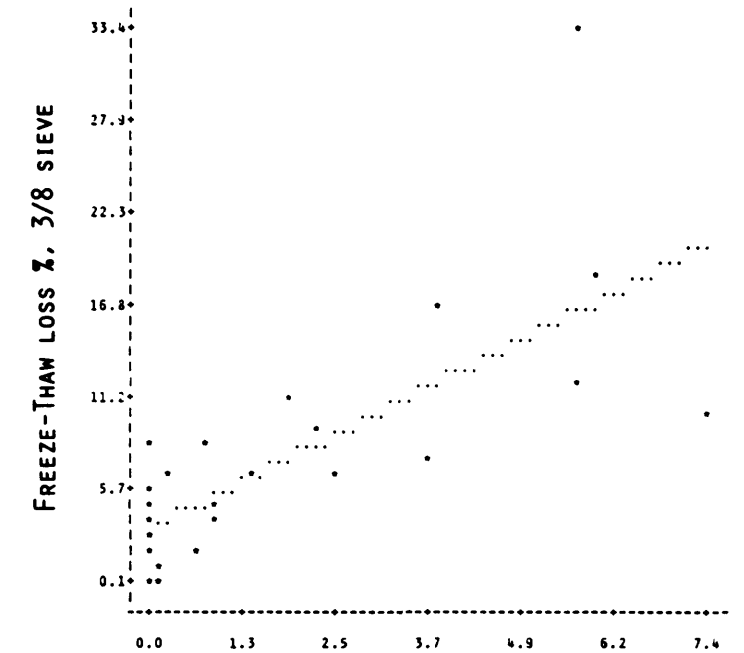

Figure 3. *Freeze-thaw loss as determined on 3/8 inch and #12 sieves. Symbols as for Figure 2.*

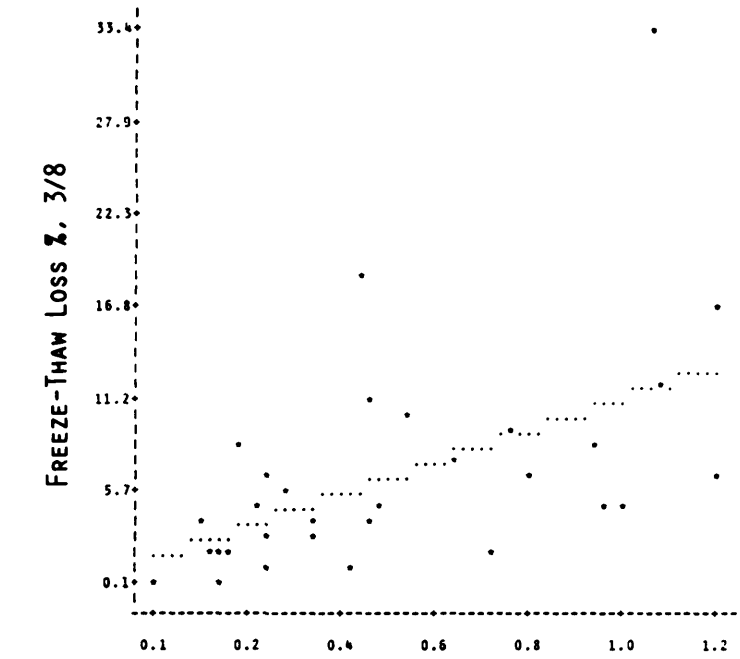

Figure 4. *Relationship of adsorption to freeze-thaw loss. Symbols as for Figure 2.*

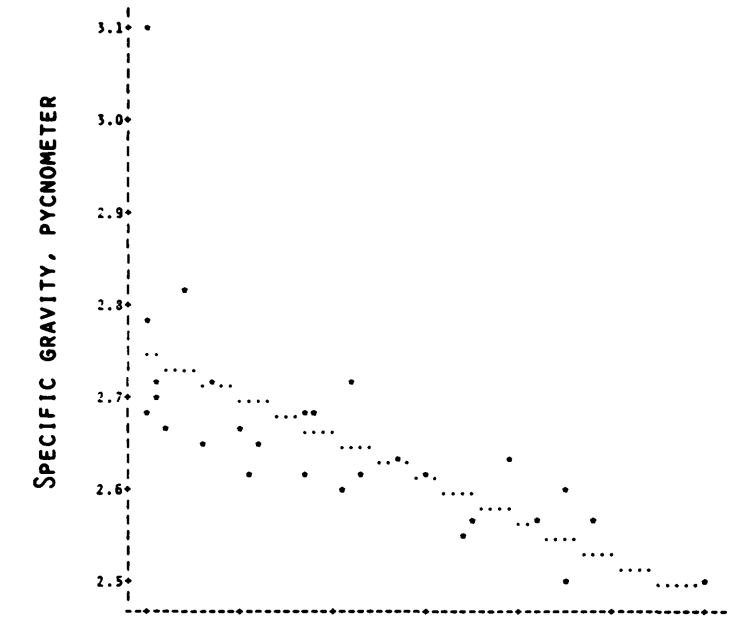

Figure 5. *Inverse relationship of absorption to specific gravity. Symbols as for Figure 2.*

CONCLUSIONS AND RECOMMENDATIONS

1. Some of the petrographic types have a present category or multiplier factor that is far out of phase with the projected behaviour of the rock.
2. The behaviour of the rock-types that give anomalous factors should be further re-evaluated by service record and additional durability tests.
3. The sample set of 31 rock-types is too small to draw definitive conclusions from. An additional 100 samples are currently being processed to improve the empirical relationship by increasing the statistical base.
4. It is suggested that rather than the 1, 3, 6, and 10 factors now in use, each rock type should be assigned a whole number factor ranging from 1 to 10.
5. As a check to the standard PN, the results of adsorption, vacuum absorption, specific gravity, and impact loss obtained for the entire sample as part of routine testing should be used in an empirical relationship derived in this research to give a 'calculated PN'. Where the two PNs differ by a certain percentage, the sample should be subjected to 'umpire tests' or re-tested. The allowable percentage difference and the 'umpire tests' should be established.

ACKNOWLEDGMENTS

The samples used in the first phase of the study were provided by the Ontario Ministry of Transportation and Communications. Mr. Chris Rogers of the ministry was instrumental in selecting and preparing the sample set.

The author was assisted in the laboratory by Barbara Phaneuf and Gayna Lee Sinclair, students in the Geology Department, University of Windsor, who did most of the routine laboratory testing.

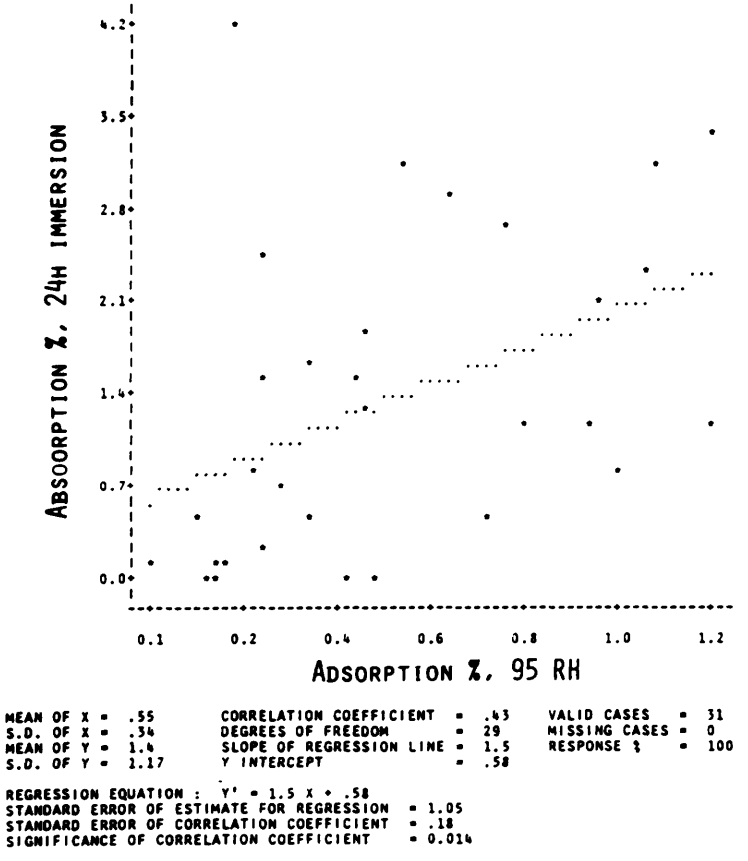

Figure 6. *Independence (lack of correlation) of adsorption and absorption properties. Symbols as for Figure 2.*

Table 3. *Regression coefficients, correlation matrix, and empirical equation, derived from stepwise regression analysis of test results.*

A. REGRESSION COEFFICIENTS

Var.	Variable Label	Mean	S.D.	Coeff.
DV	MTC Category	2.90	2.62	
K	Constant			-5.922
IV1	Adsorption %	0.55	0.35	-1.510
IV2	Absorption, %, Boil	1.83	1.44	0.859
IV3	Spec. Grav., Pyc.	2.67	0.12	2.032
IV4	Freeze-thaw Loss, %, 3/8	6.77	6.65	0.208
IV5	Impact Loss 2, %, Dry	23.53	10.67	0.053

Coefficient of Multiple Correlation = .889 (Corrected = .876)

B. CORRELATION MATRIX

	DV	IV1	IV2	IV3	IV4
IV1	0.353				
IV2	0.731	0.519			
IV3	-.484	-.288	-.699		
IV4	0.800	0.531	0.622	-.411	
IV5	0.654	0.258	0.471	-.410	0.583

C. EMPIRICAL EQUATION

Calculated P.N. = - 5.922
Category - 1.510 x Adsorption %
+ 0.859 x Vacuum Absorption %
+ 2.032 x Specific Gravity
+ 0.208 x Freeze-Thaw Loss %
+ 0.053 x Impact Loss, Dry, %

Table 4. *Comparison of calculated durability factors and Ministry of Transportation and Communications petrographic numbers (PN).*

Rock Type	MTC PN	Calc. PN	MTC Type
Hard Gneiss	1	0.86	4
M. Hard Carb.	1	2.51	21
Hrd. Sandy 1	1	0.87	2
Hrd. Sst.	1	2.15	3
Hard Volc.	1	0.43	7
Md. Hd. Sst.	1	3.26	22
Granite	1	1.29	8
M.H. Snd. Carb.	1	1.85	21
Md. Hd. Carb.	1	1.87	1
Quartzite	1	0.86	5
Hrd. Snd. Carb.	1	0.82	3
Gwcky & Arkose	1	-0.08	6
Trap	1	0.41	9
Hrd. Sandy Carb.	1	1.41	2
Hard Crs Carb.	1	1.31	23
Hard Carb.	1	1.67	1
Soft Carb.	3	4.13	40
Dw Carb.	3	4.17	42
Unwth. Cht.	3	1.72	26
Encrusted	3	1.24	52
Sft. Wth. Carb.	3	2.58	24
Brit. Granite	3	2.49	27
Sft. Gneiss	3	2.22	25
Sft. Sandy Carb.	3	4.09	41
Lchd. Chrt.	6	5.69	45
Shaley-Clay	6	5.38	43
Siltstone	6	2.51	56
Friab. Sst.	6	6.41	46
Friab. Gneiss	6	7.19	50
Clay	10	7.64	62
Shale	10	9.01	61

REFERENCES

ASTM
1981: Annual ASTM Standards, Part 14; American Society for Testing and Materials, C127, C88.

Bayne, R.L., and Greenland, C.W.
1949: A Study of Aggregate Test Results Related to the Performance of Concrete Pavements; Ontario Department of Highways.

Bayne, R.L. and Brownridge, F.C.
1955: Petrographic Analysis for Determining Quality of Coarse Aggregates; Proceedings, 36th Convention Canadian Good Roads Association, p. 114-122.

Benson, P.E., and Ames, W.H.
1975: The Precision of Selected Aggregate Test Methods; Trans. Res. Rec. No. 539, p. 85-93.

Bloem, D.L.
1966: Soundness and Deleterious Substances; Significance of Tests and Properties of Concrete and Concrete Aggregates; American Society for Testing and Materials, Special Technical Publication 169-A, p. 497-512.

Brink, R.H., and Timms, A.G.
1966: Weight, Density, Absorption and Surface Moisture; Significance of Tests and Properties of Concrete and Concrete Aggregates; American Society for Testing and Materials, Special Technical Publication 169-A, p. 432-442.

British Standards Institute
1975: Methods for Sampling and Testing Mineral Aggregates, Sands, and Fillers; BS 812.

DePuy, G.W.
1965: Petrographic Investigations of Rock Durability and Comparisons of Various Test Procedures; Journal American Association Engineering Geology, Vol. 2, p. 31-46.

Dhir, R.K., Ramsay, D.M. and Balfour, N.
1971: A Study of the Aggregate Impact and Crushing Value Tests; Journal of the Institute of Highway Engineers, November 1971, p. 1727.

Dolar-Mantuani, L.
1972: Harmful Constituents in Natural Concrete Aggregates in Ontario; 24th International Geology Congress, Montreal, Proceedings Sect. 13, p. 227-234.

Dolch, W.L.
1966: Porosity: Significance of Tests and Properties of Concrete and Concrete Aggregates; American Society for Testing and Materials, Special Technical Publication 169-A, p. 443-461.

Dunn, J.R., and Hudec, P.P.
1965: The Influence of Clays on Water and Ice in Rock Pores; Phase 4 of Physical Research Project No. 4, Acceptability Tests for Coarse Aggregates, Bureau of Physical Research, New York State, Department of Public Works, Report RR65-5.

Dunn, J.R., and Hudec, P.P.
1966: Water, Clay and Rock Soundness; Ohio Journal of Science, Volume 66, No. 2.

Hanks, J.N.
1962: The Effects of Simple Factors on the Reproducibility of the Los Angeles Abrasion Test; Proceedings First Conf. Aust. Rd. Res. Bd., volume 1, pt. 2 p. 982-994.

Hudec, P.P.
1976: Development of Durability Test for Shales in Embankments and Swamp Backfills; University of Windsor R.R. #216, Ontario Ministry of Transportation and Communications, Research and Development Division.

1980a: Durability of Carbonate Rocks as Function of Their Thermal Expansion, Water Sorption, and Mineralogy; ASTM Spec. Tech. Pub. 691, p. 497-508.

1980b: Effect of De-icing Salts on Deterioration and Dimensional Changes of Carbonate Rocks; American Society for Testing and Materials, Special Technical Publication 691, p. 629-640.

Hudec, P.P., and Rogers, C.A.
1976, The Influence of Rock Type, Clay Content and the Dominant Cation on the Water Sorption Capacity of Carbonate rocks; Abstract, Geological Association of Canada, Annual Meeting, Edmonton, May 1921.

Hudec, P.P., and Sitar, N.
1975: Effect of Water Sorption on Carbonate Rock Expansivity; Canadian Geotechnical Journal, Vol. 12, p. 179-186.

Larson, T.D., and Cady, P.D.
1969: Identification of Frost-susceptible Particles in Concrete Aggregate; Natural Hwy. Res. Prog. Rept. No. 66, 62p.

Larson, T.D., *et al.*
1964: A Critical Review of Literature Treating Methods of Identifying Aggregates Subject to Destructive Volume Change When Frozen in Concrete and a Proposed Program of Research; Highway Research Bd. Spec. Rept. No. 80.
1965: Identification of Concrete Aggregates Exhibiting Frost Susceptibility; NCHRP Rept. 15, 66p.
1968: Methods for Aggregate Evaluation; Pennsylvania Department of Highways and Bureau of Public Works, Rept. 1.
1969: Methods for Aggregate Evaluation; Pennsylvania Department of Highways and Bureau of Public Works, Rept. 2.

Litvan, G.G.
1973: Pore Structure and Frost Susceptibility of Building Materials; Research Paper No. 584 of Division of Building Research, Natural Resource Council, Canada.

MacInnis, C., and Beaudoin, J.J.
1969: Effect of Degree of Saturation on the Frost Resistance of Mortar Mixes; ACI Journal, Vol. 65, p. 203-208.

Mather, B.,
1960: Petrology of Concrete Aggregates; Proceedings, 11th Symposium on Highway Engineering Geology at Florida State University, Published by Florida Geological Survey, p. 9-22.

Mielenz, R.C.
1958: Discussion of the Method of Petrographic Examination of Aggregate Employed by the Laboratories of the Department of Highways of Ontario; Internal Rept. July 8, 1958.
1978: Petrographic Examination; Significance of Tests and Properties of Concrete and Concrete Aggregates; American Society for Testing and Materials, Special Technical Publication 169-B, p. 539572.

New York Department of Public Works,
1963: A Further Investigation of Abrasion; Physical Research Project 4, Research Report 63-1, New York Department of Public Works, Albany, N.Y.

Powers, T.C.
1955: Basic Consideration Pertaining to Freezing and Thawing Tests; American Society for Testing and Materials, Proceedings, Vol.55, p.1132-1155.
1975: Freezing Effects in Concrete; ACI Special Publication 47, p. 1-11.

Proctor and Redfern Limited
1974: Mineral Aggregate Study, Central Ontario Planning Region; Ontario Ministry of Natural Resources.

Rhoades, R., and Mielenz, R.D.
1948: Petrographic and Mineralogic Characteristics of Aggregates; Symposium on Mineral Aggregates, American Society for Testing and Materials, Special Technical Publication 83.

Rogers, C.A.
1978: Aggregate Durability Tests in Ontario: Precision and Correlation with Field Performance; Ontario Ministry of Transportation and Communications, Materials and Lab Services Section, Unpublished Draft Report.

Stewart, N.B.
1969: Detailed Petrography - An Aid in the Evaluation of Gravel Aggregates for Freeze-Thaw Resistance; Proceedings, 5th Forum on Geology of Industrial Minerals, Harrisburg, Pennsylvania, Pennsylvania Geological Survey, Mineral Resource Report 64, p. 55-89.

Sweet, H.H.
1948: Physical and Chemical Tests of Mineral Aggregates and Their Significance; Symposium on Mineral Aggregates, American Society for Testing and Materials, Special Technical Publication 83, p. 49-73

Verbec, G., and Landgren, R.
1960: Influence of Physical Characteristics of Aggregates on Frost Resistance of Concrete; American Society for Testing and Materials, Proceedings, Vol. 60, p. 1063-1079.

Yedloky, R.J., and Dean, J.R.
1961: Petrographic Features of Sandstones that Affect Their Suitability for Road material; Journal of Sedimentary Petrology, Vol. 31, p. 372-389.

Grant 118 Surface Electromagnetic Mapping in Selected Positions of Northern Ontario

O.M. Ilkisik, D.T. Hsu, J.D. Redman, and D.W. Strangway
Department of Geology, University of Toronto

ABSTRACT

In the summer of 1981, an audio-magnetotelluric (AMT) survey was completed in four locations in northern Ontario. Apparent resistivities, for frequencies from 13 Hz to 8570 Hz, were measured at 101 stations.

A survey in Moody Township near Lake Abitibi clearly outlined the clay properties and thickness, and also showed that, at the lower frequencies, we are able to map the electrical resistivity of the basement beneath the clay and/or esker cover. At one locality, the response of the bedrock is strongly anisotropic, perhaps reflecting anisotropy of the metasediments. If this proves to be the case, it then will be possible to recognize steeply dipping metasediments with the AMT method when they are not exposed.

In Marter Township near Engelhart, two survey profiles mapped a deposit of clay-rich overburden, and located high resistivities over a large esker. These profiles were taken in an area where the overburden had been examined by a rotary drilling program in 1979 by the Ontario Geological Survey. Our results can be interpreted to be in general agreement.

Measurements in the Elk Lake area appear to be strongly affected by two contact zones, and they show inhomogeneity and anisotropy. The major feature in the area is the Montreal River Fault, which runs under the town of Elk Lake. The shape of the profiles suggests that the fault dips to the southwest. However additional field work is needed to examine the complexities introduced by major fluid-filled faults.

Surveys in Bowman Township, near Matheson, were conducted on a two-dimensional grid and the data consistently showed the presence of four layers. A thin resistive surface layer a few metres thick is followed by a very conductive layer of clay. Bedrock is at a depth of 50-100 m and is very resistive; the resistivity drops sharply at depths of several kilometres. This survey provided a map of the resistivity and the thickness of the clay-rich glaciolacustrine sediments and clearly outlines near surface features such as an esker.

In addition to the AMT survey, we have collected 42 clay samples from sites in Larder Lake and in Marter Township to study their electrical properties. Laboratory measurements show that in the Kirkland Lake area, the clays have resistivities on the order of 20 ohm-m, in agreement with the high frequency AMT data over clay-rich overburden.

INTRODUCTION

An audio-magnetotelluric (AMT) survey in northern Ontario was carried out during the summer of 1981. The purpose of the survey was to conduct surface electromagnetic mapping in selected positions in the clay belts of northern Ontario, where a large proportion of the Early Precambrian volcanic-sedimentary formations are mantled by glaciolacustrine deposits. The main interest was to characterize the electrical structure of the extensive clay-covered regions, the electrical properties of the clay itself, and to test the capability of penetrating through this conductive top layer to identify anomalies in the bedrock below. There are major problems encountered using some types of conventional EM mapping methods. A second interest was to study the region covered by the Huronian Supergroup, its resistivity characteristics, and the possibility of determining its thickness and thus mapping the surface topography of the Early Precambrian basement.

The work in northern Ontario concentrated in Bowman Township near Matheson, in Moody Township near Lake Abitibi, in Marter Township near Engelhart and around James Township near Elk Lake (Figure 1). The audio-magnetotelluric method was used successfully in each of these areas, to map the thickness of clay-rich overburden and to unambiguously determine some of the characteristics of the underlying bedrock.

Additionally, we have collected 42 clay samples from sites in Larder Lake and in Marter Township to study the electrical properties and their frequency dependence.

One profile in Moody Township (A, Figure 1) in the Great Clay Belt, and two in Marter Township (B and C) in the Little Clay Belt, are composed of 15, 9 and 8 sites respectively. An extensive, reverse-circulation, rotary drilling program was completed in 1979 (Averill and Thompson 1981). The surficial geology in Marter Township is therefore well known. The fourth profile, which is along Highway 560 near the town of Elk Lake and extends south to Willet Township, includes 19 AMT stations. Eleven of these are located in the area covered by the Huronian Supergroup.

A detailed grid survey including 50 sites was completed in Bowman Township and the eastern part of Currie Township to map the resistivity variation both laterally and vertically.

AMT METHOD AND FIELD PROCEDURE

Natural fields in the audio-frequency band (10 - 10^4 Hz) are due to thunderstorm energy propagating in the earth-ionosphere cavity. They occur more or less worldwide and propagate around the world. This implies that the AMT sources can be approximated as plane waves vertically incident to the earth's surface. Cagniard (1953) showed how natural electromagnetic fluctuations could be used as sources for probing the electrical structure of the earth. Using this approach, it was possible to measure the ratio of the electric field to the magnetic field and thus to determine the apparent resistivity. At one particular frequency the apparent resistivity (ρ_a) is defined using the relationship:

$$\rho_a = \frac{1}{\omega\mu}\left\{\frac{E}{H}\right\}^2$$

E: electric field in volts/m
H: magnetic field in ampereturns/m
ω: angular frequency ($2\pi f$)
μ: magnetic permeability

Information on the variation of apparent resistivity with depth is related to electromagnetic wave penetration, referred to as skin depth. The skin depth is an inverse function of frequency. It is given as:

$$\delta = 503\left\{\frac{\rho}{f}\right\}^{1/2}$$

δ: skin depth in m
ρ: resistivity in ohm-m
f: frequency in hertz

To obtain the electrical structure of the earth, depth sounding data, derived from the apparent resistivity as a function of frequency, have to be modelled by either one-, two- or three-dimensional models. For a one-dimensional structure, the model consists of horizontal layers with the resistivity and thickness of each layer as model parameters. Two-dimensional structures can have resistivity variations in the direction perpendicular to the geologic strike and/or with depth. Three-dimensional modelling, which is closest to many real geologic situations, can have structures in any form with various resistivities; however computing models in three dimensions is expensive. For mapping purposes, one-dimensional interpretation at stations distributed on a grid is a necessary step in order to get a plan view of any three-dimensional structure that may be present.

Instrumentation to operate in the audio-frequency range (10 – 10^4 Hz) was first described by Strangway and Vozoff (1969) and by Strangway *et al.* (1973). This instrumentation has since been improved and in the recent past, several surveys have been conducted in various parts of North America (Strangway *et al.* 1980).

In the surveys reported here, an 82 m dipole was employed for measuring the electric field. The magnetic field was measured with two induction coils, one optimized for the low frequency range and the other optimized for the high frequency range. The magnitude of the apparent resistivities was measured at the discrete frequencies of 13, 22, 36, 83, 140, 210, 473, 858, 2140, 5050 and 8570 Hz (referred to in some of the figures as channel A,B,C,D,K,E,F,G,H,I and J respectively). Two orthogonal data sets at each site were measured to search for lateral anisotropies. The data sets indicated as NS and EW in the figures have the electric dipole laid out in north-south and east-west orientation respectively and the magnetic coils lined up perpendicular to these dipole orientations. The data were plotted in log ρ - log f format for a general qualitative overview.

The errors in apparent resistivity measurements for real field data determined from tests of repeatability are sometimes of the order of 30-40 percent. In this survey, anomalously low apparent resistivities, associated with low source signal levels, were sometimes found at 2140 and 5050 Hz. Low apparent resistivities at 13 and 22 Hz caused by wind noise was a problem in some measurements, particularly in Marter Township. Interference from power lines at 60 Hz was occasionally a problem in Bowman and in Marter Townships. Those poor quality data points were identified by examining the sounding curves in the field, and were removed or remeasured.

SURFICIAL GEOLOGY

The clay belts are an important subdivision of the Canadian Shield physiographic province and record the site of glacial Lake Barlow-Ojibway. Surficial geology is shown in Figure 1. In Marter Township, a reverse-circulation rotary drilling program was completed in 1979 (Averill and Thompson 1981). The surficial geology in that area is thus well known. Glacial Lake Barlow-Ojibway, a major proglacial body of meltwater, covered the area during part of the Wisconsin recession. The Matheson till (Table 1) is the lowermost unit known in the area; it consists of sandy boulder till with minor gravel and lies directly on bedrock of Precambrian age. It is an almost continuous sheet except for local discontinuities around bedrock hills. Glaciofluvial deposits overlie the Matheson till or lie directly on bedrock. They are confined mainly to broad north-trending esker ridges and broad sand and gravel plains. The most extensive deposits of Lake Barlow-Ojibway are the varved clays and silts which form plains and an interconnected network surrounding bedrock outcrops. In general, the lower part of the Barlow-Ojibway formation consists of bedded silt and the upper part of laminated clay. Shore and nearshore deposits ranging from fine sand to gravel and boulders form the uppermost part of this formation. Clay and till glaciolacustrine sediments known as the Cochrane Formation, cover the northern part of the research area. The youngest unit of Wisconsin age consists of organic deposits which contain shell, marl and peat (Hughes 1961).

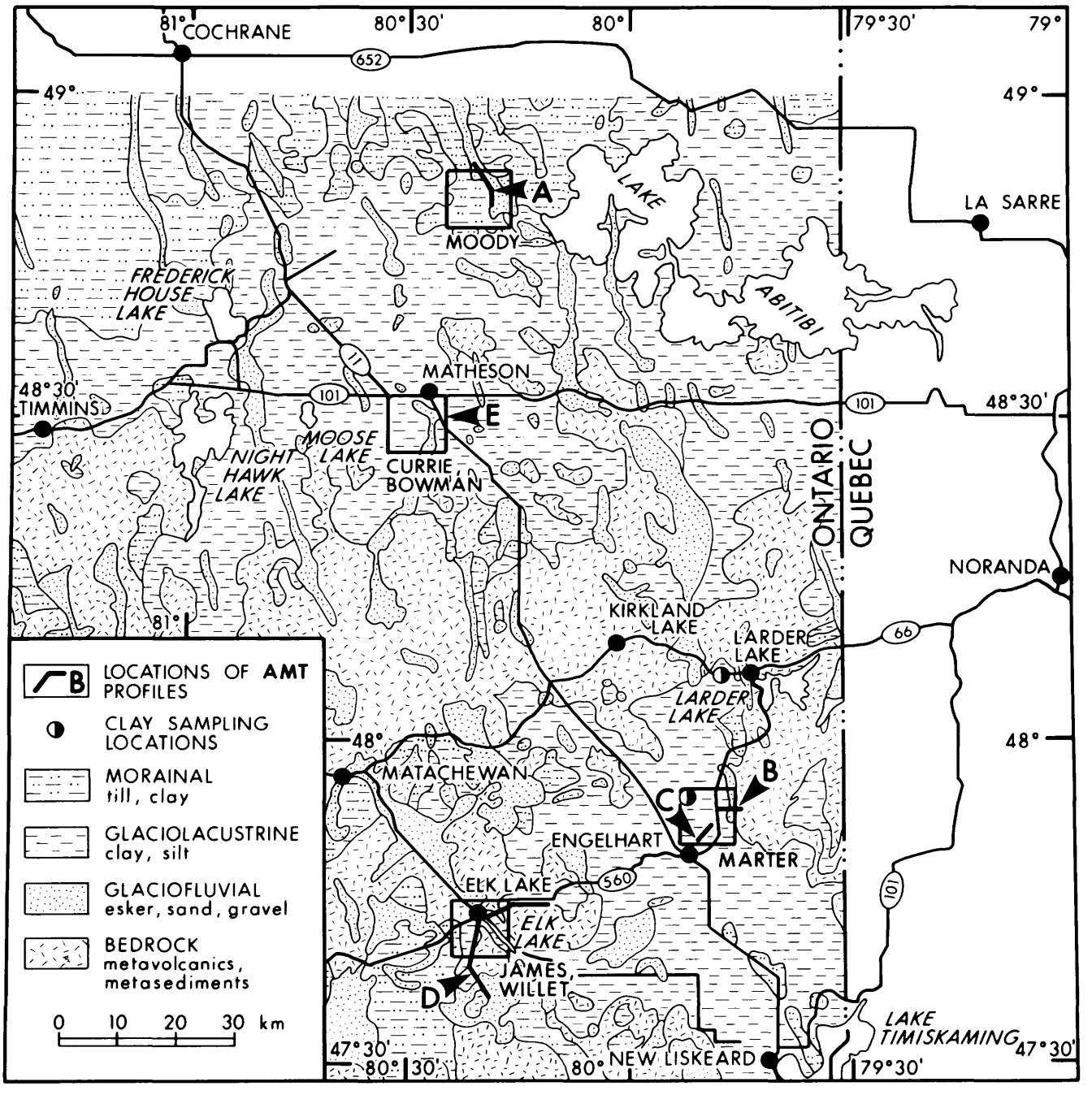

Figure 1. *Geographic location and simplified surficial geology map (modified from Roed and Hallett 1979; Lee 1979a,b).*

Table 1. *Wisconsin deposits in study area (after Averill and Thompson 1981; Hughes 1961).*

ORGANIC DEPOSIT

- Shell, marl, peat

COCHRANE FORMATION

- Clay till, glaciolacustrine sediments

BARLOW-OJIBWAY FORMATION

- Silt, sand

- Varved clay, massive clay (megavarve)

GLACIOFLUVIAL DEPOSITS

- Sand, gravel, esker

MATHESON FORMATION

- Sandy boulder till, gravel

BEDROCK GEOLOGY

The bedrock geology of the individual study areas is shown in Figures 2a-d. The oldest rocks in the Superior Province, where most of the survey was carried out, are volcanic and sedimentary rocks of Early Precambrian age. These rocks were deposited in a number of easterly trending eugeosynclines which are possibly of different ages and tectonically independent. Early Precambrian mafic metavolcanics strike east and consist of massive and pillowed flows, with minor related breccia and tuff. The lavas are conformably overlain by greywacke and argillite. All of these rocks are overlain unconformably by thinly bedded alternations of greywacke, shale with a few beds of quartzites, and conglomerate of variable thickness at or near the base. The Early Precambrian rocks are folded along easterly trending axes. These folds appear to be modified in places by crossfolds of various orientations, and are cut by several easterly trending faults and some younger faults trending northwest, north-northwest, and northeast. The youngest rocks of Early Precambrian age are felsic intrusions which are primarily granitic and syenitic in composition. The Huronian Supergroup of Middle Precambrian age is a sequence of sedimentary and volcanic rocks that lies unconformably on the Early Precambrian basement, which was deeply eroded and has a rugged topography. The Huronian rocks are undeformed or very gently folded. The Cobalt Group, the uppermost group of the Huronian Supergroup, is composed of four formations, of which the lowest two are most extensively exposed and best known. The Gowganda Formation consists of paraconglomerate, argillite, siltstone, subarkose and greywacke. It overlaps the other parts of the Huronian and lies unconformably on Early Precambrian rocks. The Lorrain Formation overlies the Gowganda conformably and is composed predominantly of quartzite and arkose.

INTERPRETATION

AMT data interpretation consists of two main stages. The first is a general qualitative overview of the data obtained, and is usually first done in the field. It is convenient to represent the measurements on a (log ρ log f) scale. By polynomial fitting, the bad readings can be detected and poor data rejected. The pseudosections based on the polynomial fits provide a rough idea of the two-dimensional distribution of resistivity. The residual plots, frequency-by-frequency, represent the resistivity values determined by subtracting the mean value for each line from the observed value. In the case of some two-dimensional effects, the anisotropy (TE/TM) plots provide a meaningful picture.

The second stage of interpretation is the fitting of a layered earth model at each station by one-dimensional inversion methods to get the best parameters that fit the data obtained. We have been using a nonlinear, least-squares estimation method (Marquardt 1962; Hsu 1981) to invert AMT data.

Another simple form of presentation for AMT data in the depth domain is the Bostick transformation (Bostick 1977). The result is an approximate depth-resistivity cross-section which contains information on the quality of data and the homogeneity of the subsurface. The application of this transformation, as well as the inversion method, to invert the data, saves labor, time and money and provides the maximum use of the data.

In stratified environments, one-dimensional modelling along a survey line is generally enough to give a two-dimensional configuration, but apparent resistivities can be influenced by lateral anomalous conductors. In such a case, layered model interpretations would be in error (Kryzan and Strangway 1977). Two- or three-dimensional modelling can have structures in any form with various resistivities. For mapping purposes, one-dimensional interpretation for stations distributed on a grid is necessary in order to get a plan view of any three-dimensional structures present. However, some two-dimensional test models have been set up by using network solution techniques (Madden and Thompson 1965), helping us to understand the actual apparent resistivity curves.

MOODY TOWNSHIP (PROFILE A)

Profile A is north-south, roughly parallel to an esker ridge. Ground moraine, essentially till and clay, dominates. The strike of the bedrock formations is approximately perpendicular to the profile. The north part (north of site A-9) of

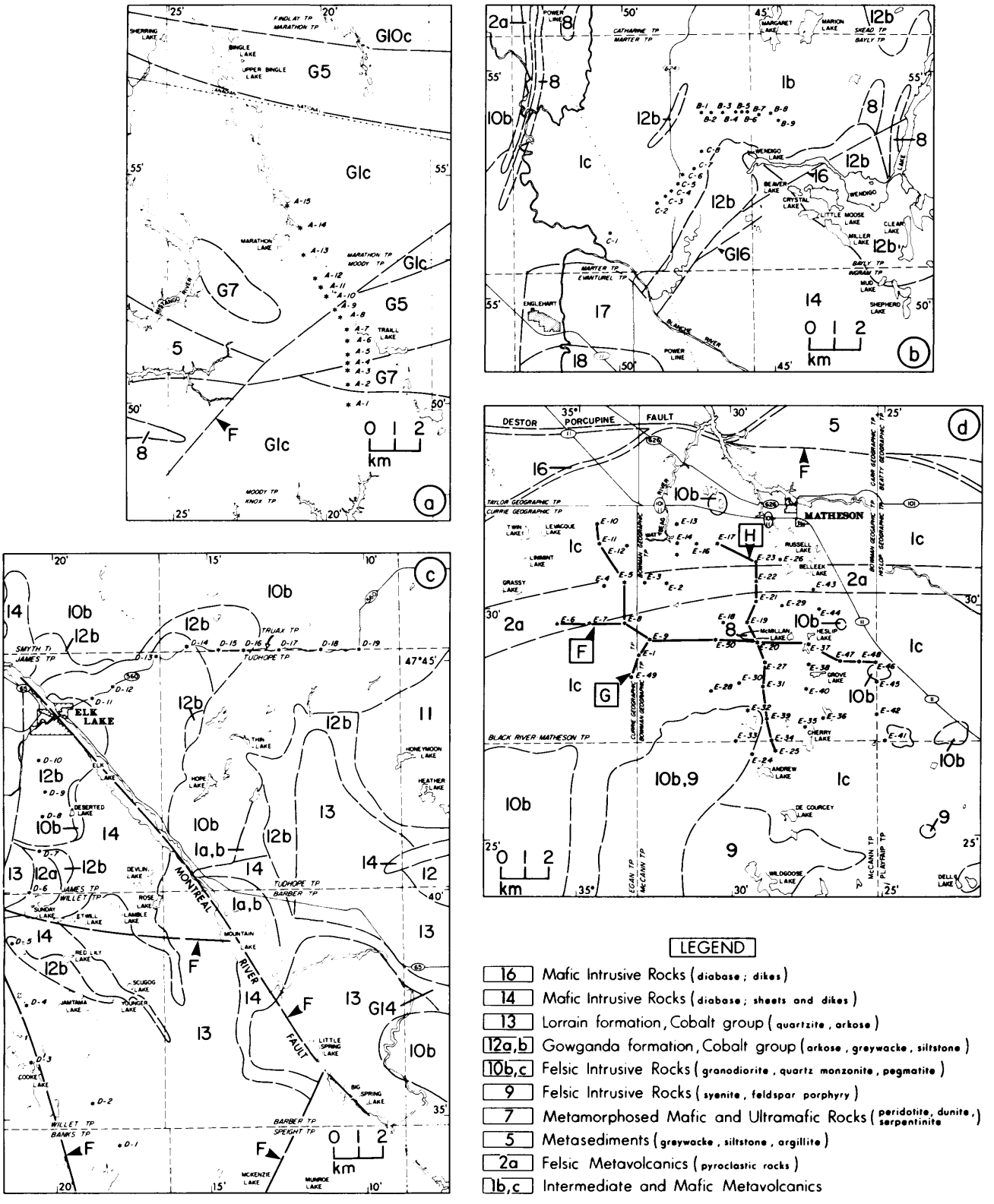

Figure 2. *Bedrock geology maps (after Pyke et al. 1973) and the locations of AMT sounding sites:* ***a.*** *Profile A in Moody Township;* ***b.*** *Profiles B and C in Marter Township;* ***c.*** *Profile D in Elk Lake area;* ***d.*** *Grid E in Matheson Township.*

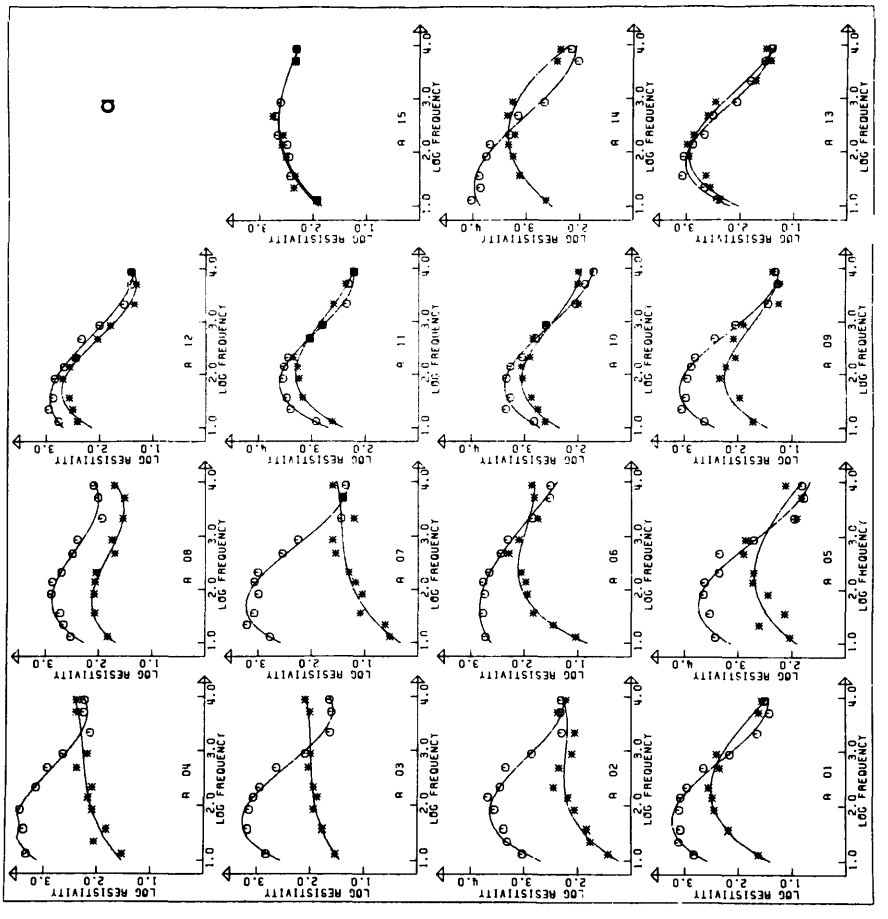

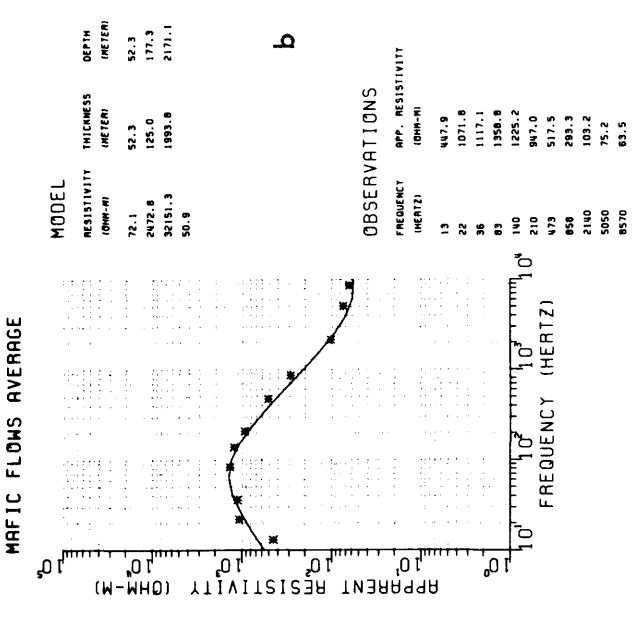

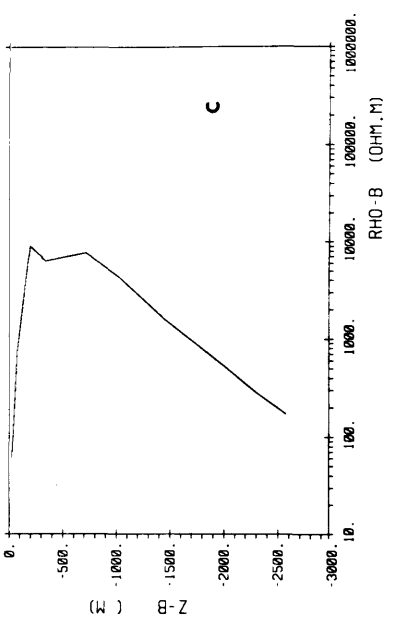

Figure 3. a. *AMT sounding curves of Profile A. Circles are NS (northerly) orientation and stars are EW (easterly) orientation data;* ***b.*** *One-dimensional inversion model for line segment on metavolcanic rocks. Apparent resistivities are averaged using data from sites A-10, A-11, A-12 and A-13;* ***c.*** *Bostick resistivity depth cross-section computed from the same averaged data.*

Profile A overlies metavolcanics. The field data for both northerly and easterly orientations (Figure 3a) are very similar at sites A-10, A-11, A-12, A-13 and A-15. This indicates that there are no significant two-dimensional effects in this part of the profile. It can therefore be reasonably approximated by a one-dimensional structure. An average, which is computed by averaging the square root of apparent resistivities at each frequency for each of these sites and then averaging for the section, is used to represent the resistivity variation with depth in this profile segment. The fitted model using the one-dimensional inversion technique suggests that there is about 50 m of overburden with a resistivity of around 70 ohm-m (Figure 3b). A highly fractured weathered layer about 100 m thick with resistivity about 2400 ohm-m lies beneath. The uppermost part of the bedrock has a resistivity of approximately 32 000 ohm-m. The Bostick transformation shows that the resistivity of the bedrock drops to 2000 ohm-m at a depth of about 2000 m (Figure 3c).

The sounding curves of Profile A in Moody Township show that there is very strong anisotropy at sites south of site A-9. This phenomenon occurs without exception in the low frequency range, and implies a peculiar characteristic of the metasediments and metamorphosed mafic and ultramafic rocks (G5 and G7 respectively in Figure 2a). The rocks are more resistive in the NS (north-trending) electrode orientation than in the EW (east-trending) orientation. This may be due to the two-dimensional structure of this area. The resistivities of the metavolcanics and of the metasediments are not significantly different in NS orientation. However, in the EW orientation, the metasediments tend to be more conductive than the metavolcanics, suggesting a preferred direction of fracturing or of structure. At least two faults, one through A-9 and one near A-3, have been suggested by other geophysical interpretations (Pyke *et al.* 1973). Easterly trending, vertically bedded Early Precambrian rocks could be an explanation of the anisotropic behaviour of the apparent resistivity data.

On the other hand, sand associated with narrow esker ridges interfingers laterally with glaciolacustrine clays. The stations in the southern part of Profile A are on the glaciolacustrine cover, but are not far from an esker ridge. This local and near surface resistivity variation could have produced an edge effect in the southern part of Profile A and hence could be a cause of this anisotropy.

The study suggests that the most probable explanation is that the metasediments are themselves strongly anisotropic. In this case it will be possible to characterize steeply dipping metasediments with the AMT method even when they are not exposed. Additionally, it should be possible to map bedrock in detail beneath regions covered by eskers using the AMT method. Similar mapping would not be possible using conventional expanding electrode array systems because of the lateral effects and the need for deep penetration.

MARTER TOWNSHIP (PROFILES B AND C)

The sounding curves of Profiles B and C in Marter Township all show a general similarity in both the NS and the EW orientations. The overall similarity of sounding indicates that the basement volcanic rocks and overburden are both homogeneous in the area. Only Wisconsin deposits are present as glacial overburden. Profile B crosses the south end of the Munro esker east of site B-6. This is a major feature that can be traced northward 300 km to James Bay. In Marter Township, the esker is confined to regional bedrock highs and consists entirely of sand (drill hole No. 6, Averill and Thompson 1981). Pseudosections along Profile B are given in Figure 4a. Apparent resistivities of about 1000 ohm-m were obtained on the esker at higher frequencies. A one-dimensional interpretation was not done for site B-6 because of the obvious two-dimensional structure in the vicinity. A depth-resistivity cross-section compiled using the Bostick transformation method is given in Figure 4b. Together with one-dimensional inversion fits along Profile B, these data reveal that the sand and gravel in this area is up to 100 m thick. Its resistivity ranges from 800 to 3000 ohm-m. The bedrock generally has a layer several hundred metres thick, of medium resistivity, overlying a highly resistive unfractured section of bedrock with resistivities up to 100 K ohm-m. There may be minor clay beds deep beneath the very thick sand and gravel in the eastern part of the profile area.

The pseudosections of Profile C in Figure 5a show the same homogeneity in both orientations as those of Profile B, also implying that there is no major lateral variation. The high frequency readings, however, are different from those in Profile B and are about 100 ohm-m, or less. The pseudosections and residual plots of Profile C reveal that the apparent resistivities are continuously decreasing southwesterly. This implies either that the overburden is getting thicker, or that the resistivity of the top conductive layer is getting lower. Drill hole No. 5 (Averill and Thompson 1981) is located at the same site as C-4 and has been used to control the model of the site and to determine the resistivities of the layered earth. The cross-section shown in Figure 5b was obtained by a one-dimensional interpretation at each site and reveals a basin structure corresponding to that detected by drilling. The basin has its edge at the northeast end of the line near site C-8. The model suggests that there is a 50 m thick overburden at the southwest end of the survey line near site C-1 and that the thickness decreases northeasterly to about 30 m at site C-5. The bedrock resistivity, from the model, is very homogeneous at about 20 000 - 60 000 ohm-m throughout the survey line.

ELK LAKE AREA (PROFILE D)

In the Elk Lake area, station locations were chosen to sample different rock types in the northern part of the profile. The apparent resistivity profiles in Figure 6a show that, in this part of the survey line from site D-13 to D-19, the structure is very complicated electrically. Site D-15 and D-16 lie on a sliver of Cobalt Group sedimentary rocks about 2000 m wide, sandwiched between younger mafic intrusive rocks (14 in Figure 2c) and older felsic

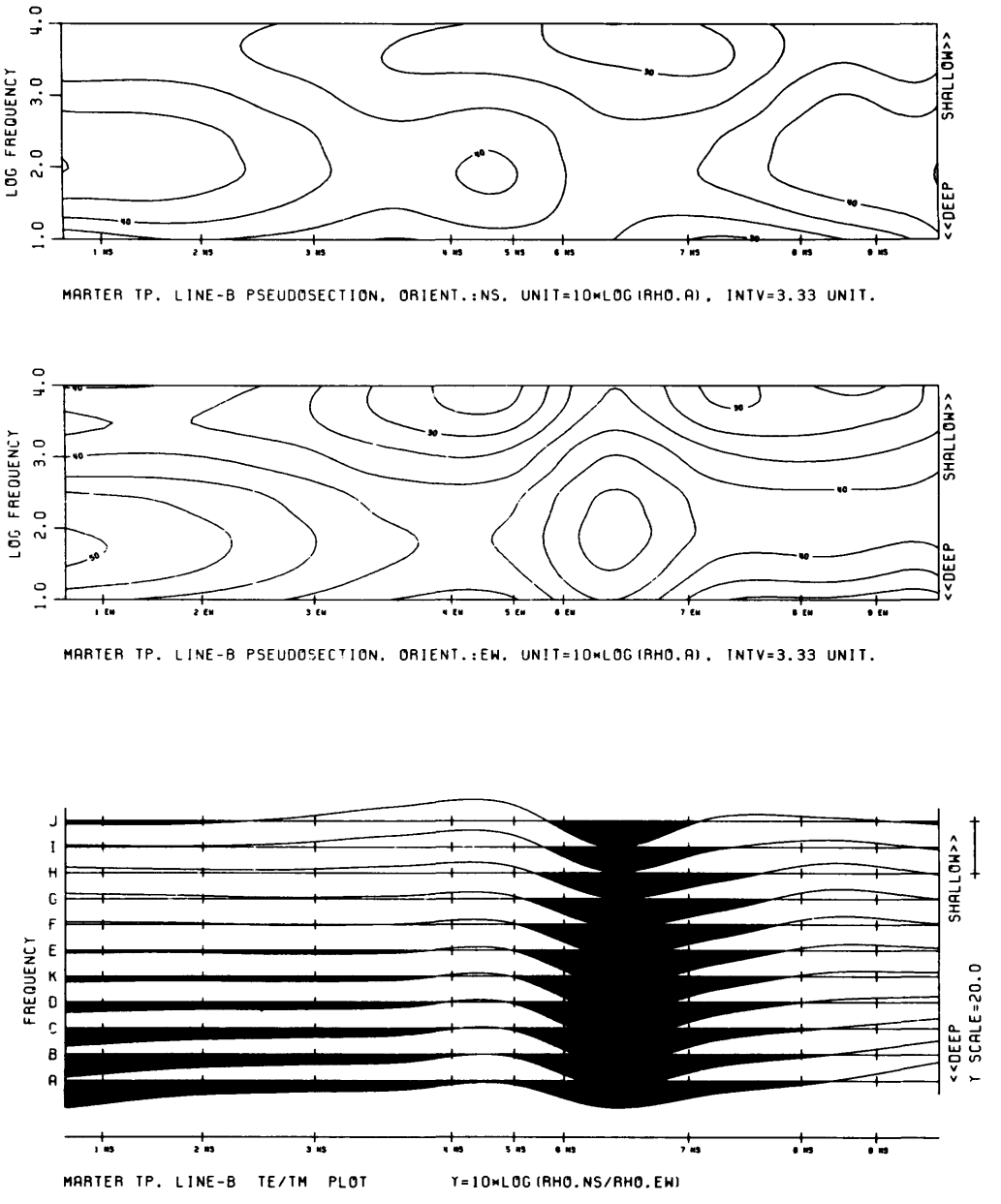

Figure 4a. *Apparent resistivity pseudosections and TE/TM plot for Profile B. Station locations along the horizontal axis and frequency on the vertical axis.*

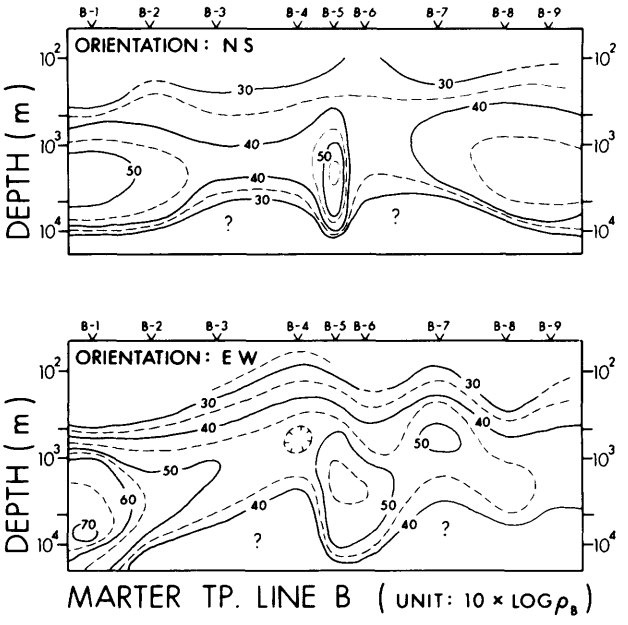

Figure 4b. *Bostick resistivity cross-sections along Profile B, (unit is 10 log a).*

intrusive rocks (10b). The measurements in the section appear to be strongly affected by the two contact zones and show inhomogeneity and anisotropy. The mafic intrusive rocks (sites D-11 to D-14) tend to be more resistive than Cobalt Group sedimentary rocks and felsic intrusive rocks (sites D-17 to D-19). The major feature in the area is the Montreal River Fault running under the town of Elk Lake. It is reflected in the apparent resistivity readings at site D-10 and in the high frequency readings of D-11. The shape of the profiles suggests that the fault dips to the southwest. The section on the southern part of the survey line lies on the Cobalt Group sedimentary rocks. Similarity is shown from site to site, especially in the low frequency range. The model fit of an averaged apparent resistivity set in Figure 6b, computed from sites D-1, D-2, D-3, D-4, D-5, D-6, D-8 and D-9, suggests that the top Cobalt sedimentary rocks have a thickness of about 280 m and a resistivity of about 2000 ohm-m. Beneath them could lie a highly fractured weathered layer, with resistivity less than 1000 ohm-m and about 100 m thick. The underlying Early Precambrian metavolcanics have resistivity values in the 25 000 ohm-m range.

BOWMAN TOWNSHIP (GRID SURVEY E)

In Bowman Township, the main features of the surficial geology are a clay-covered plain, eskers and bedrock outcrop (Figure 7b). Each unit shows different electrical characteristics. The three subdivisions are clearly outlined on contour maps of apparent resistivities in Figures 7a and 7c. A contour map of frequency J (Figure 7a) generally reflects the surficial geology, and shows a highly conductive clay-covered plain in the northwestern part of the area with resistivities less than 100 ohm-m. A high-resistivity region in the southwestern part of the area has resistivities higher than 3000 ohm-m. An intermediate resistive region is located to the east of the other two regions. The contour maps at lower frequencies such as the map of frequency C (Figure 7c) shows roughly the same pattern as that of frequency J, indicating that they are affected by the surface material.

The averaged apparent resistivity pseudosections for three Profiles F, G and H are given in Figure 7d. Sounding curves for the northwest segment of the map and the pseudosection for line G, show a typical two-layer structure: an extremely conductive layer on top of an extremely resistive half space. High frequency readings of 20-30 ohm-m reflect the top conductive clay-rich overburden. The similarity of two sets of data for the NS and EW orientations indicates the homogeneity in the glaciolacustrine plain. Anisotropy generally appears at esker-complex sites, for example E-37 on Profile F and E-24 and E-25 on Profile H. Apparent resistivities at high frequencies are mostly about 100-300 ohm-m, then rise to around 10 000 ohm-m at some sites. Strong anisotropy was observed at sites near bedrock outcrops. High apparent resistivities in the 10 000 ohm-m range were obtained at high frequencies, indicating the thin overburden and the very resistive bedrock.

The averaged data from the two orientations was employed to determine a best estimate of the electrical structure at each site. It is a good approach to interpreting data from such a glaciolacustrine-deposit covered plain because of the obvious one-dimensionality shown on the two sets of data. The top two layers, with resistivities of 10 to 40 ohm-m and thicknesses in the 20-100 m range, are very conductive clay-containing overburden of varying composition. The composition varies from a sand and boulder-rich resistive unit to a very conductive clay unit. The third highly resistive layer at 20-100 m beneath the surface is associated with bedrock having resistivity in the 10 000 - 50 000 ohm-m range. For those sites on eskers and those near bedrock outcrop, one-dimensional interpretation may be risky and misleading when strong anisotropy exists. The determination of the top layer resistivity is reliable, because of the general agreement of high frequency data on both directions.

Three block maps, showing surface resistivity, bedrock topography, and bedrock resistivity, and a contour map of bedrock toppgraphy were created by using the appropriate model parameters of the one-dimensional interpretation (Figure 8a-d). Those sites with apparent resistivity differences at frequency D of more than a factor of 5 were left out due to the unsuitability for one-dimensional modelling. The real surface resistivity map (Figure 8b) which is similar to the frequency J apparent resistivity contour map in Figure 7a, reflects the resistivity variation of surface material in the top few tens of metres. The three types of material with their characteristic resistivities are clearly outlined. The bedrock topography map was cre-

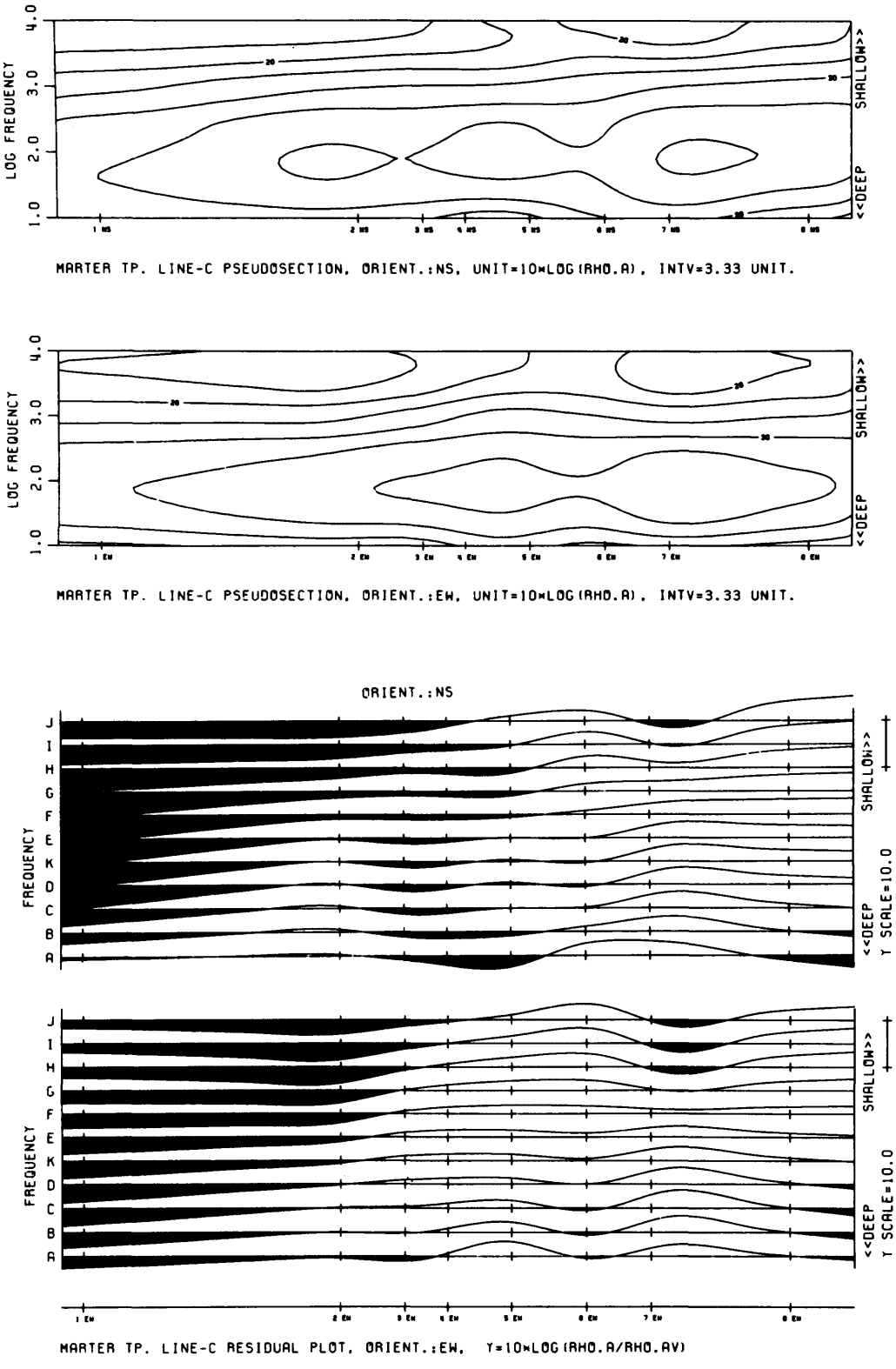

Figure 5a. *Apparent resistivity pseudosections and residual plots for Profile C.*

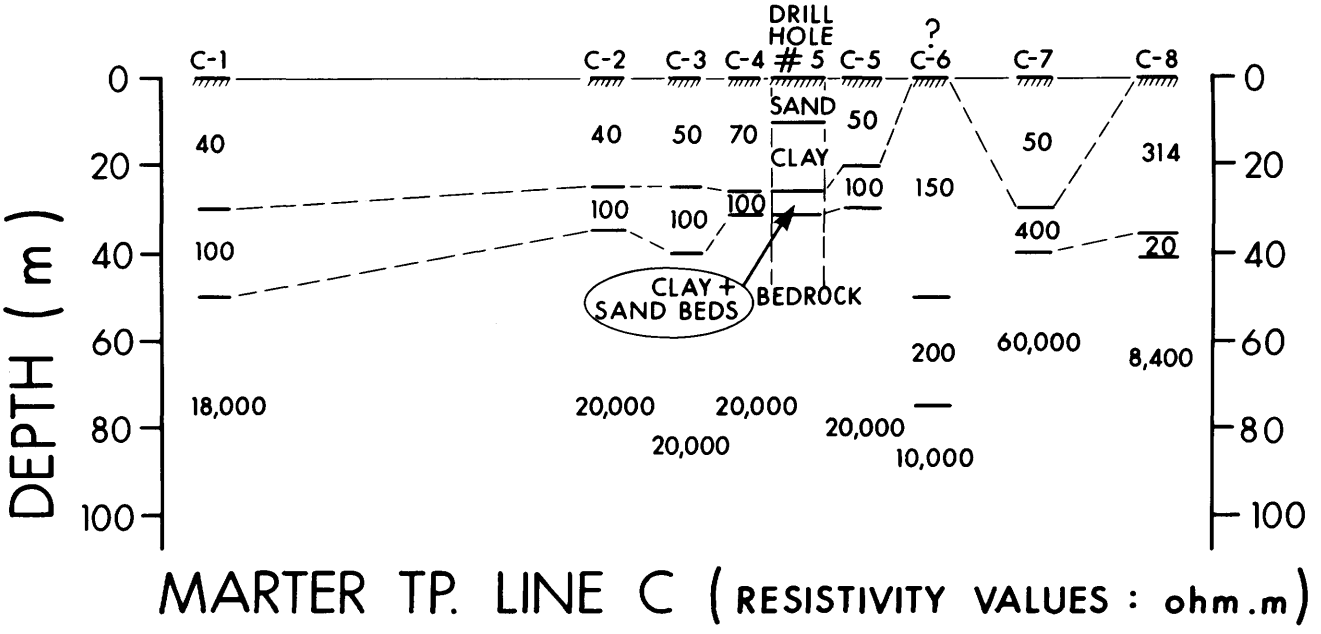

Figure 5b. *Two-dimensional configuration for Profile C derived from one-dimensional inverse models.*

ated by contouring the thickness of the top one or two conductive layers, representing the thickness of overburden in one-dimensional interpretation. Elevation correction was not applied and the surface was assumed to be flat, which is roughly the case in this area. The maps show that a bedrock valley, 100 m below surface in the northwest quadrant of the area, trends northwesterly near sites E-4, E-5, E-8 and E-9. Another bedrock topographic low at the southeastern corner of the area is near sites E-35, E-36 and E-42. These two bedrock topographic lows could imply that valleys in the older metavolcanics are separated by the younger intrusive rocks. The bedrock topography in the rest of the survey area has no significant variation in elevation. The area of bedrock exposures has an overburden thickness of less than 20 m. The areas covered by clay and by sand and/or gravel show no signficant differences in bedrock topography; all the bedrock in both these areas is in the range of a few tens of metres below the surface. The bedrock resistivity map (Figure 8a) indicates that the resistivities of bedrock in this area are extremely high in the range of 10 000 to 100 000 ohm-m. The lateral variation is not significant. Comparing the bedrock resistivity map (Figure 8a) with the bedrock geology map (Figure 2d), the felsic metavolcanics (2a) in this area tend to be more resistive than the intermediate and mafic metavolcanics (1c). The felsic metavolcanics form a ridge of high resistivity, trending roughly east in the north-central part of the area. The intrusive rocks in the south (10b, 9) have homogeneous resistivity of about 10 000 ohm-m.

ELECTRICAL PROPERTIES OF CLAY

In applying EM exploration techniques, in areas where there is an extensive clay cover, it would be useful to have a better understanding of the electrical properties of the clays. The clays are the most conductive component of the overburden, with the exception of saline alluvium, which is not known to exist in the area studied. In the Kirkland Lake area, the clays have resistivities on the order of 20 ohm-m, whereas the sands, gravels and tills have resistivities in the range of 100 to 1000 ohm-m. Thus, clay is the most important component of the overburden, in terms of limiting the depth of exploration by EM methods.

Mehran and Arulanandan (1977) measured a strong frequency dependence for the resistivity of kaolinite, illite, and a silty clay in the frequency range 50 Hz to 100 KHz. The conductivity dispersion, which was defined in this case as the difference between the conductivity at 100 KHz and at 50 Hz, was dependent upon the water content, the type of electrolyte, and the electrolyte concentration. The measured conductivity dispersions were on the order of 30 to 60 percent, decreasing with increasing

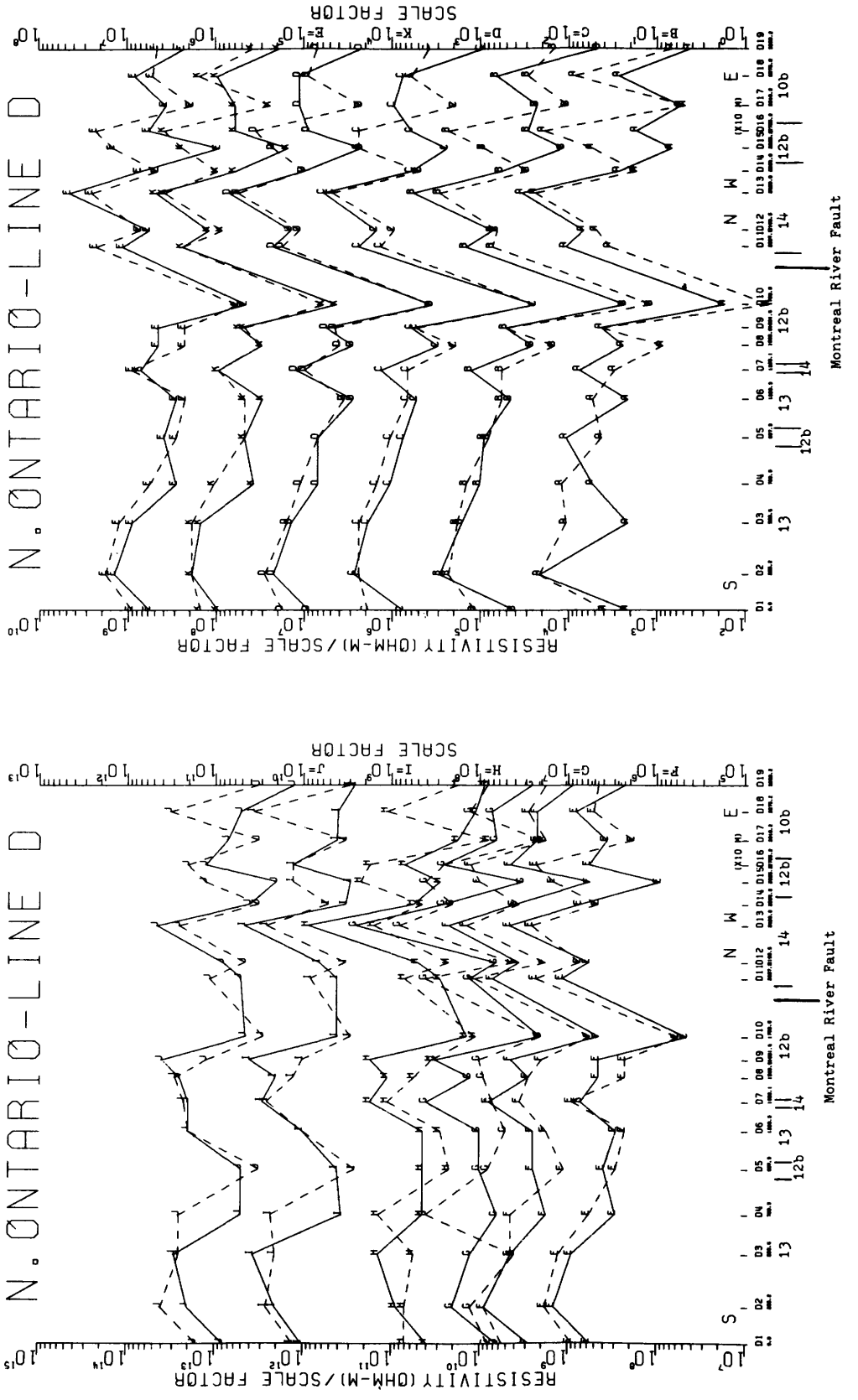

Figure 6a. *Apparent resistivity profiles along Profile D for each frequency channel. Each curve is offset from the others so that the individual profiles can be followed (NS oriented data; Solid lines; EW oriented data, dashed lines).*

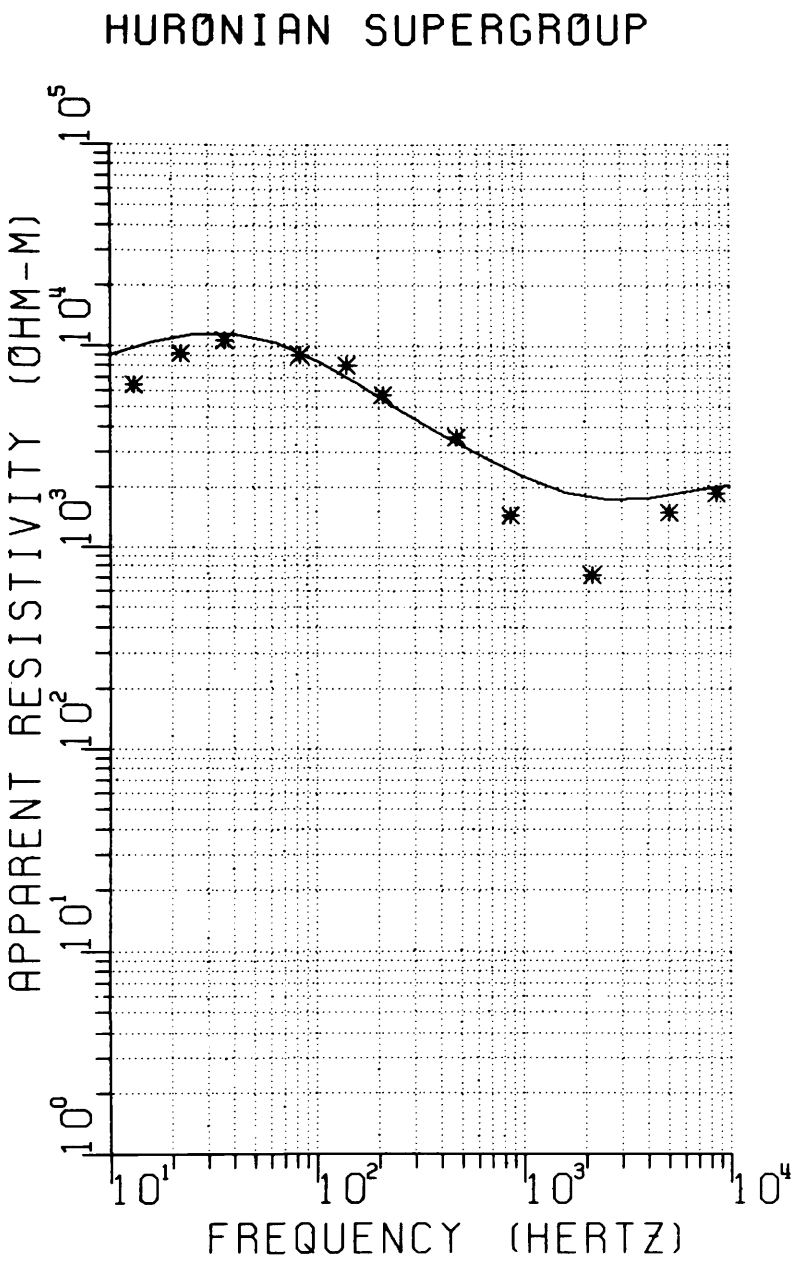

MODEL

RESISTIVITY (OHM-M)	THICKNESS (METER)	DEPTH (METER)
2059.3	281.2	281.2
1554.1	157.2	438.4
24338.1	7968.7	8407.1
2561.2		

OBSERVATIONS

FREQUENCY (HERTZ)	APP. RESISTIVITY (OHM-M)
13	6474.3
22	9226.4
36	10753.2
83	9013.2
140	8076.8
210	5760.1
473	3548.6
858	1440.2
2140	727.4
5050	1503.3
8570	1863.5

Figure 6b. *One-dimensional model for line segment on Huronian Supergroup metasediments. Apparent resistivities are averaged using data from sites D-1 to D-9.*

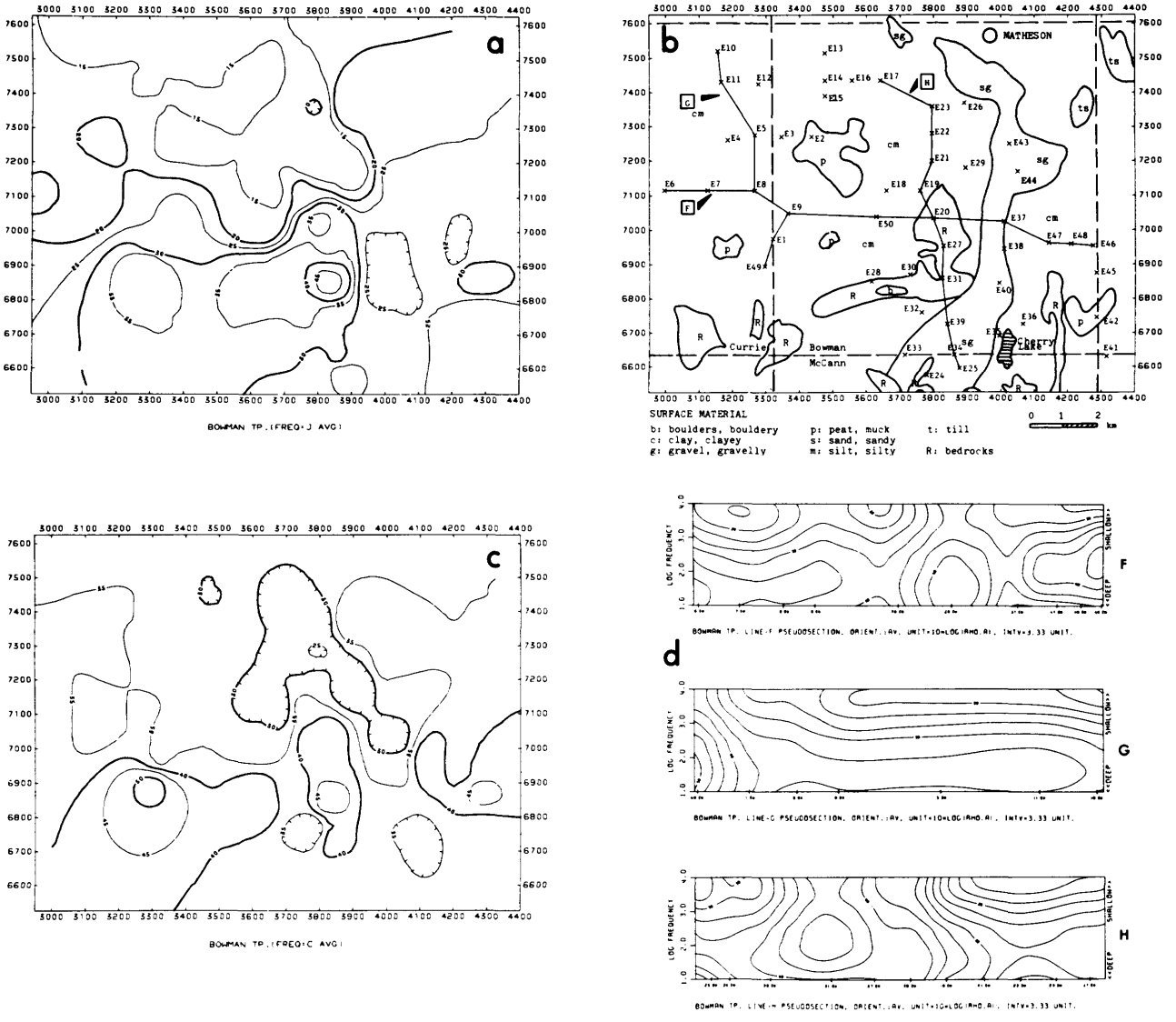

Figure 7. a. *Contour map of apparent resistivities at high frequency (J = 8570 Hz);* ***b.*** *Surficial geology of the survey area in Bowman Township; (x) represent AMT site location;* ***c.*** *Contour map of apparent resistivities at low frequency (C = 83 Hz);* ***d.*** *Averaged apparent resistivity pseudosections for Profiles F, G and H.*

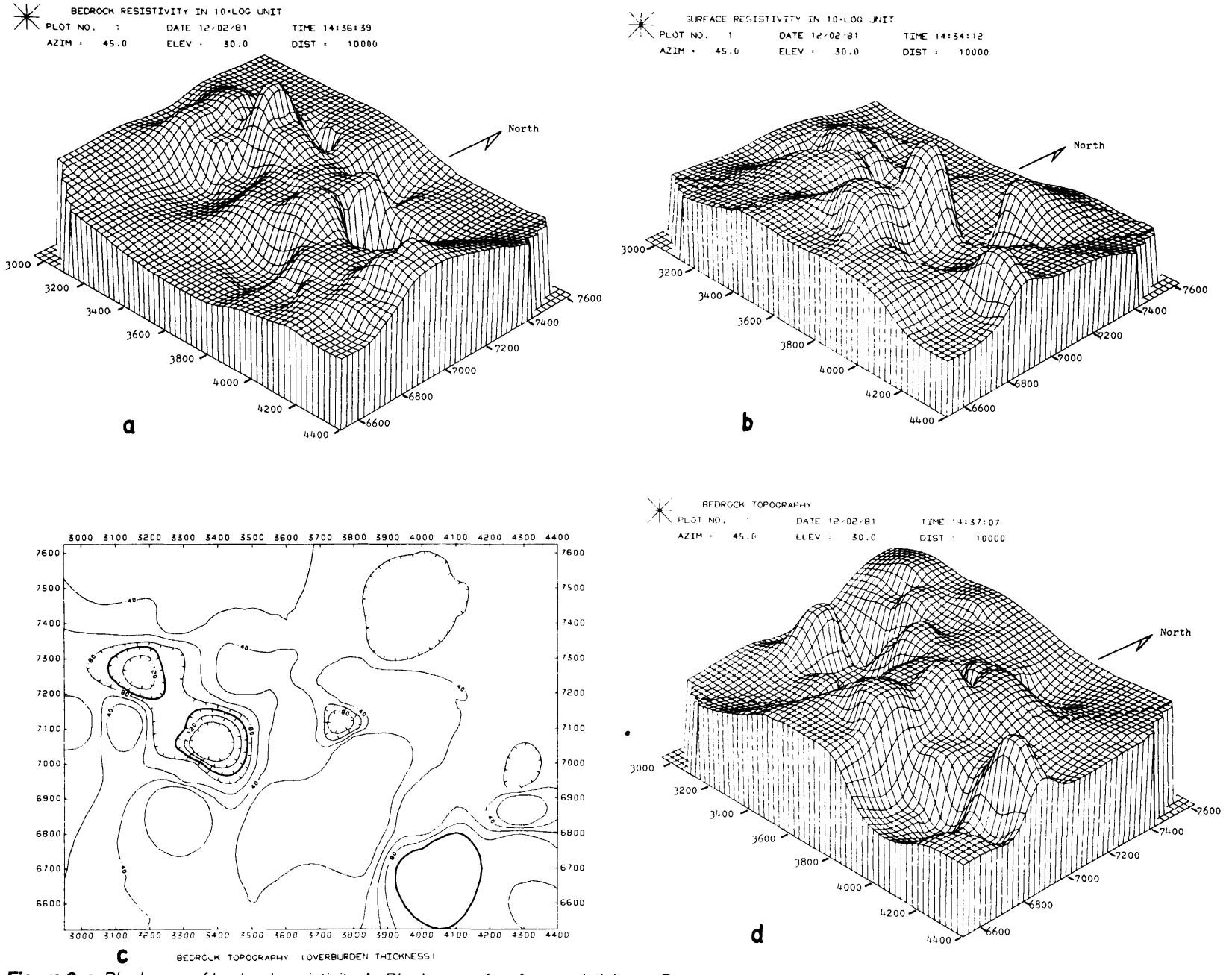

Figure 8. a. *Block map of bedrock resistivity;* ***b.*** *Block map of surface resistivity;* ***c.*** *Contour map of bedrock topography;* ***d.*** *Block map of bedrock topography. Block maps were created by model parameters of the one-dimensional interpretation.*

with increasing water content and with increasing electrolyte concentration. Silty clay gave the highest dispersion and illite the lowest. If a similar conductivity dispersion phenomenon exists in the glaciolacustrine clays, it could cause serious limitations in the interpretation of some EM methods. Thus it would be useful to have measurements of the magnitude and the frequency dependence of the resistivities of clays from northern Ontario.

Samples were collected from nine sites near Larder Lake, Matheson, and Engelhart. Some samples were taken from a vertical soil profile that was exposed in the Larder Lake dump and others were collected from road cut exposures and from exposures along rivers.

In collecting the samples, an attempt was made to preserve the samples in their original state. When a suitable site was found, the surface material was removed to expose fresh undisturbed clay. Samples were obtained by pressing a plastic tube (2.5 cm diameter by 2.5 cm length) into the face of the clay. The sample was then placed in a plastic bag that was heat-sealed later in the day, so as to preserve the original moisture content of the sample.

The complex resistivity was measured over the frequency range 5 Hz to 10^6 Hz. This range more than covers the frequencies used in most EM exploration methods. The samples were encapsulated during the measurement process to prevent them from drying.

All the measurements were carried out using the HP4192A impedance meter. Four terminal measurements were made between 5 Hz and 10 KHz, and above 10 KHz a two terminal technique, employing platinum electrodes, was used. Two of the samples measured gave the results shown in Figure 9. The resistivity magnitude changes little with frequency. Sample KL-36 had a clay content of 26 percent, a water content of 13 percent, and a resistivity of 24 ohm-m at 100 Hz and 22 ohm-m at 100 KHz. Sample KL-11 had a clay content of 77 percent, a water content of 31 percent, and a resistivity of 36 ohm-m at 100 Hz and 34 ohm-m at 100 KHz.

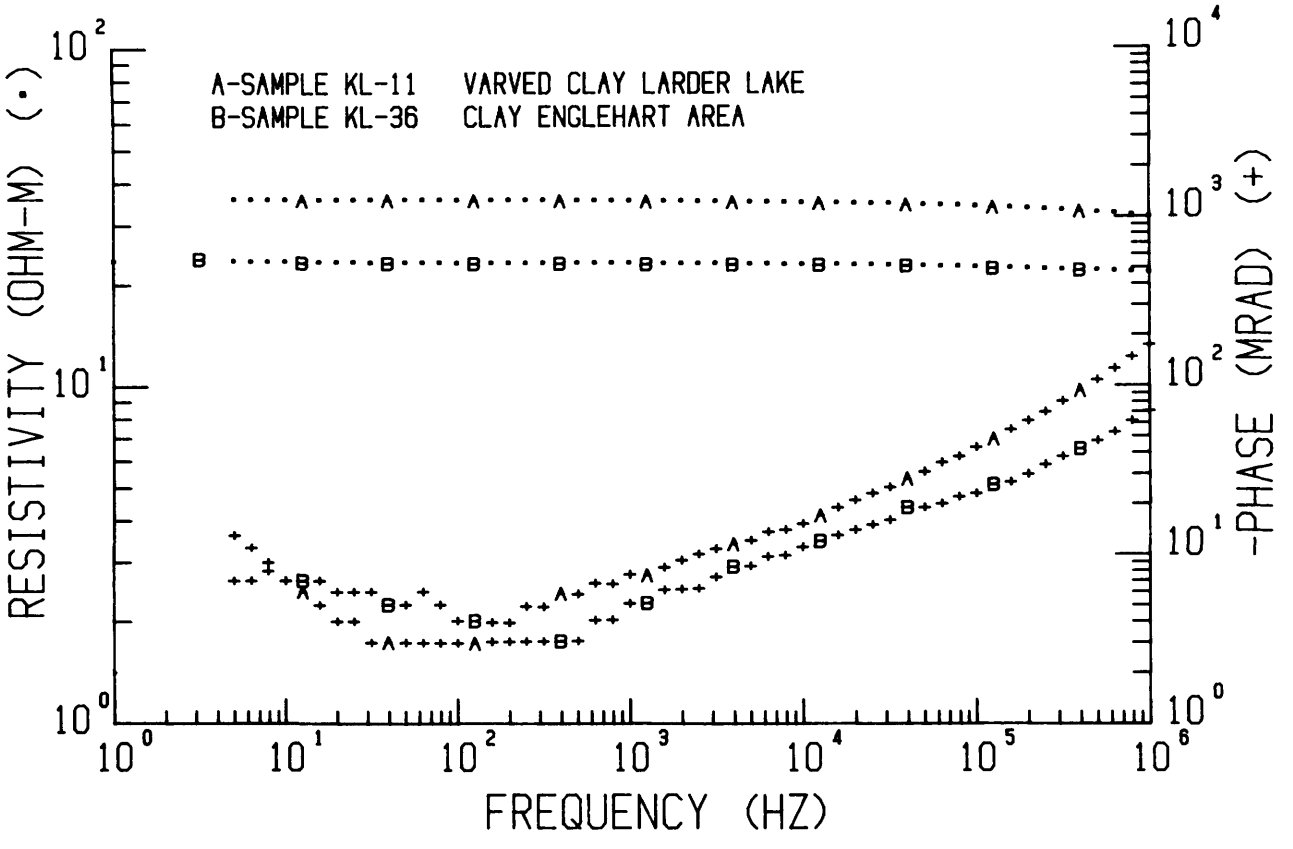

Figure 9. *The dependence of the resistivity magnitude and phase on frequency for two clay samples, one of which was a varved clay. The dots and crosses are the actual measurements.*

CONCLUSIONS

With the AMT method, we have been able to characterize, in the areas surveyed, the conductivity structure of clay-rich overburden and Precambrian Shield rocks underneath.

In Moody Township near Lake Abitibi, the survey showed a strong and uniform electrical anisotropy in an area believed to be underlain by metasediments. If this is true, then it will be possible to map out concealed, steeply dipping metasediments with the AMT method. There are many highly resistive eskers in northern Ontario which could be used as electrical sounding windows into the bedrock using this method.

Good correlation with known surficial geology in Marter Township near Engelhart was obtained when estimating the overburden thickness with the AMT approach. The ability to sound through conductive overburden and to detect conductors beneath has been proved to be possible. The resolving power, however, has to be improved by careful field measurements and careful model parameter selection. An approximate depth-resistivity diagram could be computed by applying the Bostick transform to field data to aid in interpreting survey results.

There are narrow conductive zones within the bedrock in the Elk Lake area that are interpreted as conductive fault zones. To determine the thickness of Huronian Supergroup rocks overlying Early Precambrian basement, further detailed studies are required.

Maps produced by using grid survey data in Bowman Township near Matheson show a conductive region (clay-rich overburden) in the northwestern part of the area. A high resistivity region (bedrock outcrop) occurs in the southwestern part, and an intermediate resistivity region (esker) occurs east of the other two locations. Some bedrock valleys in the northwestern part of the area were detected at depths of 50 - 100 m. Bedrock resistivity is typically 10 to 100 Kohm-m. High frequency data give resistivities of 20 to 30 ohm-m over clay-rich overburden. This value is in general agreement with resistivities measured in clay samples. The value of the clay resistivity seems fairly uniform in study areas ranging from Lake Abitibi to Engelhart.

ACKNOWLEDGMENTS

The authors express sincere thanks to R. Barlow for many ideas and information. They also wish to thank S. Yunsheng and S. Tanoli who assisted in the field work. M. Ilkisik, one of the authors, also wishes to thank A. Jones for his kind permission to use his Bostick Transform program. Geophysical data processing was done using the University of Toronto Computer Services computers.

REFERENCES

Averill, S.A. and Thomson, I.
1981: Reverse Circulation Rotary Drilling and Deep Overburden Geochemical Sampling in Marter, Catherine, McElroy, Skead, Gauthier and Hearst Townships; District of Timiskaming, Ontario Geological Survey, Open File Report 5335, 276p.

Bostick, F.X., Jr.
1977: A Simple and Almost Exact Method of MT Analysis (Abstract); Workshop on Electrical Methods in Geothermal Exploration, Utah.

Cagniard, L.
1953: Basic Theory of the Magnetotelluric Method of Geophysical Prospecting; Geophysics, Vol. 18, p. 605-635.

Hsu, D.T.
1981: One-Dimensional and Two-Dimensional Interpretation of Audiomagnetotelluric Data; Unpublished M.Sc. Thesis, University of Toronto.

Hughes, O.L.
1961: Preliminary Report on Borings Through Pleistocene Deposits, Cochrane District, Ontario; Geological Survey of Canada, Paper 61-16.

Kryzan, A. and Strangway, D.W.
1977: Magnetotelluric Studies in the Geotraverse Area; Unpublished Proceedings, 1977 Geotraverse Conference, University of Toronto, 121-131.

Lee, H. A.
1979a: Northern Ontario Engineering Geology Terrain Study Data Base Map: Iroquois Falls; Ontario Geological Survey, Map 5027, Scale 1:100 000.

1979b: Northern Ontario Engineering Geology Terrain Study Data Base Map: Kirkland Lake; Ontario Geological Survey, Map 5030, Scale 1:100 000.

Madden, T. and Thompson, W.
1965: Low-Frequency Electromagnetic Oscillations of the Earth-Ionosphere Cavity; Rev. Geophy. Space Phys. Vol. 3, p. 211-254.

Marquardt, D.W.
1962: An Algorithm for Least Squares Estimation of Nonlinear Parameters; Journal Society Indust. Applied Mathematics, Vol. 11, p.431-441.

Mehran, M. and Arulanandan, K.
1977: Low Frequency Conductivity Dispersion in Clay-Water-Electrolyte Systems; Clays and Clay Minerals, Vol.25, p. 39.

Pyke, D.R., Ayres, L.D. and Innes, D.G.
1973: Timmins-Kirkland Lake, Districts of Cochrane, Sudbury and Timiskaming; Ontario Geological Survey, Map 2205, Geological Compilation Series, Scale 1 inch to 4 miles.

Roed, M.A. and Hallett, D.R.
1979: Northern Ontario Engineering Geology Terrain Study Data Base Map: Elk Lake; Ontario Geological Survey, Map 5020, Scale 1:100 000.

Strangway, D.W. and Vozoff, K.
1969: Mining Exploration with Natural Electromagnetic Fields; Mining and Groundwater Geophysics, Geological Survey of Canada, Economic Geology Report, Vol. 26, p. 109-122.

Strangway, D.W., Redman, J.D. and Macklin, D.
1980: Shallow Electrical Sounding in the Precambrian Crust of Canada and the United States; in The Continental Crust and its Mineral Deposits, edited by D.W. Strangway, Geological Association of Canada, Special Paper 20.

Strangway, D.W., Swift, C.M. and Holmer, R.C.
1973: The Application of Audio Frequency Magnetotellurics (AMT) to Mineral Exploration; Geophysics, Vol. 38, p.1159-1175.

Grant 113 Field Investigation of Factors Controlling Changes of Ground Water Pressure in Clay Slopes

T.C. Kenney
Department of Civil Engineering, University of Toronto

ABSTRACT

Under Grant 113, research was directed towards answering the question: "by what magnitudes and at what rates do ground water pressures change in natural clay slopes?" The answers are dependent on the properties of the clay and on hydraulic boundary conditions in each slope.

Using consolidation theory, predictions were made of changes in ground water pressure based on the postulate that these changes were the direct result of changes of hydraulic conditions near the ground surface. Two factors considered to be very influential in this regard are the availability of water at the ground surface and the permeability of the clay.

The results of field measurements at a site near New Liskeard, Ontario, are in agreement with the predictions. Minimum values of ground water pressure were measured at the end of winter (at the end of prolonged periods of zero infiltration) and maximum values were measured during early summer or late autumn. Very small changes occurred at depths greater than 5 m in this soft, massive clay.

It is concluded that for soils having small values of permeability, small seasonal changes in ground water pressure can be expected, and small seasonal changes of slope stability will occur. Conversely, if the body of clay is pervious as the result of a system of open joints, larger and more rapid seasonal changes of ground water pressure can be expected, and larger changes of slope stability will occur.

INTRODUCTION

The objective of this project is to determine through theoretical and field investigations the primary factors controlling the magnitudes and rates of change of ground water pressures in clay slopes. With such knowledge there will be a better understanding of the reasons for changes of slope stability caused by climatic variations, and suitable remedial measures can be developed where hazardous conditions exist.

In Canada and Scandinavia, the greatest frequencies of landslides in clays occur in the spring and autumn periods of the year when there is abundant surface water caused by melting of snow and heavy precipitation. It can be concluded that, during these periods, ground water pressures reach their maximum annual values.

There are very few records of measurements of ground water pressures in clay slopes over extended periods of time. Kankare (1969) reported measurements at several sites along the Kimola Canal in Finland, over time periods of several years, where rapid increases of ground water pressure could be related to spring snow melt and prolonged precipitation. Kenney and Chan (1977) reported the results of measurements made over a period of five years at a research site at New Liskeard. Most of the piezometers at the New Liskeard site were located at depths greater than 7 m below the ground surface, and at these locations the gound water pressures were found to remain very steady. At locations shallower than 7 m there were fluctuations of pressure which were largest near the ground surface.

The subject of changes in ground water pressures that result from changes in conditions of water infiltration at the ground surface has been considered by Kenney (1980) on the basis of theory of fluid conduction by compressible media (theory of consolidation). Kenney determined that changes of groundwater pressure, attributable to changes of hydraulic conditions at the ground surface, would occur very slowly if the soil had small values of permeability. Conversely, much more rapid changes would occur if the soil was pervious. The rate of change of ground water pressure is also dependent on the compressibility property of the soil.

In summary, the following points can be made.

(1) The frequency of landslides in clays is greatest during the wettest times of the year.

(2) Measurements of ground water pressures in a small number of clay slopes indicate that although there can be rapid pressure increases at shallow depths, the pressures at one site remain very steady at depths greater than 7 m below the ground surface. Theoretical considerations suggest that rapid changes of ground water pressure cannot occur as a result of climatic events if the soil is impervious (such as an intact clay), but can occur if the soil is relatively pervious (such as a clay possessing a system of open joints).

(3) Combining (1) and (2) above, the postulate emerges that in the absence of open joints in a clay slope, neither rapid nor large changes of ground water pressure will occur on a seasonal time frame and, therefore, the stability of the slope will remain relatively constant. Conversely, if a clay slope has a surface zone containing open joints, the filling (or draining) of these joints with water can cause and transmit rapid changes of pressure throughout the zone of open-jointed clay, causing rapid changes of stability of the slope.

RESEARCH PROGRAM

The research program was planned as a two-year investigation. The field work for the first year had three components. The first was measurement of changes of ground water pressure, particularly near the ground surface, in a clay slope near New Liskeard, Ontario. Measurements were taken during the summer months during and following periods of rainfall, and during springtime after the ground surface had thawed. The second component of work was the investigation of the structure of the clay and its changes with depth. Exposures of the clay were examined and shallow pits were excavated for further examination. Simple water conductivity tests were conducted in augered holes in an attempt to measure the fluid-conductivity properties of near-surface zones of soil.

It was expected that the result of the first year's field work and analytical work would provide a clear indication whether or not rapid changes of ground water pressure could be related to, and require, the existence of open joints in the clay. If the first year's work had indicated the existence of open joints as a primary factor controlling rapid changes of ground water pressure, the second year's work would focus on methods to reduce the influence of the open joints by such means as draining the joints or filling them with impervious material.

In fact, the first year's work has indicated that the clay at the New Liskeard slope experiences relatively small changes of groundwater pressure, even at shallow depths, and that although there is a surface-weathered zone which is jointed, the joints appear to be tight except very close to the ground surface.

It is concluded that the New Liskeard clay, because of its very small value of permeability, undergoes small seasonal changes of ground water pressure and, therefore, also small seasonal changes of stability in spite of the fact that the site has experienced normal seasonal climatic changes. This would be expected of other clay slopes having comparable values of permeability coefficient. No information was gained concerning clay slopes in which the soils had large values of mass permeability as the result of the existence of open joints.

THEORETICAL ESTIMATES

Ground water flow through clay can be considered as a case of flow of an incompressible fluid (water) through a compressible porous medium (soil). Where the soil remains saturated the change of total flux of water being conducted through the soil plus the rate of change of volume of void space occupied by water must be zero. This is the process of consolidation or swelling, and changes of piezometric level occurring during the process can be estimated approximately through the use of the following consolidation equation describing one-dimensional flow:

$$\frac{\delta h}{\delta t} = \frac{k_z \delta^2 h}{m \gamma_w \delta z^2} \qquad \text{Equation 1}$$

where h is peizometric elevation (elevation of water surface in a piezometer standpipe), t is time, k is coefficient of hydraulic conductivity, m is coefficient of volume change of soil expressed as change of porosity per unit change of effective stress, γ_w is unit weight of water and z is the vertical axis.

Within a deposit of clay which is not subjected to external loading, changes of piezometric level will only occur as the result of changes of hydraulic conditions at the ground surface. At the ground surface the hydraulic condition is governed by the rate of water infiltration, which is influenced by the availability of water, the hydraulic gradient at the ground surface ($i = -\delta h/\delta z$) and the coefficient of hydraulic conductivity of the soil. During any period of time, when the infiltration rate is less than the discharge rate, the peizometric level will decrease and the phreatic surface (locus of points at which ground water pressure is zero) will fall. Conversely, when the infiltration rate exceeds the discharge rate, piezometric levels will increase and the phreatic surface will rise. The highest possible position of the phreatic surface is the ground surface. In the case of New Liskeard clay, what is the approximate rate of precipitation required to provide for maximum rate of infiltration? This can be estimated using approximate values of hydraulic gradient and coefficient of hydraulic conductivity: the maximum value of hydraulic gradient is $i = 1$, and an approximate value of hydraulic conductivity is $k = 1 \times 10^{-7}$ cm/s, giving a precipitation rate of 1×10^{-7} cm/s or about 0.1 mm/day, which is appreciably smaller than the average rate of precipitation at the site. This means that with normal precipitation at the site, and with the existence of pervious organic soils at the ground surface to provide storage for surface water, at most times during the year there will be available sufficient water to satisfy the needs for maximum infiltration. When the ground surface is frozen, however, the infiltration rate will be zero.

Equation 1 indicates that the rate of change of piezometric levels within the soil depends on two soil properties: k the coefficient of hydraulic conductivity, and m the coefficient of volume change. If the soil were infinitely incompressible ($m = 0$), changes of piezometric level would occur instantaneously without water having to be conducted into the soil. However, because soils have compressible structures their volume changes when ground water pressures change, and therefore water must be conducted into or out of the soil to effect changes of ground water pressure. The more compressible the soil structure the slower will be changes of ground water pressure.

Figure 1 presents the results of an estimate of changes of piezometric level below an area of infiltration for which equation 1 was used. The calculations were made for the winter period when normally the ground surface is frozen and there is zero infiltration. Immediately before freeze-up, piezometric levels are at, or close to, their maximum annual values, whereas at the end of winter they are at, or close to, their minimum annual values. Therefore, the changes of piezometric level occuring during the winter period are indicative of maximum annual changes, and estimates can be compared to the results of field measurements. The calculations involve the following assumptions:

(1) hydraulic gradient immediately before freeze-up is i = 0.5,
(2) hydraulic gradient at the ground surface immediately after freezeup is i = 0 (zero infiltration),
(3) water movement is vertical, and
(4) the value of the soil property $k/m\gamma_w$ is 0.10 m^2/day based on laboratory tests on undisturbed samples.

In Figure 1 the period of time equal to 100 days approximates the length of winter, during which infiltration would be zero. Based on these theoretical estimates the following remarks can be made.

(1) Changes of piezometric levels are greatest near the ground surface and decrease substantially at increasing distances below the ground surface. The maximum change of piezometric level in this soil was estimated to be at a depth of about 2 m (corresponding to a maximum change of ground water pressure of about 20 kPa), and significant changes did not occur beyond a depth of about 5 m.

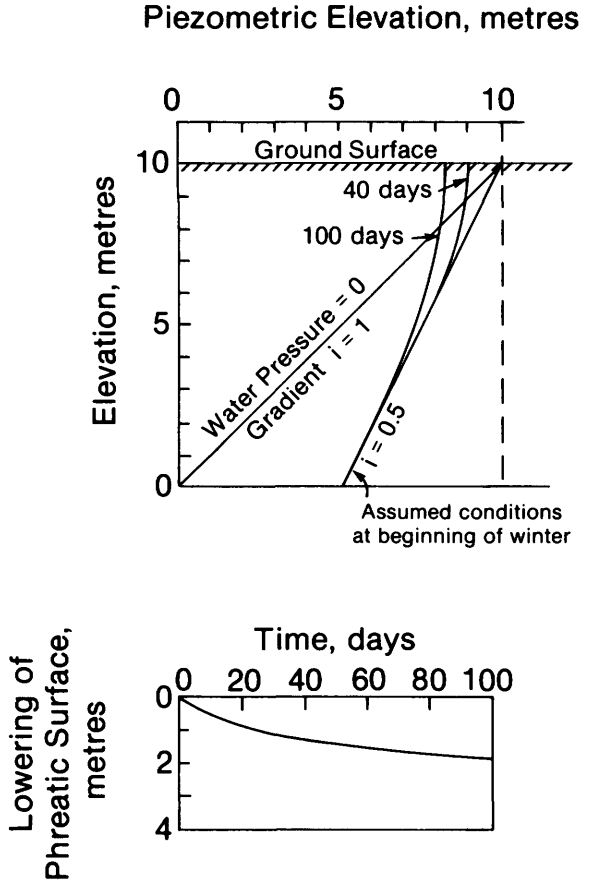

Figure 1. *Predicted changes of piezometric elevation and phreatic surface for condition of zero infiltration.*

(2) The rate of change of piezometric level is maximum at the ground surface and decreases substantially with increasing depth.

(3) The rate of change of piezometric level is proportional to the permeability of the clay and inversely proportional to its volume compressibility. Should a clay become weathered and a system of open joints develop, the coefficient of hydraulic conductivity will increase substantially whereas the coefficient of volume compressibility is likely to decrease, and both effects will cause the soil to react more quickly to changes of hydraulic conditions at the ground surface. The effect of weathering and the development of a system of open joints would increase both the range of changes of piezometric level and the depth to which changes would occur.

FIELD MEASUREMENTS

A suitable site at which measurements of changes of piezometric level can be made is located near New Liskeard, Ontario, where, for purposes of another research program, 70 piezometers had been installed and measurements made over a time period of about eight years. These measurements proved valuable to this project. The site is on the eastern bank of Wabi Creek on the property of the New Liskeard College of Agriculture Technology. The soils are soft, lacustrine sediments of glacial Lake Barlow and their characteristics have been described by Kenney and Chan (1973).

Precipitation at the site averages about 760 mm of water per year, distributed as 50 mm per month during winter and spring and 75 mm per month during summer and autumn.

In Figure 2 are presented the results of typical measurements of piezometric elevation made in the infiltration area at the head of the slope during the time period 1972-1978. For three piezometers, the total range of measurements taken during this time period are shown. To obtain more information three electric piezometers were installed at shallow depths and continuous measurements were taken during the month of August, 1981. The measurements remained constant during this period in spite of varied climatic conditions. These results are consistent with the maximum measurements obtained during the time period 1972-1978 and appear to describe the upper limit of piezometric elevations at this location.

Also plotted in Figure 2 are the depths of the phreatic surface during the period 1974-1978, based on interpretations of the piezometric measurements.

Comparison of these data with the predictions shown in Figure 1 indicate that they are in good agreement. This suggests that the factors recognized in making the theoretical estimates and discussed in the previous section are in fact the principal factors affecting changes of ground water pressure.

CLAY STRUCTURE

The clay at New Liskeard has a jointed structure to a

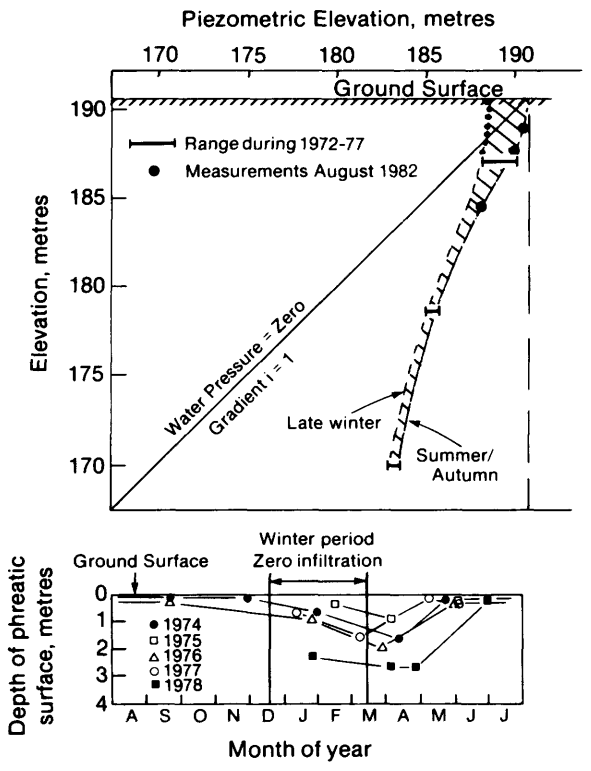

Figure 2. *Measured changes of piezometric elevation and phreatic surface below infiltration area.*

depth of about 3 m from the ground surface, the strength and frequency of the joints decreasing with depth. This was observed in exposures in the area of the site and in shallow excavations at the site.

Of considerable importance to this project was whether or not the joints were open and gave the clay a much increased value of hydraulic conductivity. From visual inspection the joints seemed to be open to a depth of about 0.5 m, and below that depth they seemed to be closed. Attempts to perform shallow permeability tests were not successful.

As explained in the following section, additional field attempts will be made to determine the variation with depth of soil properties which control the ground-water-pressure behaviour of the soils (namely $k/m\gamma_w$).

FUTURE WORK

Two further pieces of work are planned for this project. One is to install electrical piezometers at shallow depths and to obtain regular measurements over a time period of a year. The second is to attempt to measure the soil property $k/m\gamma_w$ by means of in situ dissipation tests. The test would consist of thrusting a piezometer into the soil to a particular depth, thereby generating an excess water pressure in the soil and monitoring the rate of decrease of water pressure. The measured rate of decrease of water pressure would be dependent on the geometry of the apparatus and on the soil property $k/m\gamma_w$.

CONCLUSIONS

The results of the first year's work have indicated that the clay at the New Liskeard slope experiences relatively small seasonal changes of ground water pressure, even at shallow depths. Although there is a surface-weathered zone which is jointed, observations of the joints and an interpretation of the changes of ground water pressure seem to indicate that the joints are tight except very close to the ground surface.

The finding that the seasonal changes of ground water pressure are small indicates also that the seasonal changes of slope stability would be small. The ability of a soil to react quickly to changes of hydraulic conditions at the ground surface is dependent on its value of $k/m\gamma_w$. An in situ dissipation test is being developed and will be used in attempts to measure this property in the field with piezometer probes. If it is successful it will provide a means of determining whether or not a soil profile will react quickly to changes of hydraulic boundary conditions, and from this conclusions can be drawn concerning the likelihood of large seasonal changes of ground water pressure and of important seasonal changes of slope stability.

ACKNOWLEDGMENTS

The author wishes to thank K.C. Lau and D. Lau for their technical assistance in regard to the field work.

REFERENCES

Kankare, E.
1969: Geotechnical Properties of the Clays at the Kimola Canal with Special Reference to the Slope Stability; State Institute for Technical Research, Helsinki, Finland, Publication 152.
Kenny, T.C.
1980: Long-Term Groundwater Pressures in Soft-Clay Slopes; SMFE, Proceedings of Sixth Panamerican Conference, Lima, Peru, 1979, Vol. 3, p. 83-89.
Kenney, T.C. and Chan, H.T.
1973: Field Investigation of Permeability Ratio of New Liskeard Varved Soil; Canadian Geotechnical Journal, Vol. 10, No. 3, p. 473488.
1977: Seasonal Changes of Groundwater Pressure and Stability of a Natural Slope in Varved Clay; Department of Civil Engineering, University of Toronto Publication 77-01, p. 43.

Grant 109 Interpretation of Gravity Data from New Liskeard, Ontario

L. Mansinha and D.A. Wilkinson
Department of Geophysics, University of Western Ontario

ABSTRACT

A study was made of the New Liskeard gravity high using gravity and density data collected by the Ontario Geological Survey. The regional-residual problem was tackled with a statistical trend surface refinement technique which enables the fitting of a representative regional surface by minimizing the distorting effects of local anomalies. Prior to the interpretation of the residual anomaly, the contribution of the surface geology was estimated and removed. The remainder of the residual anomaly is thought to be caused by an intrusive body. A non-linear least squares refining program was incorporated into the modelling process. Three models of the intrusive body are presented: in two models the burial depth is constant; in the third, the model units are of varying depth. Common to the first two models is the rather unusual feature that they are partitioned into essentially two separate units. This partition is attributed to the presence of a major fault system which is postulated as being instrumental in controlling the shape of the intrusive body. The third model, while still appearing to be influenced by the fault system, does not display the fragmentary nature of the two previous models. In this model the intrusion resembles the undulating sill-like structures postulated for other diabase intrusions in Ontario.

INTRODUCTION

The New Liskeard gravity high is located northwest of the town of same name in Ontario, roughly at the centre of the region bounded by Latitudes 47°N and 47°55'N and Longitudes 79°30'W and 80°30'W. This is one of the higher gravity anomalies in northeastern Ontario. The high can be seen in the Bouguer anomaly map (Figure 1) as the only peak with a –10 mgal contour. The peak value is greater than – 8 mgals. The Bouguer anomaly map was compiled with data provided by the Ontario Geological Survey. A large part of this data was obtained during a survey conducted in the summer of 1977. Some 2808 gravity stations were established using four Lacoste-Romberg gravimeters (G-28, G-294, G-329, G-417). The gravity stations were tied to control stations established by the Earth Physics Branch of Energy, Mines, and Resources Canada at North Bay, Marten River, Temagami, Latchford, and Cobalt.

The gravity observations were augmented by 1219 surface density samples collected during this survey and a previous one in 1973.

The interpretations of the gravity anomaly in terms of subsurface density models is the purpose of this project. This report is highly condensed, and the reader is referred to Wilkinson (1981) for more detail.

PROJECTION AND GRIDDING

The data were obtained from the National Gravity Data Centre in Ottawa in the form of Bouguer anomaly values with the station location given as latitude and longitude. The locations were projected onto a flat surface using spherical stereographic projection. In this projection the meridians are straight lines and there is no angular distortion. The mapping equations are

$$X = \frac{2R(\cos A \sin B - \sin A \cos B \cos C)}{1 + \sin A \sin B + \cos A \cos B \cos C}$$

$$Y = \frac{2R \cos B \cos C}{1 + \sin A \sin B + \cos A \cos B \cos C}$$

where,

R = radius of datum sphere
A = latitude of coordinate origin
B = latitude of data point
C = difference in longtitude between origin and data point

The value of R was chosen to be the radius vector of the international ellipsoid.

$R = R_0(1 - 0.003367 \sin^2 A + 0.0000071 \sin^2 2A)$

where,

R_0 = equatorial axis = 6 378 160 m

For simplicity the spherical approximation of the ellipse was used in the projection method. The error introduced was less than 1 m for any data point (Richards and Adler 1972).

For subsequent processing application it is necessary that the data be uniformly distributed on a sampling grid. This is accomplished by fitting interpolating surfaces to the observed irregularly distributed data and then reading off the surfaces at the grid points. It will be assumed here that the interpolating surface Z(x,y) possesses the minimum curvature property, where the total squared curvature

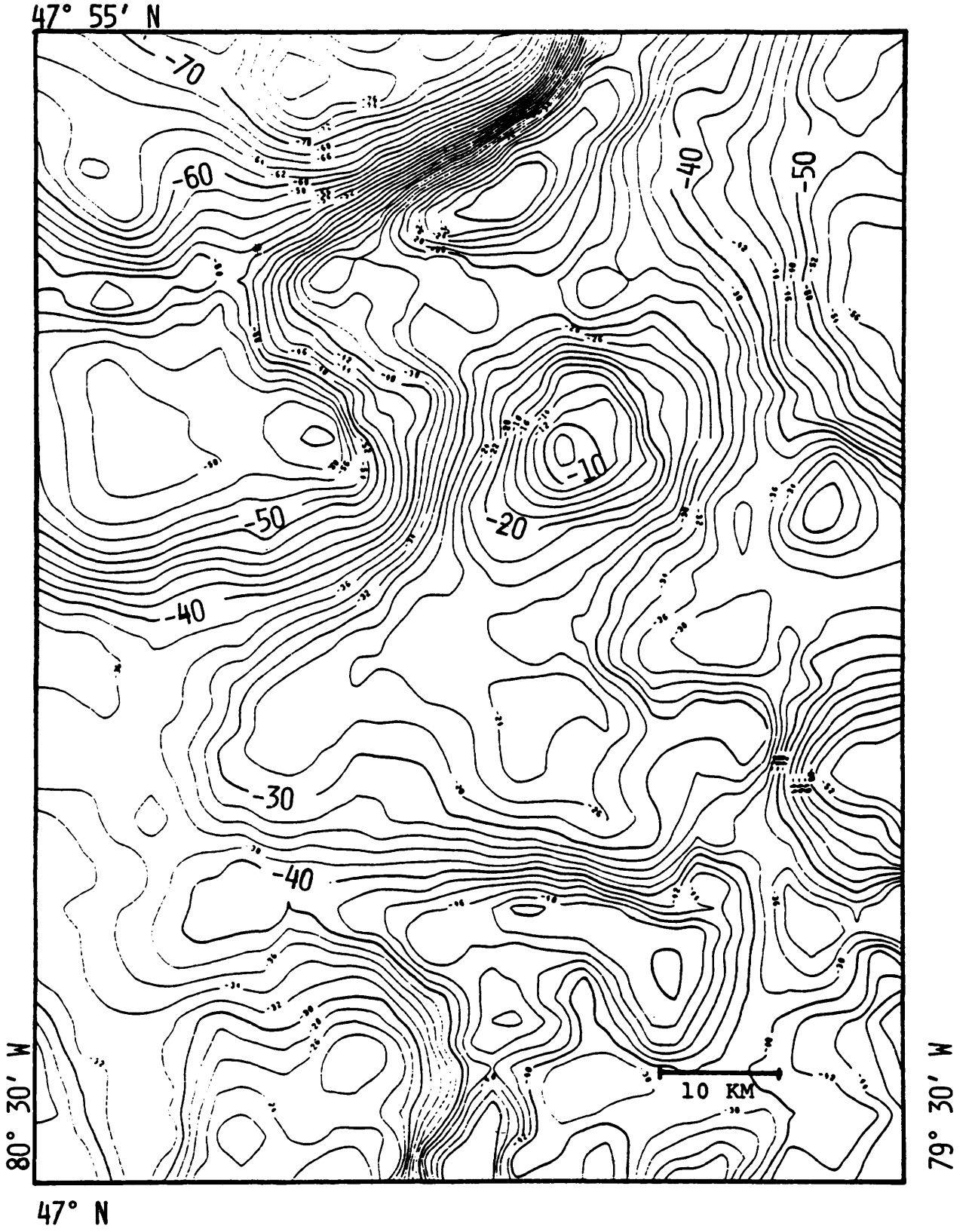

Figure 1. *Bouguer anomaly map of the New Liskeard gravity high and the surrounding region. The high is located to the top and right of the centre of the figure.*

$$C(Z) = \iint \left\{ \frac{\delta^2 Z}{\delta x^2} + \frac{\delta^2 Z}{\delta y^2} \right\} dxdy$$

is a minimum (Briggs 1974). This condition defines a surface through the sample points, which is the smoothest possible; therefore it should contain the least number of spurious values. The program was written by Harrison (1978), based on Briggs (1974) and Swain (1976).

The gravity observation stations had an average separation of about 2 km. The Bouguer anomaly map (see Figure 1) was produced with a grid interval of 2 km. The main anomaly maps, such as Figure 4, were produced with a 1 km grid.

DETERMINATION OF THE REGIONAL SURFACE

There is a continuing discussion in the literature on the method of separation of the residual from the regional anomaly (Gupta and Ramani 1980). Here we assume that the regional is a low order polynomial surface, essentially a trend surface. First the order of surface is chosen, usually 2 or 3; then the surface of the specified order is determined by a least squares "best-fit" method. However, the fitted surface would still be contaminated with the residual component. We have assumed that the regional and residual belong to two different statistical populations. After the fitting of the regional surface, the standard deviation of the residual is calculated. Original data values lying more than two standard deviations away from the fitted regional surface are assumed to be due to local structures and are modified to reduce their effect on the fitted regional surface. A new regional surface is then fitted and the process repeated until the standard deviation falls below a preset value.

Several 'modification' schemes were tried. The following scheme was adopted: the orginal data value which is more than two standard deviations away from the fitted regional is replaced with a point which is one standard deviation away. Using this scheme, a satisfac-

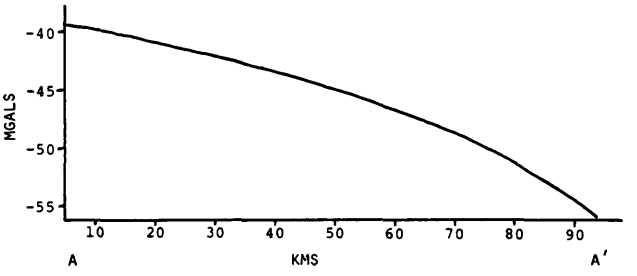

Figure 3. *A cross-section of the regional surface along the line AA' in Figure 2.*

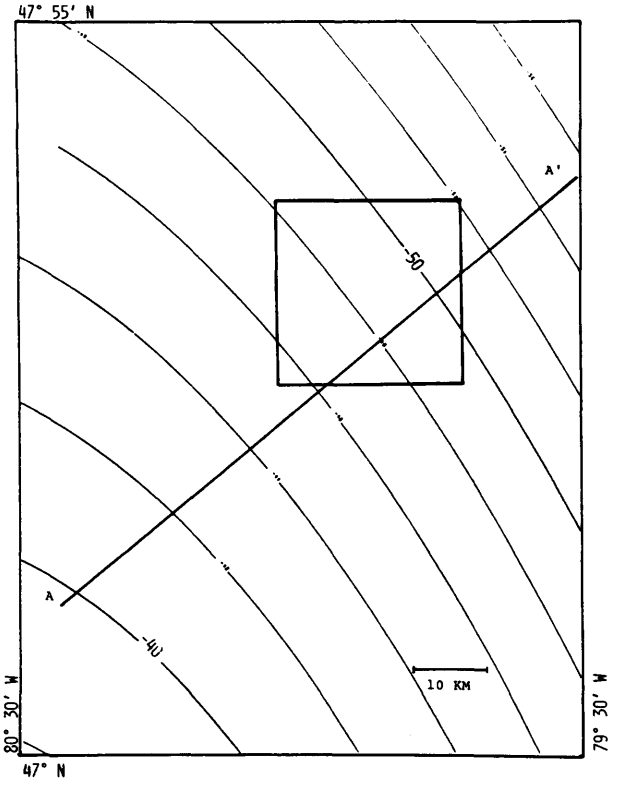

Figure 2. *Contour map of the regional anomaly. The surface slopes from the southwest to the northeast. The inset square outlines the gravity high to be interpreted in detail.*

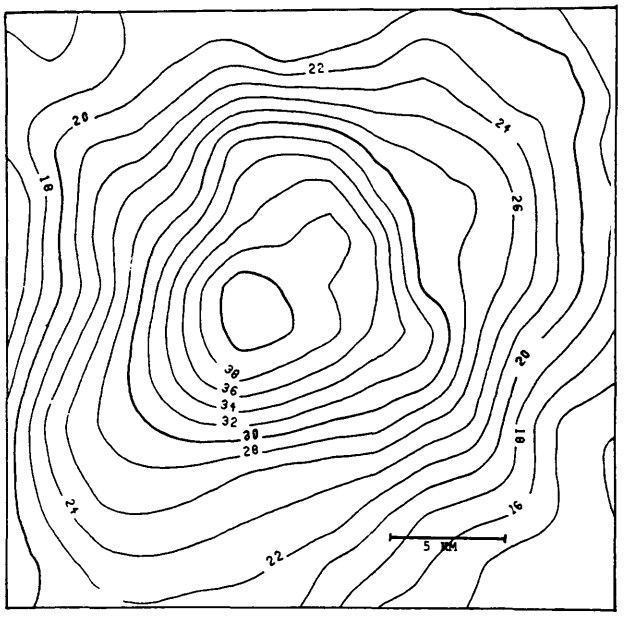

Figure 4. *The residual anomaly after removing the regional from the Bouguer anomaly. The contours are in mgal.*

tory regional surface was determined within about eight iterations.

To avoid edge effects, gravity values from a much larger area were used to determine the regional surface. We have used all the values within 78°W and 82°W, 45°N and 49°N. The total number of values used was 6985 points.

The final regional surface determined was

$$f(x,y) = 57.150425 + 0.455121\,x + 0.06233\,y - 0.002221\,x^2 - 0.000507\,xy - 0.00021\,y^2 + 0.000002\,x^3 + 0.00001\,x^2y.$$

A contour map of this surface is presented in Figure 2. The inset rectangle outlines the extent of the New Liskeard gravity high. The profile of the regional surface along AA' is shown in Figure 3. Note that the regional surface is smooth and shows no influence of the local anomalies. The removal of the regional from the observed Bouguer gravity data defines the residual anomaly to be interpreted (Figure 4).

CONTRIBUTIONS OF SURFACE GEOLOGY

The variation of density due to near surface geological structure has an effect on the Bouguer anomaly. Our purpose in calculating the geological contribution was twofold: (1) to see if the extension of surface geology to a reasonable depth could explain the residual anomaly; and (2) to correct the total residual so that the anomalous effect of the main causative body could be isolated. The surface geology contribution is shown in Figure 5. To

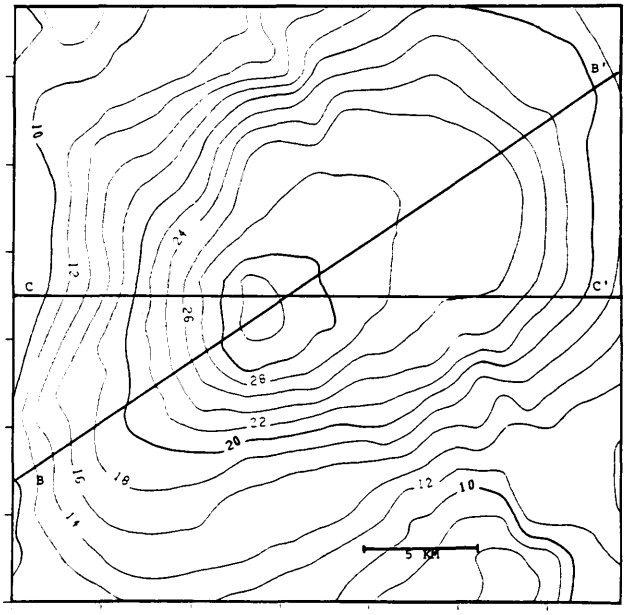

Figure 6. *The residual after removal of the effects of surface geology.*

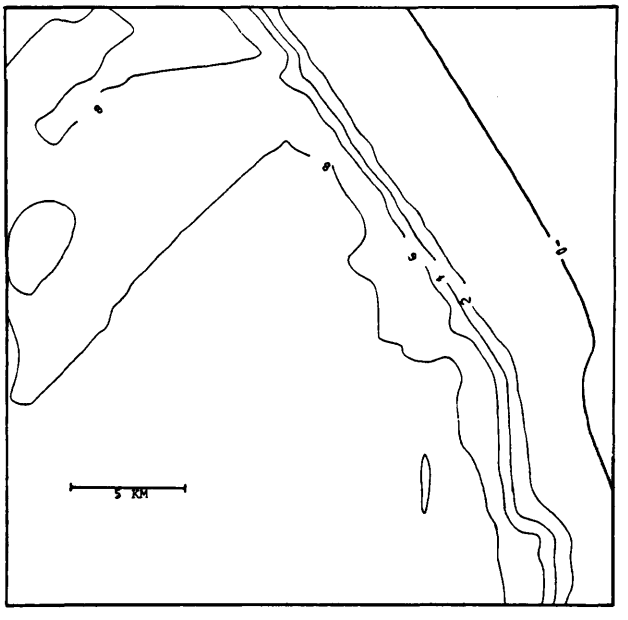

Figure 5. *The effects of surface geology. The contour values are in mgal.*

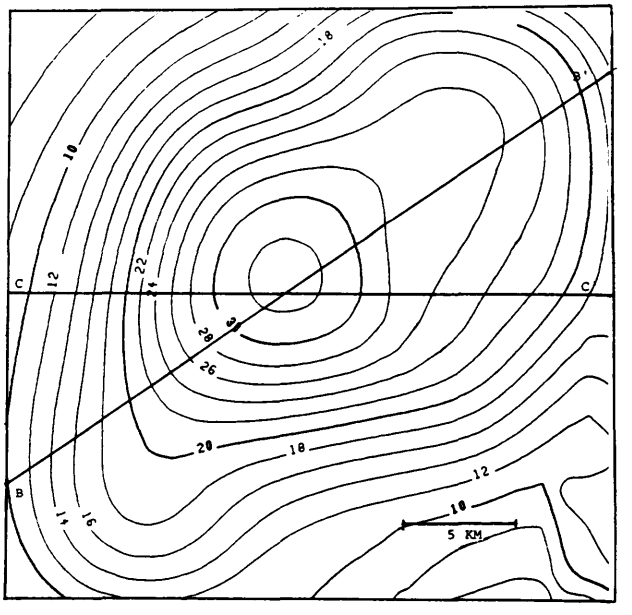

Figure 7. *The anomaly produced by Model I.*

effect the calculations, the surface was divided into a number of polygons, based on surface geology. Each polygon was assigned a thickness and a density based on the geologic formation and inferred structure. The contributions of all the polygons were summed to give the map shown in Figure 5. As can be seen, the maximum contribution of the near surface geology amounts to 8 mgal, compared to the peak value of the residual of 40 mgal, about 20 percent. The peak anomaly is now reduced to about 32 mgal.

INTERPRETATION

The procedure for interpretation of the residual anomaly (Figure 6) is now almost routine. To start, a reasonable "guess" is made of the distribution of density which may be the source of the anomaly. By considering prisms of varying depths to top, depths to bottom, and density, a model can be found which satisfactorily explains the observed values. The non-uniqueness of such solutions is well known. An infinite number of models can be found. It is necessary to apply some constraints and select a few of the possible models.

The constraint here is that an outcrop of intrusive diabase is found near the peak of the anomaly. This suggest that the causative body is an intrusion. However, the size and shape of the anomaly implies that the body is not shallow. Three different models were tried.

MODEL I

A total of 35 rectangular prisms were used, with the top surface of all the prisms fixed at 3 km. The density was assumed to be 3.01 g/cm^3. After the initial "guess" model, refinement procedure consisted of varying the depth of the bottom of each prism. It became apparent that for a good fit, several blocks of a lower density have to be incorporated into the model.

The refining of the "guess" models was effected through a nonlinear iterative program. The anomaly due to Model I is shown in Figure 7. A visual comparison with the observed residual in Figure 6 shows that the agreement is good. The profile of Model I and the gravity anomaly along line BB' is shown in Figure 8.

MODEL II

The depth to the top of the rectangular prisms was set at 4 km. The number of prisms used was 38. The density was set at 3.01 g/cm^3. However, to keep the depth to the bottom of the prism within reasonable limits, a higher density had to be used in the lower part of some of the blocks. The results are shown in Figure 9, and the profile along BB' in Figure 10.

It can be seen that the two models are quite similar. Both appear to be divided into two parts, by a northwest-trending fault.

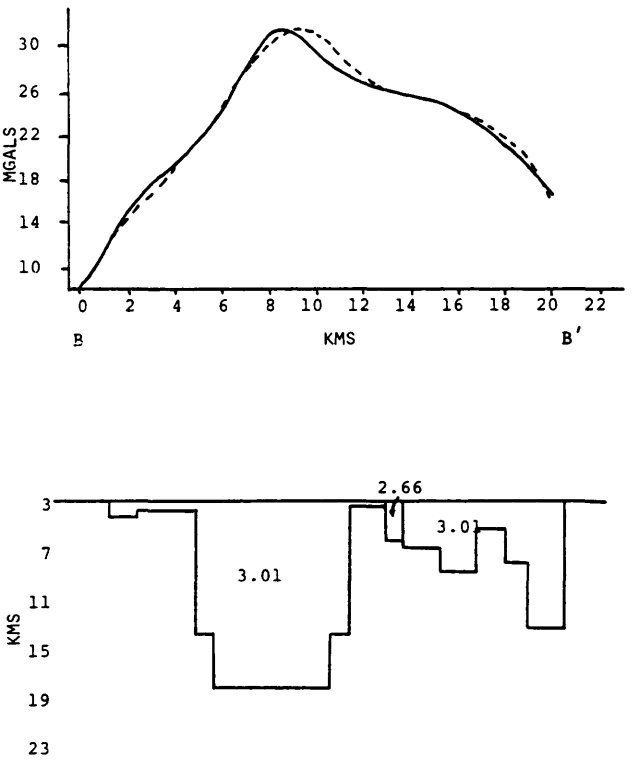

Figure 8. *Comparison of the observed residual and that computed from Model I along line BB' of Figure 7. The lower part of the figure shows the cross section of the model along the same line.*

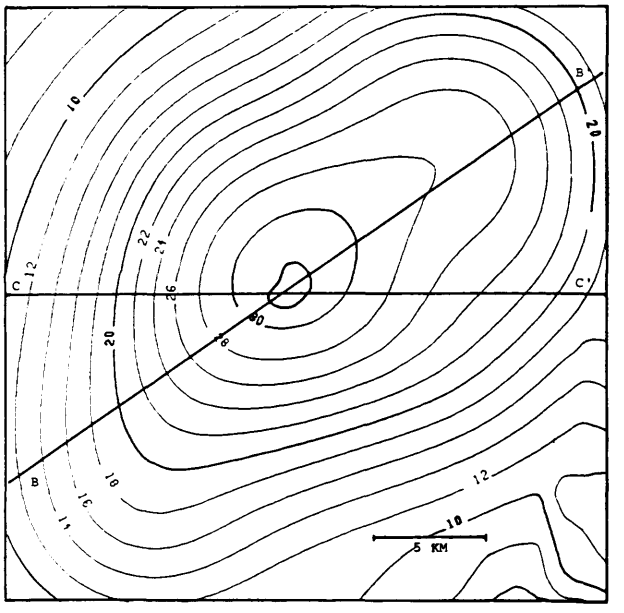

Figure 9. *The anomaly produced by Model II.*

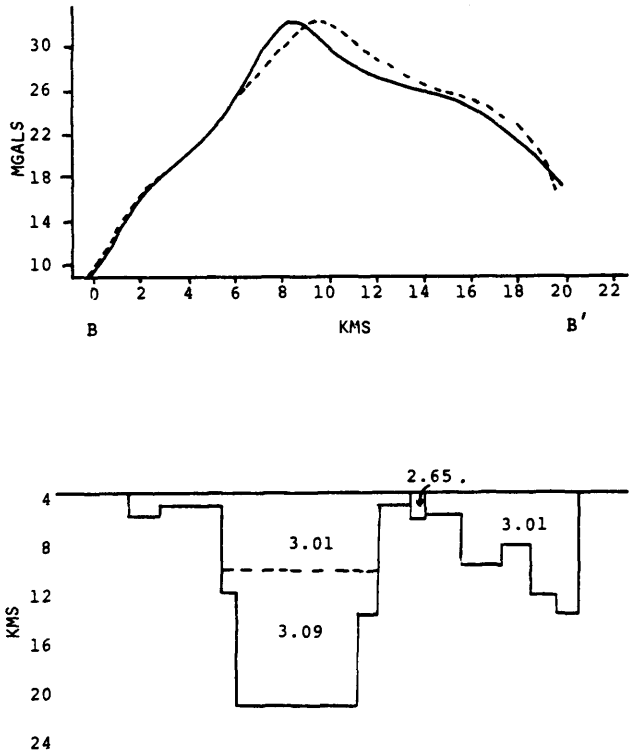

Figure 10. *Comparison of the observed anomaly with that due to Model II along line BB' of Figure 9. The cross-section of the model is also shown on the same line. Note that the depth to the top of Model I is 3 km (see Figure 8) compared to 4 km for Model II.*

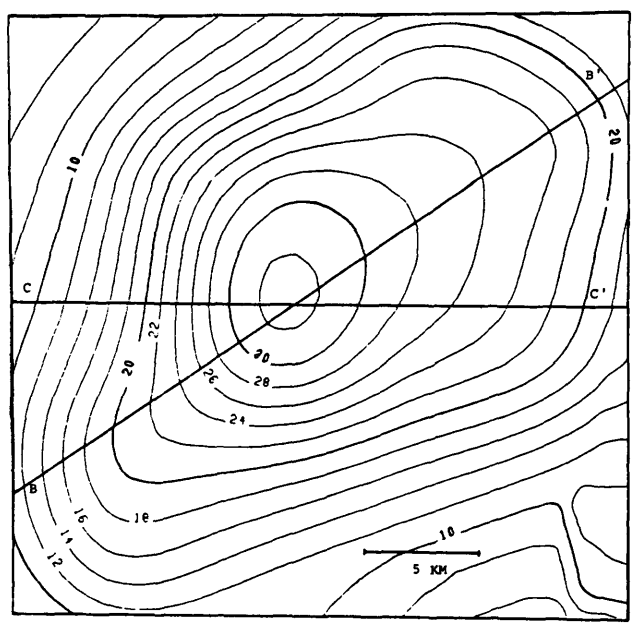

Figure 11. *The anomaly produced by Model III.*

MODEL III

A total of 34 polygonal prisms were used in this model. The density was set at 3.01 g/cm^3. Both the tops and the bottoms of the prisms were allowed to vary. The gravity anomaly caused by such a density distribution is shown in Figure 11, and the profile along BB' is given in Figure 12.

CONCLUSIONS

Due to the non-uniqueness of model fitting procedures in the interpretation of gravity anomalies, the three models are to be taken as suggestions only. The surface exposure of the diabase was not considered in the models and this probably affected the near surface part of the models. However, there is little doubt that much of the anomaly is caused by density variation at depth. The common characteristic of all three models suggests that either the causative body is bisected by a fault, or was structurally controlled by a pre-existing fault.

The iterative trend surface method of fitting the regional and the non-linear least squares model refining methods are, we believe, novel to the interpretation of gravity data.

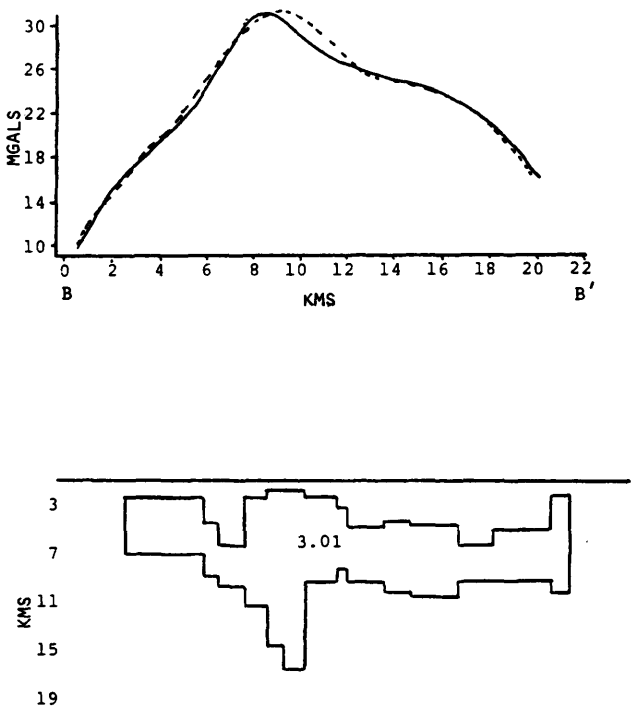

Figure 12. *Comparison of the observed and computed anomalies along line BB' of Figure 11 for Model III. The cross-section of the model is also shown.*

ACKNOWLEDGMENTS

We have profited from discussions on several occasions with R. Barlow and V. Gupta of the Ontario Geological Survey. Professor G. West of the University of Toronto made available to us copies of certain theses and computer programs during the course of this project.

REFERENCES

Briggs, I.C.
1974: Machine Contouring Using Minimum Curvature; Geophysics, Vol. 39, p. 38-48.
Gupta, V.K., and Ramani, N.
1980: Some Aspects of Regional-Residual Separation of Gravity and Anomalies in a PreCambrian Terrain; Geophysics, Vol. 45, p. 14121426.
Harrison, C.J.
1978: The Design and Application of Two-Dimensional Digital Filters; unpublished M.Sc. Thesis, University of Western Ontario.
Richards, P., and Adler, R.K.
1972: Map Projections for Geodesists, Cartographers and Geographers; American Elsevier, New York.
Swain, C.J.
1976: A Fortran IV program for Interpolating Irregularly Spaced Data Using the Difference Equations for Minimum Curvature; Computers and Geosciences, Vol. 1, p. 231-240.
Wilkinson, D.A.
1981: An Interpretation of Gravity Data from New Liskeard, Ontario; unpublished M.Sc. Thesis, University of Western Ontario.

Grant 57 A Micro-Earthquake Survey of the Gobles Oil Field Area of Southern Ontario.

R.F. Mereu
Department of Geophysics, University of Western Ontario

ABSTRACT

In August, 1980, the installation of a three-station seismic network in the vicinity of the Gobles oil field was completed. Data from these stations are telemetered via telephone lines directly to the Geophysics Department of the University of Western Ontario where they are recorded continuously on magnetic tape.

During the period from August, 1980, to May, 1982, over 225 earth tremors or micro-earthquakes in the 0.5 to 3.5 magnitude range were detected by the array. A detailed analysis of the location of the events showed that they do not correlate with the positions of oil and gas wells but rather lie along two fault lines that are almost perpendicular to each other. An analysis of the first motions of the seismic traces showed that the faults are text-book type faults which generate both compressional and dilatational onsets. The observations to date are consistent with the hypothesis that the events are induced or triggered by the fluids which are pumped in and out of the wells from secondary recovery activities.

INTRODUCTION

A few years ago, the Geophysics Department of the University of Western Ontario received a number of reports of "felt vibrations" or minor tremors from residents in the Gobles oil field area just east of Woodstock, Ontario. Further information on preliminary studies of these tremors was given by Mereu (1980). In August, 1980, the installation of a three-station seismic network over the oil field was completed by the University of Western Ontario (Figure 1). The instrument package at each station was made up of a 1 Hz vertical Mark Products seismometer, an amplifier and a voltage-to-frequency converter. Power came from dry cells which needed to be replaced only once per year. The frequency-modulated signals from the three Gobles stations are multiplexed and telemetered directly to the Geophysics Department of the University of Western Ontario via telephone lines. These signals are at present being monitored continuously on a 24-hour basis with magnetic tape. Events of interest are stored on an edited tape.

RESULTS

During the period August, 1980, to May, 1982, a total of over 225 earth tremors or micro-earthquakes in the 0.5 to 3.5 magnitude range were detected by the University of Western Ontario seismic network. Of these, most were in the 1 to 2 magnitude range. Two of the events were of magnitude greater than 3 and occurred on October 16, 1980, and August 28, 1981. An isoseismal survey, which we carried out in cooperation with the Earth Physics Branch of Energy, Mines, and Resources Canada, showed that these large events were felt by residents in a 300 km^2 area at distances greater than 10 km from the epicentre. No significant damage was reported although near the epicenter some dishes fell from the shelves.

A detailed analysis of the location of the larger well recorded events showed that they do not correlate with the positions of the oil and gas wells but are confined to two distinctly separated areas. The smaller area lies 1-1.5 km northwest of the town of Gobles. The larger area lies to the southeast of the town as is shown in Figure 1. The solutions obtained are consistent with the sources being located in either Cambrian or Precambrian formations. An analysis of the first motions of the seismic traces showed that the faults generating the signals were text-book type faults with compressive and dilatational onsets being observed. Two typical examples are given in Figures 2a and 2b. In Figure 2a the first motion at station 1 and station 2 is compressional (up) while at station 3 it is dilatational (down). In Figure 2b the first motion is compressional only at station 1. All of the events were categorized according to their first motion pattern. Each event was then plotted with a different symbol according to its pattern as shown in Figure 1. An examination of this figure shows that the symbol pattern is consistent with different types of sources lining up along two lines which are almost perpendicular to each other. These lines are a good indicator for the position of active faults. Not all the events observed fit the first motion patterns illustrated in Figure 2 (a and b). One notable exception was the large magnitude 3.2 event of August 28, 1981, which not only did not lie in the area of the other events but also had all its first motions at all three stations as "down" motions. On several occasions multiple events of almost identical signatures and patterns were observed over a few minutes or hours. On many events the amplitude at station 3 was abnormally small indicating that station 3 lay close to the auxiliary plane (plane perpendicular to the fault plane).

DISCUSSION AND CONCLUSIONS

The oil field near Gobles, Ontario, now operated by

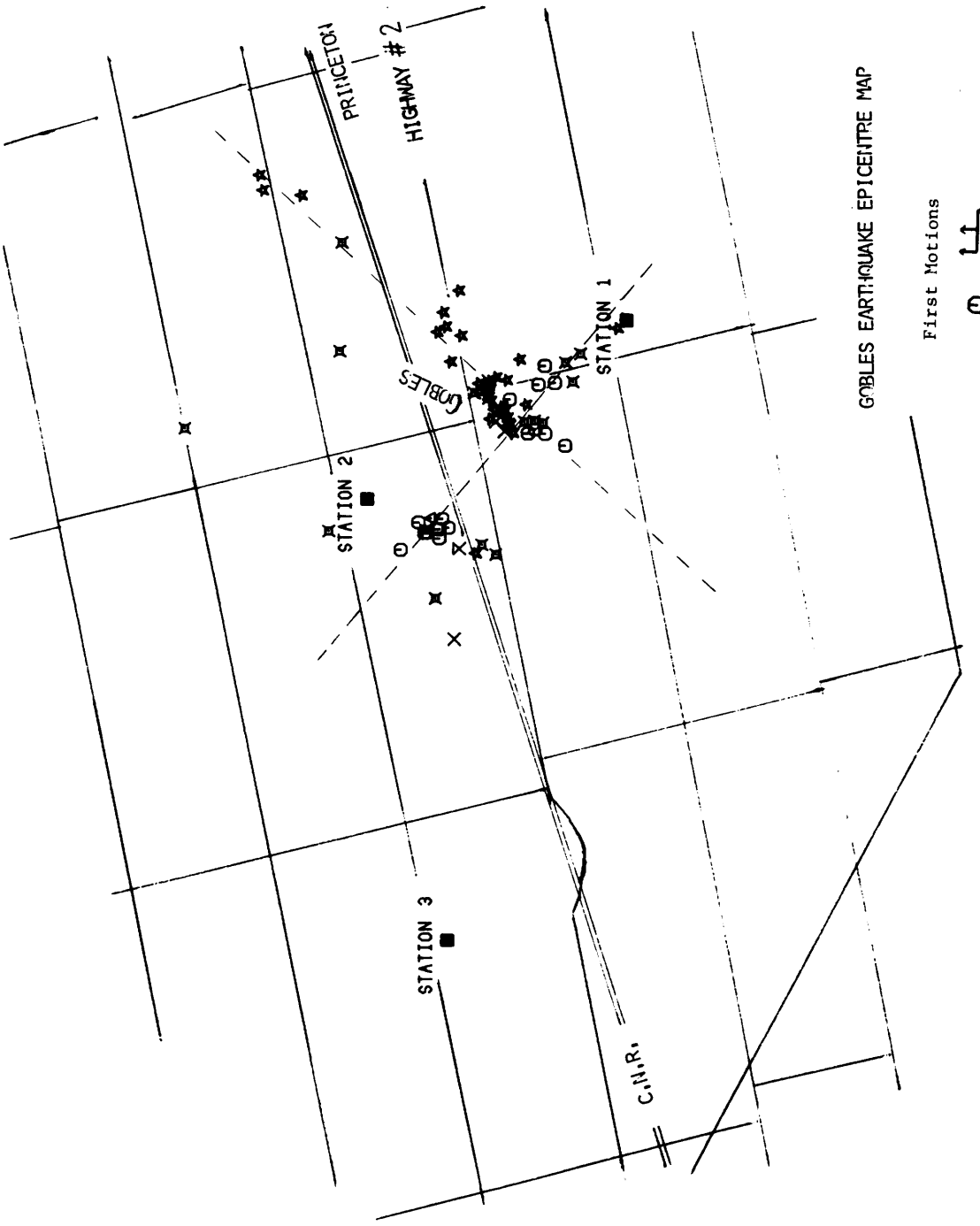

Figure 1. *Epicentre map showing the location of the Gobles earthquakes. Different symbols are used to categorize the earthquakes according to their first motion pattern. Dotted lines indicate possible fault positions.*

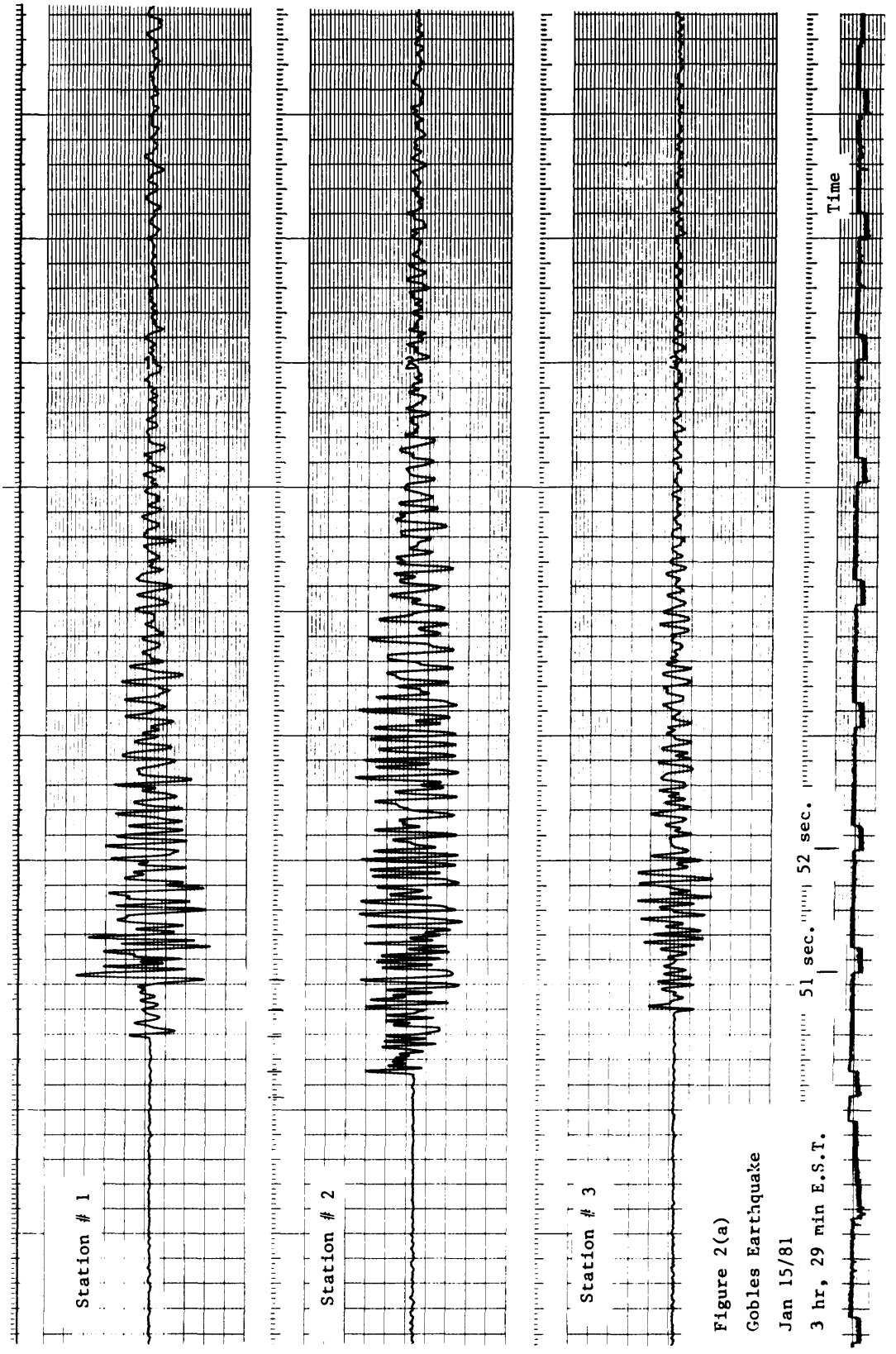

Figure 2a. *Seismic traces of Gobles earthquake January 15, 1981.*

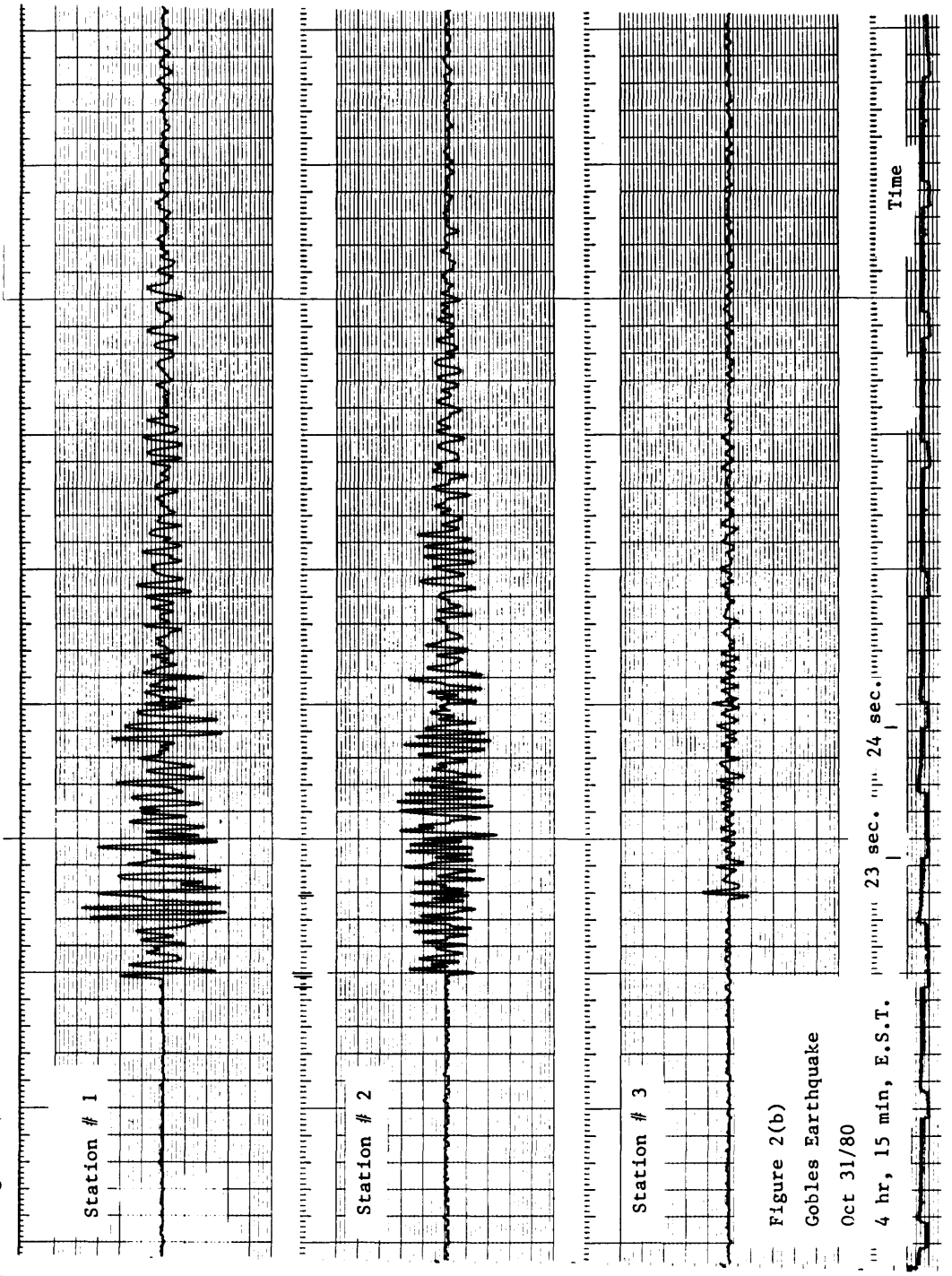

Figure 2b. *Seismic traces of Gobles earthquake October 31, 1980.*

Rayrock Resources Limited, has been producing oil and gas from about 70 wells since 1960 from a depth of 880 m (2900 feet) in the Gull River Formation just above the Cambrian. Secondary recovery operations began in the late 1960s. All our observations to date are consistent with the hypothesis that the seismic events are induced or triggered by fluids which are pumped in and out of wells from the secondary recovery activities in a manner similar to the induced events which were observed in recent years in Denver, Colorado (Evans 1966, Rayleigh *et al.* 1976), or in New York State (Fletcher and Sykes 1977). Our results indicate that at least two active faults are generating the events. It is interesting to note that the highway and railway tracks cross the region in the quiet zone between the two areas of high seismicity on either side of Gobles. It is quite possible that the heavy freight trains may be relieving the stresses below the tracks before they have time to build up to cause an earthquake. The causes of earthquakes, their prediction and their prevention by fluid injection are world problems which are still not understood very well. It is our hope that the study conducted here may provide information to help solve some of these problems.

ACKNOWLEDGEMENTS

The author would like to thank J. Brunet, B. Price, A. Yapp, S. Ojo, T. Mok, and F. Aibangee of the University of Western Ontario Geophysics Department for their technical assistance in connection with the instrumentation and operation of the seismic network at Gobles. Special thanks are also given to Mr. Gregor and Mr. Swick of the town of Princeton and Mr. Birtch of Woodstock for giving us permission to install seismic instruments on their properties. The author would also like to thank Dr. P.A. Palonen and Mr. R. Rebansky of the Ontario Ministry of Natural Resources at London, and Mr. Gaizwinkler of Rayrock Resources Limited for the very helpful discussions and technical information received in connection with the activities at the Gobles oil field.

REFERENCES

Evans, D.M.
1966: The Denver Area Earthquakes and Rocky Mountain Disposal Well; Mountain Geologist, Vol. 3, p.23-26.
Fletcher, J.B. and Sykes L.R.
1977: Earthquakes Related to Hydraulic Mining and Natural Seismic Activity in Western New York State; Journal of Geophysical Research, Vol. 82, p.3767-3780.
Mereu, R.F.
1980: Grant 57 A Micro-Earthquake Survey of the Woodstock-Kitchener Area; Ontario Geological Survey, Miscellaneous Paper 93, p.163-169.
Rayleigh, C.B., Healy, J.H. and Bredehoeft J.D.
1976: An Experiment in Earthquake Control at Rangely, Colorado; Science, Vol. 191, p.1230-1237.

Grant 92 Impact of Groundwater on Mining Activities in the Niagara Escarpment Area

R.L. Nadon and J.E. Gale
Department of Earth Sciences, University of Waterloo

ABSTRACT

A field, laboratory, and numerical modelling study was undertaken to determine the impact of groundwater on mining activities and underground space development in the Paleozoic rock units of the Niagara Escarpment near Milton, Ontario. Five holes were drilled, at a site next to the Dufferin quarry, penetrating the Amabel dolostone, the Reynales dolostone, the Cabot Head shale, the Manitoulin limestone, the Whirlpool sandstone, and the top part of the Queenston shale. The hydrogeologic characteristics of these formations were determined by a series of borehole injection tests, formation pumping tests, and laboratory tests on core samples. Results indicate the presence of an unconfined dolostone aquifer with an average hydraulic conductivity of 2×10^{-3} cm/sec, and a confined sandstone aquifer with a conductivity of 5×10^{-5} cm/sec, separated by a shale and limestone aquitard having a conductivity of less than 10^{-7} cm/sec.

Numerical model simulations of the groundwater flow system indicated that, for a 2 km^2 underground mine located in the dolostone cap rock, the inflow rates would range from 500 ℓ/min to over 2000 ℓ/min with significant dewatering of the unconfined aquifer occurring within a distance of 1500 m of the mine boundaries. Similar calculations for the confined sandstone aquifer gave inflow rates of less than 140 ℓ/min with no significant dewatering. Hence, it is concluded that groundwater conditions do not pose a problem for mining operations in either the upper dolostone unit or in the lower limestone-sandstone unit. However, while groundwater conditions do not pose a problem for subsequent space development in the limestone-sandstone unit, the groundwater conditions could adversely affect space development in the upper dolostone unit.

INTRODUCTION

The concept of combining underground aggregate mining and space development within the Paleozoic rock units of Niagara Escarpment of southern Ontario (Figure 1) has been the subject of much interest in recent years (Proctor and Redfern 1974; Acres 1974; 1976; Ontario Mineral Aggregate Working Party 1976). In these reports underground mining was identified as a possible alternative to aggregate extraction by large scale open pit mining as it is now practiced at several sites along the escarpment. The argument put forward is that underground mining provides for the protection of the Niagara Escarpment's unique natural environment and at the same time allows access to a large source of raw material of vital importance to this highly urbanized region.

Although it is more costly to produce aggregate material by underground mining techniques, mining experience in the Kansas City region has demonstrated that the economics of such a scheme can become very attractive if subsequent use of the mined space for suitable commercial and industrial purposes is introduced. As pointed out by Legget (1978), underground space development in the Hamilton-Niagara area would help slow the rate at which fertile fruitlands are being lost to warehousing and other industrial activity. Another positive factor in the economics of underground space is the energy efficiency of these facilities (McCreath and Mitchell 1978; Stauffer 1975). These authors reported on a number of examples where energy savings of 50 to 90 percent have been achieved by relocating commercial operations such as cold storage facilities in the subsurface.

GEOTECHNICAL CONSIDERATIONS

An evaluation of the technical feasibility of underground aggregate mining and space utilization in the Niagara Escarpment rock units requires data on the engineering properties of the host rockmass and the hydrogeological conditions of the site in question. Previous studies have shown that in the Paleozoic rock units of southern Ontario, including those making up the Niagara Escarpment, high horizontal stresses present major problems in both surface and subsurface excavations (Palmer and Lo 1976). Rock squeezing due to stress relief has resulted in the cracking of tunnel liners (Bowen *et al.* 1976; Lo and Morton 1976). High horizontal stresses are also considered to be responsible for the formation of pressure ridges observed in the floor of the Dufferin quarry (White *et al.* 1973). Also, natural erosion of the Niagara Escarpment along with deformation of the rock face due to stress relief has created slope stability problems at the powerhouse and access road at the Sir Adam Beck generating station in Niagara Falls (Carmichael *et al.* 1978).

Although a number of studies have contributed to an understanding of the rock engineering conditions in southern Ontario, very little is known about the general groundwater conditions and the hydrogeological characteristics of individual rock units in the Paleozoic sedimentary sequence. Experience has shown that adverse groundwater conditions have been a limiting factor in

many underground excavations (Thompson 1966; Trefzager 1966). Knowledge of the groundwater conditions is particularly critical in cases where subsequent use of the mined-out space is planned. Large inflows into excavations would interfere with the mining operation and long term maintenance of underground facilities. The expense of pumping, grouting, and other remedial work necessary in such cases would severely strain the economics of such a project. In addition, high inflows into a mine could result in extensive dewatering of the rockmass. This would create problems near areas where wells are used for domestic and commercial water supply.

CURRENT STUDY

A field and laboratory study was initiated in May, 1980, to provide the data necessary to evaluate the feasibility of underground mining and space development in the Niagara Escarpment rock units. The field work was carried out at a site on the Niagara Escarpment near Milton, Ontario (see Figure 1). The overall project includes an assessment of both the engineering properties of the bedrock units as well as the groundwater conditions at this site. In this paper we report on the first phase of this project which consisted of a detailed study of the hydrogeological characteristics of the bedrock units at the test site.

The test site is located 7 km west of Milton, on the Niagara Escarpment between the Dufferin quarry and the Indusmin quarry (Figure 2). Five boreholes, DQ-1 to DQ-5, were drilled for the hydrogeological component of this study. The orientation, length and diameter of the holes are tabulated in Figure 2. Three of the boreholes (DQ-1, DQ-3, DQ-5) were diamond drilled and provided core samples from the geologic units intersected.

GEOLOGIC SETTING

The Niagara Escarpment represents the outer rim of the geologic structure known as the Michigan Basin. The cap rock of the escarpment is a massive, resistant, bed of dolostone which overlies a sequence of thinner shale, limestone, and sandstone beds (Figure 3). Outcrops of the cap rock unit are abundant at the test site, and only thin accumulations of surficial materials, consisting mostly of sand and gravel, occur in bedrock depressions.

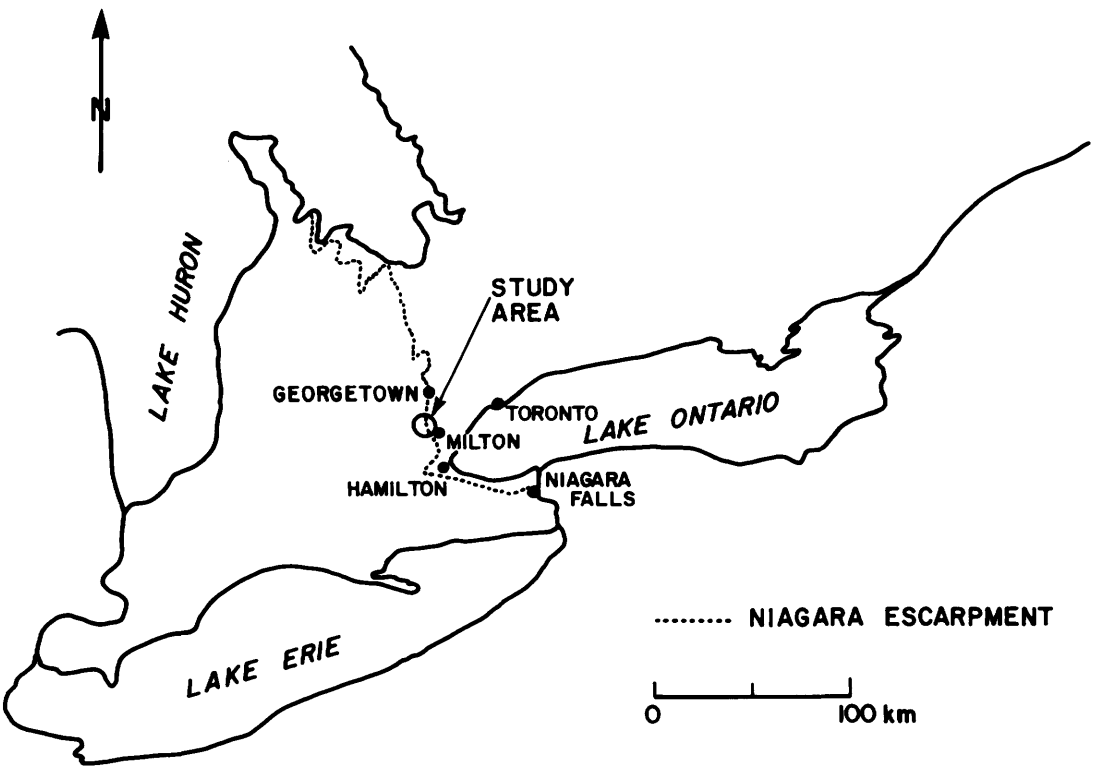

Figure 1. *Location of Niagara Escarpment and study area.*

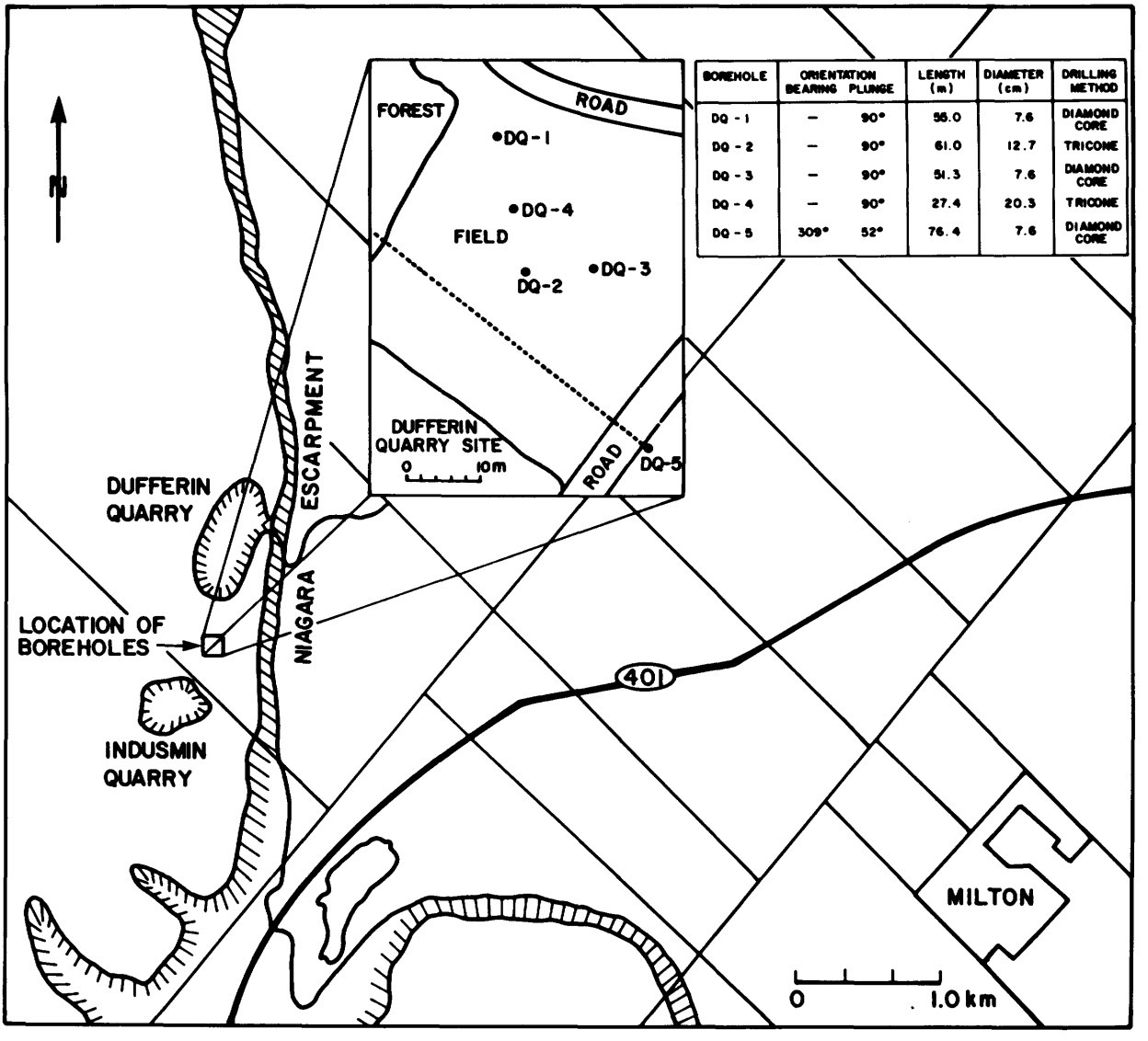

BOREHOLE	ORIENTATION BEARING	PLUNGE	LENGTH (m)	DIAMETER (cm)	DRILLING METHOD
DQ - 1	–	90°	56.0	7.6	DIAMOND CORE
DQ - 2	–	90°	61.0	12.7	TRICONE
DQ - 3	–	90°	51.3	7.6	DIAMOND CORE
DQ - 4	–	90°	27.4	20.3	TRICONE
DQ - 5	309°	52°	76.4	7.6	DIAMOND CORE

Figure 2. *Location of test site and boreholes.*

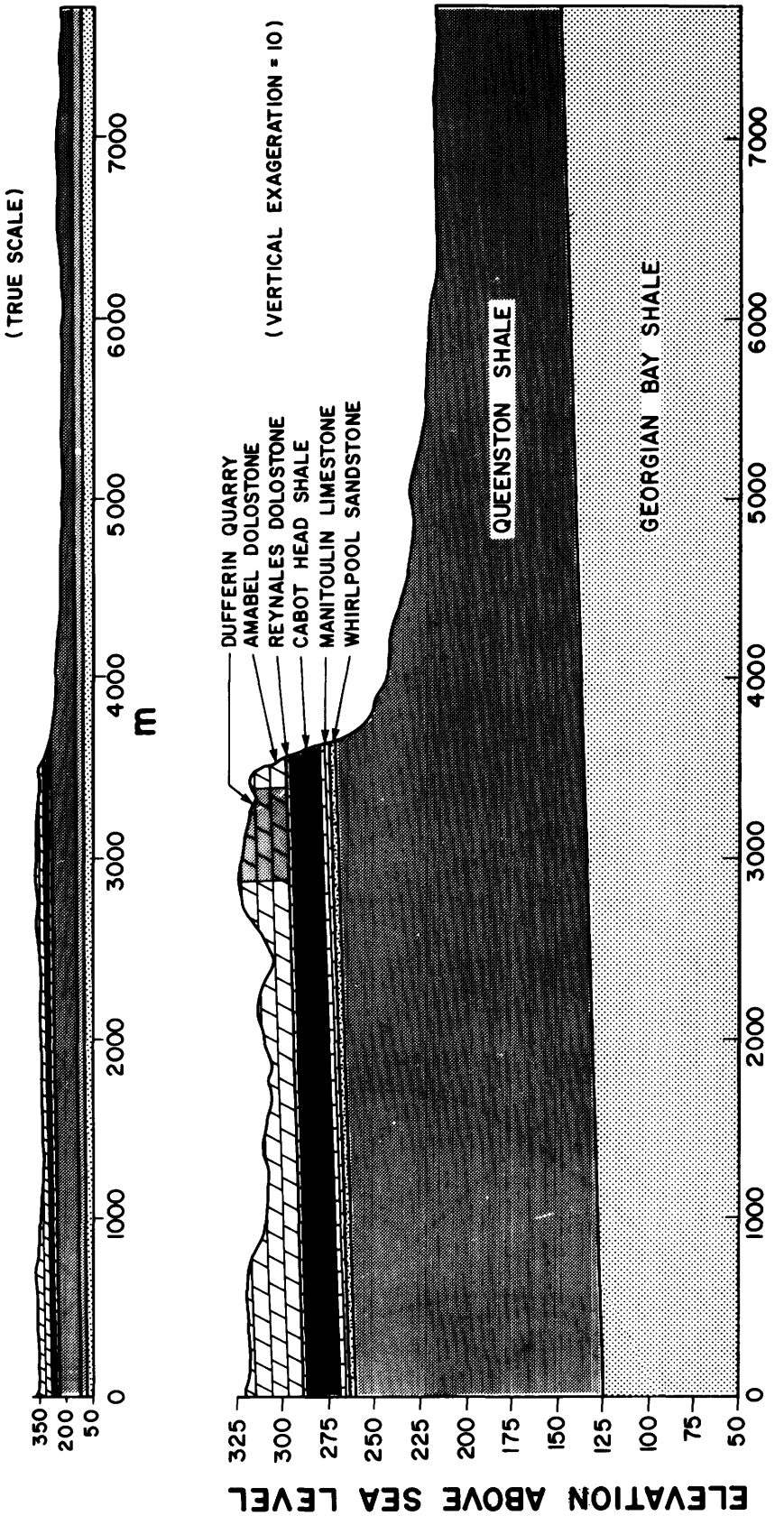

Figure 3. *Vertical cross-section of the Niagara Escarpment at the test site.*

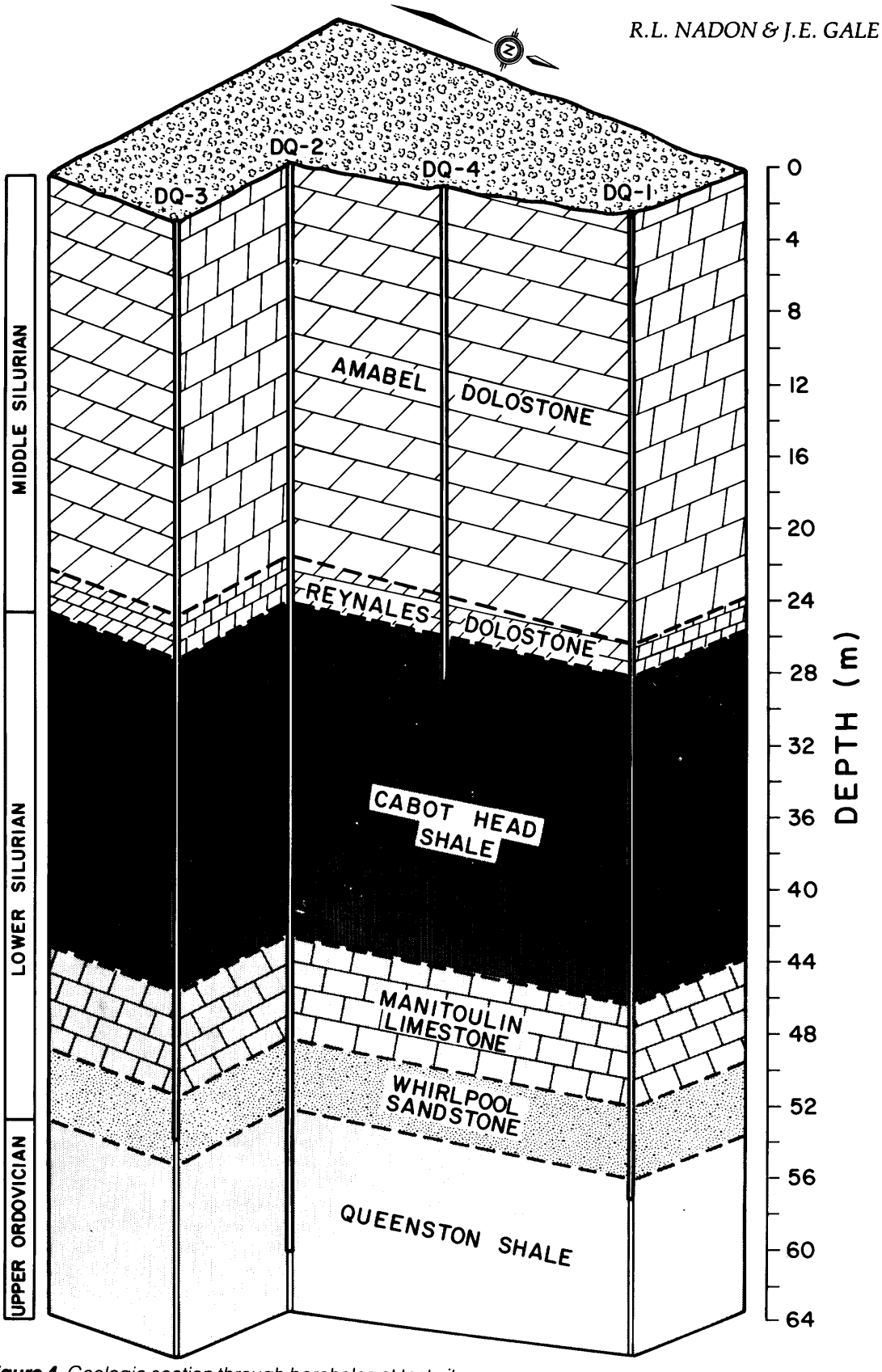

Figure 4. *Geologic section through boreholes at test site.*

At the test site, the cap rock, which includes the Amabel and Reynales Formations, has a total thickness of 26 m and is characterized mostly by massive beds of light grey-buff, fine to medium crystalline dolostone (Figure 4). The beds are highly fossiliferous, composed largely of bioclastic material, forming in some sections a highly porous rock matrix. However, for the most part, the dolostone rock mass is fairly dense and is dissected by abundant horizontal bedding discontinuties, and by more widely spaced vertical and sub-vertical fractures. Outcrop and borehole surveys have shown that these vertical fractures have preferred orientations as can be seen in the rose diagram in Figure 5.

Underlying the cap rock is the Cabot Head Formation which is 18.5 m thick and consists predominantly of grey-green, finely laminated shale. In several locations the shale is very soft, approaching the consistency of a plastic clay.

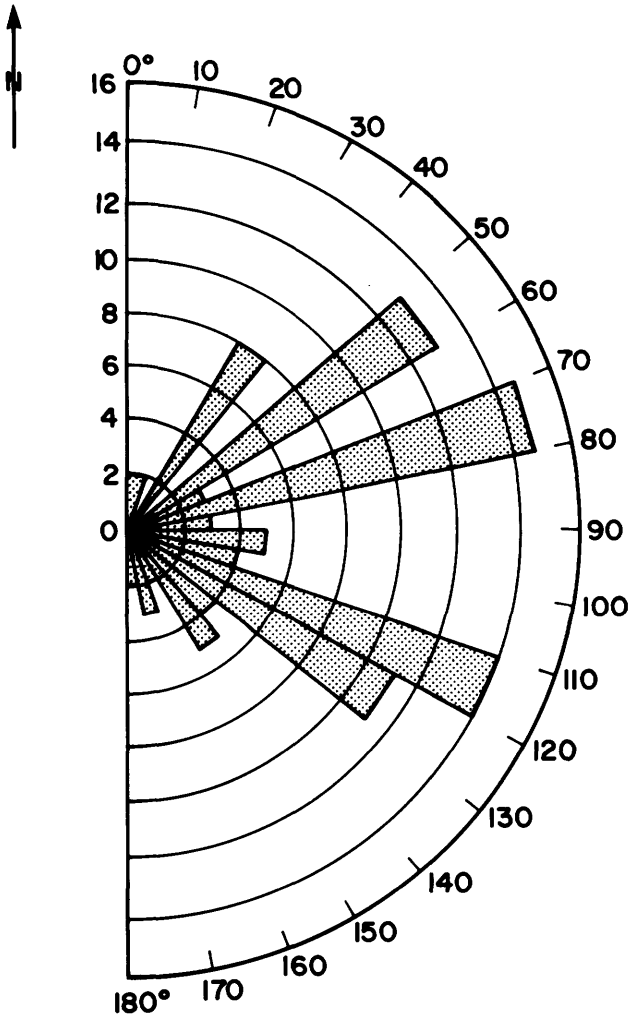

Figure 5. *Orientation of vertical and subvertical fractures in Amabel Formation.*

At the base of the Cabot Head Formation, the soft shale becomes increasingly calcareous to a point where the rock is more suitably called argillaceous limestone. This somewhat arbitrary point is considered the upper contact of the Manitoulin Formation. The Manitoulin Formation is 5.7 m thick and consists of fine crystalline, argillaceous, dolomitic limestone beds, 5 to 60 cm in thickness, separated by several thin shale beds. The Manitoulin limestone is underlain by the Whirlpool Formation, which is 4 m thick and consists of thick-bedded, light brown-grey, fine grained, well sorted, quartz sandstone. Very thin, dark grey to black shale seams occur throughout this sandstone. Very few natural fractures were found in the sandstone drill cores although some vertical and horizontal fractures were found in an exposure near the Indusmin quarry. The orientation of these fractures is shown in Figure 6. The spacing of vertical fractures in the Whirlpool sandstone is variable but sections of unfractured rock, 2 to 5 m in length, are very common. The wide spacing of the vertical fractures could explain why none were intersected in the boreholes at the test site.

The Queenston shale, over 130 m thick in the Milton region (Bolton 1957), underlies the Whirlpool sandstone. Only the top 7 m of the Queenston Formation, consisting mostly of dark red, hematitic, fissile, calcareous shale, interbedded with very finely crystalline, grey-green, highly argillaceous limestone, were intersected by the boreholes at the test site.

HYDROGEOLOGY

Owing to the presence of thick shale formations within the Niagara Escarpment, the potential of underground mining for aggregate production and (or) space development is, from the outset, limited to two specific zones. These are: Zone A, at the base of the Amabel dolostone cap rock, and Zone B, within the Whirlpool sandstone and Manitoulin limestone.

The hydrogeological setting of these two zones differs greatly. The dolostone cap rock, being exposed at the surface, is subject to direct recharge from surface water, whereas the Whirlpool and Manitoulin Formations, bounded above and below by thick shale beds, are hydraulically isolated from any significant source of groundwater recharge.

The hydrogeological setting is illustrated in Figures 7a and 7b, which present the results of 67 borehole packer injection tests (Figure 8) performed at the test site. Changes of hydraulic conductivity with depth show a close correlation to changes in lithology. Relatively high hydraulic conductivity values ranging from 10^{-5} to 10^{-3} cm/sec were measured in the dolostone cap rock; low values ranging from 10^{-9} to 10^{-7} cm/sec were obtained for the interval of rock consisting of the Cabot Head shale and Manitoulin limestone, and intermediate values in the range of 10^{-4} to 10^{-5} cm/sec were measured in the Whirlpool sandstone unit and the upper few metres of the Queenston shale. Although no tests were performed deeper in the Queenston Formation, water well records

indicate that only the upper part of the shale produces fresh water, and that over most of its thickness, only very low yields are obtained and the groundwater is highly mineralized. Therefore, the hydraulic conductivity values for the Queenston shale are probably similar to those in the Cabot Head Formation and no greater than 10^{-8} cm/-sec.

At the test site, the water table was encountered in the Amabel Formation at a depth of about 12 m below the ground surface. Hydraulic head measurements made during packer testing (see Figure 7a) indicate that the piezometric surface for the Whirlpool sandstone is very low, located about 40 m below the ground surface. Thus, within the thickness of rock that comprises the Niagara Escarpment in the Milton area, the groundwater regime may be described as a multiaquifer system consisting of an unconfined dolostone aquifer under which lies a shale and limestone aquitard, and a confined sandstone aquifer which in turn is underlain by a shale aquitard corresponding to the Queenston Formation.

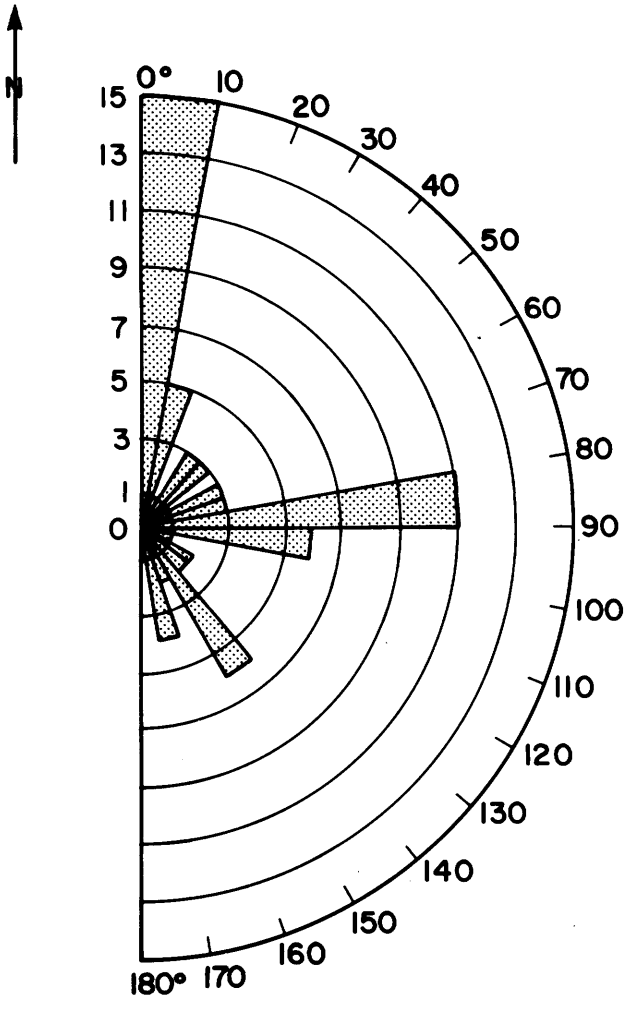

Figure 6. *Orientation of vertical fractures in Whirlpool Formation*

The hydrogeologic characteristics of the Amabel dolostone and Whirlpool sandstone were further studied by conducting pumping tests of durations ranging from 7 hours to over 40 hours. Transmissivity values obtained for the unconfined dolostone aquifer and confined sandstone aquifer were in the order of 15 m^2 day and 0.1 m^2 day respectively. Figure 9 shows the drawdown in water levels measured in observation well DQ-1 while pumping DQ-4 at a rate of 6 ℓ/min.

Attempts were made to analyse the pumping test data for the purpose of determining if the permeability of the rock formations were anisotropic in the horizontal plane as is often the case in fractured rock masses. The test data indicate that groundwater flow in the dolostone cap rock is controlled to a large extent by the location and orientation of fractures. However, due to the limited number of wells available for observing groundwater behaviour, no definite permeability anisotropy could be identified. Based on the results of the field tests, it is believed that highly anisotropic conditions exist on a small scale in this rock unit, where preferential flow of groundwater occurs primarily along fracture planes. However, it appears that the dolostone formation contains a sufficient number of well interconnected fractures, so that over large distances, the rock mass behaves essentially in a way similar to a granular isotropic porous medium.

Water level responses during a pumping test in the Whirlpool sandstone suggest that large scale anisotropic permeability conditions do exist in this formation. The permeability of the rock mass is greatest in a north-south direction, which coincides with the orientation of the main vertical fracture set observed in this formation (see Figure 6). However, since these observations are site specific, generalizations should not be made. Additional field work would be necessary in order to determine if these conditions prevail throughout the Whirlpool Formation.

Based on a knowledge of the hydrogeologic properties of each rock type in the Niagara Escarpment and from field observations made in the study area, a conceptual model, shown schematically in Figure 10, of the groundwater flow system was developed. Over most of the study area, infiltration of water into the dolostone cap rock unit occurs rapidly. Evidence of this is shown in Figure 11, which is the hydrograph for well DQ-1 plotted together with the daily precipitation measurements taken at a nearby station during the period August, 1979, to March, 1980. Major rain events in December and April show a same day sudden rise in water levels, demonstrating the immediate effects of recharge. The water which infiltrates into the saturated portion of the dolostone cap rock, is confined to this unit by the underlying Cabot Head shale and thus flows horizontally towards the escarpment where it discharges, forming several springs located along the contact of the dolostone and shale formations.

The Whirlpool sandstone and the top few metres of the Queenston shale are the only other rocks at the test

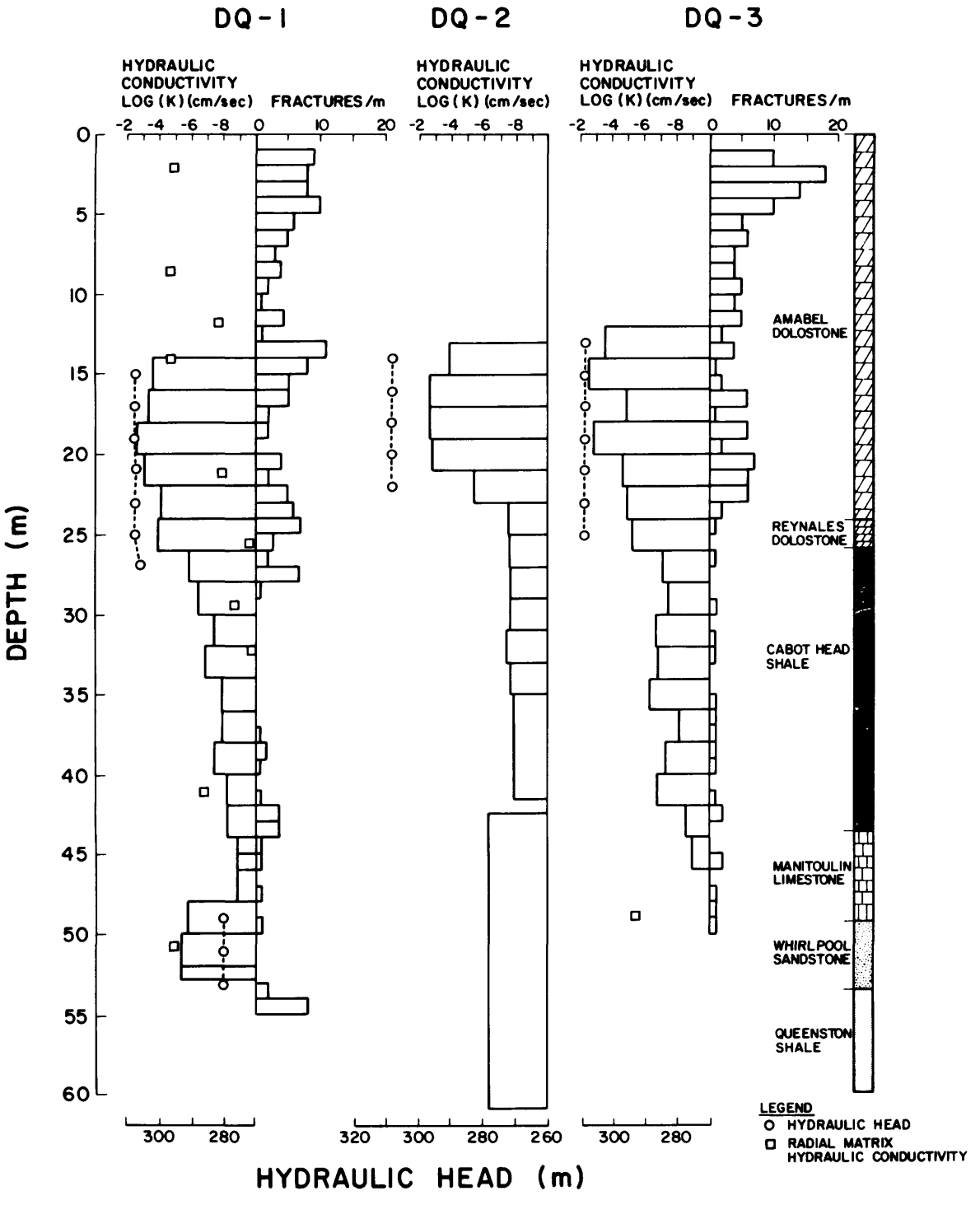

Figure 7a. *Borehole injection test results and fracture histogram for DQ-1, DQ-2, and DQ-3.*

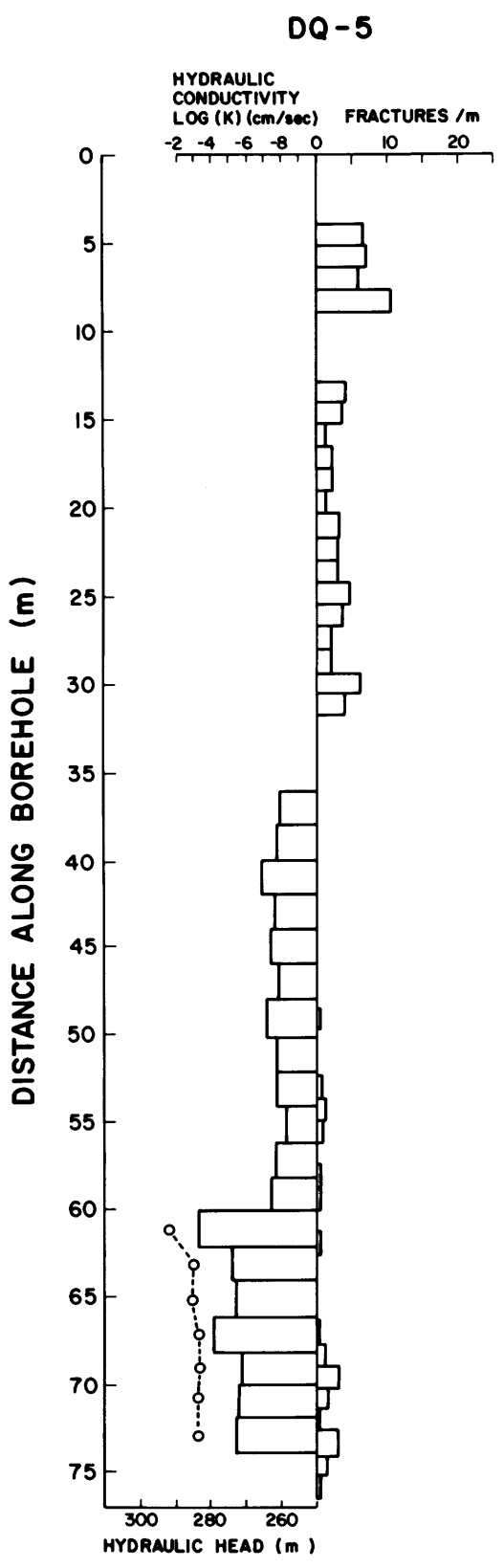

Figure 7b. *Borehole injection test results and fracture histogram for DQ-5.*

site in which significant groundwater flow occurs. These rocks are confined above by the Cabot Head – Manitoulin unit and below by the remainder of the Queenston shale. The only source of recharge is downward leakage of groundwater from the dolostone cap rock through the Cabot Head – Manitoulin unit. The unusually high vertical hydraulic gradient which exists across this unit is proof of its low permeability and of its ability to hydraulically isolate

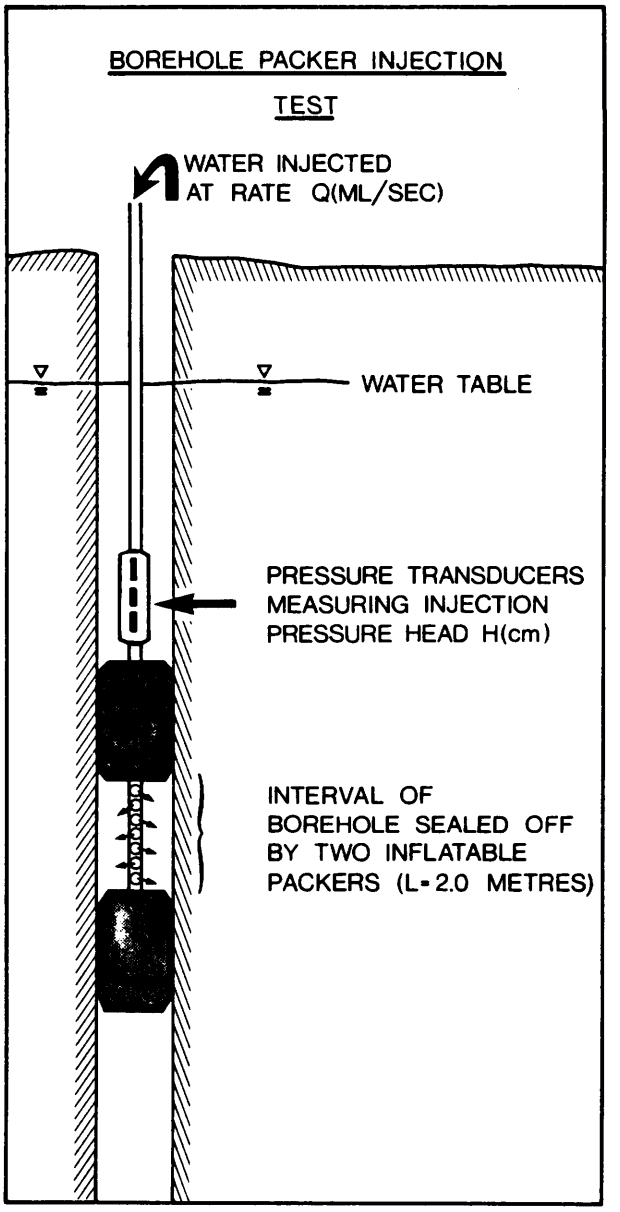

Figure 8. *Principle of borehole packer injection test.*

the dolostone and sandstone aquifers. Hydraulic head measurements in the Whirlpool sandstone (see Figure 7a) indicate that groundwater flow is horizontal. From the limited data available, it appears that the direction of flow is also easterly towards the escarpment.

MINE SEEPAGE AND ROCK MASS DEWATERING

Based on the groundwater flow system illustrated in Figure 10, a two-dimensional finite element model (Frind 1976) was used to calculate the rate of groundwater seepage and the resulting extent of rock mass dewatering for a hypothetical underground mine located within Zone A and Zone B in the escarpment section. The finite element grid used for groundwater flow simulations in both of these zones is shown in Figure 12. A complete discussion of the boundary conditions and inherent assumptions of the numerical model is found in Nadon (1981).

ZONE A

The configuration of the water table in the dolostone cap rock formation is determined primarily by two parameters: (1) the rate of surface recharge (qF), and (2) the hydraulic conductivity of the rock mass (K). Several simulations of the groundwater flow system were made using various combinations of these two parameters in order to determine what set of values generated a water table configuration most consistent with actual field conditions. The simulated water table configuration is illustrated in Figure 13 for a hydraulic conductivity value of 2×10^{-3} cm/sec and a surface recharge rate of 30 cm/year. The water table configurations in a vertical section along flow line A-A' (Figure 13), for nine simulations, are shown in Figure 14. These results show that for a range of surface recharge rates typical of southern Ontario (10 to 50 cm/year), only a very narrow range of hydraulic conductivities, between 1×10^{3} cm/sec and 3×10^{-3} cm/sec, provide acceptable results. Simulations that were most consistent with surface topography and known water table

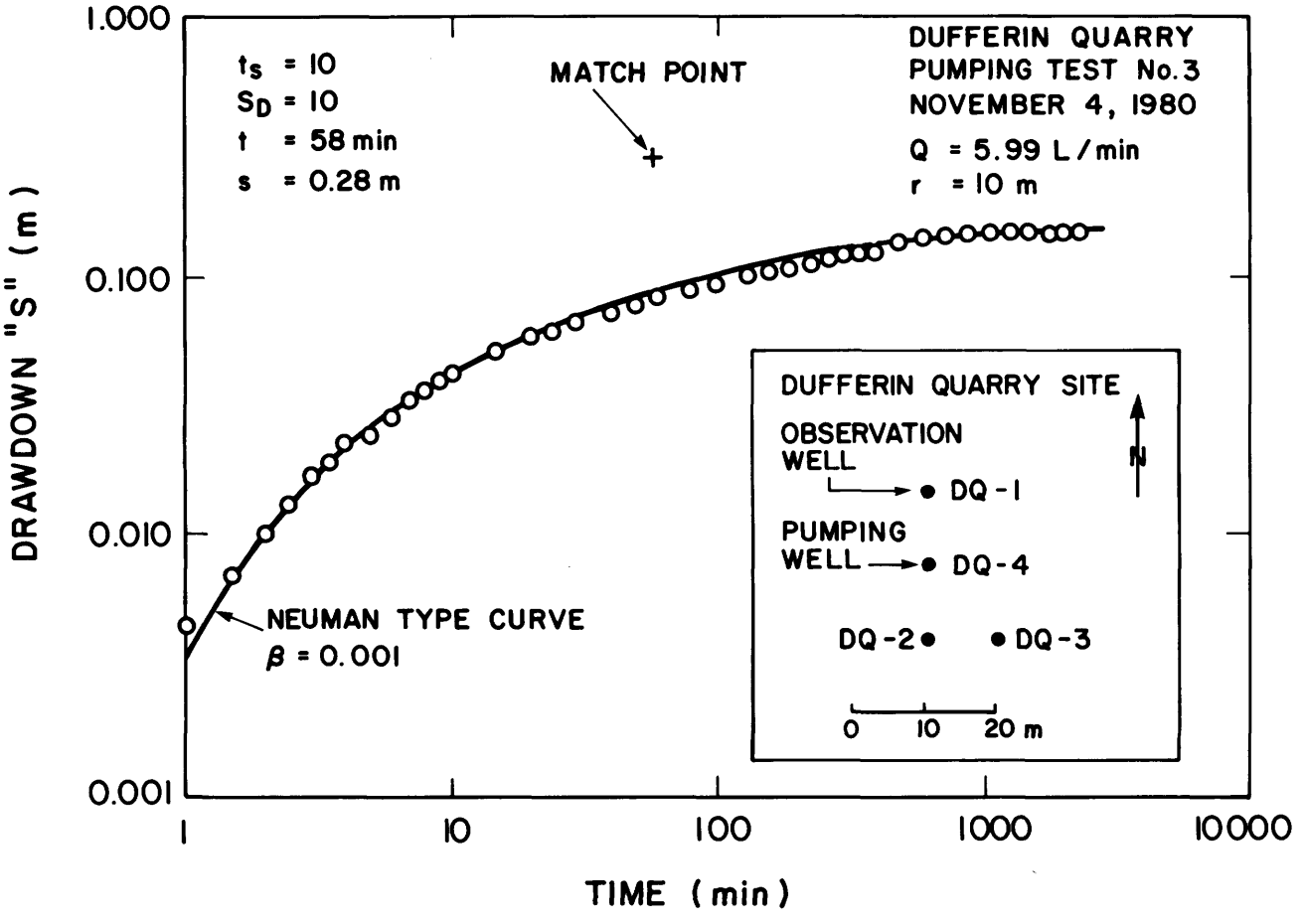

Figure 9. *Drawdown curve for observation well DQ-1.*

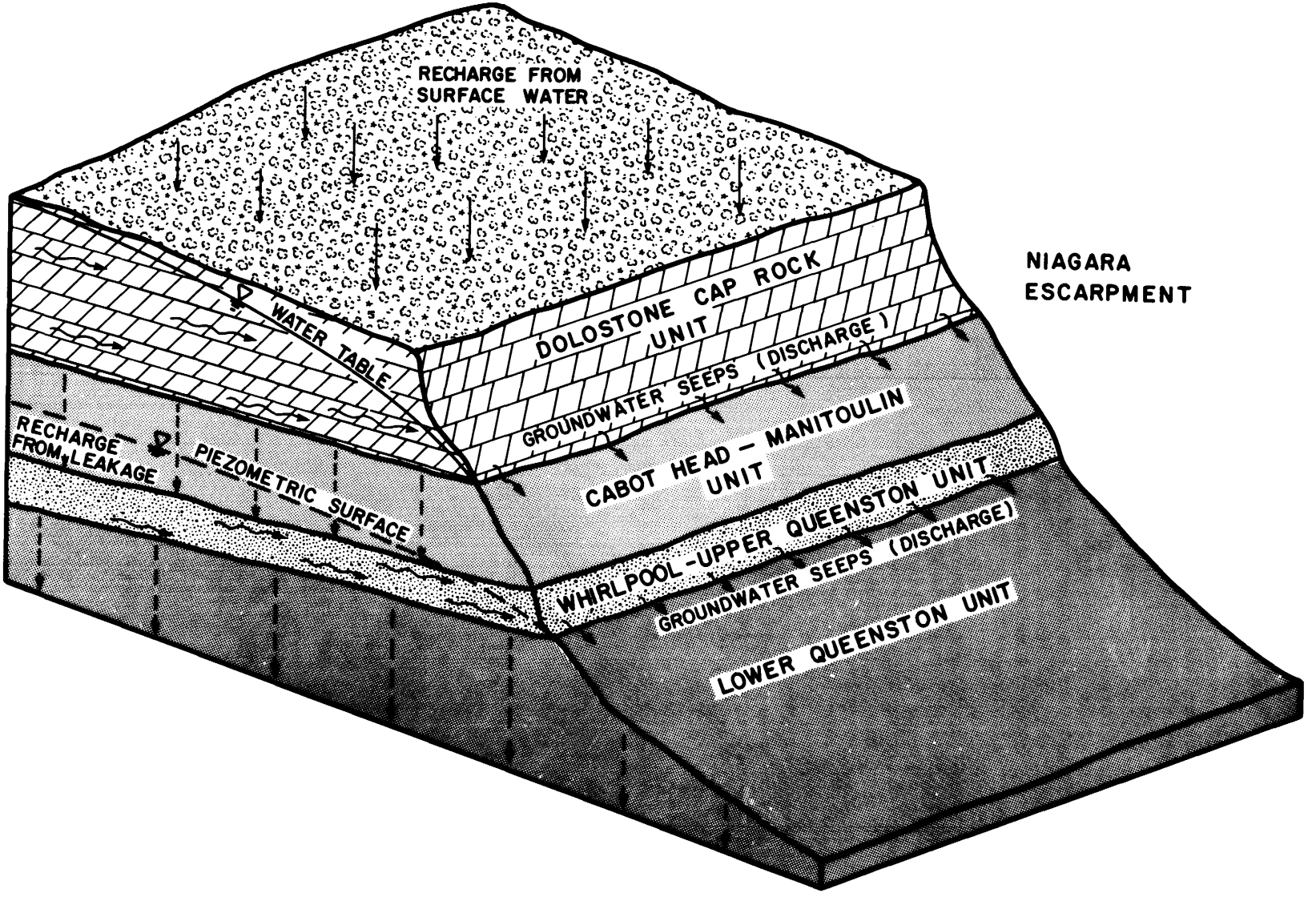

Figure 10. *Idealized groundwater flow system for study area.*

elevations were obtained by using either (1) $K = 2 \times 10^{-3}$ cm/sec and qF = 50 cm/year, or (2) $K = 3 \times 10^{-3}$ cm/sec and qF = 50 cm/year. These hydraulic conductivity values correspond very closely to those measured in field tests. With these two sets of parameters, the water table generated by the model forms a subdued expression of the general topographic trends in the region of study.

To check the validity of the numerical model, the rate of groundwater seepage into the Dufferin quarry, as calculated by the model, was compared to actual monthly average pumping rates recorded during the period 1977 to 1980. As listed in Table 1, the average pumping rates for the four year period range from 1044 to 2388 ℓ/min which correspond very closely to the seepage rates predicted by the model, 1330 and 2140 ℓ/min, for the indicated set of parameters.

Within the dolostone cap rock unit, an extensive underground room and pillar mine would have the same influence on the groundwater flow system as would a quarry of the same dimensions. Because of the relatively high permeability of the dolostone rock, and the limited thickness of the unit, complete and rapid dewatering of the rock mass above the mine would occur as the mine face advanced. Furthermore, since the rate of advancement of the mining front is much slower than the rate at which groundwater pressures in the rock mass equilibrate, the problem of predicting groundwater inflows and effects of dewatering need only be considered for steady-state conditions.

Table 1. *Comparison of measured and predicted inflow rates for the Dufferin quarry.*

MEASURED PUMPING RATES - DUFFERIN QUARRY

Year	Monthly Averate Q (l/min)
1977	2388
1978	1497
1979	1200
1980	1044

PREDICTED INFLOW RATE - DUFFERIN QUARRY

K (cm/sec)	qF (cm/year)	Q (l/min)
2×10^{-3}	30	1330
2×10^{-3}	50	2140

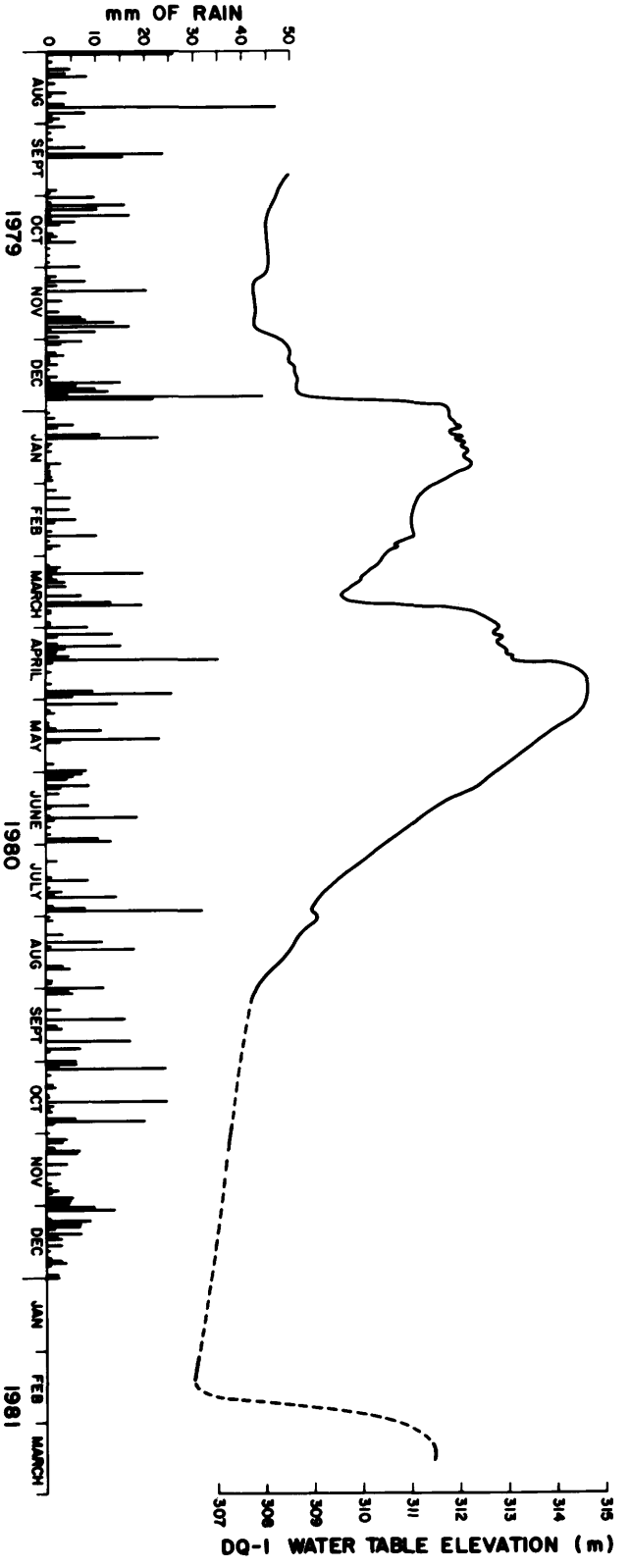

Figure 11. *Hydrograph for borehole DQ-1 and daily precipitation distribution.*

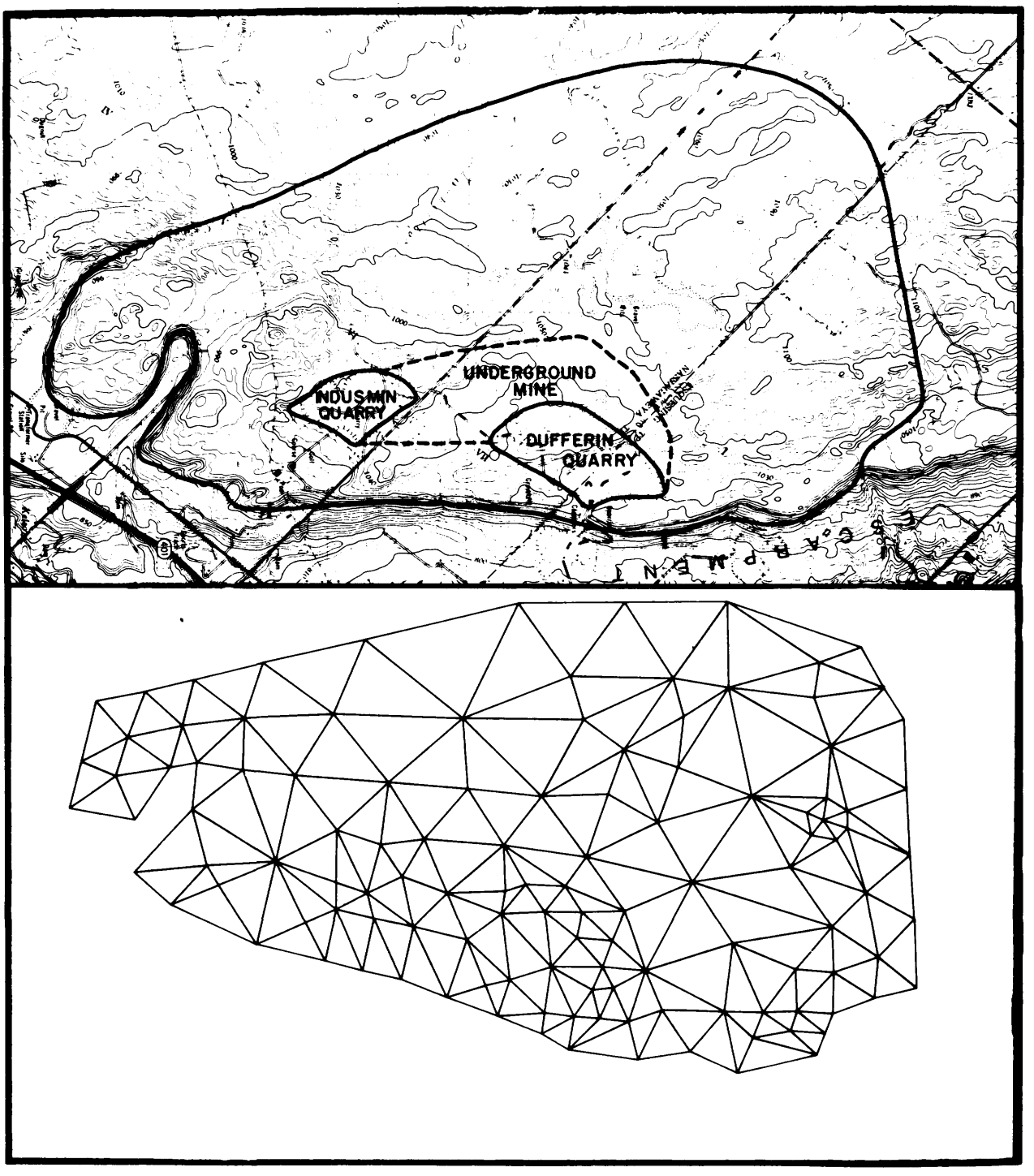

Figure 12. *Finite element grid and area of study.*

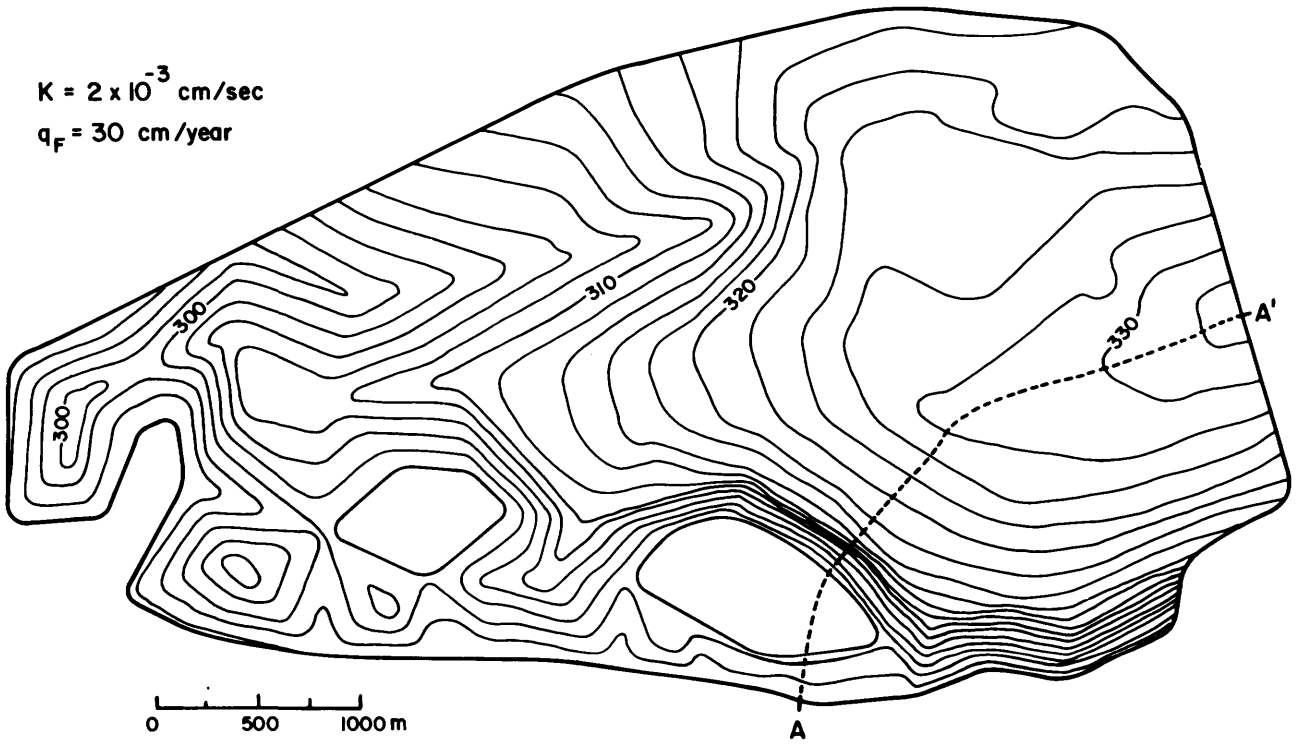

Figure 13. *Hydraulic head distribution in Amabel dolostone considering drainage into quarries.*

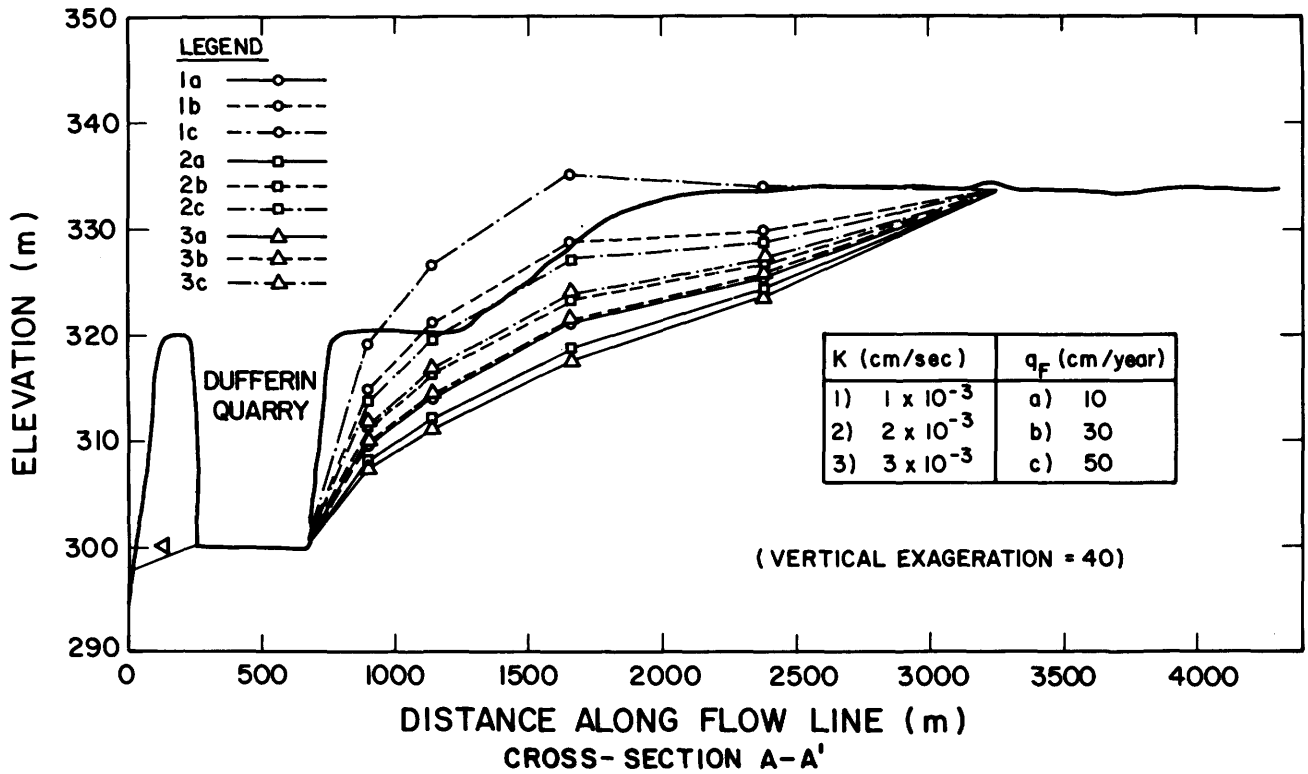

Figure 14. *Water table configuration along flow line A-A'.*

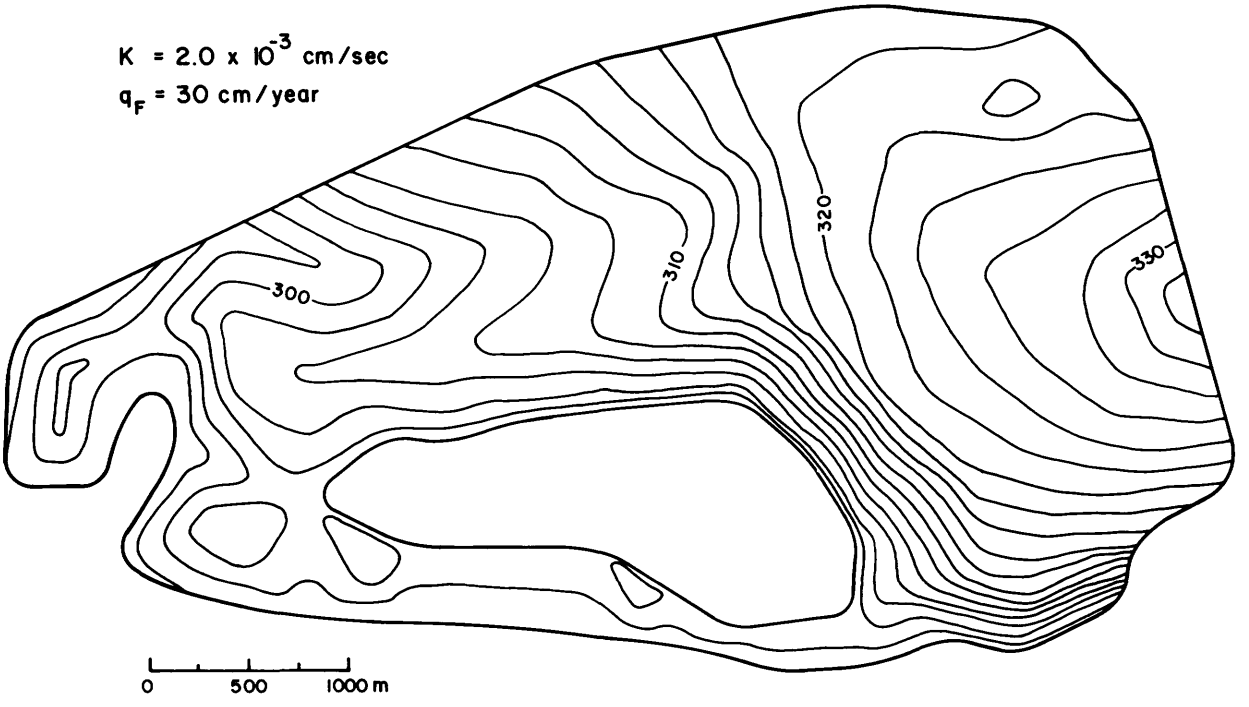

Figure 15. *Hydraulic head distribution in Amabel dolostone considering drainage into underground mine.*

Figure 15 is a contour map of hydraulic heads at steady-state conditions, produced by the model, showing the effects of drainage into a hypothetical underground mine 2 km^2 in area (see Figure 12 for location of mine). Hydraulic head gradients towards the mine are greatest along the northwest face and gradually decrease in magnitude towards the south. The extent of dewatering of the dolostone rock mass caused by drainage into the mine is illustrated in Figure 16. Beyond a distance of about 1500 m, the drawdown of the water table is insignificant (less than 1 m).

The magnitude of groundwater discharge into the mine, as calculated by the model, ranges from 560 to 2200 ℓ/min for the set of parameters indicated in Figure 17. The discharge varies proportionately with respect to both the hydraulic conductivity and rate of surface recharge.

ZONE B

The key parameters controlling the groundwater conditions in the confined Whirlpool sandstone formation are: (1) recharge from leakage through the overlying aquitard, and (2) the hydraulic conductivity of the sandstone rock mass.

From field test results, we know that the hydraulic conductivity of the Cabot Head – Manitoulin aquitard is very low and therefore the recharge to the Whirlpool sandstone can be expected to be also very low. This, combined with the intermediate hydraulic conductivity values of the sandstone unit, would lead one to presume that seepage rates for a mine located in this zone would be considerably lower than those predicted for a mine in Zone A.

Some indication of the magnitude of inflows that could be expected for an underground mine in Zone B were obtained by calculating the volume of groundwater discharging along the face of the Niagara Escarpment. Table 2 presents the values of total groundwater discharge along 3000 m of the Niagara Escarpment, calculated using the model, for a wide range of aquifer and aquitard hydraulic conductivities. For the worst case (higher aquifer and acquitard permeability), the discharge along the escarpment is only 140 ℓ/min (30 gallons/min). From field and laboratory tests, there are indications that the vertical conductivity of the acquitard is no greater than 10^{-10} cm/sec. If this should be the case, then groundwater discharge along the escarpment would be at least an order of magnitude lower (14 ℓ/min) and therefore essentially insignificant from a mining point of view.

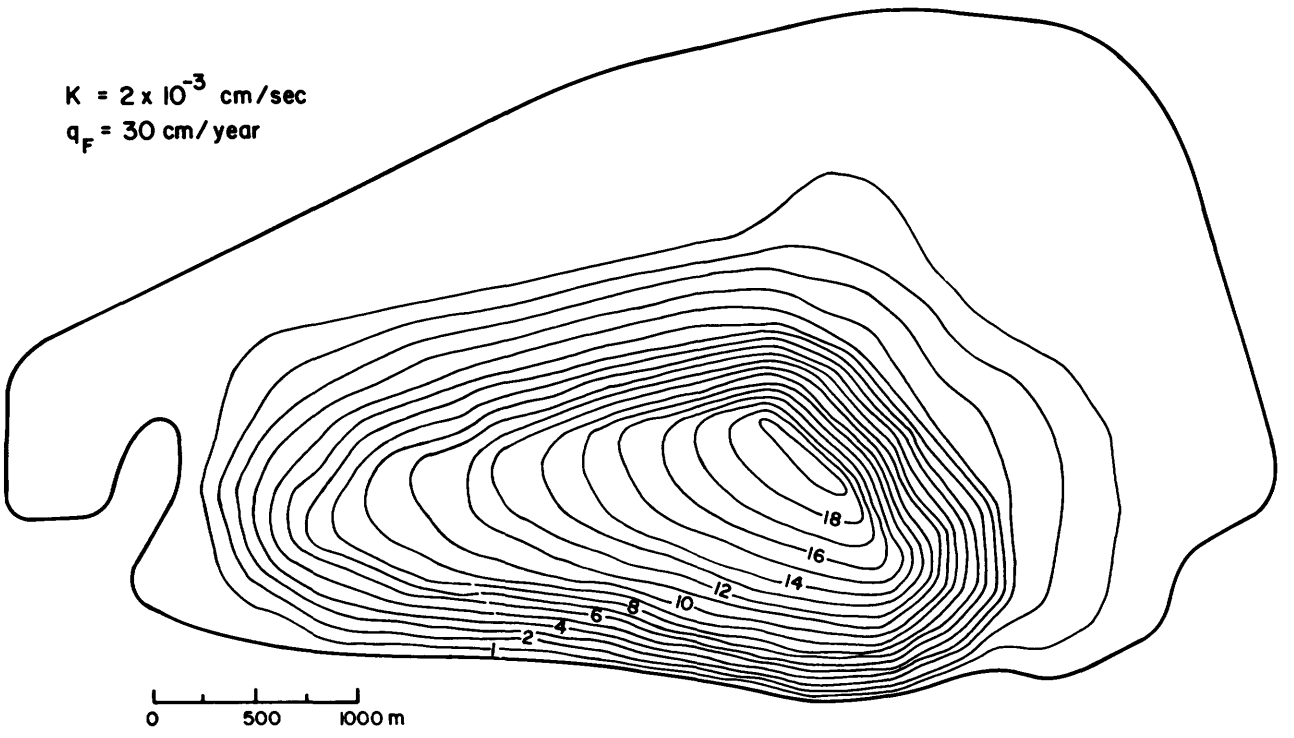

Figure 16. *Extent of dewatering of Amabel dolostone caused by drainage into underground mine.*

DISCUSSION AND CONCLUSION

The recharge characteristics and the relatively high permeability of the dolostone cap rock means that considerable inflow of groundwater into underground excavations would be inevitable. For a mine with a floor area on the order of 2 km^2, average inflows as high as 2000 to 3000 ℓ/min (440-660 gallons/min) should be anticipated. Large fluctuations in water levels in this unit throughout the year suggest that inflows into excavations would be equally variable. Very high inflows could occur during spring thaw when water levels are at their highest. The greater permeability of the dolostone rock mass near the ground surface would, during such periods, further contribute to increased seepage.

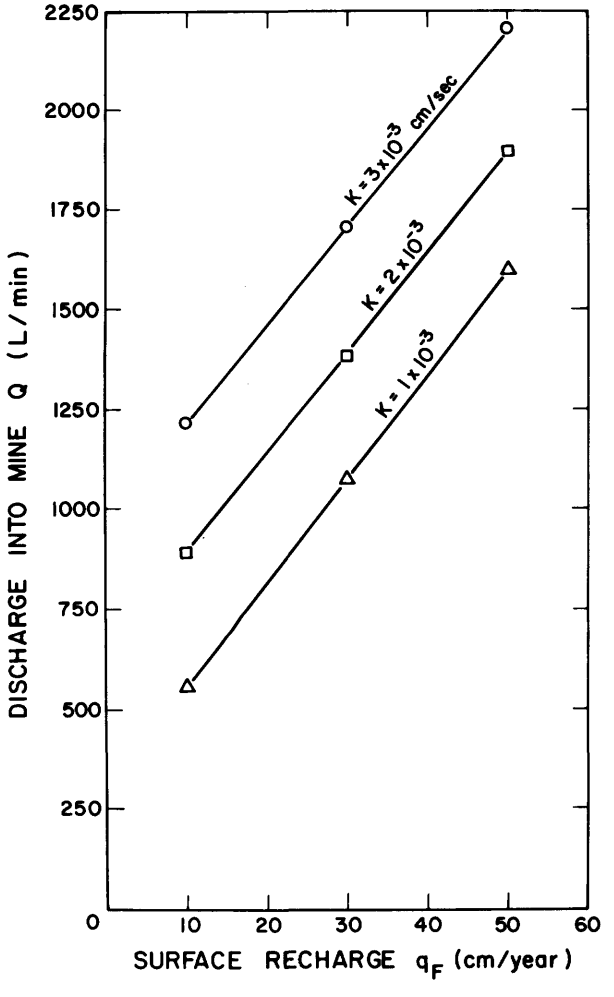

Figure 17. *Effects of hydraulic conductivity and surface recharge flux on groundwater discharge into underground mine.*

Table 2. *Discharge of groundwater from the Whirlpool-Upper Queenston unit along Niagara Escarpment.*

HYDRAULIC CONDUCTIVITY CM/SEC		DISCHARGE (L/MIN)
CONFINED AQUIFER	AQUITARD	
1×10^{-3}	1×10^{-9}	140
1×10^{-4}	1×10^{-9}	17.7
1×10^{-4}	1×10^{-10}	13.9
1×10^{-5}	1×10^{-10}	1.3
1×10^{-6}	1×10^{-10}	0.06

Both the Dufferin and Indusmin quarries adequately deal with groundwater inflows by pumping from pits excavated in the floor of the quarries. It is conceivable that, for an extensive underground mine, a suitable layout of trenches could be constructed in order to provide gravity drainage, thus avoiding major pumping expenses.

Based on modelling results, extensive dewatering of the unconfined aquifer would be restricted to the immediate surroundings of the mining operation. Within the dolostone cap unit, no significant drawdown of the water table would occur beyond a distance of 1000 to 2000 m. Therefore, no major interference problems should be encountered on a regional scale due to groundwater drainage into an underground mine.

An evaluation of the feasibility of underground mining based on the groundwater conditions of the dolostone cap rock unit requires that consideration be given to the purpose of the project. If the main concern is only with the extraction of mineral aggregate material, then considerable moisture can be tolerated in the mine and the construction of trenches and installation of pumps could adequately deal with the groundwater inflows. However, if the intent is to make use of the excavated rooms, once the mining has been completed, for storage purposes or for other industrial or commercial applications, wet conditions would be undesirable and the remedial work necessary to improve the conditions, such as grouting or permanent dewatering, could involve major expenses.

For the purpose of underground space development, mining within the Whirlpool sandstone and Manitoulin limestone formations is clearly more desirable than in the Amabel dolostone formation. The low permeability shale units located above and below effectively seal the Whirlpool and Manitoulin Formations from major groundwater movement. The small volumes of groundwater that would seep into a mine could be handled with proper ventilation of the rooms.

Although, from a hydrogeological perspective, the Whirlpool and Manitoulin Formations are ideal for underground space development, limitations may exist for mining within these rocks because of a variety of geotechnical problems. The limited thickness of these units, the

presence of deformable shale formations both above and below, and the presence of high horizontal stresses are the most obvious concerns.

ACKNOWLEDGMENT

D. Cameron, G. Jones, J. Smedley, and A. Sweezey provided assistance in the field. S. Andrews assembled the manuscript, N. Bahar and L. Kritzer drafted the figures, and P. Fisher prepared the photographs. A special thanks is extended to Doug Wilson and the staff of Dufferin Materials and Construction Limited for their generous assistance and cooperation during testing at the Dufferin quarry site.

REFERENCES

Acres Consulting Services Limited
1974: Underground Space Utilization; Acres Research and Development program, unpublished report.
1976: Underground Aggregate Mining Preliminary Feasibility Study; Ministry of Treasury, Economics and Intergovernmental Affairs, Niagara Escarpment Commission.

Bolton, T.E.
1957: Silurian Stratigraphy and Paleontology of the Niagara Escarpment in Ontario; Geology Survey of Canada, Memoir 289, 145p.
1964: Pre-Guelph Silurian Formations of the Niagara Peninsula; American Association of Petroleum Geologists, Guidebook, Geology of Central Ontario, p. 55-80.

Bowen, C.F.P., Hewson, F.I., Macdonald, D.H., and Tanner, R.G.
1976: Rock Squeeze at Thorold Tunnel; Canadian Geotechnical Journal, Vol. 13, p. 111.

Carmichael, T.J., Gorman, G., Mckay, D., and Kragewski, J.
1978: Engineering Geology at Niagara Hydroelectric Plants; p. 93-105 in Toronto 78, Field Trips Guidebook, Geological Association of Canada — Mineralogical Association of Canada.

Frind, E.O.
1976: Transient Two-dimensional Confined-Unconfined Aquifer Model; Unpublished Short User's Guide, Department of Earth Sciences, University of Waterloo.

Legget, R.
1978: Energy, Geology and the Underground; Geoscience Canada, Vol. 5, No. 3, p. 119-123.

Lo, K.Y., and Morton, J.D.
1976: Tunnels in Bedded Rock with High Horizontal Stresses; Canadian Geotechnical Journal, Vol.13, p. 216.

McCreath, D.R., and Mitchell, D.E.
1978: Build Underground and Conserve Energy: Fact or Fiction; Engineering Journal.

Nadon, R.N.
1981: Impact of Groundwater on Mining Activities in the Niagara Escarpment Area; unpublished M.Sc. Thesis, University of Waterloo, 144p.

Ontario Mineral Aggregate Working Party
1976: A Policy for Mineral Aggregate Resource Management in Ontario; Ontario Ministry of Natural Resources.

Palmer, J.H.L., and Lo, K.Y.
1976: In Situ Stress Measurements in Some Near-Surface Rock Formations, Thorold, Ontario; Canadian Geotechnical Journal, Vol. 13, p. 1

Proctor and Redfern
1974: Towards the Year 2000 - A Study of Mineral Aggregate in Central Ontario; Ontario Ministry of Natural Resources.

Stauffer, Sr., T.
1975: Kansas City: A Model of Underground Development; unpublished paper presented at Seminar - The New Industrial Space - Queen's Park, Toronto, Ontario.

Thompson, T.F.
1966: San Jacinto Tunnel; p.104-107 in Engineering Geology in Southern California, Association Engineering Geology, Special Publication.

Trefzager, R.E.
1966: Tecolote Tunnel; p. 108-113 in Engineering Geology in Southern California, Association Engineering Geology, Special Publication.

White, O.L., Karrow, P.F., and Macdonald, J.R.
1973: Residual Stress Relief Phenomena in Southern Ontario; p. 323-348 in Proceedings, 9th Canadian Rock Mechanics Symposium, Montreal.

Grant 78 Terrain Characteristics and Physical Processes in Small Lagoon Complexes

J.E. Otto[1] and R.W. Dalrymple[2]

[1]Department of Geological Sciences, Brock University
[2]Department of Geological Sciences, Queen's University

ABSTRACT

New vibracore results from the head of the Sixteen Mile Creek lagoon permit the extension of the Bottom Sand and Gray Clay stratigraphic units from the lagoon into the channel and marsh areas. The Gittja is not present in the marsh, and is replaced stratigraphically by an orange clay interpreted to be a buried soil. Halton Till underlies the Bottom Sand in this area. Pollen analyses support earlier suggestions that the Gittja accumulated in a marshy environment whereas the Brown Clay (a downstream facies equivalent to the upper part of the Gittja) and the overlying Gray Clay formed in deeper, open water. A peak in pine pollen is present just below the Gray Clay (possibly as a result of Indian agricultural practices), and the post-clearing rise in *Ambrosia* occurs in the lower part of the Gray Clay.

Reconnaissance coring in the Fifteen Mile and Twenty Mile Creeks lagoons shows that identical stratigraphic sequences exist in all three lagoons, and that the transitions from Gittja to Brown Clay (1675 ^{14}C years B.P.), and from Brown Clay and Gittja to Gray Clay (post 440 ^{14}C years B.P.), are synchronous throughout the area. Consequently the transitions are reinterpreted to be the result of rapid rises in the level of Lake Ontario brought about by "sudden" climatic changes producing greater precipitation, or by deforestation in the case of the upper contact.

The trace element geochemical results for the Sixteen Mile Creek lagoon are characterized by high variability and generally weak correlations with sediment grain size, organic content, stratigraphic position, and distance downstream. Ca and Zn show the most pronounced enrichment in the surficial sediments, but Cu and P also increase upwards locally. Ni and Zn tend to be concentrated in the finer sediments whereas Ca is more abundant in coarser material. Only P shows a weak positive correlation with organic content. Cu, Zn and Ni all increase in abundance down the length of the lagoon as does Ca after falling from a maximum in the stream channel to a minimum in the marsh. Most of the trace elements are, however, more abundant in the Twenty Mile Creek lagoon.

INTRODUCTION

The lower Great Lakes are surrounded by a large number of small lagoon-marsh complexes which occupy the lower reaches of stream valleys that were flooded as lake levels have risen during the last several thousand years. These lagoons commonly act as safe harbours for pleasure boats, and at certain times are important sites of sport fishing. In addition, they have great aesthetic and wildlife value, and the area bordering them is often prime residential land. Despite their obvious importance, however, there has been no in-depth study of historical or modern-day processes and sedimentation patterns in these lagoon-marsh complexes. As a result, little is known concerning the types of sediment accumulating in the lagoons or marshes, the role of the lagoons as traps for sediment-attached pollutants transported by the streams, or the life-expectancy and course of future development of the lagoons.

The study summarized here was undertaken to provide a firmer basis for answering these questions. One lagoon, the Sixteen Mile Creek lagoon located 5 km west of St. Catharines, was selected for detailed sedimentological and geochemical investigation. The lagoons on the adjacent Fifteen Mile and Twenty Mile (Jordan Harbour) Creeks, as well as the valley of the small Eighteen Mile Creek, were also investigated in reconnaissance fashion in order to assess how representative the data obtained from the Sixteen Mile Creek lagoon are.

Previous results from this project have been summarized in various abstracts (Otto and Dalrymple 1980, 1981b, 1982), and outlined in greater detail in last year's annual Summary of Research (Otto and Dalrymple 1981a). These reports have been concerned primarily with documenting the stratigraphy (Figure 1) and characteristics (Table 1) of the sediments filling the Sixteen Mile Creek lagoon, and with establishing a tentative history of lagoon infilling. Work during the past year has focused on extending the coring into the marsh and stream channel areas at the head of the Sixteen Mile Creek lagoon, and on undertaking reconnaissance coring in the Fifteen Mile and Twenty Mile Creeks lagoons. All of the laboratory analyses have now been completed, including those for textural (grain size) attributes, moisture content, organic content, and major and trace element abundances, on all samples from both previously and newly collected cores. Pollen analyses have also been completed, and several new ^{14}C dates have been obtained from the Brock University ^{14}C Dating Laboratory. It was learned that all of the previously-reported ^{14}C dates were approximately 2000 years too old because of an error in the standard used. Revised dates are listed on Figure 1, and all new dates

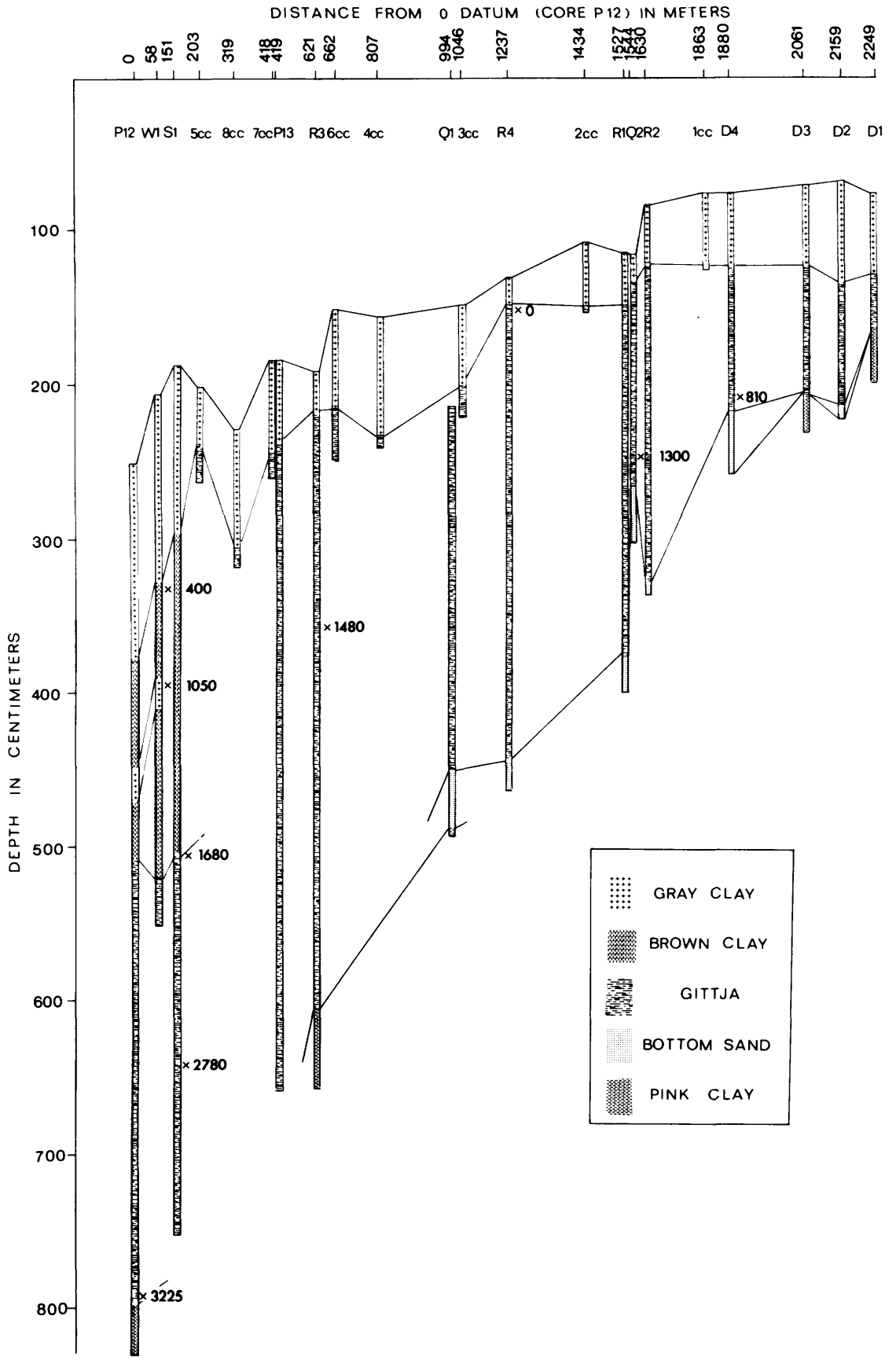

Figure 1. *Stratigraphy of the Sixteen Mile Creek lagoon (modified after Otto and Dalrymple 1981a). Depths are measured from the water surface. Locations of radiocarbon dates marked by x's.*

Table 1. *Average characteristics of the stratigraphic units beneath the Sixteen Mile Creek lagoon (data from Otto and Dalrymple 1981a).*

Unit	Thickness	Mean Grain Size	Percent Sand	Percent Silt	Percent Clay	Moisture Content	Organic Content	Additional Features
Gray Clay	20–130 cm	6.3–9.5ϕ	3%	43%	54%	39°	6°	bioturbated and massive
Brown Clay	0–210 cm	9.2ϕ	0%	40%	60%	54°	9°	weakly laminated
Gittja	35–415+cm	7.2–9.6ϕ	2%	45%	53%	47°	5–35%	finely interlaminated organics and muds; organic content increases upward
Bottom Sand	0–40 cm	33.0–4.9ϕ	28%	30%	32%	--		organic laminae present
Pink Clay	?	5.1–7.4ϕ	15%	54%	31%	26%	2–9%	massive and dense

reported have been corrected. Detailed examination of all of the data is well advanced, particularly with respect to the history of lagoon infilling, and a revised history of sedimentation is given below.

SIXTEEN MILE CREEK LAGOON

STRATIGRAPHY OF THE MARSH ON SIXTEEN MILE CREEK

The headward end of the Sixteen Mile Creek lagoon is bordered by 25 000 m^2 of nearly flat marsh which is covered by dense stands of bulrush (*Typha*). This area is submerged to variable depths during floods, but is dry for much of the summer. It slopes very gently lakeward, and the marsh merges with the open water of the lagoon. The adjacent part of the lagoon is extremely shallow (<0.5 m) for the first 200 m, and is termed the "delta" region. The marsh is traversed by a single, sinuous channel that is less than 1 m deep relative to the marsh surface. Almost imperceptible levees flank it. The channel terminates at the lagoonward end of the marsh, and does not extend across the delta as a submerged feature.

During July of 1981, six 9.5 cm diameter cores approximately 2 m in length were obtained from the channel-marsh-delta region (Figure 2) using a portable vibracorer modelled after the design described by Lanesky *et al.* (1979). From these cores, four stratigraphic units were identified. From the base up these are: 1) till; 2) sandy gravel to sand with intermixed mud; 3) "orange" clay; and 4) gray clay. The characteristics of these units are summarized in Table 2.

The lowest unit recovered in cores 1 and 5 (Figure 2) is a compact, pebbly sandy silt that varies in colour from brown to pink. Red shale pebbles were found to be present in one core, set in a matrix exhibiting conchoidal fracture. Despite its organic content, this unit is believed to be a till, and is likely equivalent to the Late Wisconsin Halton Till which Feenstra (1972) has mapped throughout the area. Stratigraphically it would seem reasonable to suggest that this till is equivalent to the Pink Clay (see Figure 1, Table 1); however, the Pink Clay does not contain pebbles, and diatoms have been found in it, suggesting that it is lacustrine rather than glacial in origin.

Abruptly overlying the till is a unit which varies in composition from very coarse sandy gravel (maximum recovered pebble sizes are 6 cm) to fine sand, with variable admixtures of silt and clay throughout. The grain sizes in this unit generally show a pronounced fining-upward trend: in its lower portions mud is mixed together with gravel and sand, but in its upper part, mud occurs locally as discrete beds, 1-5 cm thick, interlayered with fine sand. This unit is undoubtedly a fluvial deposit because of its coarseness. It is present in all of the cores collected from the head of the lagoon, but is usually buried beneath younger, clayey sediments (see below). In core 5, the most proximal channel core, however, the fine-grained variant of this unit (interlayered mud and sand = alternating stagnant water and floods?) floors the present channel. The Bottom Sand that occurs locally beneath the finer fill of the lagoon (see Figure 1, Table 1; Otto and Dalrymple 1981a) is the stratigraphic equivalent of this unit.

An orange-coloured sandy clay silt overlies the sandy gravel with a sharp contact in the central and

Table 2. *Average characteristics of the stratigraphic units recovered in vibracores from the channel, marsh and delta of the Sixteen Mile Creek lagoon.*

Unit	Thickness	Mean Grain Size	Recent Gravel	Percent Sand	Recent Silt	Recent Clay	Moisture Content	Organic Content
Gray Clay	52-145 cm	6.2-8.2Φ	-	9%	60%	31%	33%	5%
Brown Clay	37-57 cm	4.8Φ	-	29%	46%	25%	21%	3.5%
Sandy Gravel	82-101 cm	0.7-5.0Φ	12%	48%	29%	11%	19%	3%
Till	?	5.7Φ	-	24%	58%	18%	17%	2%

northern part of the marsh area (cores 2, 3, 4 and 6, Figure 2). This clay appears massive and contains orange-coloured streaks and oxidized root remains, which indicate that it represents an ancient soil horizon formed in an oxidizing environment. The sandy nature of this unit relative to the present marsh sediment (gray clay, Table 2) suggests that it formed prior to the capture of the Sixteen Mile Creek by the Twenty Mile Creek, when the discharge and coarse sediment load of the Sixteen Mile Creek would have been larger. No correlative unit to this orange clay has been found in the lagoon, indicating that it does not extend much beyond the location of core 6 (see Figure 2).

The uppermost unit is a clayey silt (gray clay) that contains abundant, coarse organic detritus in its upper portions, particularly in the present-day marsh. This clay occurs on the marsh surface (cores, 1, 2 and 4, Figure 2) where it is deposited during flooding, and in the lower reaches of the channel (core 3, Figure 2). Its presence in the latter area indicates that the Sixteen Mile Creek is presently unable to transport coarse debris to the delta. This gray clay is continuous with the Gray Clay that floors all of the present-day lagoon.

It is interesting to note that actively-forming gittja has not been found in either the marsh or the shallowly-submerged, vegetated portion of the delta; and a similar situation also exists in the lagoons and marshes of the Fifteen Mile, Eighteen Mile, and Twenty Mile Creeks. Earlier reports of modern gittja deposition in the Fifteen Mile Creek lagoon (Otto and Dalrymple 1981a) based on spot checks, were not substantiated. The reason for the absence of modern gittja is not known.

PALYNOLOGY

Core S1, located near the mouth of the lagoon (see Figure 1) was sampled in detail for pollen analysis. Because of the relatively young age of all of the sediments (see Figure 1), no major arboreal floral changes were recorded, and *Pinus, Fagus, Quercus, Acer* and *Ulmus* are the most abundant constituents throughout. There is, however, a slight, though erratic, upward increase in *Pinus* at the expense of the hardwoods through the Gittja and Brown Clay, with a noticeable peak in the Brown Clay approximately 10 cm below the Gray Clay. A similar pine peak has been found by McAndrews (1972, 1976) who dated it at 580 years B.P. It is attributed to Indian agricultural land-clearing practices rather than to a climate deterioration such as would be associated with the Little Ice Age (McAndrews 1976).

By contrast, the nonarboreal components show significant changes through the core. The Gittja is characterized by abundant Gramineae (grass) and bulrush pollen, which is consistent with the previous interpretation that it accumulated in a very shallow water to marshy environment (Otto and Dalrymple 1981a). At the contact with the overlying Brown Clay, these pollen types decrease drastically while the number of algal spores increases suddenly. This suggests that the Brown Clay was formed in a deeper, open water lagoon. The rise in *Ambrosia* (ragweed) pollen that followed European settlement and clearing of the land for agriculture (circa 1850; McAndrews and Boyko 1972) occurs over the depth range from 75 to 100 cm, 5-30 cm above the base of the Gray Clay.

Distinct diagenetic differences between the Gray Clay and the underlying units were also noted. In the Gittja and Brown Clay, pollen are abundant and contain authigenic pyrite, whereas in the Gray Clay pollen abundances are low and pyrite is absent. These observations indicate that the Brown Clay – Gray Clay boundary marks a change from a reducing to an oxidizing environment: pyrite is only stable in a reducing environment (Garrels and Christ 1965), whereas pollen is destroyed by oxidizing conditions (Tschudy 1969). The scarcity of arboreal

pollen in the upper part of the Gray Clay is probably also a result of forest clearing by the European settlers, and increased sedimentation rates (see below).

STRATIGRAPHY OF ADJACENT LAGOONS AND INTERLAGOON CORRELATIONS

A limited number of cores have been collected from the Fifteen Mile Creek and Twenty Mile Creek lagoons for comparative purposes: three short (1.5 m long) cores from the Fifteen Mile Creek lagoon (Figure 3a); and one short and two long (7-8 m long) cores from Twenty Mile Creek lagoon (Jordan Harbour) (Figure 3b). The lithologic units recognized in each lagoon are described in Table 3.

FIFTEEN MILE CREEK LAGOON

Only three lithologic units were encountered in the short cores from this lagoon (Table 3a). From the base up they are: gittja, brown clay, and gray clay. The gittja consists of interlaminated organic-poor and organic-rich silty clay, and was encountered throughout the length of the lagoon. At the downstream end of the lagoon (core 1, Figure 3a), the gittja is overlain by a thin, brown silty clay which does not extend headward as far as core 2. This brown clay, and the gittja in the remainder of the lagoon, is in turn overlain by a gray silty clay which covers the bottom of the present-day lagoon. The gray clay is extensively bioturbated; recovered organisms have been identified as *Donatia* (M. Dickman, Brock University, personal communication), a beetle which feeds on the submerged and underground stems and roots of aquatic plants such as *Nymphaea* (water lily), *Sagittaria* (arrow-head) and *Potamogeton* (pondweed).

Radiocarbon dating of samples from the base of the brown clay indicates that the gittja-brown clay transition occurred at about 1675 years B.P., while gray clay deposition commenced sometime after 470 years B.P., based on a date obtained just below the top of the brown clay.

TWENTY MILE CREEK LAGOON

Five lithologic units were penetrated by the long cores: "bottom" clay, "bottom" sand, gittja, brown clay, and gray clay (Table 3b). The lowest unit in the lagoon is a dense, light gray sandy clay silt ("bottom" clay) that is interpreted as a post-glacial lacustrine deposit. It is overlain abruptly by a muddy sand ("bottom" sand) which is believed to be of fluvial-deltaic origin. This is in turn gradationally transitional upwards into the gittja, a unit composed of alternating layers of brown silty clay and organic-rich sediment. Only core C-11 (Figure 3b) penetrated the lowest two units, but gittja was recovered in all of the cores and presumably extends throughout the lagoon. In core T1 a uniform, brown silty clay lies above the gittja, but elsewhere in the lagoon the gittja passes upward into a bioturbated, gray silty clay. This gray clay also covers the brown clay in the downstream portion of the lagoon.

^{14}C dating shows (Figure 4) that gittja deposition commenced shortly before 3225 years B.P. and continued until 1670 years B.P. when the brown clay began to accumulate near the mouth of the lagoon. After this, brown clay and gittja deposition progressed simultaneously until shortly after 440 years B.P. when formation of the gray clay began.

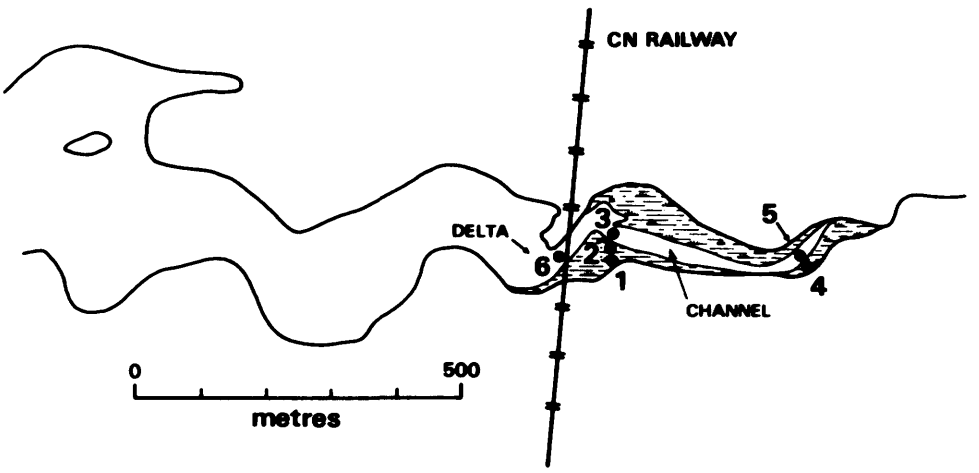

Figure 2. *Headward reaches of the Sixteen Mile Creek lagoon showing the distribution of marsh and the location of the six vibracores.*

INTERLAGOON CORRELATION

Based on the grain size, colour and organic content (see Tables 1 and 3), and on the stratigraphic distributions just described (Figure 4), a one-to-one lithological correlation of units is possible between the three lagoons. The Pink Clay and Bottom Sand of the Sixteen Mile Creek lagoon are equivalent to the "bottom" clay and "bottom" sand in Twenty Mile Creek lagoon (Jordan Harbour), and similar units are expected to exist in the Fifteen Mile Creek lagoon but have not been sampled by the available short cores. The gittja, brown clay and gray clay occur in all three lagoons, and always with the same distribution: gittja initially occurs everywhere in the lagoon but is replaced in its upper part at the lakeward end of the lagoon by brown clay before gray clay mantles everything. Formalization of these units according to recognized stratigraphic procedure is being considered.

Comparison of the radiocarbon dates given above and in Figure 1 (see also Figure 4) also shows that the transitions between the upper three units are synchronous in all three lagoons, within the accuracy of the dates. By averaging the radiocarbon dates from all three lagoons, it is estimated that the brown clay-gittja transition occurred at approximately 1675 years B.P. The date of the brown clay and gittja to gray clay transition can be bracketed between approximately 440 years B.P. (average of dates from the upper 10 cm of the brown clay) and 1850 A.D. (the date of the *Ambrosia* rise; McAndrews and Boyko 1972). All samples from the gray clay gave modern ages. No attempt has been made to estimate the "hard water effect" (incorporation of old carbon from local carbonate rocks) on these dates as Mott and Farley-Gill (1978) have done, as no dates were obtained on the rise in *Ambrosia* pollen. However, the modern ages for the gray clay and the fact that the 440 year B.P. age is bracketed stratigraphically by the pine peak in the brown clay, which is dated at 580 years B.P. by varve counting (McAndrews 1976), and the rise in *Ambrosia*, indicates the the effect of hard water is probably small. This synchroneity of the dates in the three lagoons strongly indicates that the factor(s) responsible for the stratigraphic succession must be of regional significance, having effected all lagoons similarly (i.e., changes in Lake Ontario and/or climate), rather than of local influence (e.g., capture of Sixteen Mile Creek by Twenty Mile Creek; J.J. Flint, Brock University, personal communication, 1980).

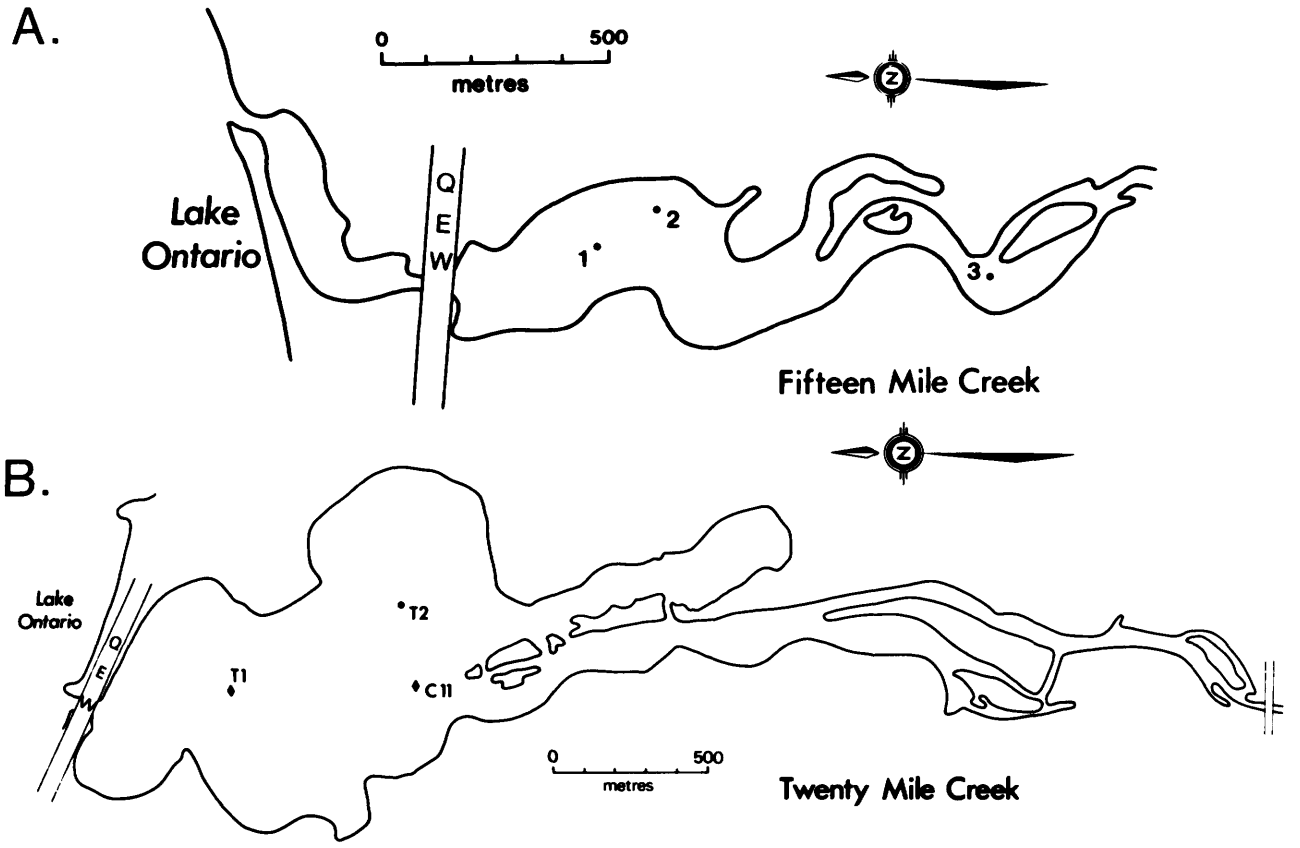

Figure 3. *Sketch maps of the (A) Fifteen Mile Creek lagoon and (B) the Twenty Mile Creek lagoon (Jordan Harbour) showing the locations of the short (solid dots) and long (solid diamonds) cores. QEW = Queen Elizabeth Highway.*

REVISED HISTORICAL SYNTHESIS

The history of sedimentation in the Sixteen Mile Creek lagoon has been summarized by Otto and Dalrymple (1981a, b) and later described in detail by Otto and Dalrymple (1982). With the very recent discovery that the radiocarbon dates used were in error, and with the recognition that all three lagoons possess identical stratigraphies, the transitions from Gittja to Brown Clay, and from Brown Clay and Gittja Clay in the Sixteen Mile Creek lagoon can not be attributed to changes in the level of Lake Ontario induced by modifications in the outlets of the post-glacial upper Great Lakes and/or to the capture of the Sixteen Mile Creek as was done previously. Other causative factors must be found.

The sedimentological and paleontological data strongly indicate that the four upper units were deposited in the following environments: Bottom Sand - fluvial channel and/or delta; Gittja - a very shallow water to marshy environment; Brown Clay - deeper, open-water lagoon; and Gray Clay - open water lagoon. This sequence is indicative of progressive deepening of the lagoon and transgression of the environments, as might be expected given that the level of Lake Ontario has risen considerably because of isostatic rebound of the St. Lawrence River outlet. This cannot be the only cause of the deepening however, as the transitions from Gittja to Brown Clay, and from Brown Clay to Gittja to Gray Clay are either sharp or occur over a very short (several centimetres) distance implying that the changes were rapid. It is reasonable to presume that the rate of isostatic uplift of the outlet has been decreasing exponentially over the past few thousand years as the deflection of the crust from its equilibrium position decreases. If deposition could keep pace with rising lake levels during the early history of the lagoon, as indicated by the great, unbroken thickness of gittja, why were there two, apparently rapid, deepenings in the more recent past when the rate of lake level rise should have been less? The two possible explanations are that some other factor raised the level of Lake Ontario

Table 3. *Average characteristics of the stratigraphic units present in the Fifteen Mile Creek and Twenty Mile Creek lagoons.*

Unit	Thickness	Mean Grain Size	Percent Sand	Percent Silt	Percent Clay	Moisture Content	Organic Content
A - Fifteen Mile Creek Lagoon							
Gray Clay	15-40 cm	9.0Φ	tr	32%	68%	-	7%
Brown Clay	19 cm	8.9Φ	tr	35%	65%	-	6%
Gittja	?	8.6Φ	1%	37%	62%	-	13%
B - Twenty Mile Creek Lagoon (Jordan Harbour)							
Gray Clay	34-74 cm	7.9Φ	1%	49%	50%	51%	5%
Brown Clay	130 cm	-	-	-	-	49%	-
Gittja	319-414 cm	8.3Φ	4%	51%	45%	54%	3-20%
"Bottom" Sand	77 cm	4.2Φ	55%	25%	20%	-	8%
"Bottom" Clay	?	6.0Φ	20%	60%	20%	-	5%

relatively suddenly on two occasions, or that the sediment supply to all three lagoons decreased.

It is tentatively suggested here that the two transitions are climatically induced. Palynological studies by many workers indicate that the areas draining into the Great Lakes have been continuously forested over the last 10 000 years until colonial times, and it is reasonable to assume that sediment supply from such heavily forested terrain would be either constant or only slightly variable in response to precipitation changes (Lewis and Anderson 1976). On the other hand, it is known from historical records that the level of Lake Ontario may rise and fall by as much as 2.0 m as a result of short-term (several years) variations in annual precipitation anywhere within the entire Great Lakes drainage network (International Great Lakes Levels Board 1973). Therefore, the events at approximately 1675 years B.P. and 440 years B.P. may represent the onset of lengthy periods of increased precipitaton over Lake Ontario, or further "upstream", which led to semi-permanent rises in lake level. It should be noted that the 1675 year B.P. event corresponds closely with the end of the Sub-Atlantic climatic episode (1690 years B.P., Bryson *et al.* 1970), and the 440 year B.P. date falls close to either the start of the Neo-Boreal episode (1550 A.D., Baerreis and Bryson 1965; Bryson and Wendland 1967) if it is left uncorrected, or to the Pacific I - Pacific II transition (1450 A.D.) if the Stuiver and Suess (1966) conversion to calendar dates is applied. Too little is known about the effects of these climatic changes in the Great Lakes areas, however, to substantiate such correlations, and they must remain tentative until further work is done.

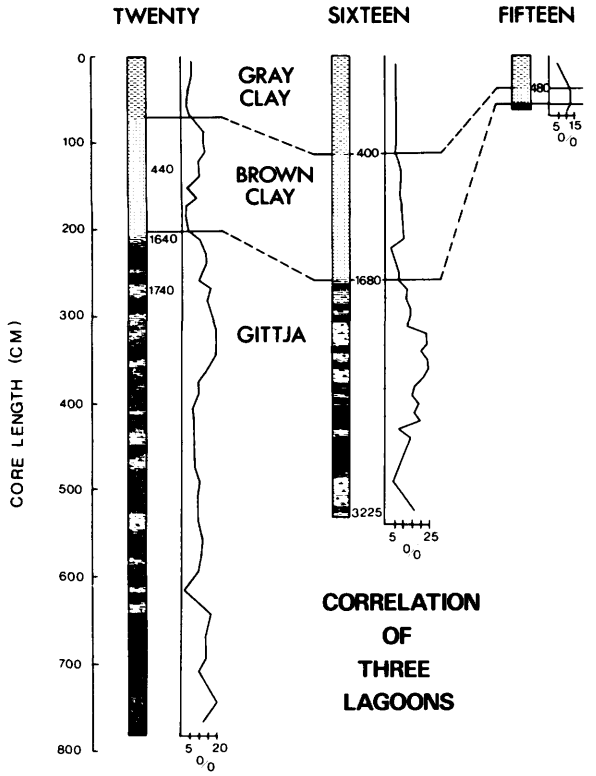

Figure 4. *Correlation of stratigraphic units in cores from the downstream end of the three lagoons. Radiocarbon dates and the vertical variation in organic content are also shown for each core.*

Alternatively, the post 440 year B.P. commencement of gray clay deposition could be the result of deforestation which spanned the period from 1775 to 1825 A.D. (Wickland and Mathews 1963), as all parts of the Gray Clay give modern ages. The observation that *Ambrosia* begins to increase in abundance between 6 and 16 cm above the transition would suggest that this explanation is less likely, but McAndrews (1976) has shown that the influx of *Ambrosia* postdates settlement elsewhere in southern Ontario. If the gray clay is the product of land clearing and increased sediment supply, then some other explanation for the apparent deepening (Gittja - Gray Clay) must be found, unless the depositional environment of the gittja has been misinterpreted.

The capture of the upper half of the Sixteen Mile Creek drainage basin by Twenty Mile Creek, 1500-2000 years B.P. (J.J. Flint, Brock University, personal communication, 1980) spanned the 1675 years B.P. climatic change but is not responsible for the gittja to brown clay transition for the reason already outlined. A more subtle reflection of the capture may, however, be present in the sediments of the Sixteen Mile and Twenty Mile Creeks lagoons. In the Sixteen Mile Creek lagoon, the organic content of the gittja increases upward to a maximum a short distance below the brown clay (or just below the gray clay at more headward localities) (see Figure 4 in Otto and Dalrymple 1981a) while the reverse trend is generally true in Twenty Mile Creek lagoon (Jordan Harbour) (see Figure 4). This is consistent with a gradual decrease through time in the terrigenous clastic input to the Sixteen Mile Creek lagoon, and a corresponding increase in input to Jordan Harbour.

In the Sixteen Mile Creek lagoon, sedimentation rates in the gray clay since deforestation, reach 69.2 cm/century near the mouth, assuming that the beginning of the *Ambrosia* rise at a depth of 90 cm occurred in 1850 A.D. (McAndrews and Boyko 1972). This value is approximately three times the pre-settlement rate if differences in compaction (i.e., water content) are considered, and is also more than three times the corresponding mean annual sedimentation rate in the main body of Lake Ontario (Kemp *et al.* 1974). The rate obtained here for the post-settlement period may be high however, because the *Ambrosia* pollen may have been mixed to a greater depth by the intense bioturbation prevalent in the Gray Clay.

SEDIMENT GEOCHEMISTRY

The geochemical data from the sediments in the Sixteen Mile Creek lagoon were summarized briefly in last year's report (Otto and Dalrymple 1981a). In the past year, addi-

tional analyses have been performed on sediments from the marsh and channel of the Sixteen Mile Creek and from core C-11 in the delta region of Jordan Harbour (Figure 3b). Interpretation and integration of the new results with previous data is currently in progress, but certain interesting trends have emerged, particularly in the gray clay.

In an attempt to determine the extent of anthropogenic loading in the Sixteen Mile Creek lagoon, concentrations of the five analyzed trace elements (P, Ca, Zn, Cu, and Ni) were regressed against the abundance of *Ambrosia* pollen in core S-1 (Figure 1). Surprisingly, the correlations were generally found to be weak although uniformly positive, with only Ca showing a statistically significant relationship (significance level (α< 1 percent for n = 8). Zn is the next most strongly correlated, having r = 0.50 (n = 8) which is significant at approximately the 20 percent level. In other cores (particularly D1 and W1, Figure 1; see also Figure 8 in Otto and Dalrymple 1981a) copper and phosphorous also show an upward increase through the gray clay. The absence of a uniform, strong correlation with *Ambrosia* may be attributed to several factors: the input of abundant pollutants post-dates the rise of *Ambrosia*; bioturbation has disturbed the distributions; and/or the variation in trace element concentrations may be controlled more strongly by other sediment characteristics such as grain size and organic content.

In order to assess this latter possibility, trace element concentrations in the gray clay were regressed against phi mean grain size and organic content. Ni showed the strongest positive relationship within grain size (r = 0.96, for n = 13; α< 1 percent) while Zn also correlated positively with grain size but only at the 10 percent significance level. These elements increase in abundance as the grain size becomes finer, and are probably bound to the clay fraction of the sediment. Ca, by contrast, shows a significant negative correlation with the phi mean size (r = 0.63; α< 5 percent) indicating that it occurs as coarser particles probably composed of limestone or dolomite. P and Cu do not show any correlation with grain size. None of the five elements exhibit a strong correlation with organic content; Ca and P show the highest positive correlation coefficients however. Similar relationships for all elements with both grain size and percent organics were also found in the gittja.

Because of the large amount of scatter in the data, areal variations in trace element concentrations within the surficial sediments of the Sixteen Mile Creek and Twenty Mile Creek lagoons were analyzed by averaging all available samples from the uppermost 20 cm within specified geomorphic areas (Table 4). This reduces the influence of anomalously high or low concentrations and produces more uniform trends. Consequently the patterns differ somewhat from those reported last year (Otto and Dalrymple 1981a).

In the Sixteen Mile Creek lagoon-marsh complex (Table 4), Zn, Cu and Ni all show progressive downstream increases in concentration with maxima near the mouth of the lagoon. Ca is most abundant in the channel at the head, but from the marsh it too increases in abundance

Table 4. *Areal variations in average concentrations of selected elements within the uppermost 20 cm of the sediment profile.*

Environment	Phosphorous (%)	Calcium (%)	Zinc (ppm)	Copper (ppm)	Nickel (ppm)
Sixten Mile Creek					
Channel	0.25	3.95	56.4	27.6	19.1
Marsh	0.22	1.09	119.5	28.8	20.8
Delta	0.24	1.22	147.4	58.7	21.7
Mouth	0.23	2.19	181.2	63.0	25.4
Twenty Mile Creek					
Delta	0.24	2.02	221.4	110.7	23.3

down the lagoon. Phosphorous values are more or less constant throughout.

At least some of the areal variation in Ni, Zn and Ca concentrations can be explained by the grain size dependences documented above. The channel sediments are the coarsest, hence the high Ca and low Ni and Zn, whereas the gray clay near the mouth is finer than in the delta region (see Figure 6 in Otto and Dalrymple 1981a), resulting in higher Ni and Zn values. This cannot, however, explain the downstream increase in Cu and Ca, and some other factor such as input from the Queen Elizabeth Highway is required.

Finally, it is interesting to note that the concentrations of all elements, P excepted, are slightly to significantly higher in the delta region of the Twenty Mile Creek lagoon than they are in the corresponding portion of the Sixteen Mile Creek lagoon. This may be due to the larger size and more intense development of the drainage basin of the Twenty Mile Creek which passes through several towns on its way to Lake Ontario. The average values for Zn and Cu in the Sixteen Mile Creek lagoon are also lower than the values reported from surficial sediments in Lake Ontario (Kemp and Thomas 1976), no doubt because of the lack of urban development in the Sixteen Mile Creek drainage basin.

ACKNOWLEDGEMENTS

The authors gratefully acknowledge J.J. Flint, Brock University, for his advice and assistance, and J. Terasmae and H. Melville for providing the ^{14}C dates and loaning field equipment. The portable vibracorer was constructed with a grant from the Advisory Research Committee, Queen's University, to the second author.

REFERENCES

Baerreis, D.A., and Bryson, R.A.
1965: Climatic Episodes and the Dating of the Mississippian Cultures; Wisc. Archeol., Vol. 46, p. 203-220.

Bryson, R.A., Baerreis, D.A., and Wendland, W.M.
1970: The Character of Late-Glacial and Post-Glacial Climatic Changes; p.53-74 in Pleistocene and Recent Environments of the Central Great Plains, edited by W. Dort Jr., and J.K. Jones Jr., University Press of Kansas, Lawrence.

Bryson, R.A., and Wendland, W.M.
1967: Tentative Climatic Patterns for some Late Glacial and Post-Glacial Episodes in Central North America; University of Wisconsin, Department of Meteorology, Technical Report, Vol. 34, No. 1202(07), p. 271-302.

Feenstra, B.H.
1972: Quaternary Geology of the Niagara Area, Southern Ontario; Ontario Geological Survey, Preliminary Map P. 764, Geological Series, scale 1:50 000.

Garrels, R.M., and Christ, C.L.
1965: Solutions, Minerals, and Equilibria; Harper and Row, New York, 450p.

International Great Lakes Levels Board
1973: Regulation of Great Lakes Water Levels; Report to the International Joint Commission, 294p. + 7 Appendicies.

Kemp, A.L.W., Anderson, T.W., Thomas, R.L., and Mudrochova, A.
1974: Sedimentation Rates and Recent Sediment History of Lakes Ontario, Erie and Huron; Journal Petrology, Vol. 44, p. 207-218.

Kemp, A.L., and Thomas, R.L.
1976: Cultural Impact on the Geochemistry of the Sediments of Lakes Ontario, Erie and Huron; Geoscience Canada, Vol. 3, p. 191-207.

Lanesky, D.E., Logan, B.W., Brown, R.G., and Hine, A.C.
1979: A New Approach to Portable Vibracoring Underwater and on Land; Journal Sedimentary Petrology, Vol. 49, p. 654-657.

Lewis, C.F.M., and Anderson, T.W.
1976: Basin Deposits; a Record of Long Term Coastal Evolution (Recession) in the Great Lakes?; p.109-115 in Proceedings Workshop on Great Lakes Coastal Erosion and Sedimentation, edited by N.A. Rukavina, Burlington.

McAndrews, J.H.
1972: Pollen Analyses of the Sediments of Lake Ontario; 24th International Geological Congress, Montreal, Canada, Section 8, p. 223-227.
1976: Fossil History of Man's Impact on the Canadian Flora: an Example from Southern Ontario; Supplement to Canadian Botanical Association, Bulletin, Vol. 9, 5p.

McAndrews, J.H., and Boyko, M.
1972: Dating Recent Sediment in Lake Ontario by Correlation with a Varve-Dated Pollen Diagram; Abstracts, 15th Conference Great Lakes Research, International Association of Great Lakes Research, p. 12651274.

Mott, R.J., and Farley-Gill, L.D.
1978: A Late-Quaternary Pollen Profile from Woodstock, Ontario; Canadian Journal of Earth Sciences, Vol. 5, p. 1101-1111.

Otto, J.E., and Dalrymple, R.W.
1980: Sedimentation in the Sixteen Mile Creek Lagoon; Ontario Geological Survey, Geoscience Research Seminar Abstracts, p. 14.
1981a: Terrain Characteristics and Physical Processes in Small Lagoon Complexes; Ontario Geological Survey, Miscellaneous Paper 98, p. 202-215.
1981b: Sedimentation History and Geochemistry of the Sixteen Mile Creek Lagoon; Ontario Geological Survey, Geoscience Research Seminar Abstracts, p. 11.
1982: Sedimentation in the Sixteen Mile Creek Lagoon and the Recent History of Lake Ontario; Geological Association of Canada, Program with Abstracts, Vol. 7, p. 71.

Stuiver, M., and Suess, H.E.
1966: On the Relationship between Radiocarbon Dates and true Sample Ages; Radiocarbon, Vol. 8, p. 534-540.

Tschudy, R.H.
1969: Relationship of Palynomorphs to Sedimentation; p.79-96 in Aspects of Palynology, edited by R.H. Tschudy, and R.A. Scott, Wiley-Interscience, Toronto.

Wickland, R.E., and Mathews, B.C.
1963: The Soil Survey of Lincoln County; Report 34 of the Ontario Soil Survey, Canada Department of Agriculture and the Ontario Agricultural College, 48p.

Grant 114 Source, Correlation and Thermal Maturation History of Hydrocarbon Mineral Deposits of Southern Ontario

S.J. Pollock, J.F. Barker, R.W. Macqueen, and P. Fritz
Department of Earth Sciences, University of Waterloo

ABSTRACT

Hydrocarbon gas chemistry relations between natural gases in the Ontario parts of the Appalachian and Michigan basins, and natural gases in the deeper US parts of these respective basins, support the postulation that natural gases in the Ontario parts of the Appalachian and Michigan basins have distal sources within their respective basins. Carbon and hydrogen isotope data indicate that most natural gases in Ontario are more mature than their host rocks and hence have distal mature sources of possibly similar maturity. Preliminary organic geochemical analyses indicate a genetic grouping of oils related to the stratigraphic level of their reservoirs. Additional organic and isotopic analyses of liquid and solid hydrocarbons are planned. Sufficient thermal maturation for petroleum generation has been found only in Middle Silurian and lower strata.

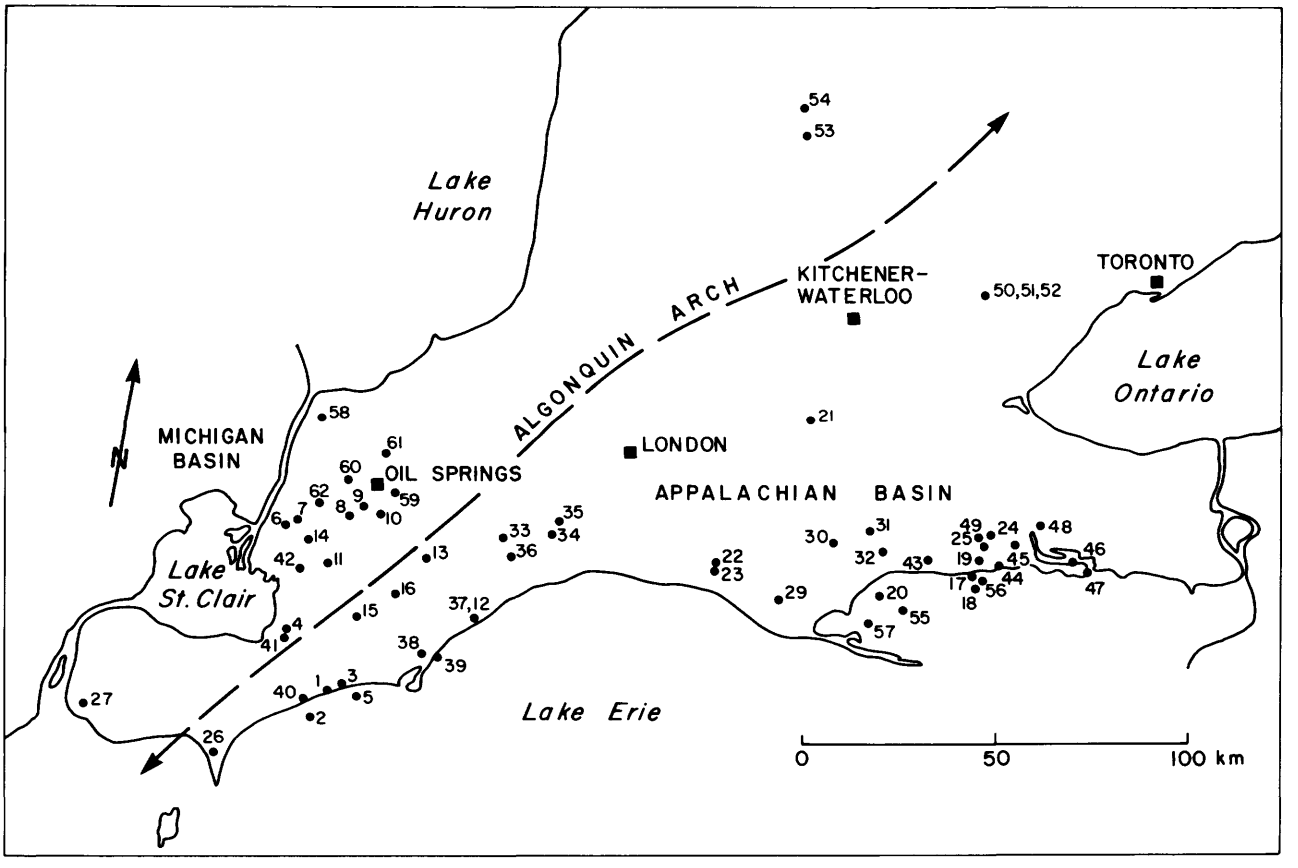

Figure 1. *Gas sample location map showing basins and approximate position of Algonquin Arch.*

Table 1. *Analyses of natural gases from southern Ontario for major components and carbon and hydrogen isotope ratios.*

+ $\delta^{13}C = \left(\frac{R\ sample}{R\ standard} - 1\right) \times 1000\ ^{o}/_{oo}$, where $R = \frac{^{13}C}{^{12}C}$. Carbon standard is P.D.B.

Similarily for $\delta^{2}H$, $R = \frac{^{2}H}{^{1}H}$, Hydrogen standard is S.M.O.W.

* Total $C_4H_{10} = iC_4H_{10} + nC_4H_{10}$

a Contaminated by higher hydrocarbons

	Natural Gas Chemistry - Analyses are expressed as Volume Percents								Carbon and Hydrogen Isotope Ratios of Hydrocarbon Gases Analyses are expressed in the Usual δNotation +					
									$\delta\ ^{13}C\ ^{o}/_{oo}$			$\delta\ ^{2}H\ ^{o}/_{oo}$		
Sample No.	Methane CH_4	Ethane C_2H_6	Propane C_3H_8	Iso Butane iC_4H_{10}	Normal Butane nC_4H_{10}	Nitrogen N_2	Oxygen O_2	Carbon Dioxide CO_2	Methane CH_4	Ethane C_2H_6	Propane and Butane $C_3H_8 + C_4H_{10}$	Methane CH_4	Ethane C_2H_6	Propane + Butane $C_3H_8 + C_4H_{10}$
Upper Silurian														
5	79.1	3.7	1.6	0.8*				0.01	-37.8	-29.6				
6	68.9	12.3	10.4	6.5*		1.7		0.3	-51.0	-35.1	-28.3			
8	83.0	7.1	4.2	2.8*		2.7		0.2	-45.2	-32.5	-27.6			
11	83.9	6.4	3.2	1.6*		4.8		0.5	-42.9	-33.1	-29.9			
15	78.4	10.0	5.5	1.6*		4.5			-39.1	-27.7				
16	78.9	5.5	2.4	2.2*		10.9								
26	92.3	4.18	1.35	0.07	0.17	3.21	<0.04	<0.03	-37.2	-34.6	-30.4	-169	-157	-142
33	82.10	6.50	2.94	0.33	0.57	7.04	0.53	<0.03	-41.4	-34.5	-31.0	-163	-174	-134
34	81.68	6.40	2.91	0.29	0.62	7.35	0.44	<0.03	-40.8	-33.5	-30.5	-196	-171	-144
36	84.33	5.77	2.65	0.33	0.65	6.47	0.06	0.05	-40.2	-34.6	-31.1	-193	-162	-143
38	78.94	10.63	4.85	0.84	1.09	3.99	0.24	<0.03	-40.1	-28.1	-26.9	-171	-134	-130
42	79.50	7.54	3.88	0.57	0.73	6.55	0.30	0.07	-47.4	-36.5	-31.1	-231	-180	-142
Upper and Middle Silurian														
1	78.7	5.3	3.1	1.6*				0.2	-39.9	-34.7	-32.2			
10	74.7	9.8	6.7	4.0*		4.5		0.3	-36.9	-30.9	-28.1			
14	78.8	8.1	4.3	1.9*		4.9		0.05	-42.9	-34.8	-31.0			
27	84.6	6.81	2.88	0.23	0.47	5.58	<0.04	0.05	-41.4	-34.3	-30.5	-191	-154	-142
37	83.99	5.13	1.99	0.17	0.47	7.69	0.45	0.04	-39.2	-34.6	-30.7	-177	-166	-143
59	83.76	7.44	4.10	0.87	0.78	2.94	<0.04	<0.03	-49.0	-34.0		-238	-151	-130
62	91.46	4.80	2.55	0.43	0.44			0.32	-52.3	-35.1		-241	-141	-129

Table 1. *Continued.*

Sample No.	Natural Gas Chemistry - Analyses are expresses as Volume Percents: Methane CH_4	Ethane C_2H_6	Propane C_3H_8	Iso Butane iC_4H_{10}	Normal Butane nC_4H_{10}	Nitrogen N_2	Oxygen O_2	Carbon Dioxide CO_2	Carbon and Hydrogen Isotope Ratios of Hydrocarbon Gases — Analyses are expressed in the Usual δNotation†: $\delta^{13}C$ °/₀₀ Methane CH_4	$\delta^{13}C$ °/₀₀ Ethane C_2H_6	$\delta^{13}C$ °/₀₀ Propane and Butane $C_3H_8 + C_4H_{10}$	$\delta^{2}H$ °/₀₀ Methane CH_4	$\delta^{2}H$ °/₀₀ Ethane C_2H_6	$\delta^{2}H$ °/₀₀ Propane + Butane $C_3H_8 + C_4H_{10}$
Middle Silurian														
2	79.1	3.7	1.7	0.8*				0.01	-39.0	-35.1	-31.7			
3	80.8	4.6	2.2	1.0*				0.01	-40.3	-35.6	-31.5			
7	83.4	5.9	3.2	1.9*		5.6			-43.5	-32.2	-28.6			
9	81.6	5.7	4.9	2.0*		5.3			-49.2	-33.5	-28.0			
29	88.5	4.41	1.40	0.03	0.11	5.29	<0.04	<0.03	-41.1	-36.7	-31.6	-205	-176	-132
30	86.4	6.70	2.31	0.05	0.28	5.57	<0.04	<0.03	-45.4	-38.2	-32.6	-258	-225	-149
31	87.4	5.09	1.52	0.02	0.18	6.08	<0.04	<0.03	-42.8	-37.1	-31.8	-229	-191	-135
39	84.61	5.82	2.01	0.31	0.47	5.31	<0.04	0.35	-38.1	-33.1	-29.2	-164	-145	-76
40	83.45	4.32	1.55	0.16	0.47	4.90	0.27	0.21	-37.3	-34.1	-30.0	-168	-144	-125
58	89.81	4.13	2.23	0.60	0.51	2.90	0.11	0.27	-52.5	-35.7	-27.2	-227	-142	-115
60	86.51	5.41	2.92	0.91	0.61	3.43	<0.03	<0.03	-47.6	-33.2	-25.4			
61	66.81	8.18	9.52	1.36	3.19	11.33	0.16	0.05	-48.8	-38.8	-32.5	-276	-225	-182
Middle and Lower Silurian														
32	89.96	3.26	0.92	0.02	0.12	6.21	<0.04	<0.03	-39.2	-35.5	-30.5	-181	-135	
43	85.18	3.69	0.96	0.07	0.13	9.49	0.15	<0.03	-38.4	-35.8	-30.5	-180	-152	-125
44	83.23	7.43	2.80	0.19	0.48	5.71	0.09	<0.03	-45.8	-37.1	-32.0	-229	-197	-138
45	83.63	7.12	2.66	0.18	0.44	5.54		<0.03	-45.0	-37.0	-31.7	-240	-190	-139
47	83.20	7.04	2.74	0.18	0.42	6.15	0.05	<0.03	-45.7	-38.1	-32.1	-204	-248	-146
48	85.15	5.04	1.66	0.11	0.34	7.00	<0.03	<0.03	-43.6	-37.1	-32.1	-225	-201	-137
49	85.02	6.35	2.32	0.16	0.38	6.22	<0.03	<0.03	-44.2	-37.7	-31.9	-229	-207	-139
56									-44.3	-37.2	-31.7	-234	-189	-148
Lower Silurian														
17	82.1	6.9	4.7	4.1*		<2.2			-43.8	-35.4	-30.0			
18	89.3	4.1	2.7	3.9*					-41.5	-39.7				
19	81.6	6.9	4.7	4.0*		<3.0			-44.4	-34.9	-30.4			

Table 1. *Continued.*

Sample No.	Natural Gas Chemistry - Analyses are expresses as Volume Percents								Carbon and Hydrogen Isotope Ratios of Hydrocarbon Gases Analyses are expressed in the Usual δNotation+					
									$\delta\ ^{13}C\ ‰$			$\delta\ ^{2}H\ ‰$		
	Methane CH_4	Ethane C_2H_6	Propane C_3H_8	Iso Butane iC_4H_{10}	Normal Butane nC_4H_{10}	Nitrogen N_2	Oxygen O_2	Carbon Dioxide CO_2	Methane CH_4	Ethane C_2H_6	Propane and Butane $C_3H_8 + C_4H_{10}$	Methane CH_4	Ethane C_2H_6	Propane + Butane $C_3H_8 + C_4H_{10}$
20	84.3	4.0	3.8	3.9*		< 4.0			-43.6	-39.5	-29.2			
22	<80								<-36.8[a]					
23	<85								<-37.9[a]					
24	<80								<-39.1[a]					
25	<80								<-37.9[a]					
46	79.39	7.99	4.14	0.31	0.81	6.37	0.24	<0.03	-46.5	-37.8	-32.3	-260	-206	-137
55									-39.0	-36.0	-30.4	-181	-162	
57									-39.7	-36.5	-31.5	-198	-172	-141
Middle Ordovician														
41	83.10	5.53	2.58	0.20	0.67	2.98	0.26	0.09	-38.5	-34.5	-31.2	-185	-166	-142
50									-39.9	-33.5	-30.2	-175	-164	-111
51									-34.7	-32.3	-30.0	-182	-161	-106
52									-40.3	-34.5	-30.1	-185	-153	-134
53									-38.4	-32.4	-30.1	-161	-142	-123
54									-38.7	-32.2	-30.1	-167	-151	-125
Cambrian														
4	82.8	4.7	2.4	1.2*				0.06	-41.0	-35.6	-32.1			
12	81.5	5.1	0.4	4.7*		8.4		< 0.01	-38.1	-35.1	-32.6			
13	79.6	8.0	6.1	1.6*		4.7		< 0.01		-31.6[a]				
21	77.4	8.8	6.7	5.5*		<1.5		0.06	-44.4	-37.4	-33.2			

NATURAL GAS GEOCHEMISTRY

Even though natural gases are simple mixtures of relatively few components, considerable information can be derived from the study of the chemical and isotopic composition of natural gases.

To date, a total of 62 natural gas samples have been collected using air displacement methods. The sample locations are shown in Figure 1; the chemical and isotopic data are given in Table 1.

HYDROCARBON GAS GEOCHEMISTRY

The hydrocarbon gases analyzed for their volume percents were methane (CH_4), ethane (C_2H_6), propane (C_3H_8) and iso and normal butane (iC_4H_{10}, nC_4H_{10}). Considering these gases individually there are no distinct compositions or trends in natural gas composition with respect to reservoir rock age and/or geographic location within Ontario. The only exception is that Cambrian natural gas has a greater content of ethane and of higher hydrocarbons than most other natural gases in southern Ontario; however, unlike most of Ontario's gas deposits Cambrian gases are usually oil associated.

The samples from the eastern Lake Erie area generally have ethane:propane percent volume ratio greater than 2.0, whereas samples from the Windsor-Sarnia and western Lake Erie areas are generally between 0.5 and 3.0 (Nantais 1982). A similar grouping was found for the iC_4/nC_4 ratio. Eastern and western Lake Erie areas, or Appalachian basin samples, usually have iC_4/nC_4 ratios less than 1.0, averaging 0.5; Windsor-Sarnia or Michigan basin sample values are usually greater than 1.0, averaging 1.2 (Nantais 1982). There is also a different correlation between C_2/C_3 versus iC_4/nC_4 ratios for the basins as shown in Figure 2. It is now clear that there are regional variations in hydrocarbon gas chemistry in southern Ontario. Comparison of (C_2/C_3)versus (iC_4/nC_4) of samples from the Ontario parts of the Michigan and Appalachian basins, to samples from deeper parts of the respective basins (Table 2), supports the earlier postulation that the natural gas accumulations in the Ontario parts of the Michigan and Appalachian basins have distal sources within their respective basins.

A tertiary plot with the volume percent of CH_4, C_2H_6 and $C_3H_8 + C_4H_{10}$ at the apices (Figure 3) shows a trend which roughly bisects the diagram at the CH_4 apex. Any interpretations at this stage are preliminary, but a possible explanation of the trend is that ethane and propane plus butane are formed and destroyed or removed at comparable rates, and that the plotted position only changes vertically with relative methane content. Three means of changing the relative methane content are increasing thermal maturation, bacterial alteration, and preferential migration of CH_4.

Table 2. *Comparison of gaseous hydrocarbon chemistry in the Michigan and Appalachian Basins, using the ratio $(C_2H_6/C_3H_8)/(iC_4H_8/nC_4H_{10})$ (from Nantais 1982).*

Basin	Michigan		Applachian	
Location	Canada	U.S.A.	Canada	U.S.A.
number of samples	16	4	15 of 16	15 of 19
age	Silurian	Silurian	all ages	all ages
ratio range	<3.5	1.69-3.0	3.5-8.0	>3.5

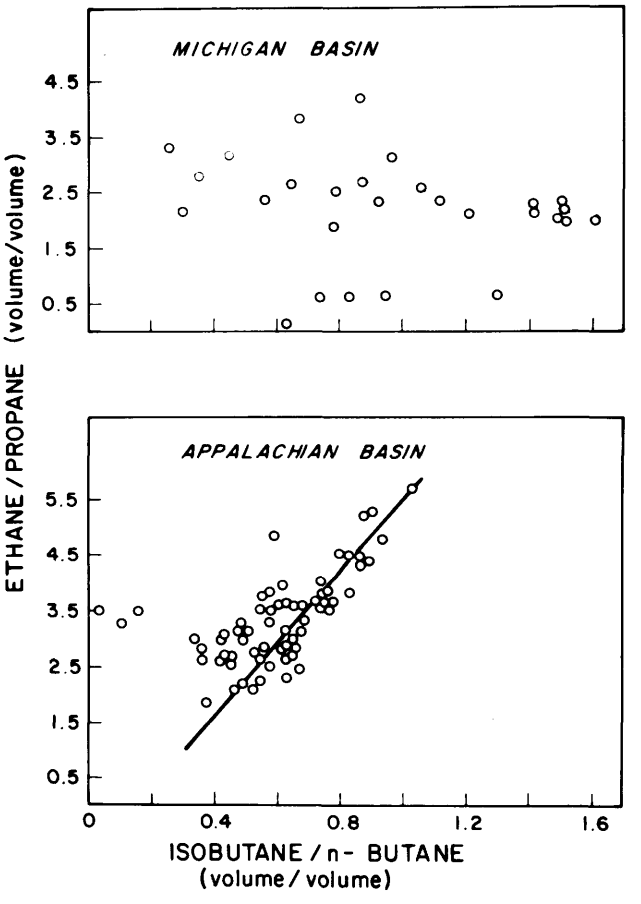

Figure 2. *Plot of ethane/propane vs. isobutane/normal butane (after Nantais 1982), showing differences in hydrocarbon gas chemistry of the natural gases in the Ontario parts of the Michigan and Appalachian basins.*

NON-HYDROCARBON GAS GEOCHEMISTY

Ontario natural gases generally contain minor amounts of nitrogen and trace amounts of carbon dioxide and oxygen. There are no significant differences or trends in CO_2 and O_2 content with respect to reservoir rock age or location. Nantais (1982) found an increase in nitrogen content from offshore Lake Erie to onshore. This agrees with the trend of nitrogen content increasing westwards in the Appalachian basin (Roth 1968). According to the gas facies for dominant non-hydrocarbon gases in the Western Canada Basin (Hunt 1979), southern Ontario is in the immature facies. Isotopic data presented in the next section strongly suggests that the hydrocarbon gases are mature. This discrepancy is under investigation.

The small but potentially commercial helium content of Ontario's natural gases was studied in a B.Sc. thesis by Moses (1981). In summary it is generally believed that He in natural gas originates from radioactive decay in rocks and a Precambrian basement He source is postulated. The primary factors influencing He content are reservoir age, pressure and proximity to faults.

Hydrogen sulphide occurs mainly in gases reservoired in the Guelph formation in the western Lake Erie region although several other widely separated occurrences were reported in Paper 70-2 (Ontario Department of Mines and Northern Affairs 1970). When present, H_2S content is usually less than 1 percent. Hunt (1979) regards the amount of reservoir H_2S that is of prelithification biogenic origin as being negligible. According to Hunt (1979) the most likely origin of reservoir H_2S is thermal alteration of organic sulfur compounds in both source and reservoir beds plus thermocatalytic reduction of sulphate when in contact with pooled hydrocarbons. H_2S generation from these thermal sources is not significant until temperatures are in the range of 100°C and does not peak before 170°C. Legall (1980) concluded that the maximum paleotemperature of Paleozoic strata in southern Ontario was 90°C. A thermal source for the H_2S in the

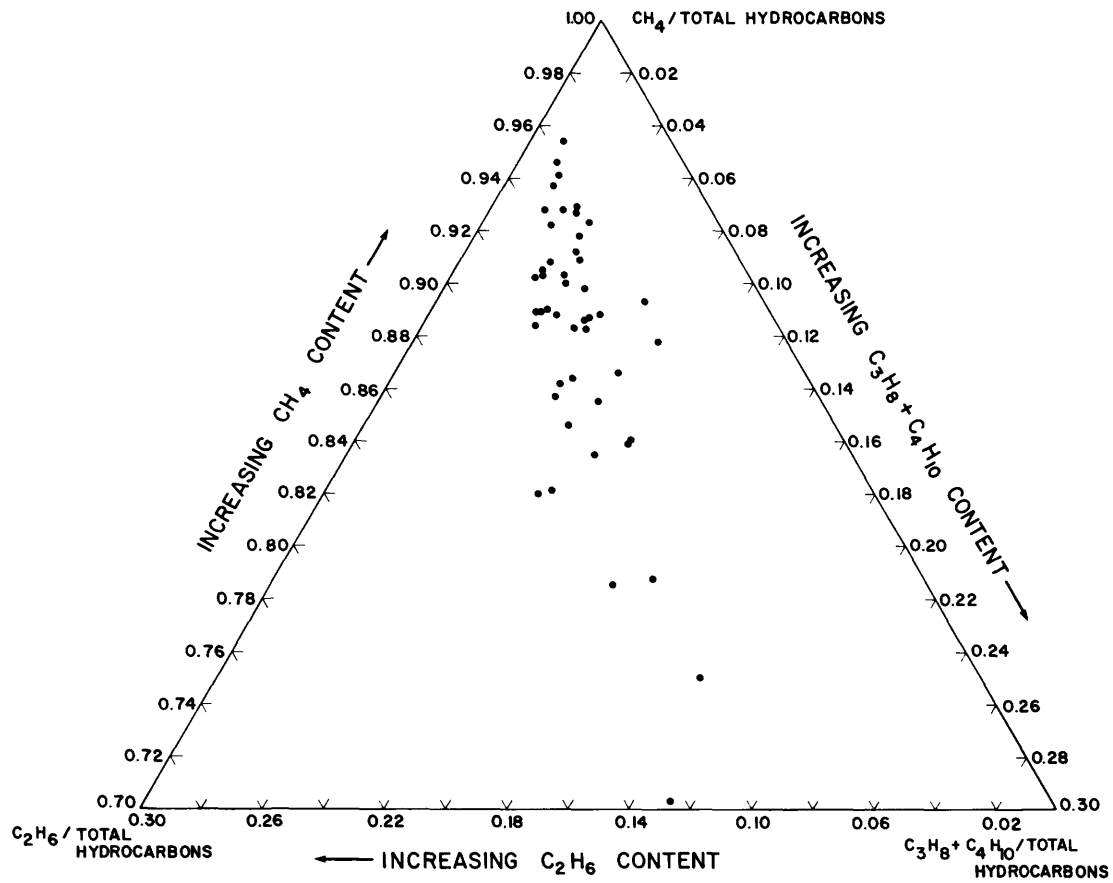

Figure 3. *Tertiary plot of CH_4, C_2H_6, C_3H_8 + C_4H_{10} in the sample gases of southern Ontario. A possible interpretation is that C_2H_6 and C_3H_8 + C_4H_{10} contents change at comparable rates, and plotted position changes with relative methane content.*

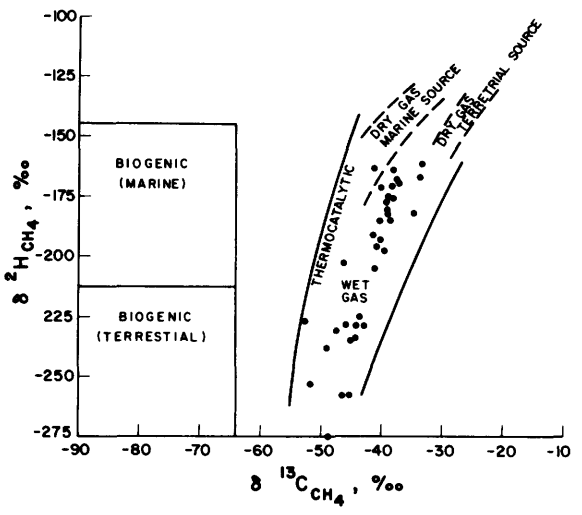

Figure 4. *The origin of CH_4 as indicated by $\delta^{13}C_{CH4}$ vs. $\delta^{2}H_{CH4}$ (after Schoell 1980). Isotopic data shown that the CH_4 in southern Ontario's natural gas is of a mature thermocatalytic origin.*

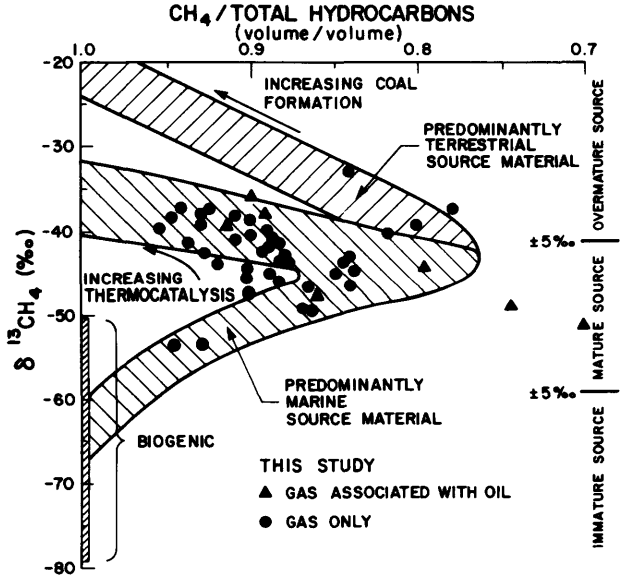

Figure 5. *Maturation of CH_4 as indicated by $\delta^{13}C_{CH4}$ and CH_4 content (after Stahl 1973). Use of Stahl's model suggests that natural gas accumulations in southern Ontario are mature to overmature and hence more mature than host rocks. This suggests a distal source.*

western Lake Erie region would support a distal mature natural gas source. The planned sulphur isotope studies should identify the H_2S source and thus provide information concerning gas migration.

CARBON AND HYDROGEN ISOTOPIC GEOCHEMISTRY OF HYDROCARBON GASES

There is neither a relation between the isotopic composition of any gaseous hydrocarbon and reservoir age nor between the isotopic composition and the volume percent of a hydrocarbon gas, even when one considers age (see Table 1). For the higher hydrocarbons there is a very much smaller variation in $\delta^{13}C$ than for CH_4 and a suggestion of a systematic increase in ^{13}C content with increasing hydrocarbon chain length. Similar trends are seen for hydrogen isotopes, but with some exceptions.

There is a significant correlation between the ^{13}C and ^{2}H composition of methane which is illustrated in Figure 4. Figure 4 indicates that virtually all of southern Ontario's methanes are thermocatalytic and have isotopic compositions similar to that of CH_4 found in wet mature gases. Most of Ontario's natural gas accumulations are dry and the sedimentary rocks are immature to only marginally mature (Legall 1980). This suggests that most of Ontario's natural gas has a mature and hence distal source. If large amounts of C_{2+} gases were formed with the CH_4, they were lost during migration.

Using a world wide data base Stahl (1973) proposed a model for the maturation of natural gas. This is adopted in Figure 5 which is a plot of $\delta^{13}C_{CH4}$ vs CH_4/total hydrocarbons (vol/vol). Assuming this model is applicable to carbonate-evaporite clastic sequences, Figure 5 indicates that Ontario natural gas deposits are mature to overmature and therefore have a distal source. There is an empirical relationship between the maximum total hydrocarbon/methane ratio and the $\delta^{13}C_{CH4}$ value for each of the gas types: oil associated, non-associated and coal (Deines 1980). These relationships are shown as contours on Figure 6. Figure 6 suggests that of the oil associated samples 4, 6, 12, 21, 37, 42, 61), only samples 6 and 61 were formed in association with their presently pooled oils and hence have local origins. Figure 6 does not clearly indicate whether or not gases other than samples 6 and 61 were formed in association with oil, with subsequent loss of wet gas during migration.

As stated earlier, hydrocarbon gas chemistry shows regional variations and supports the postulation that the natural gas accumulations in the Ontario parts of the Michigan and Appalachian basins have distal sources within their respective basins. The results of "Statistical Analysis Systems" procedures for one way analysis of variance and F tests, shown in Table 3, show both similarities and dissimilarities in the isotope data from the Windsor-Sarnia, eastern Lake Erie, and western Lake Erie regions. Similarities could result from similar source material of similar maturity. Dissimilarities can be explained in terms of increments of gas accumulation from various maturity stages (Fuex 1977). The most outstand-

Table 3. *Statistical analysis of isotopic compositions of natural gases from three different areas of southern Ontario.*

Isotopic composition of hydrocarbon gas/gases compared	Sample Areas: Windsor-Sarnia	Western Lake Erie	Eastern Lake Eri
$\delta^{13}C_{CH_4}$	A *	B	C
	-45.6 **	-39.2	-43.0
	(16)	(14)	(18)
	[0.50 ± 0.20]	[1.44 ± 0.20]	[0.65 ± .20]
$\delta^{13}C_{C_2H_6}$	A	A	B
	-34.4	-33.2	-37.1
	(16)	(14)	(18)
	[0.78 ± 0.25]	[0.82 ± 0.25]	[0.50 ± 0.25]
$\delta^{13}C_{C_3H_8 + C_4H_{10}}$	A	B	B
	-29.4	-30.7	-31.3
	(14)	(12)	(17)
$\delta^{2}H_{CH_4}$	A	B	A
	-219	-175	-218
	(6)	(8)	(14)
$\delta^{2}H_{C_2H_6}$	A	A	B
	-156	-157	-189
	(6)	(8)	(14)
$\delta^{2}H_{C_3H_8 + C_4H_{10}}$	A	A	A
	-133	-137	-139
	(6)	(7)	(12)

* Statistical Grouping.

The one-way analysis of variance and F tests are done separately for the carbon, and hydrogen isotopic compositions of each gas with respect to the three sample areas. Similar letters indicate that the areas do not differ significantly at the 95% confidence level, but only for a particular gas and its carbon or hydrogen isotopic composition.

** Mean Isotopic Composition, °/₀₀.

( ) Number of samples.

[ ] Ro calculated from mean $\delta^{13}C$ (Stahl, 1975).

ing feature of Table 3 is the enrichment of ^{13}C and ^{2}H in the CH_4 of the western Lake Erie area. This may indicate an accumulation of overmature CH_4; however, bacterial alteration of the reservoired CH_4 could also produce this enrichment.

Stahl and Carey (1975) found that there is a relationship between the vitrinite reflectance (R_o) of marine source material and $\delta^{13}C$ for C_1, C_2 and C_3 gases. The R_o values calculated for the geographic areas, Windsor-Sarnia, western Lake Erie, and eastern Lake Erie (Table 3), are in sufficient agreement to indicate at least one marginally mature to mature and hence distal source. The R_o of 1.4 ± 0.2 calculated from the mean $\delta^{13}C_{CH4}$ for the western Lake Erie region suggests overmature source rocks for the CH_4 in this region; however, this R_o may be falsely overestimated if bacterial alteration has enriched these methanes in ^{13}C.

ORGANIC GEOCHEMISTRY OF LIQUID AND SOLID HYDROCARBONS

Core and recent well cuttings samples obtained from the Petroleum Resources Section, Ontario Ministry of Natural Resources, as well as core samples from the former oil producing Fletcher Field, obtained from Consumers' Gas System have been analyzed for total organic carbon (TOC) content. Considerable effort was necessary to select a suite of about 21 samples (TOC > 0.5 percent) suitable for independent organic geochemical assessment by T.G. Powell (Geological Survey of Canada, Calgary) of source potential and thermal maturation of Ontario sedimentary rocks. These samples are in addition to 32 rock samples previously sent to Powell.

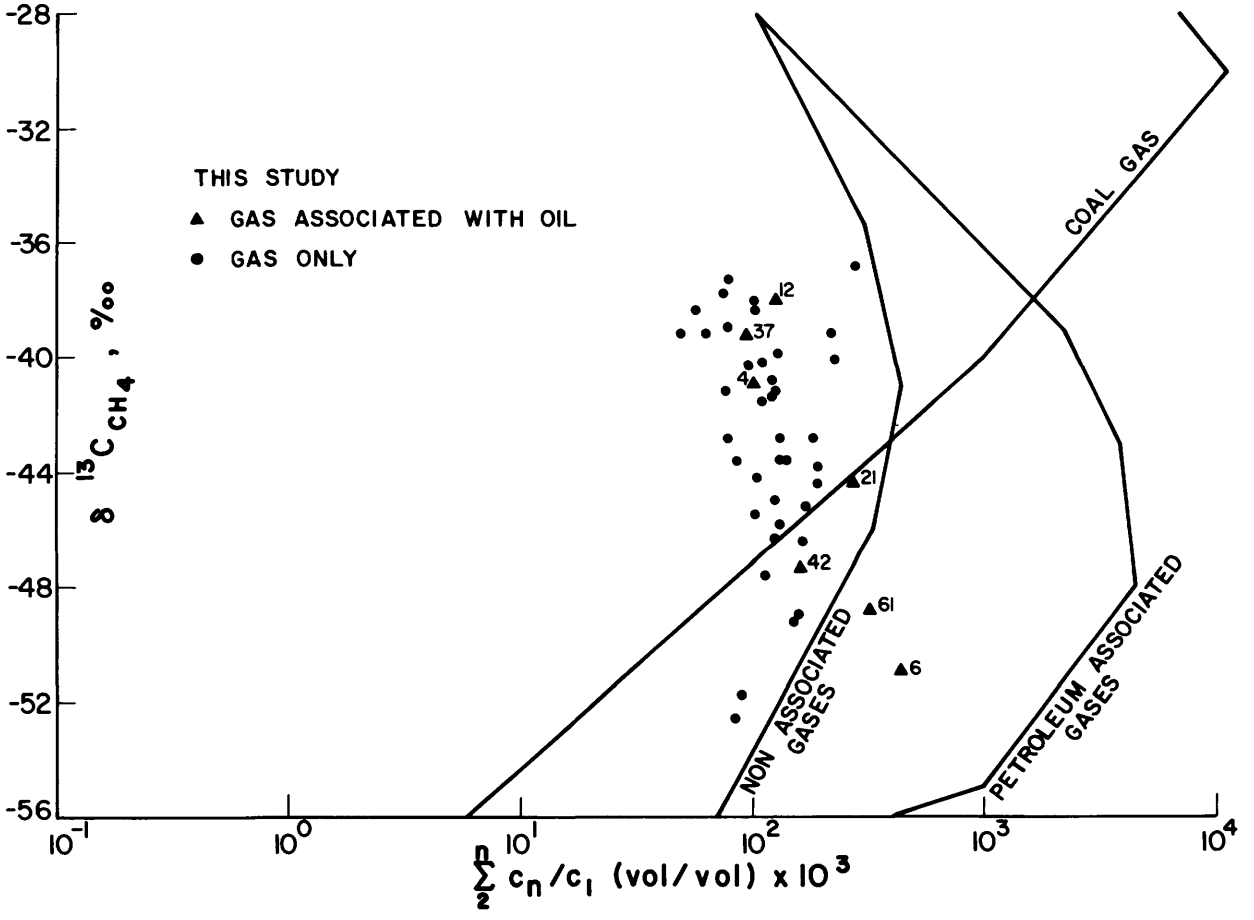

Figure 6. *Relationship between total hydrocarbon/methane and $\delta^{13}C_{CH4}$ (after Deines 1980). Contours show empirical maximums for different gas types (from Deines 1980).*

Table 4. *Sediment maturation parameters and inferred hydrocarbon potential in Paleozoic sedimentary rocks of southern Ontario.*

System \ Method		Conodont Colouration (CAI)	Bitumen Character	Kerogen Reflectance R_o( )	Thermal Alteration Index	Inferred Hydrocarbon Potential
	U				2-	
Devonian	M	1.5 (Immature)	Immature-Mature		1+, 2-, 2-,	Immature
	L					
	U		Immature		2+	Immature-Marginally Mature
Silurian	M	1.5	Immature-Marginally Mature		2, 2, 2, 2+, 2+, 2+	Marginally Mature
	L				2, 2+, 3-	
Ordovician	U	1.5	Mature	0.44-0.56 (Immature-Marginally Mature)	2-, 2-, 2-, 2, 2, 2+	Marginally Mature
	M	2			2+, 2+, 2+, 2+, 3-, 3-, 3-, 3-	
Cambrian	U		Mature		2+, 2+, 2+, 2+, 3-, 3+	Mature?

Preliminary analyses of a suite of 17 oils from Lower and Middle Paleozoic reservoirs by Powell allows them to be divided into three genetic groups based upon the character of their saturate fractions and supported to some extent by analyses of the gasoline range fraction. These groups are related to the stratigraphic level of their reservoirs. The only exception is the Mosa oil which, although occurring in a Silurian reservoir, resembles oils occurring elsewhere in Ordovician and Cambrian reservoirs. The peculiar hydrocarbon distributions of the Silurian oils are consistent with a source from a hypersaline environment such as in the Salina Formation. Cambrian and Ordovician oils appear to be the most mature. An additional fifteen oil samples have been sent to T.G. Powell, and analyses are forthcoming.

ISOTOPIC GEOCHEMISTRY OF LIQUID AND SOLID HYDROCARBONS

A procedure for combustion of oil or source rock fractions using a Parr bomb has been developed. This procedure has been proven to give reproducible ^{13}C analyses; it is currently being tested for ^{2}H reproducibility. A similar procedure for sulphur isotope analyses of oil or source rock fractions is also being investigated. The analytical techniques necessary for source rock separations are presently in place at Waterloo or in the laboratories of T.G. Powell.

Powell has separated the saturate, aromatic, resin, and asphaltene fractions of 32 oil samples and isotopic analyses of these fractions are forthcoming. Oil, gas, and distal gas source rock samples from deeper within the US parts of the Appalachian and Michigan basins will be sought to complete the understanding of hydrocarbon deposits in Ontario.

THERMAL MATURATION STUDIES OF SEDIMENTARY ROCKS

The interval from the top of the Middle Silurian to the top of the Paleozoic sequence was found to be at the immature or, at most, incipient maturation level, and so is not a favourable source for the oil and gas deposits found within this sequence (Table 4). Lower Ordovician to Middle Silurian rocks generally lie within the liquid "window" at an intermediate level of thermal maturation favourable for petroleum generation (Table 4). Powell's previous analyses (Barker *et al.* 1979) and those of Gunther (*in* Riediger 1981) indicate rather uniform maturation levels in all Collingwood shale samples but very different kerogen compositions at two sites. The geological controls of these variations are to be addressed.

P.R. Gunther, Petro Canada Limited, Calgary, is currently proceeding with visual kerogen examination and reflectance measurements in support of this research. Where vitrinite (a coal maceral) is not present — a situation anticipated in the Lower Paleozoic rocks of southern Ontario — reflectance measurements can be made on other kerogen materials. Greater caution is required in interpretation of such kerogen reflectance measurements.

ACKNOWLEDGMENTS

The authors would like to thank Pentti Palonen and the Ontario Ministry of Natural Resources Inspectors without whose assistance gas and oil sample collection would not have been possible, and Ronald Kellerman for the gas chromatographic analyses. Core material was provided by Consumers' Gas Company Limited and Stephen Calhoun and Charles Perity provided additional advice and information. Isotope analyses were conducted in the Isotope Laboratory under the supervision of Robert Drimmie. The assistance of T.G. Powell (Geological Survey of Canada) and Paul Gunther (Petro Canada Limited) is acknowledged.

REFERENCES

Barker, J.F., Legall, F.D., Barnes, C.R., and Fritz, P.
1979: Grant 39: Source, Correlation and Thermal Maturation History of Hydrocarbon Mineral Deposits of Southern Ontario; Ontario Geological Survey, Miscellaneous Paper 87, p. 7-10.

Deines, P.
1980: The Isotopic Composition of Reduced Organic Carbon; Chapter 9, p. 329-406, in Handbook of Environmental Isotope Geochemistry, Vol. 1, edited by Fritz, P. and Fontes, J.C., Elsevier Scientific Publishing Company, 545p.

Fuex, A.N.
1977: The Use of Stable Carbon Isotopes in Hydrocarbon Exploration; Journal of Geochemical Exploration, Vol. 7, p. 155-188.

Hunt, J.M.
1979: Petroleum Geochemistry and Geology; W.H. Freeman and Company, 617p.

Legall, F.D.
1980: Organic Metamorphism and Thermal Maturation History of Paleozoic Strata, Southern Ontario; Unpublished M.Sc. Thesis, University of Waterloo, 166p.

Moses, R.J.
1981: The Occurrence of Helium in Southern Ontario Natural Gases; Unpublished B.Sc. Thesis, University of Waterloo, 57p.

Nantais, P.T.
1982: Geochemistry of Natural Gases in Southern Ontario; Unpublished B.Sc. Thesis, University of Waterloo, 64p.

Ontario Department of Mines and Northern Affairs.
1970: Petroleum Resources, Gas Analyses — Ontario Gas Wells; Ontario Department of Mines and Northern Affairs, Paper 70-2, 194p.

Riediger, C.L.
1981: Evaluation of the Oil Shale Potential of the Collingwood Shale; Unpublished B.Sc. Thesis, University of Waterloo, 48p.

Roth, E.E.
1968: Natural Gases of Appalachian Basin; in Natural Gases of North America: A Summary, American Association of Petroleum Geologists, Memoir 9, Vol. 2, p. 1702-1715.

Schoell, M.
1980: The Hydrogen and Carbon Isotopic Composition of Methane from Natural Gases of Various Origins; Geochemica et Cosmochimica Acta, Vol. 44, p. 649-661.

Stahl, W.
1973: Carbon Isotope Ratios of German Natural Gases in Comparison with Isotope Data of Gaseous Hydrocarbons From Other Parts of the World; in Advances in Organic Geochemistry, edited by Tissot, B. and Bienner, F., Editions Technip, Paris, p.453-462.

Stahl, W., and Carey, B.D.
1975: Source Rock Identification by Isotope Analyses of Natural Gases from Fields in the Val Verde and Delaware Basins, West Texas; Chemical Geology, Vol. 16, p. 257-267.

Grant 96 Mineralization in the Whitewater Group, Sudbury Basin

D.H. Rousell
Department of Geology, Laurentian University

ABSTRACT

Rocks of the Whitewater Group, of early Proterozoic (Aphebian) age, constitute the fill of the Sudbury Basin and consist of three formations which are, from oldest to youngest: Onaping, massive heterogenous breccia; Onwatin, argillite and siltstone; and Chelmsford, mainly greywacke.

Mineralization is as follows: (1) disseminated sulphides in the Onaping Formation (pyrrhotite is the major sulphide mineral and occurs as fragments; others are chalcopyrite, sphalerite, galena, pyrite and marcasite); (2) Zn, Cu, Pb, Ag and Au mineralization in a carbonate-chert unit at the base of the Onwatin Formation (Vermilion and Errington Mines); (3) pyrite and local base metals in the Onwatin Formation; (4) anthraxolite veins in the Onwatin Formation; and (5) mineralized quartz veins in the South Range (Pb, Zn, and Ag at Moore Lake; Zn and Pb at Foisey; and Cu, Au, and Co at Papineau) and in the North Range (Pb, Zn, and Cu at Proulx). Analyses of material from two former gold properties (Creighton and Gordon Lake) yielded no Au values. Mineralized quartz-carbonate veins in a mafic sill, located at the Onwatin-Chelmsford contact, contain Cu, Zn and Au.

If the Sudbury structure is volcanogenic, the pyrrhotite fragments in the Onaping Formation may have been derived from pre-existing sulphide-rich rocks and the Vermilion-Errington deposits from metal- and sulphur-rich volatiles which escaped to the surface. If the Sudbury structure is of meteorite impact origin, the pyrrhotite fragments may have been derived from the base of the transient crater and, in part, from Huronian "target" rocks. The Vermilion-Errington deposits may represent sedimentary-exhalative deposits of the Remac-type; brines, trapped at the base of the transient crater could have risen to the surface and deposited the Vermilion member under anoxygenic conditions. Pyrite in the Onwatin Formation could have precipitated under similar conditions.

The quartz veins of the area are believed to have been emplaced during the time of major deformation, and the anthraxolite veins to have formed by remobilization and concentration of carbonaceous material during metamorphism.

INTRODUCTION AND GEOLOGICAL SETTING

The Sudbury Basin is renowned for the nickel-copper mines located at or near its outer rim. The rocks within the basin also contain a variety of mineral occurrences including two former base metal mines and two gold properties. Little new information on the mineralization within the basin has appeared in the last 25 years and many of the occurrences are poorly known. The purpose of this study is to characterize this mineralization and determine its origin, within the framework of basin evolution.

The Sudbury Basin is situated near the junction of three structural provinces of the Candian Shield: it lies within the Southern Province, with the Superior Province to the northwest and the Grenville Province to the southeast (Figure 1). The basin is elliptical in plan view, 58 km long and 26 km wide, with the long axis trending N65°E. The outer segments may be divided into three ranges: East, North, and South.

Rocks of the Whitewater Group, of early Proterozoic (Aphebian) age, comprise the fill of the basin and have no known equivalents outside the basin. The group consists of three formations which are, from oldest to youngest, the Onaping, Onwatin and Chelmsford Formations. Contacts between the formations are gradational and conformable. A distinctive breccia, consisting mainly of quartzite fragments as much as 80 m in length, occurs at the base of Onaping Formation (Stevenson 1961, 1972; Peredery 1972). Igneous rocks underlie, penetrate and locally form the matrix of the basal breccia. These igneous rocks may be related to the micropegmatite phase of the Nickel Irruptive (Stevenson 1963), or the oxide-rich phase of the Nickel Irruptive (Peredery and Naldrett 1975), or may represent melt rocks formed by meteorite impact (Peredery 1972). Above the basal unit, the Onaping Formation consists of a massive upward-fining breccia containing fragments which include devitrified glass, quartzite, quartz, granite, gneiss and gabbro. The Onwatin Formation is composed of argillite and siltstone. A carbonate-chert unit (Vermilion member), the distribution of which is not fully known, occurs at the base of the Onwatin Formation. The Chelmsford Formation consists largely of greywacke with minor argillite and siltstone and represents a proximal turbidite sequence (Rousell 1972). The rocks of the Whitewater Group contain abundant carbonaceous material and this imparts a dark colour to them.

The Nickel Irruptive was emplaced between the

Onaping Formation and the footwall rocks, outcrops in the form of an elliptical ring, and outlines the basin perimeter. The nickel-copper ores, consisting mainly of pyrrhotite, pentlandite and chalcopyrite are within a distinctive inclusion-bearing facies of the irruptive, known as the Sublayer (Souch *et al.* 1969, Naldrett *et al.* 1972, Pattison 1979). The Sublayer occurs between the Nickel Irruptive and the footwall, and in radiating dikes known as Offsets.

The basin was formed approximately 1.9 Ga ago (Gibbins and McNutt 1975a), and its origin is controversial (Stevenson and Stevenson 1980, Rousell 1981). It was long regarded as being of volcanic origin, and is still regarded as such by some. Dietz (1962) proposed that the basin was excavated by meteriorite impact.

The Sudbury Basin was deformed by an orogenic event 1.6 to 1.8 Ga ago (Gibbins and McNutt 1975b). The basin, once less elliptical than its present form in plan view, was flattened by a push directed toward the northwest. A penetrative tectonic foliation and lineation were developed in the Onaping Formation and locally in the Nickel Irruptive of the South and East Ranges (Brocum and Dalziel 1974; Rousell 1975). In the South Range, isoclinal similar folds, overturned to the northwest, are present in the basal breccia of the Onaping Formation (Stevenson 1960) and at the contact of the Onaping and Onwatin Formations (Martin 1957; Rousell 1975). Further to the northwest the deformation intensity decreased and rocks of the Onwatin and Chelmsford Formations developed a cleavage and formed open folds with vertical axial planes. Still further to the northwest the deformation was slight as only a local and weak foliation is present in the Onaping rocks of the North Range. Later episodes of brittle deformation produced a complex joint pattern (Rousell and Everitt 1981).

The locations of all mineral occurrences within the Whitewater Group that are known to the writer are shown on Figure 1. The mineralization may be grouped as follows: (1) disseminated sulphides in the Onaping Formation; (2) sulphides in a carbonate-chert unit; (3) pyrite and local base metals in the Onwatin Formation; (4) anthraxolite veins; and (5) mineralized quartz (carbonate) veins. The mineralization is diagramatically represented in the columnar section of Figure 2.

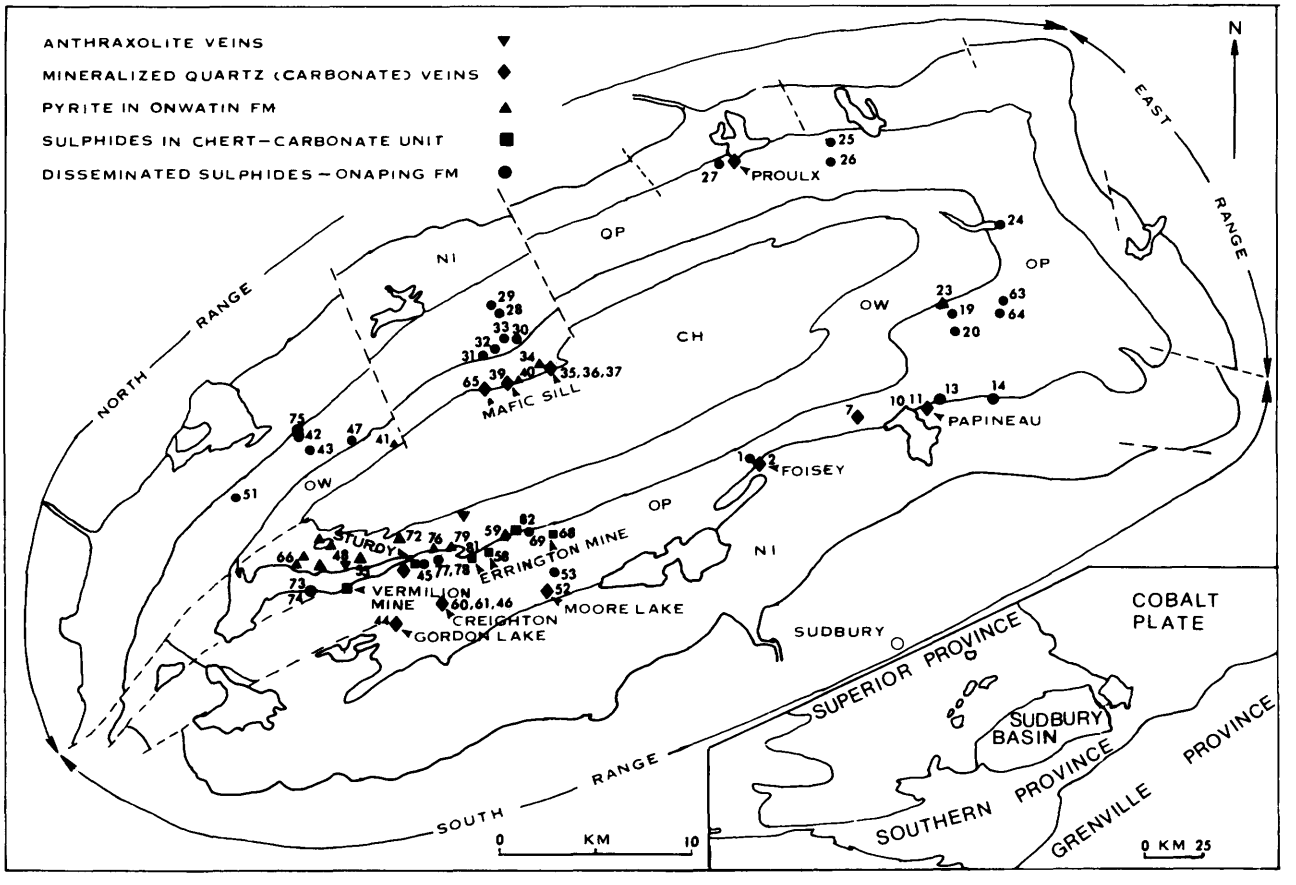

Figure 1. *Geological map of the Sudbury Basin showing the location of mineral occurrences in the Whitewater Group. Numbers correspond to specimen numbers in the tables (prefixed by W in the tables). Ni, Nickel Irruptive; OP, Onaping Formation; OW, Onwatin Formation; and CH, Chelmsford Formation. Inset map indicates the regional setting of the basin.*

DISSEMINATED SULPHIDES IN THE ONAPING FORMATION

Disseminated sulphides are present throughout the entire Onaping Formation, including the igneous rocks that occur below and locally form the matrix of the basal quartzite breccia. The sulphides occur mainly in the form of discrete fragments but there are also sulphide patches and sulphide grains within rock fragments. The sulphide fragments are tectonically elongated in the South and East Ranges. Several of the occurrences are exposed in trenches and pits and one occurrence is exposed by an adit approximately 37 m in length (locally known as "Morley's mine", locality 75 on Figure 1). The sulphide content of these occurrences is variable and some occurrences apparently were reported on the basis of accessibility. Muir (1980) and Lafleur (1981) noted that sulphides in the North Range are most abundant in the upper portion (black member) of the formation.

The sulphide fragments seldom exceed 0.5 cm in length, and generally constitute less than 10 volume percent of the rock. Polished section examination indicates that pyrrhotite is the major sulphide mineral with individual grains 0.5 mm or less in diameter. Chalcopyrite is common and is frequently enclosed by pyrrhotite but, in general, comprises less than 1 percent of total sulphides. Sphalerite, galena, marcasite and pyrite occur in minor amounts. The most abundant sulphide minerals in the Sudbury Ni-Cu mines are pyrrhotite, chalcopyrite and pentlandite (Hawley 1962); in the Nickel Irruptive the most abundant are pyrite, chalcopyrite, pyrrhotite, and pentlandite (Duke and Naldrett 1976). Thus the sulphide mineralization in the Onaping Formation resembles that in the mines in that pyrrhotite and chalcopyrite are the commonest sulphide minerals, it differs from that in the Nickel Irruptive in that the order of abundance is essentially reversed, and it differs from both in the apparent absence of pentlandite.

Desborough and Larson (1970) identified the following sulphide minerals in specimens of the Onaping Formation from the South Range and the Onaping Falls area (locality 42, Figure 1) in the North Range: pyrrhotite, nickel marcasite, "pure" pyrite, nickel pyrite, sphalerite, and chalcopyrite. Pyrrhotite is the most abundant sulphide mineral and it is locally replaced by nickel pyrite and nickel marcasite. The nickel and cobalt contents of grains of pyrrhotite, pyrite and marcasite were determined in three specimens by means of electron microprobe analysis. The Ni content of pyrrhotite is of particular interest; the range for eight grains is 0.1 to 0.35 weight percent and the average is 0.28 weight percent nickel. The ranges of nickel content of pyrrhotite from seven specimens from the Nickel Irruptive (Duke and Naldrett 1976) and from several Sudbury Ni-Cu mines (Hawley 1962) are 0.5 to 1.2 weight percent, and 0.76 to 2.65 weight percent, respectively. The corresponding average nickel contents are 0.81 and 1.62 weight percent, respectively. Thus the nickel content of pyrrhotite is apparently low in the Onaping Formation, higher in the Nickel Irruptive and still higher in the Ni-Cu ores.

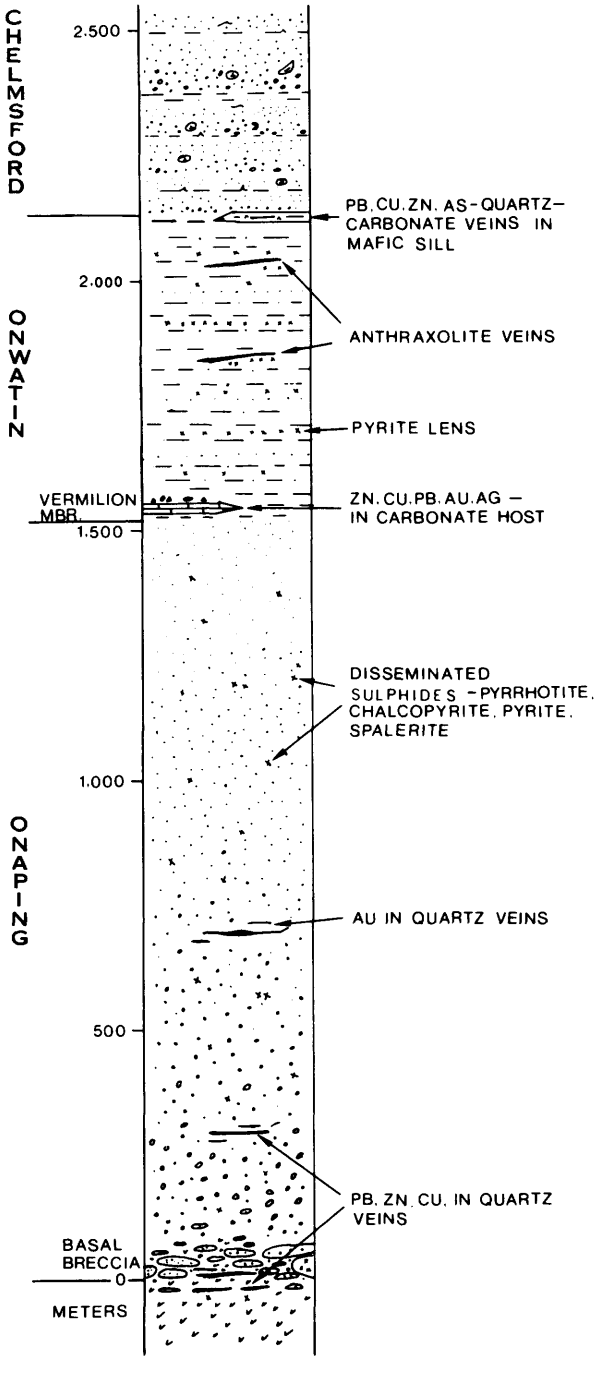

Figure 2. *Diagrammatic representation of mineralization in the Whitewater Group.*

Table 1 sets out chemical data for 28 specimens of the Onaping Formation and 3 specimens of the igneous matrix of the basal breccia. Specimen W1, near the base of the formation, contains relatively high values of Zn, Pb, and As, and W69, near the top of the formation, contains high values of Zn, Pb, Ba, and As. Average values of the analyses of Table 1 (igneous rocks omitted) are given in Table 4. The numbers shown in parentheses in Table 4 are averages obtained by omitting certain high values (Zn in W69 and Pb in W1, W69) and are used for comparison with other published data. Trace element data from the Onaping Formation reported by Arengi (1977) and Sadler (1958) are given in Table 4 in terms of average values. Arengi's (1977) data indicate somewhat higher average Zn, Ni and Cr values and Sadler's (1958) data show higher average values of Cu, Ni and Pb compared to the average values obtained in this study (see Table 4).

The average abundance of certain elements in the earth's crust and five common rock types (Krauskopf 1967, 1979) are given in Table 4 for comparative purposes. It is difficult to compare the Onaping Formation with common rock types because of the heterogeneous nature of the unit (Peredery 1972). Based on the chemical analyses of six selected specimens, Stevenson (1972) concluded that the Onaping Formation ranges in composition from rhyodacite near the base to dacite toward the top. This corresponds most closely to the 'intermediate' rock type of Table 4. The average values of Cu, Zn, Co and Cr in the Onaping Formation are at least twice as great as the average values of these elements in intermediate rocks; Ni and Pb values are not appreciably different. The average As value in the Onaping Formation is notably high and is approximately 13 times greater than the average value of intermediate rocks. The data of Arengi (1977) and Sadler (1958) indicate average Ag values that are approximately 100 times greater than the average Ag values in intermediate rocks; however, the material analyzed by the writer yielded much lower Ag values (see Table 1).

SULPHIDES IN A CARBONATE-CHERT UNIT

The Vermilion Mine, the Sturdy property and the three shafts of the Errington Mine are located in the southwestern corner of the basin (see Figure 1). These Zn-Pb-Cu-Ag-Au deposits occur over a length of 11 km, are in a carbonate-chert unit located at the base of the Onwatin Formation and are on the site of a magnetic high (GSC 1960) that extends to the northeast and beyond the mines. Burrows and Rickaby (1930) discussed the early history of the mining operations, Martin (1957) described the geology of the mines, and excellent coloured plans and sections were presented by Thomson (1956, after Martin 1957).

These properties have had a chequered history of exploration and development and have changed hands several times. Mineralization was first discovered by James Stobie in 1897 at Stobie Falls on the Vermilion River (between localities 79 and 81, Figure 1, and no longer exposed). Several small shafts, in the vicinity of Errington No. 1 shaft (Locality 79, Figure 1), indicate early activities. After considerable diamond drilling, the Errington No. 1 shaft was sunk in 1926 (approximately 152 m) followed by the sinking of No. 2 shaft (approximately 457 m) and No. 3 shaft (approximately 125 m). The Vermilion orebody, situated beneath Vermilion Lake, was discovered in 1929 by diamond drilling. An extensive surface installation was constructed that included a mill and flotation plant. Operations ceased in 1931 because of a fall in metal prices. In 1952, the Errington Mine was dewatered and the properties reopened. The Vermilion Mine shaft was completed in 1953 (approximately 381 m). Operations apparently stopped in 1957 (S.N. Charteris, Falconbridge Nickel Mines Limited, personal communication). One of the reasons for the lack of success was a problem in recovery because of the fine-grained nature of the ore. Giant Yellowknife Mines Limited, the present owner of the property, completed a drilling program in 1979 at the Vermilion Mine in order to obtain fresh material for recovery tests.

The ore occurs in a distinct unit called the "Vermilion Formation" (Martin 1957). Arengi (1977) relegated the unit to member status because diamond drill hole data indicated lateral discontinuity; the writer concurs with this view. Figure 3 is a diagrammatic representation of the Vermilion member and it is based on the description by Martin (1957). The basal argillite (0-30 m thick) is a massive siliceous and carbonaceous rock containing pyrite as fine disseminated grains and thin layers; upper and lower contacts are gradational. The argillite is supposedly replaced by the overlying carbonate from the top down, and the former may be thin or absent when the latter is thick. The carbonate rock, as much as 30 m in thickness, hosts most of the ore, and varies from fine to coarse grained; it locally exhibits pisolitic texture and in places is prominently layered (see photograph in Thomson 1956, p.50). A cherty carbonate zone marks the gradation from carbonate to chert breccia. Carbonate replaces chert breccia and locally this process is almost complete. The chert breccia consists of black chert fragments, generally less than 5 cm in length, set in a matrix of white recrystallized chert. The uppermost unit of the member (approximately 6 m thick) consists of interbedded argillite, limestone and dolomite.

The ore sulphides consist of pyrite, sphalerite, galena, chalcopyrite, marcasite, and pyrrhotite. There are two types of ore: disseminated ore and massive pyrite ore. The disseminated ore occurs in the carbonate rock, and the mineralization is fine-grained and intimately mixed. The massive pyrite ore is generally high in Zn and low in Cu. It occurs mainly at the base of the carbonate rock, and apparently replaces the underlying argillite; massive pyrite is also present at the base of the Vermilion member. Small pyrrhotite-rich pods occur at the top of the Onaping Formation. Chalcopyrite locally replaces pyrite and pyrrhotite and also replaces chert breccia and chert carbonate. Accordingly, the highest copper values tend to be at the top and bottom of the deposits. Quartz veins in the ore zone display coarse sphalerite, galena and chalcopyrite; the veins are barren outside the ore zone.

Table 1. *Chemical analyses of specimens from the Onaping Formation.*

	ppm								ppb	%
Spec. No.	Cu	Zn	Ni	Co	Pb	Ba	Cr	As	Ag	Au	Fe_2O_3
W1	60	650	65	50	960	614	105	152	0.8	ND	8.0
W13	15	130	ND	130	ND	41	36	3	ND	ND	1.8
W14	50	25	11	45	ND	569	41	1	ND	10	3.0
W19	30	110	60	30	5	652	92	9	ND	10	1.1
W20	15	100	13	20	ND	470	88	13	ND	30	10.0
W24	20	50	13	20	2	254	76	8	ND	ND	9.0
W25	160	35	55	55	ND	158	95	10	ND	ND	7.2
W26A	245	55	80	60	3	175	127	12	ND	ND	12.8
W28	55	200	60	65	25	813	99	21	ND	70	7.7
W29	270	370	65	55	15	141	102	2	0.3	ND	9.3
W30	17	50	60	30	5	749	87	4	ND	ND	7.3
W31	20	65	55	52	10	586	83	15	ND	ND	7.5
W32	45	35	70	37	8	764	102	4	ND	ND	7.7
W33	35	125	60	25	25	466	91	15	0.2	ND	10.0
W42	75	35	70	30	13	622	110	90	0.5	ND	9.2
W43	35	10	70	65	10	496	98	9	ND	ND	8.0
W45	ND	ND	11	200	ND	679	93	49	ND	ND	0.1
W47	85	80	58	60	7	496	96	9	ND	ND	8.3
W51-1	30	10	62	50	ND	674	102	17	ND	ND	7.2
W51-2	265	180	12	121	217	1474	9	27	0.7	ND	4.3
W53	80	65	60	85	17	215	113	0.3	0.3	ND	5.7
W58	85	95	58	45	25	440	92	5	ND	ND	3.3
W63	45	87	55	30	3	725	103	19	ND	ND	6.9
W64	65	155	72	32	15	1040	133	0.1	ND	ND	8.3
W69	325	2.32*	147	100	6250	2839	146	302	4.1	ND	4.9
W73	40	45	70	20	ND	340	69	14.9	-	-	14.4
W74-2	40	30	115	20	ND	550	74	6.1	-	-	11.7
W75-1	92	200	145	50	140	290	103	15.1	-	-	4.3
W75-2	70	48	78	30	30	1040	108	4.9	-	-	8.6
W77	72	270	70	25	ND	920	86	ND	-	-	11.4
W78	60	375	60	25	90	550	83	5.7	-	-	11.7

Notes:
1. Total Fe as Fe_2O_3
2. ND - not detected, dash - not analyzed
3. Location of specimens shown on Figure 1 (W omitted for brevity)
4. Percent *
5. W13, W14 and W75-2 - igneous matrix of basal quartzite breccia

The rocks in the mines are strongly folded and faulted and the structure is complex. The folds are isoclinal, doubly plunging and overturned to the northwest with the axial planes dipping steeply to the southeast. Some of the folds are asymmetrical with a long southeastern limb and a short northwestern limb; the orebodies are located on the southeastern limbs and hinges of the folds. The folds appear to be of the similar type. The carbonate rocks of the Vermilion member probably behaved in a ductile manner and flowed toward the fold hinges; the brittle chert brecciated. The rocks are offset by reverse faults, disposed parallel to the axial planes of the folds, with as much as 150 m dip-slip movement.

Some investigators have stressed that the ore bodies lie in a major fault or shear zone (Burrows and Rickaby 1930, Thomson 1956), implying a relationship between faulting and ore. In general, the rocks of the South Range lack primary layering but possess a tectonic foliation oriented parallel to the faults. Thus it is difficult to recognize faults on the surface except at the southwestern rim of the basin. Deformation in the basin increases in intensity toward the southeast (Rousell 1975). The rocks in the mines are probably no more intensely faulted than are those to the southeast.

Burrows and Rickaby (1930) located five outcrops of ore on a map of the Errington property; only two of these are now exposed. One (locality 82, Figure 1) consists of a lenticular gossan, as much as 2 m wide, enclosed by slate of the Onwatin Formation. Mottled grey and white dolomite, with an average grain diameter of 0.5 mm, comprises approximately 90 percent of the rock together with minor quartz and sulphides. A chemical analysis of specimen W82 (Table 2) indicated a 0.9 percent Zn content. The Vermilion member is well exposed at the northwestern edge of a ridge occupied by the Errington No. 1 shaft. Chert breccia consists of black chip-like fragments of chert, as much as 5 cm in length, set in a matrix of white, very fine-grained quartzite with individual grains approximately 0.05 cm in diameter. This rock is not mineralized (W81, Table 2). A dense, fine-grained siliceous rock is associated with the chert breccia. Most of the exposure consists of a medium to coarse grained, massive dolomitic rock containing abundant sulphides including sphalerite, pyrite, galena and chalcopyrite. Chemical analyses of this material (W81-2, W81-3, Table 2) indicate a high Zn content together with significant Pb, Cu, and As values.

Table 2 includes chemical analyses of a specimen from the Errington No. 3 dump (W68) and the average of four specimens from the Vermilion Mine dump (Arengi 1977). The Zn, Pb, and Cu values indicate that much of the material in these dumps is mineralized.

The Vermilion member is covered by surficial deposits outside the ore zone and the lateral extent of the member can only be traced by drilling. According to Arengi (1977), argillaceous limestone, 1-4 m thick, was encountered in three drill holes in the North Range (northeast of the mafic sill and southwest of Proulx, Figure 1); in the South Range a drill hole (near locality 7, Figure 1) penetrated approximately 30 m of argillaceous limestone and cherty limestone, and two other drill holes, southwest of the above hole and northwest of Errington No. 3 shaft, penetrated 2 m of these rocks. Average metal values for four specimens from the South Range drill holes are given in Table 2 and indicate low metal values.

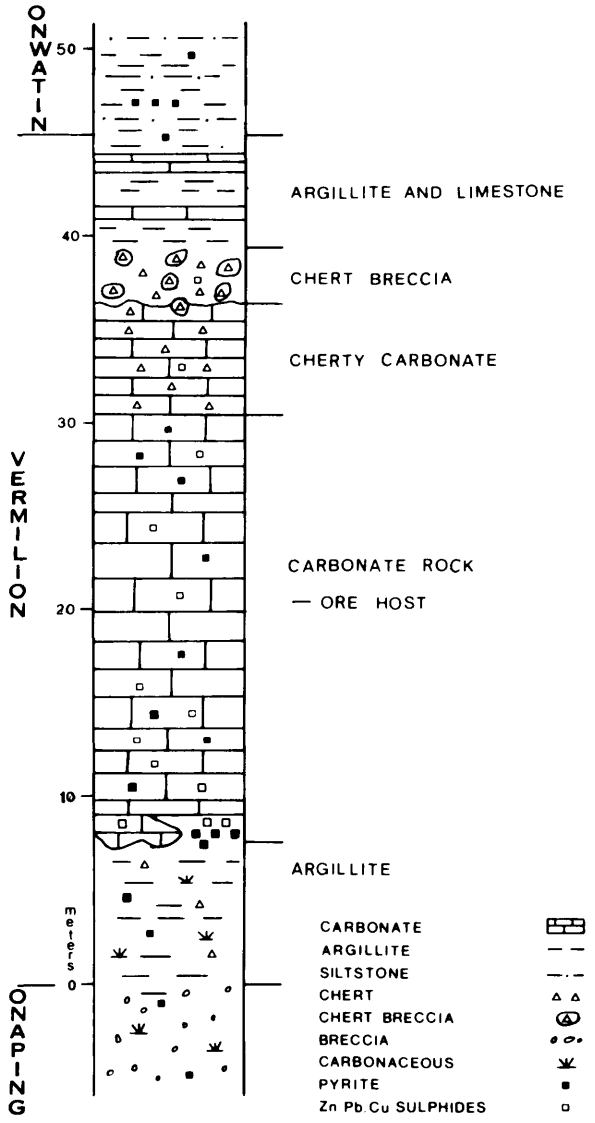

Figure 3. *Stratigraphy and mineralization in the Vermilion member.*

Table 2. *Chemical analyses of specimens from the Vermilion member and average values from published data.*

	ppm									ppb	%
Spec. No.	Cu	Zn	Ni	Co	Pb	Ba	Cr	As	Ag	Au	Fe_2O_3
W68	1300	3.0*	28	14	525	45	26	42	4.1	30	4.0
W81-1	70	45	ND	40	ND	ND	0.6	27	-	-	0.7
W81-2	9000	3.8*	20	60	1.6*	ND	4	7800	-	-	11.7
W81-3	2000	4.1*	100	35	8000	460	30	1100	-	-	31.3
W82	120	9000	10	20	175	25	ND	76.6	-	-	8.6
Vermilion Mine dump[6]	1.03*	3.45*	62	193	1.43*	215	68	-	71	-	-
Vermilion Mbr[7]	34	390	62	30	111	248	70	-	11	-	-
Errington Mine[8]	1.07*	4.31*			1.47*				59.4	594	
Vermilion Mine[8]	8000	3.83*			1.14*				47.6	703	

Notes:
1. Total Fe as Fe_2O_3
2. dash - not analyzed
3. Location of specimens shown on Figure 1 (W omitted for brevity)
4. Percent - *
5. W68 - Errington #3 dump, W81 - outcrop at Errington No. 1 and W82 - outcrop between Errington No. 2 and No. 3
6. Average of 4 samples (Arengi 1977)
7. Average of 4 samples from two DDH's in the central portion of the South Range (Arengi 1977)
8. Average values of ore grade (Thomson 1956)

PYRITE AND BASE METALS IN THE ONWATIN FORMATION

The Onwatin Formation is rich in pyrite. This pyrite occurs as abundant silt-size grains arranged parallel to the bedding plane and as massive stratiform lenses, generally 1 to 3 cm thick, but locally as thick as 20 cm. The presence of pyrite along cleavage planes indicates remobilization. Pyrite cubes, as much as 2 cm in diameter, occur in local masses and are the result of recrystallization. This type of occurrence is common north of Vermilion Lake and many are exposed in trenches and pits.

Chemical data for eleven specimens of the Onwatin Formation are given in Table 3. All specimens, except W23, are from the western portion of the basin as the formation is poorly exposed elsewhere. Apart from modest Zn values in W59, none of the specimens contain an appreciable metal content. Table 4 sets out the average values of the data of Table 3 and the average metal content of shale. In the Onwatin Formation the average values of Co, Ba, As, and Ag are greater, Zn values are somewhat less and Cu, Ni, Pb and Cr values are approximately the same as the average values in shale.

Table 4 gives average values of Sadler's (1958) chemical data for (1) Onaping-Onwatin transition zone and basal Onwatin argillite, and (2) Onwatin Formation, and average values of Arengi's (1977) data for the Onwatin Formation. All these values are higher than the average values of shale particularly Ag. The transition zone – basal argillite grouping of Sadler is very high in Cu, Ni, Co, and Pb; Sadler's data for the Onwatin Formation indicate high Cu and Pb values; and Arengi's data for the

Table 3. *Chemical analyses of specimens from the Onwatin Formation.*

	ppm								ppb	%
Spec. No.	Cu	Zn	Ni	Co	Pb	Ba	Cr	As	Ag	Au	Fe_2O_3
W23	12	50	45	45	6	2619	87	33	0.3	ND	8.3
W34	ND	20	30	ND	7	383	102	12	0.6	ND	2.3
W40	30	40	65	45	15	543	128	3	ND	ND	4.5
W41-2	4	10	50	20	17	337	110	14	0.6	ND	3.4
W48-1	90	75	155	68	8	287	77	34	0.3	ND	4.6
W55-1	50	60	26	51	ND	471	121	2	0.3	ND	3.1
W59	55	1250	100	85	35	4828	120	42	ND	10	9.4
W66	90	25	45	21	5	756	84	10	0.5	ND	2.9
W72	105	55	95	125	120	920	50	162	-	-	11.7
W76-1	58	105	30	15	ND	4200	109	ND	-	-	8.6
W79	45	20	55	75	30	770	46	99	-	-	5.7

Notes: 1. Total Fe as Fe_2O_3

2. ND - not detected, dash - not analyzed

3. Location of specimens shown on Figure 1 (W omitted for brevity)

Onwatin Formation indicate high Cu and Cr values and very high Zn values compared to average values in shale.

The specimens chemically analyzed by Sadler (1958) and Arengi (1977) yielded considerably higher metal values than the specimens of the Onwatin Formation analyzed by the writer. Much of the material of these investigators came from drill holes which apparently intersected relatively mineral-rich zones.

ANTHRAXOLITE VEINS

An anthraxolite vein occurs in the Onwatin Formation in Lot 10, Concession I, Balfour Township. The anthraxolite is a black, dense, platy material and contains considerable pyrite and some quartz. The anthraxolite consists of approximately 95 percent carbon (Burrows and Rickaby 1930). The vein was exposed by an inclined shaft 30 m in length and two smaller inclined shafts. The deposit generated considerable local interest before the turn of the century as it was thought the material could be used as a fuel. However, it proved unsuitable due to the high ash content. Another similar anthraxolite vein occurs in Lot 5, Concession VI, Fairbank Township (see Figure 1, Locality 48).

QUARTZ (CARBONATE) VEINS

In the South Range, sulphide-bearing quartz veins occur at the contact of the Nickel Irruptive and the Onaping Formation (Foisey and Papineau properties) and in the basal felsic breccia of the Onaping Formation (Moore Lake occurrence). Gold-bearing quartz veins are present in the lower part of the Onaping Formation. In the North Range mineralized quartz (carbonate) veins occur in the basal felsic breccia of the Onaping Formation (Proulx property), in shear zones in the Onaping Formation (Lafleur 1981), and in a mafic sill located at the Onwatin-Chelmsford contact. Quartz veins are prominent in the South Range but are relatively scarce in the North Range. Mineralized quartz veins have not been reported in the East Range.

Figure 4 is a stereographic plot of poles to 47 quartz veins, all but four of which are from the South Range. In general, the veins dip steeply and the rose diagram of the strikes indicates two dominant trends, N53°E and N83°E. In the southwestern portion of the South Range the lithologic contacts and the foliation strike approximately N53°E; in the eastern part of the South Range the strike of the contacts and foliation turn (at Foisey property, Figure 1) and strike approximately N83°E. In the former locality quartz veins strike at N53°E and in the latter locality at

Table 4. *Average values of chemical data from the Onaping Formation and the Onwatin Formation and certain common rocks.*

	ppm									ppb	%
	Cu	Zn	Ni	Co	Pb	Ba	Cr	As	Ag	Au	Fe
Onaping[3]	85	955 (129)	48	47	272 (16)	553	80	28	-	-	6.1
Onaping[4]	58	376	106	60	16	-	447	-	10	-	-
Onaping[5]	154	97	118	33	60	-	76	-	7 (<1)	-	-
Onwatin[6]	49	155 (46)	63	50	22	1465	94	37	0.33	-	5.9
Transition[7]	394	163	223	70	70	-	134	-	4	-	-
Onwatin[8]	168	1320 (120)	144	55	62	-	129	-	~2	-	-
Onwatin[9]	230	1917 (695)	133	49	53	778	225	-	10	-	-
Crust[10]	50	70	75	22	12.5	500	100	1.8	0.07	3	5.4
Granite[10]	12	50	0.8	3	20	700	20	1.5	0.04	2	2.7
Intermediate[11]	32.5	66	35	8.5	15	-	36	2.2	0.06	4	-
Basalt[10]	100	100	150	48	3.5	300	200	2	0.1	4	8.6
Ultramafic[11]	15	40	2000	175	0.55	-	1800	0.75	0.055	5.5	-
Shale[10]	50	90	80	20	20	600	100	10	0.1	3	4.7

Notes:
1. Number in ( ), located below the row, is the average obtained by omitting analyses with high values.
2. Dash - not analyzed published or relevant.
3. Average of 28 analyses from Table 1 (W13, W14 and W75-2 omitted). Omissions for ( ) are: Zn - W69 and Pb - W1, W69.
4. Average of 7 analyses from two DDH's located in the central portion of the North Range (Arengi 1977).
5. Average of 7 analyses from four DDH's and three outcrops; 6 analyses from the NE portion of the South Range and 1 from the East Range. Omission for ( ) is: Ag - 42ppm (Sadler 1958).
6. Average of 11 analyses from Table 3. Omission for ( ) is: Zn - W59.
7. Onaping-Onwatin transition zone and basal argillite of Onwatin Fm. Average of 5 analyses from three DDH's located in NE part of South Range (Sadler 1958).
8. Average of 11 analyses from several DDH's and outcrops - North and South Ranges. Omissions for ( ) are: Zn - 5610, 5160, 1480 and 1340ppm (Sadler 1958).
9. Average of 6 analyses from three DDH's - two located as in note 5 and one in the North Range immediately east of locality 35, Figure 1. Omission for ( ) is: Zn - 7420 ppm (Arengi 1977).
10. From Krauskopf (1979).
11. From Krauskopf (1967).

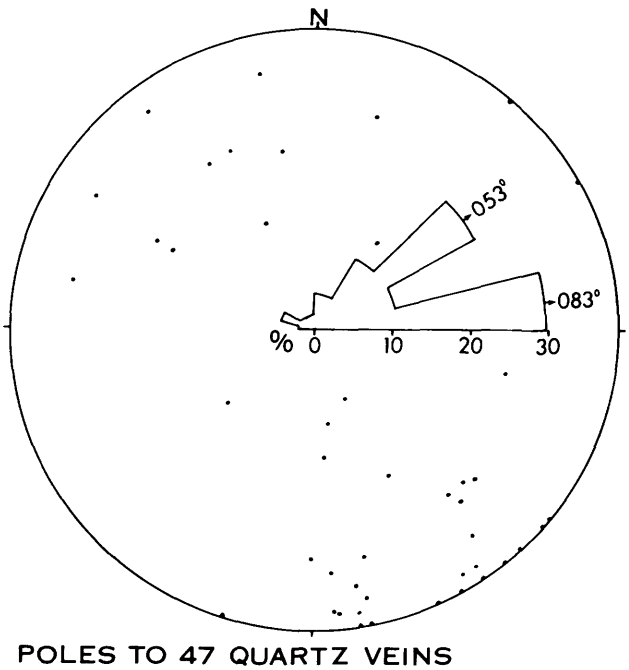

Figure 4. *Lower hemisphere equal-area plot of poles to 47 quartz veins in the Whitewater Group. Rose diagram indicates preferred orientations of the strikes of the veins.*

N83°E. Accordingly, quartz veins in the South Range strike parallel to lithologic contacts and the foliation.

SULPHIDE-BEARING QUARTZ VEINS

The Foisey property is located in Lot 2, Concession III, Rayside Township. There are a number of quartz veins in the vicinity of the property. The best mineralized vein is approximately 1 m in thickness and is within the igneous rock which forms the matrix of the basal felsic breccia of the Onaping Formation. Black sphalerite, together with some galena and chalcopyrite, form local blebs as much as 3 cm across. Polished section examination indicates that sphalerite, galena, and chalcopyrite comprise approximately 90 percent, 9 percent, and 1 percent of the total sulphides, respectively. Sphalerite occurs as masses over 1 cm across, galena occurs as tiny (0.01 mm) inclusions in the sphalerite and as individual grains 0.01 mm in diameter, and chalcopyrite occurs as grains 0.01 mm in diameter within the sphalerite. Chemical analyses of a specimen of the vein (W3-1A, Table 5) indicate high values of Zn and Pb and the presence of minor amounts of Ag and Au. The Co content is also high compared to the average Co content of common rock types (see Table 4). An analysis of the igneous country rock (W3-2, Table 5) indicates the metal content of this rock is low.

The geological setting of the Papineau property (located in Lot 3, Concession V, Blezard Township) is somewhat similar to that of the Foisey property but the sulphide mineralogy is different. Quartz veins and blebs as much as 5 m in thickness are very numerous in this locality, and they occur within an igneous rock (micropegmatite ?) that is below the basal breccia of the Onaping Formation. At the Papineau shaft a 2.5 m wide quartz vein contains massive arsenopyrite and some pyrite. Mauve-coloured carbonate material contains chalcopyrite, malachite and azurite. Polished section examination reveals that over 90 percent of the sulphides consist of arsenopyrite, and less than 10 percent is chalcopyrite. Chemical analyses of two specimens from the vein (W10-A and W10-B, Table 5) indicate relatively high Cu values, moderately high Au and Co values and traces of Ag. Specimen W10-B gave the highest Au value of any specimen analyzed in the present study. A few tens of metres north of the shaft is a trench 65 m long and 3 m wide. Broken vein material contains arsenopyrite and a chemical analysis of this material (W11, Table 5) indicates relatively high Au, Co and Ba values.

The Moore Lake occurrence (Lot 4, Concession V, Creighton Township) consists of several quartz veins, approximately 10 cm in width, within the basal breccia of the Onaping Formation. Galena occurs in masses as much as 5 cm in width together with black sphalerite, pyrite and minor chalcopyrite. The presence of these minerals was confirmed by polished section examination. A chemical analysis of a specimen from the vein (W52-2, Table 5) shows high Pb and Zn values and the highest Ag value of any chemically analyzed specimen in the study. The country rock contains considerable pyrite but a chemical analysis (W52-1, Table 5) indicates low metal values.

The Proulx property is located in the North Range (Lot 3, Concession I, Bowell Township) and on the south shore of Nelson Lake (formerly Trout Lake). Burrows and Rickaby (1930) briefly described the occurrence. A shaft was sunk to a depth of at least 20 m and two quartz veins 1.5 and 2.4 m in thickness contain appreciable amounts of sphalerite, galena and chalcopyrite. The country rock is the basal felsic breccia of the Onaping Formation. At present there is no trace on the surface of the shaft or of quartz veins.

Lafleur (1981) reported the presence of north-northwesterly trending shear zones in the Onaping Formation in Dowling Township. Some shears extend more than 20 m along strike and contain galena, sphalerite, chalcopyrite and pyrite. Chemical analyses of five samples from one set of veinlets (near locality 42, Figure 1) contained as much as 8.88 percent Zn, 11.8 percent Pb and 0.42 percent Cu (Lafleur 1981).

GOLD-BEARING QUARTZ VEINS

The Gordon Lake and Creighton "gold mines", apparently abandoned around the turn of the century, occur in the southwestern portion of the basin (see Figure 1). Both were briefly described by Blue (1893).

The Gordon Lake Mine is located in Lot 2, Concession IV, Fairbank Township; a prominent outcrop of quartz-rich rock on the west side of the Gordon Lake

Road is presumably the site of the "mine". The quartz-rich rock is penetrated by a 10 m long adit and there is a 22 m long trench. The rock is pale pink, medium grained, and contains numerous quartz veins and blebs as much as 30 cm wide. The quartz-rich unit is approximately 12 m in thickness, dips steeply to the southeast, and is internally folded. In thin sections the pink quartz rock consists of strained quartz grains, together with some plagioclase grains, in a fine grained mosaic of recrystallized quartz. Locally the quartz is highly fractured. Pyrite and limonite are abundant. A light green rock consisting of carbonate, quartz, and chlorite occurs beneath the quartz-rich unit. The writer tentatively interprets the quartz rock as a quartzite fragment from the basal breccia of the Onaping Formation that has been emplaced in its present position in the Onaping Formation by faulting. Chemical analysis of three specimens from the property (W44-1, W44-2, W44-3, Table 5) indicate no Au nor significant amounts of any other metal.

The Creighton Mine is located in Lot 11, Concession V, Creighton Township. During the time of operation gold

Table 5. *Chemical analyses of specimens from quartz veins and host rocks*

	ppm								ppb	%
Spec. No.	Cu	Zn	Ni	Co	Pb	Ba	Cr	As	Ag	Au	Fe_2O_3
W3-1A	160	8.5*	22	200	6750	464	59	1400	7.6	60	4.6
W3-2	10	130	25	80	45	637	34	22	ND	NN	2.7
W7-1	15	85	27	30	10	1628	91	4	0.2	ND	4.9
W10-A	5000	0.5	6	160	25	77	18	1.3*	1.7	869	2.5
W10-B	3000	0.8	40	580	80	125	29	10.1*	3.4	2400	17.9
W-11	150	ND	10	305	3	1477	4	45	0.4	820	3.8
W35-1	55	165	22	70	115	440	25	38	1.4	ND	8.9
W36-1	60	10	40	230	ND	46	31	18.6*	7.3	1610	35.8
W37	1.0*	2500	40	280	420	1	17	ND	1.5	ND	0.9
W39-1	3	5	10	165	ND	6	16	4400	ND	10	3.2
W39-2	2	55	50	37	5	341	22	109	0.6	30	5.9
W44-1	ND	25	15	87	310	221	17	ND	0.7	ND	0.06
W44-2	ND	ND	32	155	ND	21	12	35	ND	ND	0.9
W44-3	2	5	55	45	2	739	131	10	ND	ND	6.1
W46	30	75	31	40	ND	395	66	15	ND	ND	2.1
W52-1	45	50	25	200	15	83	52	900	ND	ND	2.7
W52-2	50	1.93*	56	160	2.73*	70	37	4.5*	264	ND	6.3
W60	20	150	132	120	10	1546	492	82	ND	ND	1.9
W61-1	160	10	36	62	15	213	96	10	ND	ND	7.7
W61-2	5	3	22	215	ND	59	15	1	ND	ND	0.01
W61-3	40	7	38	133	11	662	18	24	ND	ND	3.3
W61-4	40	95	54	68	15	19	9	ND	ND	ND	9.3
W65	135	50	25	40	ND	62	10	28	0.7	ND	6.4

Notes:
1. Total Fe as Fe_2O_3
2. ND - not detected
3. Locations of specimens shown on Figure 1 (W omitted for brevity)
4. Percent - *
5. Quartz veins: W3-1A - Foisey; W10-A, W10-B, W11 - Papineau; W36-1, W37, W39-1, W65 - in mafic sill; W44-1, W44-2 - Gordon Lake; W52-2 - Moore Lake; and W60, 61-2, 61-3, 61-4 - Creighton
6. Host rocks: W3-2 - micropegmatite; W7-1 - acid dike; W35-1, W39-2 - mafic sill; W44-3 - schist; W46 - mafic dyke; and W52-1, W61-1 - Onaping Formation.

values* were apparently between $4 and $20 per ton of ore (Blue 1893). An abandoned shaft (surface dimensions 5.5 m by 3 m) is located on the property and there is a large dump. Quartz vein material extends over a width of 12 m with as much as 4 m of continuous exposure. The vein is exposed for 100 m along strike until it disappears into a swamp. The country rock, the Onaping breccia, contains some disseminated sulphides and the quartz veins contain some pyrite and limonite. Table 5 gives a chemical analysis of the country rock (W61-1) and analyses of three specimens of the quartz veins (W61-2, W61-3, and W61-4). No Au was detected and the values of the other metals are low. Similar results were obtained from a specimen from a quartz vein near the Creighton Mine (W60).

SULPHIDE-BEARING QUARTZ-CARBONATE VEINS IN A MAFIC SILL

A mafic sill as much as 30 m in thickness, and exposed at three localities over a length of 4 km, occurs at the Onwatin Formation-Chelmsford Formation contact. The sill is located in Balfour Township in the North Range. The rocks are strongly altered but primary pyroxene is locally preserved. The sill is the locus of mineralized quartz-carbonate veins and these have been explored by numerous pits and trenches. The veins are as thick as 1.7 m and are irregular, and vein material is commonly intimately mixed with the mafic rocks. The carbonate is buff-coloured, weathers to a chocolate brown, and is probably ankerite or siderite. Pyrite, commonly in the form of cubes, locally weathers to limonite and hematite. Arsenopyrite is a prominent mineral, occurs in local masses a few centimetres across, and as narrow veinlets in quartz and in the mafic rock. Chalcopyrite is locally present and weathers to malachite.

Table 5 sets out chemical analyses of two specimens of the mafic rock and four specimens of quartz-carbonate veins. Both specimens of the mafic rock (W35-1, W39-2) contain disseminated pyrite but neither have significant metal values; W39-2 contains traces of Au. Specimen W36-1 is from a vein with massive arsenopyrite and has a high As content and contains appreciable Au and some Ag. Specimen W37 is from a vein with visible chalcopyrite and displays high Cu and Zn values and a modest Pb content. Specimens W39-1 and W65 apparently represent material from barren veins although W39-1 has a moderately high As content.

ORIGIN OF MINERALIZATION

Previous investigators of the mineralization in the Whitewater Group assumed that the basin was formed by volcanism, and they related the mineralization to this process. These early ideas are reviewed here and, in addition, the mineralization is considered in terms of the meteorite impact theory of basin origin.

*In 1893 the price of gold was $20 per ounce.

SULPHIDES IN THE ONAPING FORMATION

According to Sangster and Scott (1976) sulphide fragments are not uncommon in felsic pyroclastic rocks associated with Precambrian massive sulphide deposits. These fragments may form by several processes including brecciation of original sulphide layers by slumping or later volcanic explosions, or brecciation by explosion of sulphides in volcanic pipes. Sulphides in the Onaping Formation consist mainly of pyrrhotite fragments and the formation is considered by some (e.g. Stevenson 1972) to represent a felsic pyroclastic rock. Accordingly, sulphide-rich material must have been present prior to brecciation and incorporation into the unit.

Pattison (1979) proposed that the Ni-Cu ore of the basin originated as a result of meteorite impact. In brief, a transient crater penetrated as deep as the upper mantle where sulphide-rich pods were presumably present. The sulphides, together with silicate rocks formed an impact melt that travelled up the crater wall; the sulphides separated from the melt due to density differences and produced the ore bodies. Some of the sulphide material of the pods may have been brecciated and incorporated into the fall-back breccia (Onaping Formation) to form the pyrrhotite fragments. Metasedimentary and tuffaceous rocks of the Elsie Mountain and Stobie Formations (Huronian Supergroup), exposed to the south of the basin, locally contain as much as 10 percent sulphide, mainly pyrrhotite and some pyrite and chalcopyrite (Innes 1972). These formations may have been "target" rocks for meteorite impact and some of the sulphide material may have become part of the fall-back breccia. The genetic connection between the pyrrhotite in the Onaping Formation and that in the Ni-Cu ores, the Nickel Irruptive and the Huronian rocks remains unresolved. Some of the sulphides in the Onaping Formation, particularly the sphalerite and galena, may be related to the Vermilion-Errington deposits.

VERMILION-ERRINGTON DEPOSITS AND MINERALIZATION IN THE ONWATIN FORMATION

The Vermilion-Errington deposits were originally thought to lie in a major shear zone and to represent irregular pods scattered thoughout masses of quartz-carbonate rock. The mineralization was interpreted in terms of the classical hydrothermal concept, that is, the sulphides were supposedly derived from mineral-bearing solutions emanating from the Sudbury Nickel Irruptive and at lower temperatures than the Ni-Cu ores, also derived from the irruptive (Burrows and Rickaby 1930).

Further studies, after the reopening of the mines in 1952, led to the realization that the deposits were stratigraphically and structurally controlled. The ore occurs mainly on the south limb of folds that are the site of thrust faults. "Maximum dragging and brecciation of the Vermilion formation occurs in such locations, and the best structural conditions to catch mineralization of epigenetic origin" (Martin 1957, p. 368). Martin (1957) further stated

that some or most of the chert, carbonate and pyrite may have been the result of hot-spring activity during the last phase of Onaping volcanism. Thomson (1956) suggested that the host rocks may have been sedimentary in origin, that the chert breccia might have been the result of slumping or later deformation, and that these brecciated units would have been amenable to mineralization.

Card and Hutchinson (1972) elaborated on these earlier concepts and considered the deposits in terms of regional volcanic-tectonic cycles. The Onaping Formation was regarded as a product of explosive volcanism during a second cycle. During the later phases of this cycle two metal- and sulphur-rich phases supposedly formed: a melt which differentiated at depth to form the Nickel Irruptive and the Ni-Cu ores outside the basin, and a volatile phase which escaped to the surface to form the Vermilion-Errington deposits inside the basin.

Arengi (1977) suggested that the deposition of the Onaping Formation (fall-back breccia) resulted in a flat crater floor. Disruption of the floor, possibly due to the emplacement of the Sudbury Nickel Irruptive, gave rise to local highs on which carbonate banks developed (Vermilion member); basal argillites and siltstones of the Onwatin Formation were deposited between the banks.

Sangster (1970) divided Canadian stratabound Pb-Zn deposits into two types: the Mississippi Valley type and the Remac type (after the Reeves-MacDonald Mine, in the Kootenay Arc structural province of B.C.). The second type was later referred to as Alpine type (Sangster and Scott 1976). The former deposits occur in relatively undeformed platform carbonates and are located between or at the margins of basins. The ores are younger than the host carbonate and were emplaced in permeable zones formed by processes such as brecciation, fracturing and dolomitization. The rocks of the Remac deposit are highly deformed; the ore is fine- to medium-grained and banded, and the carbonate host is composed of alternating light bands and dark graphite-bearing bands of dolomite. In general, the stratigraphic succession for Kootenay Arc Pb-Zn deposits, from bottom to top, is: quartzite, thin-bedded limestone and dolomite, local chert, and black carbonaceous shales (see Høy 1982). The succession suggests that the rocks were deposited in the centre of a basin and in a deep-water euxinic environment rich in H_2S; metal-bearing solutions precipitated sulphides in the form of a layer on the seafloor and syngenetic with the host rocks (Sangster 1970).

The stratigraphic succession associated with the Vermilion-Errington deposits, namely basal argillite, banded carbonate with mineral layers and bitumen, chert and black carbonaceous pyritic shale (Onwatin Formation) suggests these deposits may be of the Remac type. The basal argillite, interpreted by Martin (1957) to be a volcanic mud leached by hot acids, may represent an alteration halo. The Vermilion-Errington deposits may be sedimentary-exhalative deposits (Carne and Cathro 1982) and the "volatile phase" of Card and Hutchinson (1972) might actually be metal-rich brines. Moreover, the process could have been triggered by meteorite impact. The impact site might have been a shallow sea; seawater penetrated to the bottom of the deep transient crater and became trapped by the fall-back breccia. The crater then filled with seawater and the outer rim gave rise to a closed basin much larger than the present remnant basin. Abundant carbonaceous material suggests bottom waters were stagnant and anoxygenic. The trapped brines incorporated base metals and rose upward, deposited minor quantities of Pb and Zn as they passed through the Onaping Formation, and, on reaching the basin floor, precipitated the Vermilion member around local vents. Some metals were apparently precipitated in between the vents in the basal argillites and siltstones of the Onwatin Formation. Reducing conditions apparently prevailed throughout the deposition of the upper Onwatin Formation but pyrite was the only sulphide precipitated.

Later tectono-metamorphism folded and faulted the Vermilion-Errington deposits, remobilized some of the sulphides and locally remobilized and concentrated organic material to form the anthraxolite veins.

QUARTZ (CARBONATE) VEINS

Rocks of the Onaping Formation in the South Range are characterized by a tectonic foliation and numerous quartz veins whereas those of the North Range are undeformed and quartz veins are scarce. The strike of the quartz veins in the South Range is parallel to the strike of the tectonic foliation and the veins are not geometrically related to a prominent northwesterly trending joint set (Rousell and Everitt 1981). Accordingly, the veins were likely emplaced during the major deformation of the basin (approximately 1.7 Ga) rather than during a later episode of brittle deformation.

The exact time of emplacement of the mineralized mafic sill and the enclosed quartz-carbonate veins is not known. A similar mafic sill occurs in the Onwatin Formation south of the Chelmsford outcrop belt. Cleavage in the Onwatin Formation passes into sill rocks suggesting the sill was emplaced before or during basin deformation.

ACKNOWLEDGMENTS

D.G. Innes, consulting geologist, drew my attention to several mineral occurrences. Field and laboratory assistance was provided by Willard Desjardins, Lorraine Dupuis, O.O. Kehinde-Phillips, Edward Ludwig and Violet Smith, all of Laurentian University. Susan Cunningham typed the manuscript.

REFERENCES

Arengi, J.T.
1977: Sedimentary Evolution of the Sudbury Basin; unpublished M.Sc. thesis, University of Toronto, 141p.

Blue, A.
1893: The Creighton Gold Mine; Third Annual Report of the Ontario Bureau of Mines, p. 45-47.

Brocum, S.J. and Dalziel W.D.
1974: The Sudbury Basin, the Southern Province, and the Penokean Orogeny; Geological Society of America Bulletin, Vol. 85, p. 1571-1580.
Burrows, A.G. and Rickaby, H.C.
1930: Sudbury Basin Area; Ontario Department of Mines, Vol. 38, Part 3, 55p.
Card, K.D. and Hutchinson, R.W.
1972: The Sudbury Structure: Its Regional Geological Setting; p. 67-78 in New Developments in Sudbury Geology, J.V. Guy-Bray, editor, Geological Association of Canada, Special Paper 10.
Carne, R.C. and Cathro, R.J.
1982: Sedimentary Exhalative (sedex) Zinc-Lead-Silver Deposits, Northern Canadian Cordillera; The Canadian Mining and Metallurgical Bulletin, Vol. 75, p. 66-78.
Desborough, G.A. and Larson, R.R.
1970: Nickel-Bearing Iron Sulphides in the Onaping Formation, Sudbury Basin, Ontario; Economic Geology, Vol. 65, p. 728-730.
Dietz, R.S.
1962: Sudbury Structure as an Astrobleme; Abstract, Transactions of the American Geophysical Union, Vol. 42, p. 445-446.
Duke, J.M. and Naldrett, A.J.
1976: Sulphide Mineralogy of the Main Irruptive, Sudbury, Ontario; Canadian Mineralogist, Vol. 14, Part 4, p. 450-461.
Gibbins, W.A. and McNutt, R.H.
1975a: The Age of the Sudbury Nickel Irruptive and the Murray Granite; Canadian Journal of Earth Sciences, Vol. 12, p. 1970-1989.
1975b: Rubidium-Strontium Mineral Ages and Polymetamorphism at Sudbury, Ontario; Canadian Journal of Earth Sciences, Vol. 12, p. 1990-2003.
GSC
1960: Aeromagnetic Map 706G; Geological Survey of Canada
Hawley, J.E.
1962: The Sudbury Ores: their Mineralogy and Origin; The Canadian Mineralogist, Vol. 7, Part 1, 207p.
Høy, Tygve
1982: Stratigraphic and Structural Setting of the Stratabound Lead-Zinc Deposits in Southeastern B.C.; The Canadian Mining and Metallurgical Bulletin, Vol. 75, p. 114-134.
Innes, D.G.
1972: Proterozoic Volcanism and Associated Sulphide-bearing Metasediments in the Sudbury Area, Ontario; unpublished B.Sc. thesis, Laurential University, 87p.
Krauskopf, K.B.
1967: Source Rocks for Metal-Bearing Fluids; p. 1-33 in Geochemistry of Hydrothermal Ore Deposits, H.L. Barnes, editor, Holt, Rinehart and Winston, 670p.
1979: Introduction to Geochemistry; McGraw-Hill, 617p.
Lafleur, Jean
1981: Cascaden, Dowling and Trill Townships, District of Sudbury; p. 80-83 in Summary of Field Work, 1981 by the Ontario Geological Survey, edited by John Wood, O.L. White, R.B. Barlow and A.C. Colvine, Ontario Geological Survey, Miscellaneous Paper 100, 255p.
Martin, W.G.
1957: Errington and Vermilion Lake Mines; p. 363-376 in Structural Geology of Canadian Ore Deposits, Vol. 2, 6th Commonwealth Mining and Metallurgical Congress.
Muir, T.L.
1980: Morgan Lake - Nelson Lake Area; p. 79-82 in Summary of Field Work, 1980, by the Ontario Geological Survey, edited by V.G. Milne, O.L. White, R.B. Barlow, J.A. Robertson and A.C. Colvine, Ontario Geological Survey Miscellaneous Paper 96, 201p.
Naldrett, A.J., Hewins, R.H. and Greenman, L.
1972: The Main Irruptive and Sub-Layer at Sudbury, Ontario; Prceedings of the 24th International Geological Congress, Vol. 4, p. 206-213.
Pattison, E.F.
1979: The Sudbury Sublayer; Canadian Mineralogist, Vol. 17, p. 257-274.
Peredery, W.V.
1972: Chemistry of Fluidal Glasses and Melt Bodies in the Onaping Formation, p. 49-59 in New Developments in Sudbury Geology, J.V. Guy-Bray, editor, Geological Association of Canada, Special Paper 10.
Peredery, W.V. and Naldrett, A.J.
1975: Petrology of the Upper Irruptive Rocks, Sudbury, Ontario; Economic Geology, Vol. 70, p. 164-175.
Rousell, D.H.
1972: The Chelmsford Formation of the Sudbury Basin - a Precambrian Turbidite; p. 79-91 in New Developments in Sudbury Geology, J.V. Guy-Bray, editor, Geological Association of Canada, Special Paper 10.
1975: The Origin of Foliation and Lineation in the Onaping Formation and the Deformation of the Sudbury Basin; Canadian Journal of Earth Sciences, Vol. 12, p. 1379-1395.
1981: Sudbury and the Meteorite Theory; Geoscience Canada, Vol. 8, p. 167-169.
Rousell, D.H. and Everitt, R.A.
1981: Jointing in the Sudbury Basin, Ontario; p. 381-391 in Proceedings of the Third International Conference on Basement Tectonics, D.W. O'Leary and J.L. Earle, editors. Basement Tectonics Committee, Incorporated, Denver, Colorado.
Sadler, J.F.
1958: A Detailed Study of the Onwatin Formation; unpublished M.Sc. thesis, Queen's University, Kingston, 184p.
Sangster, D.F.
1970: Metallogenesis of some Canadian Lead-Zinc Deposits in Carbonate Rocks; Proceedings of the Geological Association of Canada, Vol. 22, p. 27-36.
Sangster, D.F. and Scott, S.D.
1976: Precambrian, Strata-Bound, Massive Cu-Zn-Pb Sulphide Ores of North America; p. 129-222 in Handbook of Stratabound and Stratiform Ore Deposits, Vol. 6, K.H. Wolf, editor, Elsevier Scientific Publishing Company, 585p.
Souch, B.E., Podolsky, T. and Geological Staff
1969: The Sulphide Ores of Sudbury: their Particular Relationship to a Distinctive Inclusion-Bearing Facies of the Nickel Irruptive; p. 252-261 in Magmatic Ore Deposits, H.D.B. Wilson, editor, Economic Geology Monograph 4.
Stevenson, J.S.
1960: Origin of Quartzite at the Base of the Whitewater Series, Sudbury Basin, Ontario; International Geological Congress, Report of 21st Session Norden, Part 26, p. 32-41.
1961: Recognition of the Quartzite Breccia in the Whitewater Series, Sudbury Basin; Transactions of the Royal Society of Canada, 3rd series, Vol. 55,p. 57-66.
1963: The Upper Contact Phase of the Sudbury Micropegmatite; Canadian Mineralogist, Vol. 7, p. 413-419.
1972: The Onaping Ash-Flow Sheet, Sudbury, Ontario, p. 41-48 in New Developments in Sudbury Geology, J.V. Guy-Bray, editor. Geological Association of Canada, Special Paper 10.
Stevenson, J.S. and Stevenson, L.S.
1980: Sudbury, Ontario, and the Meteorite Theory; Geoscience Canada, Vol. 7, p. 103-108.
Thomson, J.E.
1956: Geology of the Sudbury Basin; Ontario Department of Mines, Vol. 65, Part 3, p. 1-56.

Grant 56 Geochemistry and Field Relations of Lode Gold Deposits in Felsic Igneous Intrusions

P.A. Studemeister, R. Kerrich, and W.S. Fyfe
Department of Geology, University of Western Ontario

ABSTRACT

At Gutcher Lake, 30 km north of Wawa, Ontario, a stock of trondhjemite intrudes a succession of Archean rocks which are metamorphosed to the greenschist facies. The stock is 4 km^2 in area, and is partly enveloped by an aureole of epidote-hornblende hornfels up to 1 km wide. Within the contact aureole, chlorite is pseudomorphic after biotite; chlorite + calcite + quartz are pseudomorphic after hornblende + epidote; iron content in epidote decreases from core to rim; serrated hornblende has rims of actinolite; and albite varies in composition from An_0 to An_7. Within the stock, chlorite is pseudomorphic after biotite, and feldspar is mottled with white mica + quartz + calcite and has clear rims of albite. Fractures filled with quartz, ankerite, calcite, chlorite, and muscovite cross-cut the stock and its contact aureole. Retrogressive metamorphism of hornfels and trondhjemite near gold-bearing veins which transect the margin of the stock added Si, Fe, K, H_2O + CO_2, S, Rb, and Au; leached Na, and shifted (Fe^{+2}/Fe_t) from 0.7 to 0.9.

Initial contact metamorphism of volcanic rocks at T = 450°C to 550°C and P < 2 Kbar culminated in an aureole of epidote-hornblende hornfels. Subsequent regional metamorphism at T = 325°C to 450°C and P = 2 to 3 Kbar overprinted a lower greenschist assemblage on the stock and its aureole. The retrogression of hornfels and trondhjemite by metamorphogenic fluids triggered the precipitation of native gold, pyrite, and quartz along fractures.

INTRODUCTION

The purpose of this study is to elucidate the relationship between metamorphism and formation of gold-bearing veins near a stock at Gutcher Lake, near Wawa, Ontario. The Gutcher Lake stock is a trondhjemite body with a partly enveloping aureole of epidote-hornblende hornfels. The stock intrudes Archean rocks of the Wawa "greenstone" belt in the Canadian Shield, 200 km north of Sault Ste. Marie in Ontario (Figure 1). Concentrations of chalcopyrite and native gold occur in sulphide stringers and veins in layered rocks juxtaposed against the north margin, or stratigraphic top, of the stock (Studemeister and Colvine 1978). Native gold is also disseminated with minor sulphide minerals in quartz-carbonate veins cross-cutting the stock and its contact aureole.

The only past producer in the study area is Amherst Mines Limited, which produced 76 kg of gold prior to 1940 from an auriferous quartz-ankerite vein transecting the east margin of the stock (Bruce 1940). Similar but undeveloped gold-bearing veins outcrop near the south margin of the intrusion; Ego Mines Limited reported that sections of veins assay at least 6.86 g/t gold (Northern Miner 1974). Ego Mines Limited reported 348 000 tonnes averaging 1.60 percent copper and 3.77 g/t gold (Northern Miner 1979) for a cluster of stratiform and vein base metal concentrations in layered rocks adjacent to the north margin.

METAMORPHIC ZONES

The Archean succession around the Gutcher Lake stock consists of steeply dipping metavolcanics and metasediments (Figure 2). This succession is divided into two metamorphic zones based on the distribution of biotite and hornblende. The biotite zone has a clear spatial association with the Gutcher Lake stock and is a contact aureole. This zone has hornfelsic to schistose textured rocks with essential amphibole, epidote, quartz, albite, biotite, chlorite, and magnetite.

The chlorite zone surrounds the biotite zone and is developed on a regional scale, extending outside the study area. This metamorphic zone consists of schistose rocks with essential chlorite, actinolite, calcite, epidote, quartz, albite, and muscovite. The biotite-hornblende isograd is within 1 km of the margin of the Gutcher Lake stock. The ensuing discussion of petrology is based mainly on investigation of mafic metavolcanics, the most common rock type in both metamorphic zones.

CHLORITE ZONE

MINERAL PARAGENESIS

The essential minerals in mafic metavolcanics of the chlorite zone are ferruginous prochlorite with 15 to 30 percent FeO_t; light green actinolite with less than 3 percent Al_2O_3; pistacite epidote with 9 to 15 percent Fe_2O_3; albite with less than 2 percent molecular anorthite; calcite; and quartz (Tables 1 and 2). The mica mineral in felsic metavolcanics and tuffaceous metasediments is phengitic muscovite, and less commonly paragonite. Accessory minerals in the "greenstone" succession of the

chlorite zone include ankerite, pyrite, magnetite, sphene, chloritoid, apatite, and schorlite tourmaline.

The mineral assemblage prevailing in mafic metavolcanics of the chlorite zone is regarded as an equilibrium assemblage because minerals are intimately intergrown, have uniform compositions, and are aligned parallel to the regional schistosity. There are no replacement textures, reaction rims around minerals, or compositional zoning other than epidote in which iron content increases from core to rim.

REGIONAL METAMORPHISM

The major calcium-bearing minerals coexisting with chlorite in mafic metavolcanics of the chlorite zone are calcite, actinolite, and epidote. Most rocks have essential yet variable quantities of all three minerals. Hence, the mineral assemblage that developed in mafic volcanic rocks during regional metamorphism was governed by the following reaction:

$$5\,(Mg,Fe)_9Al_6Si_5O_{20}(OH)_{16} + 38\,CaCO_3 + 77\,SiO_2 \rightleftarrows 9\,Ca_2(Mg,Fe)_5Si_8O_{22}(OH)_2 + 10\,Ca_2Al_3Si_3O_{12}(OH) + 26\,H_2O + 38\,CO_2 \quad (1)$$

(Chlorite + Calcite + Quartz ⇄ Actinolite + Epidote + Fluid)

Pure albite, low alumina actinolite, ferruginous chlorite, phengitic muscovite, and calcite are typical minerals of the chlorite subfacies of the greenschist facies the world over (Turner 1981; Myashiro 1973). Temperatures prevailing in the chlorite zone during regional metamorphism are 325°C to 450°C, with reference to the stability fields of these minerals at P = 2 to 3 Kbar (Turner 1980; Liou *et al.* 1974; Schiffman and Liou 1980).

The lithostatic pressure prevailing during regional greenschist metamorphism is estimated with the sphalerite geobarometer applied on sphalerite-chalcopyrite-pyrrhotite-pyrite assemblages in the "greenstone" succession near the Gutcher Lake stock. Experimental studies by Scott (1973; 1976) and Hutchinson and Scott (1981) reveal that the FeS content in sphalerite varies regularly with pressure when the FeS activity is buffered

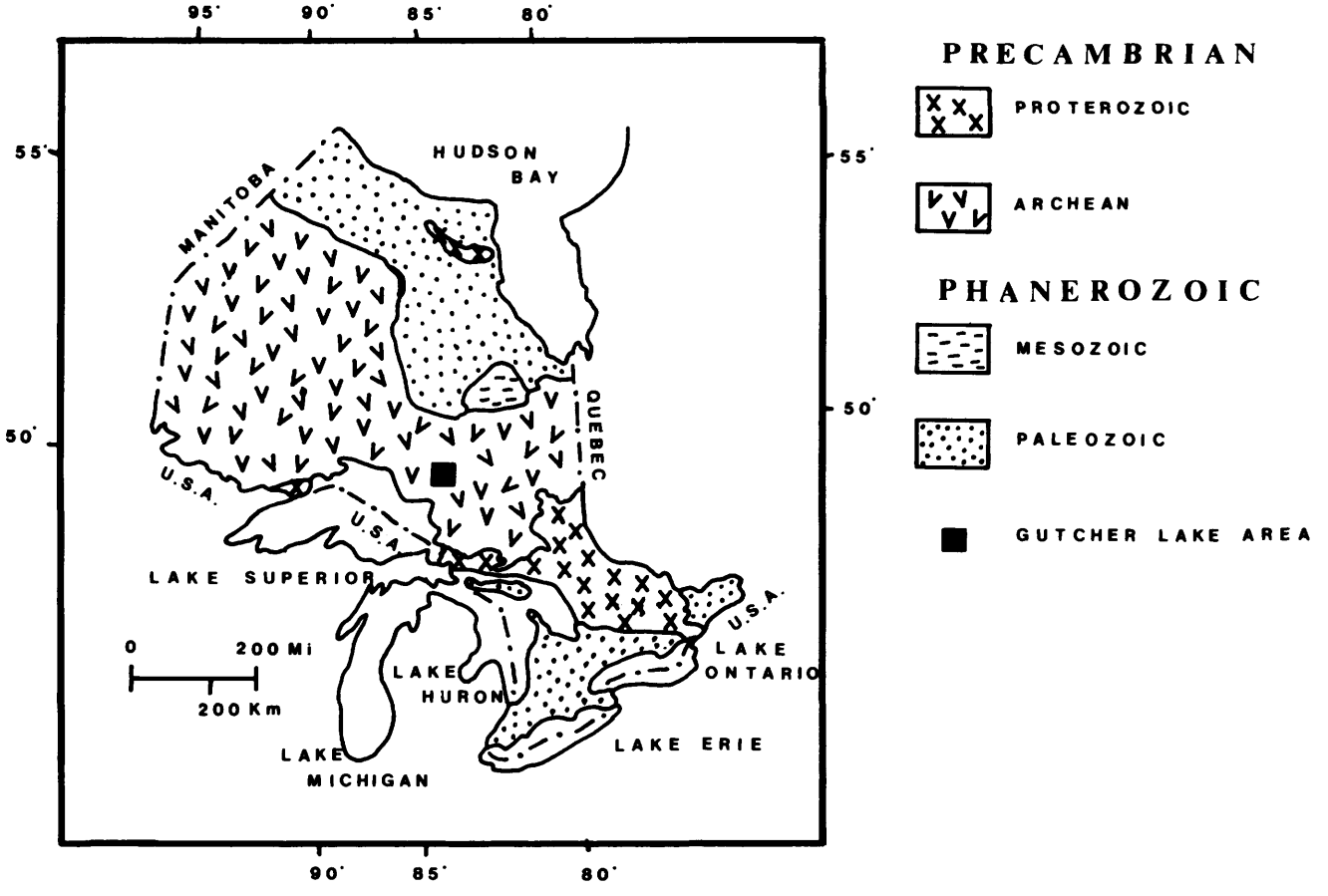

Figure 1. *Location of the Gutcher Lake area.*

Table 1. *Electron microprobe analyses of chlorite and amphibole in mafic metavolcanics of the chlorite zone.*

	CHLORITE				ACTINOLITE			
(wt%)	1A	1B	2A	3A	1A	1B	3A	3B
SiO_2	25.63	25.63	27.81	27.05	53.59	54.01	55.44	54.92
TiO_2	0.00	0.00	0.00	0.00	0.00	0.04	0.00	0.00
Al_2O_3	20.36	20.08	20.41	20.04	0.93	1.53	1.22	1.19
Cr_2O_3	0.01	0.08	0.00	0.00	0.07	0.00	0.20	0.03
FeO_t	28.48	26.74	18.59	23.68	15.89	15.21	13.82	13.18
MnO	0.36	0.31	0.00	0.36	0.36	0.29	0.16	0.38
MgO	13.75	13.84	20.77	17.09	13.46	14.09	14.55	15.83
CaO	0.13	0.12	0.02	0.06	12.77	12.19	13.18	12.61
Na_2O	0.00	0.00	0.00	0.00	0.00	0.13	0.00	0.14
K_2O	0.02	0.00	0.00	0.00	0.04	0.00	0.02	0.03
Cl	0.01	0.07	0.00	0.00	0.04	0.00	0.00	0.00
TOTAL:	88.85	86.87	87.60	88.28	97.15	97.49	98.59	98.31
			CHEMICAL	FORMULA				
Si	5.435	5.510	5.633	5.603	7.887	7.865	7.930	7.866
Al	2.565	2.490	2.367	2.397	0.113	0.135	0.070	0.134
Al	2.523	2.597	2.505	2.494	0.049	0.128	0.136	0.067
Ti	0.000	0.000	0.000	0.000	0.000	0.004	0.000	0.000
Mg	4.346	4.435	6.217	5.276	2.953	3.058	3.102	3.379
Fe	5.051	4.808	3.149	4.102	1.956	1.852	1.653	1.579
Mn	0.065	0.056	0.000	0.063	0.045	0.036	0.019	0.046
Cr	0.002	0.014	0.000	0.000	0.008	0.000	0.023	0.003
Na	0.000	0.000	0.000	0.000	0.000	0.037	0.000	0.039
Ca	0.030	0.028	0.004	0.013	2.014	1.902	2.020	1.935
K	0.005	0.000	0.000	0.008	0.008	0.000	0.004	0.005
O	28	28	28	28	23	23	23	23

FeO_t : Total iron is reported as FeO.

O : Number of oxygen ions used to calculate chemical formulas from anhydrous microprobe analyses.

Specimen 1: E-42-4A; 2: EW-33-6; 3: E-35-6.

Table 2. *Electron microprobe analyses of epidote and albite in metavolcanics of the chlorite zone.*

	EPIDOTE				ALBITE			
(wt%)	1Core	1Rim	2Core	2Rim	1A	1B	4A	5A
SiO_2	38.65	38.75	38.43	38.57	69.09	68.45	68.98	68.65
TiO_2	0.10	0.00	0.05	0.00				
Al_2O_3	25.06	24.56	26.34	25.80	19.35	19.44	19.22	19.57
Cr_2O_3	0.00	0.03	0.00	0.05				
Fe_2O_3	9.81	10.01	7.68	8.21				
MnO	0.13	0.13	0.00	0.00				
MgO	0.00	0.08	0.05	0.00				
CaO	23.14	24.22	26.22	25.71	0.19	0.29	0.25	0.21
Na_2O	0.00	0.00	0.00	0.00	11.76	11.59	11.50	11.66
K_2O	0.00	0.02	0.00	0.00	0.06	0.04	0.08	0.03
Cl	0.00	0.00	0.00	0.00				
TOTAL:	96.89	97.80	98.77	98.34	100.45	99.81	100.03	100.12
				CHEMICAL	FORMULA			
Si	6.126	6.114	5.993	6.040	12.013	11.980	12.035	11.975
Al	0.000	0.000	0.008	0.000	3.965	4.009	3.951	4.023
Al	4.680	4.566	4.831	4.761				
Ti	0.012	0.000	0.006	0.000				
Mg	0.000	0.019	0.012	0.000				
Fe	1.170	1.189	0.901	0.968				
Mn	0.017	0.017	0.000	0.000				
Cr	0.000	0.004	0.000	0.006				
Na	0.000	0.000	0.000	0.000	3.965	3.933	3.890	3.943
Ca	3.929	4.094	4.380	4.313	0.035	0.054	0.047	0.039
K	0.000	0.004	0.000	0.000	0.013	0.009	0.018	0.007
O	25	25	25	25	32	32	32	32
				MOLECULAR	PERCENTAGE			
AB					98.79	98.42	98.37	98.85
AN					0.88	1.36	1.18	0.98
OR					0.33	0.22	0.45	0.17

Fe_2O_3 : Total iron is reported as Fe_2O_3.

O : Number of oxygen ions used to calculate chemical formulas from anhydrous microprobe analyses.

Specimens 1, 2, and 4 are mafic metavolcanic rocks; specimen 5 is a felsic metavolcanic rock. 1: E-42-4A; 2: EW-33-6; 4: E-65-1; 5: E-23-11B.

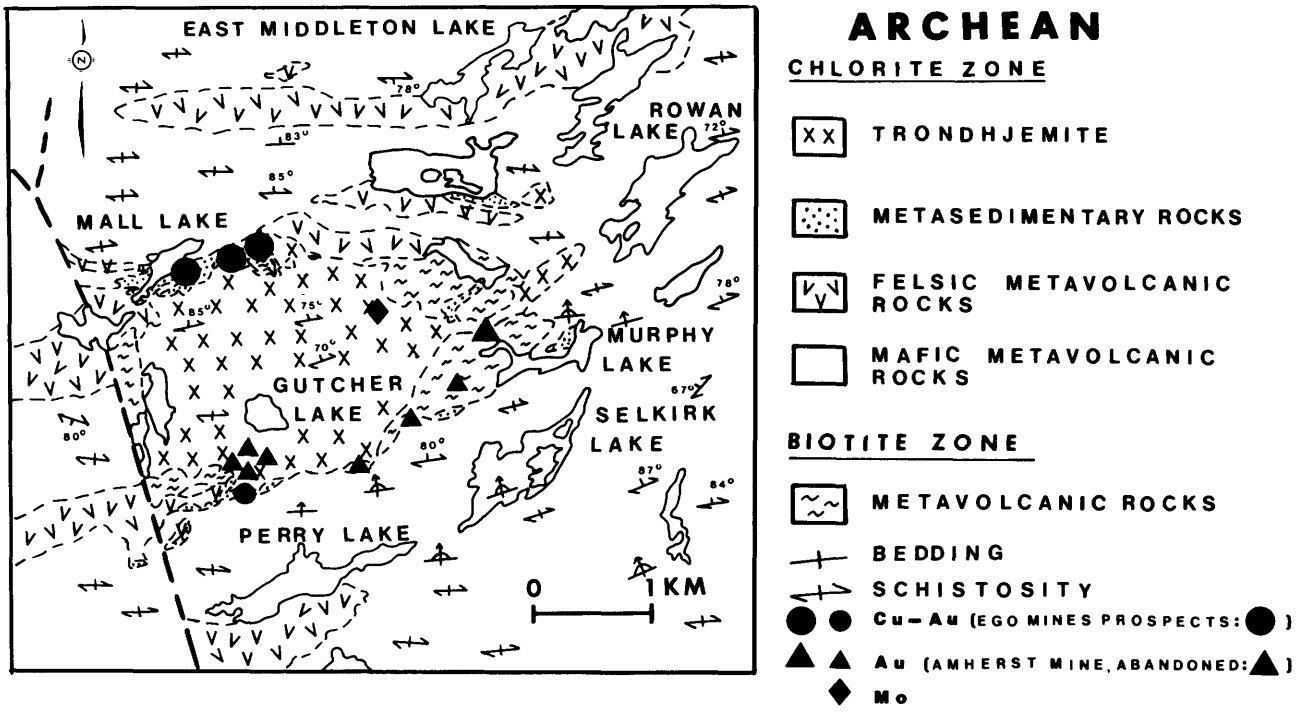

Figure 2. *Geology of the Gutcher Lake area.*

by pyrite and hexagonal pyrrhotite. Application of the sphalerite geobarometer to sulphide mineral assemblages in metamorphic terrains has provided reliable estimates of pressures prevailing during regional metamorphism (Bristol 1974; Scott 1976).

Sphalerite coexists with pyrite, pyrrhotite, and chalcopyrite in veins fringed by pyrite-albite-muscovite-chlorite-calcite-quartz assemblages near the stock (Studemeister 1982). Electron microprobe analyses reveal that this sphalerite contains between 16.6 and 18.6 percent mole FeS, and averages 17.6 mole percent FeS (Figure 3). With the temperature of sphalerite-chalcopyrite-pyrrhotite-pyrite equilibration fixed by the metamorphic grade of the enclosing rocks, T = 325°C to 450°C, the lithostatic pressure is between 1.6 and 3.1 Kbar (Figure 4), applying the stability curves of Scott (1976) and Hutchinson and Scott (1981).

BIOTITE ZONE

MINERAL PARAGENESIS

Within the biotite zone, which partly envelopes the Gutcher Lake stock, mafic metavolcanics are hornfelsic to schistose and consist of amphibole, epidote, quartz, albite, biotite, chlorite, magnetite, and pyrrhotite. Amygdular rocks have quartz- and amphibole-filled amygdules, whereas similar rocks in the chlorite zone have cal-

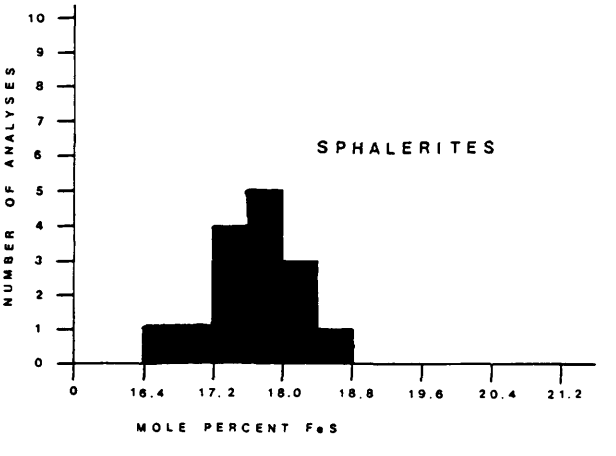

Figure 3. *Histogram for the FeS content in sphalerites.*

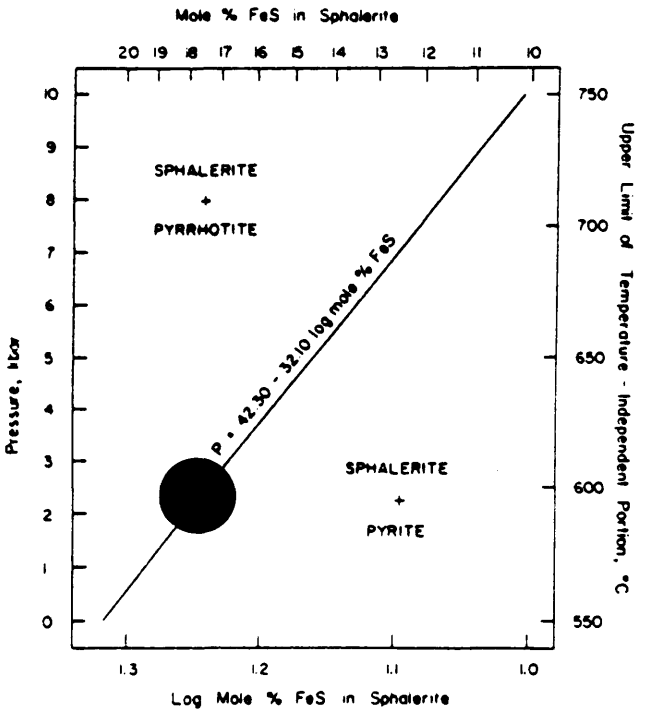

Figure 4. *Pressure versus mole percentage FeS projection onto the FeS-ZnS join of the temperature-independent portions of the sphalerite + pyrite + hexagonal pyrrhotite solvus isobars. (After Hutchinson and Scott 1981).*

• *Average FeS in sphalerites from the Gutcher Lake area.*

cite and quartz fillings. Epidote-hornblende hornfels passes into calcite-actinolite-chlorite rocks near quartz-carbonate veins, adjacent to the margin of the stock, and near the biotite-hornblende isograd.

Textural and compositional criteria suggest that the mineral assemblage prevailing in the biotite zone is in disequilibrium. These criteria are:

(1) Amphibole, epidote, and albite have variable composition. Amphibole has 1 to 10 percent Al_2O_3; 40 to 55 percent SiO_2; and hornblende cores with actinolite rims (Table 3, Figure 5). Iron content in epidote decreases from core to rim, in opposite sense to zoned epidote of the chlorite zone (Table 4). Albite varies between An_0 and An_7 (Table 4).

(2) Single or multi-phase pseudomorphs of essential minerals consist of chlorite, calcite, quartz, and actinolite. Amphibole porphyroblasts have margins that are serrated or dismembered with an enveloping halo of fine grained chlorite, calcite, quartz, and actinolite (Figures 6a, 6e, and 6f). Chlorite pseudomorphs after biotite are common (Figure 6b). Epidote may have embayed borders and overgrowths of fine grained chlorite, calcite, and quartz.

(3) Fractures, up to several metres wide and filled with quartz, calcite, ankerite, chlorite, and muscovite, cross-cut epidote-hornblende hornfels (Figures 6c and 6d).

(4) The regional schistosity is overprinted on biotite-epidote-amphibole assemblages (Figure 6e), and a gradation from granoblastic to schistose textures accompanies an increase in chlorite, calcite, and actinolite content.

The aforementioned criteria suggest the overprinting of an albite-muscovite-chlorite-actinolite-calcite-quartz assemblage on a pre-existing and pre-tectonic assemblage of hornblende, epidote, quartz, calcium-bearing albite, biotite, magnetite, and pyrrhotite.

RETROGRESSION OF CONTACT AUREOLE

The retrogression of epidote-hornblende hornfels may be generalized by the following reaction:

$$Ca_2(Mg,Fe)_5Al_1Si_7O_{22}(OH)_2 + 2\,Ca_2Al_3Si_3O_{12}(OH) + 2\,NaAlSi_3O_8 + K_2O + 6\,CO_2 + 4\,H_2O \rightarrow (Mg,Fe)_5Al_3Si_2O_{10}(OH)_8 + K_2Al_6Si_6O_{20}(OH)_4 + 6\,CaCO_3 + 11\,SiO_2 + Na_2O \quad (2)$$

(Hornblende + Epidote + Albite + Fluid → Chlorite + Muscovite + Calcite + Quartz + Fluid)

The sequence of metamorphic events in the biotite zone was (1) initial contact metamorphism, followed by (2) overprinting of regional metamorphism (Figure 7). Contact metamorphism of mafic volcanic rocks near the Gutcher Lake stock at T = 450°C to 550°C and P < 2 Kbar culminated in an aureole of pyrrhotite-magnetite-biotite-albite-quartz-epidote-hornblende hornfels. Metamorphic conditions during contact metamorphism are ascribed to the biotite subfacies of the greenschist facies (Turner 1980). The absence of pyroxene, calcium plagioclase, cordierite, and garnet suggests that conditions of the amphibolite facies were not attained.

Regional greenschist metamorphism overprinted on the aureole an albite-muscovite-actinolite-chlorite-quartz-calcite assemblage. Condition during retrogression correspond to the chlorite subfacies of the greenschist facies with T = 325°C to 450°C (Turner 1981; Miyashiro 1973; Schiffman and Liou 1980; Liou *et al.* 1974). The retrogression of epidote-hornblende hornfels was only partial as attested to by the preservation of hornblende, iron-rich epidote, and biotite. Complete retrogression was hampered by a negative ΔS_r for reaction (2), and the impermeability of hornfels which restricted access to fluids.

GUTCHER LAKE STOCK

MINERAL PARAGENESIS

The Gutcher Lake stock has sharp and irregular contacts with the surrounding succession of metavolcanics and metasediments. It is classified as trondhjemite because the ratio of modal alkali feldspar to plagioclase is less than 1:8, and the plagioclase composition is albite-oligoclase with less than 15 percent An (Table 5). The interior of the stock is generally blasto-hypidiomorphic-granular; quartz and feldspar are recrystallized and mildly foliated (Figures 8a and 8b). This massive trondhjemite is medium grained and leucocratic, and consists of pla-

Table 3. *Electron microprobe analyses of amphibole in mafic metavolcanics of the biotite zone.*

(wt%)	7Rim	7Core	13A	13B	14ACore	14ARim	14BCore	14BMarg.	14BRim
SiO_2	50.29	48.57	46.78	45.32	44.75	52.40	49.37	50.89	53.23
TiO_2	0.12	0.08	0.35	0.32	0.40	0.00	0.14	0.14	0.03
Al_2O_3	2.94	4.27	7.48	8.54	9.10	2.69	5.14	4.73	2.22
Cr_2O_3	0.11	0.13	0.02	0.02	0.00	0.00	0.11	0.13	0.00
FeO_t	21.12	21.39	20.75	22.19	19.00	15.58	17.70	16.66	17.77
MnO	0.80	0.76	0.59	0.58	0.43	0.29	0.23	0.28	0.37
MgO	10.62	10.21	8.98	8.07	11.91	14.18	11.80	11.56	11.90
CaO	11.43	11.21	11.84	11.91	11.06	13.02	12.77	12.58	12.57
Na_2O	0.37	0.72	0.75	1.04	0.52	0.21	0.38	0.43	0.14
K_2O	0.04	0.11	0.26	0.40	0.48	0.14	0.09	0.07	0.07
TOTAL:	97.84	97.45	97.80	98.39	97.65	98.51	97.73	97.47	98.30
				CHEMICAL	FORMULA				
Si	7.565	7.374	7.071	6.887	6.733	7.618	7.332	7.510	7.799
Al	0.435	0.626	0.929	1.113	1.267	0.382	0.668	0.490	0.201
Al	0.087	0.138	0.404	0.417	0.347	0.079	0.232	0.333	0.182
Ti	0.014	0.009	0.040	0.037	0.045	0.000	0.016	0.016	0.003
Mg	2.381	2.310	2.023	1.828	2.671	3.073	2.612	2.543	2.599
Fe	2.657	2.716	2.623	2.820	2.391	1.894	2.198	2.056	2.177
Mn	0.102	0.098	0.076	0.075	0.055	0.036	0.029	0.035	0.046
Cr	0.013	0.016	0.002	0.002	0.000	0.000	0.013	0.015	0.000
Na	0.108	0.212	0.220	0.306	0.152	0.059	0.109	0.123	0.040
Ca	1.842	1.823	1.918	1.939	1.783	2.028	2.032	1.989	1.973
K	0.008	0.021	0.050	0.078	0.092	0.026	0.017	0.013	0.013
O	23	23	23	23	23	23	23	23	23

FeO_t : Total iron is reported as FeO.

O : Number of oxygen ions used to calculate chemical formulas from anhydrous microprobe analyses.

Specimen 7: EW-36-2; 13: E-17-5; 14: E-21-4A.

Table 4. *Electron microprobe analyses of epidote and albite in metavolcanics of the biotite zone.*

	EPIDOTE				ALBITE			
(wt%)	7Rim	7Core	13A	13B	15A	15B	14A	14B
SiO_2	37.69	38.77	38.48	37.58	68.38	69.01	67.24	67.46
TiO_2	0.04	0.09	0.14	0.19				
Al_2O_3	26.31	24.93	25.11	23.87	19.61	19.32	20.05	20.77
Cr_2O_3	0.00	0.00	0.00	0.05				
Fe_2O_3	8.18	10.86	9.77	11.19				
MnO	0.21	0.15	0.21	0.23				
MgO	0.00	0.04	0.03	0.00				
CaO	24.38	23.32	23.76	23.09	0.61	0.18	1.01	1.63
Na_2O	0.00	0.00	0.00	0.00	11.54	11.39	11.45	10.98
K_2O	0.01	0.00	0.00	0.00	0.06	0.09	0.00	0.01
Cl	0.00	0.01	0.03	0.00				
TOTAL:	96.82	98.17	97.53	96.20	100.20	99.99	99.75	100.85
			CHEMICAL	FORMULA				
Si	5.983	6.089	6.078	6.051	11.937	12.036	11.815	11.730
Al	0.017	0.000	0.000	0.000	4.034	3.971	4.152	4.256
Al	4.904	4.614	4.676	4.529				
Ti	0.004	0.011	0.010	0.023				
Mg	0.000	0.009	0.007	0.000				
Fe	0.977	1.283	1.161	1.356				
Mn	0.028	0.020	0.028	0.031				
Cr	0.000	0.000	0.000	0.006				
Na	0.000	0.000	0.000	0.000	3.906	3.852	3.901	3.701
Ca	4.146	3.924	4.021	3.983	0.114	0.034	0.190	0.304
K	0.002	0.000	0.000	0.000	0.013	0.020	0.000	0.002
O	25	25	25	25	32	32	32	32
			MOLECULAR	PERCENTAGE				
AB					96.84	98.63	95.35	92.37
AN					2.83	0.86	4.65	7.58
OR					0.33	0.51	0.00	0.05

Fe_2O_3 : Total iron is reported as Fe_2O_3.
O : Number of oxygen ions used to calculate chemical formulas from anhydrous microprobe analyses.
Specimens 7, 13, and 14 are mafic metavolcanic rocks. Specimen 15 is a felsic metavolcanic rock. 7: EW-36-2; 13: E-17-5; 14: E-21-4A; 15: E-68-3.

gioclase, quartz, and chlorite with accessory muscovite, calcite, epidote, sphene, apatite, alkali feldspar, and biotite.

Massive trondhjemite grades into schistose trondhjemite along the margin of the stock. This marginal phase has a fine-grained and leucocratic matrix of quartz, albite, muscovite, calcite, and chlorite that wraps around anhedral quartz and albite porphyroclasts (Figures 8e and 8f). The most common feldspar is albite with less than 2 percent An (Table 5). Compared to massive trondhjemite, schistose trondhjemite has more muscovite and calcite and is more foliated.

Textures and compositions suggest that the mineral assemblage in the trondhjemite of the Gutcher Lake stock is in disequilibrium. These criteria are:

(1) Zoned feldspar has mottled cores with up to 15 percent An, and clear rims of albite (Table 5).

(2) Feldspar is partly or wholly pseudomorphed by muscovite, albite, quartz, and calcite (Figures 8a to 8e).

(3) Biotite is pseudomorphed by chlorite with minor epidote and quartz.

(4) Fractures, up to several metres wide and filled with quartz, ankerite, calcite, muscovite, chlorite, and epidote, cross-cut the stock (Figure 8b, Figure 9).

(5) The regional schistosity is overprinted on the trondhjemite (Figures 8e and 8f), and a gradation from massive to schistose textures accompanies an increase in muscovite, calcite, chlorite, albite, and quartz content.

The mineral paragenesis corresponds to a fine grained chlorite-calcite-muscovite-albite-quartz assemblage overprinted on a pre-existing and pre-tectonic biotite-quartz-plagioclase assemblage. Mineral transformation is moderate in the interior and intense along the margin of the stock. Inward decrease in intensity of schistosity and abundance of alteration minerals is consistent with regional compression to which the less altered interior of the stock responded as a more competent and resistant block than the hydrated margin of the stock.

RETROGRESSION OF TRONDHJEMITE

The retrogression of the trondhjemite may be generalized by the following mineral reaction:

$$20\,(0.9\,NaAlSi_3O_8 + 0.1\,CaAl_2Si_2O_8) + 2\,K_2(Mg,Fe)_5Al_4Si_5O_{20}(OH)_4 + 2\,K_2O + 12\,H_2O + 2\,CO_2 \rightarrow 4\,K_2Al_6Si_6O_{20}(OH)_4 + 32\,SiO_2 + 1\,(Mg,Fe)_{10}Al_4Si_6O_{20}(OH)_{16} + 2CaCO_3 + 2\,NaAlSi_3O_8 + 8\,Na_2O \quad (3)$$

(Plagioclase + Biotite + Fluid → Muscovite + Quartz + Chlorite + Calcite + Albite + Fluid)

The chlorite-muscovite-calcite-albite-quartz assemblage of alteration corresponds to the chlorite subfacies of the greenschist facies with T = 325°C to 450°C. Hence, retrogression of the trondhjemite was contemporaneous with the retrogression of the stock's contact aureole during regional greenschist metamorphism.

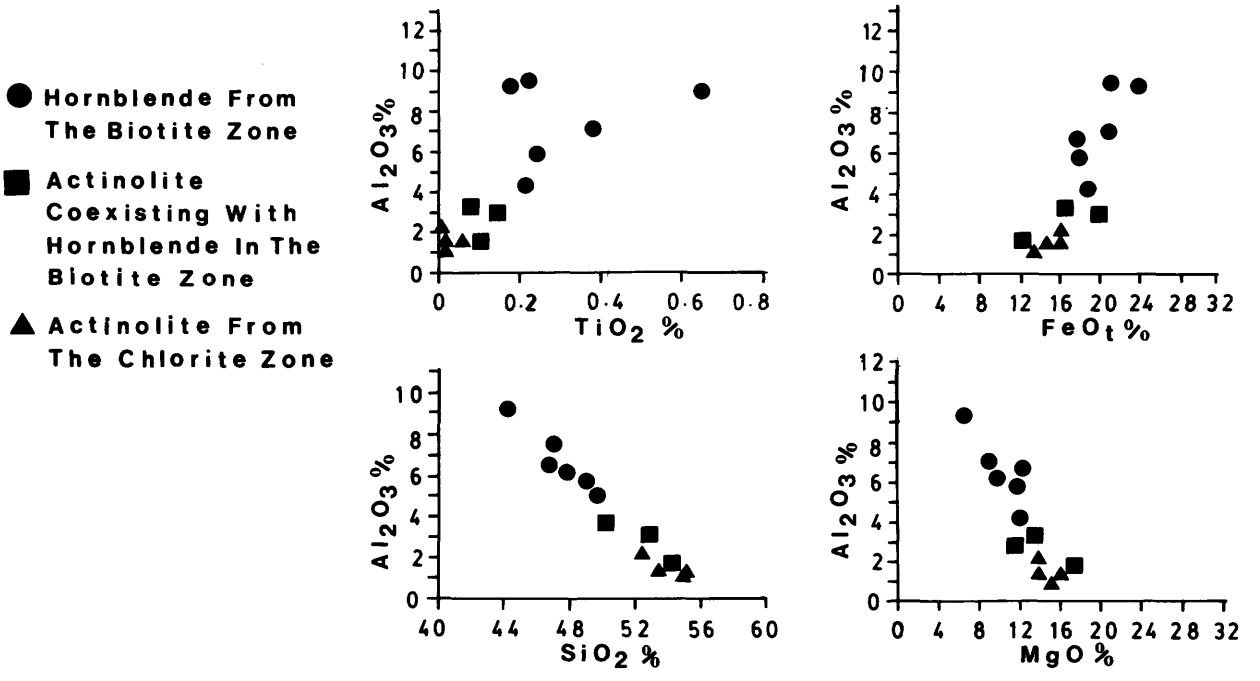

Figure 5. *Compositional variation of amphibole.*

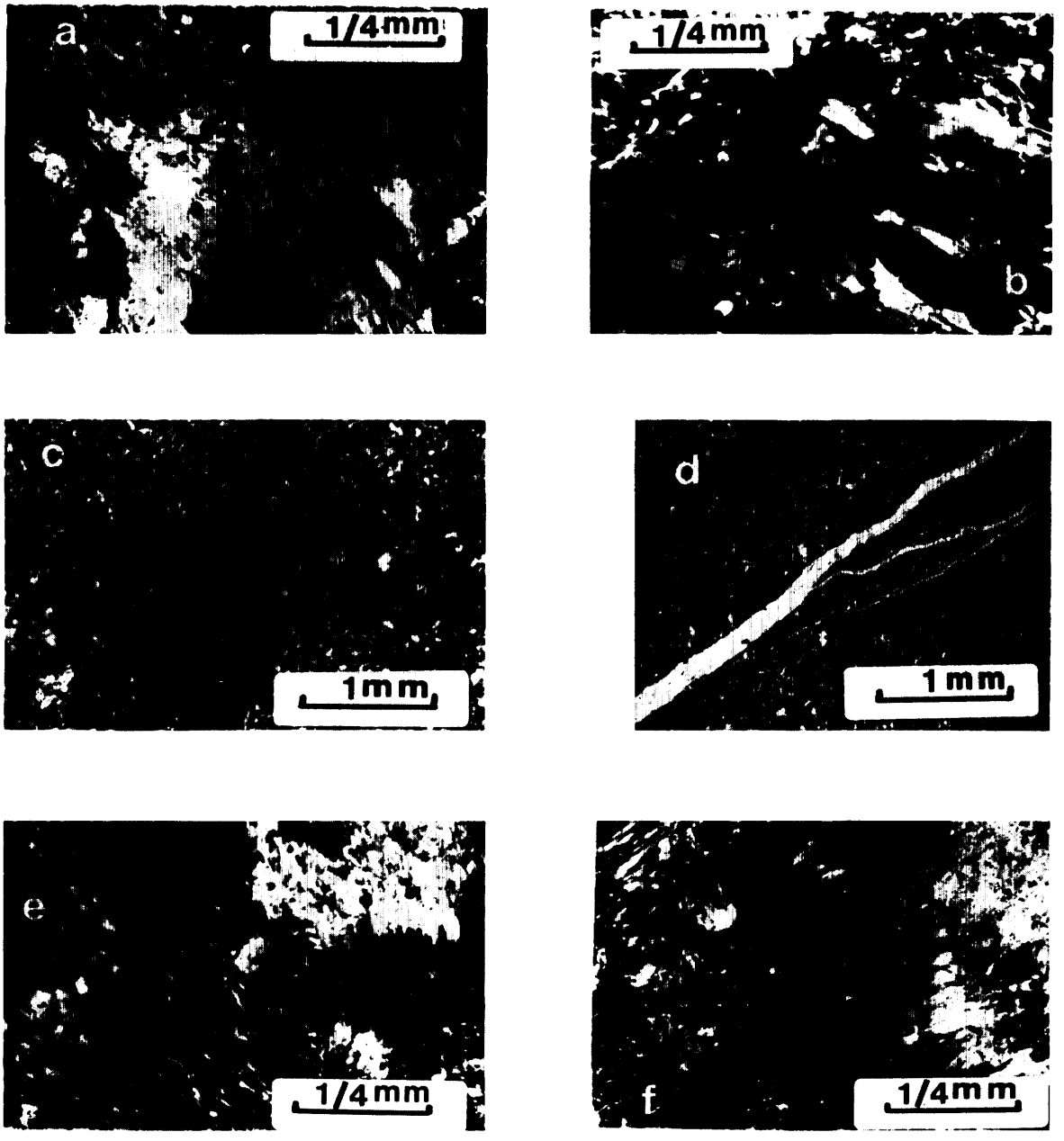

Figure 6. *Photomicrographs of textures in rocks of the biotite zone. All photos taken through crossed polarizers.*
a. *Poikiloblastic hornblende (grey) with margins pseudomorphed by an intergrowth of chlorite, quartz, calcite, and actinolite (dark grey), near Ruth Lake.*
b. *Chlorite (dark grey) pseudomorphic after biotite (light grey) in a pyrite-chlorite schist near Mall Lake.*
c. *Microfracture, filled with chlorite, quartz, and calcite, cross-cutting epidote-hornblende hornfels, near Murphy Lake.*
d. *Microfracture, filled with quartz and calcite, cross-cutting hornfels near Ruth Lake.*
e. *Hornblende (pale grey) with serrated and dismembered margins, partly enclosed by a chloritic sheath (dark gray), near Ruth Lake.*
f. *Hornblende (light grey) with radiating plumes of fine-grained chlorite, quartz, and calcite (dark gray), near Ruth Lake.*

Table 5. *Electron microprobe analyses of plagioclase in trondhjemite of the Gutcher Lake stock.*

	PLAGIOCLASE									
(wt%)	16Core	16Rim	17Core	17Rim	18A	18BRim	19A	19B	20Rim	20Core
SiO_2	69.40	67.80	67.65	68.09	68.63	69.10	69.83	67.47	68.68	67.03
Al_2O_3	19.08	19.85	20.75	20.33	20.22	19.50	19.70	20.98	19.23	20.75
CaO	2.23	1.13	1.45	0.71	0.82	0.09	0.09	0.36	0.05	1.80
Na_2O	9.55	11.24	10.68	11.18	10.76	10.65	10.89	10.71	11.40	10.74
K_2O	0.00	0.00	0.00	0.00	0.00	0.03	0.00	0.28	0.03	0.00
TOTAL:	100.26	100.02	100.53	100.31	100.43	99.37	100.51	99.80	99.39	100.32
	CHEMICAL FORMULA									
Si	12.058	11.868	11.772	11.859	11.915	12.075	12.069	11.799	12.043	11.715
Al	3.906	4.905	4.255	4.172	4.137	4.015	4.012	4.323	3.974	4.274
Na	3.217	3.815	3.603	3.775	3.622	3.608	3.649	3.631	3.876	3.639
Ca	0.415	0.212	0.270	0.132	0.153	0.017	0.017	0.067	0.009	0.337
K	0.000	0.000	0.000	0.000	0.000	0.007	0.000	0.062	0.007	0.000
O	32	32	32	32	32	32	32	32	32	32
	MOLECULAR PERCENTAGE									
AB	88.57	94.74	93.02	96.61	95.96	99.36	99.55	96.55	99.59	91.52
AN	11.43	5.26	6.98	3.39	4.04	0.46	0.45	1.79	0.24	8.48
OR	0.00	0.00	0.00	0.00	0.00	0.18	0.00	1.66	0.17	0.00

O : Number of oxygen ions used to calculate chemical formulas from anhydrous microprobe analyses.

Specimens 16, 17, and 18 are massive trondhjemite. Specimen 19 is schistose trondhjemite. Specimen 20 is a wallrock to the main vein at the Porter-Premier prospects. 16: E-70-6F; 17: E-18-3; 18: E-19-3; 19: E-33-8; 20: E-36-2.

GOLD-BEARING QUARTZ-CARBONATE VEINS

The morphology of gold-bearing quartz-carbonate veins transecting the periphery of the Gutcher Lake stock is exemplified by the main vein at the Porter-Premier prospects, southwest of Gutcher Lake (Figure 9). The east-striking, steeply dipping vein cross-cuts trondhjemite and contains a succession of pyrite-quartz lodes enclosed by fine-grained schistose wallrocks. These leucocratic wallrocks of quartz, calcite, muscovite, paragonite, albite, chlorite, and pyrite grade outward from the vein into massive trondhjemite mottled with white mica and calcite. The gold-bearing vein at the Amherst mine near Murphy Lake is an east-southeast striking, steeply dipping fracture filled with quartz, ankerite, pyrite, pyrrhotite, chalcopyrite, sphalerite, chlorite, and muscovite that transects the margin of the Gutcher Lake stock. The massive quartz-ankerite vein is fringed by fine grained mesocratic calcite-quartz-chlorite wallrocks that grade outward into epidote-hornblende hornfels.

Gold-bearing quartz-carbonate veins distributed about the margin of the Gutcher Lake stock are manifestations of the retrogression of epidote-hornblende hornfels and trondhjemite. The mineral transformation recorded in wallrocks about these veins involved attack by CO_2-H_2O fluids and can be represented by reactions (2) and (3). Excess fluid-to-rock volumes adjacent to fractures shifted equilibrium to pyrite-albite-muscovite-chlorite-calcite-quartz assemblages.

GEOCHEMISTRY OF RETROGRESSION

MASS BALANCE CALCULATIONS

Gresens' (1967) equation of metasomatism was used to assess the changes in element abundances during retrogression of trondhjemite and epidote-hornblende hornfels in wallrocks near gold-bearing veins in the study area. Specimens were collected along two lines perpendicular to sections of vein cross-cutting mafic metavolcanics at the Amherst mine, and trondhjemite at the Porter-Premier prospects, respectively (Tables 6a, b and 7a, b). Rocks in each suite have relatively uniform Al_2O_3 to TiO_2 ratios (Tables 6a and 7a) suggesting that the abundance of aluminum and titanium did not change significantly during retrogression. The volume factor, F_v, used in mass balance calculations was therefore the weighted average of $(F_v)_{Al}$ and $(F_v)_{Ti}$. Results of calculations are plotted as chemical change versus distance from vein (Figures 10a, b, and 11a, b); integrating the area between $\Delta X_i = 0$ and the extrapolated chemical change curve provides an estimate of the net change in element abundance.

Wallrocks near gold-bearing veins experienced the following changes in element abundances (Figures 10a, b, and 11a, b):

(1) addition of Si, Fe, K, $H_2O + CO_2$, S, and Rb; and

(2) loss of Na.

Calcium and magnesium were quantitatively leached from wallrocks fringing the vein at the Porter-Premier prospects, but were quantitatively added to wall-

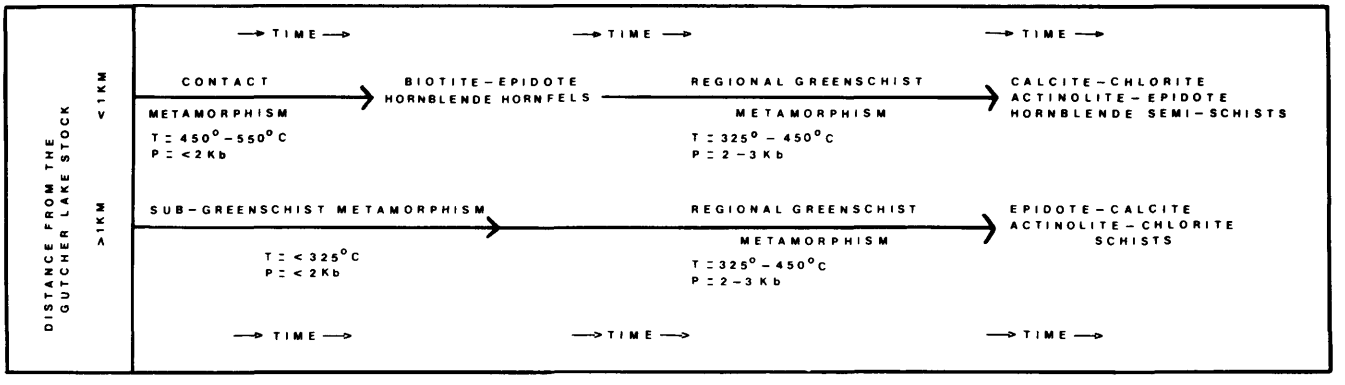

Figure 7. *Temporal evolution of metamorphism in the Archean succession.*

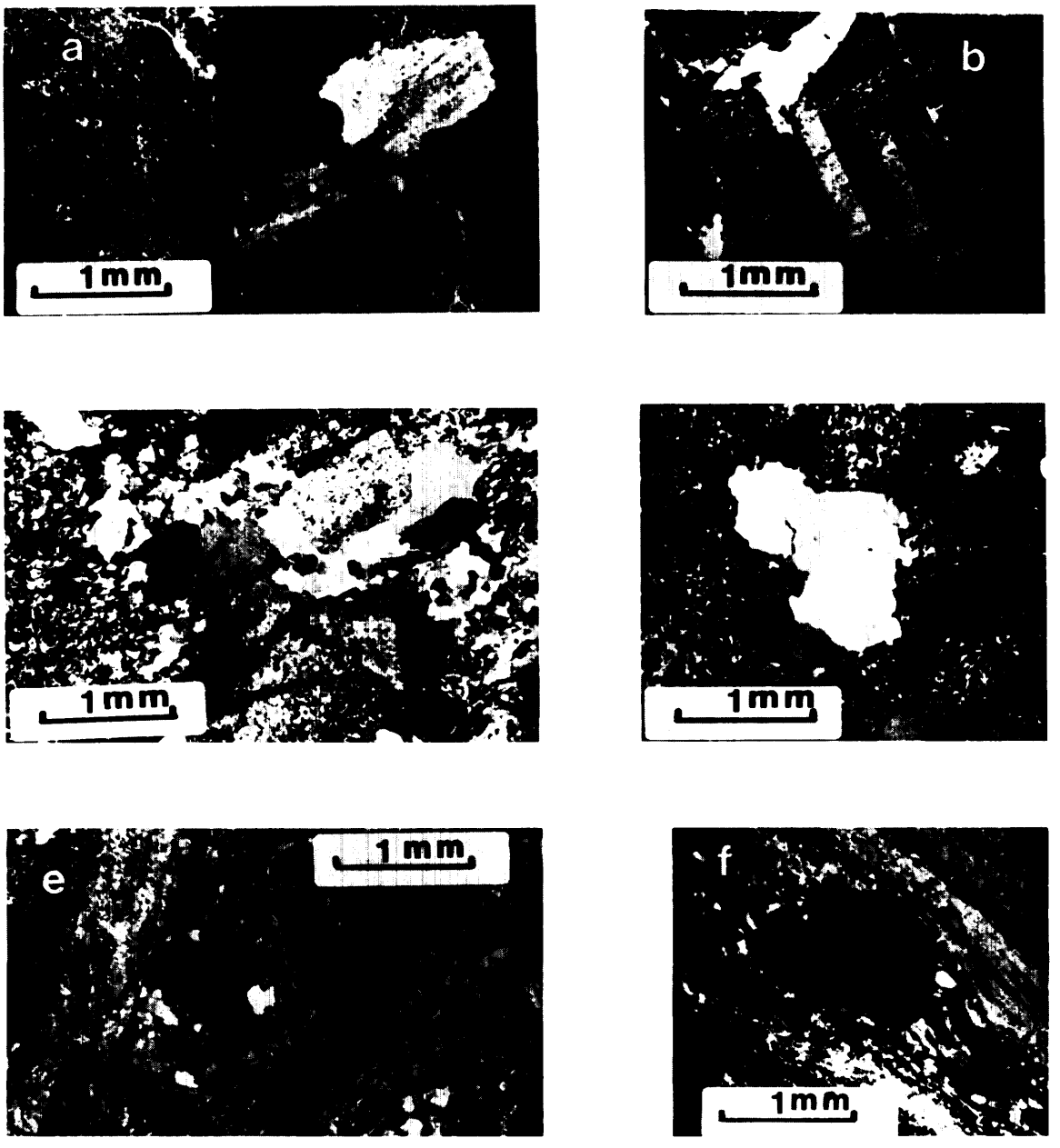

Figure 8. *Photomicrographs of textural variation of the stock. All photos taken through crossed polarizers.*
a. *Anhedral quartz and subhedral plagioclase mildly mottled with white mica, massive trondhjemite near Gutcher Lake.*
b. *Amoeboid quartz interstitial to subhedral plagioclase, massive trondhjemite near Gutcher Lake.*
c. *Calcite-albite-quartz-white mica pseudomorph after feldspar, trondhjemite east of Gutcher Lake.*
d. *Anhedral assemblage of quartz (grey) and feldspar (spotted brown) mottled with white mica, trondhjemite east of Gutcher Lake.*
e. *Fractured quartz porphyroclast wrapped by foliated fine-grained matrix, marginal trondhjemite near Mall Lake.*
f. *Quartz porphyroclast (black) fringed by pressure shadows of calcite, marginal trondhjemite south of Gutcher Lake.*

Table 6a. *Chemical analyses of wallrocks about the main gold-bearing vein at the Porter-Premier prospects, southwest of Gutcher Lake.*

SPECIMEN:		7K	7J	7I	7H	7G	WALLROCKS 7F	7E	7D	7C	7A	7B	CORE 364
	(wt%)												
SiO_2		63.28	61.37	63.23	63.71	63.81	64.65	64.23	64.42	62.88	78.49	82.34	90.07
TiO_2		0.45	0.42	0.44	0.43	0.43	0.44	0.41	0.46	0.47	0.29	0.23	0.09
Al_2O_3		15.23	14.13	15.05	14.74	14.98	15.20	15.24	15.49	15.86	8.19	7.17	2.89
Fe_2O_3		4.39	4.51	4.12	4.49	4.12	4.23	3.93	3.98	4.72	5.42	3.27	1.16
MnO		0.06	0.08	0.06	0.06	0.05	0.04	0.04	0.04	0.04	0.01	0.02	0.02
MgO		1.24	1.56	1.39	1.30	1.41	1.35	1.27	1.09	1.02	0.15	0.28	0.49
CaO		3.90	4.80	3.37	3.90	3.75	2.88	3.06	2.67	2.57	0.64	0.73	1.42
Na_2O		5.42	4.77	4.75	4.82	4.70	4.67	4.60	4.91	4.92	2.25	2.04	1.33
K_2O		1.15	0.97	0.95	0.78	0.83	1.07	1.30	1.54	1.49	1.11	1.09	0.99
P_2O_5		0.05	0.04	0.04	0.05	0.04	0.04	0.04	0.05	0.06	0.00	0.00	0.00
L.O.I.		5.24	7.44	5.99	5.83	5.61	4.89	6.24	5.64	5.70	3.45	2.85	2.34
TOTAL:		100.42	100.09	99.39	100.11	99.73	99.46	100.36	100.29	99.73	100.00	100.02	100.80
S		0.03	0.11	0.02	0.03	0.04	0.07	0.18	0.41	1.27	3.09	1.53	0.14
	(ppm)												
Y		16	14	12	15	11	13	7	14	19	8	9	6
Zr		101	101	104	97	94	100	96	104	110	82	70	46
Nb		54	46	32	42	40	36	19	37	33	33	32	42
Cr		34	20	15	23	12	14	15	21	42	25	7	3
Ba		229	196	202	170	159	179	210	211	205	138	126	24
Sr		309	258	362	312	296	282	295	300	396	231	210	63
Rb		25	23	25	21	20	27	34	33	33	28	25	3
Pb		0	9	12	9	7	5	2	6	8	13	5	8
Co		24	26	18	20	26	24	25	24	26	56	55	93
Zn		10	11	13	26	32	36	26	14	7	13	12	14
Cl							<50	50	<50	<50	<50	<50	150
S.G.		2.75	2.76	2.78	2.76	2.75	2.74	2.75	2.76	2.78	2.75	2.77	2.66
(Al_2O_3/TiO_2)	:	33.84	33.64	34.21	34.28	34.84	34.55	37.17	33.67	33.75	28.24	31.17	32.11

Fe_2O_3 : Total iron is reported as Fe_2O_3.
L.O.I. : Volatiles (wt%) lost on ignition at ∿1000°C, uncorrected for oxidation of iron.
S.G. : Specific gravity of rock specimen.

Table 6b. *Chemical changes in wallrocks about the main gold-bearing vein at the Porter-Premier prospects, southwest of Gutcher Lake.*

ROCK PAIR:	7K → 7J	7J → 7I	7I → 7H	7H → 7G	7G → 7F	7F → 7E	7E → 7D	7D → 7C	7C → 7A	7A → 7B
$(F_v)_w^{Al,Ti}$	1.07	0.93	1.03	0.99	0.99	0.99	0.97	0.97	1.93	1.14
					(gms/100 gms of pair parent rock)					
SiO_2	+ 2.63	- 2.14	+ 1.92	- 0.77	- 0.04	- 0.83	- 1.52	- 2.98	+ 86.97	+ 16.06
TiO_2	+ 0.01	- 0.01	0.00	- 0.01	0.00	- 0.03	+ 0.04	0.00	+ 0.08	- 0.03
Al_2O_3	- 0.06	- 0.03	+ 0.02	+ 0.04	+ 0.01	- 0.06	- 0.16	+ 0.01	- 0.22	+ 0.04
Fe_2O_3	+ 0.45	- 0.65	+ 0.47	- 0.43	+ 0.05	- 0.33	- 0.06	+ 0.63	+ 5.63	- 1.67
MnO	+ 0.03	- 0.02	0.00	- 0.01	- 0.01	0.00	0.00	0.00	- 0.02	+ 0.01
MgO	+ 0.44	- 0.26	- 0.06	+ 0.09	- 0.08	- 0.09	- 0.21	- 0.09	- 0.73	+ 0.17
CaO	+ 1.25	- 1.64	+ 0.62	- 0.20	- 0.91	+ 0.16	- 0.46	- 0.16	- 1.35	+ 0.20
Na_2O	- 0.30	- 0.32	+ 0.18	- 0.18	- 0.09	- 0.10	+ 0.18	- 0.10	- 0.62	+ 0.09
K_2O	- 0.11	- 0.08	- 0.15	+ 0.04	+ 0.23	+ 0.22	+ 0.20	- 0.08	+ 0.63	+ 0.14
P_2O_5	- 0.01	+ 0.01	0.00	- 0.01	0.00	0.00	+ 0.01	+ 0.01	+ 0.06	0.00
L.O.I.	+ 2.75	- 1.83	- 0.03	- 0.30	- 0.79	+ 1.31	+ 0.22	- 0.03	+ 0.89	- 0.18
S	+ 0.09	- 0.09	+ 0.01	+ 0.01	+ 0.03	+ 0.11	+ 0.22	+ 0.83	+ 4.63	- 1.33
					(gms/10^6 gms of pair parent rock)					
Y	- 1	- 3	+ 3	- 4	+ 2	- 6	+ 7	+ 5	- 4	+ 2
Zr	+ 8	- 4	- 5	- 4	+ 5	- 5	+ 5	+ 4	+ 47	- 2
Nb	- 5	- 16	+ 11	- 3	- 5	- 17	+ 17	- 5	+ 30	+ 4
Cr	- 13	- 6	+ 9	- 11	+ 2	+ 1	+ 5	+ 20	+ 6	- 17
Ba	- 19	- 7	- 28	- 13	+ 18	+ 30	- 5	- 11	+ 59	+ 7
Sr	- 32	+ 81	- 43	- 20	- 18	+ 11	- 3	+ 87	+ 45	+ 10
Rb	0	0	- 4	- 2	+ 7	+ 7	- 2	- 1	+ 21	+ 1
Pb	+ 10	+ 2	- 3	- 2	- 2	- 3	+ 4	+ 2	+ 17	- 7
Co	+ 4	- 9	+ 3	+ 6	- 2	+ 1	- 2	+ 1	+ 81	+ 7
Zn	+ 2	+ 1	+ 14	+ 6	+ 4	- 10	- 12	- 7	+ 18	+ 1
Cl					- ∿25	+ ∿25	- ∿26	- ∿1	+ ∿46	+ ∿4

$(F_v)_w^{Al,Ti}$: volume factor used in mass balance calculations is a weighted average of $(F_v)^{Al}$ and $(F_v)^{Ti}$

Table 7a. *Chemical analyses of wallrocks about the gold-bearing vein at the Amherst mine, Murphy Lake.*

		←Θ→	WALLROCKS	←Θ→		CORE
SPECIMEN:	22B	22C	22D	22E	22F	502
(wt%)						
SiO_2	56.47	61.20	54.22	71.88	7.50	63.90
TiO_2	1.07	0.88	1.11	1.12	0.05	0.00
Al_2O_3	13.50	12.13	14.45	14.39	0.68	0.01
Fe_2O_3	16.90	15.33	18.24	3.86	10.35	7.15
MnO	0.20	0.16	0.22	0.06	0.61	0.08
MgO	3.60	3.58	5.56	1.77	13.35	0.50
CaO	1.10	0.00	0.02	0.18	25.32	0.01
Na_2O	1.31	1.48	0.00	0.34	0.00	0.00
K_2O	0.45	0.24	0.72	3.27	0.00	0.02
P_2O_5	0.03	0.02	0.02	0.03	0.00	0.00
L.O.I.	5.15	5.30	5.94	3.44	41.88	14.03
TOTAL:	99.78	100.32	100.50	100.34	99.74	85.70
S	0.63	0.57	0.07	0.31	0.05	13.70
(ppm)						
Y	35	29	33	23	18	1
Zr	90	81	90	80	40	0
Nb	46	16	16	29	30	1
Cr	79	59	81	75	2	10
Ba	59	32	100	354	0	1
Sr	33	23	21	37	11	0
Rb	16	13	23	76	2	5
Pb	0	11	13	6	4	1540
Co	51	51	37	35	11	332
Zn	177	157	229	36	35	44200
S.G.	2.86	2.68	2.77	2.73	2.95	3.15
(Al_2O_3/TiO_2) :	12.62	13.78	13.02	12.85	13.60	ø

Fe_2O_3 : Total iron is reported as Fe_2O_3.
L.O.I. : Volatiles (wt%) lost on ignition at ∿1000°C, uncorrected for oxidation of iron.
S.G. : Specific gravity of rock specimen.

Table 7b. *Chemical changes in wallrocks about the gold-bearing vein at the Amherst mine, Murphy Lake.*

ROCK PAIR:	22B → 22C	22C → 22D	22D → 22E	22E → 22F
$(F_v)_w^{Al,Ti}$:	1.22	0.80	1.02	19.85
	(gms/100 gms of pair parent rock)			
SiO_2	+ 13.49	- 16.37	+ 18.04	+ 88.99
TiO_2	- 0.06	+ 0.04	+ 0.02	- 0.05
Al_2O_3	+ 0.37	- 0.18	+ 0.02	+ 0.20
Fe_2O_3	+ 0.63	- 0.25	- 14.36	+218.14
MnO	- 0.02	+ 0.02	- 0.16	+ 13.02
MgO	+ 0.49	+ 1.02	- 3.78	+284.58
CaO	- 1.10	+ 0.02	+ 0.16	+542.92
Na_2O	+ 0.38	- 1.48	+ 0.34	- 0.34
K_2O	- 0.18	+ 0.36	+ 2.57	- 3.27
P_2O_5	- 0.01	0.00	+ 0.01	- 0.03
L.O.I.	+ 0.90	+ 0.61	- 2.48	+894.87
S	+ 0.02	- 0.51	+ 0.24	+ 0.76
	(gms/10^6 gms of pair parent rock)			
Y	- 2	- 2	- 10	+ 363
Zr	+ 3	- 7	- 10	+ 778
Nb	- 28	- 3	+ 13	+ 615
Cr	- 12	+ 8	- 6	- 32
Ba	- 22	+ 51	+ 256	- 354
Sr	- 7	- 6	+ 16	+ 199
Rb	- 1	+ 6	+ 53	- 33
Pb	+ 13	0	- 7	+ 80
Co	+ 7	- 20	- 2	+ 201
Zn	+ 3	+ 32	- 193	+ 715

$(F_v)_w^{Al,Ti}$: volume factor used in mass balance calculations is a weighted average of $(F_v)^{Al}$ and $(F_v)^{Ti}$.

rocks at the Amherst vein. These results suggest that calcium and magnesium are locally derived elements; leached from some sections of wallrock, remobilized, and then precipitated as carbonate minerals elsewhere. Changes in the abundance of Zr, Nb, Y, Ba, Cr, Co, Sr, and Cl also vary between wallrock traverses (Studemeister 1982) suggesting that these elements were not leached or added by fluids on a substantial scale during retrograde metamorphism.

OXIDATION STATE OF IRON

Wallrocks near quartz-carbonate veins in the study-area have $Fe^{+2}/Fe_t \cong 0.9$ compared to background rocks with $Fe^{+2}/Fe_t \cong 0.66$ (Figure 12), suggesting attack by a reducing fluid. Assuming that the reducing agent was hydrogen produced by the dissociation of water cooling from T = 500°C and P = 1 Kbar to T = 300°C and P = 2 Kbar, the water-to-rock ratio required to shift Fe^{+2}/Fe_t from 0.7 to 0.9 in wallrocks of the Amherst vein is about 5:1 (Studemeister 1982). The water to rock ratio was calculated with the method of Kerrich *et al.* (1977) using experimental data on the fayalite-quartz-magnetite-water system by Eugster and Skippen (1967).

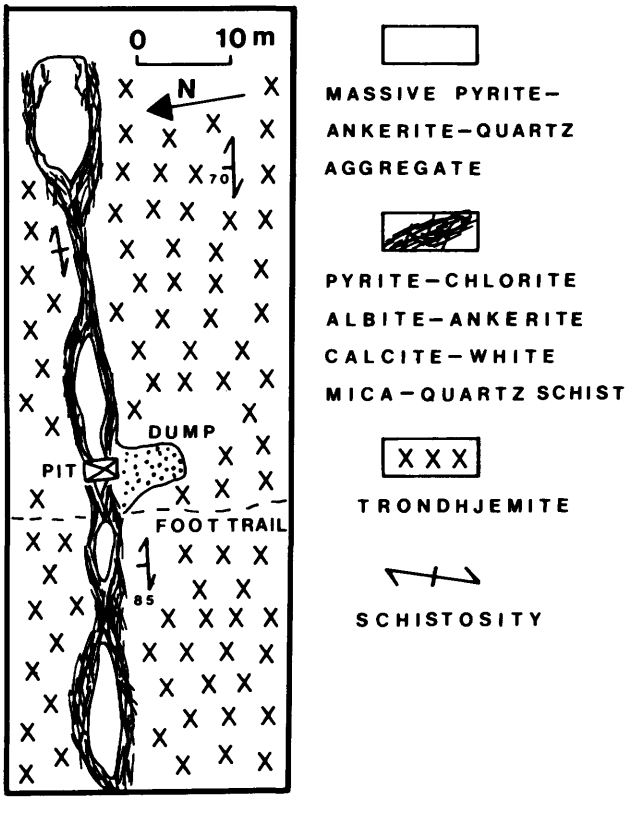

Figure 9. *Geologic sketch map of the main gold-bearing vein at the Porter-Premier prospects, southwest of Gutcher Lake.*

OXYGEN ISOTOPE RELATIONS

The oxygen isotope composition of quartz, $\delta^{18}O_{Qtz}$, in gold-bearing veins in the study area is between 11.5 and 14.1 ‰ (Table 8). Vein quartz has two-phase fluid inclusions consisting of a liquid with a gas bubble, presumably carbon dioxide. Primary fluid inclusions, identified by criteria outlined in Roedder (1967; 1976), have filling factors, F = volume liquid/(volume liquid + gas), between 0.75 and 0.80. These primary inclusions have homogenization temperatures between 275 and 340°C (Figure 13). The uniform filling factors suggest that the gold-bearing fluid was under hydrostatic pressure and not boiling at time of trapping (Roedder 1967; 1976). The homogenization temperatures, measured at atmospheric pressure, is therefore a minimum estimate of the trapping temperature.

Applying the $\Delta Qtz\text{-}H_2O$ fractionation equation of Taylor (1967) with T = 400°C, the fluid that equilibrated with $\delta^{18}O_{Qtz}$ = 11.5 to 14.1 ‰ has $\delta^{18}O_{H2O}$ = 6 to 9 ‰. The isotopic composition of the fluid does not distinguish between metamorphic and magmatic waters because the $\delta^{18}O_{H2O}$ overlaps both fields. However, a metamorphic origin is likely because veins cross-cut the stock, its contact aureole, and are lined with a greenschist mineral assemblage.

EXPLORATION STRATEGIES FOR GOLD

Future exploration strategies for gold in Ontario will require reliable guidelines for the discovery of sub-surface orebodies because most orebodies exposed at the surface have probably been discovered. The present cost of diamond drilling is about $100 to $150 per metre, and an exploration program can easily exceed $200 000 in drilling costs. Improved selection of sites for exploratory drilling based on criteria recognizable in the field would improve the chances of a major discovery and save mining companies thousands of dollars.

This research suggests the following exploration strategies for vein-type gold deposits in Archean "greenstone" belts:

(1) Exploration should focus on greenstone successions with producing or past producing base and precious metal mines.

(2) Felsic intrusions with contact aureoles that are overprinted by regional greenschist facies metamorphism are prime targets, particulary if the retrograde aureoles have associated sulphide concentrations.

(3) The most favourable site for gold deposits are along the margins of stocks and their contact aureoles, along narrow pyritic zones of intense retrogression.

(4) Disseminated magnetite or pyrrhotite in contact aureoles may generate magnetic anomalies with ground or airborne magnetic surveys, and these anomalies delineate rocks favoured to host major gold deposits.

(5) The massive interiors of intrusions, and greenstone successions remote from contact aureoles, are less likely to host major gold veins.

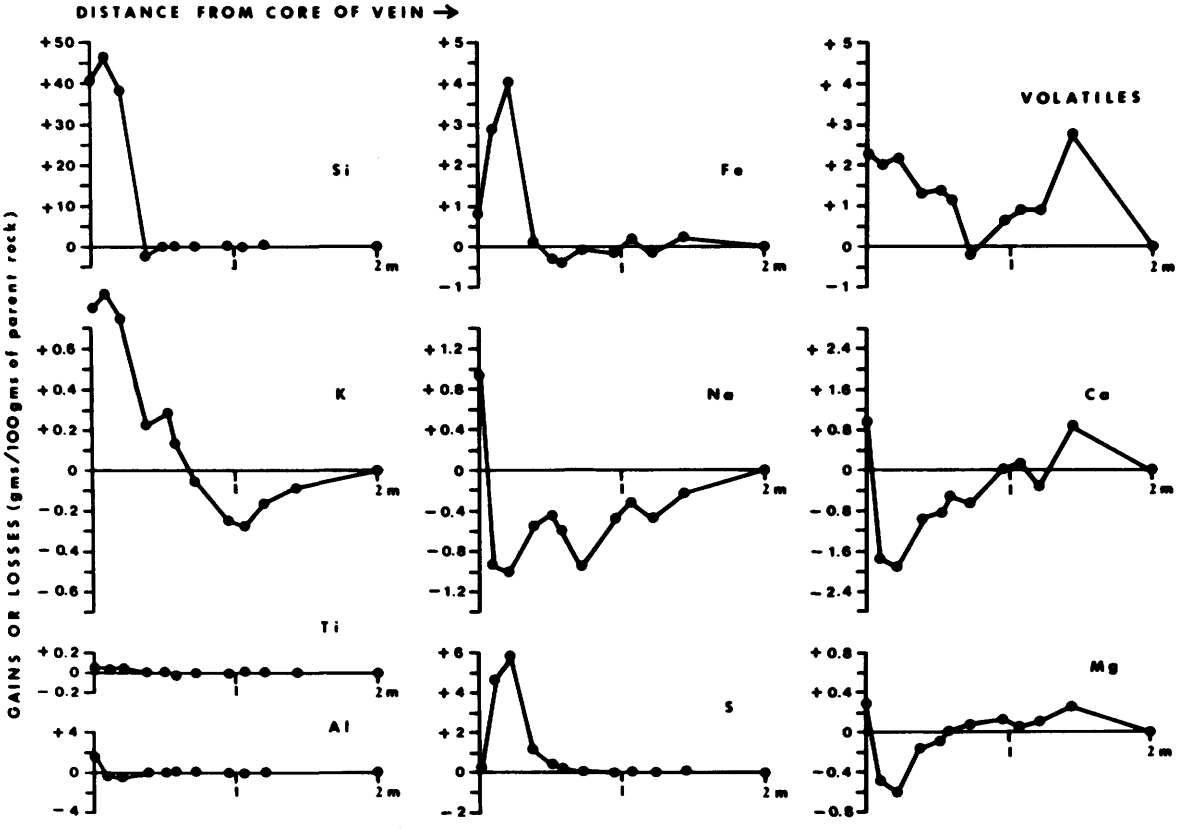

Figure 10a. *Changes in major element abundances in wallrocks about the main gold-bearing vein at the Porter-Premier prospects.*

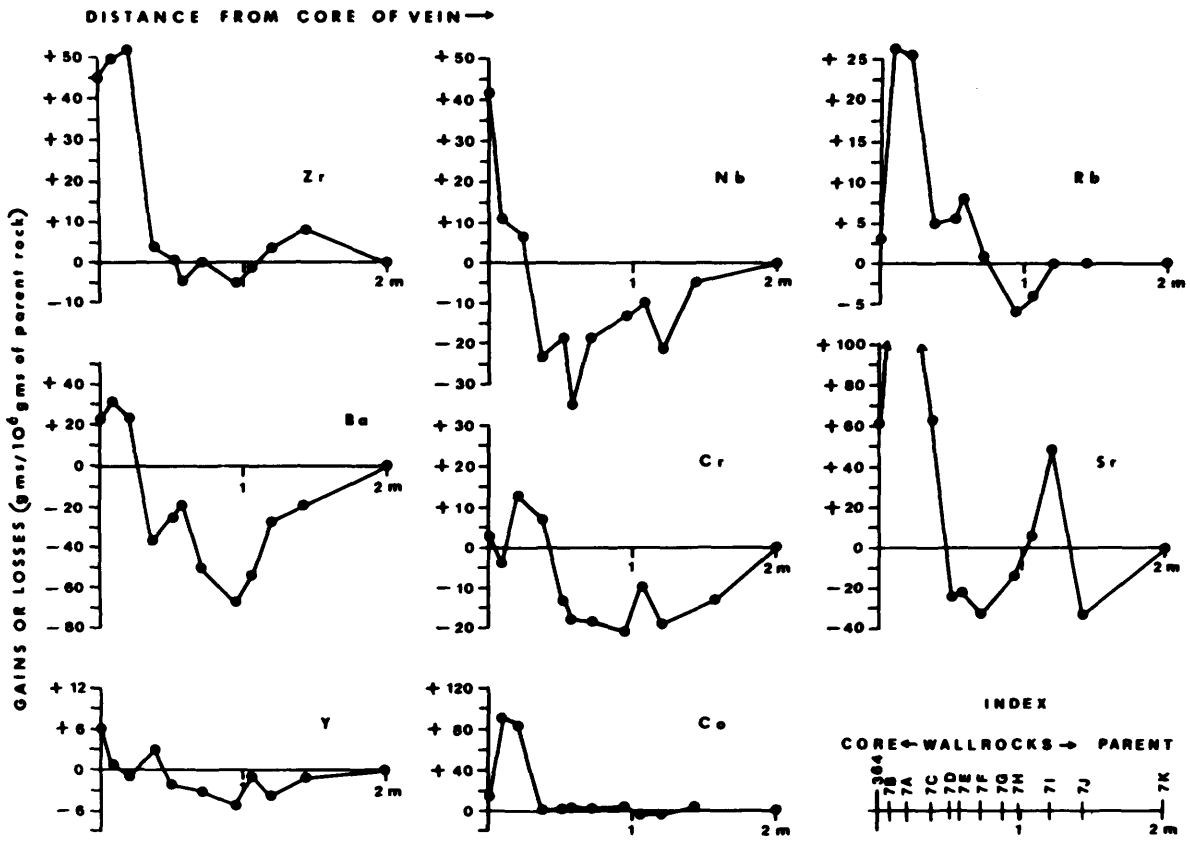

Figure 10b. *Changes in trace element abundances in wallrocks about the main gold-bearing vein at the Porter-Premier prospects.*

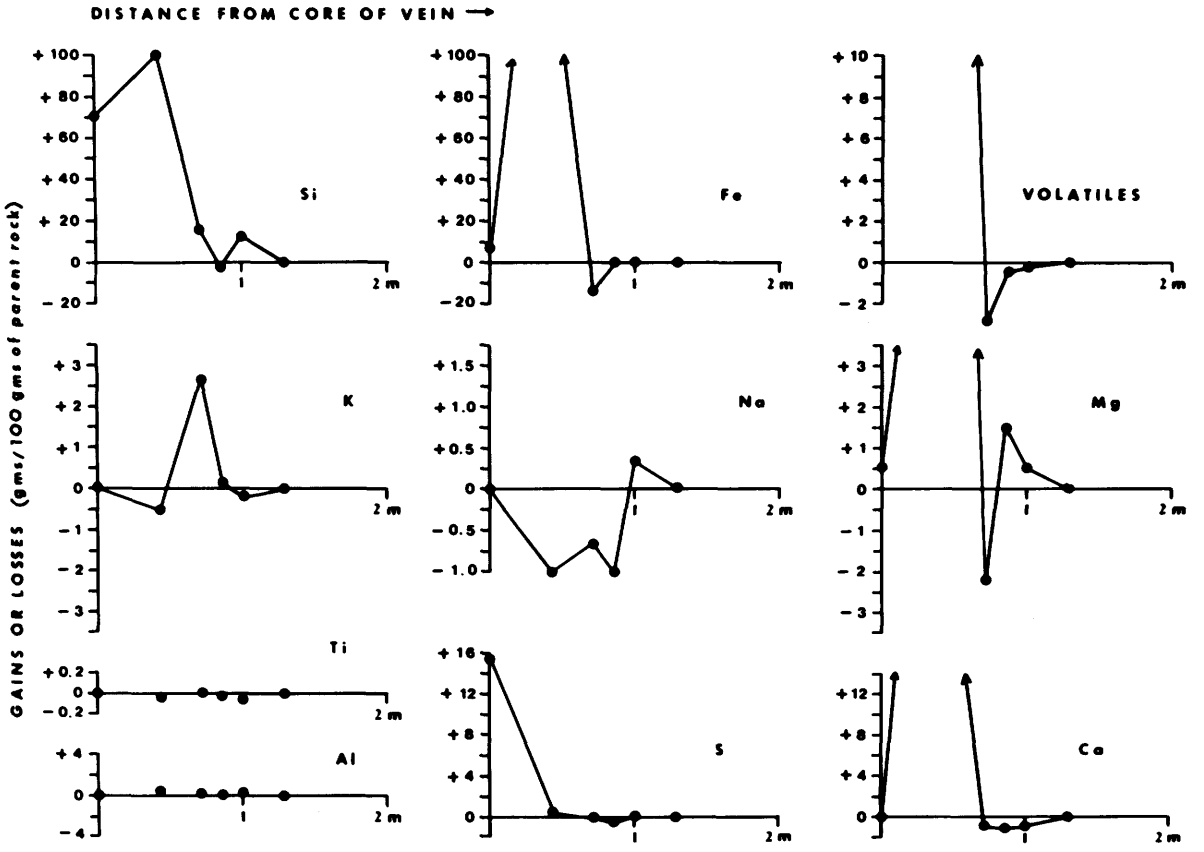

Figure 11a. *Changes in major element abundances in wallrocks about the gold-bearing vein at the Amherst mine.*

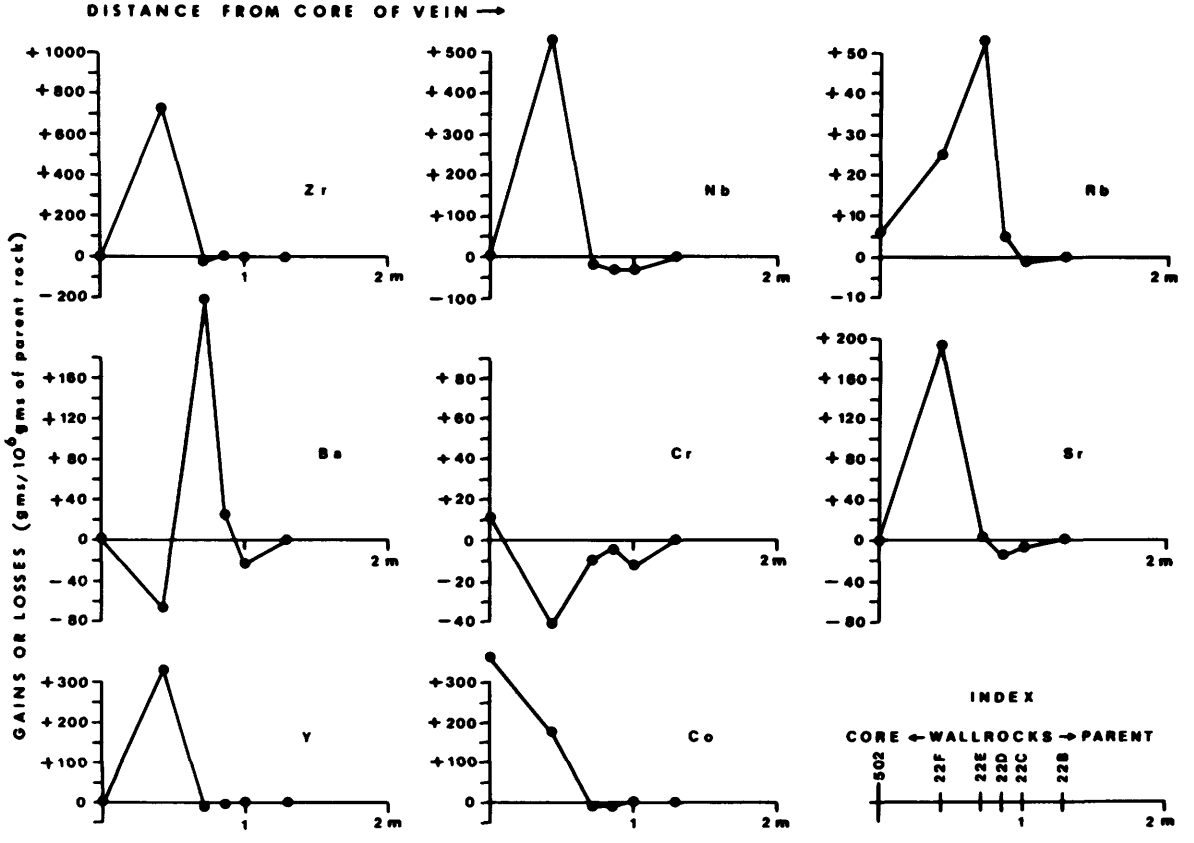

Figure 11b. *Changes in trace element abundances in wallrocks about the gold-bearing vein at the Amherst mine.*

Table 8. *Oxygen isotope composition of quartz from veins.*

PROSPECT	SPECIMEN	$\delta^{18}O_{Qtz}$ ‰	BRIEF DESCRIPTION
I) Ego Mines Cu-Au Prospects:			
Main Zone	E-30-10	14.10	Barren quartz vein.
W-8 Zone	E-27-7	12.44	Au-Cpy-Py-Qtz vein.
	E-24-3C	12.61	Cpy-Py-Qtz vein.
C Zone	E-51-3	12.77	Cpy-Py-Ank-Qtz vein.
	E-51-8	12.61	Cpy-Po-Py-Qtz vein.
II) Amherst Au Mine:			
Amherst Vein	E-50-2	12.73	Sph-Cpy-Po-Py-Qtz vein.
III) Porter-Premier Au Prospects:			
No. 1 Vein	E-36-6	11.52	Py-Qtz vein.
No. 2 Vein	E-15-4	12.56	Py-Qtz vein.

(Analyst: R. Kerrich, University of Western Ontario).

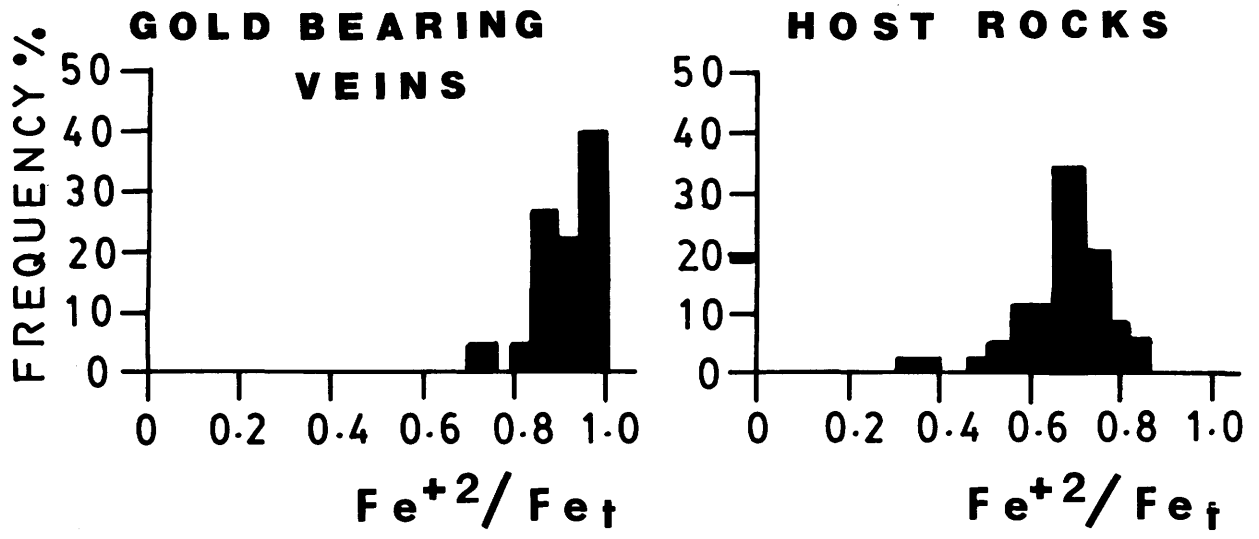

Figure 12. *Histograms for the oxidation state of iron in rocks.*

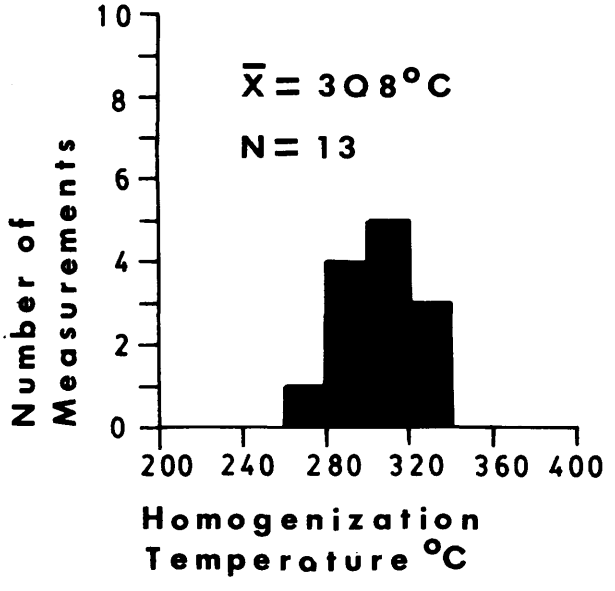

Figure 13. *Histogram for the homogenization temperatures of two-phase fluid inclusions in vein quartz.*

CONCLUSIONS

(1) The "greenstone" succession around a trondhjemite stock near Wawa is divided into two metamorphic zones: the biotite zone and the chlorite zone.

(2) The chlorite zone is of regional dimensions and has an equilibrium mineral assemblage that corresponds to the chlorite subfacies of the regional greenschist facies.

(3) The biotite zone partly envelopes the trondhjemite stock and is a contact aureole. These rocks have a dis-equilibrium mineral assemblage corresponding to an epidote-hornblende hornfels facies overprinted by the regional greenschist facies.

(4) The stock consists of trondhjemite that is overprinted by regional greenschist metamorphism, and has gold-bearing veins distributed about its margin.

(5) Gold-bearing veins transecting trondhjemite and epidote-hornblende hornfels of the stock are manifestations of retrogression by CO_2-H_2O fluids during regional greenschist metamorphism.

(6) Exploration for vein-type gold deposits should focus on greenstone successions with rapid changes in metamorphic facies. Targets for exploration are felsic intrusions with associated sulphide concentrations and with contact aureoles that are retrograded, generating magnetic anomalies which can be detected by geophysical surveys.

ACKNOWLEDGEMENTS

Gratefully acknowledged are R.W. Hodder, A.C. Colvine, R.P. Sage, and V.G. Milne for valuable discussions and assistance at various stages of the research. Special thanks are due to R. Barnett for instructions and guidance in the use of the electron microprobe; to B. McKinnon for guidance in the analyses of rocks by XRF and by wet chemistry; and to A. Noon for preparation of photographic plates.

REFERENCES

Bristol, C.C.
1974: Sphalerite Geobarometry of some Metamorphosed Orebodies in the Flin Flon and Snow Lake Districts, Manitoba; Canadian Mineralogist, Vol. 12, p. 308-315.

Bruce, E.L.
1940: Geology of the Goudreau-Lochalsh Area; Ontario Department of Mines, Annual Report Vol. 49, Pt. 3, 50p.

Eugster, H.A. and Skippen, G.B.
1967: Igneous and Metamorphic Reactions involving Gas Equilibria; p. 492-520, in Researches in Geochemistry, edited by P.H. Abelson, Vol. I, John Wiley and Sons, New York, 511p.

Gresens, R.L.
1967: Compositional-Volume Relationships of Metasomatism; Chemical Geology, Vol. 2, p. 47-65.

Hutchinson, M.N. and Scott, S.D.
1981: Sphalerite Geobarometry in the Cu-Fe-Zn-S System; Economic Geology, Vol. 76, p. 143-153.

Kerrich, R., Fyfe, W.S., and Allison, I.
1977: Iron Reduction around Gold-Quartz Veins, Yellowknife District, Northwest Territories, Canada; Economic Geology, Vol. 72, p. 657-663.

Liou, J.G., Kuniyoshi, S., and Ito, K.
1974: Experimental Studies on the Phase Relations between Greenschist and Amphibolite in a Basaltic System; American Journal of Science, Vol. 274, p. 613-632.

Miyashiro, A.
1973: Metamorphism and Metamorphic Belts; John Wiley and Sons, New York, 492p.

The Northern Miner
1974: Ego Gold Discovery Shows Real Potential; Northern Miner Press, March 7, 1974, Vol. 60.
1979: Ego is Re-evaluating Property; Northern Miner Press, October 18, 1979, Vol. 65, No. 32, p. B29.

Roedder, E.
1967: Fluid Inclusions as Samples of Ore Deposits; p. 515-574, in Geochemistry of Hydrothermal Ore Deposits, edited by H.L. Barnes, Holt, Rinehart, and Winston, N.Y., 670p.
1976: Fluid Inclusion Evidence on the Genesis of Ores in Sedimentary and Volcanic Rocks; p. 67-110, in Handbook of Stratabound and Stratiform Ore Deposits, Geochemical Studies, edited by K.H. Wolf, Vol. 2, Elsevier Publishing Company, 363p.

Schiffman, P. and Liou, J.G.
1980: Synthesis and Stability Relations of Mg-Al Pumpellyite $Ca_4Al_5MgSi_6O_{21}(OH)_7$; Journal of Petrology, Vol. 21, p. 441-474.

Scott, S.D.
1973: Experimental Calibration of the Sphalerite Geobarometer; Economic Geology, Vol. 68, p. 466-474.
1976: Application of the Sphalerite Geobarometer to Regionally Metamorphosed Terrains; American Mineralogist, Vol. 61, p. 661-670.

Studemeister, P.A.
1982: An Archean Felsic Stock with Peripheral Gold and Copper Occurrences, Abotossaway Township, District of Algoma, Ontario; unpublished Ph.D. Thesis, University of Western Ontario, London, Ontario.

Studemeister, P.A. and Colvine, A.C.
1978: Geology and Mineralization of the Gutcher Lake Stock; p. 218-221, in Summary of Field Work, 1978, edited by V.G. Milne, O.L. White, R.B. Barlow, and J.A. Robertson, Ontario Geological Survey, Miscellaneous Paper 82, 233p.

Taylor, H.P.
1967: Oxygen Isotope Studies of Hydrothermal Deposits; p. 109-142, in Geochemistry of Hydrothermal Ore Deposits, edited by H.L. Barnes, Holt, Rinehart, and Winston, New York, 670p.

Turner, F.J.
1981: Metamorphic Petrology: Mineralogical, Field, and Tectonic Aspects; 2nd edition, McGraw-Hill Book Company, New York, 524p.

Grant 124 Model Studies of Electromagnetic Prospecting

G.F. West
Department of Physics, University of Toronto

ABSTRACT

The purpose of this program is to use computer and analogue methods for modelling the response characteristics of electromagnetic (EM) prospecting systems. This is done to improve the capability of EM mineral prospecting methods for searching the Earth more deeply for prospective targets and for the separation of these targets from geological "noise". The analogue scale modelling apparatus developed under Ontario Geoscience Research Grant 8 has been used both for academic and industrial applications. Improvements in computer modelling programs have followed two different, but complementary, directions. The first direction is the development of new modelling routines capable of simulating the EM responses of complex geological targets. The second direction is aimed at making these routines more quickly available and more easily accessible to the geophysical community. This is being done by developing a standardized input/output routine, a graphics package, and a data archival system.

INTRODUCTION

The purpose of this research program is to improve understanding of the response characteristics of EM systems to deeply buried conductors, and to improve the ability to differentiate between geological "noise" and conductive mineralization. This research is being carried out by companies using the analogue modelling facilites, and by A. Dyck, J. Macnae, P. Walker and M. Bloore of the Department of Physics. Detailed results are being published in the "Research in Applied Geophysics" series of the Geophysics Laboratory, University of Toronto.

MODELLING FACILITIES

SCALE MODEL LABORATORY[1]

The scale model laboratory established in late 1970s at the University of Toronto has seen moderate use in both research and industrial applications. During the summer of 1981, the tank was in almost continuous use for the generation of model profiles by M. Vallée (1981) for his research. Subsequent to this the facility has been used extensively by both Crone Geophysics Limited and by Lamontagne Geophysics Limited. Crone Geophysics used the facility for modelling the response of a borehole PEM system to complex conductors and as an aid in interpretation of anomalies detected in the Noranda area of Quebec. Lamontagne Geophysics used it for type curve generation of conductor models not possible by using existing computer programs.

A current problem limiting the use of the modelling facility is that approximately one week of training by University of Toronto staff has been required before a new operator can effectively use the apparatus. This has deterred several potential industrial users from running models. To date, the model facility has been used for theses by four students, and five industrial projects have been completed.

STANDARDIZATION OF COMPUTER MODELLING PROGRAMS[2]

Interpretation of EM data by trial and error fitting of models through interactive computing is a viable alternative to curve matching with a suite of previously prepared responses. Modelling techniques will be useful to the geophysicist-at-large only when he is guaranteed the type of access which will render this approach convenient and cost-effective. The VAX computer programs PLATE and SPHERE, are recent examples of what can be done on a mainframe computer, but what is really required is a more general scheme which transcends the use of just these two models. Alternatively, microcomputer implementations are useful in certain situations, but are necessarily hampered by speed and memory limitations. Work in progress at the University of Toronto (in co-operation with the Geological Survey of Canada) is concerned with extending the EM modelling capabilities on the VAX with a general purpose input/output package which is sufficiently flexible to accommodate existing programs as well as future software developments. Features of the package will include: (1) a standard system for parameter input and result output which is independent of the model and prospecting technique; (2) flexible graphics output; (3) a data archiving system; and (4) a standard system for remote communication with microcomputers.

Features (1) and (3) already have been implemented. The data, comprising a parameter or result file, is

[1]By G.F. West, M. Bloore, J. Macnae.
[2]By A.V. Dyck, M. Bloore.

described by the user in a simple, high-level form, and then Fortran subroutines to read and write the file are generated automatically. These subroutines may be compiled and incorporated into a program. Each subroutine reads or writes a group of related data items, so many input/output statements may be replaced with a single call. Each file is internally titled to identify the description which goes with it and data is stored in a compact form to conserve space in archival storage.

The next step will be a general plotting package which will read data and description files and produce plots according to a standard form, defined in the description file, or to the user's individual specifications. Plotting directions may be stored in the data description file, in a separate plot description file, or may be obtained interactively. These directions will include the content and placement of titles, the type, position, and labeling of axes, and the selection of data items and array slices to plot. This data selection facility will be extended to allow creation, examination and modification of files. A parameter file description, for example, might contain default values for its items, and when a file is generated from it, the user could change some of these to produce new input to a program.

COMPUTER MODELLING[1]

Work has been done on extending the applicability of the thin plate modelling program, PLATE (Dyck *et al.* 1980), to more complex geological configurations. The method used is based on the one pioneered by Annan (1974), in which the current distribution of the plate is approximated by an arbitrary number of trial functions. The work done here has been directed primarily at solving for the response of more than one thin plate and at solving for the inductive response of a thin plate embedded within a horizontally stratified space (Walker 1981). To this end, some of the subroutines used in PLATE have been rewritten and improved in order to reduce computational errors. A program which computes the interactions between two plates has been written and tested. The results produced by this program were found to concur with those produced in the scale model laboratory (Figures 1, 2, and 3) for weak and moderate interactions. For configurations in which strong interactions were present, problems resulted. These problems were caused partly because of conditioning problems, and partly because not enough trial functions were included to properly account for the coupling. Similar problems also occur in PLATE when sources or receivers are placed very close to the conductor.

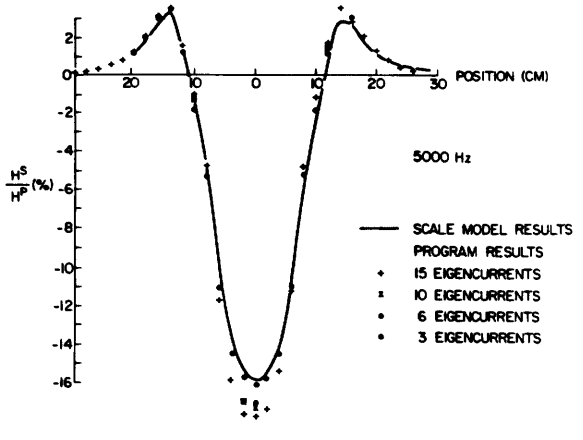

Figure 1. *A comparison of the in-phase anomaly for two plates produced by the program and from scale model experiments.*

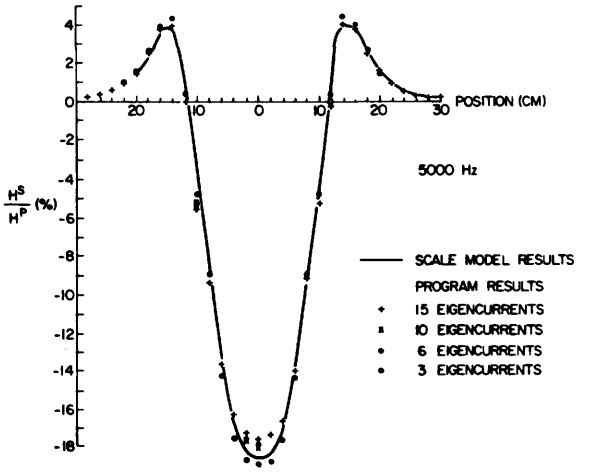

Figure 2. *A comparison of the quadrature anomaly for two plates produced by the program and from scale model experiments.*

To rectify this problem and to enhance the flexibility of the model, the problem is being reformulated by invoking the finite element method. By using this method, many more trial functions can be included in the solution of the problem than is practical by using the present formulation. This should allow the fields close to the plate to be computed more accurately, and allow strong interactions between plates to be more accurately determined. The finite element method will also make it possible to model the responses of nonrectangular planar objects in addition to rectangular objects which are now being modelled.

A program which computes the response of a thin plate in a stratified space has also been written but has been found to be impractical. The problem with the program is that the Green's functions for the problem required lengthy computation, and because of this, the time required to generate any results is formidable. However, in solving this problem, a program which computes both

[1]By P. Walker.

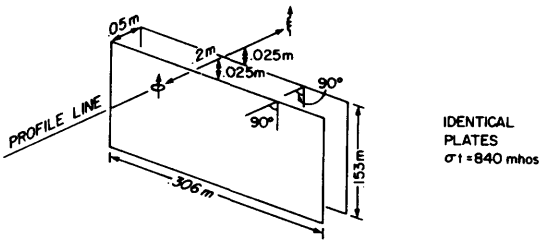

Figure 3.*HLEM configuration used to compare the results of the program with scale model experiments for multiple conductors.*

electric and magnetic fields due to dipole electric and magnetic sources anywhere within a layered earth was written. This program has been extended by Scott Holladay to include the effects of anisotropic media and both routines have been useful for checking results of less general stratified Earth routines.

J. Hanneson's (1981) program which calculates the response of a thin sheet in a conductive host medium has been used during the past year to compute phasor diagrams for HLEM interpretations for Gulf Minerals Limited.

RESEARCH IN APPLIED GEOPHYSICS SERIES

The research sponsored by the Ontario Geological Survey in Grant 8 (now completed) and in Grant 124 (this report) is made available to the public in a series of reports: the Research in Applied Geophysics series of the Geophysics Laboratory, University of Toronto. During the last year, over six hundred copies of these reports were ordered and delivered to companies and individuals outside the University.

REFERENCES

Annan, A.P.
1974: The Equivalent Source Method for Electromagnetic Scattering Analyses and its Geophysical Applications; unpublished Ph.D. thesis, Memorial University of Newfoundland, 242p.

Dyck, A.V.
1981: A Method for Quantitative Interpretation of Wideband Drill-Hole EM Surveys in Mineral Exploration; Research in Applied Geophysics, No. 23, Geophysical Laboratory, University of Toronto.

Dyck, A.V., Bloore, M., Vallée, M.A.
1980: User Manual for Programs Plate and Sphere; Research in Applied Geophysics, No. 14, Geophysical Laboratory, University of Toronto.

Hanneson, J.E.
1981: The Horizontal Loop EM Response of a Thin Vertical Conductor in a Conducting Half Space; Research in Applied Geophysics, No. 19, Geophysics Laboratory, University of Toronto.

Vallée, M.-A.
1981: Scale Models on Transient Response of Multiple Conductors; Research in Applied Geophysics, No. 20, Geophysics Labratory, University of Toronto.

Walker, P.
1981: The Inductive Response of Thin Plates in a Stratified Space; Research in Applied Geophysics, No. 21, Geophysics Laboratory, University of Toronto.

Grant 62 Direct Dating of Ore Minerals

Derek York[1], A. Masliwec[1], C.M. Hall[1], P. Kuybida[1], W.J. Kenyon[1], E.T.C. Spooner[2], and S.D. Scott[2]

[1]Department of Physics, University of Toronto
[2]Department of Geology, University of Toronto

ABSTRACT

Pyrite appears to be the most promising of the common sulphides for direct $^{40}Ar/^{39}Ar$ age analysis. Geco Mine pyrites, on an argon isotope correlation plot, give an age of 2.5 ± 0.1 Ga, in agreement with ages on associated micas. Mississippi Valley Type (MVT) pyrites show a strong linear correlation on such a plot, but with greater scatter than would be due solely to experimental error. The easiest interpretation, however, is that the MVT deposit was formed prior to about 450 Ma ago. A laser-probe dating device has been developed which greatly speeds up age analysis. When this is linked up in the near future with an ultra-sensitive new mass spectrometer, it should be far easier technically to determine the ages of a variety of sulphides.

INTRODUCTION

One of the most difficult problems in geochronology is the precise dating of sulphide ore deposits. Usually the approach adopted would be to date silicate material presumed to be cogenetic with the ore (Kinkel *et al.* 1965). However, since such material is not always available, and since it is by no means always clear that the silicates and ore minerals are in fact contemporaneous, the present project was begun to see if sulphide minerals themselves could be dated with the rapidly developing $^{40}Ar/^{39}Ar$ method.

Little other work has been done on the direct dating of sulphides. It was attempted, with some promise, by Reesman and Hurley (1968), who used the Rb-Sr method. However, no follow-up work has been reported. Recently, Luck and Allegre (1981) have shown that some deposits may be dateable with the Re-Os method. The pioneering work of Shepherd and Darbyshire (1981) on the Rb-Sr dating of fluid inclusions in quartz looks promising.

Our initial work showed that pyrites appeared to be the most useful of the common sulphides for $^{40}Ar/^{39}Ar$ dating. An argon isochron-type plot for pyrites from the Geco Mine in northwestern Ontario gave an age of 2.50 ± 0.12 Ga. This agreed, within experimental error, with the age of 2.61 ± 0.02 Ga found by $^{40}Ar/^{39}Ar$ dating of flecks of biotite found in intimate association with the ore minerals. The scatter in the pyrite data was greater than would be expected from experimental contributions alone. This result, however, was deemed to be very encouraging (York *et al.* 1982).

Because it seemed likely that, in dating a fragment of sulphide mineral, one would often really be dating mostly the fluid inclusions in the sulphides, we have developed methods of simultaneously measuring Ca and Cl concentrations as well as K and Ar contents (York *et al.* 1981b) since the K:Cl:Ca ratios should be a useful indicator of the importance of fluid inclusions.

Initial results have demonstrated that there is a distinct possibility of directly dating sulphides with the $^{40}Ar/^{39}Ar$ method. However, the results also showed that the analysis required a much greater level of skill and effort than that required for the usual dating of biotites and hornblendes. This is largely because of the extremely low levels of K and Ar in sulphides. To overcome the technical difficulties and to study fluid inclusions more specifically, we have concentrated on bringing into operation a laser probe system. The state of this development is described below. We note here that, now that the feasibility of such a continuous-laser dating probe has been demonstrated (York *et al.* 1981a), a grant of about a quarter of a million dollars has been received from the Natural Sciences and Engineering Research Council of Canada (N.S.E.R.C.) to purchase and develop an ultrasensitive mass spectrometer which will form a much-improved analyser end of the laser probe.

EXPERIMENTATION

The evolution of our experimental methods of handling sulphides has been described earlier (York *et al.* 1981b). All sulphide samples were irradiated in the McMaster University reactor along with the Zartman hornblende standard (Zartman 1964). One to two gram size samples were used and cadmium cladding was used to reduce the hazard level of the induced radioactivities. The irradiated samples were then fused in an ultra-high vacuum system and the purified argon was subsequently analyzed on an MS10 mass spectrometer. Mineral separations were performed with extreme care so that silicate contamination was removed as completely as possible.

RESULTS

The data for the MVT pyrites are shown in Table 1 and Figure 1. The data from sixteen pyrite samples, from a

single hand specimen of ore from the St. Joe mine in southeast Missouri, are shown in Figure 1 on an isotope correlation plot. If all the samples were of the same age, and if trapped initial argon was of uniform composition, and if the samples had remained closed systems, then the data points should lie, within experimental errors, on a straight line. On this type of plot, the reciprocal of the intercept on the y-axis would give the $^{40}Ar/^{39}Ar$ ratio in the argon initially trapped in the sulphides. The reciprocal of the x-intercept would give the age of the sulphides. As may be seen from Figure 1, the sulphide data are obviously linearly correlated, but are equally obviously scattered about a straight line with a significantly higher dispersion than would be expected on experimental ground alone. These pyrites clearly contain geochronological information, but the systems evidently do not satisfy the aforementioned criteria which are the prerequisites for the production of a well-defined straight line on such an isotope correlation plot. The most likely explanation of the excess scatter in Figure 1 is that the different pyrites trapped somewhat different types of argon at crystallization.

If we try to extract age information from Figure 1, we conclude that the simplest interpretation is that this MVT ore formed soon after deposition of the enclosing late Cambrian dolostones.

As anticipated in our original proposal, a continuous-laser has been set up and tested as a device for melting minerals. Using this, our methods of analysis are being revolutionized.

The first use of any kind of laser as a dating device was described by Megrue (1973). He used a pulsed ruby laser to date minute volumes of neutron-irradiated meteorites. Later, Schaeffer and his co-workers did important developmental work in showing how this approach could be used to unlock the many episodes of history which are trapped in lunar breccias (Plieninger and Schaeffer 1976). Our innovation has been to use a continuous laser (as opposed to a pulsed one) to melt the samples. We have shown that it is easier to use than a pulsed laser and has the enormous advantage that step-heating of the sample is straightforward (York *et al.* 1981a).

A Spectra-Physics, Model 171-08, 15 watt, argon-ion continuous laser was purchased for the project. The light from this is focussed, via a lens system, through the camera tube of a binocular microscope onto the sample. The sample, an irradiated mineral, is contained in a small glass tube with optically flat faces. The sample tube is attached to the mass spectrometer inlet system (Figure 2), so that as the laser power is increased, the evolved gases may be passed through a titanium sponge getter and the argon may be leaked into the mass spectrometer for analysis.

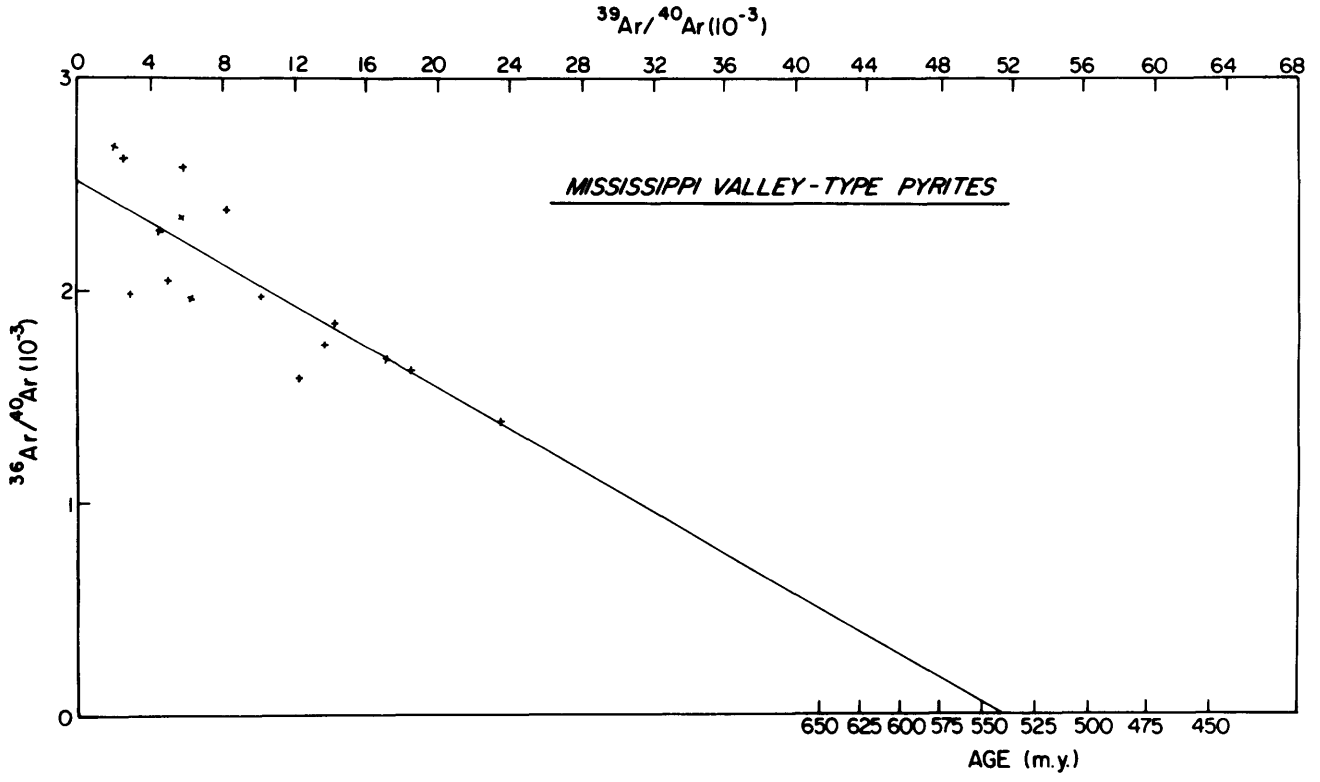

Figure 1. *Argon correlation plot for MVT pyrites.*

Table 1. *Analytical data for Mississippi Valley type pyrite.*

Sample No.	K(p.p.m.)	$^{36}Ar(10^{-10}cc/gm)$	$^{40}Ar/^{36}Ar$
OGS17	78.10	15.9	509
OGS19	23.62	13.7	437
OGS45	19.70	14.2	382
OGS46	102.30	17.0	567
OGS92	113.00	16.4	576
OGS93	71.60	32.8	428
OGS96	114.10	7.3	542
OGS130	431.2	19.8	712.8
OGS135	352.3	26.9	579.8
OGS136	45.5	12.2	484.7
OGS137	64.6	33.9	505.7
OGS138	533.8	40.9	599.1
OGS142	89.5	21.9	528.9
OGS143	22.9	25.7	369.7
OGS144	115.3	27.9	428.0
OGS145	26.4	30.1	463.4

It has been shown to be a simple matter to melt micas, hornblende, and slate with this laser. With the arrangement shown in Figure 2, it is straightforward to bring a variety of sample grains successively under the laser beam, degas them and hence date them. Through protective goggles, it is possible to observe samples down the microscope and see them melt as the laser power is increased.

The laser has been brought into the orebody dating project initially for the dating of silicate materials. Muscovite and slate samples from the Kidd Creek Mine, near Timmins, were melted with the laser. Three laser fusions were carried out on the irradiated mica, so that three ages were obtained. Only one grain of muscovite (0.5-1.0 mm size) was melted in each run. As a comparison, two other fusions were carried out on the same mica using the usual radio-frequency fusion system. The results (Table 2) show that, within expected experimental errors, the much more rapidly obtained laser dates agree completely with the more conventionally determined ages. An age of about 2.6 Ga is indicated for the last cooling of the Kidd Creek deposit.

Step-heating is an important tool in $^{40}Ar/^{39}Ar$ dating. We have been able to show that with the laser it is straightforward to get $^{40}Ar/^{39}Ar$ age spectra information via step-heating. With the power level set at 1 watt, the laser beam was focussed to a beam spot size of roughly 600 μm and shone onto a chip (≅ 3 mm) of slate from the Kidd Creek mica. After five minutes of this heating, the $^{40}Ar/^{39}Ar$ ratios in the gases evolved were measured. This procedure was then repeated with laser power settings of 1.5, 2.0 and 2.65 watts. The results are shown in Figure 3 where the laser age spectrum is compared with two spectra obtained in the usual way by radiofrequency heating. It is clear that the agreement is complete within expected experimental errors. These results substantiate the muscovite data, referred to earlier, that indicated the last cooling of the Kidd Creek deposit occurred about 2.6 Ga ago.

One way of checking orebody ages is to date alteration products (if they are available) formed by the ore-bearing solutions. The clay mineral illite is one such alteration product. To test whether reliable $^{40}Ar/^{39}Ar$ ages can be obtained rapidly and reliably on such material with the

laser, we have carried out laser step-heating analyses of illite from McClean Lake formed by the uranium-bearing ore-forming fluids. The result is illustrated in Figure 4, in which a very convincing age spectrum indicates that this illite was formed approximately 1.32 Ga ago, suggesting strongly that this is the original age of formation of the uranium deposit. This agrees well with the estimate of Cumming and Rimsaite (1978) which was based on U-Pb dating of uranium-bearing minerals. The illite turned out to be particulary easy to date, having lots of radiogenic argon which is clearly strongly held, yet having extremely small amounts of contaminating argon (initial or modern atmospheric), judging by its very low ^{36}Ar content.

SUMMARY

Our research so far has shown the following:

(1) The most promising sulphides for direct dating by the $^{40}Ar/^{39}Ar$ approach are pyrites.

(2) Contaminating argon, with a $^{40}Ar/^{36}Ar$ ratio very different from modern atmospheric composition, is found in pyrites. Isochron-type plotting is therefore essential to remove the effects of this contamination.

Table 2. *Comparison of age data for Kidd Creek muscovite, determined using laser and radio-frequency heating.*

Analysis	$^{40}Ar^*/^{39}Ar$	Age (b.y.)
R. F. fusion	578±4	2.64±0.01
	562±8	2.60±0.02
Laser	561±7	2.60±0.02
(Single grain)	540±47	2.55±0.12
	550±9	2.57±0.02

$^{40}Ar^*$ = radiogenic ^{40}Ar.

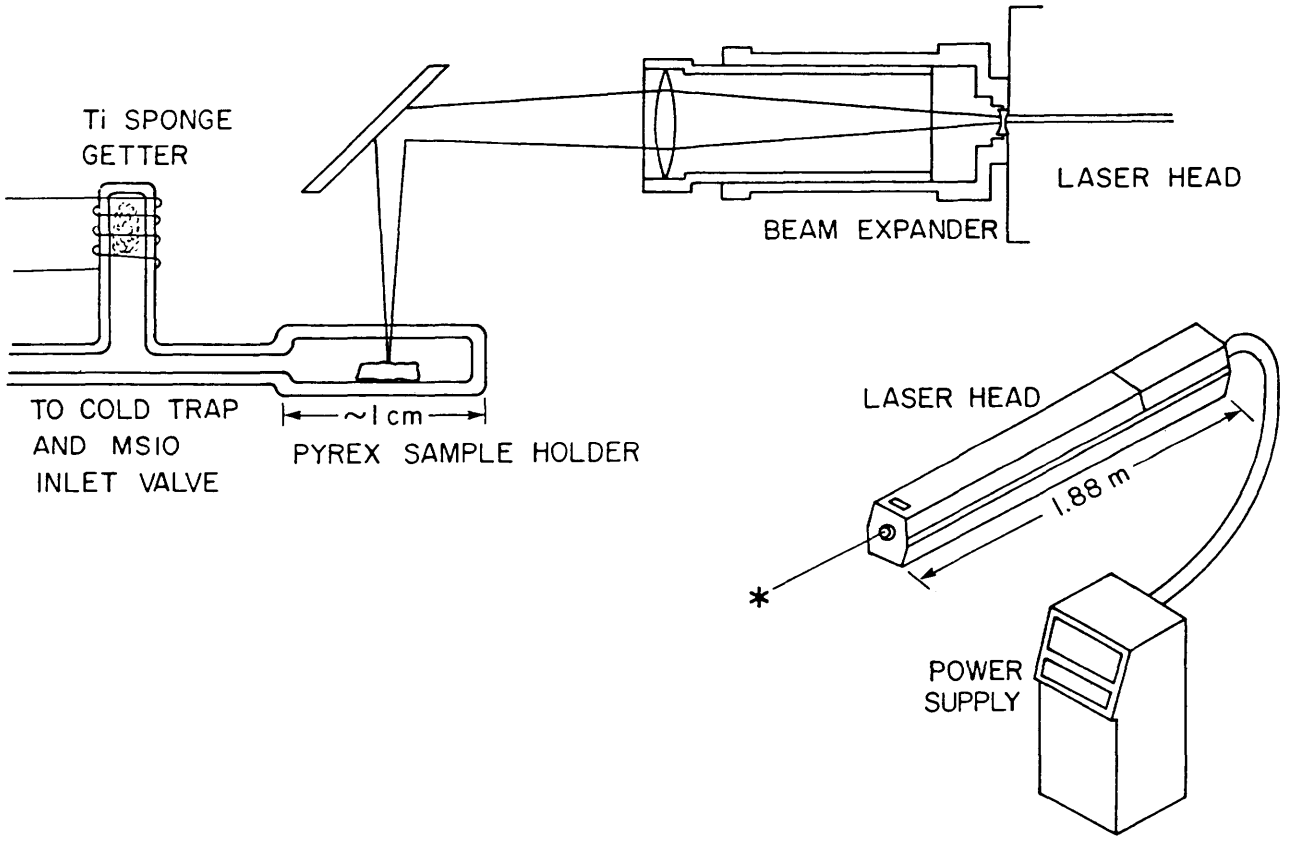

Figure 2. *Laser fusion system. In the present version, the laser light beam passes through the camera tube of a binocular microscope onto the sample.*

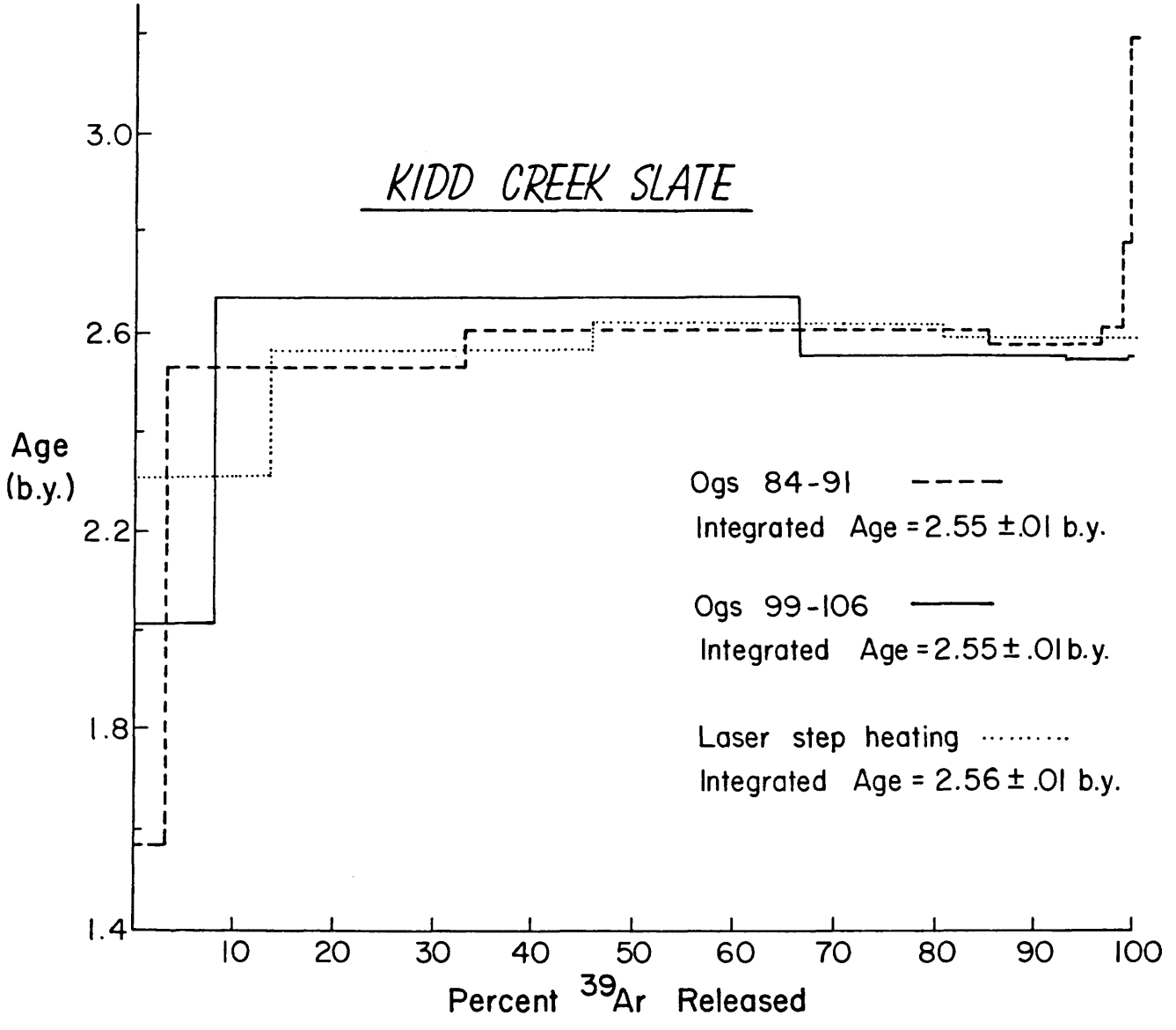

Figure 3. *Laser step-heating age spectrum of the Kidd Creek slate compared with the spectra produced in two runs done by conventional radio-frequency heating.*

(3) While Geco Mine pyrites gave the correct age for the deposit, within reasonable experimental error, the MVT pyrites displayed too much scatter about an isochron-type line to be unequivocally dated. However, the data suggest that this southeast Missouri deposit formed prior to 450 Ma ago. It is clear that these pyrites possess definite geochronological information and more analyses might well produce data with significantly less scatter.

(4) The continuous-laser probe dating system has been shown to be easy to use. It enables ages to be obtained far more quickly than can be done in the usual way with a radio-frequency heater. The continuous nature of the laser enables one to perform step-heating runs in a simple, rapid way. Most importantly, it can be used as a milliprobe dating device.

(5) With the aid of a new N.S.E.R.C. major equipment grant which has been received, a new ultra-sensitive mass spectrometer will be developed as an integral part of the laser-probe system. This will convert the present device from a milliprobe to a microprobe dater.

(6) It appears to be straightforward to date illite and it may be possible to make good estimates of ore-deposition age when such a clay mineral is available as an ore-fluid induced alteration product.

(7) We conclude that pyrites, at least, hold out very good prospects for direct dating. However, the low argon concentrations mean that sophisticated measuring techniques are required. With the one-hundred-fold increase in sensitivity that we will have with our new system, it should be possible to analyze sulphides in the near future with the same ease technically as one now can deal with biotites and hornblendes.

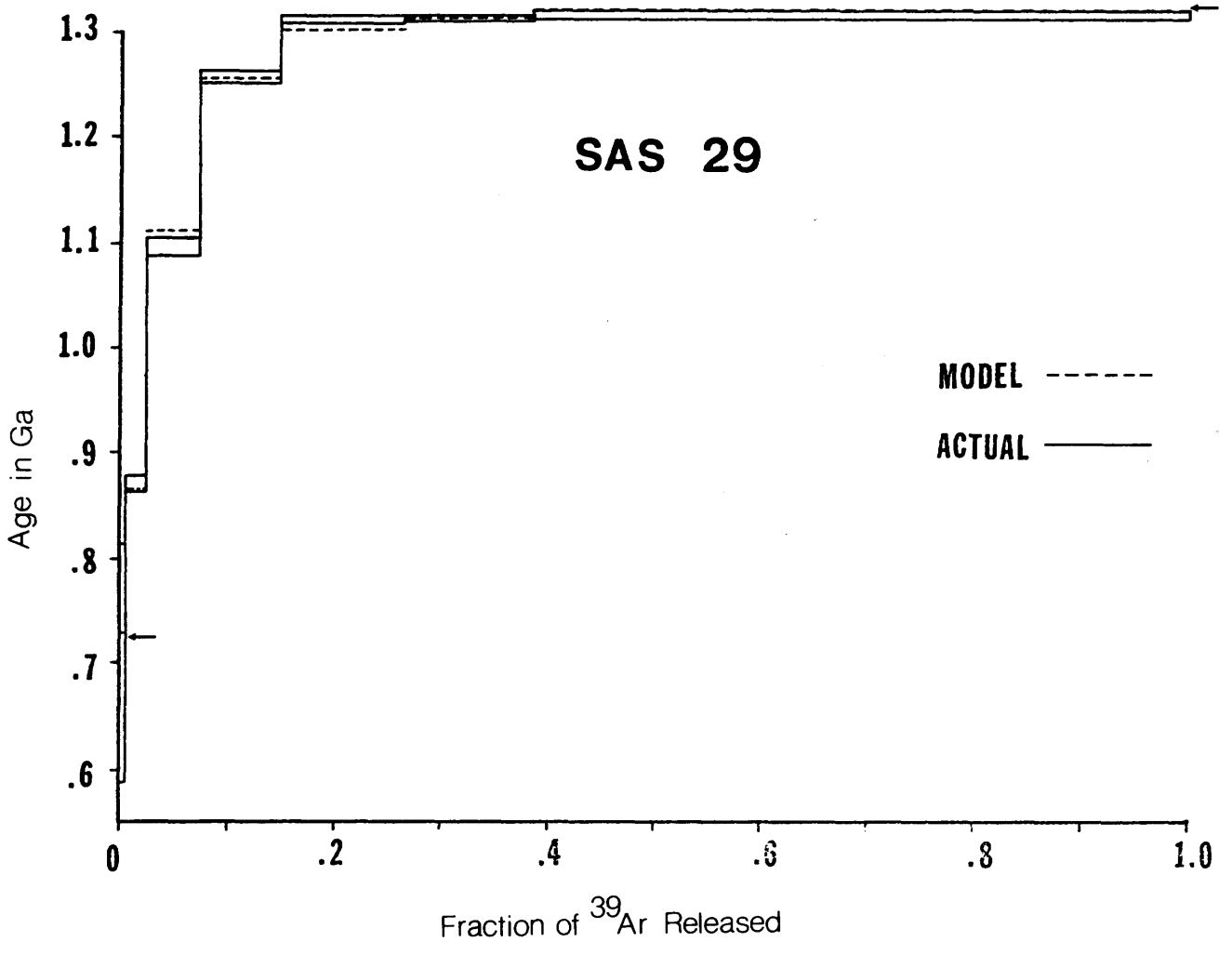

Figure 4. *Laser-derived age spectrum for McClean illite.*

ACKNOWLEDGMENTS

This ore-dating project is principally funded by the Ontario Geoscience Research Grant Program, but is also significantly supported by N.S.E.R.C. grants. We are indebted to Drs. F.W. Beales and P. Coad for provision of some samples. The McMaster University reactor personnel were extremely helpful with all irradiations.

REFERENCES

Cumming, G.L. and Rimsaite, J.
1979: Isotopic Studies of Lead-Depleted Pitchblende, Secondary Radioactive Minerals and Sulphides from the Rabbit Lake Uranium Deposit, Saskatchewan; Canadian Journal of Earth Sciences, Vol. 16, p. 1702-1715.

Kinkel, A.R., Thomas, H.H., Marvin, R.F., and Walthall F.G.
1965: Age and Metamorphism of some Massive Sulfide Deposits in Virginia, North Carolina and Tennessee; Geochimica et Cosmochimica, Vol. 29, p. 717-724.

Luck, J.M. and Allegre, C.J.
1981: $^{187}Re/^{187}Os$ Dating of Molybdenites; EOS Translations, American Geophysical Union, Vol. 62, p. 430.

Megrue, G.H.
1973: Spatial Distribution of $^{40}Ar/^{39}Ar$ Ages in Lunar Breccia 14301; Journal of Geophysical Research, Vol. 78, p. 3216-3221.

Plieninger, T., and Schaeffer, O.A.
1976: Laser Probe $^{39}Ar/^{40}Ar$ Ages of Individual Mineral Grains in Lunar Basalt 15607 and Lunar Breccia 15465; Proceedings 7th Lunar Science Conference, Vol. 2, p. 2055-2066.

Reesman, R.H. and Hurley, P.M.
1968: The Rb-Sr Analyses of some Sulfide Mineralization; Earth and Planetary Science Letters, Vol. 5, p. 23-26.

Shepherd, T.J. and Darbyshire, D.P.F.
1981: Fluid Inclusion Rb-Sr Isochrons for Dating Mineral Deposits; Nature, Vol. 290, p. 578-579.

York, D., Hall, C.M., Yanase, Y., Hanes, J.A., and Kenyon, W.J.
1981a: $^{40}Ar/^{39}Ar$ Dating of Terrestrial Minerals with a Continuous Laser; Geophysical Research Letters, Vol. 8, No. 11, p. 1136-1138.

York, D., Masliwec, A., Hall, C.M., Kuyibida, P., Kenyon, W.J., Spooner, E.T.C., and Scott, S.D.
1981b: The Direct Dating of Ore Minerals; Grant 62, p. 334-340 in Geoscience Research Grant Program, Summary of Research 1980-81, edited by E.G. Pye, Ontario Geological Survey, Miscellaneous Paper 98, 340p.

York, D., Masliwec, A., Kuybida, P., Hanes, J.A., Hall, C.M., Kenyon, W.J., Spooner, E.T.C., and Scott, S.D.
1982: $^{40}Ar/^{39}Ar$ Dating of Pyrite; submitted to Nature.

Zartman, R.E.
1964: A Geochronologic Study of the Lone Grove Pluton from the Llano Uplift, Texas; Journal Petrology, Volume 5, p. 359-409.

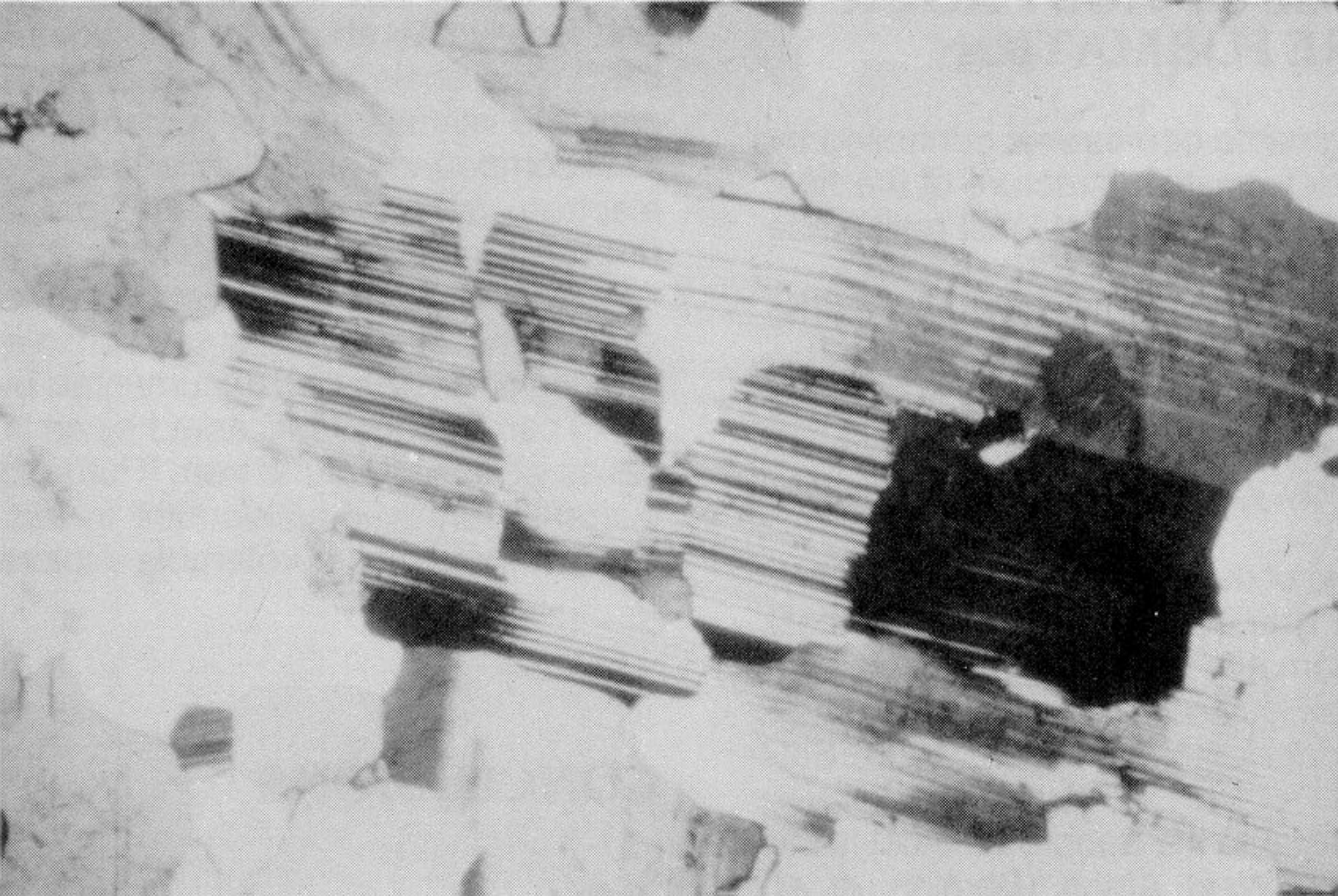

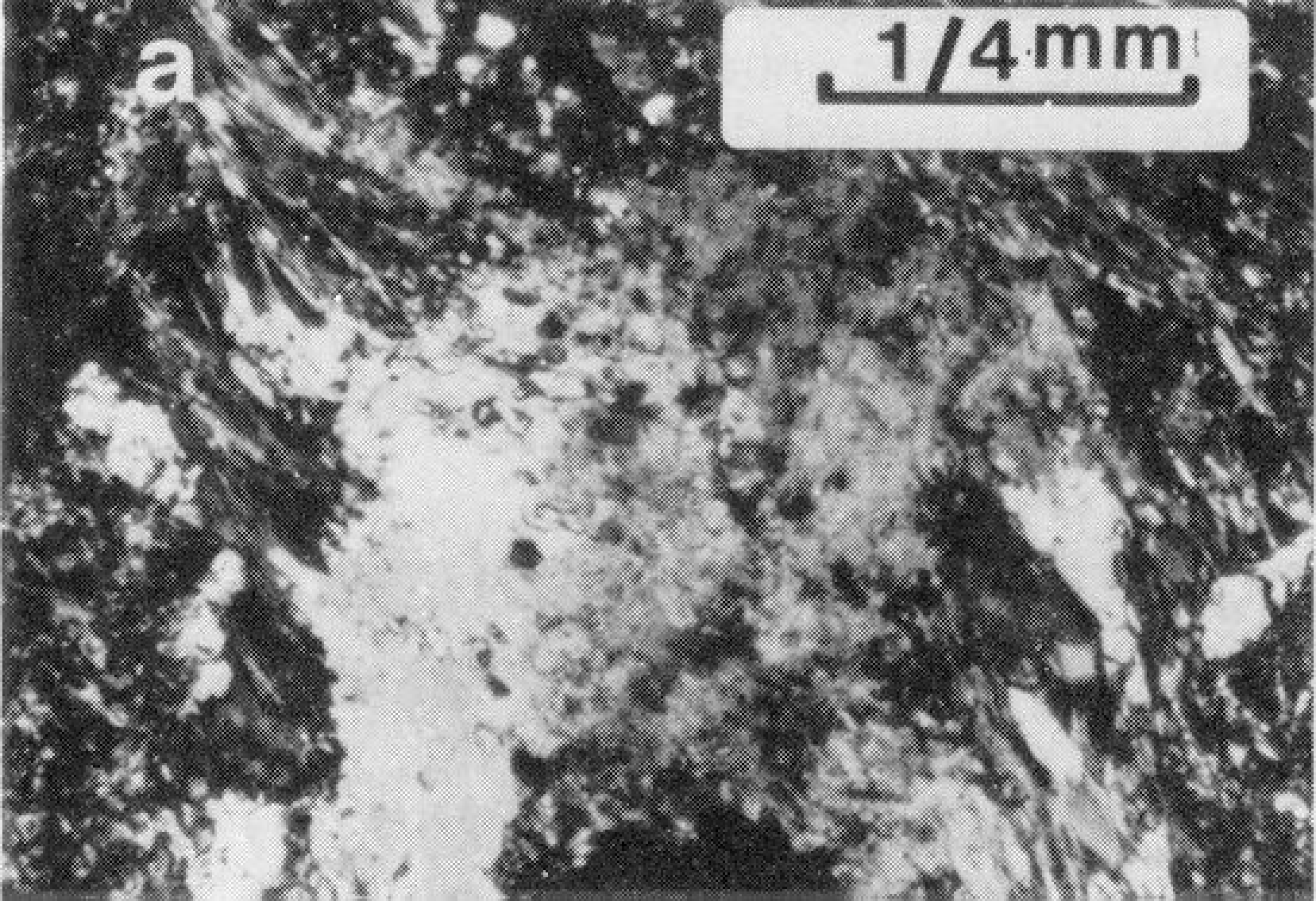
a
1/4 mm

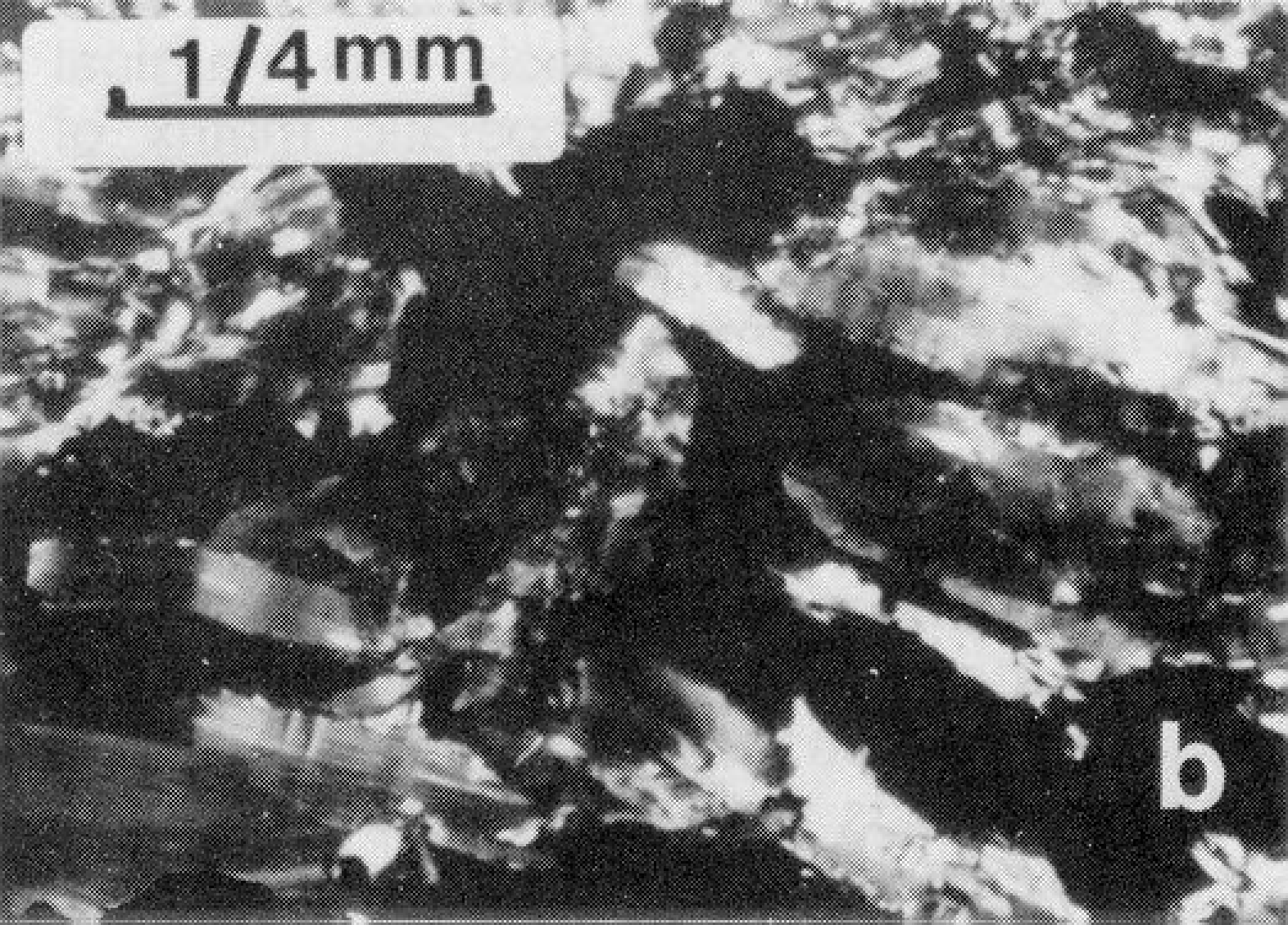
1/4 mm
b

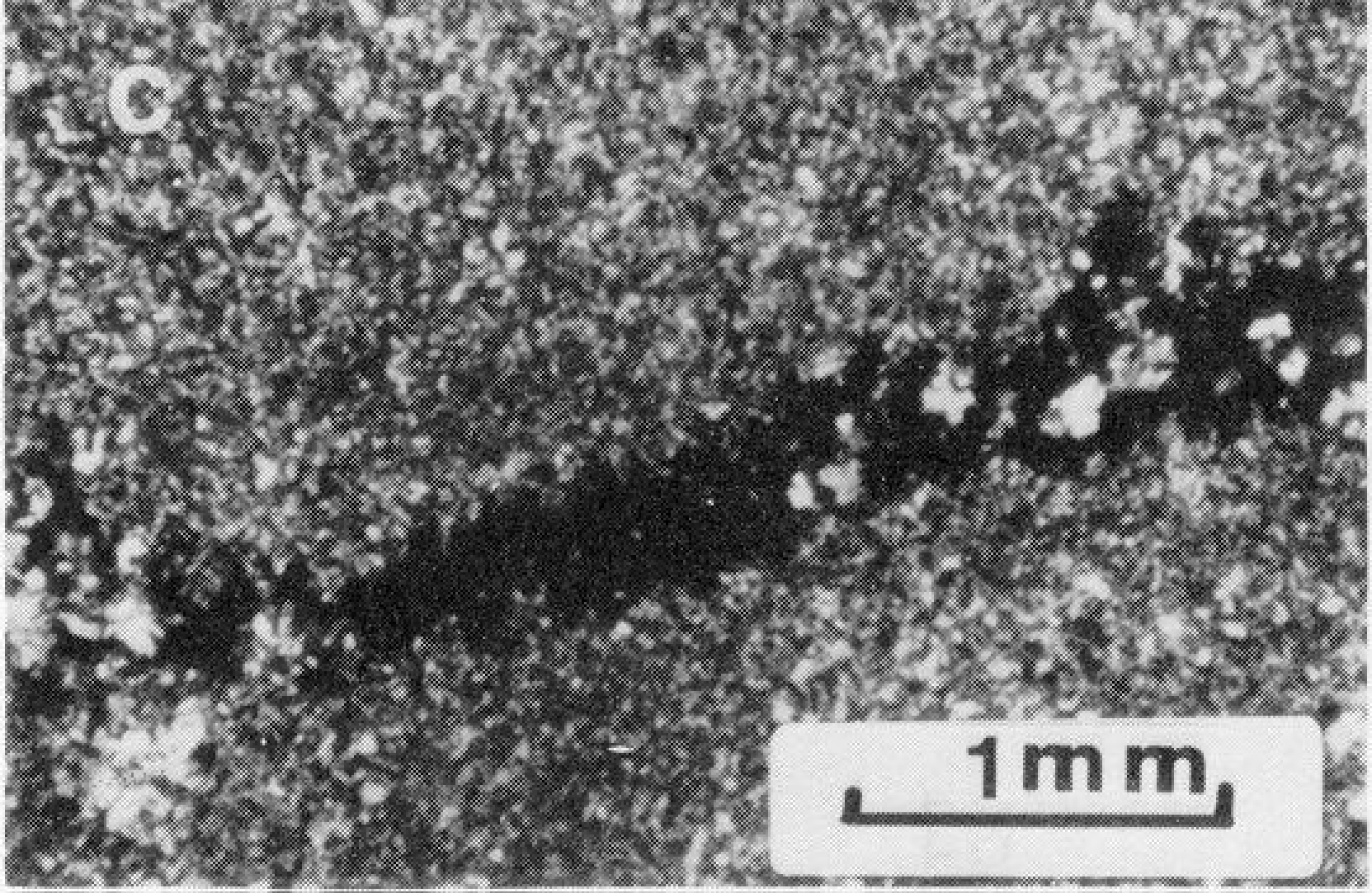
C
1mm

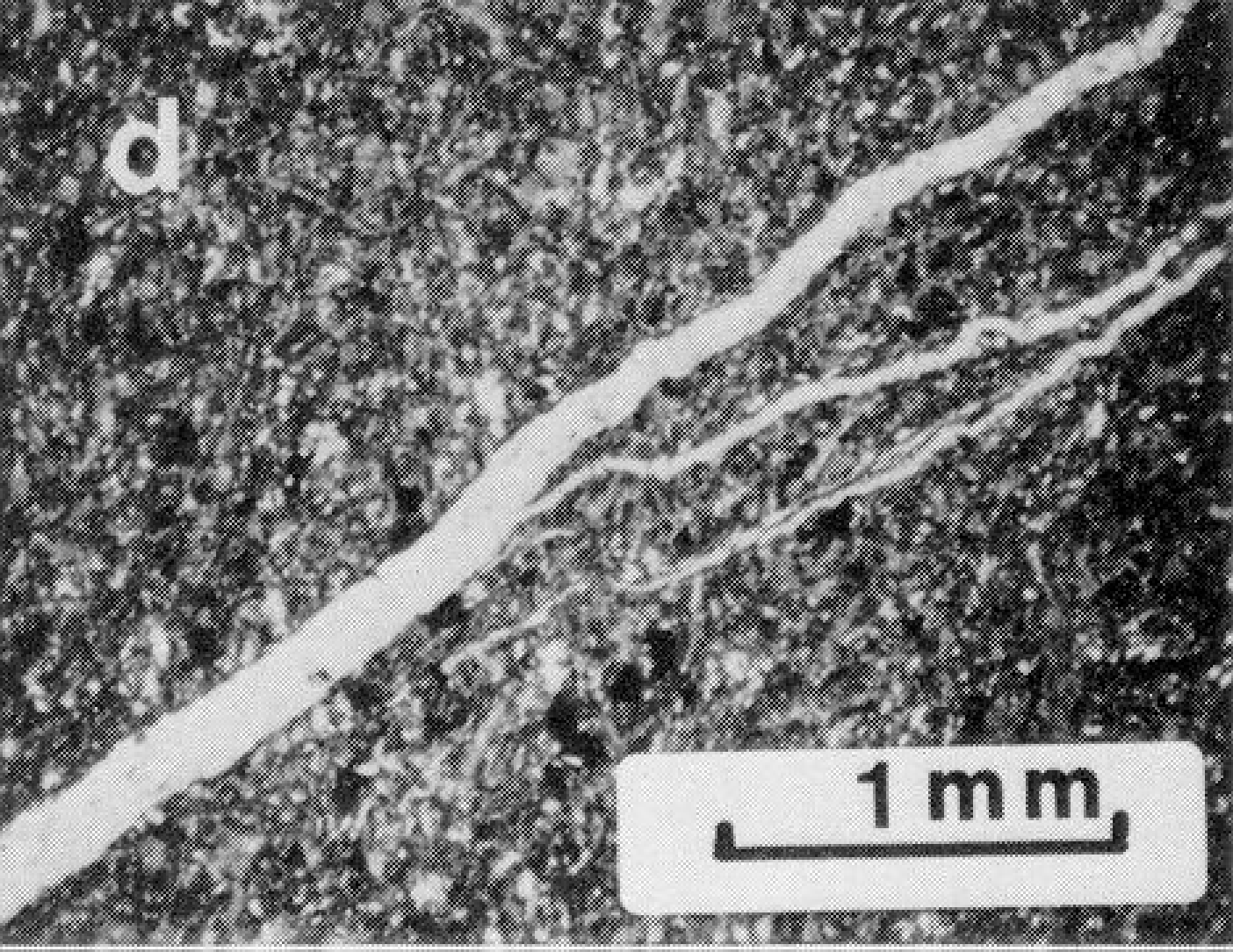
d
1 mm

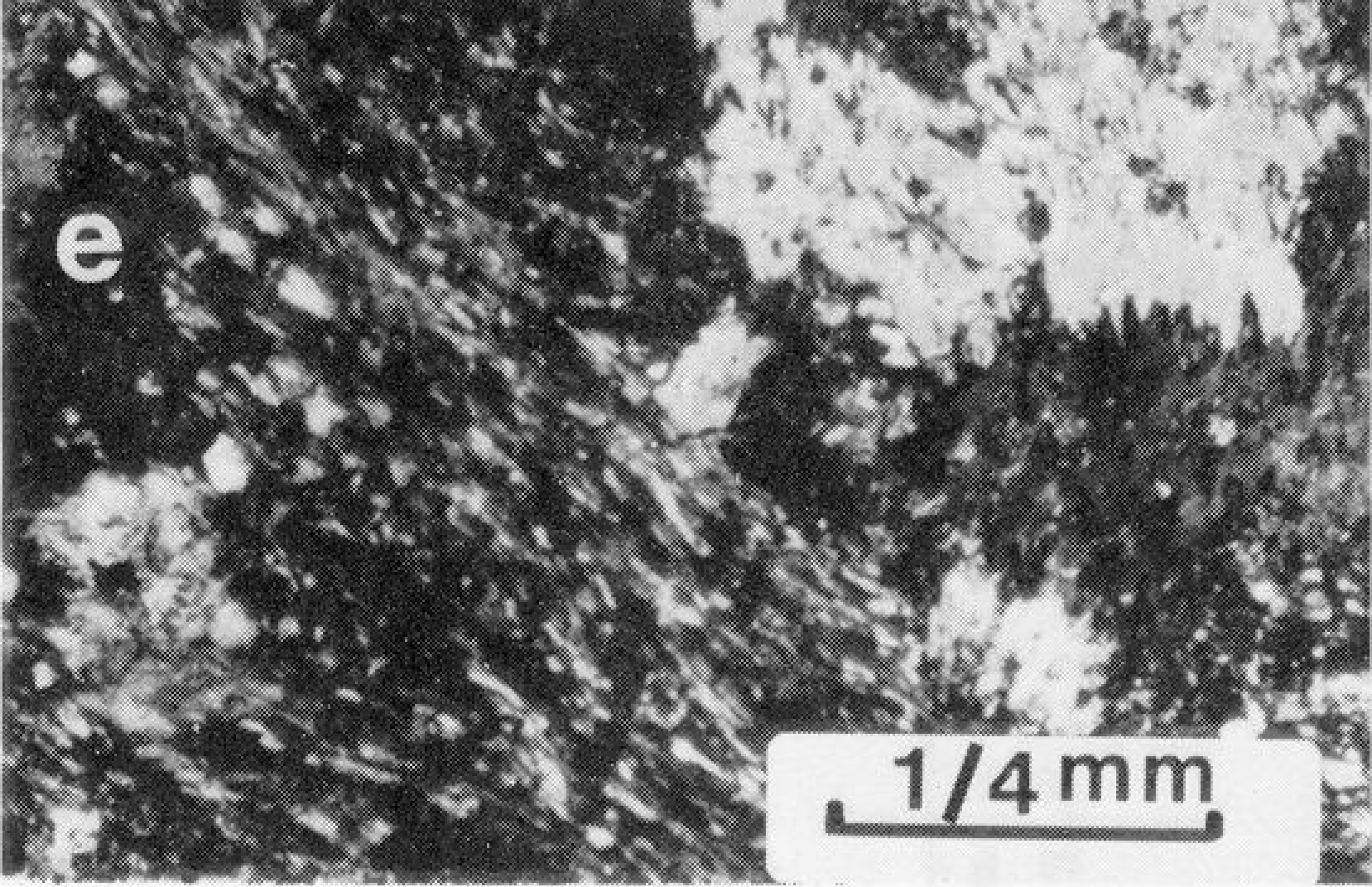
e
1/4 mm

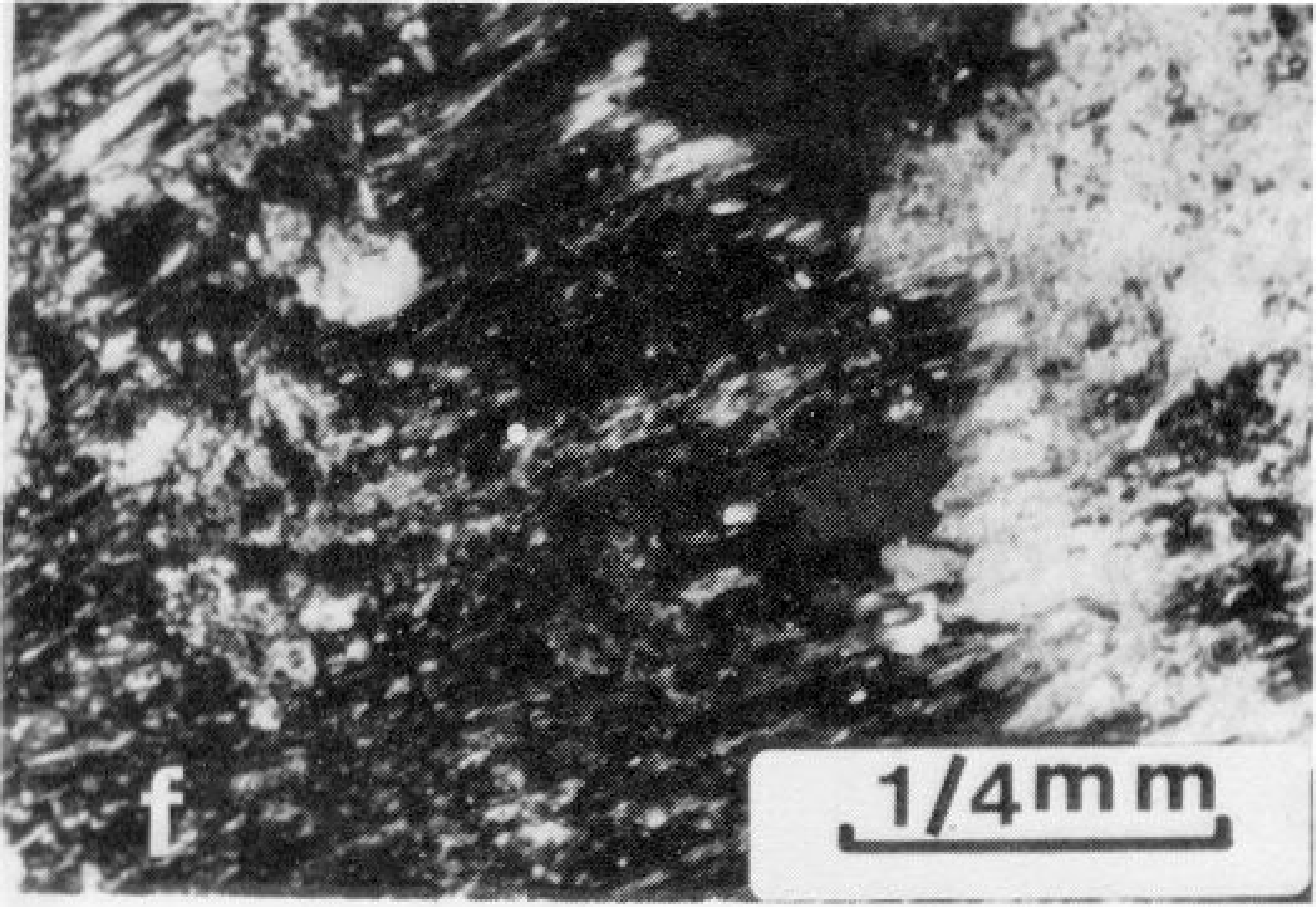
f
1/4mm

a
1 mm

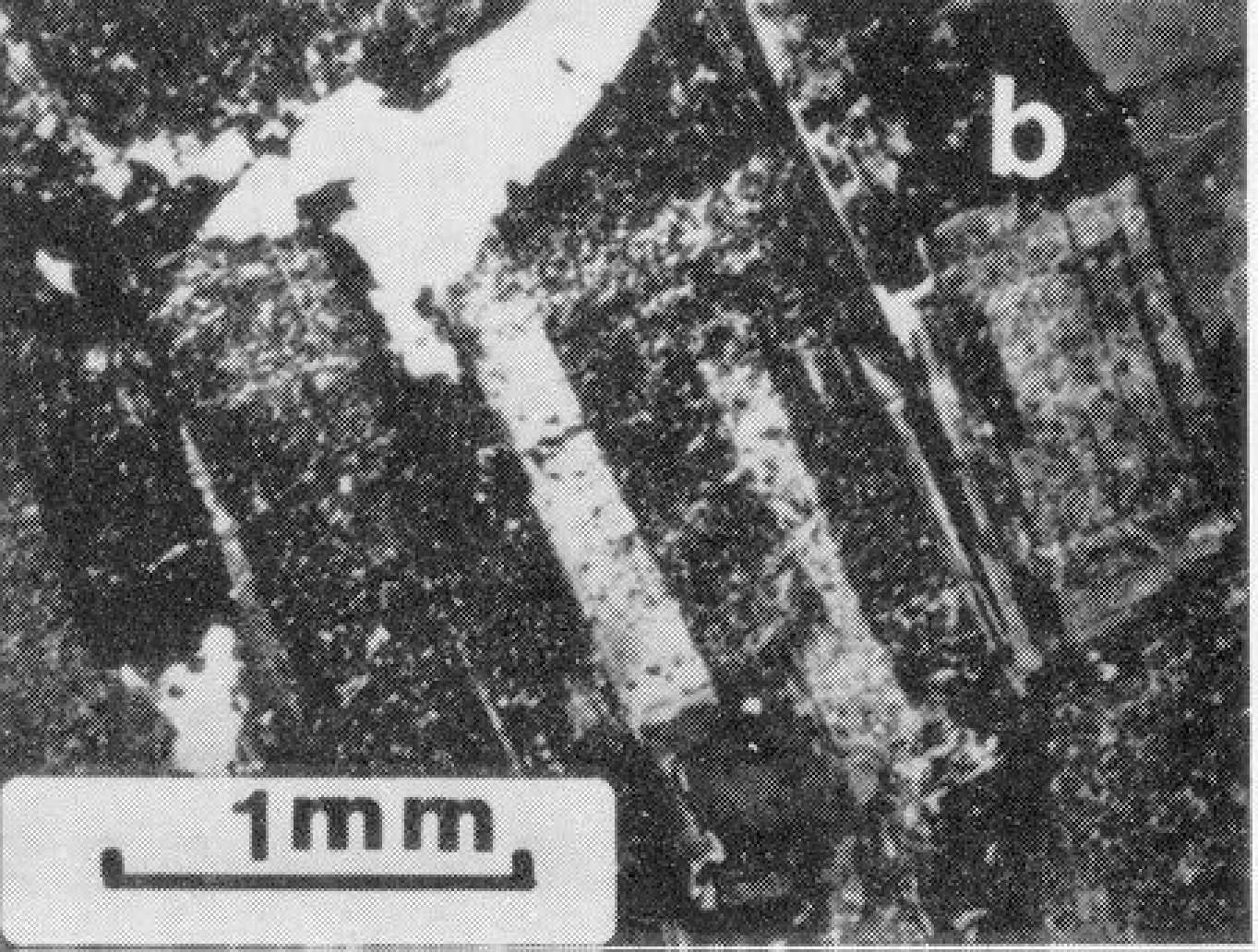
b
1mm

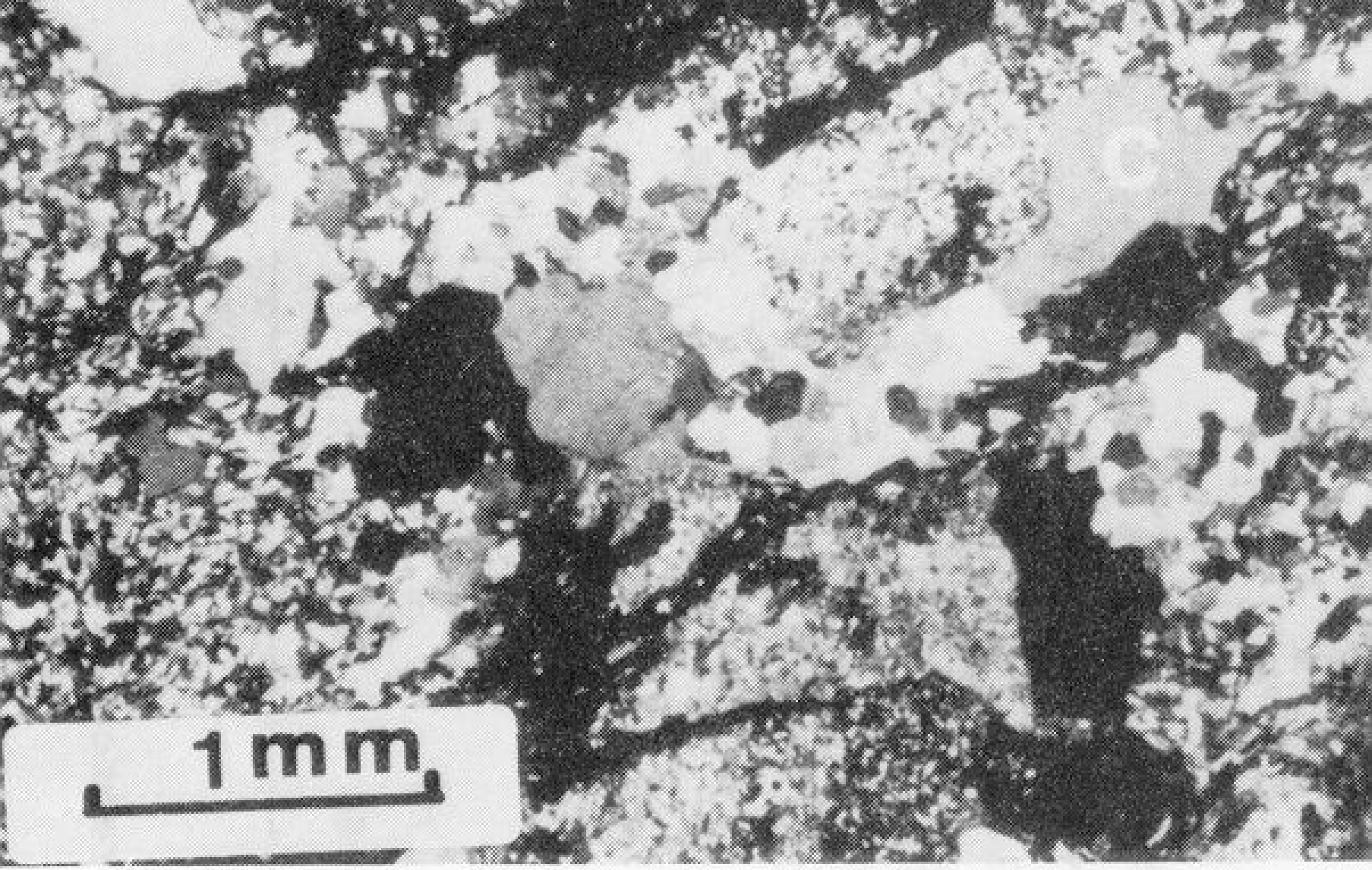
1 mm

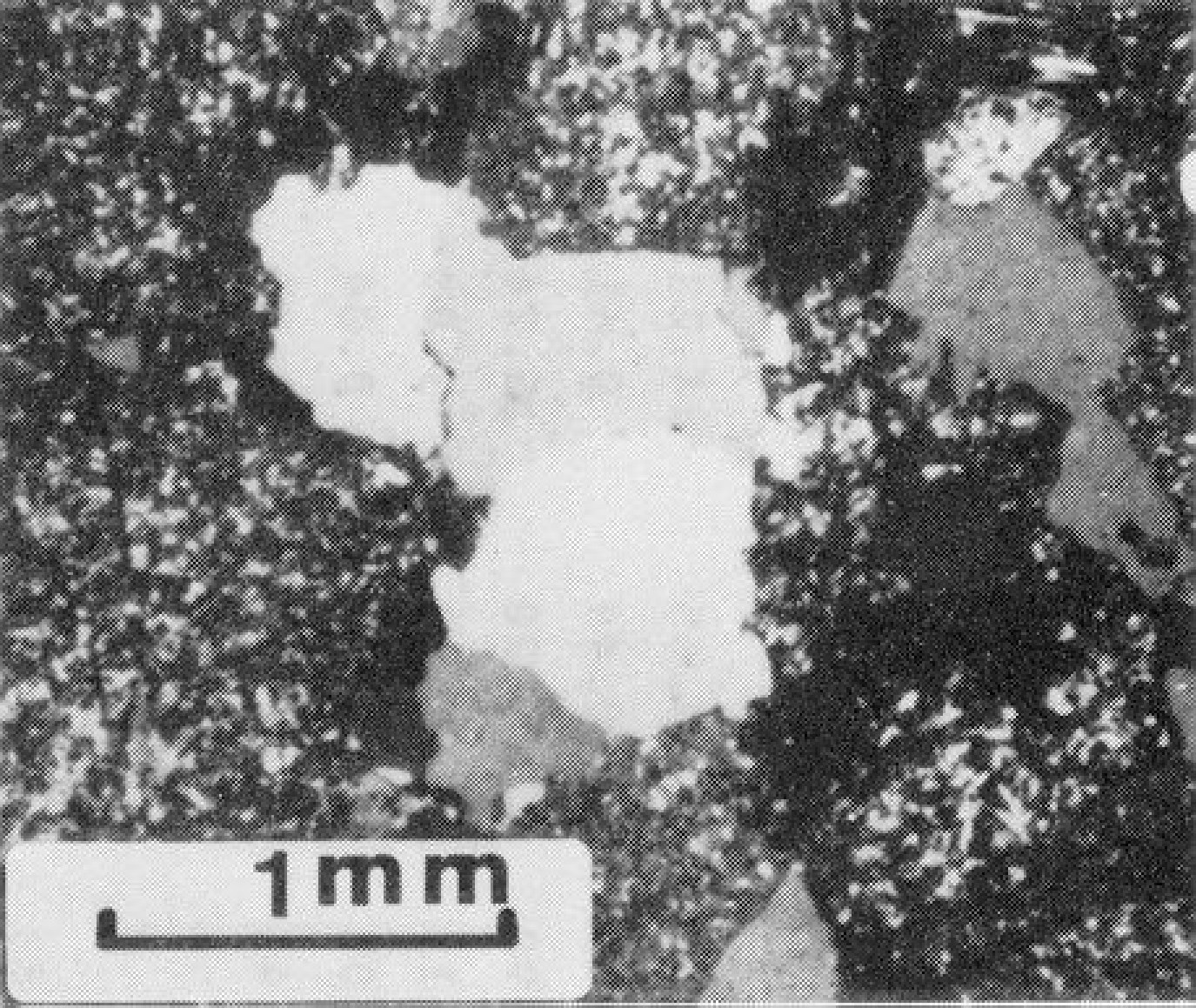
1 mm

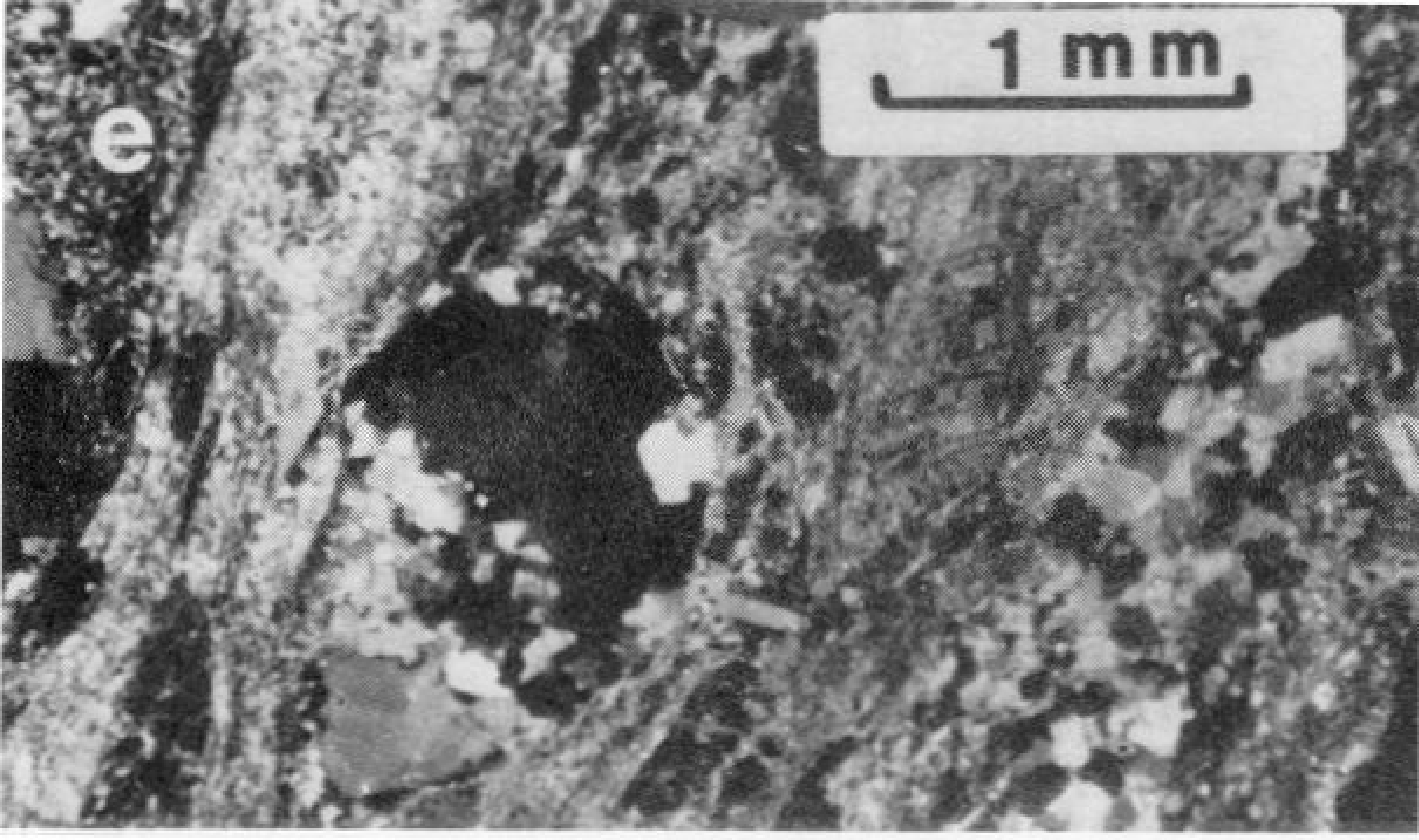
e
1 mm

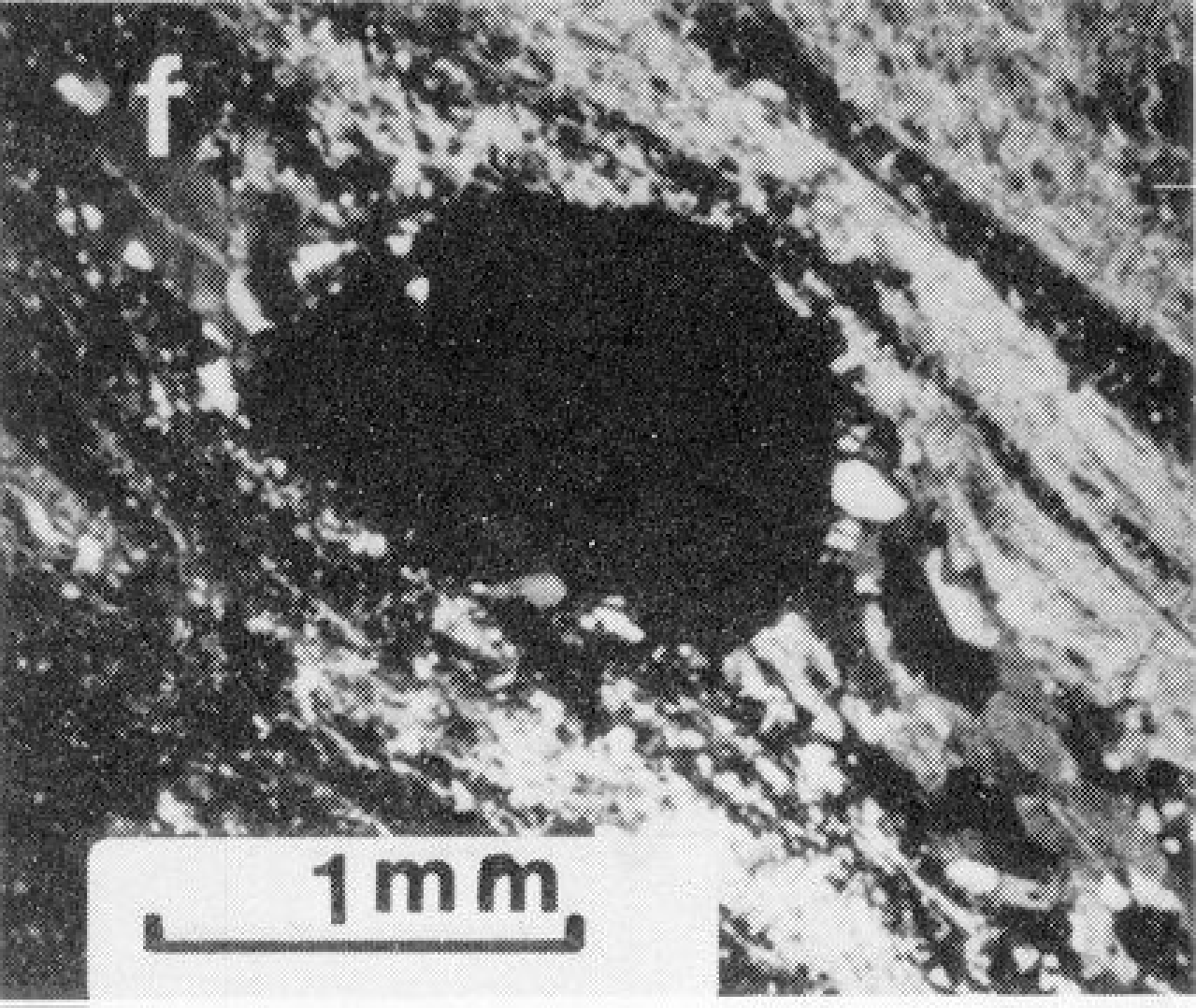
f
1mm